Strategies for hepatitis C virus elimination; from point of care testing to investigation of a natural vaccine model

Weronika Witkowska
BSc, MRes

A thesis submitted in fulfilment of the requirements for the degree of Doctor of Philosophy

MRC – Centre for Virus Research
Institute of Infection Immunity and Inflammation
College of Medical, Veterinary and Life Sciences
University of Glasgow

September 2019

Abstract

Hepatitis C virus (HCV) is a major cause of chronic viral hepatitis with over 70 million people affected worldwide. Recent advances in direct acting antivirals for HCV treatment have resulted in sustained virological response rates of more than 90%. Thus, the World Health Organisation (WHO) has developed a global strategy for elimination of the virus by 2030. Major barriers to elimination include the lack of a point-of-care (POC) test for immediate linkage to care and the development of a HCV vaccine.

This first part of this thesis covers experiments aimed towards the development of a novel POC test based on loop mediated isothermal amplification (LAMP). The second section of the thesis addresses the novel phenomenon of secondary spontaneous clearance (SSC), studied as a natural vaccine model to decipher the immune responses involved in spontaneous resolution following treatment relapse.

A double-blind study of HCV LAMP was conducted on RNA samples of all major HCV genotypes and viral loads. The sensitivity and specificity of the assay was 90% and 98%, respectively within less than 25 minutes of incubation which fulfils current WHO recommendations. We developed a user-friendly read-out based on a pregnancy-test like lateral flow device. LAMP has minimal equipment and training requirements with previous field studies making it ideal for a future HCV POC test.

The two cases of SSC post-treatment relapse were studied in comparison with four treatment failure (TF) patients. In both SSC cases, low levels of neutralising antibody were detected at the time of diagnosis but on relapse, a robust and sustained response was generated that reduced the infectivity of autologous viral pseudoparticles expressing HCV envelope proteins – a feature not present in any control patients. Furthermore, significant differences in levels of Th-1 cytokines were noted prior to treatment in SSC but not TF. This natural vaccine model (prime on acute infection, boost on relapse) adds weight to the importance of adaptive immune responses in resolving HCV infection.

Table of Contents

List of Tables

List of Figures

Publications

- Publications arising from this thesis

Witkowska W, Davis C, Sabir S, Garrett A, Bradley-Stewart A, Reboud J, Xu G, Yang Z, Gunson R, Thomson E.C, Cooper J. Loop mediated isothermal amplification: a powerful tool for rapid, cheap hepatitis C point-of-care diagnosis. 2019. *PLOS Biology* (Manuscript submitted).

Witkowska W, Swann R.E, Cowton V, Cole S, Asamaphan P, Sabir S, Davis C, Niebel M, McGregor E, McLauchlan J, Patel A.H, Cooper J, Thomson E.C. Secondary spontaneous clearance of acute hepatitis C following treatment relapse. 2019. *Lancet Gastroenterol Hepatol*. (Manuscript in preparation).

Acknowledgement

First and foremost, thank God for helping me through this journey.

I am forever indebted to my Master's project supervisor, Dr Tamer Abdelrahman, without whom I would never dream of completing a PhD project. Thank you for making me believe.

This work would not have been possible without the unwavering support from my supervisor, Dr Emma Thomson. Apart from our insightful meetings and many in-depth discussions I can never repay her for the positive attitude and enthusiasm towards my work. It was very inspirational, especially in difficult times. I truly could not have asked for a better supervisor.

I would also like to thank my second supervisor, Prof Jon Cooper, for his support and valuable time, especially in the last few months of my studies. I would never imagine I would have the chance to do research in Biomedical Engineering. Thank you for this wonderful opportunity and for inspiring me to do better.

My gratitude goes to other members (past and present) of the Thomson's group: Dr Chris Davis, Dr Shirin Ashraf, Mr Marc Niebel, Dr James Shepherd, Dr Suleman Sabir, Dr Sultan Alotaibi, Dr Walt Adamson and Dr Patawee Asamaphan. I am grateful for your mentoring, insightful scientific discussions, kindness, joined experiments and sharing resources. It has been a pleasure to work alongside every single one of you.

I am also very appreciative of the support I received from the collaborators at the School of Biomedical Engineering, especially Dr Julien Reboud. I am thankful for his feedback on my work progress whether through meetings, skype or email. I am also thankful for the kindness and support I received from my colleagues at the School of Engineering: Miss Alice Garrett, Dr Eloise Larson, Dr Zoe O'Hara, Dr Robert Wilson, Dr Gaolian Xu, Dr Zhugen Yang, Dr Shantimoy Kar and Dr Xiaoxiang Yan amongst others.

I would also like to express my gratitude to members of the Patel's group, especially Dr Vanessa Cowton and Mrs Sarah Cole. Without your guidance, assistance and materials provided this work would not have been possible.

My thanks also goes to my assessors – Prof Manuel Salmeron-Sanchez and Prof Arvind Patel. Thank you for your advice during our annual meetings

My gratitude also goes to other CVR members especially Dr Ania Owsianka and Dr Connor Bamford. Your knowledge and advice was very inspirational – thank you for all your help throughout the years and the materials you have provided.

I would like to thank Prof Rory Gunson and Dr Amanda Bradley-Stewart from the West of Scotland Specialist Virology Centre for providing samples for the double-blind study.

I am also thankful to my taekwondo instructor – Mr Karim Belgacem – for teaching me how to persevere. I believe that working through this PhD project is a true testament to that.

Finally I cannot thank enough my incredible family for their support and understanding, especially my mum and dad, my friends for their kind words and gestures to keep me going and my wonderful partner, Kris, for the emotional support and for never ceasing to believe in me.

Last, but not least to my dog, Roxi – thank you for the many distractions during the write-up period! It certainly helped alleviate all of my anxiety☺.

Author's declaration

This work was completed at the University of Glasgow between October 2015 and May 2019 and has not been submitted for another degree. All work presented in this thesis was obtained by the author's own efforts, unless otherwise stated.

Next generation sequencing was carried out by Dr Christopher Davis, post-doctoral researcher in the Thomson's laboratory.

The bioinformatics pipelines used for NGS data analysis were developed by Dr Sreenu Vattipally.

The neutralisation, Sanger sequencing and GNA-ELISA experiments for P76 were carried out by Dr Rachael Swann.

The phCMV expression vector was developed by Dr Vanessa Cowton, a post-doctoral researcher in the Patel's laboratory at the Centre for Virus Research.

The original paper and PMMA devices were based on templates designed by Miss Alice Garrett, Dr Gaolian Xu, Dr Shantimoy Kar and Dr Xiaoxiang Yan, researchers at the School of Engineering.

Abbreviations

Aa	Amino acid
Ad6	Adenovirus vector serotype 6
Ad24	Adenovirus vector serotype 24
ADCC	antibody-dependent cellular cytotoxicity
ALT	alanine aminotransferase
AP	Accelerating Primer
APC	antigen presenting cells
AP Ori	AP original
AP Rev	AP reverse
ARFP	alternative reading frame protein
ARV	anti-retroviral
BIP ori	original BIP
BLP	backward loop primer
BOC	boceprevir
bp	Base pair(s)
cAg	Core Antigen
CCL20	lectin 20
cDNA	complementary DNA
CE	European Conformity
Chad3	chimpanzee adenovirus 3
CLDN-1	Claudin-1
CLIAs	chemoluminescence immunoassays
Con1	genotype 1b clone
CTLA-4	cytotoxic T lymphocyte associated antigen-4
CypA	Cyclophilin A
DAAs	Direct Acting Antivirals
DCs	Dendritic cells
DEG	degenerate published primers
DMEM	Dulbecco's modified Eagle's medium
DMSO	Dimethyl sulfoxide
dNTPs	Deoxyribonuleotide triphosphates
dsRNA	double-stranded RNA
EAP	Early Access Program
EASL	The European Association for the Study of the Liver
ECLs	electrochemoluminescence immunoassays

EIAs	enzyme immunoassays
ELISA	enzyme-linked immunoassay
EMCV	encephalomyocarditis virus
ER	Endoplasmic Reticulum
FDA	Food and Drug Administration
FLP	forward loop primer
GAGs	glycosaminoglycans
Gal-9	Galectin 9
GM-CSF	Granulocyte macrophage colony stimulating factor
GNA	Galanthus nivalis agglutinin
Gt	genotypes
HBV	hepatitis B virus
HC5	healthy control 5
HC7	healthy control 7
HCC	Hepatocellular Carcinoma
HCV	Hepatitis C virus
HCVcc	HCV cell culture system
HCVpp	HCV pseudoparticle system
HICs	high-income countries
HIV	human immunodeficiency virus
HRP	Horseradish peroxidase
HTZ	Holtzman
HVR-1	hypervariable region 1
HVR-2	hypervariable region-2
IFN	interferon
IFN gamma	Interferon gamma
IgG	Immunoglobulin G
IgVR	intergenotypic variable region
IL2	Interleukin 2
IL-28	Interleukin 28
IRES	internal ribosome entry site
ISGs	Interferon Stimulated genes
IU/ml	international units per ml
KIRs	Killer cell immunoglobulin-like receptors
LAMP	Loop-Mediated Isothermal Amplification
LB2	Lysis Buffer 2
LCV	Leuco-crystal violet

LD	lipid droplets
LDV	ledipasvir
LICs	low income countries
LMICs	low-and-middle income countries
MADAs	Metal-Amplified Density Assays
Mab	monoclonal antibody
MAVs	mitochondrial antiviral
MF59C.1	gpE1/gpE2 with ‘oil in water emulsion’
MFI	Median Fluorescence Intensity
MHC	major histocompatibility complex
mi-122	microRNA-122
MLV	Murine Leukemia Virus
MSM	men-who-have-sex-with-men
MVA	modified vaccinia Ankara
nAb	neutralising antibodies
NANBH	non-A, non-B hepatitis
NASBA	nucleic acid sequence-based amplification
NAT	nucleic acid testing
NEB	New England Biolabs
NHC	New healthy control
NGS	next generation sequencing
NK	natural killer
NPHV	Non-Primate Hepacivirus
Nr	Norway rats
NTC	no template control
OCLN	Occludin
ORF	open reading frame
PBMC	Peripheral blood mononuclear cells
PBS	phosphate buffered saline
PD-1	Programmed death 1
pDCs	plasmacytoid dendritic cells
PEG-IFN	pegylated IFN
PIs	Protease Inhibitors
$PI_4KIII\alpha$	phosphate kinase III α
PKR	protein-kinase R
PMMA	Poly-methyl methacrylate
POCTs	Point-of-care tests

PRRs	pattern recognition receptors
PWID	people who inject drugs
RBV	ribavirin
RC	replication complex
RDTs	rapid diagnostic tests
RdRp	RNA dependent RNA polymerase
RFU	relative fluorescent units
RIG-1	retinoic-acid-inducible gene I
RNA	Ribonucleic acid
ROC	Receiver Operating Characteristic
RPMI	Roswell Park Memorial Institute
RT	Real Time
RT-PCR	reverse transcriptase real time PCR
RV	replication vesicles
RVR	rapid virological response
SA-PE	streptavidin-phycoerythrin
SC	spontaneous clearance
SDM	Site-directed mutagenesis
SMV	Simeprevir
SNPs	single-nucleotide polymorphisms
SOF	Sofosbuvir
SP	signal peptidase
SSC	Secondary Spontaneous Clearance
$STAT^{-/-}$	signal transducers and activators of transcription
SVR	sustained virological response
SPP	signal peptide peptidase
SRB1	scavenger receptor B1
TAE	Tris-acetate-EDTA buffer
TIM-3	T cell immunoglobulin and mucin domain 3
TIR	Toll-Interleukin receptor
TLRs	toll-like receptors
Tm	melting temperature
TMB	tetramethylbenzidin
TPA	time point A
TRAIL	tumour necrosis factor-related apoptosis inducing ligand
T regs	Regulatory CD4+T cells
TRIF	Toll-Interleukin receptor domain containing adapter inducing IFN-

TVR	telaprevir
UTR	Untranslated Region
VEL	velpatasvir
VLDL	Very Low-Density Lipoprotein
WHO	World Health organisation
WoSSVC	West of Scotland Specialist Virology Centre

Amino acid	Three letter code	One letter code
Alanine	Ala	A
Arginine	Arg	R
Asparagine	Asn	N
Aspartic acid	Asp	D
Cysteine	Cys	C
Glutamine	Gln	Q
Glutamic acid	Glu	E
Glycine	Gly	G
Histidine	His	H
Isoleucine	Ile	I
Leucine	Leu	L
Lysine	Lys	K
Methionine	Met	M
Phenylalanine	Phe	F
Proline	Pro	P
Serine	Ser	S
Threonine	Thr	T
Tryptophan	Trp	W
Tyrosine	Tyr	Y
Valine	Val	V

1 Introduction

1.1 Overview of hepatitis C virus infection

Hepatitis C (HCV) is a single-stranded positive-sense RNA virus belonging to the genus Hepacivirus within the *Flaviviridae* family (Choo et al. 1991). The *Flaviviridae* family also contains three other genera; Flavivirus (including Zika, Dengue, Japanese encephalitis and Yellow fever viruses), Pegivirus (including GB virus-A and human pegiviruses) and Pestivirus (including Border Disease virus and Bovine Viral Disease virus). The most closely related virus to HCV is the recently identified non-primate hepacivirus (NPHV) found in horses, dogs, rodents, bats and cattle (Kapoor et al. 2011). Despite relatedness of these viruses, HCV has a very narrow species tropism with humans and chimpanzees being the only known hosts.

First identified in 1989, HCV was found to be one of the aetiological agents of non-A non-B hepatitis acquired by patients following transfusion (Choo et al. 1989). The main mode of transmission of HCV is direct contact with infected blood through injection drug use or unscreened blood products, although vertical and sexual transmission has also been reported. The high replication rate of the error-prone RNA-dependent RNA-polymerase which has no proof-reading activity accounts for the variability of the HCV genome with at least 8 genotypes and over 60 subtypes described.

HCV is a major cause of chronic viral hepatitis with over 70 million people affected worldwide. Only 15-25% cases clear HCV infections spontaneously within the first six months following exposure, while the remaining 75-85% develop chronicity (Micallef, Kaldor & Dore 2006). The large burden of chronic infection is partially attributable to the mostly asymptomatic nature of HCV, which may only become apparent after 20-40 years when serious clinical manifestations, including liver steatosis, fibrosis, cirrhosis, and hepatocellular carcinoma (HCC) tend to develop (Perz et al. 2006). HCV is also associated with extrahepatic manifestations including increased resistance to insulin and Type II diabetes.

1.2 HCV genome

The HCV particle is approximately 50-60 nm in size and is structurally similar to that of other members of the *Flaviviridae* family. The glycoproteins E1 and E2 are anchored within the envelope lipid bilayer, which surrounds the nucleocapsid and is made up of repetitive subunits of the Core protein. This layer of Core encompasses a single strand of positive-sense RNA (Figure 1.1). The entire HCV genome is about 9.6 kb in size and encodes a large polyprotein of approximately 3010 amino acids, although the length is genotype and subtype-dependent (Choo et al. 1991). As a member of the *Hepacivirus* genus, the HCV genome is flanked by a 5' untranslated region (5'UTR) and a 3' untranslated region (3'UTR). These are the most conserved parts of the HCV genome and play important roles in RNA replication and translation. The 5'UTR is approximately 341 nucleotides in length with four structural domains and more than 90% sequence identity amongst different genotypes (Bukh, Purcell & Miller 1992). The first domain plays a role in RNA replication while the latter three are involved in translation and contain the internal ribosome entry site (IRES) (Brown et al. 1992; Honda, Brown & Lemon 1996; Smith et al. 1995). Domain IV contains a stem-loop with the start codon, AUG, which initiates translation of the viral polyprotein (Honda, Brown & Lemon 1996). The 3'UTR is located directly after a stop codon and varies in length from 200 to 235 nucleotides. It has three main regions namely; variable, poly(U/UC) and a highly conserved, 96 nucleotides long, X-region (Kolykhalov, Feinstone & Rice 1996; Tanaka et al. 1995; Yamada et al. 1996). The latter region is tightly associated with regulation of the translation process.

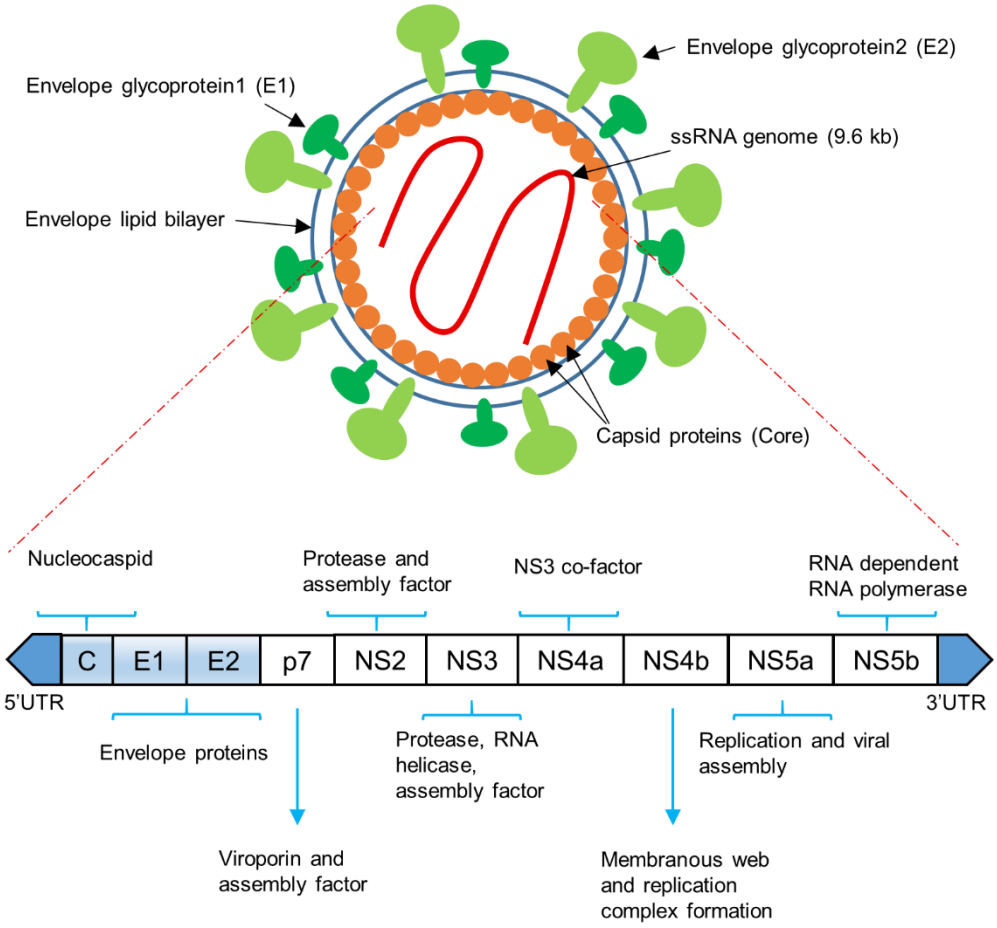

Figure 1.1 The structure and organisation of the HCV particle and genome
The viral particle consists of a lipid bilayer with embedded envelope glycoproteins, E1 and E2. The inner layer of the virus is made up of capsid proteins which form a protective layer surrounding the single stranded 9.6 kb positive sense RNA. This RNA encodes for a single polyprotein with various functions in the HCV life cycle as stated.

HCV has a single open reading frame (ORF), which encodes 11 proteins, including three structural proteins; Core, E1, E2, and seven non-structural proteins; p7 viroporin, NS2, NS3, NS4A, NS4B, NS5A, and NS5B (Figure 1.1 and Figure 1.2) (Choo et al 1991). The 11th 'F' protein results from a frameshift in the Core-coding region (Varaklioti et al. 2002; Walewski et al. 2001). Single proteins are separated from the large polyprotein through co and post-translational processing by the host and viral-encoded proteases (Hijikata et al. 1991). Each protein has a unique role in the viral life cycle and replication. The non-structural proteins are the targets of the recently-developed direct-acting antiviral drugs (DAAs). The structural proteins are key in vaccine development studies due to their position on the surface of the viral particle and central role

in viral evasion of the immune system. The functions and characteristics of these proteins are discussed in detail below.

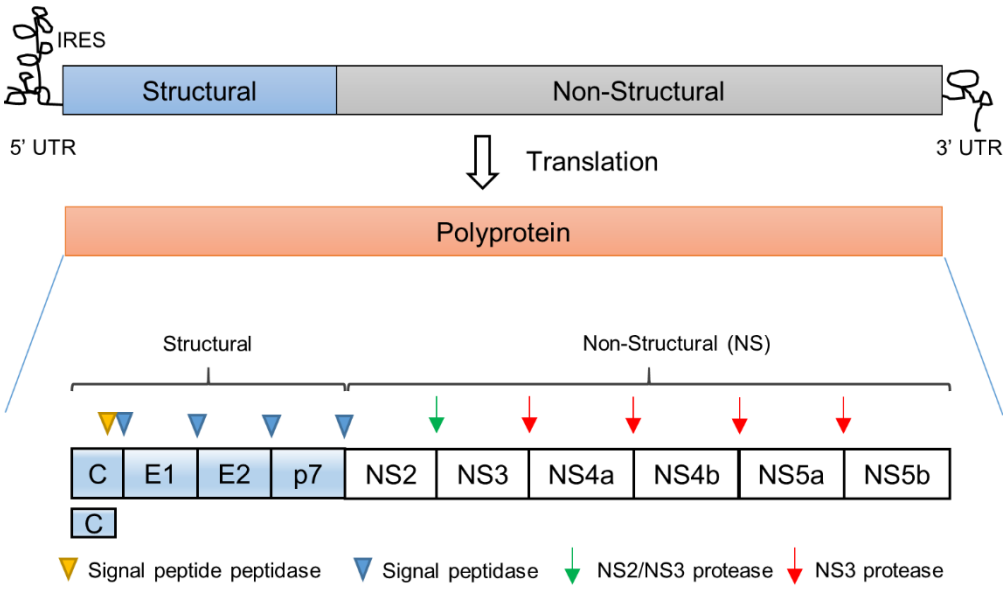

Figure 1.2 Hepatitis C virus genome organisation
The hepatitis C virus encodes for a large polyprotein with a single open reading frame. The entire genome of 9.6 kb is flanked by a 5' untranslated region of about 340 nt in length containing the internal ribosomal entry site (IRES) and by the 3' untranslated region of 250 nt in length. The open reading frame encodes for at least 10 viral proteins divided into structural and non-structural. Once translated, the polyprotein is cleaved into individual components by host signal peptide peptidase at the C-terminus of Core indicated by the yellow triangle and host signal peptidases indicated by the blue triangle. The remaining proteins are cleaved by viral NS2-3 protease (indicated by the green arrow) and viral NS3 protease (indicated by the red arrow) Adapted from (Bartenschlager, Cosset & Lohmann 2010).

1.2.1 Core and Alternative Frameshift proteins

Core is the most conserved HCV protein amongst all genotypes (Hitomi et al. 1995). Differences in the Core protein amongst genotypes may be associated with different rates of progression to disease, particularly steatosis (Kato et al. 2004). It is the first encoding protein located at the N terminus with a signal sequence located at the C terminus before the E1 envelope glycoprotein. The signal sequence allows the uncleaved polyprotein to translocate into the Endoplasmic Reticulum (ER)(Bartenschlager et al. 1994). Within the ER lumen, E1 is cleaved at the N-terminus by host signal peptidase (SP) producing the immature Core protein known as p23 (Yasui et al. 1998). Subsequent cleavage by signal peptide peptidase (SPP) results in release of the immature core protein from the ER anchor, producing a 179 aa long mature core protein (21 kDA). This forms the building blocks of the viral nucleocapsid which is involved in RNA packaging and viral budding. The mature Core protein consists of two domains; a

hydrophilic Domain I and a hydrophobic Domain II (Boulant et al. 2005). The highly basic hydrophilic domain is located within the first 120 aa of the N-terminus and has a role in RNA binding. The hydrophobic Domain II (aa 120 – aa 175) forms two alpha helices and assists in the association of Core with the ER and lipid droplets (LD).

Core protein has additional pleiotropic functions. The interaction of Core with a wide variety of proteins (both viral and cellular) may lead directly to liver disease. For example, the interaction of Core protein with components of the JAK/STAT signalling pathway lead to a reduction of IFN-alpha and decreased expression of Interferon Stimulated genes (ISGs), which inhibit viral infections (Lin et al. 2006). Core protein can also significantly suppress the immune response by binding to the complement receptor gC1qR present on the surface of many immune cells. This results in reduced production of Interleukin-12, a cytokine involved in the differentiation and stimulation of T cells (Kittlesen et al. 2000). Core also contributes to liver fibrosis via an interaction with Toll-like receptor 2, leading to increased deposition of extracellular matrix within hepatocytes, which subsequently impairs liver function.

Translation of the Core gene in an alternative reading frame may result in the production of the alternative reading frame protein (ARFP) or F protein. It is not entirely clear if this protein has an effect *in vivo*, but studies of chimpanzees where silent mutations were incorporated into ARFP, showed a clear decrease in liver pathology and virus production (Vassilaki et al. 2008). Core also plays a role in altering gene expression and apoptosis (Nguyen, Sankaran & Dandekar 2006).

1.2.2 E1E2 envelope glycoproteins

The host-derived envelope of HCV consists of two type I transmembrane proteins known as E1 and E2 (Michalak et al. 1997). The E1 and E2 proteins form a heterodimer and play a crucial role in both viral cell entry through interaction with hepatocyte receptors, and membrane fusion (Tong et al. 2018). The interaction of HCV with the cellular receptors Claudin-1, Occludin, CD81, and Scavenger receptor class-1 type 1 have been shown to be mediated via E2 while the role of E1 has not been fully elucidated (Douam et al. 2014; Petracca et al. 2002). One role of E1 is interaction with apolipoproteins, especially ApoE, which

aids viral cell entry (Mazumdar et al. 2011). The 160 amino acid N-terminal ectodomain of E1 forms a trimer confirmation on the surface (Falson et al. 2015). Although it contains a fusion-like domain, it does not fulfil the criteria for a class II fusion protein.

The recently-solved crystal structure of E2 revealed a globular, compact form differing greatly from the typically extended confirmation of class II fusion proteins common in other *Flaviviruses* (Khan et al. 2014; Kong et al. 2013). The ordered sections of E2 are dominated by ß-sheets linked by hydrophobic interactions and disulphide bonds. The majority of the E2 ectodomain is either unstructured or primarily composed of flexible loops (Khan et al. 2014; Kong et al. 2013).

Since E1 and E2 are both located on the surface of the HCV particles, they are exposed to the immune system and are thus excellent candidates for vaccine design. E1 and E2 are highly glycosylated with 4 and 9-11 N-linked sites, respectively, which help evade the antibody-mediated immune responses by protecting key HCV epitopes (Figure 1.3) (Falkowska et al. 2007).

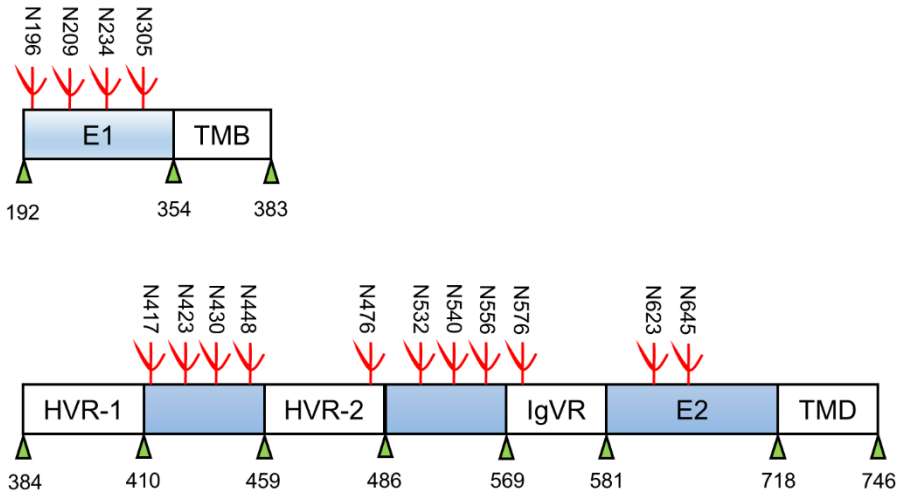

Figure 1.3 N-linked glycosylation sites on the E1 and E2 glycoproteins
The green triangles with numbers represent the amino acid positions of the polyprotein based on a genotype 1a reference strain (Genbank accession no. AF009609). The red branches represent the N-linked glycans with the amino acid position. HVR-1 – hypervariable region 1, HVR-2 – hypervariable region 2, TMD – transmembrane domain, IgVR – intergenotypic variable region. Adapted from Patel *et al* 2015 (Patel et al. 2015).

The crystal structures of the truncated form of E2 bound by antibodies provide the building blocks for vaccine development (Khan et al. 2014; Kong et al. 2013). E2 is highly disordered and flexible with highly variable immunogenic regions known as the hypervariable region 1 (HVR-1), hypervariable region-2 (HVR-2) and intergenotypic variable region (IgVR). To date, most broadly neutralising antibodies (nAb) have been shown to bind with globular or discontinuous epitopes rather than linear epitopes on the E2 protein (Angus & Patel 2011). Recent work led to the identification of three key nAb binding regions on the surface of E2, which include sites associated with CD81 binding (Drummer et al. 2006; Owsianka et al. 2006; Roccasecca et al. 2003; Sautto et al. 2013). These regions are located between amino acids 412-423 (Region 1), 434-446 (Region 2), 523-535 (Region 3) and 611-617 (Region 4) with the first three regions being adjacent to one another, facilitating CD81 binding as shown by X-ray crystallography (Figure 1.4) (Khan et al. 2014; Kong et al. 2013). Although many nAbs bind Region 1 of the CD81 binding residues of E2, they do so in different ways. Less than 2.5% of chronic patients develop similar antibodies, possibly due to HVR variability and glycan shielding, as well as E2 flexibility. E2 forms at least two different conformations in this region (Alexander W. Tarr et al. 2007). AP33 is an antibody originally developed in mice with a pangenotypic neutralisation profile and a threefold more potent humanised version known as MRCT10.v362 (Homer Pantua et al. 2013; Alexander W. Tarr, et al. 2006). The first E1 antigenic epitope structure was identified using the broad nAb IGH526. This antibody binds to a highly flexible region with an alpha-helical epitope (Kong et al. 2015).

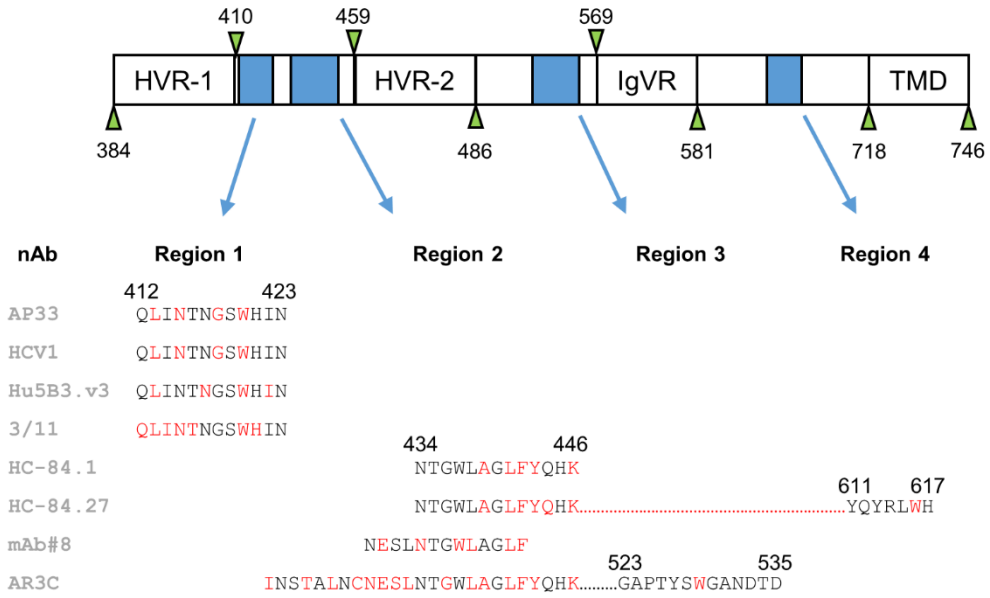

Figure 1.4 Four regions of the E2 glycoprotein implicated in nAb and CD81 receptor binding
The epitope sequences of each antibody is given below the region. Red indicates the contact residues discovered through structural analysis. The dots indicate two portions of a discontinued epitope. Amino acid numbering is based on the genotype 1a reference sequence (Genbank Accession no. AF009606). nAb – neutralising antibody, HVR-1/2 – hypervariable region 1/2, IgVR – intergenotypic region, TMD – transmembrane domain. Adapted from Patel *et al* 2015 (Patel et al. 2015)

1.2.3 p7

The small hydrophobic protein p7, separates the HCV structural proteins, Core and E1E2 from the non-structural proteins, NS2-NS5B. It belongs to a family of proteins known as Viroporins and is essential for virus assembly and release from infected cells (Steinmann et al. 2007). Oligomerization of Viroporins enables them to form pores or ion channels in cell membranes, thereby altering the ionic gradient and disturbing physiological cell functions (Scott & Griffin 2015). This, in turn, allows p7 to create a favourable environment for the viral life cycle stages, namely HCV assembly and egress (Nieva, Madan & Carrasco 2012).

1.2.4 Non-structural proteins

The non-structural proteins play a vital function in cleavage of the large polyprotein and subsequent viral replication and are not incorporated into newly synthesised virus particles (Suzuki & Suzuki 2016). The NS2 protein is cleaved at the N-terminal by host signal peptidase and subsequently inserts into the ER membrane, leaving the C-terminal in the cytoplasm. This allows the cysteine

protease activity to auto-cleave at the NS2/NS3 junction. In addition, NS2 is involved in viral assembly by acting as a scavenger protein for interactions with the E1, E2, p7, NS3-4A and NS5A proteins.

The NS3 protein is a 70 kDA protein, which acts as a serine protease at the N-terminus, cleaving the remaining non-structural proteins, namely at the junctions of NS3/4A, NS4A/4B, NS4B/5A, and NS5A/5B. NS3 protein function is dependent on the formation of a complex together with its 8-kDa cofactor, NS4A. NS3 also contains a C-terminal domain, which acts as an RNA helicase, unwinding double-stranded RNA (dsRNA) during replication. Binding of the NS3 helicase occurs at the poly (U) region of the 3'UTR with unwinding of dsRNA occurring in a 3'-5' direction during viral replication. The NS3/4A complex inserts into the ER membrane via the N-terminus of the NS4A protein through a transmembrane α-helix.

The NS4B, 27-kDA protein, plays a crucial role in intercellular membrane remodelling by forming self-oligomerised structures which act as platforms for the viral replication complex (RC). NS4B also initiates the formation of the membranous web, a multivesicular structure partially derived from the ER where viral RNA replication occurs.

Although the NS5A protein has no known enzymatic activity, it plays a crucial role in the assembly of viral replication complex through multiple interactions with host proteins. These interactions include for example phosphatidylinositol-4 phosphate kinase III α ($PI_4KIII\alpha$) which is involved in cellular signalling pathways and membrane trafficking. The phosphorylation status of NS5A is dependent on $PI_4KIII\alpha$ activity. In addition, the C-terminus of the protein helps in the production of infectious viruses by mediating interaction with Core proteins.

The NS5B is a 65-kDa RNA dependent RNA polymerase (RdRp), the enzymatic core of viral replication. NS5B produces negative strand RNA directly from the original RNA genome, which acts as a template for the subsequent production of positive-strand RNA genomes. Because RdRp has no proofreading or exonuclease activity, it is a million times lower in fidelity than eukaryotic DNA polymerases (Suzuki & Suzuki 2016).

1.3 HCV replication

HCV replication is initiated upon viral binding with hepatocytes, which are the primary infection site. ApoE is responsible for the initial attachment of HCV with hepatocytes via Heparan sulfate proteoglycan syndecan-1/syndecan-4 or scavenger receptor B1 (SRB1) (Barth et al. 2003; Scarselli et al. 2002). The LDL receptor has also been proposed as an initial point of contact due to the close association of the virus with Low and Very Low-Density Lipoproteins (V/LDL) (Agnello et al. 1999). The envelope glycoproteins, E1 and E2, primarily interact with glycosaminoglycans (GAGs) and subsequently with SRB1, CD81 tetraspanin and the tight junction proteins Claudin-1 and Occludin (Dubuisson, Helle & Cocquerel 2008; Pileri et al. 1998; Ploss et al. 2009; Scarselli et al. 2002) (Figure 1.5). These receptors synergistically allow for HCV endocytosis into the hepatocyte in a clathrin-dependent manner. Inside the hepatocyte, HCV particles reaches the endosome, where the low pH initiates viral uncoating and single-stranded RNA is released into the cytoplasm (Zeisel, Felmlee & Baumert 2013). The viral RNA is subsequently translated at the ribosomal units in the Endoplasmic reticulum (ER) via the 5'untranslated region, which contains the internal ribosomal entry site (IRES). This results in the formation of the large polyprotein of over 3000 amino acids in length, which is cleaved into individual proteins by cellular and viral proteases. All viral components of HCV are directly (or indirectly for NS4A protein via NS3) associated with ER membranes and together with the host factors form a 'membranous web' where viral replication takes place. These host cell factors include Cyclophilin A (CypA), phosphatidylinositol 4-kinase IIIα and microRNA-122 (mi-122). The RNA-dependent RNA polymerase in complex with other non-structural proteins replicates the HCV genome from a negative strand intermediate, which acts as a template. Newly formed RNA can subsequently re-enter the translation stage to produce more proteins or become packaged into the capsid made-up of Core proteins decorated by the structural proteins, E1 and E2. The progeny virus gains envelope protein through budding with the host ER lipid bilayer. HCV is closely associated with the VLPL synthesis pathway, which facilitates viral maturation and subsequent release into the bloodstream with apoE (Bartenschlager et al. 2011). This explains the apolipoprotein coating of HCV circulating in the

bloodstream. Another route of hepatocyte infection is direct cell-to-cell transmission, which can facilitate evasion of the immune system.

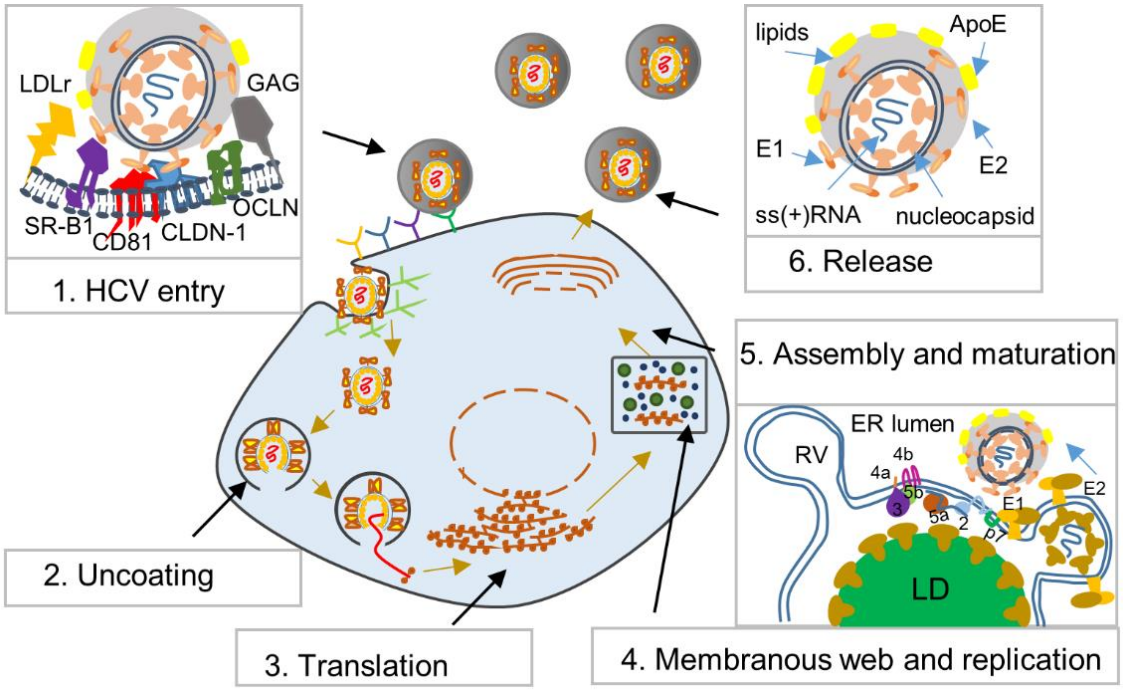

Figure 1.5 HCV life cycle
The HCV replication cycle is initiated by the binding of E1 and E2 envelope glycoproteins with glycosaminoglycans (GAGs) and the (very) low-density-lipoprotein (VLDL) (Step 1). A subsequent interaction with the scavenger receptor B1 (SR-B1), the CD81 tetraspanin, Claudin-1 (CLDN-1) and Occludin (OCLN) facilitates clathrin-mediated HCV entry into hepatocytes. Uncoating of the HCV particle occurs due to the low endosomal pH which also induces the conformational changes of E1E2 (Step 2). The released viral RNA is translated through the internal ribosomal entry site, located in the 5' untranslated region, at the endoplasmic reticulum (ER) (Step 3). The resulting 3000 amino acid long polyprotein is cleaved by cellular and viral enzymes into 10 individual proteins which associate with the ER membranes. Here, the NS4B and possibly NS5A proteins contribute to the formation of membranous replication vesicles (RV) which accumulate in what is known as the 'membranous web'. RNA replication initiates with a negative strand intermediate acting as a template for positive RNA strand production. These positive RNA strands are either used for translation of the polyprotein or are assembled into new viral particles. Assembly and maturation takes place within close vicinity of lipid droplets (LD) (Step 5). The VLDL synthesis pathway facilitates in viral maturation, association of HCV with LD and ApoE and the subsequent release of the newly produced viruses out of the cell (Step 6). The diagram was adapted from Bartenschlager *et al* 2010 (Bartenschlager, Cosset & Lohmann 2010).

1.4 Distribution, diversity, and modes of transmission

1.4.1 Epidemiology

HCV-related morbidities cause a significant number of deaths throughout the world. The number of viral hepatitis-related deaths increased from 0.89 million in 1990 to 1.45 million in 2013, the majority of which were caused by HCV and HBV (96%) (Stanaway et al. 2016). This pattern of increase is anticipated to continue unless the treatment of HCV is upscaled considerably (Razavi et al. 2014). The increased number of deaths is likely related to the expansion of injections both in health care settings and in people who inject drugs (PWID) (Magiorkinis et al. 2009). As it takes at least 10 years to develop HCV-related diseases, any increase in mortality may reflect an increase in infection rate 20-60 years before. In some countries, an increased incidence of HCV infection has also been reported in men-who-have-sex-with-men (MSM) and PWID (Conrad et al. 2015; Wandeler et al. 2015). Recent systematic reviews estimate that 115 million people are positive for anti-HCV antibodies and 71.1 million people are chronically infected worldwide (Blach et al. 2017; Gower et al. 2014), although lack of data in some regions of the World may make accurate estimations difficult (Niebel et al. 2017).

1.4.2 Genome diversity

HCV is associated with high genetic diversity and is classified into 8 different genotypes which differ by 30-35% at the genomic level (Simmonds 2004). The genotypes of HCV are further subdivided into over 90 known subtypes (Simmonds 2004). The error-prone RNA-dependent polymerase results in a high replication rate of 10^{12} virus particles/day (Powdrill et al. 2011). Within infected individuals, HCV circulates as a pool of related, but genetically diverse variants referred to as quasispecies (Farci, Bukh & Purcell 1997). Viral diversity contributes to both immune escape and resistance to anti-viral therapies.

While HCV has a global distribution, the genotype prevalence differs greatly from country to country and throughout different areas of the world (Messina et al. 2015). Genotype 1 and 3 have the highest prevalence around the world accounting for 44% and 25% of all infections, respectively (Blach et al. 2017). Genotype 1 is the most common genotype found in most European countries,

whereas genotype 3 mostly occurs in South Asia and in countries like Pakistan and India. The most recently discovered genotype 8 was discovered in Punjab, India (Borgia et al. 2018). Most genotype 2 and 6 cases are found in East Asia while genotype 4 infections are found in North, East and Central Africa and the Middle East. Genotype 5 contributes to the fewest number of all HCV infections with approximately 1.4 million cases worldwide, mostly in South Africa (Messina et al. 2015).

1.4.3 Transmission

The majority of HCV transmission occurs through contact with contaminated blood and blood products, which can be divided into three main routes: transmission occurring via unscreened transfusions, sharing needles by people who inject drugs (PWID) and unsafe medical practices during the administration of therapeutic drugs (Alter 2002; CDC 1998). Prior to the development of successful HCV screening tests, the dominant route of transmission occurred via unsafe medical practices with an estimated 3.8% of blood donors being infected before 1986 (Donahue et al. 1992). In high-income countries (HICs), the current risk of contracting HCV via blood transfusion is 0.001%, due to effective screening tests. This risk is at least 10 times higher in low income countries (LICs) (Donahue et al. 1992; Kupek 2004). Currently, the main route of transmission in HICs is intravenous drug use with 70-80% of infections in the last 30 years occurring through this route (Alter 2002; Dore et al. 2003). The prevalence of HCV amongst PWID is as high as 70-90% in some populations (Thorpe et al. 2000). The unsafe use of medical equipment, including contaminated needles for administration of drugs, occurs in up to 2 million individuals every year (Hauri, Armstrong & Hutin 2004). Low-income countries have the highest risk of transmission via this route due to lack of sterile needles and unsafe medical procedures with drugs often administered by untrained individuals. Egypt has the highest prevalence of HCV on a country level primarily due to contaminated needle use for the treatment of schistosomiasis between 1960 and 1987 (Frank et al. 2000). Outside of the main routes of transmission, both vertical transmission from an infected mother to foetus and sexual transmission have been reported. The former has been estimated to occur in approximately 5% of infected mothers although some studies have reported the risk to be as high as 20% (Mast et al. 2005; Roberts & Yeung 2002). It may be

most likely in mothers with a high viral load or in those co-infected with HIV. Sexual transmission mostly occurs in high-risk groups with multiple sexual partners or high-risk practices, particularly in MSM or with HIV co-infection (Alter et al. 1989; Magder et al. 2004; Rooney & Gilson 1998; Sánchez-Quijano et al. 1990). Outside of the high-risk criteria, sexual transmission remains relatively low-risk (Cavalheiro et al. n.d.; Magder et al. 2004).

1.5 Treatment regimens for hepatitis C virus

1.5.1 Old treatment regimens

HCV treatment regimens have changed rapidly since its discovery in 1989 (Choo et al. 1989). The first pilot study of 10 patients involved treatment with interferon (IFN) and was conducted in 1986 when HCV was referred to as the causative agent of 'non-A, non-B hepatitis' (NANBH) (Figure 1.6) (Alter et al. 1975; Hoofnagle et al. 1986). Two controlled trials followed the discovery of HCV employing three times weekly conventional IFN with sustained virological response (SVR) in approximately 10-25% of patients treated (Di Bisceglie et al. 1989; Davis et al. 1989). Another milestone in HCV treatment history occurred when ribavirin (RBV) was added to the IFNα2b treatment regimen in 1998. This resulted in 38% of patients being successfully treated after 48 weeks compared to 13% when IFN was used as the sole treatment option (McHutchison et al. 1998). In 2001, combination therapy was further improved by replacing IFN with pegylated IFN (PEG-IFN) which has a longer half-life, thus resulting in increased cure rates amongst patients (approximately 55%) (Fried et al. 2002).

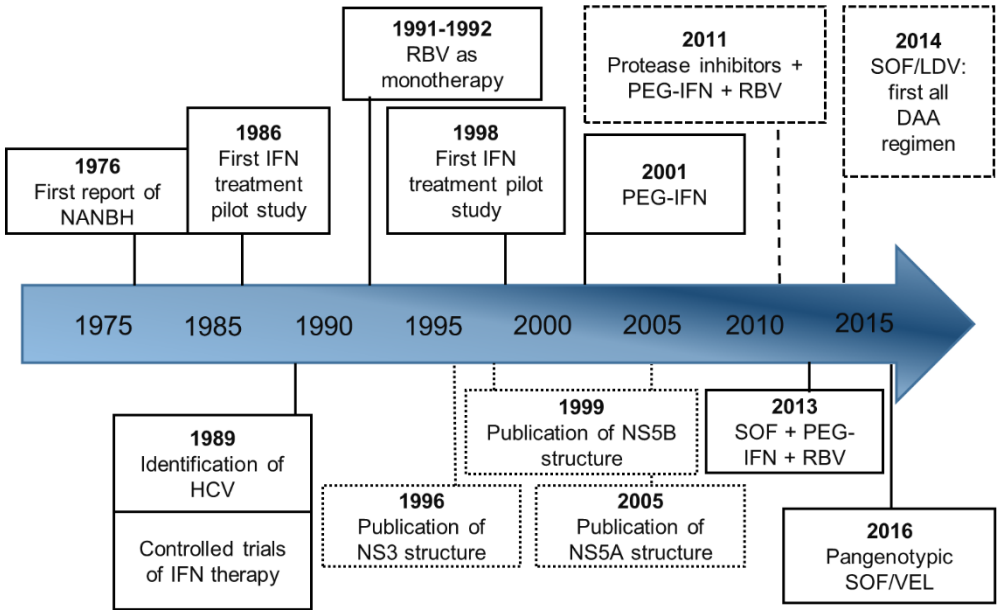

Figure 1.6 Timeline of events leading to advancements of HCV treatment regimens
NANBH – non-A, non-B hepatitis, NS – nonstructural protein, PEG-IFN, pegylated interferon, SOF – sofosbuvir, LDV – ledipasvir, VEL – velpatasvir, RBV – ribavirin. Adapted from Hepatitis C virus protocols (Law n.d.).

This combination therapy remained the standard treatment for HCV for a decade. The major drawbacks of the treatment combination were a less than ideal SVR rate, which differed greatly between genotypes, and numerous side-effects including reduced neutrophil and red blood cell count, flu-like symptoms, lack of energy/physical weakness and depression (Poynard et al. 1995). Classification of outcomes of treatment with PEG-IFN/RBV are shown in (Figure 1.7). SVR is defined as an undetectable viral load at least 12 weeks after the end date of therapy and is associated with clinical cure. Various studies with long term follow up of patients post-therapy have shown that a negative viral load after 6 months predicts absence of viral relapse in over 95% of patients (Lau et al. 1998; Marcellin 1997). Other treatment outcomes include, null response (when the patient does not respond and there are no changes in viral load of >2 $\log_{10}$ IU/ml), partial response (when the patient viral load decreases >2 $\log_{10}$ IU/ml, but remains detectable throughout treatment) and viral relapse (when the patient has undetectable levels of virus while on treatment but relapses 6 months following the end of therapy). Viral breakthrough (not shown on the figure) occurs when the patient initially has an undetectable viral load level as a

result of receiving treatment, which then becomes detectable while the patient is still receiving therapy.

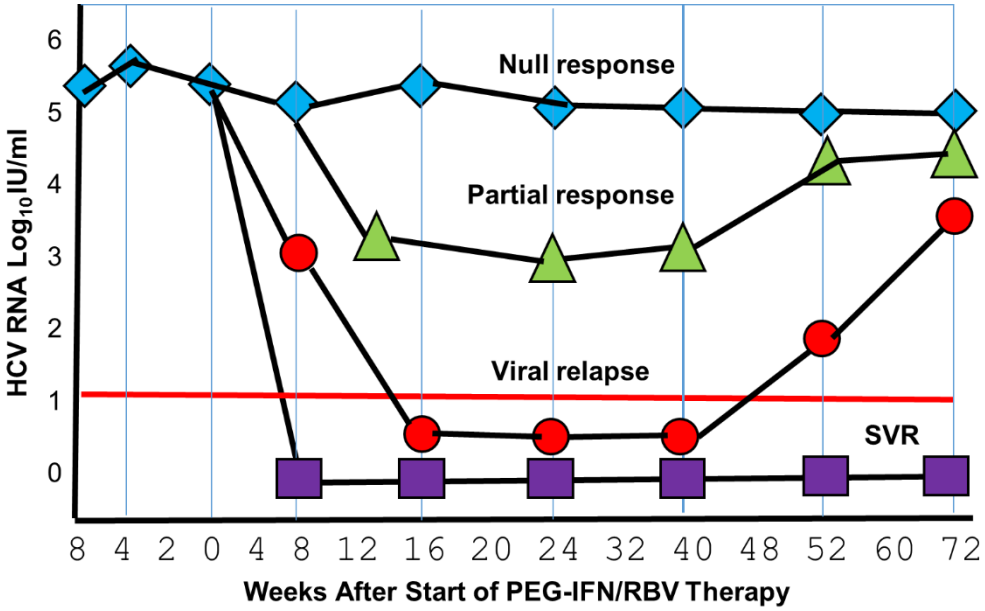

Figure 1.7 Outcomes of PEG-IFN and RBV combination therapy for HCV
Pegylated Interferon and Ribavirin (PEG-IFN and RBV) were the 'old' standard of care for treatment of HCV usually given over the course of 24-48 weeks. During the course of HCV, patients displayed various outcomes which were determined based on viral load of HCV RNA in $\log_{10}$ international units per ml (IU/ml) by qPCR. Null response (blue diamond) is when patients would display no changes (or changes of <2 $\log_{10}$ IU/ml of HCV RNA) over the course of treatment. Partial response indicated by green triangles is when patients' viral load decreased more than 2 $\log_{10}$ IU/ml of HCV RNA but stayed detectable throughout the course of treatment. Viral relapse (red circles) occurred when patients had undetectable levels of HCV RNA throughout the course of the treatment but became positive again for HCV RNA within 6 months from the end of treatment. SVR or sustained virological response occurs when patients have undetectable levels of HCV RNA 12 or 24 months after the end of treatment. The purple line on the graph indicates an undetectable viral load level. Adapted from Feld *et al* 2005 (Feld & Hoofnagle 2005a).

1.5.2 Direct Acting Antivirals

In 2011, a new wave of drugs known as Direct Acting Antivirals (DAAs) replaced previous standard treatments for HCV. As the name implies, the drugs act on the virus by directly targeting HCV proteins and functions and consequently different stages of the viral life cycle. The DAAs have been classified into four categories based on the proteins they act upon, namely, NS3/4A Protease Inhibitors (PIs), NS5A Inhibitors, Nucleoside/Nucleotide NS5B Polymerase Inhibitors, and Non-Nucleoside NS5B Polymerase Inhibitors. The first agents used in clinical practice were the NS3/NS4A protease inhibitors telaprevir (TVR) and boceprevir (BOC) which increased SVR rates to 65-75% in combination with PEG-IFN and RBV (Jacobson et al. 2011; Poordad et al. 2011). The FDA approval of these drugs led

to the development of yet another NS3/NS4A protease inhibitor Simeprevir (SMV) with similar SVR rates when used in combination with PEG-IFN and RBV, but fewer side-effects (Manns et al. 2014). A major breakthrough in the DAA treatment occurred with the development of the first NS5B polymerase inhibitor, Sofosbuvir (SOF), which is a nucleotide analogue. Nucleotide analogue drugs work by causing premature termination of RNA synthesis by incorporation into the growing RNA strand (Membreno & Lawitz 2011). SOF in combination with PEG-IFN and RBV achieved SVR rates of 90% in patients infected with genotype 1 or genotype 4. This high cure rate may be a reflection of the high barrier to resistance of nucleotide analogue NS5B polymerase inhibitors (Lawitz et al. 2013). Furthermore, SOF with RBV alone achieved SVR rates of 95% and 82% when used for genotype 2 and genotype 3 infected patients, respectively (Jacobson et al. 2013; Lawitz et al. 2013). The next major breakthrough arrived with the introduction of all-oral drug regimens, eliminating the need for IFN. Combinations of two or more types of DAAs were used to prevent the selection of resistant variants. The first all-oral combination treatment for genotype 1 was approved in 2014 and involved the use of SOF and the NS5A inhibitor ledipasvir (LDV). SVR rates for this combination treatment were 94-99%, even when RBV was not included and in treatment failure patients (Afdhal et al. 2014; Afdhal, et al. 2014). Most recently, the use of SOF in combination with velpatasvir (VEL), an NS5A inhibitor has led to improved potency and pangenotypic activity. Figure 1.8 lists all the currently approved DAAs and their protein target as well as all drugs undergoing clinical trials.

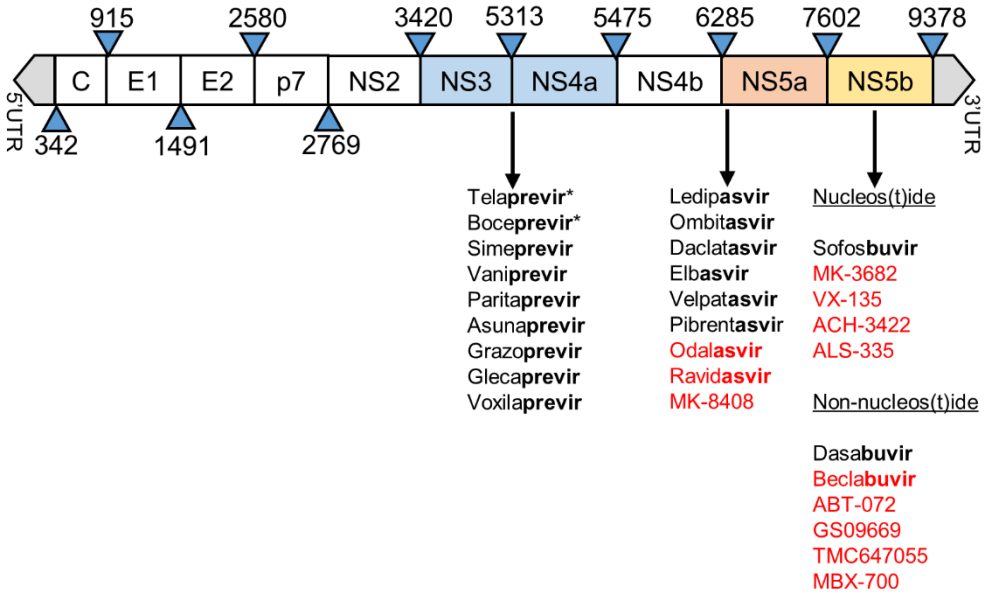

Figure 1.8 Direct acting antivirals for HCV treatment and their targets
Direct acting antivirals for HCV treatment are divided into four classes of drugs; NS3-4A inhibitors ('-previr'), NS5A inhibitors ('-avir') and NS5B inhibitors ('-buvir') further subdivided into nucleos(t)ide and non-nucleos(t)ide inhibitors. Drugs highlighted in red are currently undergoing clinical trials. The star symbol indicates previously approved drugs which have now been discontinued.

1.6 The immune responses and viral escape

The acute phase of HCV infection occurs during the first 6 months following exposure during which time a small proportion (10-40%) of individuals spontaneously clear infection while the majority progress to chronicity (Seeff 2002; Thomas & Seeff 2005). HCV RNA can usually be detected in blood within 7 to 14 days post exposure following an initial eclipse period. This is then followed by the appearance of HCV Core antigen (p22) for 6-10 weeks, prior to anti-HCV antibody appearance. In spontaneous clearers, HCV RNA and HCV antigen levels become undetectable typically within the first 6 months, while in progressors, HCV RNA increases rapidly and persists throughout the course of infection (Figure 1.9). Differences in immune outcome have been linked with innate and adaptive immune responses.

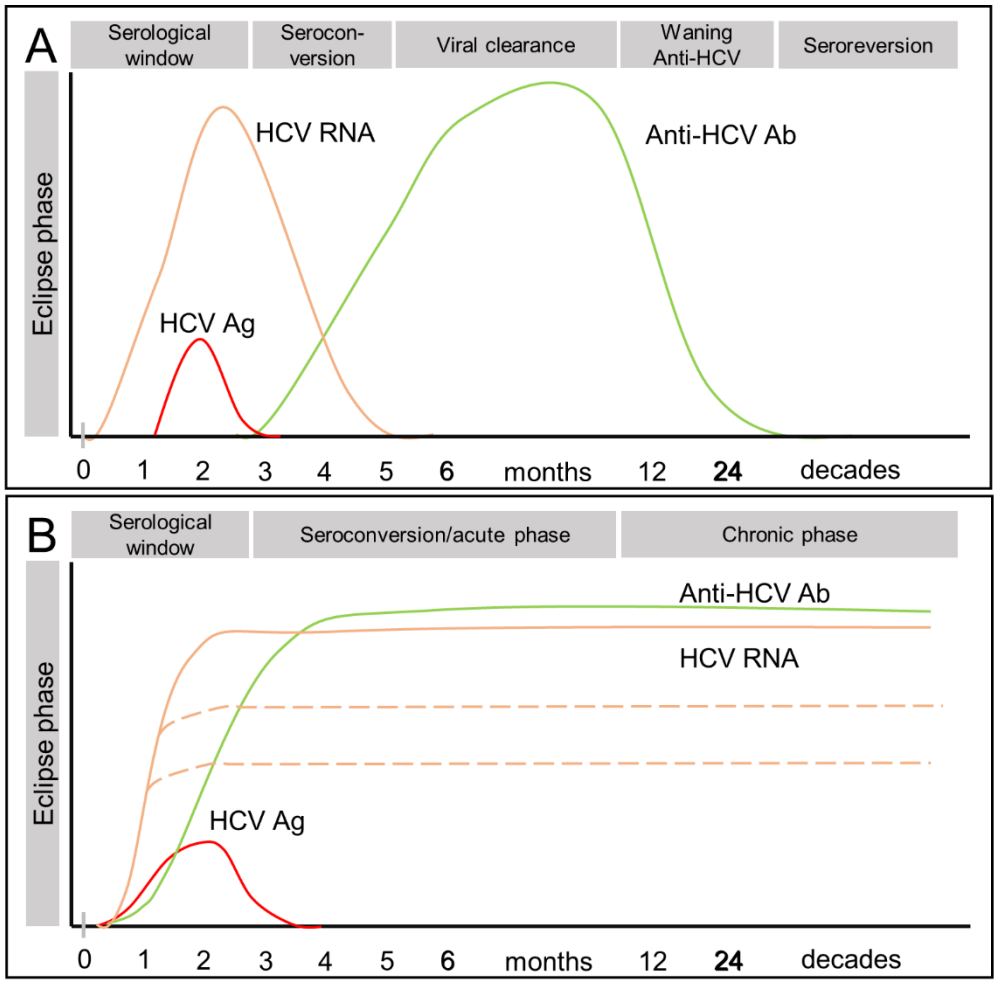

Figure 1.9 Natural history of HCV infection
A indicates approximate time course of HCV infection in a spontaneous clearer **B** indicates a chronic HCV infection. HCV Ag – HCV antigen, Ab – antibody. Adapted from WHO's guidelines on hepatitis B and C virus testing.

1.6.1 Innate immunity

The first line of host defence, termed innate immunity, occurs immediately after the onset of HCV RNA replication. Early innate immune responses include the production of IFN-stimulated genes (ISGs) in the liver and recognition by natural killer (NK) cells in peripheral blood (Thimme et al. 2001a). Initially HCV RNA is detected by pattern recognition receptors (PRRs) via toll-like receptors (TLRs) and other proteins, including toll-like receptor 3 (TLR3), protein-kinase R (PKR) and retinoic-acid-inducible gene I (RIG-I). These proteins act via activation of a Toll-Interleukin receptor (TIR) domain containing adapter inducing IFN-β (TRIF) in the case of TLR3 or via mitochondrial antiviral signalling proteins (MAVs) which subsequently leads to secretion of type I IFNs (Horner & Gale 2013). Auto- and paracrine IFN stimulation results in the expression of ISGs via the JAK-STAT signalling pathway, both in infected cells and surrounding cells, including Kupffer cells, plasmacytoid dendritic cells (pDCs) and myeloid dendritic cells (Lau et al. 2013; Takahashi et al. 2010; Wieland et al. 2014). This anti-viral signalling reduces viral replication and prevents infection occurring from cell to cell (Lau et al. 2013). NK cells play a key role in innate immunity by mediating killing of HCV infected cells. This function is performed via the production of granzyme and perforin and via tumour necrosis factor-related apoptosis (TRAIL). Killer cell immunoglobulin-like receptors (KIRs), present on NK cells, interact directly with MHC Class I ligands on infected cells (Jost & Altfeld 2013). The genetic allele KIR2DL3 has been linked with increased secretion of IFNγ and spontaneous clearance (SC) of HCV infection (Amadei et al. 2010). Several other host factors have been linked with resolution of infection either positively, for example, female gender, or negatively including co-infection with HIV, kidney pathologies, chronic use of alcohol and obesity (Feld & Hoofnagle 2005b). The strongest innate host factor associated with viral clearance known to date (detected via genome-wide association studies) are single-nucleotide polymorphisms (SNPs) near the IL28β (IFNλ4) locus. The most crucial SNP is rs12979860. A favourable CC allele is linked to SC and a positive outcome following IFN-based therapy. Unfavourable alleles include the heterozygous CT or homozygous TT (Afdhal et al. 2011; Suppiah et al. 2009; Thomas et al. 2009). More recently a novel dinucleotide mutation that can produce or interrupt an ORF of IFNλ4 has also been linked to predicting the outcome of HCV infection. Lack of expression of IFNλ4 is favourable for SC (Prokunina-Olsson et al. 2013).

1.6.2 Adaptive immunity

Adaptive immune responses play a major role in determining the outcome of HCV infection. Of particular importance is the role of antigen presenting cells (APC), primarily Dendritic cells (DCs), which bridge the transition of innate immune responses to adaptive immunity. Adaptive immune responses are not apparent until 6-8 weeks for cellular immunity and 8 weeks onwards for humoral responses, which may result in the formation of quasispecies and consequent evasion of the immune response (Organization 2016b).

1.6.2.1 Humoral responses

A rapid and sustained immune response is essential for SC; a delayed humoral response may partly explain why the majority of patients develop chronicity (Netski et al. 2005; Thimme et al. 2001b; Vernelen et al. 1994). Although the role of humoral immune response has been only partly explored, several studies highlight the importance of nAb responses in SC. Chronic disease has been associated with low titres of nAb with narrow reactivity against various HCV genotypes, while SC is often associated with a rapid, high titre and broadly reactive response (Bjoro et al. 1994; Dowd et al. 2009; W O Osburn et al. 2014; Pestka et al. 2007; Raghuraman et al. 2012). When serum levels of Ab are lowered, for example following administration of the CD20 B cell inhibitor rituximab, viral titre tend increase, resulting in more rapid disease progression, a phenomenon which is reversed following restoration of initial Ab levels (Ennishi et al. 2008). In studies using animal models, passive immunisation with nAbs help to control HCV infection, a finding also reflected in humans where accidental contamination of blood products with HCV occurred (Bresee et al. 1996; Farci et al. 1996; Morin et al. 2012; Yu et al. 2004). Despite this, studies in chimpanzees have revealed that not all cases of SC are associated with effective Ab responses (Bassett et al. 1999; Major et al. 1999). Humoral immune responses can also act via antibody-dependent cellular cytotoxicity (ADCC). This phenomenon occurs when Ab are simultaneously bound to infected cells through the variable region and to Fc receptors on NK cells through the Fc region. This NK cell interaction leads to release of cytokines, degranulation and subsequent lysis of the infected cell. The presence of ADCC-inducing Abs targeting the E2

glycoprotein has been reported both in acute and chronically infected patients(Nattermann et al. 2005).

A major flaw in humoral immunity to HCV is that it is often delayed, resulting in weakened responses during primary infection (Dowd et al. 2009). Moreover, anti-HCV Abs mostly target the HVR portion of the E2 glycoprotein, which has a high mutation rate and can often act as an immunological decoy (Weiner et al. 1992). Many key nAb epitopes are shielded by glycosylation sites on the envelope glycoproteins as well as closely associated lipoproteins (Helle et al. 2007).

1.6.2.2 Cellular responses

Cellular adaptive immune responses in HCV infection are crucial in determining the outcome of disease. T cells in patients who progress to chronicity tend to recognise a smaller repertoire of CD8 and CD4 T cell epitopes. In contrast, SC is often associated with concurrent recognition of up to 9 CD8 and up to 14 CD4 T cell epitopes (Cooper et al. 1999; Day et al. 2002; Lechner et al. 2000a). The T cell response is typically directed against the NS proteins. Different epitopes may act as targets even in patients with the same HLA type (Lauer et al. 2002, 2004; Smyk-Pearson et al. 2006). This potent broadly-active helper T cell and cytotoxic T cell response changes during chronic disease when the epitope repertoire becomes narrower and weaker (Day et al. 2002; Dustin, Cashman & Laidlaw 2014). A major evasion mechanism is the ability of the HCV virus to accumulate mutations in CD8 T cell epitopes which become fixed within the quasispecies (Bowen & Walker 2005; Cox et al. 2005; Erickson et al. 2001). These polymorphisms typically occur during the acute phase of viral infection.

The genetic repertoire of HLA alleles is responsible for the selective presentation of target epitopes (Gaudieri et al. 2006; Timm et al. 2004). Some HLA types are favourable, for example HLA*B27 and HLA*B57, which are highly linked to SC. This occurs due to presentation of epitopes with a high fitness cost upon accumulation of mutations (Dazert et al. 2009; Neumann-Haefelin et al. 2006). CD8 T cells typically exert their function by eliminating HCV-infected cells via two mechanisms; the non-cytolytic pathway involving inhibition of replication without killing target cells or the cytolytic killing mediated by perforin/granzyme pathway or surface death receptor via Fas/FasL (Klenerman

& Thimme 2012). In HCV infection the non-cytolytic pathway is primarily mediated by production of IFNγ. The initial stages of infection in progressors may be characterised by a 'stunned' phenotype where CD8 T cells have an impaired ability to produce IFNγ and are consequently unable to control HCV replication (Lechner et al. 2000a). In SC, following production of IFNγ, a rapid reduction of the viral load and ALT levels are observed. This observation is directly linked with an increase in CD4+T cells and subsequent elimination of HCV (Thimme et al. 2001a). CD4 T helper cells play a vital role in maintaining HCV specific CD8 T cells. In a study on chimpanzees, reduction of T helper cells resulted in low cytokine production from CD8 T cells and reduction of CD8 T cell specific to HCV, leading to viral escape mutations (A Grakoui et al. 2003). In chronic infection CD8 T cells express exhaustion markers such Programmed death 1 (PD-1),cytotoxic T lymphocyte associated antigen-4 (CTLA-4) and T cell immunoglobulin and mucin domain 3 (TIM-3), which result in a reversible loss in function *in vitro* (Fuller et al. 2013). High expression of PD-1 in the early phase of infection has been linked to progression to chronicity (Urbani et al. 2006). In persistent infection, CD8 T cells display a so-called 'exhausted' phenotype characterised by co-expression of PD-1, 2B4, CD160 and KLR61 (Bengsch et al. 2010; Bowen et al. 2008; Kasprowicz et al. 2008; Urbani et al. 2006). Regulatory CD4+T cells (T regs) have also been implicated in CD8+T cell exhaustion, loss of function and progression to chronicity (McMahan et al. 2010; Nakamoto et al. 2009; Penna et al. 2007). T regs typically exert their function by releasing regulatory cytokines such as IL-10 and TGF-ß and the production of TIM-3 ligand, Galactin 9 (Gal-9), which results in apoptosis of CD8 T cells and Th1 cells (Abdel-Hakeem & Shoukry 2014).

1.7 Barriers to HCV vaccine development

1.7.1 Models of infection

The recent development of the DAAs will help to cure over 90% of those who receive treatment, although the high cost, treatment accessibility worldwide and drug resistance are still major concerns. Various studies suggest that successful therapy with DAAs may not necessarily prevent liver disease, due to patients becoming re-infected. Moreover, treatment-induced cure of HCV infection does not protect against future encounters with the virus (Beinhardt et

al. 2018). Therefore, an effective vaccine remains an important goal for the elimination of HCV (Kumthip & Maneekarn 2015). Various *in vitro* and *in vivo* models have been developed in recent years in order to facilitate the development of a prophylactic HCV vaccine by studying different stages of HCV life cycle and host-viral interactions.

1.7.1.1 *In vitro* models

The first *in vitro* model of HCV replication was established in 1999, when Lohmann *et al*. discovered the minimal requirements for HCV replication by combining NS3/4A, NS4B, NS5A and NS5B proteins in a partial genome system otherwise known as the HCV subgenomic replicon (Lohmann et al. 1999). The first prototype system was derived from a genotype 1b clone (Con1), in which the structural protein-encoding genes were replaced by the neomycin phosphotransferase gene responsible for G418 antibiotic resistance. This resistance gene is driven by the HCV IRES while the non-structural genes are preceded by the IRES of encephalomyocarditis virus (EMCV) driving their expression (Figure 1.10). The initial subgenomic replicon system produced low levels of viral replication in the HCC cell line, Huh-7, until adaptive cell culture mutations increased replication by several orders of magnitude (Blight, Kolykhalov & Rice 2000; Lohmann et al. 2001). To date, subgenomic replicons of all six major genotypes (1-6) have been described, greatly facilitating the development of DAAs and studies of drug resistance (Blight et al. 2003; Saeed et al. 2012, 2013; Targett-Adams & McLauchlan 2005; Wose Kinge et al. 2014; Yu et al. 2014). A major limitation of the replicon system is the lack of infectious particle production as there are no structural proteins present, thus only viral replication stages of the HCV life cycle can be studied.

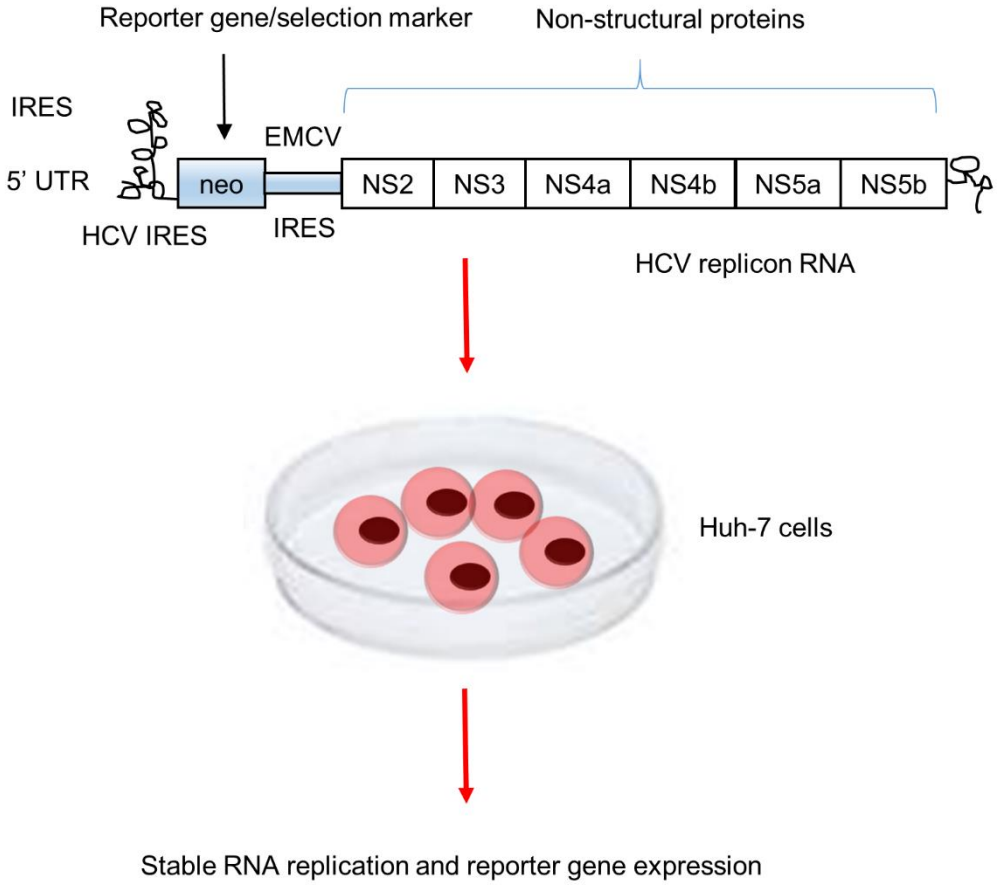

Figure 1.10 The structure and production of the HCV subgenomic replicon system
The HCV subgenomic replicon system consists of the 5'UTR containing the HCV IRES, a reporter gene/selection marker, EMCV IRES, HCV non-structural genes from NS2 to NS5B and the 3'UTR. The replicon is transfected in Huh-7 cells, which drives HCV viral replication by selecting for the resistant clones through the selection marker – for example G418 antibiotic resistance in the neomycin phosphotransferase gene, resulting in stable RNA replication *in vitro*. Alternatively a reporter gene can be used to replace the selection marker thus allowing monitoring of replication. IRES – internal ribosome entry site, EMCV – encephalomyocarditis virus, neo- neomycin phosphotransferase, 5'UTR – 5' untranslated region.

Another major milestone occurred with the development of the HCV pseudoparticle system (HCVpp), which enabled investigation of the cell entry stage of HCV life cycle. This system expresses HCV envelope glycoproteins on the surface of defective retroviral-derived particles (Birke Bartosch, Dubuisson & Cosset 2003). HCVpp are synthesised in a kidney cell line (293T) following transfection with three plasmids. The three plasmids encode for the Gag-Pol proteins of the Murine Leukaemia Virus (MLV) or human immunodeficiency virus (HIV), a reporter gene such as luciferase or GFP encoded in a retroviral genome and the E1 and E2 glycoproteins of HCV (Hsu et al. 2003) (Figure 1.11).

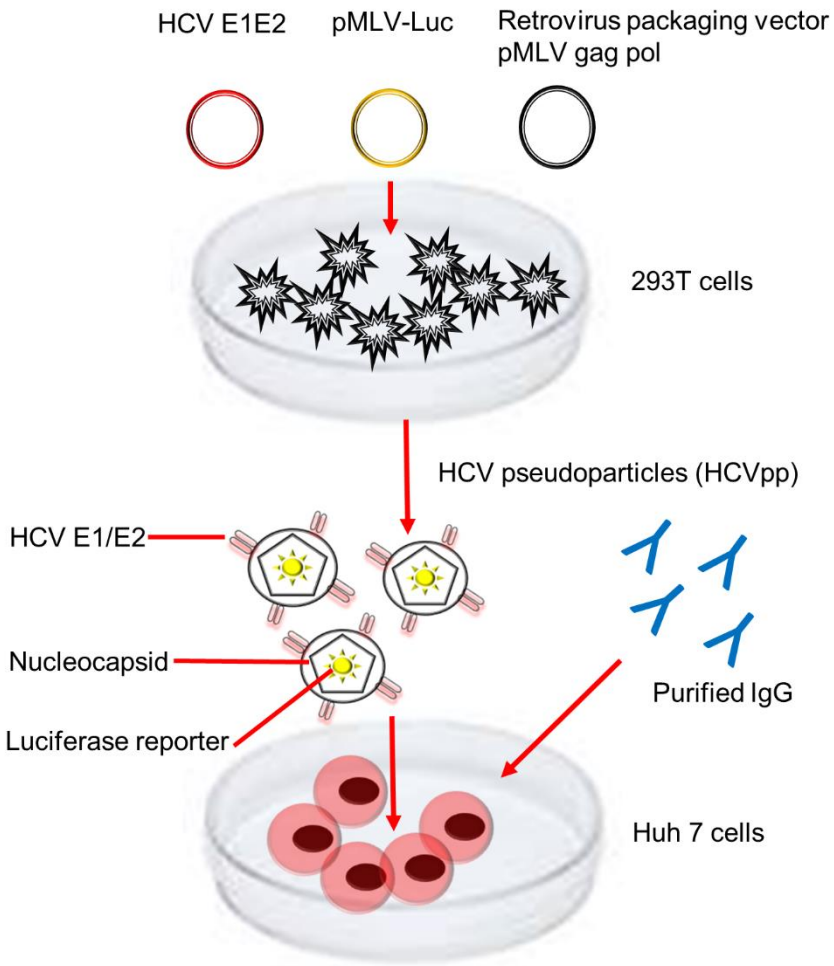

Figure 1.11 The HCV pseudoparticle system
HCV pseudoparticles (HCVpp) are produced in 293T cells following transfection with three plasmids, namely, HCV E1E2, Murine Leukaemia Virus luciferase reporter (pMLV-Luc) and the Retroviral packaging vector (pMLV gag pol). HCVpp are then used to infect permissive cell lines, such as Huh-7 cells. Replication can be monitored via the luciferase signal. Purified Immunoglobulin G (IgG) and patient sera incubated with the HCVpp can be used in the infection of Huh-7 cells in order to study neutralizing antibody responses

The HCVpp system has allowed scientists to investigate HCV entry by studying interactions between the E1 and E2 glycoproteins and receptors and attachment factors on the cell surface. Furthermore, the system has been central to the study of nAb responses to E1E2 glycoproteins in patient serum samples facilitating the identification of cross-neutralising antibodies, contributing to vaccine design (A W Tarr et al. 2006). A major limitation of the HCVpp system is the lack of association with lipoproteins, which occurs naturally in the viral life cycle, partly because the particles are produced in a kidney cell line rather than liver-derived cells. Furthermore, the particles assemble like retroviruses. The system only allows study of the viral entry stage of the life cycle.

The first cell culture system (HCVcc), which enabled the study of the complete HCV life cycle was established in 2005 (Lindenbach 2005). HCVcc systems were derived from a genotype 2a HCV isolate from a **J**apanese patient with **f**ulminant **h**epatitis thus termed 'JFH1', which produced low levels of infection in the Huh-7 hepatoma cell line (Wakita et al. 2005; Zhong et al. 2005) (Figure 1.12).

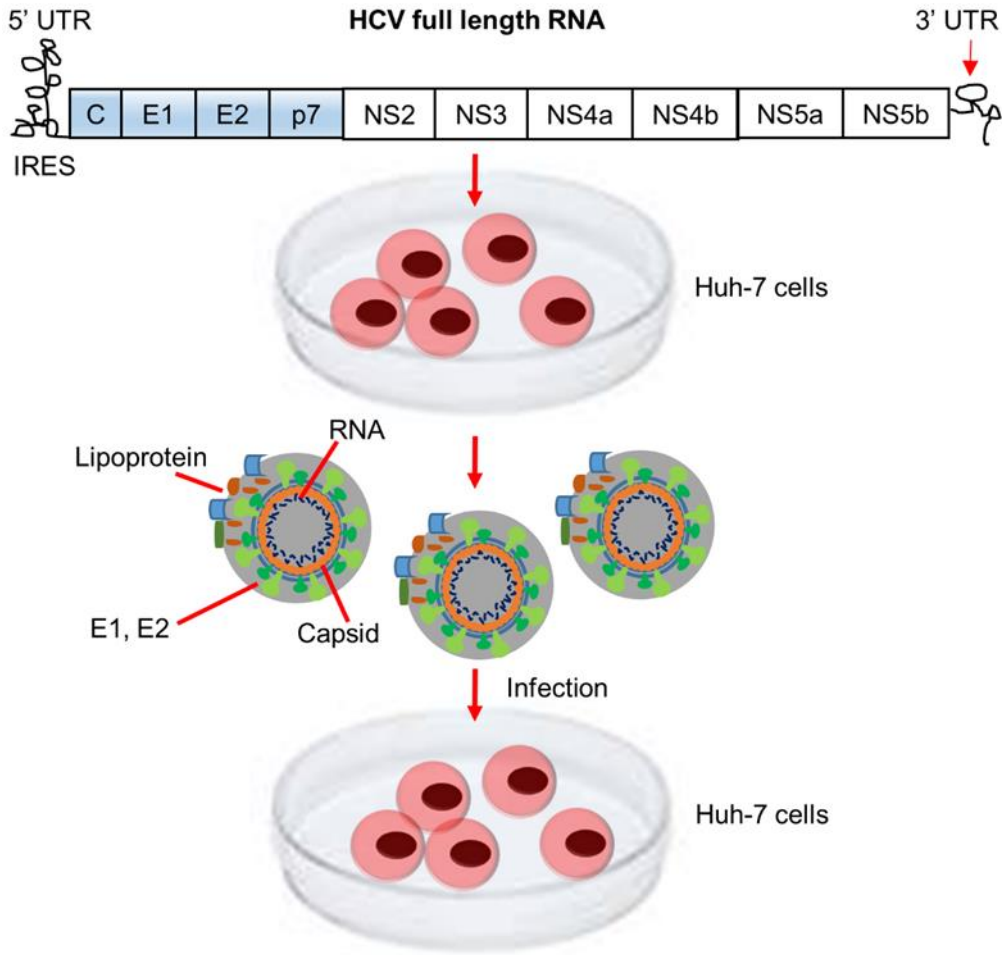

Figure 1.12 The HCV cell culture system

Studying the HCVcc system lead to the discovery of new entry factors and, due to its infectivity in chimpanzees and other *in vivo* models, enabled testing of various HCV vaccine candidates (de Jong et al. 2014; Law et al. 2008; Lindenbach et al. 2006; Prentoe et al. 2011). The replicative fitness of the HCVcc model was later improved by removing the Core to NS2 region and replacing them with the same region of another genotype 2a isolate, J6 (Lindenbach et al. 2006; Lohmann et al. 2003; Pietschmann et al. 2006). More recently, several luminescence and florescence-based reporter genomes have been created by fusing the reporter with the viral protein, NS5A or alternatively adding as additional proteins, which are cleaved by the viral protease (J. M. Gottwein et al. 2011; Judith M. Gottwein et al. 2011; Liu et al. 2012; Liu, Chen & Hagedorn 2014). In order to study DAA potency in various HCV genotypes, several intergenomic chimeras were made by replacing the genes in the J6/JFH1 backbone with genes from all other HCV genotypes (1-7), for example C-NS2, NS3/4A, NS5A and NS5B (Gottwein et al. 2007, 2013; Russell et al. 2009). Most recently, novel full length genotype 1 and 2 genomes have been cultured *in vitro* (Li et al. 2012; Ramirez et al. 2014).

1.7.1.2 Animal models

For many years, the chimpanzee (*Pan troglodytes*) was the only HCV animal model. Despite the apparent relatedness of humans to chimpanzees (98% similarity at the genome sequence level), the outcomes of HCV infection differ greatly between the two species. Only a small portion of HCV-infected humans will spontaneously clear the infection (15%) whereas most chimpanzees resolve their infection with only 30-40% progressing to chronicity (Lanford et al. 2001). Moreover, to date, fibrosis has never been reported in chimpanzees with only one case of HCC ever reported (Muchmore et al. 1988). The natural susceptibility of the chimpanzee model has not only helped to confirm the cause of non-A non-B hepatitis, but has facilitated research of the immune responses and in studying potential HCV vaccines (Bigger, Brasky & Lanford 2001; Elmowalid et al. 2007; Forns et al. 2000; Fuller et al. 2013; A. Grakoui et al. 2003; Major et al. 2002; Meunier et al. 2011; Mikkelsen et al. 2011; Weiner et al. 1990). Unfortunately, the use of this natural HCV model was discontinued in 2013 for ethical reasons as well as expense and limited availability of the animals. Efforts have been subsequently made to develop an alternative *in vivo*

model, which would mimic as many clinical features of human HCV infection as possible, desirably at a lower expense, higher reproducibility with minimal ethical constraints.

The tree shrew (*Tupaia belangeri*) is a non-primate mammal that allows low level of HCV replication with some HCV-associated manifestations (Amako et al. 2010; Feng et al. 2017). However, the *Tupaia* model is limited by the low number of animals available and lack of chronic stage of infection limiting its use in vaccine studies.

Transgenic mice can be genetically altered in order to express HCV structural or non-structural proteins or a combination of both. While this model is useful in studying viral and host protein interactions, it is not useful for studying the immune responses in vaccine studies. Moreover, random integration of the transgene results in high and uncontrolled overexpression of the proteins and is a major limitation in the reproducibility of the model.

Since mice are naturally resistant to HCV, one of the approaches of establishing infection is by transplanting them with primary human liver cells. This is not easy to achieve in immunocompetent mice as the immune system rejects the transplanted graft, thus mice models are usually immunocompromised (Bumgardner et al. 1999; Bumgardner, Heininger, et al. 1998; Bumgardner, Jiashun, et al. 1998). Another obstacle is the need for liver injury in order to allow for proliferation of human hepatocytes, which can be achieved by either chemical, surgical or genetic methods (von Schaewen, Ding & Ploss 2014). A number of immunocompromised liver xenograft mice models have been developed including the Timera, Alb-uPA-SCID and FRG mice models (Galun et al. 1995; Grompe et al. 1993; Heckel et al. 1990; Overturf et al. 1996; Sandgren et al. 1991) which allow passive immunisation studies but are nonetheless limited by their impaired immune responses and therefore cannot easily be utilised in research studying vaccine development (Meuleman & Leroux-Roels 2008).

Another approach is the use of immunocompetent models, with alternative methods of preventing graft rejection by the host. One such model is the Tolerized Rat model, which is created by injecting Huh-7 cells prior to birth,

thereby inducing tolerance towards the foreign cells (Kline et al. 1994; Ouyang et al. 2001). The rats are subsequently injected intrasplenically with the same cell line within the first day following their birth. The model supports HCV replication, albeit at a low level, with a maximum viral load of 22,500 copies/ml (Wu et al. 2005). Liver-related sequelae and HCV gene expression are also observed. The major drawback of the system is the use of cancerous liver cells rather than a primary cell line, as well as low levels of human hepatocytes, as the rat hepatocytes are also still present. The host immune system does not recognise viral antigens due to the incompatibility of the human major histocompatibility complex (MHC) on the human liver cell, limiting its use in studying immune responses (Wu et al. 2005). In recent years, efforts have focused on the adaptation of the rodent host to natural HCV infection, rather than the adaptation of the virus to the new host as described above. For this purpose Adenoviruses have been used to mediate transient expression of the human entry factors required for viral cell entry, namely CD81, SR-B1, OCLN and CLDN1 (Dorner et al. 2011). This results in entry of HCV into liver cells of the Rosa 26-Fluc mice model although impaired innate immune response signalling ($STAT^{-/-}$) is needed for low level replication lasting up to three months (Dorner et al. 2013). Unfortunately, this model system does not lead to liver-related pathologies and the level of receptors is physiologically too high (Ding et al. 2017). Furthermore, B cell development and tight-junction formation are impaired. One way to overcome this problem is by humanising the second extracellular loops of CD81 and OCLN resulting in physiological expression of chimeric HCV receptors. Despite this, low-level replication limits the usefulness of the model in studies evaluating the interaction of the virus and the host immune response. Chen *et al* recently developed an ICR-C/OTg mouse model which can be challenged with HCV-infected serum or the HCVcc system and sustains infection for over a year (Chen et al. 2014). In this model, the liver becomes moderately inflamed with both steatosis and fibrosis present, although no HCC has been reported to date. Therefore, the ICR-C/OTg mouse remains a very important HCV model amongst the current *in vivo* systems.

HCV-related viruses which establish infection in non-primate mammals including rodents, dogs and horses serve as effective fully immunocompetent HCV homolog models. One example is the GB virus originally found in tamarins which were

subjected to experimental serum infection from a case of acute hepatitis in a surgeon (G.B) (Stapleton et al. 2011). Marmosets and tamarins have been used as models for evaluating protective immune responses although infrequent chronic infection is a major drawback of this system (Bukh et al. 2008; Deinhardt 1967). Recently, next generation sequencing studies identified new HCV homologs including hepaciviruses and pegiviruses. The NPHV originally isolated from dogs is of particular interest, although horses were later identified as the natural hosts (Kapoor et al. 2011; Scheel, Simmonds & Kapoor 2015). NPHV is similar to HCV infection due to tissue tropism, establishment of chronic infection and liver-related manifestations. The major drawback of the model is the large size of the animals and associated costs. Two novel hepatotropic hepaciviruses termed NrHV-1 and NrHV-2 were also recently isolated in Norway rats (Nr) living in New York (Firth et al. 2014). NrHV can establish chronic infection only in immunocompromised mice with no type I IFN or adaptive immune responses while immunocompetent mice (such as C57BL/6J or BALB/c) resolve challenge with the virus within the first few weeks (Billerbeck et al. 2017). Therefore studies have focused on the natural host infections in the rat. Various rat lines including Spraque-Dawley, Holtzman (HTZ), Long Evan and Wistar Han have shown partial control of challenges with NrHV. Importantly, infecting HTZ rats with NrHV results in inflammation of the liver and steatosis which resembles HCV infection (Trivedi et al. 2018). NrHV infection in rats represents the first small animal model permissive to hepacivirus replication in the liver(Firth et al. 2014).

1.7.2 Vaccine development

Two HCV vaccine candidates are currently in clinical trials with the aim of elucidating humoral and cellular immune responses. The first targets the NS3-NS5 proteins and is based on an adenovirus vector with the aim of eliciting CD4 and CD8 T cell responses (Folgori et al. 2006). Initial experimental studies relied on the use of Adenovirus vector serotype 6 (Ad6) and 24 (Ad24) encoding HCV genotype 1b NS proteins. This was later boosted with plasmid DNA and chimpanzees were infected with a heterologous genotype 1a virus. The resulting broadly reactive CD8 T cell response reduced the viral loads of acute infection in 4 out of 5 animals while 2 out of 5 controls developed chronic infection (Folgori et al. 2006). Human Ad6 prime and chimpanzee adenovirus 3 (ChAd3) boost were later used in healthy humans which lead to polyfunctional cross-reactivity in

CD4/CD8 T cells for a minimum of 12 months. More importantly, T cells shared the same functions and phenotype as functional effector memory T cells (Barnes et al. 2012; Kelly et al. 2015). The ChAd3 was later used as a prime with modified vaccinia Ankara (MVA) boost in uninfected, healthy volunteers resulting in a high number of broadly reactive memory T cells (Swadling et al. 2014). This vaccine is currently in Phase II clinical trials in a cohort of PWID (NTC01436357).

The second vaccine is currently in a Phase I clinical trial and is based on recombinant gpE1/gpE2. To date, this candidate has demonstrated protective immune responses against homologous/ heterologous viruses, sometimes leading to sterilising immunity in animals (Choo et al. 1994; Meunier et al. 2011). Prior to the clinical trial, the gpE1/gpE2 with 'oil in water emulsion' (MF59C.1) adjuvant was tested in healthy volunteers. This resulted in nAb responses and CD4 T helper cell responses directed against the E1 and E2 glycoproteins (Frey et al. 2010; Law et al. 2013; Ray et al. 2010; J. A. J.-X. Wong et al. 2014).

Although both vaccine candidates elucidated high immunogenicity and protective immunity in chimpanzees and healthy volunteers, it is unclear whether these responses will protect all cases of HCV exposure. Future vaccines will most likely aim to target both humoral and cellular immune responses. Despite recent advancements in HCV vaccine development, this area of research remains challenging due to high viral diversity, lack of suitable animal models, the asymptomatic nature of acute HCV infection and lack of access to high risk cohorts for testing vaccine candidates. Another major obstacle is the translation of our current knowledge of protective immune responses into a prophylactic vaccine model.

In the context of studying vaccine models and challenges with HCV in high risk cohorts, our group was recently presented with a unique opportunity to study immune responses in a natural vaccine model. In a large cohort of acutely infected patients including MSM, infected healthcare workers and PWID, 85 patients did not spontaneously resolve within the first 3-6 months of infection and were treated with 24-48 weeks of IFN/RBV dual therapy (Thomson et al. 2011). A total of 63 (74.1%) achieved a sustained virological response, but the remaining 22 (25.9%) did not and either relapsed (8/22), had a null or partial response (12/22) or were treatment intolerant with subsequent viral relapse

(2/22). Unexpectedly, 2 out of 8 of the relapse patients subsequently spontaneously resolved the infection within 3 months after relapse with no further treatment. We have called this novel phenomenon ‘Secondary Spontaneous Clearance’ (SSC). This novel phenomenon mimics a natural vaccine model with a prime on initial infection and boost on relapse and could potentially add valuable findings to the studies of the adaptive immune responses in HCV research; both humoral and cellular.

1.8 The World Health Organisation elimination strategy

In 2013, viral hepatitis was estimated to cause 1.46 million deaths worldwide, with the majority of the burden coming from infections with hepatitis B virus (HBV) and HCV (Stanaway et al. 2016). HCV alone has a prevalence of 71 million people with chronic infection worldwide (Mohd Hanafiah et al. 2013). Preventing new infections would decrease the incidence of new infections. However without supplementary strategies, an additional 7.2 million deaths are predicted to occur between the years 2015 and 2030 due to HCV alone. In 2014, as a direct result of this burden, the World Health Assembly asked the World Health organisation (WHO) to identify possible strategic methods to eliminate HCV (and HBV) by 2030 worldwide (Resolution of Hepatitis 2014). Five target areas were identified, including, universal vaccination for HBV for new-borns, eliminating vertical transmission by vaccination or other methods, preventing horizontal transmission by ensuring safe injections and quality-assured screening of blood products, reducing harm by providing sterile needles for PWIDs and treatment of those infected (WHO 2016a). If all five targets would be reached by 2030, the overall incidence of viral hepatitis infections has been estimated to decrease by 90% with a 65% reduction in deaths. In 2016 a total of 36 countries developed national elimination strategies while 33 were preparing national plans to enact the elimination efforts. With the arrival of highly effective DAAs, a high number of deaths can be avoided even in LMICs where most infections occur. Despite the introduction of cost-effective treatment methods, most individuals are unaware of their infection status. Therefore, effective diagnosis of HCV is essential for immediate linkage to care.

1.9 Diagnosis of HCV

1.9.1 Current diagnostic algorithms

The current diagnostic algorithm for HCV is broadly divided into two categories of tests: serological testing and nucleic acid testing (NAT). The diagnostic algorithm usually starts with serological tests used to screen for anti-HCV antibodies due to their relatively low cost when compared to NATs (Figure 1.13). Serological tests have many forms including laboratory-based enzyme immunoassays (EIAs), rapid diagnostic tests (RDTs), electrochemoluminescence immunoassays (ECLs) and chemoluminescence immnoassays (CLIAs). All these tests are designed to screen for history of exposure to HCV and have to be followed up by a NAT to confirm active infection. NATs can be either qualitative or quantitative and can be replaced by testing for HCV Core Antigen (cAg). There are several purposes for NATs/cAg testing including: confirmation of current infection and monitoring response to treatment. If a patient is confirmed to have active HCV infection, further testing may be recommended including genotype testing to determine the best treatment options and fibrosis stage by non-invasive tests and liver biopsy (WHO. 2016b).

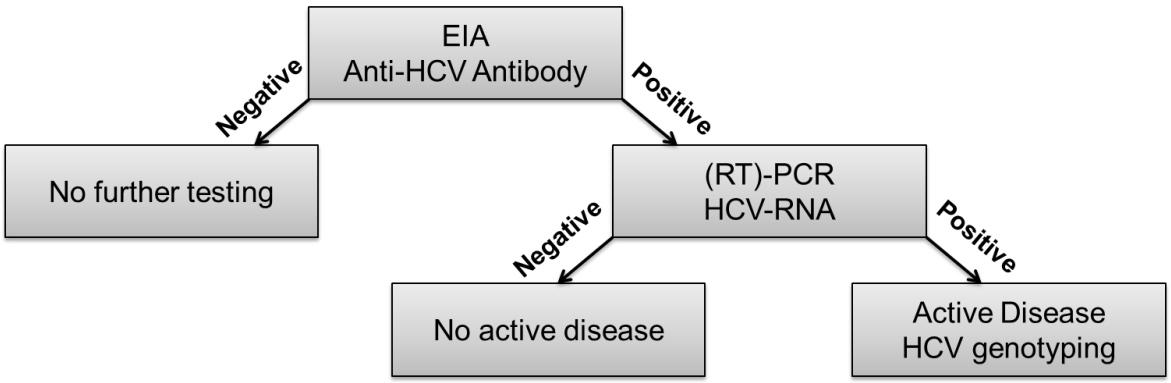

Figure 1.13 Diagnostic algorithm for hepatitis C virus
The first test identifies anti-HCV antibody by Enzyme Immunoassays (EIA) or rapid diagnostic tests (RDT). If the patient is negative, no further testing is required. With a positive anti-HCV antibody, the patient is tested further for HCV RNA by reverse transcriptase real time PCR or occasionally for HCV core antigen. If the test is negative there is no active infection and no further action is required. If the test is positive the patient is linked to care and further testing such as HCV genotyping and scoring of liver fibrosis stage is undertaken. (RT)-PCR – reverse transcriptase real time PCR.

1.9.2 The diagnostic gap

The early phase of HCV infection is mostly asymptomatic resulting in up to 80% of patients being unaware of their infection status until they develop serious manifestations including liver cirrhosis and HCC (Denniston et al. 2012; Papatheodoridis et al. 2016). Initial screening for anti-HCV antibody, while relatively cheap and sensitive, is not always reliable as seroconversion may take several weeks and is significantly more delayed in immunocompromised patients (Chevaliez & Pawlotsky 2006; Thomson et al. 2009). Furthermore, several visits to a health clinic are often required to make final diagnosis due to the multiple tests involved in the standard algorithm of HCV. This often results in patient loss to follow-up, particularly in high-risk individuals in HICs. Effective and rapid diagnosis of HCV is also limited in LMICs due to the requirement of trained medical personnel, expensive equipment and a lengthy turnaround time. Current assays often rely on venepuncture blood sampling, which can prove problematic in individuals like PWID due to collapsed veins, which is further compounded by the requirement of a cold-chain system for storage purposes. In LMICs, the nearest healthcare centre may be too distant and the infrastructure too poor for effective diagnosis (Chevaliez & Pawlotsky 2018).

With the arrival of highly effective and safe oral treatment regiments, HCV-infected patients are required to be monitored while on therapy in order to assess treatment response and to monitor for toxicity. All patients diagnosed with HCV can be treated with several new regimens even without genotype testing due to pangenotypic efficacy (Pawlotsky et al. 2018). There is now an essential need for cheap diagnostic assays with costs below $10 to facilitate large-scale diagnosis. The European Association for the Study of the Liver (EASL) suggests that an acceptable lower limit of detection of a standard laboratory-based assay should be 15 International units/ml (IU/ml). However, in order to screen patients on a large scale, RNA assays could be simplified to a limit of detection of <1000 IU/ml without compromising detection in the majority of cases tested (Pawlotsky et al. 2018). Simpler and cheaper molecular diagnostic measures are urgently required to enable treatment monitoring and improve global HCV elimination efforts.

1.10 Rapid diagnostic tests

Point-of-care tests (POCTs) or rapid-diagnostic tests (RDTs) are designed to provide results rapidly on the same day within as little as 30 minutes. They must be cheap and simple to use, without the need for high-level expertise. They often rely on the use of whole blood, serum or plasma obtained through venepuncture or fingerstick and sometimes through the use of less invasive methods such as oral fluid. POCTs have already increased the likelihood of diagnosing various infectious diseases including HIV in high-risk groups in HICs LICs (Lubelchek et al. 2005). The WHO recognises that POCTs have the potential to close the diagnostic gap in HCV testing by ensuring a direct linkage to care, especially in LMICs.

1.10.1 Immunological rapid diagnostic tests

Out of all anti-HCV Immunological rapid diagnostic tests, the OraQuick® HCV RDT is the only one approved by the U.S. Food and Drug Administration (FDA). The OraQuick® HCV Rapid Antibody Test is a lateral flow device and can be used on either saliva, blood (fingerstick or venous), serum and plasma samples. The sensitivity and specificity both ranges from up to 99.2% for oral fluids and 100% for any other specimens used, the latter of which is equivalent to the standard laboratory EIA. With a rapid turnaround time of just 20-40 minutes, the OraQuick® HCV Rapid Antibody Test can be used as an alternative to standard EIA laboratory tests (Lee et al. 2010, 2011). Table 1.1 lists more anti-HCV diagnostic tests and other RDTs. The sensitivities of the other anti-HCV kits listed range between 22-100% with the lowest one for the HCV SPOT antibody test, while the specificities range from 77-100% with the lowest in HCV one-step test ACON and HCV TRI-DOT (Al-Tahish et al. 2013; Mvere et al. 1996). Despite the high performance of these two rapid diagnostic tests, anti-HCV detection kits such as these do not identify active infection as antibodies are present for life after HCV exposure (EASL 2016). These tests therefore require a follow-up test to confirm the diagnosis. More suitable markers of active HCV infection, such as HCV antigen or RNA should be used for rapid diagnosis eliminating the need for a subsequent test for viral RNA with (RT)-PCR. Table 1.1 lists the core antigen-based Abbott ARCHITECT HCV assay, which although slightly less sensitive than HCV RNA testing, is a proposed marker of active infection (Kamal

et al. 2015). The current limit of detection is equivalent to 500-3000 IU/ml, which led to the assay becoming marked by the European Conformity (CE) (Freiman et al. 2016; Pawlotsky et al. 2018). The major limitation of the assay lies in the cost, size and skillset required to run the equipment.

Table 1.1 Characteristics of available HCV rapid diagnostic tests

Rapid Test name	Pathogen tested	Turnaround time	Method (abbreviated)	Reference
HCV one-step test device ACON HCV	HCV	N/A	Qualitative, membrane-based immunoassay	(Al-Tahish et al. 2013)
HCV TRI-DOT	HCV	Read results immediately	Fourth-generation flow-through test	(Al-Tahish et al. 2013)
The ImmunoComb II HCV test	HCV	10 min incubation + 1 min to stop the reaction	Indirect solid-phase EIA	(Al-Tahish et al. 2013)
HCV-SPOT™	HCV	5 min	Dot-blot antibody test	(Mvere et al. 1996; Nyirenda et al. 2008)
ACON rapid test strips	HCV (HIV,HBV, Syphilis)	70 min (30/30/10)	Immunochromatographic rapid strip test	(Buseri, Seiyaboh & Jeremiah 2010)
OraQuick® rapid test platform	HCV	20-40 minutes	Lateral-flow indirect immunoassay	(Lee et al. 2010)
Chembio DPP HCV test (Chembio Diagnostic Systems)	HCV (& HIV)	15-30min	Single use, disposable chamber assay (flow-through)	(Smith et al. 2011)
Multiplo Rapid HIV/HCV Antibody Test - MedMira	HCV (& HIV)	3 min	Single use, disposable chamber assay (flow-through)	(Smith et al. 2011)
Monolisa(®) HCV-Ag-Ab-ULTRA Bio-Rad	HCV	90min/30min/30min (incubation/wash/development)	Commercially available, combined HCV antigen–antibody assay (cEIA)	(Larrat et al. 2012)
Bioeasy HCV test	HCV	15-20 min (No later than 20min)	Immunochromatographic assay	(da Rosa et al. 2013)
ImunoR´apido HCV	HCV	Reading times 10-15 min (no later than 20min)	Immunochromatographic assay	(da Rosa et al. 2013)
The INNO-LIA™ HCV Score	HCV (HIV, HBV)	2,3 and 16 hours incubations possible	Third generation line enzyme immunoassay	(Kania et al. 2013)
Toyo® anti-HCV test	HCV	5–15-min incubation period	Two-site immunometric assay	(Kant et al. 2013)
Dual Path Platform (DPP) HIV-HCV-Syphilis Assay - Chembio	HIV-HCV-	10-20 min after addition of Buffer 2 to Well 2	Immunochromatographic device	(Hess, Fisher & Reynolds 2014)
The HCV ImmunoFlow	HCV	15 and 30 min after sample application	Lateral-flow rapid immunochromatographic test	(Kosack, Nick & Shanks 2014)
Miriad Rapid TP/HBV/HIV/HCV Ab Test	HCV-HBV-HCV-Syphilis	Results within 3–5 min (3 pre-steps)	Rapid Vertical Flow Technology, immunoassay	(Pai et al. 2014)
HCV Rapid Card	HCV	Reading Time : 10~15 min	Sensitive immunoassay	(V. W. Wong et al. 2014)
Chembio HCV Screen Assay	HCV	15-30min	Immunochromatographic assay	(Fisher et al. 2015)
Medmira hepatitis B (HBV,HIV,HCV Ab test)	HCV-HIV-HBV	Read results immediately	Rapid Vertical Flow Technology, immunoassay	(Fisher et al. 2015)
Abbott ARCHITECT HCV Ag assay	HCV	<60 min, (36-37 min)	Two-step chemiluminescent microparticle immunoassay (CMIA)	(Kamal et al. 2015)
The Rapid Anti-HCV Test	HCV	Results at 15 min	Immunochromatographic assay - Lateral Flow	(Sharma et al. 2015)

1.10.2 Nucleic acid-based point-of-care tests

In order to close the current diagnostic gap in HCV diagnosis, a POC test should be able to fulfil the criteria set by the WHO known as ASSURED (Table 1.2)

(Peeling 2006). Briefly, an ideal RDT requires minimal training and should have a shelf-life of at least one year at room temperature. It should be highly sensitive and specific and not be limited by the use of sophisticated laboratory equipment. Finally, a rapid sample-to-answer should be achieved by the POC tests, ideally within less than 1 hour.

Table 1.2 The ASSURED criteria for an 'ideal' rapid diagnostic test set by the WHO

A = Affordable
S = Sensitive
S = Specific
U = User-friendly
R = Robust and Rapid
E = Equipment-free
D = Deliverable
WHO – World Health Organisation

Recent innovations in technology has allowed several HCV POC tests to be developed based on nucleic-acid based testing or NAT. The GeneXpert Omni was created by Cepheid as a lightweight, small (23 cm tall) device for HCV RNA quantification from as little as 100 µl of whole blood. The major advantages of the device lie in the use of a rechargeable battery and wireless connectivity for recording results with a lower limit of detection of 40 IU/ml within 60 minutes (Grebely et al. 2017; Gupta et al. 2017; McHugh et al. 2017). For these reasons the GeneXpert Omni device has been CE-marked and WHO pre-qualified although is not yet FDA-approved.

A second POC test known as the Genedrive® device was recently developed in Manchester, United Kingdom. Similar to the GeneXpert, it is a small portable device requiring 30 µl of plasma. There is no requirement for RNA extraction and the entire process takes less than 90 minutes with a sensitivity of 99.8% for samples with viral load above 1000 IU/ml (A Llibre et al. 2018). This device fulfils the WHO's criteria for testing in decentralised environment such as in low-and-middle income countries (LMICs) but still requires expensive equipment. Other HCV POC tests based on NATs are currently under development such as the Allere™ q (Abbott, Chicago, IL) (Jani et al. 2016).

Although the new HCV POC are already closing the gap in diagnosis, they still pose several limitations. For example, the requirement of training eliminates

their use by non-medical individuals. Furthermore the cost of individual tests remain well above the desired $10 target.

There are a number of new technologies adapted to HCV infection that have the potential of filling the current gaps and limitations present in diagnostic capability. Figure 1.14 illustrates several novel assay types, which are mostly based on either NATs (RNA/DNA) or antigen detection (Park et al. 2010; Shen et al. 2011). Many of these technologies, including the Electrochemical Immunosensor Array, Metal-Amplified Density Assays (MADAs) and Loop-Mediated Isothermal Amplification (LAMP) can be quantified, which opens up the opportunity for monitoring patients receiving treatment in the future (Nyan & Swinson 2016; Subramaniam et al. 2015; Dianping Tang et al. 2010). The turnaround time for these assays ranges, in most cases, from less than 5 minutes to less than an hour. The Electrochemical Immunosensor Array, (RT)-LAMP and the Quantum Dot Barcodes offer very high sensitivities with detection limits of 0.8 ng/ml antigen, 10 IU of Nucleic acid and 10^{10} - 10^{12} M of antigen, respectively.

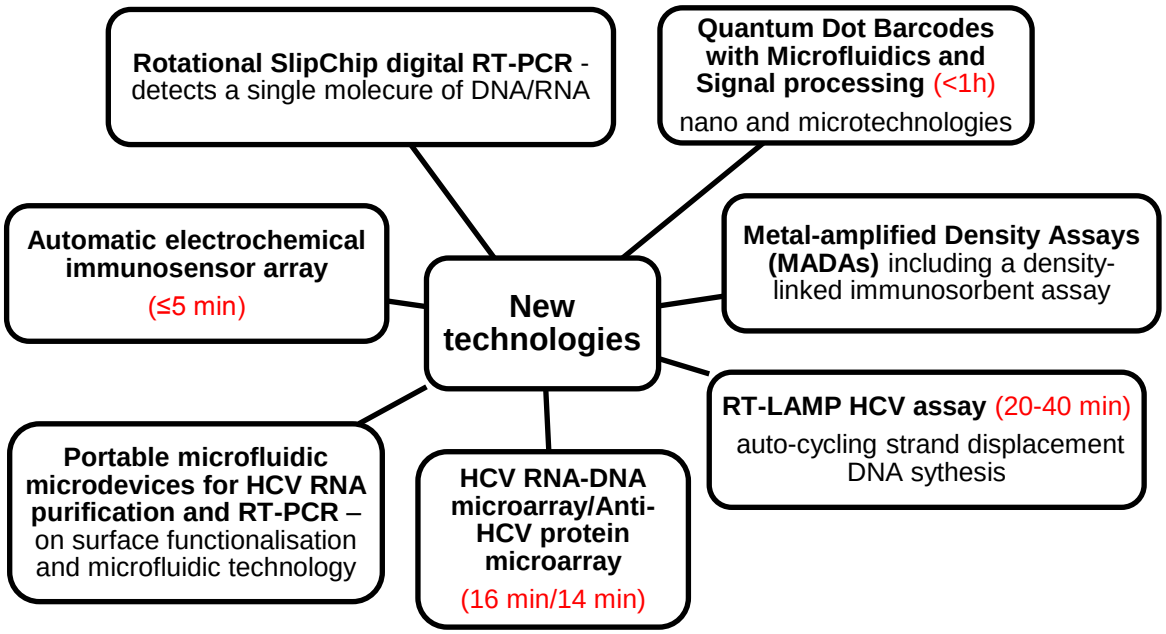

Figure 1.14 New diagnostic technologies for hepatitis C virus detection
The name of each technology is written in bold. Red indicates turnaround time followed by description of the technology with additional characteristics (Ember et al. 2011; Klostranec et al. 2007; Nyan & Swinson 2016; Shen et al. 2011; Subramaniam et al. 2015; D Tang et al. 2010; Vaghi et al. 2016).

1.10.3 Loop-mediated isothermal amplification

LAMP is a simple, rapid and cheap technique, which has been considered for POC testing for HCV and other viruses (Damhorst et al. 2015; Nyan et al. 2014; Yang et al. 2011). The major advantage of this method is amplification at a constant temperature ranging from 63-65°C within 30-60 minutes, without the need for PCR cycling at higher temperatures to denature double-stranded DNA (Notomi et al. 2000a). The high specificity of the method is ensured by designing 4 primers, termed F3 and FIP (recognising F1c and F2 regions) and B3 and BIP (recognising B1c and B2 regions), complementary to a total of 6 distinct areas within the DNA fragment. LAMP is based on a DNA polymerase with high strand displacement activity, ensuring the production of self-amplifying cauliflower-like structures, the principle of which is described briefly in Figure 1.15. The sensitivity of the assay can also be improved by integrating two additional primers, termed Loop Forward and Loop Reverse, spanning the regions between F2/B2 and F1/B1, respectively (Nagamine, Hase & Notomi 2002). This also improves the overall turnaround time of the assay. The final advantage is the simple visualization methods of LAMP products, based on, for example, turbidity, changes in colour, or nucleic-acid detection strips, allowing for examination of results with the naked eye without the need for sophisticated laboratory equipment (S Miyamoto et al. 2015; Mori et al. 2001; Reboud et al. 2019). In terms of HCV diagnosis, the addition of the AMV reverse transcriptase allows integration of an RNA reverse transcription step with the subsequent amplification of target cDNA in one simple-step (Zhao, Liu & Sun 2017). Finger-stick whole blood processing with DNA elution and a subsequent LAMP reaction has already been integrated on a cheap, simple to use filter paper-based method for malaria (Xu, Nolder, et al. 2016). In this assay, multiple LAMP reactions are performed on the same sample ensuring simultaneous detection of *Plasmodium* spp. as well as species-determination. This filter paper-based assay represents an example of a microfluidic paper-based analytical device or μPAD. Microfluidic devices or chips contain micro-channels craved into a material like glass, paper or plastic, which are joined together to achieve a required function including mixing or sorting. These functions allow for the integration of biochemical reactions in a scaled-down format, thus eliminating the need for sophisticated equipment, making microfluidic devices ideal candidates for POC tests (Zhang et al. 2017). While the paper-based malaria assay requires further optimisation, this method could

potentially be adapted for the detection of HCV with integrated RNA extraction method. With a cheap, simple to use design, the assay seems ideal for POC testing, especially in resource-limited settings and at the bedside where it would prevent patient loss due to follow-up (as the test could be performed during the first visit).

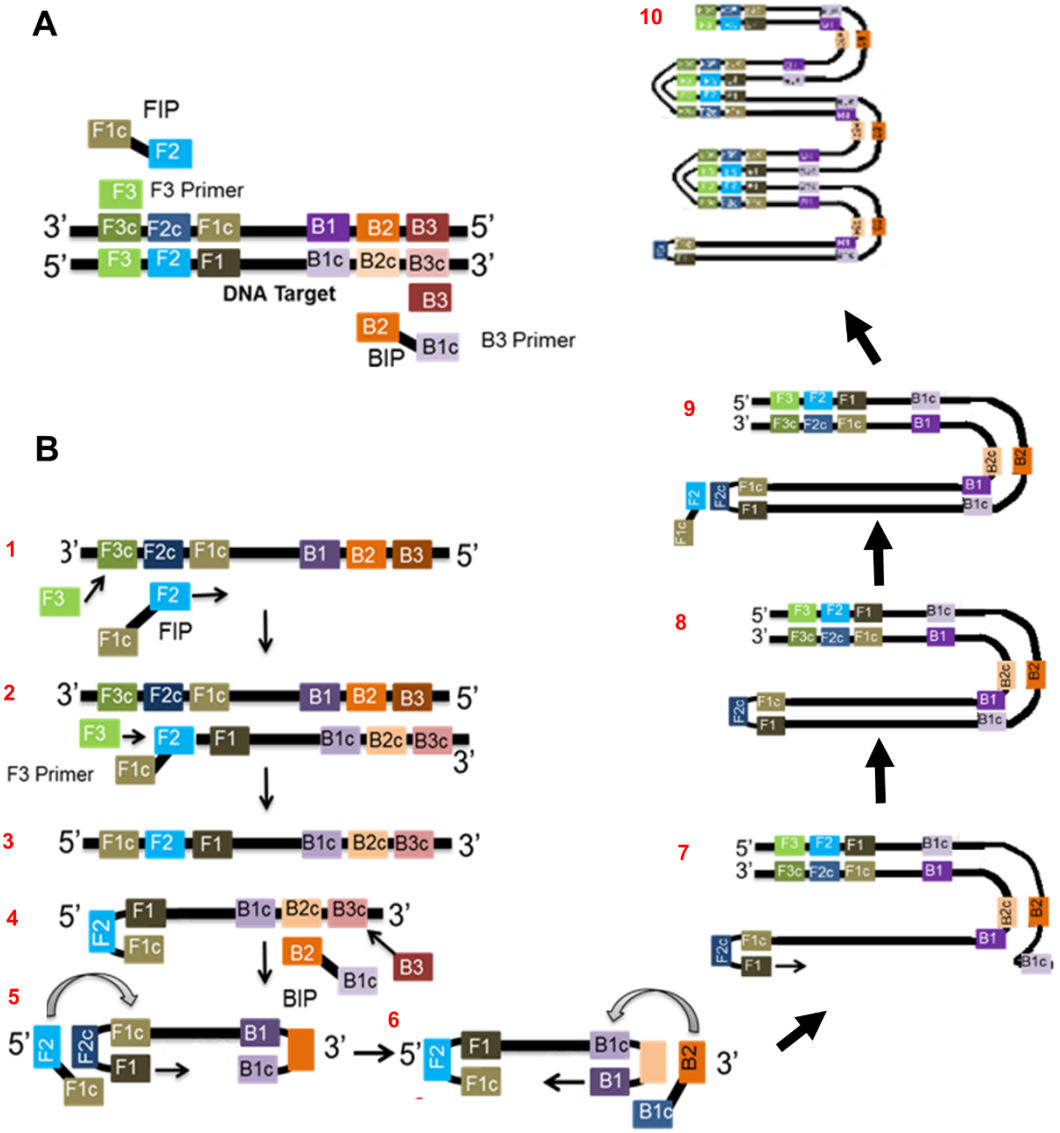

Figure 1.15 Method of loop-mediated isothermal amplification
A. The target sequence is divided into six regions recognised by the LAMP primers, named: F3/B3, F2/B2 and F1/B1. The letter 'c' indicates a complementary sequence. Two inner primers (FIP and BIP) and two outer primers (F3 and B3) are crucial for the method. FIP and BIP consist of F1c/B1c and F2/B2 sequences combined together, respectively. **B.** The LAMP method. The F2 (B2) portion of the FIP (BIP) binds to F2c (B2c) starting elongation. Strand displacement DNA synthesis occurs as the F3 primer bind to its complementary sequence and the strand elongated from FIP is replaced. A loop structure forms at the 5' end followed by the same elongation process with the BIP/B3 primers producing a loop at the 3' end. The product is used as a template for either F2 or B2 primers depending on what primer has initiated elongation. Self-primed DNA synthesis occurs.

1.11 Hypothesis and aims

This thesis aimed to study several important areas which could facilitate the WHO's elimination strategy, namely; the development of a POC test for diagnosing active HCV infection and studying the immune responses during SSC for possible implications in future vaccine studies. We hypothesized that adaptive immune responses played a role in SSC and therefore aimed to characterize both humoral and cellular responses in SSC patients and 4 control patients, 3 relapsers and 1 null patient. We aimed to correlate the immune response with viral evolution in SSC to decipher the key mechanisms involved in immune clearance. For the POC development, we hypothesized, that LAMP is a suitable candidate for a sensitive, specific and pangenotypic HCV assay. We aimed to first develop and subsequently validate the HCV LAMP assay in a cohort of HCV infected and uninfected patients in a double-blind setting. Moreover we aimed to comply with the WHO's ASSURED criteria for a POC test by evaluating different visual detection methods. The final optimised assay would be evaluated in a portable, inexpensive microfluidic platform with an integrated RNA extraction method.

2 Materials and Methods

2.1 Materials

2.1.1 Common chemicals/reagents (Catalogue no.)

1 kb DNA ladder (New England Biolabs, N3232S)

100 bp DNA ladder (New England Biolabs, N0551S)

3, 3', 5, 5'-tetramethylbenzidin (TMB) substrate (Thermo Fisher Scientific, 10301494)

Absolute Ethanol (VWR, PROL20821.330)

Agarose (Thermo Fisher Scientific, 16500-500)

Ampicillin (Sigma, A9518)

Betaine (Sigma, B0300-1VL)

ß-cyclodextrin (VWR, 7585-39-9)

Crystal Violet (Sigma, C6158)

Dimethyl sulfoxide (DMSO) (Sigma, 276855)

DNase enzyme (Thermo Fisher Scientific, AM2222)

Deoxyribonuleotide triphosphates (dNTPs) (New England Biolabs, N0447S)

Ethidium bromide (Sigma, E1510)

Evagreen (VWR, 31000-T)

Gel red dye (VWR, 41003)

Heat-inactivated foetal calf serum (Thermo Fisher Scientific, 10500-064)

HEPES buffer (Fisher Scientific, 11560496)

Histopaque (Sigma, 10771)

Isopropanol (Sigma, 24137)

Kanamycin (Thermo Fisher Scientific, 11815-024)

Nonessential amino acids (Thermo Fisher Scientific, 11140-035)

Nuclease-free water (Qiagen, 129115)

Phosphate Buffered Saline (Tissue culture grade) (Sigma, D8662)

Random hexamers (Thermo fisher scientific, N8080127)

RNase OUT enzyme (Thermo Fisher Scientific, 10777-019)

Roswell Park Memorial Institute (RPMI) medium (11875093)

Sodium sulphite (Sigma, 7757-83-7)

Triton X-100 (Sigma, T8787)

Tween-20 (Sigma, P1379)

2.1.2 Oligonucleotides

Unless otherwise indicated, oligonucleotides were synthesised by Eurofins genomics or Sigma.

2.1.3 Cell lines

Table 2.1 Cell lines used in this study

Cells	Description	Source
Huh7	Human Hepatoma cell line	Jean Dubuisson (CNRS, Institut de Biologie de Lille, Lille, France)
HEK-293T	Human Embryonic Kidney cell line	American Type Culture Collection

2.1.4 Solutions

2.1.4.1 Propagation of bacteria

Table 2.2 Bacterial propagation solutions

Solution	Components
Luria Bertani (LB) Broth	170 mM NaCl, 10 g/l Bactopeptone, 5 g/l yeast extract
LB-Agar	LB Broth plus 1.5% (w/v) agar
Super optimal broth with catabolite repression (S.O.C) medium	2% Tryptone**,** 0.5% Yeast Extract**,** 10 mM NaCl**,** 2.5 mM KCl**,** 10 mM $MgCl_2$**,** 10 mM $MgSO_4$**,** 20 mM glucose

2.1.4.2 Cell culture

Table 2.3 Tissue culture solutions

Solution (Catalogue no.)	Component
Supplemented Dulbecco's modified Eagle's medium (DMEM) (Thermo Fisher Scientific, 41966-029)	10% heat inactivated foetal calf serum, 1% nonessential amino acids, 10 mM HEPES buffer and 4 mM L-glutamine
Versene (E&O laboratories limited, 04074819)	0.6 mM EDTA in PBS, 0.002 % (w/v) phenol red
Cell Lysis Buffer 2 (LB2)	20 mM Tris-HCl pH 7.4, 20 mM iodoacetamide, 150 mM NaCl, 1 mM EDTA, 1 % Igepal CA-630

2.1.4.3 Restriction enzymes

Table 2.4 Restriction enzymes used in this study

Enzyme name	Source	Catalogue no.
Mung bean nuclease	New England Biolabs	M0250S
XbaI	New England Biolabs	R0145S
DpnI	New England Biolabs	R0176S

2.1.4.4 DNA manipulation

Tris-acetate-EDTA buffer (TAE) 50 X

121 g of TRIS, 28.5 ml of glacial acetic acid, 50 ml of 0.5 M EDTA pH 8, water up to 500 ml

2.1.5 Antibodies

Table 2.5 List of primary and secondary antibodies

Antibody	Description	Type	Reference
Anti-E2 AP33	Monoclonal non-biotinylated	Mouse	(Owsianka et al. 2005; Alexander W. Tarr, Owsianka, Timms, McClure, Richard J. P. Brown, et al. 2006)
Humanised AP33 (h-AP33)	Monoclonal known as MRCT10	Humanised mouse	(H Pantua et al. 2013)
Purified IgG from plasma	Polyclonal IgG from patient samples	Human (purified on Protein G HP SpinTrap antibody purification columns from GE Healthcare)	This study
Anti-mouse HRP conjugate	Polyclonal (Catalogue no. A4416)	Rabbit secondary antibody from Sigma	
Anti-human HRP conjugate	Polyclonal against heavy and light chains of human IgG (Catalogue no. W4031)	Goat secondary antibody from Promega	
Anti-human IgG (Fc-specific) HRP Conjugate	Polyclonal against Fc portion of human IgG (Catalogue no. A-0170)	Goat secondary antibody from Sigma	

2.1.6 Patient E1E2 mammalian expression plasmids

Table 2.6 Patient derived E1E2 in mammalian phCMV vector used in HCVpp system for this study

Name	Genotype	Infectious HCVpp?	Accession number	Additional details	Ref
H77	1a	Yes	AF001751	Wild type genotype 1a	(Yanagi et al. 1997)
UKN1B5.23	1b	Yes	AY734976	-	(Lavillette et al. 2005)
JFH-1	2a	Yes	AB047639	-	(Kato et al. 2001)
UKN 2B1.1	2b	Yes	AY734982	-	(Lavillette et al. 2005)
UKN3A13.6	3a	Yes	AY894683	-	(Lavillette et al. 2005)
UKN4.11.1	4a	Yes	AY734986	-	(Lavillette et al. 2005)
P76_TPA	1a	Yes	To follow	Sample taken from patient 76 in 2008	-
P76_TPC	1a	Yes	KU645407	Sample taken from patient 76 in 2010	-
P155_TPA	4d	Yes	To follow	Sample taken from patient 155 in 2009	-
P155_TPD	4d	Yes	To follow	Sample taken from patient 155 in 2011	-
P75_TPA	1a	Yes	To follow	Sample taken from patient 75 in 2008	-
P75_TPB	1a	Yes	To follow	Sample taken from patient 75 in 2010	-
P63_TPA	1a	No	To follow	Sample taken from patient 63 in 2008	-
P63_TPB	1a	No	To follow	Sample taken from patient 63 in 2009	-

Infectivity was tested as described in the Methods. HCVpp was considered infectious if the luciferase signal was 10 times higher than the signal of the background. HCVpp – HCV pseudoparticle

2.2 Diagnosing hepatitis C virus

2.2.1 Clinical samples.

2.2.1.1 Ethical approvals

Samples were collected under ethical approval from the Acute HCV UK cohort and the HCV Research UK cohorts. Additional anonymised samples for LAMP testing were obtained from the West of Scotland Specialist Virology Centre (WoSSVC), Glasgow Royal Infirmary (Dr Rory Gunson and Dr Amanda Bradley-

Stewart) to validate the HCV POC LAMP assay. Written consent for participation was provided and ethical approval obtained as per Declaration of Helsinki. The studies were approved by the Riverside Research Ethics Committee and the West of Scotland Research Local Ethics Committee

2.2.1.2 Early Access Program

Eight chronic hepatitis C virus whole blood samples from patients with advanced liver cirrhosis from the Early Access Program (EAP) were obtained under HCV Research UK ethical approval. EAP patients were treated with sofosbuvir and an NS5A inhibitor (daclatasvir or ledipasvir) with ribavirin. A total of five genotype 3a, two genotype 1a and one genotype 1b samples were collected.

2.2.1.3 Acute HCV Research UK

The Acute HCV Research UK study consists of two acute HCV cohorts; patients recruited at St Mary's Hospital, Imperial College London NHS Trust and Gartnavel Hospital, Greater Glasgow and Clyde. Patient whole blood samples were collected at regular intervals (approximately 1-3 months), and processed for plasma as described in section 2.3.2. Patients who did not spontaneously clear the HCV infection were treated with pegylated interferon (peg-IFN) and weight based RBV for 24-48 weeks or DAAs as per local guidelines.

2.2.1.4 Validation of point-of-care LAMP assay

Anonymised RNA samples from fifty-six HCV infected patients and four negative control patients were provided by the WoSSVC, Glasgow Royal Infirmary (Dr Rory Gunson and Dr Amanda Bradley-Stewart) to evaluate the HCV point-of-care test. Samples included a variety of different genotypes; twenty-two genotype 1a, three genotype 1b, two genotype 2, twenty-three genotype 3 and six unknown genotype samples. The HCV infection status was confirmed by the Abbott RealTime HCV assay at the WoSSVC.

For clinical sensitivity and specificity testing, the HCV LAMP test developed during this project was validated in a double-blind evaluation. The West of Scotland Specialist Virology Centre at Glasgow Royal Infirmary provided plasma samples from one hundred HCV infected patients and one hundred HCV negative

patients (Dr Rory Gunson and Dr Amanda Bradley-Stewart). The double-blind procedure involved three individuals; individual one aliquoted samples into a 96-well plate. Individual two performed blinded RNA extractions as described in section 2.2.4 and the cDNA synthesis stage as described in section 2.2.4.1. The third individual used the RNA and cDNA to evaluate clinical sensitivity and specificity by testing on the in-house developed HCV LAMP assay and the in-house qPCR assay (section 2.2.7).

2.2.2 Standards

Plasmids containing HCV replicons from various genotypes (wild type genotype 2a, genotype 1a and 3a (Saeed et al. 2012)) were used as an in-house standard for analytical sensitivity and point-of-care diagnostic optimisation experiments (provided by Dr Connor Bamford). Figure 2.1 shows a diagram of the subgenomic replicons used as standards for part of this thesis.

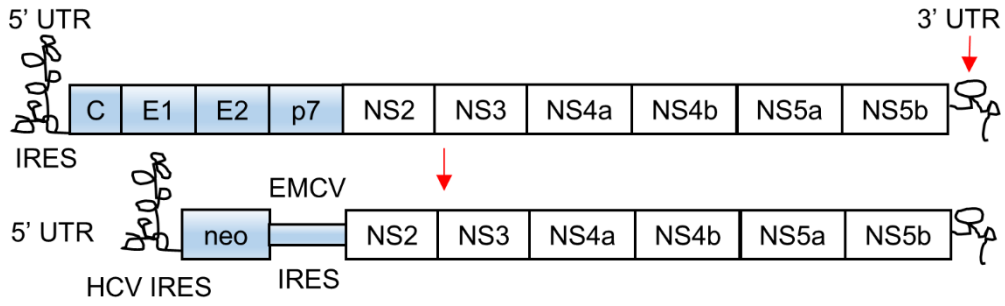

Figure 2.1 Structure of the subgenomic replicon
Subgenomic replicons are modified from a full HCV sequence (top panel) by removing the structural genes (Core, Envelope and p7) and replacing them with a reporter gene; neomycin resistance gene/firefly luciferase for genotype 1a and genotype 3a or Guassia luciferase for wild type genotype 2a. Each subgenomic replicon contains two open reading frames (ORF). Translation of the first is initiated by the HCV IRES/5' UTR and the second is by the EMCV IRES. The HCV sequences are specific to each genotype. C Core, E1/E2 – Envelope 1/2, NS – non-structural proteins, UTR – Untranslated region, EMCV – encephalomyocarditis virus, IRES – internal ribosomal entry site.

2.2.3 Transcription of HCV RNA

Standard subgenomic replicons from section 2.2.2 were used for *in vitro* HCV RNA transcription in order to obtain a high concentration of HCV RNA for optimisation of the diagnostic assay. To render the replicon non-infectious, structural genes in the plasmid were replaced by the luciferase reporter gene

and the non-structural proteins were kept intact. The plasmid also contains a T7 promoter for *in vitro* transcription initiation. In order to linearize the plasmid, a restriction digest of 10 µg of the plasmid with XbaI enzyme (New England Biolabs) was performed overnight at 37°C as per manufacturer's instructions. To create blunt ended products, 2 µl of Mung bean nuclease (New England Biolabs) was used to trim the linearised HCV DNA in CutSmart buffer for 1 hour at 30°C as per manufacturer's instructions. The DNA was column purified using the QIAquick PCR Purification kit (Qiagen) as per manufacturer's instructions and the eluted DNA concentration measured on a Nanodrop spectrophotometer (Thermo Fisher Scientific). T7 RiboMAX™ Express Large Scale RNA Production System (Promega, P1320) was used for the transcription reaction by incubating 10 µl of T7 RiboMAX 2x buffer, 1 µg of linear DNA, 2 µl of T7 RiboMAX Enzyme Mix and nuclease free water to a total volume of 20 µl at 37°C for 2 hours. DNase enzyme (1 µl) was added to each reaction for the final 15 minutes and the RNA products cleaned up on the RNeasy mini kit (Qiagen, 74104) as per manufacturer's instructions. The purified RNA samples were stored at -80°C.

2.2.4 RNA extractions

Ribonucleic acid (RNA) was extracted from 200-400 µl of plasma or whole blood samples and standards using the Agencourt RNAdvance Blood kit (Beckman Coulter, A35604) on the automated KingFisher™ Flex Purification System as per manufacturer's instructions with slight modifications; 300 µl of lysis buffer and 30 µl of Proteinase K were added directly to samples in plates and mixed thoroughly (Figure 2.2). The whole mixture was incubated at 55°C for 15 minutes. Samples were cooled for 2 minutes and 410 µl of Bind 1/Isopropanol solution was added, mixed thoroughly and separated on a magnet for 10 minutes. The supernatant was removed and the magnetic beads were washed first with 800 µl of Wash buffer and second with 800 µl of 80% Ethanol. The supernatant was discarded after each wash while samples were kept on a magnet and dried for 5 minutes at room temperature. Next, all samples were mixed with 100 µl of DNase solution and incubated at 37°C for 5 minutes. A further 200 µl of Bind 2 buffer was added, mixed and incubated for 5 minutes at room temperature. The supernatant was discarded, following 5 minutes of incubation on a magnetic rack and a further two washes with 80% Ethanol were performed. Magnetic beads were dried for 10 minutes and RNA eluted in 15-30 µl

of nuclease-free water. The magnet was used to separate the magnetic beads from the eluted samples, which were subsequently transferred to fresh tubes or plates for storage purposes.

For the point-of-care tests, RNA extraction followed a protocol with reduced steps, omitting the DNase reaction and the two subsequent washes. The point-of-care tests were manufactured as described in section 2.2.9.

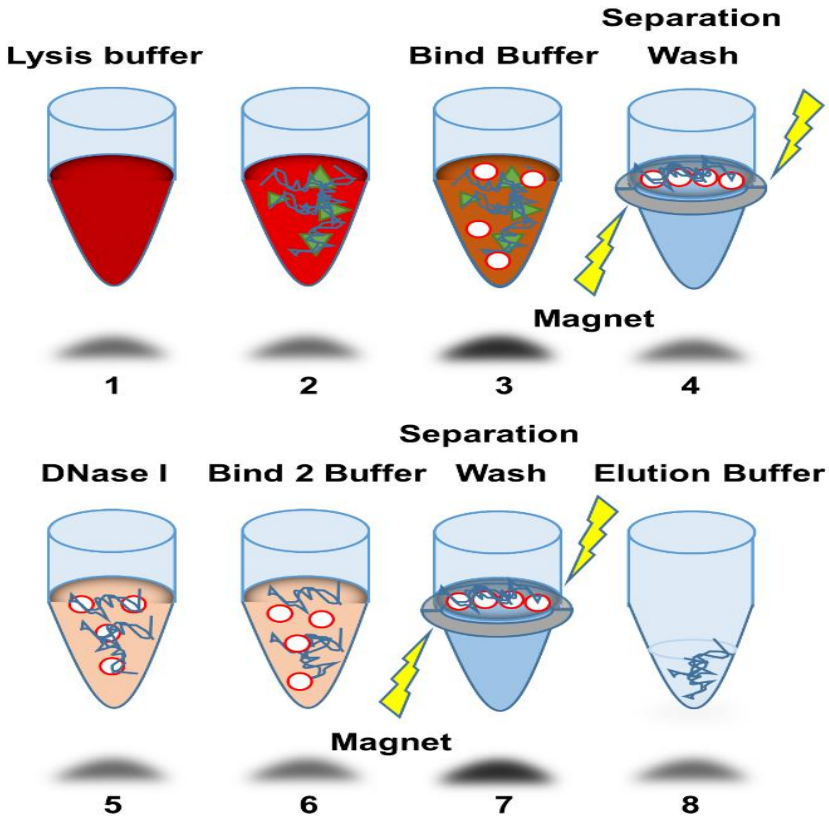

Figure 2.2 Agencourt RNAdvance Blood kit workflow

1. Addition of lysis buffer to whole blood and mixing. 2. Lysis and Proteinase K digestion. 3. Addition of Bind 1 Buffer. 4. Magnetic bead separation from waste, washing with Wash Buffer and 80% Ethanol. 5. DNase I reaction 6. Rebinding with Bind 2 Buffer. 7. Magnetic bead separation from waste and two washes with 80% Ethanol. 8. Elution. Adapted from Beckman Coulter user guide.

2.2.4.1 Using Mengovirus as an RNA extraction control

Mengovirus, otherwise known as Encephalomyocarditis virus (EMCV) is a Cardiovirus commonly used as an RNA extraction control. A Mengovirus extraction control kit (Biomerieux, 21650A) was used for evaluation of RNA extraction efficiency from the point-of-care devices as per manufacturer's instructions with slight modifications. Briefly, 10 µl of Mengovirus (2.13×10^6 copies) was spiked directly into 200 µl of plasma samples in lysis buffer. The RNA extraction was performed as above and the efficiency calculated by generating a standard curve. Standard curves were generated by spiking 10 µl of Mengovirus (2.13×10^6 copies) directly into the lysis buffer, without plasma, and following the procedure for RNA extractions. The resulting elution was serially diluted four times (10 fold) to create five dilution points. Serial 10-fold dilutions were subsequently made as above. Reverse transcriptase quantitative real-time PCR was used to determine the recovery of Mengovirus RNA using the GoTaq 1-Step RT-qPCR System (Promega, A6020). Each master mix contained 10 µl of 2x GoTaq qPCR Mastermix, 0.4 µl of reverse transcriptase enzyme, 1.25 µl of 12.5 µM forward primer (5'-GAAGTAACATATAGACAGACGCACAC-3'), 1.25 µl of 22.5 µM of reverse primer (5'-GCGGGTCCTGCCGAAAGT-3'), 0.625 µl of 6.25 µM probe (5'FAM-ATCACATTACTGGCCGAAGC-MGBNFQ-3'(Pinto, Costafreda & Bosch 2009), 5 µl of RNA template and nuclease-free water to a total volume of 25 µl. The reaction was set up with the following conditions: 10 minutes of reverse transcription at 50°C, 3 minutes at 95°C followed by 40 cycles of denaturation for 5 seconds at 95°C and annealing/extension for 12 seconds at 60°C with collection of data at the annealing/extension stage.

2.2.5 Synthesis of cDNA

SuperScript III Reverse Transcriptase (Thermo Fisher Scientific, 18080044) was used for first strand complementary DNA (cDNA) synthesis with slight modifications from the manufacturer's protocol. Briefly, 11 µl of extracted RNA samples were transferred to PCR tubes, incubated for 5 minutes at 65°C and immediately cooled on ice. Reverse transcription was carried out by adding 4 µl of 5x reverse transcription buffer, 2 µl of superscript III reverse transcriptase enzyme, 1 µl of RNAse OUT enzyme (5,000 units), 1 µl of random hexamers (10

mM) 1 µl of dNTPs (10 mM) and 1 µl of DTT (100 mM).The mixture was incubated at 25°C for 10 minutes and subsequently at 55°C for 60 minutes. Each reaction was then inactivated at 70°C for 10 minutes.

2.2.6 Synthesis of double-stranded cDNA

Double stranded cDNA synthesis was carried out using a Second Strand Synthesis kit (New England Biolabs, E7530). The entire sample from first strand synthesis reactions was mixed with 8 µl of 10x second strand synthesis buffer, 4 µl of second strand enzyme and 48 µl of nuclease-free water and incubated at 16°C for 2.5 hours.

2.2.7 HCV real-time PCR assays

Quantitative real-time PCR reactions for HCV were carried out using either Superscript III Platinum™ One-Step qRT-PCR kit (Thermo Fisher Scientific, 11732020) or TaqMan™ Fast Universal PCR Master Mix (2x) (Thermo Fisher Scientific, 4352042) as per manufacturer's instructions. All reactions were amplified using fast universal conditions on a 7500 Fast Real-Time PCR machine (Applied Biosystems). HCV viral load was quantified using the automated Abbott RealTime HCV assay at the WoSSVC

2.2.7.1 Superscript III Platinum One Step qRT PCR assays

A Superscript III Platinum One Step qRT-PCR kit was used for qRT-PCR reactions directly from RNA. The reaction mix was prepared as follows; 0.75 µl of 10 µM forward primer, TCTGCGGAACCGGTGAGTA, 0.75 µl of 10 µM reverse primer GCACTCGCAAGCACCCTATC, 0.75 µl of 5 µM probe FAM-AAAGGCCTTGTGGTACTG-MGB, 1 µl of RNA, 0.3 µl of Superscript III RT/Platinum™ Taq mix, 7.5 µl of 2x Reaction Mix, and nuclease-free water to a total reaction volume of 15 µl. The run consisted of a reverse transcription at 50°C for 15 minutes, denaturation at 95°C hold for 2 minutes followed by 40 cycles of denaturation at 95°C for 3 seconds and annealing/extension at 60°C for 30 seconds.

2.2.7.2 TaqMan™ Fast Universal PCR Master Mix

TaqMan™ Fast Universal PCR Master Mix was used for quantitative PCR from cDNA. Each master mix consisted of 5 μl of 2x TaqMan Fast Universal Mix, 0.5 μl of 18 μM forward primer, 0.5 μl of 18 μM reverse primer, 0.5 μl of 5 μM probe, 1 μl of cDNA template and nuclease-free water to a final volume of 10 μl. The run consisted of 20 seconds hold at 95°C followed by 40 cycles of denaturation for 20 seconds at 95°C and annealing/extension for 30 seconds at 60°C. The primers and probes were the same as for the above HCV RNA qRT-PCR assay.

2.2.8 Loop mediated isothermal amplification tests

2.2.8.1 Primer design

Primers were designed by studying a reference alignment of 204 pre-aligned full genome sequences of different HCV genotypes (Smith et al. 2014). The alignment was analysed to look for areas of highest conservation and the 5'UTR was picked as the most suitable region for generating in-house developed primers using PrimerExplorerV4. Published primers were based on sequences previously published by Yang et al 2011 (Table 2.7) (Yang et al. 2011). Both primer sets were manufactured by Eurogentec (Eurogentec S.A., Seraing, Belgium).

Table 2.7 In-house and published HCV LAMP primers

	In-house primers		**Published primers**	
Primer Name	**Sequence (5'-3')**	**Genome position**	**Sequence (5'-3')**	**Genome position**
F3	GAGAGCCATAGTRGTCTGC	133-151	ACTCCACCATGAATCACTC	24-42
B3	CACGGTCTACGAGACCTC	320-337	ATCAGGCAGTACCACAAGG	279-297
FIP	TCTYGCGGGGGCACG-GTGAGTWCACCGGAATYGC	232-246/159-177	AGGCTGYACGACACTCATAC-CTGTGAGGAACTACTGTCTTC	94-113/45-65
BIP	CTAGCCGAGTAGYGTTGGGTYG-CACTCGCAAGCACCCTAT	250-271/296-313	GGATMAACCCRCTCAATGCC-TCGCRACCCAACRCTAC	200-219/258-274
Floop	TCCAMGAAAGGACCCDGTC	184-202	GCCATGGCTAGACGCT	74-89
Bloop	GGCCTTGTGGTACTGCCTG	277-295	GTGCCCCCGCRAGAC	233-247
AP			TTCCGCAGACCACTATGGCTCT	134-155

The genome positions for in-house primers and published primers are based on HCV H77 genotype 1a sequence (Genbank accession number AF009606). In-house primers were developed based on PrimerExplorerV4 guidelines (obtained on the following website: https://docplayer.net/347924-A-guide-to-lamp-primer-designing-primerexplorer-v4.html accessed on 02/03/2019). AP stands for Accelerating Primer. Floop stands for Forward loop primer, Bloop stands for Backward loop primer.

2.2.8.2 Optimisation of LAMP conditions

Initial HCV-LAMP reactions were optimised by the following parameters; enzyme, primer selection, primer concentration, incubation temperature, incubation time, concentration of magnesium, concentration of dNTPs and analytical and clinical sensitivity of the assay. LAMP reactions were optimised in a final volume of 25 µl and all contained 5 µl of JFH1 standard. In addition the following reagents were added; 1 M of betaine (Sigma Aldrich, USA), 8U of *Bst* DNA polymerase large fragment (New England Biolabs, M0275S)/*Bst* 3.0 DNA polymerase (New England Biolabs, M0374S) or GspSSD DNA polymerase (Optigene, GSPSSD-001), 1X Buffer supplied with each polymerase, 2 mM-8 mM $MgSO_4$, 1.2 mM of mixed dNTPs, 1.6 µM/2 µM of inner primers (FIP/BIP), 0.8 µM/1 µM of loop primers (LF/LB) and 0.2 µM of external primers (F3/B3) for both published and in-house primer sequences. For HCV-LAMP with the published primer sequences, the reaction mixture also contained 0.8 µM of Accelerating primer (AP). Serial dilutions of the JFH1 plasmid were used to evaluate analytical sensitivity of both primer sets. HCV samples were tested for clinical sensitivity in a final volume of 25 µl containing 15 µl of ISO-001 Mastermix (Optigene,ISO-001), 5 µl of template, 2 µM of inner primers, 1 µM of loop primers and 0.2 µM of external primers (0.8 µM of AP was added when published primers were used). The reaction mixtures were incubated for 30-60 minutes at either 60°C or 65°C on a 7500 Fast Real-Time PCR machine (Applied Biosystems) using the SYBR green setting.

2.2.8.3 Internal control assays

LAMP primer sequences for the *Homo Sapiens BRCA1* target have been published elsewhere (Tanner, Zhang & Evans Jr. 2012). Primers were added to LAMP reactions as internal controls with all other conditions kept the same as the HCV LAMP assay. Table 2.8 shows the sequences and final concentrations of all primers.

Table 2.8 LAMP primer sequences used as internal controls

Target	Primer	Final concentration	Sequence (5'-3')
Homo sapiens BRCA1	BRCA1 F3	0.2 µM	TCCTTGAACTTTGGTCTCC
	BRCA1 B3	0.2 µM	CAGTTCATAAAGGAATTGATAGC
	BRCA1 FIP	0.64 µM	ATCCCCAGTCTGTGAAATTGGGCAAAATGCTGGGATTATAGATGT
	BRCA1 BIP	0.64 µM	GCAGCAGAAAGATTATTAACTTGGGCAGTTGGTAAGTAAATGGAAGA
	BRCA1 FLP	0.8 µM	AGAACCAGAGGCCAGGCGAG
	BRCA1 BLP	0.8 µM	AGGCAGATAGGCTTAGACTCAA

2.2.8.4 HCV LAMP assay

Primer set selection (in-house vs published primers) and HCV samples and controls were tested in a final volume of 25 µl. Each reaction contained 15 µl of ISO-001/ISO-001-RT Master Mix (Optigene, ISO-001RT), 5 µl of target DNA/RNA, 0.8 µM each of FIP and BIP primer, 0.4 µM each of loop-F and loop-B primers, 0.2 µM each of F3 and B3 primers and 0.4 µM of AP. To ensure uniform results, primers were added from a 10x LAMP primer stock solution. The reaction mixtures were incubated for 30-40 minutes at 65°C. Targets consisted of either patient samples or in-house standards. Real time monitoring of LAMP reactions was performed on a 7500 Fast Real-Time PCR machine (Applied Biosystems) using the SYBR green setting. The run consisted of 30-60 cycles of 60 seconds each at 65°C. Fluorescence was read at the end of each cycle and the data analysed on Matlab software version R2017, Microsoft Excel 2016 and GraphPad Prism version 7. Additional detection methods were used for LAMP products as described in section 2.2.10. For LAMP reactions directly from serum samples, 2 µl of serum template was added and the volume adjusted to 25 µl with nuclease-free water. Standard JFH1-containing plasmids were serially diluted in serum and water from 10^7 copies/ml to 10 copies/ml. Each dilution was then used for LAMP reactions.

2.2.8.5 Statistical analysis

GraphPad Prism version 7 was used to test data distribution using three normality tests; the D'Agostio-Pearson omnibus normality test, the Shapiro-Wilk normality test and the Kolmogorov-Smirnov test. Data were considered to follow a normal distribution if the p value was more than 0.05. For non-parametric data, a two-tailed Mann-Whitney test or Kruskal Wallis with Dunn's multiple comparisons test was performed on GraphPad Prism version 7. Data were considered significant if the p value was less than or equal to 0.05. For the double-blind study, a Receiver Operating Characteristic (ROC) curve of sensitivity and (1-specificity) was plotted on GraphPad Prism version 7.

2.2.9 Manufacturing HCV point-of-care diagnostic devices

2.2.9.1 Hot wax printing of filter paper devices

Filter-based fluidic devices were designed using CorelDRAW Graphics Suite 2013 software where black colour was used to represent hydrophobic areas and white for hydrophilic. The designed patterns were printed on filter paper (GE Healthcare Life Science, Whatman™, 1001-320) with wax using a Xerox ColorQube 8570 printer. Filter paper was heated at 120°C for 1-2 minutes on the hotplate in order to melt the wax and diffuse it through the filter paper. Glass fiber spots with different diameters (GE Healthcare Life Science, Whatman™, 1825-015) were positioned onto the hydrophilic parts of the filter paper to allow capturing of nucleic acid during extractions. Devices were folded to separate the washing procedures from elution as shown in Figure 2.3. Elution and LAMP reactions were performed on top of a separate plastic device manufactured as described in section 2.2.9.2. Prior to extractions, devices were tested for the movement of liquids between different areas of the printed patterns.

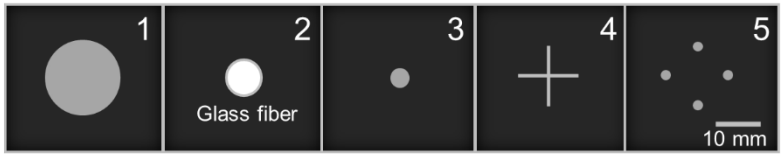

Figure 2.3 Filter paper based microfluidic device

Black squares represent hydrophobic wax areas, grey circles/crosses represent hydrophilic channels and the white circle represents glass fiber. Each panel, numbered 1-5, is folded on top of another to form a function in the nucleic acid extraction procedure. Panels 3 and 2 are folded with the glass fiber in between the hydrophilic channels on top of panel 1 for the washing stage. The sample is then dispensed onto the hydrophilic part of panel 3 and nucleic acid captured by the glass fiber. After adding wash buffer on top of panel 3, folded panels 2 and 3 are flipped to the panels 4 and 5. This allows the sample to be eluted and dispersed evenly onto four hydrophilic spots. The design and diagram were adapted from a previously published study on malaria diagnosis (Xu, Nolder, et al. 2016).

2.2.9.2 Laser cutting of plastic devices

Laser-cut devices were designed on CorelDRAW Graphics Suite 2013 software and either manufactured by CNC machining at Epigem Ltd or laser cut from Poly-methyl methacrylate (PMMA) (Stockline Plastics Ltd) on an in-house laser cutter (Laserscript). Devices were designed for LAMP reactions with detection or nucleic acid extraction processes. LAMP reaction devices contained a chamber for nucleic acid detection strips valves and LAMP chambers, which were sealed with acetate films (MicroAmp® Optical Adhesive Films, Thermo Fisher Scientific, 4311971) to prevent liquid evaporation during the amplification process. Extraction devices consisted of two layers of varying thickness (2 mm or 3 mm) and contained the same reagents as standard RNA extractions described in 2.2.4 excluding DNase and two washes. Each step of the reaction was contained in a different chamber, separated by valves, and a magnet was used to move nucleic acids captured on magnetic beads between the different stages. The layers of the extraction devices were joined together with double-sided tape or acetone and each side sealed with acetate films to prevent leakages (Figure 2.4). The eluted nucleic acid was collected and LAMP products detected by methods described below (Section 2.2.10). For optimisation purposes, different designs of plastic device were tested with water and food colouring dyes.

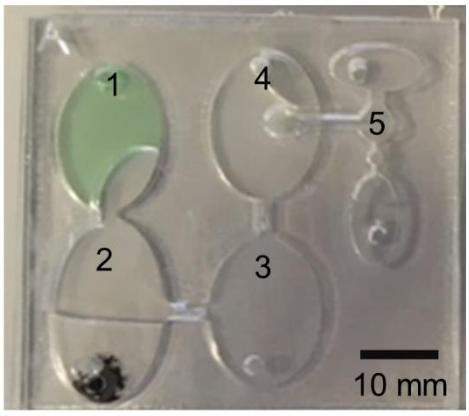

Figure 2.4 Extraction device
The diagram represents an example of an extraction device manufactured from PMMA by laser cutting. The device consisted of chambers (labelled 1-5) each for a different part of the extraction procedure as follows: 1. Lysis chamber 2 Binding chamber (with magnetic beads) 3. Wash buffer 4. 80% Ethanol wash 5. Elution chamber. The device consisted of two layers of PMMA, 2 mm and 3 mm thick, which were joined together by acetone wielding. The sample was added through an inlet in chamber 1 and the magnetic beads carrying nucleic acid were moved between the chambers using a magnet. The final elution stage was performed by dragging the magnetic beads upwards into the top layer channel and subsequently into the elution chamber. The channels were filled with 1% agarose to prevent premature leaking of solutions between the chambers.

2.2.10 Detection of LAMP products

2.2.10.1 Fluorescent DNA dyes

Evagreen is a DNA-binding dye used for quantitative qPCR and post-PCR melt curve analysis (Mao, Leung & Xin 2007). It shares the same spectrum of detection as the more commonly used SYBR Green I dye with a few advantages; it is less inhibitory to PCR, more environmentally friendly, stable and produces a better signal to noise ratio. Thus, 20x Evagreen dye (VWR) was added to initial LAMP reactions to monitor the amplification of DNA over time and find optimal reaction conditions. All reactions were run on a 7500 Fast Real-Time PCR machine (Applied Biosystems) on the SYBR Green setting.

2.2.10.2 Gel electrophoresis

For end-point detection, gel electrophoresis was used for LAMP product visualisation. Reactions were run on 1% agarose gel in TAE buffer dyed with 5 µl of ethidium bromide (stock 10 mg/ml) or 10 µl of gel red 10 000x. DNA ladder (100 bp or 1 kb) was purchased from New England Biolabs and run alongside LAMP products for 30 minutes at 120 V. Results were visualised under UV light.

2.2.10.3 Leuco-crystal violet

Leuco-crystal violet (LCV) was used as a tool for colorimetric LAMP product detection as previously described (Shigehiko Miyamoto et al. 2015). Briefly, a solution containing 0.5 mM Crystal Violet, 30 mM sodium sulphite and 5 mM ß-cyclodextrin was prepared and aliquots of 5 µl were transferred into 200 µl micro tubes. Next, the LCV mixtures were dried for 30 minutes at 50°C and subsequently under vacuum for 1 hour. Tubes were stored away from light with desiccators at -20°C until required. LAMP mixtures were added directly into LCV tubes. Reactions were incubated at 65°C for 30-45 minutes and terminated at 80°C for 2 minutes. A smartphone camera was used to take photographs at the end of the reaction to capture colour changes of each LAMP mixture.

2.2.10.4 Colorimetric LAMP detection

For visual results, WarmStart Colorimetric 2x LAMP Master Mix (New England Biolabs, M1800S) was used as per manufacturer's instructions. FIP and BIP primers were added at 1.6µM each with all other conditions kept the same as for ISO-001 Master mix. Products were analysed by visual inspection and photographs captured using a smartphone camera.

2.2.10.5 Nucleic acid detection strips

Disposable nucleic acid detection strips were purchased from Ustar (Molecular testing anywhere, China, D003-03) and used as per manufacturer's instructions with slight modifications. Briefly, forward loop primer (FLP) was labelled with FITC dye and backward loop primer (BLP) was labelled with Biotin. All primers were added at the same concentration as other LAMP assays (see section 2.2.8.4) with loop primers replaced with labelled loop primers. LAMP reactions were incubated at 65°C for 30-45 minutes and the entire reaction was added onto the sample pad of the lateral flow strip (Figure 2.5a). The sample pad was topped up with 100 µl of nuclease-free water and the lateral flow devices were run at room temperature for 10-15 minutes. The results were interpreted as shown in Figure 2.5b. Pictures were taken by a smartphone camera or alternatively the devices were scanned by the EPSON EXPRESSION 1680 Pro scanner.

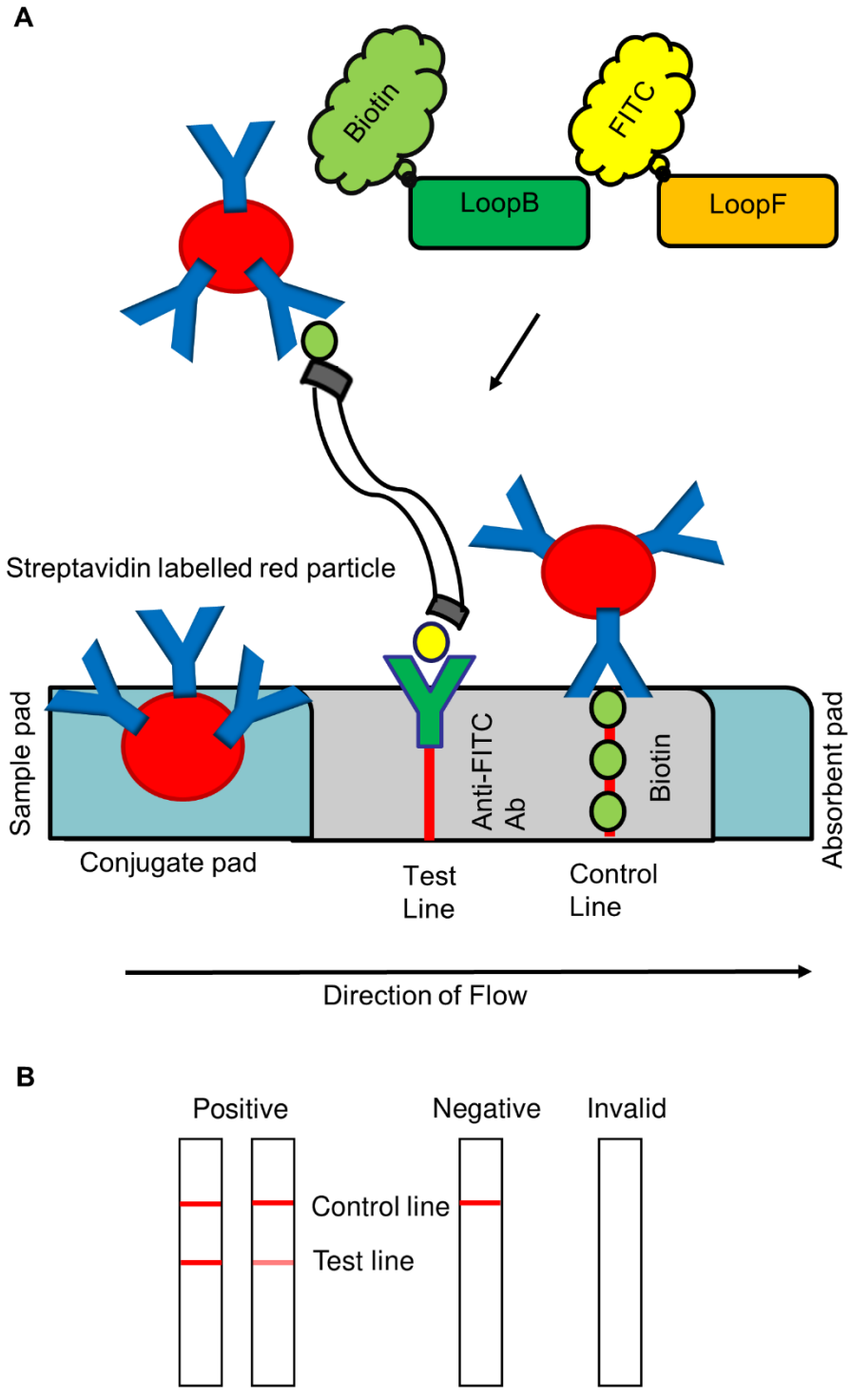

Figure 2.5 Mechanism and interpretation of nucleic acid detection strips
A. Mechanism of nucleic acid detection. Forward Loop Primer (FLP) is labelled with FITC and Backward Loop Primer (BLP) with biotin. LAMP reaction is added to the sample pad. The double stranded DNA amplicon containing both biotin and FITC moves towards the conjugate pad by capillary action, which contains red particles labelled with Streptavidin. The Streptavidin on red particles binds with biotin on the amplicon and the products move towards the test line containing anti-FITC antibodies. Here, anti-FITC antibodies capture the FITC-labelled amplicon and the red particles form a line. Any unbound red nanoparticles are captured by the biotin at the control line and form a line. **B.** Interpretation of the nucleic acid detection strips. After adding sample to the sample pad, the user should wait for the results to develop for 5-10 minutes. Two red bands indicate a positive result, one band indicates a negative result and no bands indicate an invalid test.

2.3 Studying secondary spontaneous clearance

2.3.1 Patient cohort

Patients were men-who-have-sex-with-men (MSM) with HCV-HIV coinfection recruited as part of the St Mary's Acute HCV cohort at Imperial College NHS Hospital Trust (Thomson et al. 2011). Samples were taken at several time points (TP) throughout the course of infection along with additional information including clinical and viral parameters. Patients who did not spontaneously clear infection were offered treatment consisting of 24-48 weeks of pegIFNα and weight based RBV or DAAs according to local guidelines for HCV infection. For the purpose of this thesis, samples from pegIFN/RBV treatment failures were retrieved from two patients with the rare event of secondary spontaneous clearance (SSC, n=2) and four control patients: three relapse and one null response patient (n=4).

2.3.2 Plasma separation

Whole blood samples were collected in Vacutainer®. Samples were processed by the density gradient centrifugation on a Heraeus Megafuge 40R (rotor model: 7500307/08,Thermo Fisher Scientific) as follows; 20-25 ml of blood was gently poured on top of a 10-20 ml layer of Histopaque and centrifuged for 20 minutes at 24400 x g at room temperature with no deceleration. The top plasma layer was collected and stored in 2 ml tubes at -80°C. Peripheral blood mononuclear cells (PBMC) were washed in phosphate buffered saline (PBS). The mixture was centrifuged at 1500 rpm for 5 minutes at room temperature and the supernatant discarded. Cells were resuspended in Foetal Calf Serum (1 ml for every 10 ml of blood). Freezing mix containing 20% Dimethyl sulfoxide (DMSO) and 80% Roswell Park Memorial Institute (RPMI) medium was added slowly to the resuspended cells at a final ratio of 1:1. The mixture was immediately transferred to cryovials in a pre-cooled container and stored at -80°C for 1-3 days. The cryovials were subsequently stored in liquid nitrogen. Whole blood samples were aliquoted (<1ml) and stored at -80°C prior to the density gradient centrifugation protocol.

2.3.3 RNA extractions

Extractions of RNA were carried out by the automated method described in section 2.2.4. For samples low in volume (<0.5 ml) or with low viral loads, extractions were carried out manually using the same protocol.

2.3.4 Cell culture

Cell lines were grown in supplemented Dulbecco's modified Eagle's medium (10% heat-inactivated foetal calf serum, 1% nonessential amino acids, 10 mM HEPES buffer and 4 mM L-glutamine) at 37°C and 5% CO2 atmosphere. Cells were maintained in 80 cm2 or 175 cm2 tissue culture flasks and passaged once 80-90% confluent. Flasks were washed by gently adding 5-10 ml of Versene and the cells detached by washing with trypsin diluted in Versene (final concentration of 0.025%).

2.3.5 Next generation sequencing

For next generation sequencing (NGS), a metagenomic sequencing approach was used as described previously (Thomson et al. 2016). Briefly, RNA was extracted, reverse transcribed and converted to double-stranded cDNA as described in sections 2.2.4, 2.2.4.1, and 2.2.6. A KAPA library preparation kit (KAPA BioSciences, 7961880001) was used for adapter-ligation library preparation, cDNA was end repaired and purified using AMPureXP magnetic beads (Beckman Coulter, A63881). To minimize loss of sample, the beads were retained in all steps and samples remained in the same tube until adapter ligation. Adaptor-ligated DNA was subsequently amplified in real-time with a KAPA Hifi Real-time library amplification kit (KAPA BioSciences, 7958978001). NEBnext multiplex oligos (New England Biolabs, E7780) were used to add index tags. Amplified DNA was purified on AMPureXP beads and eluted in 15 µl of nuclease-free water. A Qubit 2.0 fluorimeter was used to assess Library DNA concentration and the final size profile was verified on the Agilent 2200 Tapestation. HCV sequences were subsequently enriched using the NimbleGen SeqCap Target Enrichment system (Roche) using a panel of custom probe sets covering all known HCV genotypes across the full genome. Separate pools for low and high viral loads were generated at a total concentration of 1 µg and hybridized to probes for 48 hours.

Universal primers were used for 14 rounds of PCR and the resultant pools sequenced on the Miseq system (Illumina).

2.3.6 Bioinformatic analysis

Fastq files were mapped using an in-house mapper Tanoti (http://www.bioinfomatics.cvr.ac.uk/tanoti.php) and *de novo* assembly was carried out using dipSPAdes. HCV reference sequences were selected using a genotyping method written by Sreenu Vattipally (CREATE-KMERS) employing a kmer-based approach.

Alignments of HCV sequences were performed on MAFFT and adjusted manually if required. RaxML was used for maximum likelihood phylogenetic analysis using the GTR+G+I substitution model.

2.3.7 Generation of HCV pseudoparticles

2.3.7.1 Nested PCR for amplification of patient viral E1E2 sequences

Extracted RNA samples from section 2.2.4 were subjected to cDNA synthesis as described (2.2.4.1). Nested primers for full length E1E2 were adapted from previously published primer sequences (A W Tarr et al. 2007). Patient consensus sequences, obtained from NGS data, were aligned with the entire primer set on Serial Cloner software version 2.6.1 and nucleotides replaced, based on any mismatches found. All primers were adjusted in length for optimal PCR conditions and inner primers contained either a start or stop codon and a directional tag as shown in Table 2.9.

Table 2.9 Primer sequences for amplification of patient HCV E1E2

Primer	Sequence (5'-3')	Patient/time point amplified
Gen 4d Outer Sense	GCTTCGCCGATCTCATGGGATAC	P155 TPA, P155 TPD
Gen 4d Outer Antisense	CGACTGAGACGGCATTGATGGTG	P155 TPA, P155 TPD
Gen 4d Inner Sense I	**CACC*ATGGGTTGCTCTTTCTCTATCTTTCTCTTG	P155 TPA
Gen 4d Inner Sense II	*CACC*ATGGGTTGCTCTTTCTCTATCTTCCTCTTG	P155 TPD
Gen 4d Inner Antisense	TTATGCTTCGACCTGCGAGACCATCAGC	P155 TPA, P155 TPD
Gen 1a Outer Sense	GTGAACTATGCAACAGGGAA	P75 TPA, P75 TPB, P131 TPA, P131 TPD, P101 TPA, P101 TPB, P63 TPA, P63 TPB
Gen 1a Outer Antisense I	GCAAAGCAGAAAAACACGAG	P75 TPA, P75 TPB, P131 TPA, P131 TPD
Gen 1a Outer Antisense II	GCAAAGCAGAAGAACACGAG	P101 TPA, P101 TPB, P63 TPA, P63 TPB
Gen 1a Inner Sense	*CACC*ATGGGTTGCTCTTTCTCTATCTTC	P75 TPA, P75 TPB, P131 TPA, P131 TPD, P101 TPA, P101 TPB, P63 TPA, P63 TPB
Gen 1a Inner Antisense I	AAAGTTTCTAGATTATGCCTCCGCTTGGGAGA	P75 TPA, P75 TPB, P131 TPA, P131 TPD
Gen 1a Inner Antisense II	AAAGTTTCTAGATTACGCCTCCGCCTGGGATA	P101 TPA, P101 TPB
Gen 1a Inner Antisense III	AAAGTTTCTAGATTACGCCTCCGCTTGGGATA	P63 TPA, P63 TPB

*Start codons are underlined, stop codons are indicated in bold and directional tag is indicated by italics. Nucleotides highlighted in red were added additionally for optimal PCR conditions.

Nested PCR was performed using Phusion® Hot Start Flex DNA Polymerase (New England Biolabs, M0535S) as per manufacturer's instructions with slight modifications. Briefly, each reaction contained 0.5 µl Phusion enzyme, 10 µl 5x Phusion GC buffer, 1 µl dNTPs (10 mM), 2 µl of template, 2.5 µl of forward primer (10 µM), 2.5 µl of reverse primer (10 µM) and nuclease free water to a final volume of 50 µl per reaction. The second step of the nested PCR used the inner primers and contained undiluted 2 µl of PCR product as a template from the first step of the outer primers nested PCR reaction. Both nested PCR reactions were subjected to the following thermocycling conditions; denaturation at 98°C for 30 seconds followed by 35 cycles of denaturation at 98°C for 10 seconds, annealing for 1 minute at 68°C/72°C for outer/inner PCR, respectively. Extension was performed at 72°C for 1 minute and 30 seconds with a final 5 minutes extension at 72°C. For P75, plasma samples were limited in volume (<0.5 ml) and thus full E1E2 genes were synthesised by Eurofins genomics. Phusion® Hot Start Flex DNA Polymerase was used to obtain PCR products from the synthesised genes by utilising only the inner nested PCR primers. PCR reactions were set up as above and supplemented with 1.5 µl of DMSO and 2 µl of template at 10 ng/µl was used. The PCR reactions were incubated at 98°C for 30 seconds with 35 cycles of denaturation at 98°C for 10 seconds, annealing at 56°C/72°C for 30 seconds and extension at 1 minute at 72°C with a final extension for 10 minutes at 72°C.

2.3.7.2 Gel purification of E1E2-encoding sequences

Nested PCR products from patients were diluted in DNA loading dye (New England Biolabs, B7024S) and run on a 1% agarose gel TAE dyed with 5 µl of ethidium bromide (stock 10 mg/ml) along with 100 bp DNA ladder (New England Biolabs). Products were visualised by a UV lamp and bands of 1.8 kb were excised. DNA was purified using a GeneJet gel extraction kit (Thermo Fisher Scientific, K0701) as per manufacturer's instructions following the centrifugation method. Purified DNA was eluted in Elution buffer in a final volume of 30-50 µl.

2.3.7.3 Cloning into the directional TOPO Gateway™ entry vector

Purified nested PCR products were used for subcloning into the pENTR D-TOPO directional cloning vector (Thermo Fisher Scienfic, K240020) as per

manufacturer's instructions (Figure 2.6). Briefly, each reaction contained 1 µl of salt solution 1 µl of linearized TOPO® and between 0.5-4 µl of purified PCR product at three different molar ratios (0.5:1, 1:1 and 2:1 of insert to vector) to a final volume of 6 µl. Reactions were mixed, incubated at room temperature for 5 minutes and placed on ice. The TOPO® cloning reaction was transformed into One Shot® chemically competent *E. coli* by adding 2 µl of the mix per vial and mixing gently. The cells were incubated on ice for 30 minutes, heat-shocked for 30 seconds at 42°C and immediately placed back on ice. S.O.C Medium (Thermo Fisher Scientific, 15544034) was equilibrated to room temperature and 250 µl added to each vial. Cells were incubated at 37°C for 1 hour with shaking and 200 µl of bacterial culture was spread on a pre-warmed selective LB agar plates containing 50 µg/ml of Kanamycin. Following an overnight incubation at 37°C, 5-10 colonies were selected and cultured overnight in 5 ml LB broth containing 50 µg/ml of Kanamycin. DNA was extracted from bacterial cells using the GeneJet Plasmid Miniprep kit (Thermo Fisher Scientific, 10319699) as per manufacturer's instructions. Purified DNA was eluted in 25-30 µl of elution buffer and the presence of E1E2 sequences confirmed by Sanger sequencing (Eurofins Genomics), as described in section 2.3.7.6, by utilising M13 forward (5´-GTAAAACGACGGCCAG-3´) and M13 reverse (5´-CAGGAAACAGCTATGAC-3´) primers. Sequences were analysed on Serial Cloner 2.6.1 software by aligning to the corresponding NGS consensus and by visually examining chromatograms for miscalled nucleotides. Complete E1E2-containing clones without internal stop codons were used for downstream subcloning processes into the mammalian expression vector phCMV (B Bartosch, Dubuisson & Cosset 2003) as described below (section 2.3.7.4).

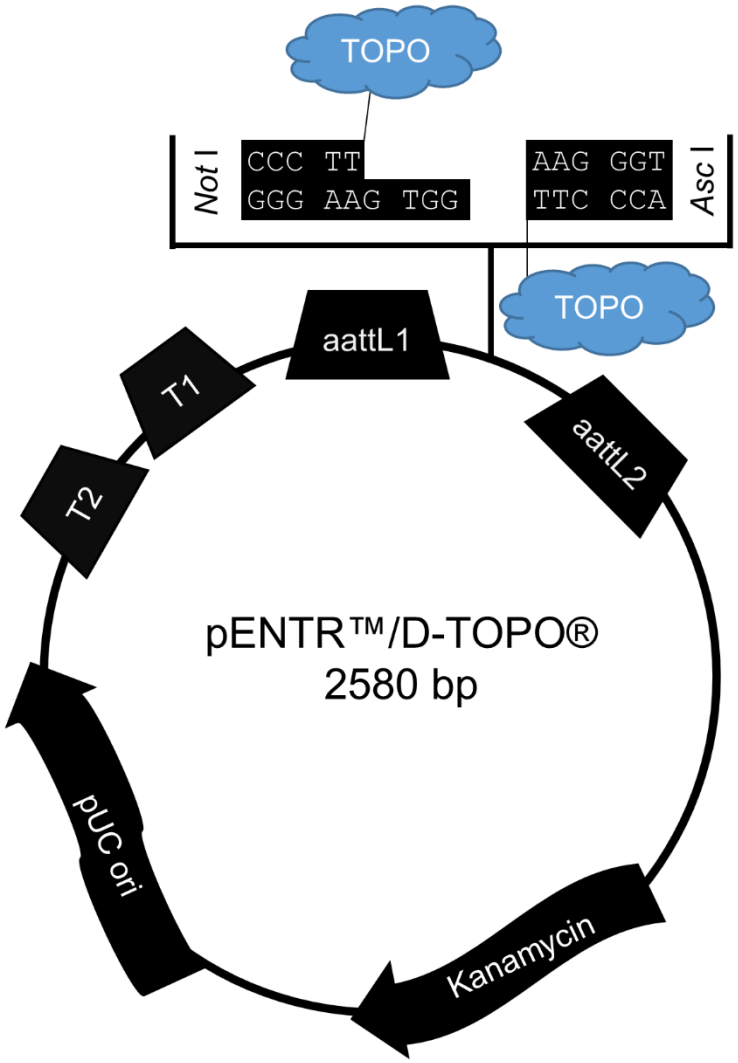

Figure 2.6 pENTR D-TOPO directional cloning vector

The figure shows the layout of the plasmid with directional cloning sites (TOPO), *aat*L1 and *aat*L2 sites (bacteriophage ƛ-derived recombination sequences enabling recombinational cloning of gene of interest in the entry vector with a Gateway® destination vector), Kanamycin resistance gene (allows selection of plasmid in *E.coli*), pUC origin of replication (allows high-copy replication and maintenance in bacterial cells). T1 and T2 transcription termination sites are present to reduce potential toxicity by preventing basal expression of the PCR insert and digestion restriction sites for digestion enzymes *Not*I and *Asc*I. Figure adapted from the Thermo Fisher website https://assets.thermofisher.com/TFS-Assets/LSG/figures/2721.jpg-650.jpg accessed 08/03/2019.

2.3.7.4 Screening for E1E2 in pENTR™/D-TOPO clones by PCR

Clones obtained on selective media described in section 2.3.7.3 were screened for the presence of E1E2 by PCR. Several clones were picked from each plate using a sterile pipette tip and inserted directly into 10x DreamTaq™ Green Buffer PCR reaction mix (Thermo Fisher Scientific, EP0711). Each reaction contained 2.5 µl of 10x DreamTaq Green Buffer, 0.5 µl of 10mM dNTP mix , 2.5 µl of 10 µM of M13 Forward primer, 2.5 µl of 10 µM of M13 Reverse primer, 0.125 µl of

DreamTaq DNA polymerase, and nuclease-free water to the total volume of 25 µl. The PCR reactions were subjected to the following thermocycling conditions; denaturation at 95°C for 10 minutes, to allow release of DNA from bacteria, followed by 35 cycles of denaturation at 95°C for 30 seconds, annealing at 52°C for 30 seconds and extension at 72°C for 1 minute. Final extension was performed at 72°C for 10 minutes. The PCR products were visualised by loading directly into 1% agarose gel for electrophoresis as described in 2.2.10.2.

2.3.7.5 Insertion into the phCMV Gateway® expression vector by recombination

Complete E1E2-encoding pENTR vectors were used to transfer E1E2 sequences into the mammalian phCMV Gateway® expression vector. Dr Vanessa Cowton supplied this expression vector based on the Gateway® Vector Conversion System (Thermo Fisher Scientific). For the recombination reaction, 1-10 µl of entry clone (150 ng) was mixed with 2 µl of the expression vector (300 ng), 4 µl of 5x LR Clonase™ reaction buffer and TE buffer, pH 8, to a final volume of 16 µl. The LR Clonase™ enzyme mix (Thermo Fisher Scientific, 11791019) was thawed on ice, vortexed briefly and 4 µl added to each reaction vial. Reactions were incubated at 25°C overnight and 2 µl of Proteinase K solution was added to each vial and incubated for 10 minutes at 37°C. For transformation, one vial of One Shot® competent cells was thawed on ice and 1-5 µl of each recombination reaction added directly. The mixtures were mixed by tapping and incubated on ice for 30 minutes. Next, the cells were heat shocked at 42°C for 30 seconds and immediately placed back on ice. S.O.C medium (250 µl) was added to each vial and cells were incubated at 37°C for 1 hour at 225 rpm in a shaking incubator. Pre-warmed LB agar plates containing 100 µg/ml ampicillin were used to spread 20-200 µl from each transformation vial. Plates were then inverted, stored overnight at 37°C and 5-10 colonies incubated further in 5 ml of LB containing 100 µg/ml ampicillin for 16 hours. Plasmids were extracted using the GeneJet Plasmid Miniprep kit (Thermo Fisher Scientific, K0503) as per manufacturer's instructions and eluted in 25-30 µl of nuclease-free water. The DNA concentrations of each expression vector were measured on Nanodrop spectrophotometer (Thermo Fisher Scientific).

The success of each recombination was determined by Sanger sequencing (Eurofins Genomics) as described below by using a phCMV forward primer (5'-

CGGTGCACATGCTTTACATGT-3', designed by Dr Vanessa Cowton) and checking for the presence of HCV E1E2 sequences.

2.3.7.6 Sanger sequencing

Sanger sequencing was carried out using the Mix2Seq kit (Eurofins Genomics) as per manufacturer's instructions. The plasmid template to be sequenced was diluted to 50-100 ng/µl and 15 µl transferred to the designated tubes from Mix2Seq kit. A further 2 µl of forward or reverse primer was added at a concentration of 10 µM. Samples were sent to Eurofins for Sanger sequencing on ABI 3730XL sequencing machines. Sequences in fasta format were analysed and compared to NGS consensus sequences on Serial Cloner software 2.6.1. Chromatograms were examined visually for misclassified bases using BioEdit version 7.04.1 for ab1 files or Adobe Acrobat Reader for pdf files.

2.3.7.7 Site-directed mutagenesis

Site-directed mutagenesis (SDM) by PCR was used directly on the mammalian expression vector (phCMV) containing sequences from time-point A (TPA) from P155 and TPA from P63. Complementary primers incorporating correct base pairing with a mutation in the middle (SDM) were designed for P155 and P63 as shown in Table 2.10. Phusion® Hot Start Flex DNA polymerase (New England Biolabs) was used for PCR as per manufacturer's instructions. Briefly, each reaction contained 1 µl of forward primer (10 µM), 1 µl of reverse primer (10 µM), 1 µl of plasmid DNA template at 1 ng/µl, 0.6 µl DMSO, 10 µl of 2x Phusion Mastermix and nuclease free water to a total volume of 20 µl per reaction. PCR reactions were subjected to the following thermocycling conditions; denaturation at 98°C for 3 minutes followed by 35 cycles of denaturation at 98°C for 10 seconds, annealing/extension at 72°C at 4 minutes 30 seconds with a final extension at 72°C for 10 minutes. PCR products were cleaned with QIAquick PCR purification kit (Qiagen, 28104) as per manufacturer's instructions; 5 volumes of Buffer PB was added to 1 volume of PRC reaction and applied to a Qiaquick column. The entire mixture was centrifuged in a table-top microcentrifuge at 17,900 g for 1 minute. Washing was performed by adding 750 µl of Buffer PE and a 1-minute centrifugation step as above. Residual buffer was removed by a further centrifiguation step and 30 µl of Buffer EB added and used for elution

into a fresh 2 ml tube. A final centrifugation step was performed for 1 minute to obtain cleaned eluted DNA. Next, DpnI enzyme was incubated with the cleaned PCR products in order to remove any dam+ plasmids and generate pure PCR-generated product. The reactions were incubated at 37°C for 1 hour and inactivated at 70°C for 10 minutes. The purified reactions were transformed into One Shot® TOP10 cells (Thermo Fisher Scientific, C404010) as per manufacturer's instructions. Clones were screened for positive mutants by Sanger sequencing as described in section 2.3.7.6.

Table 2.10 Primers used in site-directed mutagenesis

	Primer name and sequence	
Patient	**Forward (5'->3')**	**Reverse (5'->3')**
P155	*GAACTGTTGAATTTGTTGTAGT**A**AAGCAGAC	GTCTGCTTT**T**ACTACAACAAATTCAACAGTTC
P63	CTCATCTATC**G**CCACAGATTCAACTCTTC	GAAGAGTTGAATCTGTGG**C**GATAGATGAG

*Bold letters indicate the deliberate insertion of a mismatching nucleotide in complementary primers to change the amino acid

2.3.7.8 Transfection of HEK 293 T cells

HEK 293 T cells were seeded in 10 cm cell culture dishes at a density of $1x10^6$ cells per dish. Dishes were incubated at 37°C and 5% CO_2 atmosphere for 24 hours. Subconfluent cells were co-transfected with the HCV E1E2-phCMV expression vector, the pMLV gag-pol retroviral packaging vector and the pMLV-Luc transfer vector using the calcium chloride precipitation method as previously described (A W Tarr et al. 2007). Some of the phCMV vectors were generated during the course of this project (section 2.3.7) others were obtained through personal communication (Prof Arvind Patel). The morning after co-transfection, media were replaced with 6 ml of fresh DMEM supplemented with 10% heat inactivated foetal calf serum, 1% nonessential amino acids, 10 mM HEPES buffer and 4 mM L-glutamine. At 48-72 hours post co-transfection, supernatant medium was passed through a 0.45 µM filter.

2.3.7.9 Infectivity testing of HCVpp

In order to test HCVpp for infectivity, Huh7 cells were seeded at 4×10^4 cells per 96-well Immunolon-II plate (Nunc, Thermo Fisher Scientific, 167008). Cells were incubated for 24 hours at 37°C with 5% CO2 atmosphere. HCVpp generated by

HEK 293T transfections above were added in triplicate (40-50 µl) after removing cell media from each well and kept in an incubator for 3-4 hours. HCVpp were discarded and replaced with 100 µl per well of supplemented DMEM medium. Cells were incubated for 72 hours at 37°C with 5% CO2 atmosphere. Media were discarded and 50 µl of Glo Lysis buffer (Promega, E2661) was added to each well. Cells were incubated on a shaker at room temperature for 10 minutes and the cell lysate was transferred to white 96-well tissue culture plate (Sigma, CLS3912-100EA). The BrightGlo luciferase assay substrate (Promega, E2620) was added at a 1:1 ratio to each well and infectivity confirmed by measuring luminescence on a Hidex BIOSCAN Chameleon Luminometer. For neutralisation assays, luminescence signal in relative light units was normalised to background or Huh7 cell signal only (set at 1). The infectivity of each HCVpp was measured as the increase from the mean of the background or control (x mean control). Only HCVpp with relative light units at least 10-100 times higher than the uninfected Huh7 cells, were selected.

2.3.7.10 Obtaining cell lysate from HEK-293T cells

After harvesting HCVpp generated in section 2.3.7, 5 ml of Lysis Buffer 2 (LB2) was added to all 10 cm cell culture dishes. Dishes were placed on a shaker for 10 minutes and the lysate transferred to centrifuge tubes. Lysates were centrifuged at 5000 g for 10 minutes and the supernatant transferred to a clean centrifuge tubes and stored at -20°C.

2.3.8 HCVpp based assays

2.3.8.1 IgG purification

Plasma samples from healthy controls and patients from at least one time-point pre-treatment and one post-treatment time-point were analysed and used for Immunoglobulin G (IgG) purification. To inactivate viral particles, Triton X-100 was added to each sample at a 1 in 10 dilution to a final concentration of 0.05%. The mixtures were purified for IgG on Protein G HP SpinTrap antibody purification columns (Sigma, GE28-4083-47) as per manufacturer's protocol with slight modifications. All centrifugation steps were performed for 1 minute at 8000 g. Media in purification columns were resuspended and removed by centrifugation. Columns were equilibrated by adding 600 µl of binding buffer and

by a centrifugation step. Binding buffer was discarded and 100-200 µl of plasma was added to each column. Samples were mixed gently at room temperature for 4 minutes and centrifuged. A further 600 µl of binding buffer was added and centrifuged again. The step was repeated twice and residual buffer removed with a further centrifugation. The purified IgG was eluted by adding 200 µl of elution buffer and mixing by inversion. The purification columns were placed on top of fresh 2 ml tubes containing 30 µl of neutralizing buffer and centrifuged. A minimum of two elution steps per sample were performed. The final IgG concentration was measured on a Nanodrop 1000 spectrophotometer (Thermo Scientific, UK). Pierce™ Protein G Binding Buffer (10455944), Pierce™ IgG Elution Buffer (10433805) and Neutralization Buffer (1856281) were purchased from Thermo Fisher Scientific.

2.3.8.2 GNA capture ELISA

ELISA experiments used to detect antibodies to E1E2 were performed as previously described (Patel et al. 2000). Briefly, Galanthus nivalis agglutinin (GNA, Sigma, L8275-5MG) was used to coat Immulon II microtitre plates (Fisher Scientific, 10795026) overnight at 0.25 µg/well in 100 µl phosphate buffered saline (PBS). Plates were blocked in 2% skimmed milk PBST with 0.05% Tween (PBST) for 2 hours at room temperature. After three PBST washes, HEK-293T cell lysates, generated in section 2.3.7.8, were used as E2 test fraction sources, diluted 1/3 in PBS with 0.05% Tween and 2% skimmed milk (PBSTM) and captured by GNA for at least 2 hours at room temperature. Plates were washed again and purified IgG from patients and healthy controls were added at 100 µg/ml PBSTM for 1 hour. Bound antibodies were detected by Horseradish peroxidase (HRP) anti-human IgG diluted in PBSTM (Sigma A0170 or W4031) and TMB substrate. IgG from healthy controls acted as a negative control and were used to normalise ELISA plates between experiments. A dilution curve of the anti-HCV E2 mouse monoclonal antibody (MAb) AP33 (Owsianka et al. 2005; Alexander W. Tarr, et al. 2006) was included as a positive control and absorbance values were measured at 450 nm. GNA Capture ELISA was also used to detect E2 proteins in cell lysates from non-infectious HCVpp as determined by the infectivity testing in section 2.3.7.9. Experiments were performed as described above with serial-dilution of AP33 used as an E2 detection antibody.

2.3.8.3 Neutralisation assays

Immunol II 96-well plates were seeded with Huh7 cells at 4 x 10^3 cells/well. At 24 hours, 100µg/ml of purified IgG from all patient time-points were incubated with HCVpp from the general genotype panel. Heat-treated plasma from each patient time-point was incubated with autologous HCVpp from the same patient. Plasma was serially diluted from 1:50 in 1:3 dilutions in PBS. Plasma and IgG were incubated with 40 µl of HCVpp for 1 hour at 37°C and subsequently transferred to Huh7 cell plates after removing media. Plates were incubated for 3-4 hours at 37°C and replaced with fresh medium. At 72 hours, the medium was discarded, cells lysed and luciferase activity measured using the GloLysis luciferase substrate assay (Promega) as per manufacturer's instructions.

2.3.9 Cytokine assays – Luminex

For cytokine analysis, Luminex assays were performed using MULLIPLEX® MAP Human Th17 Magnetic Bead Panel Kit (Merck, HTH17MAG-14K) as per manufacturer's instructions with slight modifications. Prior to starting the experiment quality controls 1 and 2 were reconstituted in 250 µl of deionised water, vortexed and allowed to stand for 5-10 minutes. Wash buffer was prepared by equilibrating to room temperature and mixing 60 µl with 540 µl of deionised water. Plasma matrix was prepared by adding 0.5 ml of deionised water to the lyophilised matrix and allowed to stand for at least 10 minutes. Standards for human Th17 assay were prepared by adding 250 µl of deionised water to standard 7 which was mixed and allowed to stand for 5-10 minutes. Standards 6-1 were serially diluted from standard 7 by adding 50 µl to each dilution sequentially. In a 96-well plate, 200 µl of assay buffer was added to each well. The plate was sealed and mixed on a plate shaker for 10 minutes at room temperature. The assay buffer was discarded and residual liquid removed by inverting the plate onto blue roll and tapping several times. Standards and controls were added to appropriate wells (25 µl each) followed by 25 µl of assay buffer. The same volume of serum matrix was added into standard and control wells and 25 µl of neat samples were added to appropriate wells. Next, magnetic beads were mixed by vortexing and 25 µl added to each well with intermittent shaking to prevent the beads from settling. The plate was sealed, wrapped in aluminium foil and incubated with agitation on a plate shaker overnight at 4°C.

The plate was placed on a handheld magnet (EMD Millipore) for 60 seconds and the contents removed by decanting into a waste container. Residual liquid was removed by inverting the plate onto blue roll and tapping several times. The plate was washed twice by removing from the magnet, adding 200 µl of wash buffer and then placed back on a shaker for 30 seconds. The plate was held on the magnet for 60 seconds and the content removed as above. Detection antibodies were equilibrated to room temperature and 25 µl added into each well. The plate was covered in aluminium foil, placed on a shaker for 1 hour at room temperature and 25 µl of streptavidin phycoerythrin added to each well. The plate was covered in aluminium foil and placed on a shaker for further 30 minutes. The well contents were removed, washed twice as above and 100 µl of 4 % formaldehyde added to each well to ensure all HCV and other blood-borne infectious agents were inactivated. The plate was washed overnight by placing on a shaker at 4°C. The results were read on the Bio-Rad Bio-Plex Luminex machine and the data analysed using a spline curve fitting method for calculating the analyte concentration from Median Fluorescence Intensity (MFI) on the Bio-Plex software. The principle of the Luminex assay is shown on (Figure 2.7)

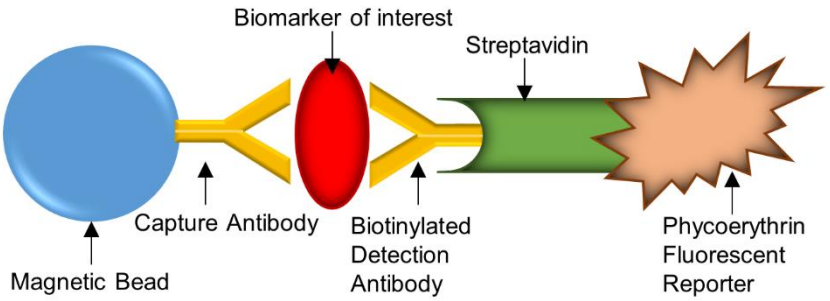

Figure 2.7 Luminex immunoassay
Fluorescently dyed beads each have a distinct code, allowing for discrimination of multiple types of biomarkers in a single suspension. Two lasers are used to detect and measure the concentration of different molecules bound to magnetic beads. The Bio-Plex Pro™ assays follow a similar principle as a sandwich ELISA. Beads conjugated to capture antibodies bind to the biomarker of interest in a given sample. A series of washes is performed to remove unbound material and a biotinylated detection antibody is used to create a sandwich complex. The detection complex forms when streptavidin-phycoerythrin (SA-PE) conjugate is added, with the phycoerythrin acting as a fluorescent reporter. Diagram adapted from Bio-Rad website: http://www.bio-rad.com/webroot/web/pdf/lsr/literature/10014905.pdf accessed on 11/03/2019.

2.3.9.1 Statistical analysis

Statistical analyses were performed using two-tailed parametric (t-test) or non-parametric (Mann-Whitney) tests on GraphPad Prism version 7. Data were considered significant if p value was less than or equal to 0.05.

3 Results

3.1 Improving diagnostic techniques for HCV testing

The isothermal amplification technique known as LAMP was utilised as a potential candidate for an HCV POC test.

3.1.1 Optimisation of HCV LAMP

In the first set of experiments, LAMP conditions including primer design, temperature, dNTP concentration and polymerase selection were varied to optimise the reaction. These initial optimisation experiments were based on published guidelines for designing LAMP assays (Eiken Chemical Co., Ltd).

3.1.1.1 Primer selection

In order to develop in-house LAMP primers for a pan-genotypic HCV assay, the most conserved region of HCV was selected, namely the 5'UTR, based on a reference alignment of 204 sequences of different genotypes (gt) as described in Materials and Methods. Figure 3.1 represents a summary of the alignment of these in-house primers with seven major HCV genotypes including; gt 1a, gt 2a, gt 3a, gt 4d, gt 5a, gt 6b and gt 7a. The binding region of the primers spans from the 5'UTR, at nucleotide 101 to the start of Core finishing at nucleotide 345. Degenerate sites were inserted in primers F3, F2, FLP, F1 and B1 in order to match with the majority of the genotypes from the reference alignment. Only one mismatch was noted in the seven major genotypes, localised in the binding area of the FLP primer; here an insertion of CD nucleotides (D representing a degenerate nucleotide, A/G/T) binds only with the CA in the gt 6b sequence. This is because all other genotypes have the two nucleotides missing which is indicated by two red underscores.

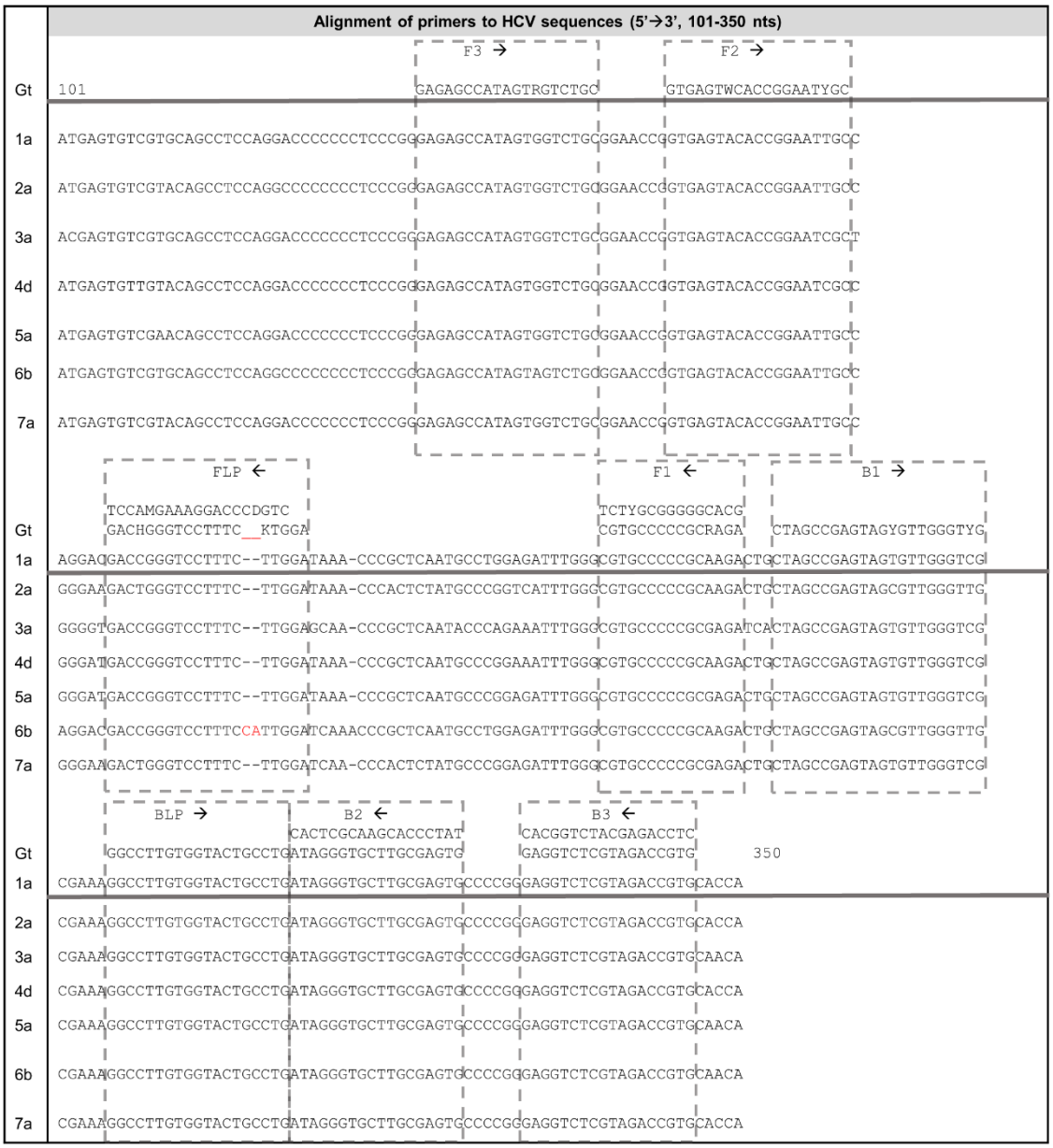

Figure 3.1 Alignment of in-house LAMP primers with major HCV genotypes
The alignment was performed using LAMP primers and seven major HCV genotypes (Genbank: AF009606, 1a, D00944, 2a, D17763, 3a, FJ462437, 4d, AF06449, 5a, D84262, 6b, EF108306, 7a) . The nucleotide numbering is based on the genotype 1a H77 reference sequence with Genbank accession number: AF009606 starting in the 5' untranslated region and finishing at the start of Core (nucleotides 101 -350). Dashed lines indicate areas of individual primer targets. Black arrows pointing right indicate forward primers and those pointing left indicate reverse primers. For reverse primers, the underlined sequence represents the complementary primer sequence. Mismatches are indicated in red. Primers FIP and BIP consists of primers F1 or B1 and F2 or B2, respectively. BLP – Backward loop primer, FLP – Forward loop primer. Degenerate nucleotides are indicated by the following letters; W – 'Weak' nucleotides A or T, S – 'Strong' nucleotides C or G, M – A/C, K – G/T, R – Purines A or G, Y – Pyrimidine C or T, B – Not A nucleotides C/T/G, D – Not C nucleotides A/G/T, H – Not G, nucleotides A/C/T, V not T, nucleotides A/C/G, N – Any, nucleotides A/C/G/T.

We also evaluated previously published HCV LAMP primer sequences (see Materials and methods). Figure 3.2 illustrates the regions targeted by these primers including the Accelerating Primer (AP) which spans the region between F1 and B1 in order to accelerate the reaction. Red letters indicate mismatches of primers with representative genotypes. There were six mismatches in F1 (two in gt 4, two in gt 2, one in gt 3 and one in gt 7), four in F2 (one in gt 3 and three in gt 7), two in FLP (one in gt 3 and one in gt 7), three in F1 (one in gt 3, one in gt 4 and one in gt 5), one in AP to gt 6b and six in the B1 target area (one in gt 2a, two in gt 3a, one in gt 6 and two in gt 7). No mismatches were observed in the B2 and B3 binding regions. Two mismatches to gt 3a were located in the last three nucleotides at the 3'end in primers F1 and BLP. The same was true for the gt 7 sequence, with mismatches in the last three nucleotides at the 3'end in two primers namely, F2 and FLP

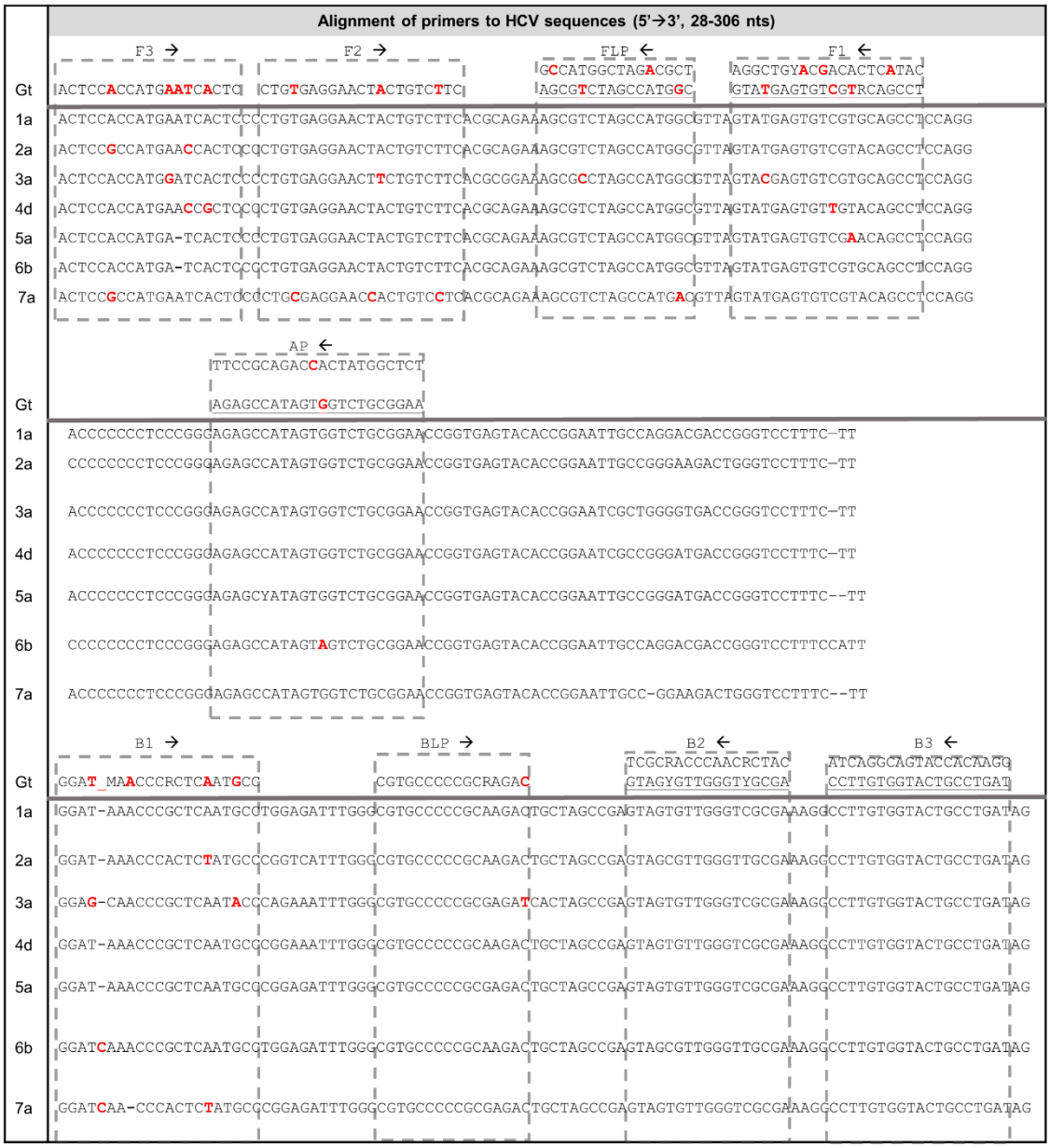

Figure 3.2 Alignment of published primers with major HCV genotypes
The alignment was performed using LAMP primers and seven major HCV genotypes (Genbank: AF009606, 1a, D00944, 2a, D17763, 3a, FJ462437, 4d, KC844046, 5a, D84262, 6b, EF108306, 7a) . The nucleotide numbering is based on genotype 1a sequence with Genbank accession number: AF009606 in the 5' untranslated region spanning between nucleotides 101 to 350. Dashed lines indicate areas of individual primer targets. Black arrows pointing right indicate forward primers and those pointing left indicate reverse primers. For reverse primers, the underlined sequence represents the complementary primer sequence. Mismatches are indicated by red. Primers FIP and BIP consists of primers F1 or B1 and F2 or B2, respectively. BLP – Backward loop primer, FLP – Forward loop primer, AP – Accelerating primer. Degenerate nucleotides are indicated by the following letters; W – 'Weak' nucleotides A or T, S – 'Strong' nucleotides C or G, M – A/C, K – G/T, R – Purines A or G, Y – Pyrimidine C or T, B – Not A nucleotides C/T/G, D – Not C nucleotides A/G/T, H – Not G, nucleotides A/C/T, V not T, nucleotides A/C/G, N – Any, nucleotides A/C/G/T

In order to select the best primer set for the HCV LAMP assay, in-house primers and previously published primers were included in experimental LAMP reactions with the same conditions enabling a direct comparison of the time to positive detection (TP). TP was defined as the earliest time, in minutes, for a given sample to reach the exponential phase of amplification observed as an exponential increase in fluorescence (the signal is directly proportional to the amount of DNA present in the sample). Primer concentrations were chosen as previously published primer (Yang et al. 2011). Figure 3.3 shows that the in-house primers had an earlier TP with the exponential phase starting around 15-16 minutes compared with approximately 17-19 minutes with published primers. However, variability of the data was noted. The selection of the optimum primer set was determined by several factors including analytical sensitivity and clinical sample detection in subsequent experiments.

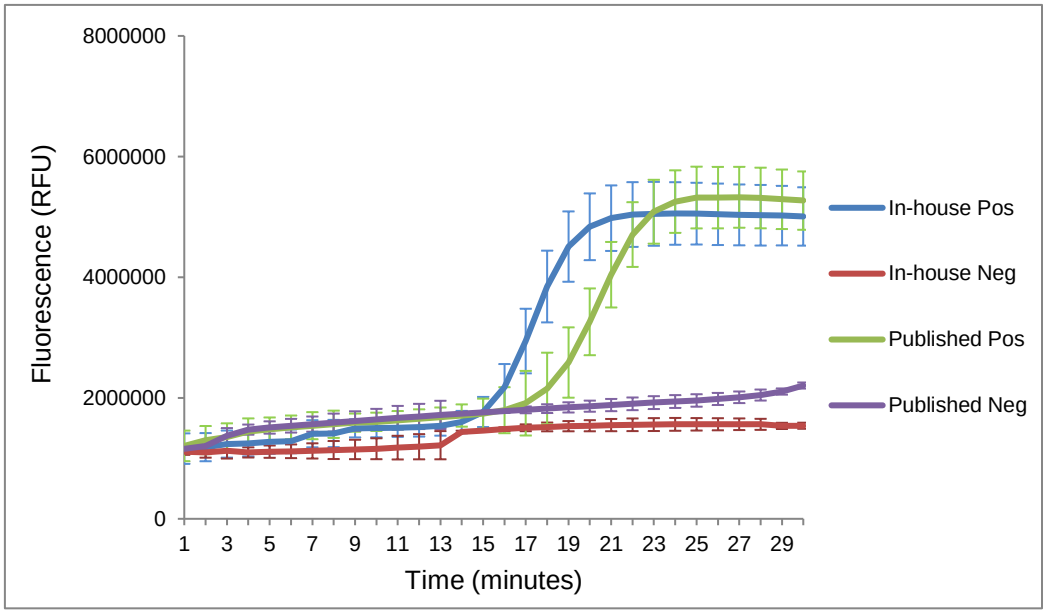

Figure 3.3 Time to detection with in-house and published primers

LAMP amplification products following real time amplification based on fluorescence signal in relative fluorescence units (RFU) with ISO-001 master mix for 30 minutes at 65°C. JFH1 plasmid replicon in quadruplicate (n=4) at 10^7 copies/ml was used as the positive (Pos) control and no template control in duplicate (n=2) as a negative control. Graph represents data from a single experiment. Primers were used at concentration of 2 µM (FIP/BIP), 1 µM (LF/LB) and 0.2 µM (F3/B3) with published primers also containing AP at 20 µM. In-house Pos (blue) represents standard JFH1 HCV LAMP assays with in-house primers. Published Pos (green) indicates standard JFH1 HCV LAMP assay with published primers. The values represent the mean and the error bars represent ±SD.

The TP of all experiments was defined based on fluorescence based on relative fluorescence units (RFU) (Figure 3.4). As HCV samples increase in fluorescence over the incubation period (value), the time to detection/positive was defined as the time with the greatest increase in fluorescence from the previous time point (highest point at the slope). As negative samples/controls do not contain the target, there are minimal differences in fluorescence between each time point and thus the fluorescence usually appears as a flat line (negative).

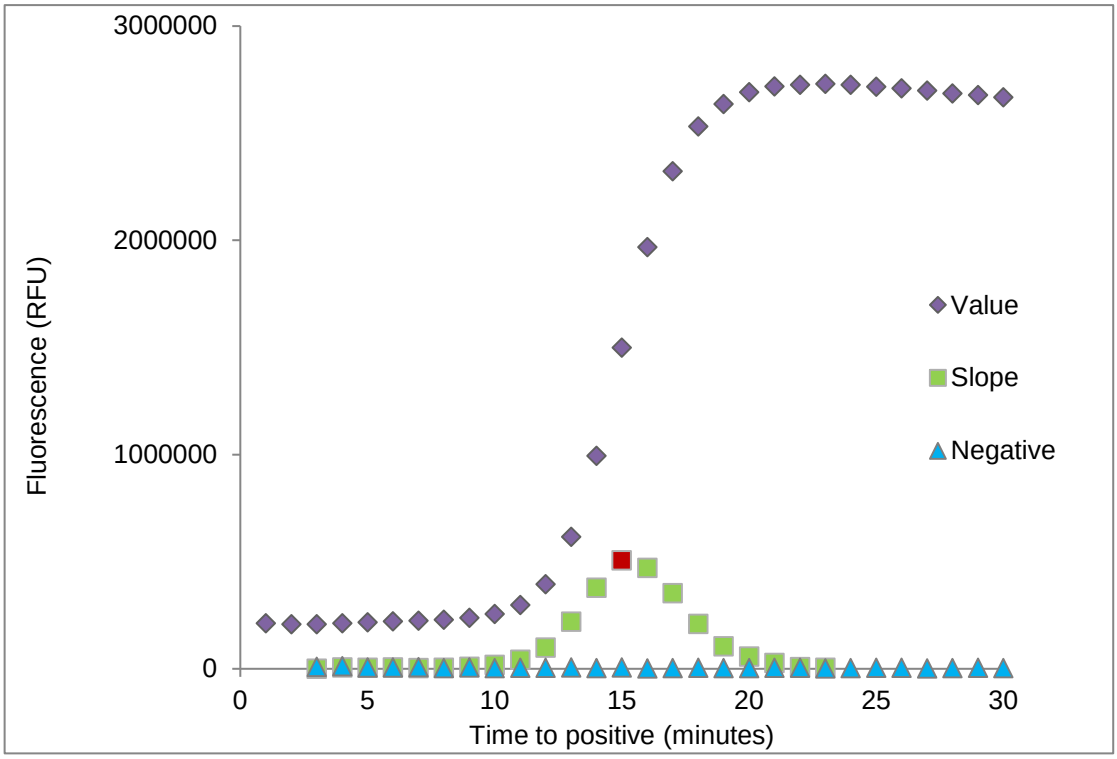

Figure 3.4 Determination of time to positive based on fluorescence

The value curve represents increase in fluorescence over a 30-minute incubation time at 65°C with HCV-positive genotype 1a replicon standard (10^6 copies/ml). The slope was calculated by subtracting fluorescence in relative fluorescence units (RFU) from the previous time point (a derivative). The highest point located on the slope is defined as time to positive for each sample tested – represented in red here. The negative is a no-template control, which resulted in minimal increase in fluorescence over-time.

3.1.1.2 Analytical sensitivity of the two primer sets

Serial dilutions of the JFH1 replicon plasmid starting at 10^7 copies/ml and finishing at 10 copies/ml were carried out to evaluate sensitivity. Figure 3.5 shows the results of the analytical sensitivity test with the previously published primer set. The lowest dilution detected by the primers was 10^2 copies/ml, detected only on one occasion. Samples at 10^3-10^4 copies/ml were detected on two occasions out of nine. The highest dilutions, 10^5 and 10^7, were detected on all occasions, other than one replicate at 10^5 copies/ml. The shorter the TP was in minutes, the higher the copy number of JFH1 replicon. The median TP was 21.5 minutes for 10^7 copies/ml, 30 minutes for 10^5, 45 minutes for 10^4, 10^3, 10^2 and 10 copies/ml and the negative control. Significant differences in TP were detected between the two highest concentrations (10^7 copies/ml and 10^5 copies/ml) and the negative control ($p<0.0001$ and $p=0.0085$, respectively), the 10 copies/ml ($p<0.0001$ and $p=0.0085$), and the 10^2 copies/ml ($p<0.0001$ and $p=0.0281$). The highest concentration (10^7 copies/ml) also had significant differences between the 10^4 copies/ml and 10^3 copies/ml ($p=0.0004$ and $p=0.012$).

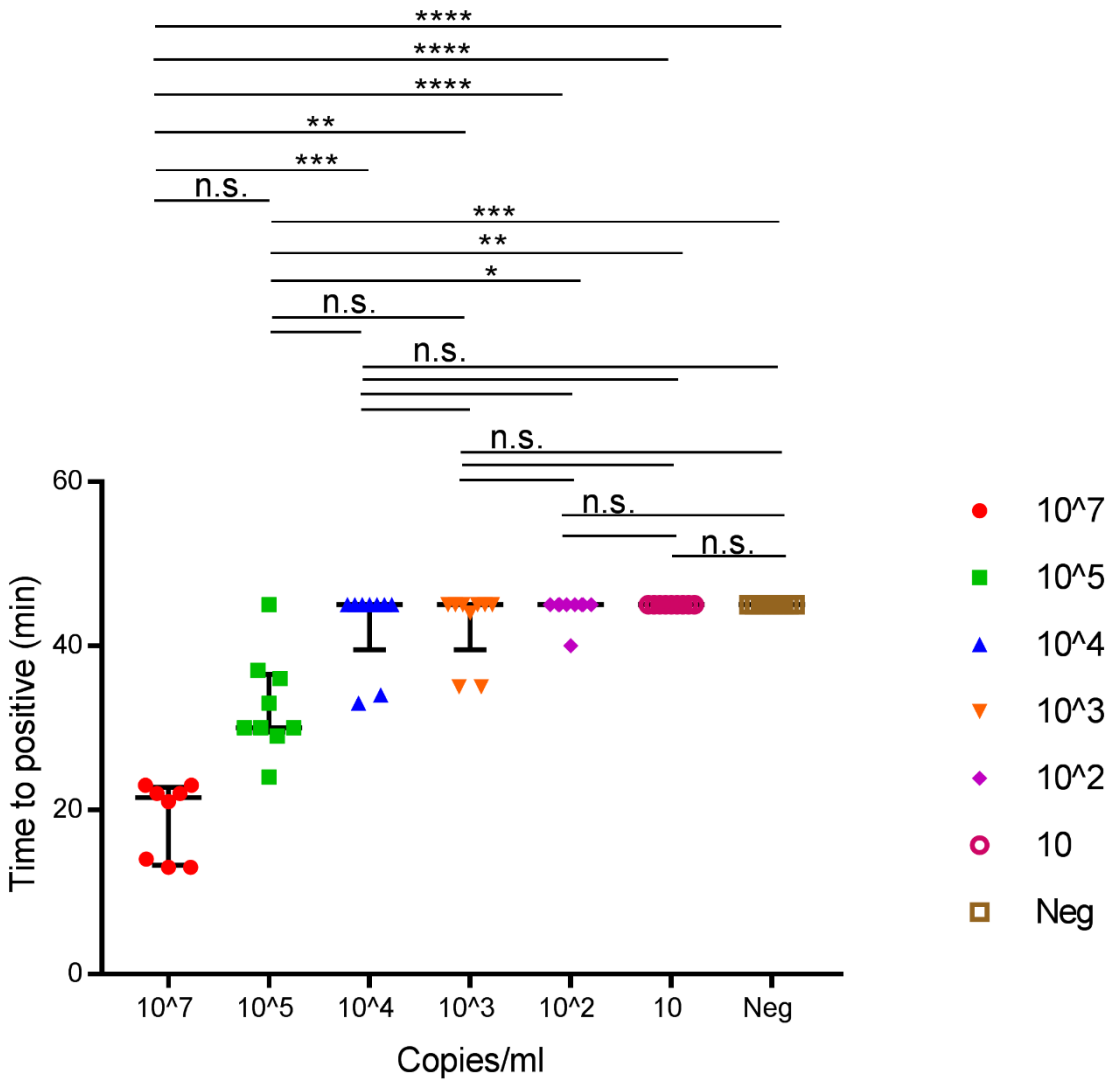

Figure 3.5 Analytical sensitivity of HCV LAMP assay with published primers
Serial dilutions of JFH1 replicon plasmid (10^7-10 copies/ml) were used as standards with no template as a negative control. Published primers developed by Yang *et* al 2011 were used at a concentration of 2 µM (FIP/BIP), 1 µM (LF/LB), 0.2 µM (F3/B3) and 0.8 µM (AP). The LAMP assay was incubated at 65ºC for 45 minutes. The values represent the median and the error bars represent interquartile range. No amplification was defined as time to positive of 45 minutes. Graph represents four independent experiments in duplicate. Kruskal-Wallis test with Dunn's multiple comparisons test was used for statistical analysis with significant differences indicated as follows: **** - p≤0.0001, *** - p≤0.001, ** - p≤0.01, * -p≤0.05, n.s. = not significant.

Figure 3.6 shows the results of the serial dilution experiment with the in-house primer set replicating the same LAMP conditions as the assay above. The median TP for all the dilutions used was: 17 minutes for 10^7 copies/ml, 32 minutes for 10^5 copies/ml, 40 minutes for 10^4 copies/ml, and 45 minutes for $10^3/10^2/10$ copies/ml and the negative control. The lowest copy number/ml detected by the in-house primers LAMP assay was 10^3, 10-fold higher than the published primer-based assay. Significant differences between the negative control and the serial dilutions were detected in the 10^7 copies/ml ($p<0.0001$), 10^5 copies/ml ($p<0.0001$) and 10^4 copies/ml ($p=0.0294$), therefore 10-fold lower than the published primer-based assay. All replicates were detected at the two highest concentrations, four were negative in the 10^4 copies/ml and seven in the 10^3 copies/ml (out of a total of nine). Concentrations of 10^2 copies/ml and lower were all negative. Significant differences were detected between the two highest concentrations (10^7 copies/ml and 10^5 copies/ml) and the three lowest concentrations, 10^2 copies/ml ($p<0.0001$ and $p=0.0042$, respectively), 10 copies/ml ($p<0.0001$ and $p=0.0042$) and the negative control ($p<0.0001$ and $p=0.0042$). The highest concentration, 10^7 copies/ml, also had significant differences between 10^4 copies/ml and 10^3 copies/ml ($p=0.0377$ and $p=0.0002$, respectively).

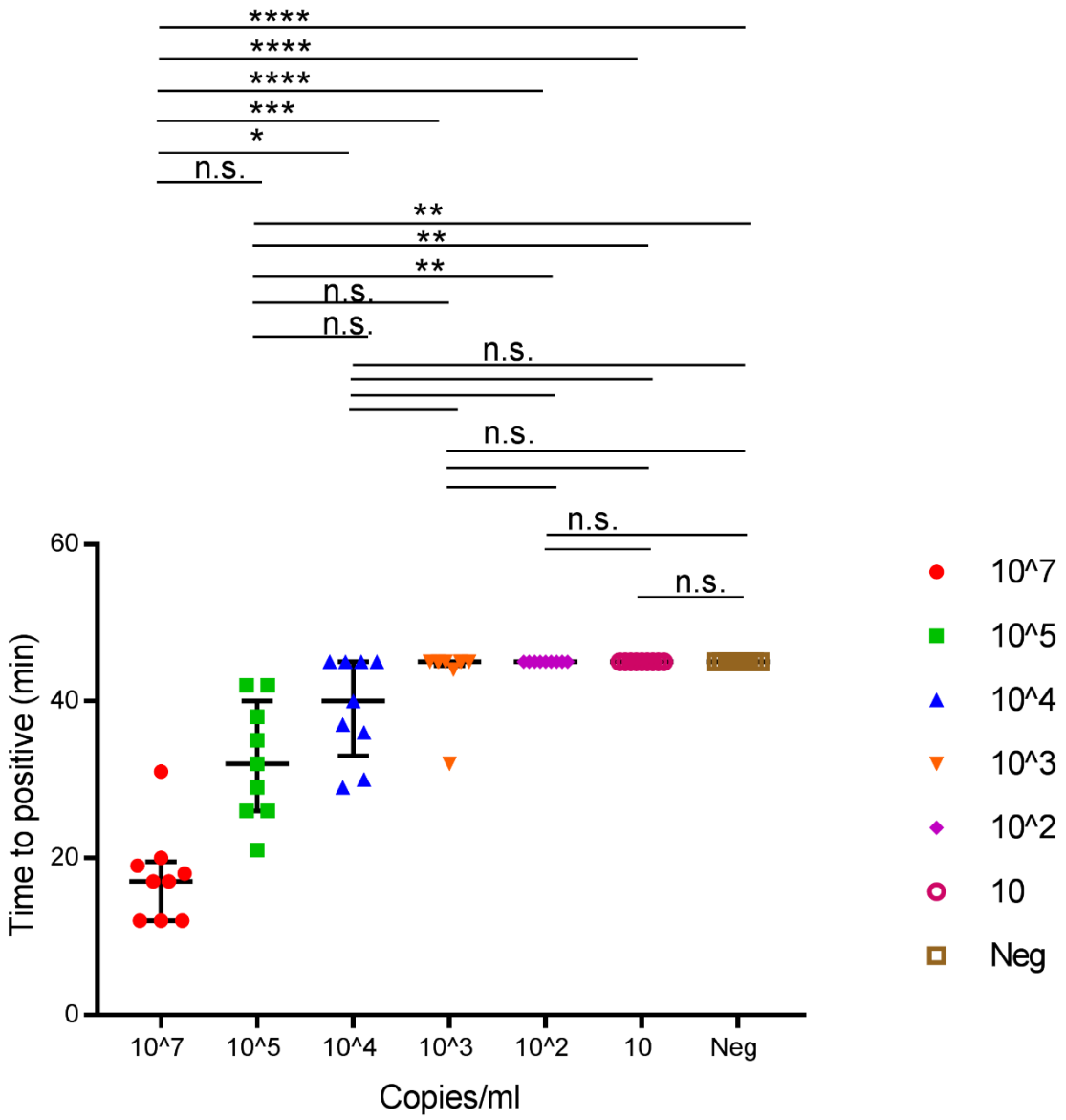

Figure 3.6 Analytical sensitivity of HCV LAMP with in-house primers
Serial dilutions of JFH1 plasmid (10^7-10^3 copies/ml) were used as standards with no template in duplicate as a negative control. In house primers were used at a concentration of 2 µM (FIP/BIP), 1 µM (LF/LB), 0.2 µM (F3/B3) and 0.8 µM (AP). The LAMP assay was incubated at 65°C for 45 minutes. The values represent the median and the error bars represent interquartile range. No amplification was defined as time to positive of 45 minutes. Graph represents four independent experiments in duplicate. Kruskal-Wallis test with Dunn's multiple comparisons test was used for statistical analysis with significant differences indicated as follows: **** - p≤0.0001, *** - p≤0.001, ** - p≤0.01, * -p≤0.05, n.s. – not significant.

Next, clinical sensitivity was assessed using both primer sets by testing eight samples from chronically infected patients from the HCV Early Access Program (EAP).Figure 3.7 shows the results of two independent experiments (A and B) of the HCV LAMP assay with the published primer sets. In the first experiment (A) six out of eight samples were detected within the 60 minutes, including, AA09, AA12, AA13, AA14 and AA15. In the second experiment, only samples AA12, AA14 and AA15 remained positive. Samples were described as positive if an exponential increase of fluorescence occurred, indicating DNA amplification.

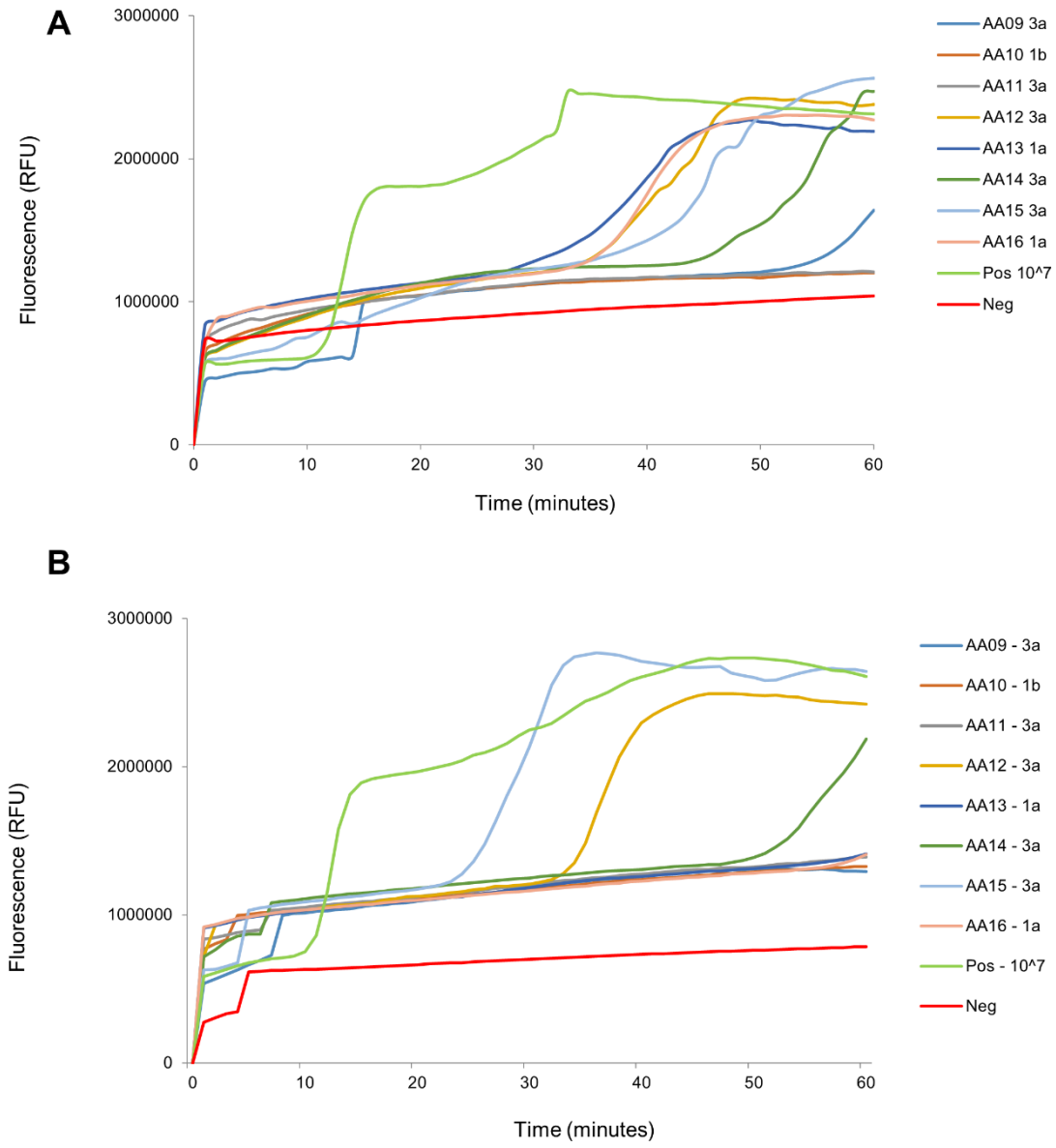

Figure 3.7 Clinical sensitivity of HCV LAMP with published primers and EAP samples
Eight chronically infected HCV patients, AA09-AA16, from the EAP were used for the evaluation of clinical sensitivity with the published primer set. Each sample is colour-coded as shown in the legend on the right along with the genotype. Pos – positive control JFH1 plasmid template at 10^7 copies/ml, Neg – negative, no template control. LAMP reactions were run using the IS0-001 Master mix with the graph representing fluorescence over time. A and B represent two separate experiments.

When the same clinical samples were tested with the in-house primer set, only two samples were detected in the first experiment, namely AA10 and AA13, although samples AA12 and AA14 started to amplify at the end of the 60 minute incubation (Figure 3.8a). These samples were genotypes 1b and 1a, respectively. In the second experiment, none of the samples were detected as positive (Figure 3.8).

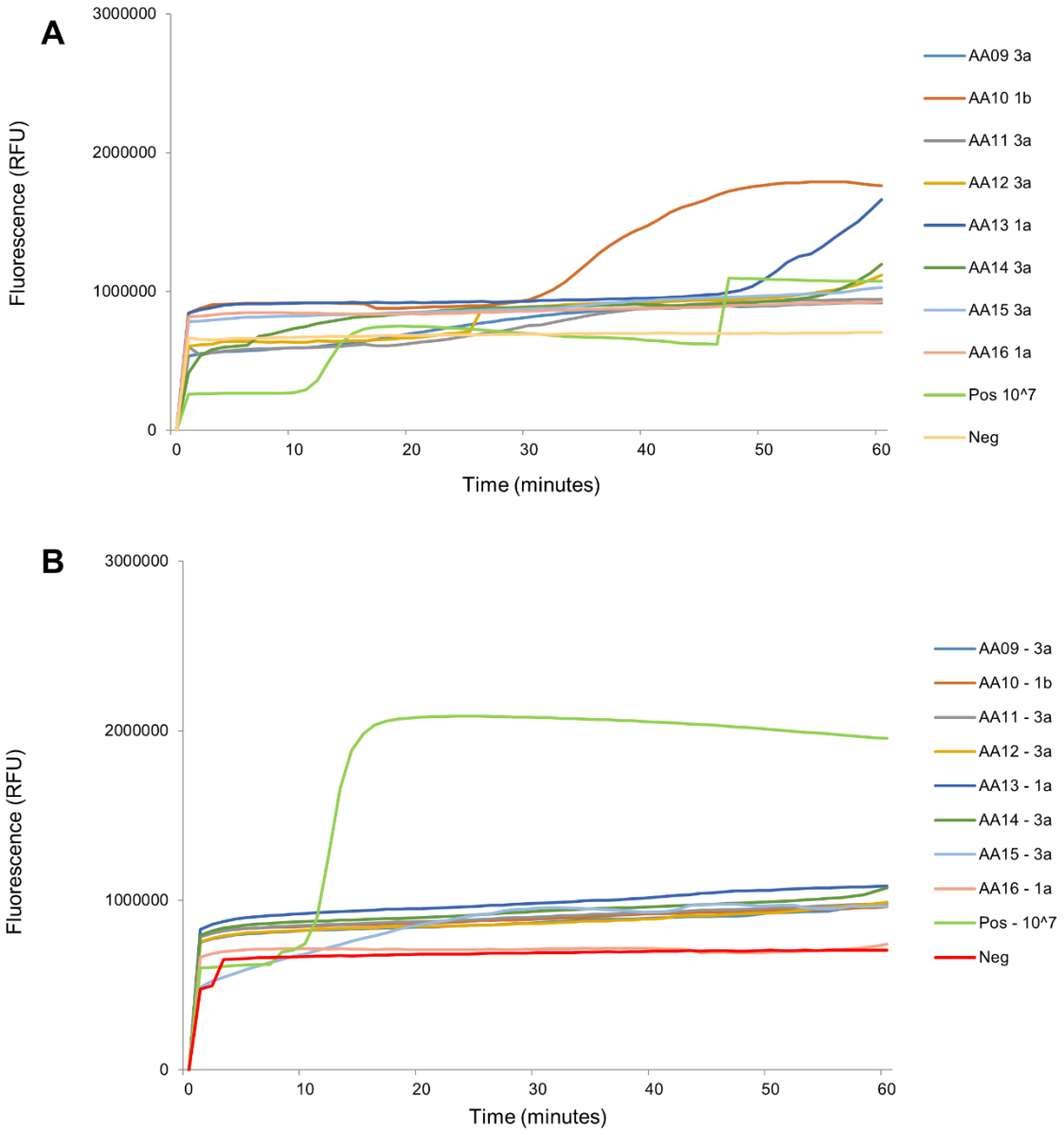

Figure 3.8 Clinical sensitivity of HCV LAMP assay with in-house primers and EAP samples
Eight chronically-infected HCV patients, AA09-AA16, from the EAP were used for the evaluation of clinical sensitivity with the published primer set. Each sample is coloured coded as shown in the legend on the right along with the genotype. Pos – positive control JFH1 plasmid template at 10^7 copies/ml, Neg – negative, no template control. LAMP reactions were run using the IS0-001 Master mix with the graph representing fluorescence over time. A and B represent two separate experiments.

In order to assess whether mismatches to primers played a part in the false negatives in clinical samples, both LAMP primer sets were aligned with the NGS consensus sequence of the clinical samples tested. The alignment of in-house primers to the clinical samples revealed that no mismatches were present. However, the alignment of published primers revealed mismatches in eight sites located in F3 (two sites), F2 (one site), FLP (one site), F1 (one site), B1 (two sites) and BLP (one site) binding regions (Figure 3.9). No mismatches were observed in the binding sites of B2, B3 and AP primers. Most mismatches occurred in the middle or at the 5'end of the primer, apart from the last nucleotide mismatch in BLP primer (change of C to T) in samples AA09, AA11, AA12, AA14, AA15 as well as the third last nucleotide (change of G to A) in B1 primer in samples AA09, AA11, AA12, AA14 and AA15. Samples AA09, AA11, AA12 AA14 and AA15 had the same number of mismatches in the same regions of different primers. Only samples AA12, AA14 and AA15 were positively identified with HCV on both LAMP experiments. Sample AA09 was detected once out of two occasions and sample AA11 was not detected as positive in both experiments. Samples AA16, AA13 and AA10 had no mismatches but were only detected once (AA13/16) or not at all (AA10) in the LAMP experiments.

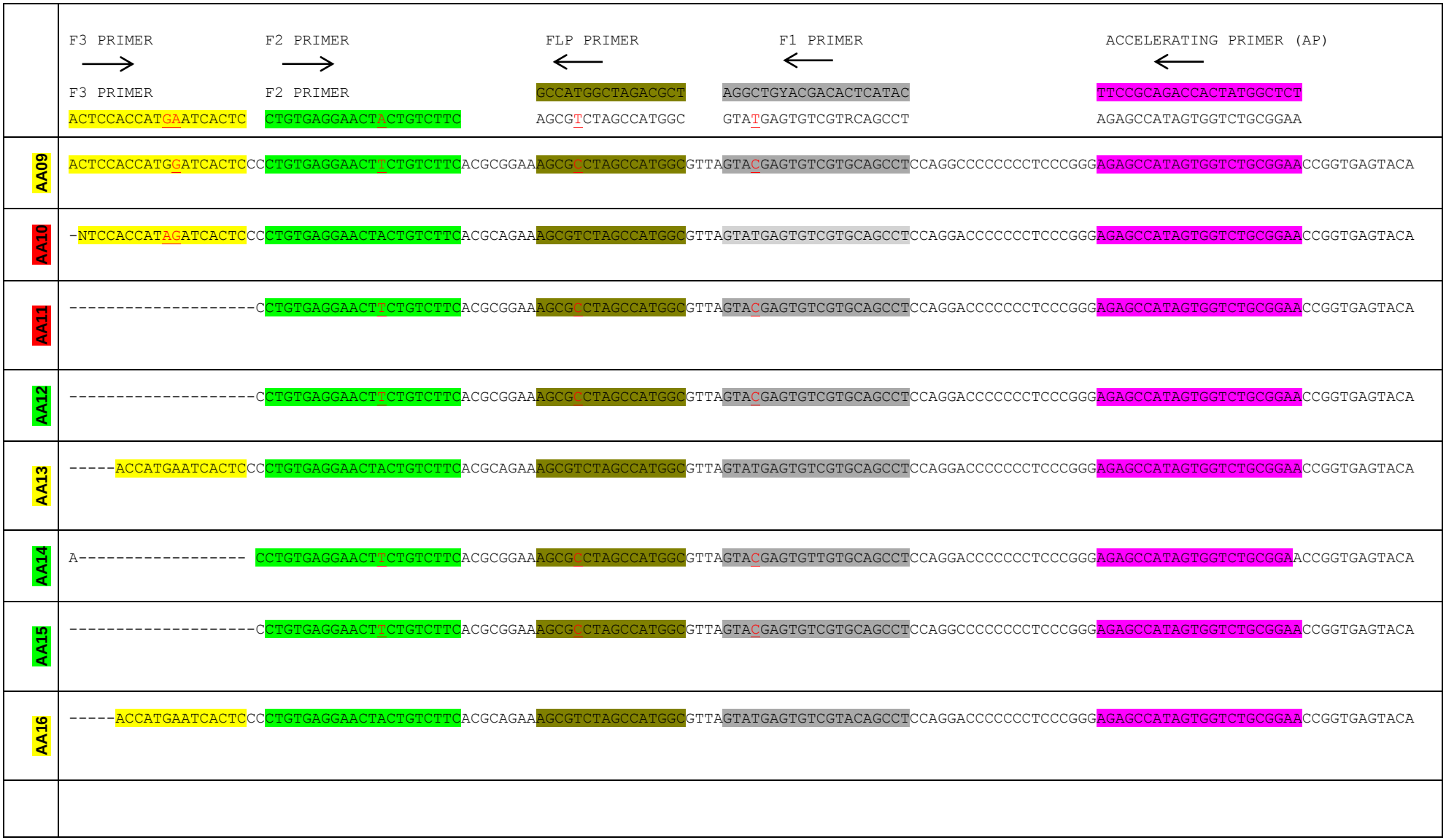
F3 PRIMER
F2 PRIMER
FLP PRIMER
F1 PRIMER
ACCELERATING PRIMER (AP)
F3 PRIMER
F2 PRIMER
GCCATGGCTAGACGCT
AGGCTGYACGACACTCATAC
TTCCGCAGACCACTATGGCTCT
ACTCCACCATGAATCACTC
CTGTGAGGAACTACTGTCTTC
AGCGTCTAGCCATGGC
GTATGAGTGTCGTRCAGCCT
AGAGCCATAGTGGTCTGCGGAA
AA09
ACTCCACCATGGATCACTCCCCTGTGAGGAACTTCTGTCTTCACGCGGAAAGCGCCTAGCCATGGCGTTAGTACGAGTGTCGTGCAGCCTCCAGGCCCCCCCCTCCCGGGAGAGCCATAGTGGTCTGCGGAACCGGTGAGTACA
AA10
-NTCCACCATAGATCACTCCCCTGTGAGGAACTACTGTCTTCACGCAGAAAGCGTCTAGCCATGGCGTTAGTATGAGTGTCGTGCAGCCTCCAGGACCCCCCCTCCCGGGAGAGCCATAGTGGTCTGCGGAACCGGTGAGTACA
AA11
----------CCTGTGAGGAACTTCTGTCTTCACGCGGAAAGCGCCTAGCCATGGCGTTAGTACGAGTGTCGTGCAGCCTCCAGGACCCCCCCTCCCGGGAGAGCCATAGTGGTCTGCGGAACCGGTGAGTACA
AA12
----------CCTGTGAGGAACTTCTGTCTTCACGCGGAAAGCGCCTAGCCATGGCGTTAGTACGAGTGTCGTGCAGCCTCCAGGACCCCCCCTCCCGGGAGAGCCATAGTGGTCTGCGGAACCGGTGAGTACA
AA13
-----ACCATGAATCACTCCCCTGTGAGGAACTACTGTCTTCACGCAGAAAGCGTCTAGCCATGGCGTTAGTATGAGTGTCGTGCAGCCTCCAGGACCCCCCCTCCCGGGAGAGCCATAGTGGTCTGCGGAACCGGTGAGTACA
AA14
A---------- CCTGTGAGGAACTTCTGTCTTCACGCGGAAAGCGCCTAGCCATGGCGTTAGTACGAGTGTTGTGCAGCCTCCAGGACCCCCCCTCCCGGGAGAGCCATAGTGGTCTGCGGAACCGGTGAGTACA
AA15
----------CCTGTGAGGAACTTCTGTCTTCACGCGGAAAGCGCCTAGCCATGGCGTTAGTACGAGTGTCGTGCAGCCTCCAGGCCCCCCCCTCCCGGGAGAGCCATAGTGGTCTGCGGAACCGGTGAGTACA
AA16
-----ACCATGAATCACTCCCCTGTGAGGAACTACTGTCTTCACGCAGAAAGCGTCTAGCCATGGCGTTAGTATGAGTGTCGTACAGCCTCCAGGACCCCCCCTCCCGGGAGAGCCATAGTGGTCTGCGGAACCGGTGAGTACA

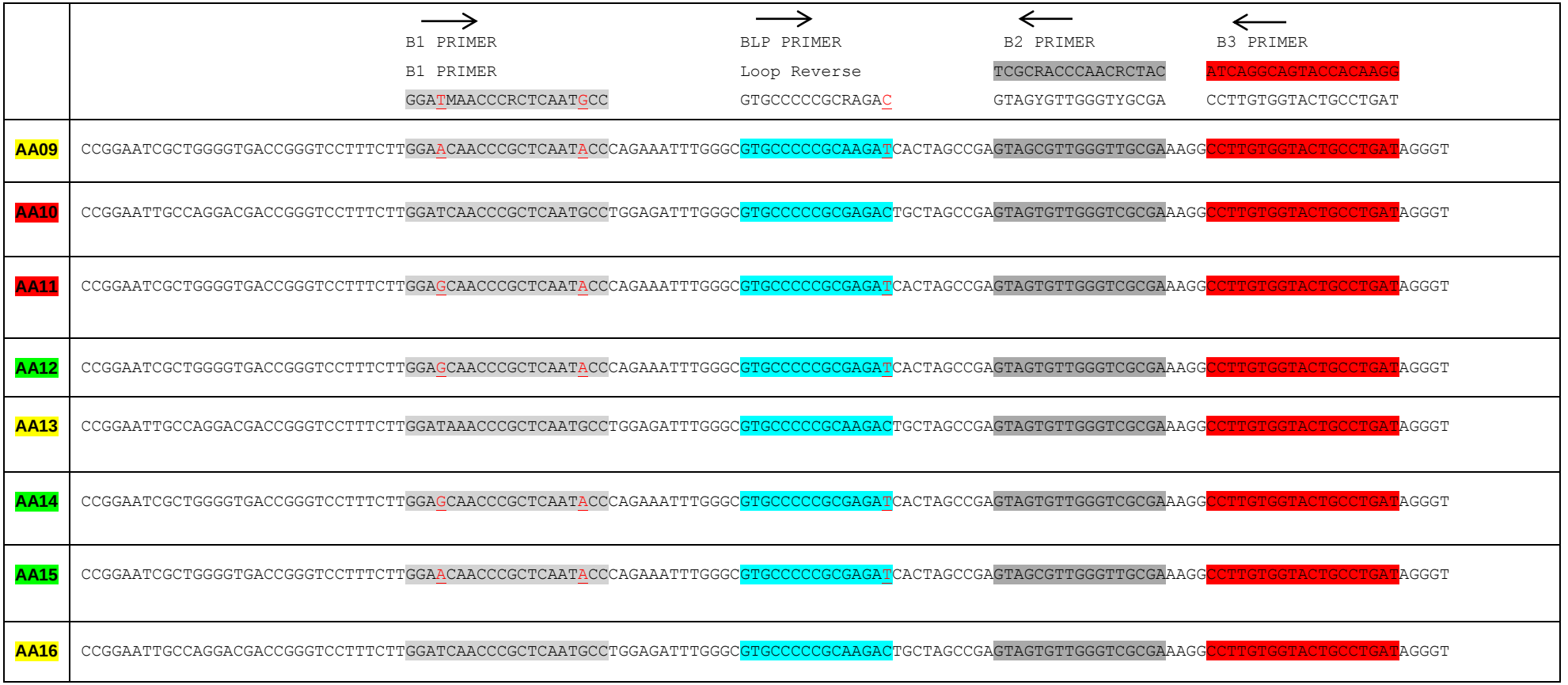

Figure 3.9 Alignment of NGS consensus sequence of clinical samples with the published LAMP primer set

Diagram represents eight chronically infected HCV patients, AA09-AA16, from the EAP aligned with the published primers. The nucleotide sequence starts at position 28 and finishes at position 309 based on sequence with Genbank accession number: AF009606. Black arrows pointing right indicate forward primers and those pointing left indicate reverse primers. Mismatches are indicated by underscored red letters. Primers FIP and BIP consists of primers F1 or B1 and F2 or B2, respectively. BLP – Backward loop primer, FLP – Forward loop primer. Samples highlighted in green were detected in two experiments out of two, in yellow in one experiment out of two and those highlighted in red missed detection in both experiments.

Overall, although both the in-house primers and the published primers had a similar TP, the latter set was able to detect more clinical samples (despite mismatches) and had higher analytical sensitivity than the former set. Therefore, future LAMP experiments focused on the published primer set.

Since mismatches in primer binding sites did not correlate with detection in the LAMP assay, other characteristics of the clinical samples were investigated. Table 3.1 lists the genotype, viral load (IU/ml) and Ct value. Samples were either gt 3 (n=5, AA09, AA11, AA12, AA14 and AA15), gt 1a (n=2, AA13, AA16) or gt 1b (n=1, AA10). The viral load ranged between 930000 and 1900000 with the lowest viral load in AA16 and the highest in AA09. This did not correlate with the viral load as the highest viral load sample, AA09, had a Ct of 37 while the lowest viral load sample, AA16, had a Ct value of 38.2. The lowest Ct value was found in sample AA10, Ct 31.0, with a viral load of 1735801, although, it was not detected by either of the two LAMP experiments. AA10 was also the only gt 1b infected sample. AA11 was a gt 3a sample also missed by both LAMP experiments with a Ct value of 33.0 and a viral load of 1735801. LAMP detected all other samples at least in one of the two experiments with Ct values ranging between 34 and 38.2.

Table 3.1 Characteristics of samples from the Early Access Program

Sample	Genotype	Viral Load (IU/ml)	Ct value
AA09	3a	1900000	37.0
AA10	1b	1735801	31.0
AA11	3a	1413795	33.0
AA12	3a	1393286	34.0
AA13	1a	1148682	34.6
AA14	3a	1028606	35.8
AA15	3a	1000000	35.1
AA16	1a	930000	38.2

In order to improve clinical sensitivity, the published primers were modified according to mismatches found earlier on in the analysis. Figure 3.2 shows all the modifications made in the primers, ensuring as many sequences in the 204 HCV sequence alignment were covered by replacing with degenerate nucleotides. Mismatches found in <10 sequences were not replaced in the primer set. The final modifications were made in F3 primer at position 35 (from A to R), FIP including two in F1 primer at position 103 and 110 (G to R and A to R, respectively) and one in F2 at position 57 (from A to W). Other changes in primers included one in B1 part of BIP at position 217 (from G to R), one in FLP at position 85 (from A to R) and one in AP at position 144 (from C to Y). The only modification in the last nucleotide was made in BLP, where the last C was removed and replaced at the front of the primer (removed from position 246, added to position 232).

Table 3.2 Original LAMP primer set and improved proposed LAMP primer set used in this study

	Published primers		Proposed 'Lit Deg' primer sequences	
Primer Name	Sequence (5' to 3')	Genome position*	Sequence (5' to 3')	Genome position
F3	ACTCCACCATGAATCACTC	24-42	ACTCCGCCATGRATCACTC	24-42
B3	ATCAGGCAGTACCACAAGG	279-297	ATCAGGCAGTACCACAAGG	279-297
FIP	AGGCTGYACGACACTCATAC-CTGTGAGGAACTACTGTCTTC	94-113/45-65	AGGCTGYACRACACTCRTAC-CTGTGAGGAACTWCTGTCTTC	94-113/45-65
BIP	GGATMAACCCRCTCAATGCC-TCGCRACCCAACRCTAC	200-219/258-274	GGATMAACCCRCTCAATRCC-TCGCRACCCAACRCTAC	200-219/258-274
FLP	GCCATGGCTAGACGCT	74-89	GCCATGGCTAGRCGCT	74-89
BLP	GTGCCCCCGCRAGAC	233-247	CGTGCCCCCGCRAGA	232-246
AP	TTCCGCAGACCACTATGGCTCT	134-155	TTCCGCAGACYACTATGGCTCT	134-155

*Genome position based on Genbank Accession No. AY460204. Nucleotide modifications are highlighted in blue.

The next experiment aimed to compare the TP values and analytical sensitivity of the original published primer set with the modified degenerate primer set. Serial 10-fold dilutions of the JFH1 plasmid were made from 10^6 copies/ml to 10^2 copies/ml and the TP measured with both primer sets. Figure 3.10 shows the results of the experiment, with an almost inverse relationship between TP and increasing concentration of JFH1 plasmid – as the copy number/ml increased the TP decreased with both primer sets. Overall the median TP at all concentrations were similar between the two primer sets with error bars overlapping and no significant differences were observed.

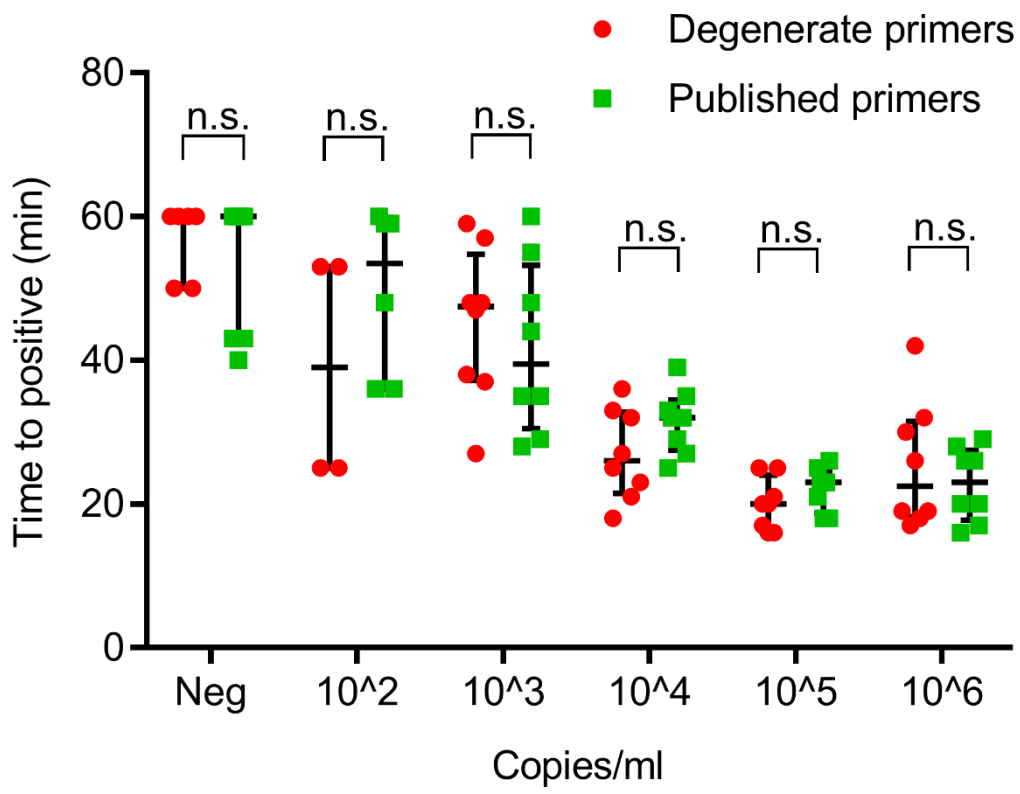

Figure 3.10 Differences in time to positive between published and degenerate primer sets
Serial dilutions of JFH1 plasmid (10^6-10^2 copies/ml) were used as standards with no template as a negative control. Primers were used at a concentration of 2 µM (FIP/BIP), 1 µM (FLP/BLP), 0.2 µM (F3/B3) and 1 µM (AP). The LAMP assay was incubated at 65°C for 60 minutes. The values represent the median and the error bars represent interquartile range. No amplification was defined as time to positive of 60 minutes. Graph represents data from four independent experiments in duplicate. A non-parametric paired Wilcoxon signed test was used for statistical analysis to compare the time to positive (TP) between the degenerate and published primer sets at each paired concentration of the JFH1 plasmid. No significant results were observed between the groups (n.s. – not significant).

In order to evaluate clinical sensitivity, the same eight samples from the EAP were retested with the adapted primer set (AA09-AA16). Figure 3.11 shows that all sample amplification in both primer sets occurred after 45 minutes. The only samples detected by published primers were, AA09 (two out of two replicates), AA11 (one out of two replicates) and AA16 (two out of two replicates). Detection with the degenerate primers was similar, although the AA11 sample was not detected and sample AA10 was only detected in one of the two replicates tested. In addition, the TP with degenerate primers was longer with all sample detections occurring only after 49 minutes of incubation. In the experiment with the published primer set, one of the negative controls also amplified after 29 minutes of incubation. Unfortunately, because of lack of samples, this experiment could not be repeated.

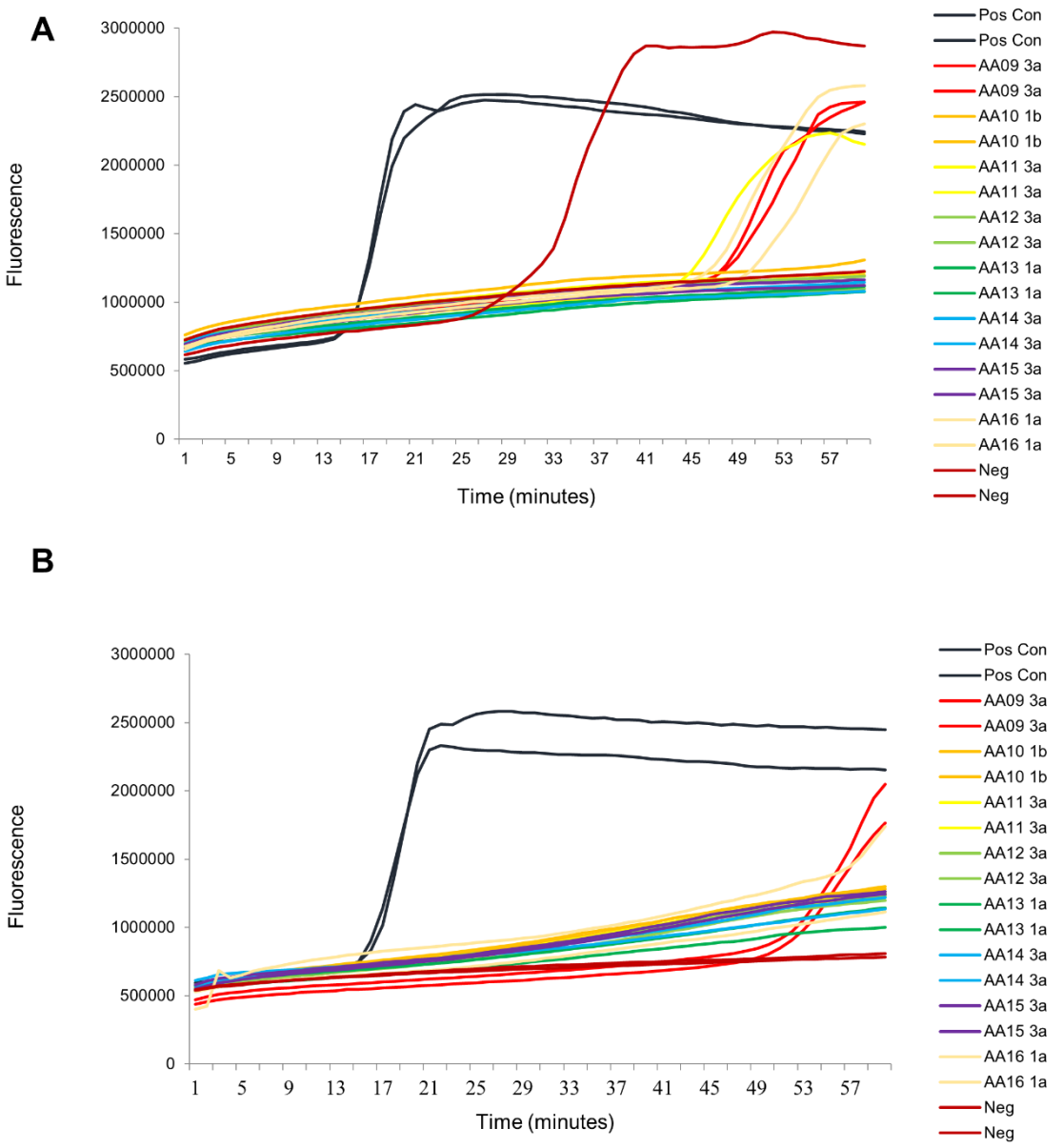

Figure 3.11 Clinical sensitivity of degenerate primers vs published primers in eight EAP samples
Diagram represents eight chronically-infected HCV patients, AA09-AA16, from the EAP. Primers were used at a concentration of 2 µM (FIP/BIP), 1 µM (FLP/BLP), 0.2 µM (F3/B3) and 1 µM (AP). The LAMP assay was incubated at 65ºC for 60 minutes with either the original published primer set (A) or the modified degenerate primer set (B). The diagrams represent fluorescence in relative fluorescence units (RFU) from one experiment with duplicate samples. Samples are colour coded as indicated on the figure legend (right side of the graphs). Pos is positive control, JFH1 plasmid at 10^6 copies/ml, Neg is no template, negative control.

Since no improvement was made in either TP of LAMP reactions or clinical sensitivity with the degenerate primer set, potential primer mismatches were reassessed for mismatches by alignment with 204 reference sequences of different HCV genotypes (Table 3.3). Prior to the modification of primers, most mismatches were found in gt 3 sequences, most commonly in F3 which matches with only 23 sequences in the previously published primer and 31 in the modified primer with mismatches in gt 1b, 2, 3, 4, 5 and 6. Primers B3 and B2 matched most sequences (201 and 196) and gt and did not require further modifications. In addition, modifications in primers B1, FLP and AP resulted in a very small improvement in the number of matching sequences namely, 1, 11 and 6 more matching sequences, respectively. Although the BLP primer matched most sequences, gt 3 sequences did not match and the modification resolved that issue. Finally primers F1 and F2 matched 124 and 133 sequences in the published primer set with mismatches in gt 3, 4, 5 and gt 3 and 6, respectively. Following modification primer F1 matched most sequences while primer F2 matched an additional 35 sequences. However, following the modification process, the entire FIP primer contained four degenerate nucleotides with three degenerate nucleotides in the F1 primer alone.

Table 3.3 Analysis of genotype mismatches in the published and degenerate HCV LAMP primer set.

Primer Name	Sequence of published primer	No of sequence matches in the alignment (/204)	Genotype mismatches	Sequence of degenerate primer	No of sequence matches in the alignment (/204)	Genotype mismatches
F3	ACTCCACCATG**A**ATCACTC	23	Gt 1b, 2, 3, 4, 5, 6	ACTCCACCATG**R**ATCACTC	31	Gt 1b, 2, 3, 4, 5, 6
B3	ATCAGGCAGTACCACAAGG	201	Matches most gt	ATCAGGCAGTACCACAAGG	201	Matches most gt
FIP	AGGCTGYAC**G**ACACTC**A**TAC-CTGTGAGGAACT**A**CTGTCTTC	F1 - 124 F2 - 133	F1 - gt 3, 4, 5 F2 - gt 3, 6	AGGCTGYAC**R**ACACTC**R**TAC-CTGTGAGGAACT**W**CTGTCTTC	F1 – matches most F2 - 168	Gt 3
BIP	GGATMAACCCRCTCAAT**G**CC-TCGCRACCCAACRCTAC	B1 - 54 B2 - 196	B1 – gt 2, 3, 6, 7 B2 – matches most gt	GGATMAACCCRCTCAAT**R**CC-TCGCRACCCAACRCTAC	B1 – 55 B2 -196	B1 – gt 2, 3, 6, 7 B2 – matches most gt
FLP	GCCATGGCTAG**A**CGCT	155	Gt 2, 3, 4, 7	GCCATGGCTAG**R**CGCT	166	Matches most gt
BLP	GTGCCCCCGCRAGA**C**	181	Gt 3	**C**GTGCCCCCGCRAGA	197	Matches most gt
AP	TTCCGCAGAC**C**ACTATGGCTCT	184	Gt 6	TTCCGCAGAC**Y**ACTATGGCTCT	190	Matches most gt

Following a reassessment of mismatches in the alignment with published and modified primer sets, only some modifications appeared to improve the number of matching sequences at a large scale. Therefore an alternative approach for the primers sequences was assessed, which is summarised in Table 3.4. For the FIP primer an alternative gt 3 and 6 primer was created, which matched a total of 27 sequences. Instead of replacing nucleotides with degenerate nucleotides in the BIP primers, two separate primers were created which were assessed in future experiments as a 50% mixture. A reverse complement of the AP primer was used to compensate for the large number of mismatches in the F3 primer. This is based on the observation noted by the authors of the published primer set which states that the AP primer forms an alternative amplification pathway making the B3 primer expendable (Yang et al. 2011). Finally the BLP degenerate primer was used to match with all gt 3 sequences as well as other genotypes.

Table 3.4 Proposed primer sequences for HCV LAMP based on the published primer set

Proposed new primers	Proposed primer sequence(s)	Comments	No of sequences matches in the alignment (/204)
FIP - F1 gt 3 FIP -F2 gt 3/6	AGGCTGCACGACACTCGTAC-CTGTGAGGAACTTCTGTCTTC	Primer designed to match gt 3 and gt 6 only	27
BIP_1 BIP_2	GGATMAACCCRCTCAATGCC-TCGCGACCCAACACTAC GGATMAACCCRCTCAAT**G**CC-TCGC**A**ACCCAAC**G**CTAC	Mix BIP_1 and BIP_2 as a 50%/50% mixture	196
AP Rev	AGAGCCATAGTGGTCTGCGGAA	To compensate for mismatches in F3 primer	184
BLP Deg	CGTGCCCCCGCRAGA	To match gt 3 sequences	197

Figure 3.12 shows the results from experiments testing the TP in minutes of the new BLP compared to the original BLP as well as assay where no BLP was added. The TP was determined in both gt 1a and gt 3 subgenomic replicon. There were minimal differences in TP in gt 1a with TP with BLP new primer at 11.5 minutes compared to 12 minutes with the original BLP or 14 minutes without the primer added. Significant differences were found between BLP New and No BLP ($p=0.0076$) and between BLP Ori and No BLP ($p=0.0211$). In a gt 3 experiment, the TP was faster with the new BLP compared to the original primer or experiments with no BLP at all (TP at 17 minutes compared to 21.5 and 22 minutes, respectively). There were significant differences between BLP New and BLP Ori ($p=0.0003$) and between BLP New and No BLP ($p=0.002$). Therefore, the new BLP was used in future experiments.

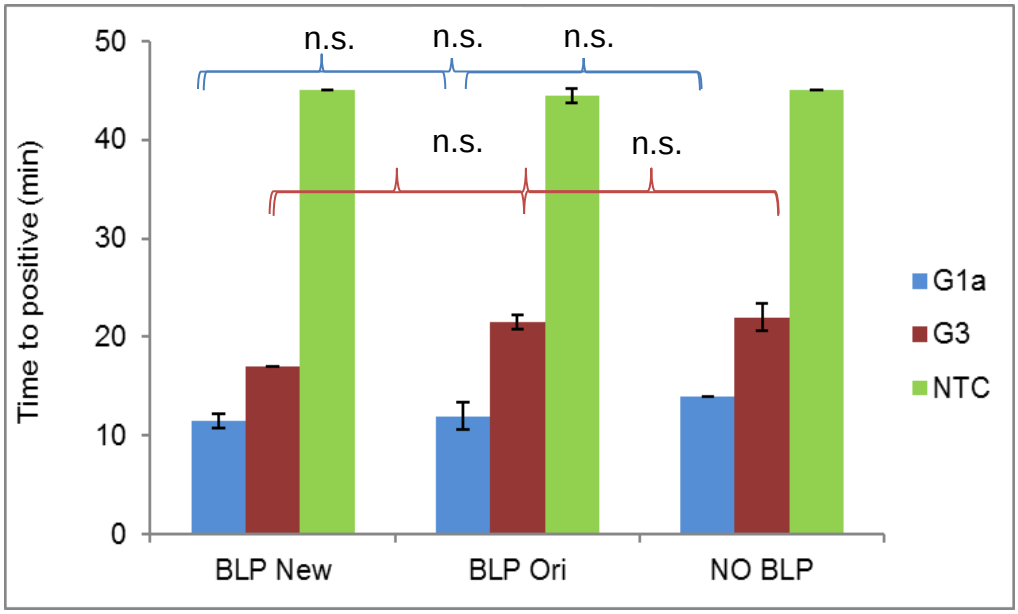

Figure 3.12 Evaluation of backward loop primer in genotype 1a and 3 replicons
Time to detection was based on genotype 1a and 3 replicon standards at 10^6 and 10^5 copies/ml, respectively. BLP New is the modified primer, BLP Ori is the original published primer and NO BLP represents assays with no LR added. All HCV-LAMP assays consisted of 0.8 µM FIP/BIP, 0.4 µM loop primers (or 0.4µM FLP only for NO BLP), 0.2 µM F3/B3 and 0.4 µM AP. Reactions were incubated for 45 minutes at 65°C. Graph represents data from two independent experiments in duplicate. Error bars represent ±SD. One-Way ANOVA with Tukey's multiple comparisons test was used for statistical analysis between the different groups in each genotype template. The p values were as follows: BLP New vs BLP Ori p=0.6324 (gt 1) and p=0.0003 (gt 3), BLP New vs no BLP p=0.0076 (gt 1) and p=0.0002 (gt 3), BLP Ori vs No BLP p=0.0211 (gt 1) and p=0.6324 (gt 3). Results were significant if p≤0.05. No amplification was given a TP of 45 minutes. NTC – No template control

Next, we assessed the TP in minutes with the AP reverse (AP Rev) vs the AP original (AP Ori) and no AP in the HCV LAMP reactions. Figure 3.13 shows the TP with gt 1 subgenomic replicon (A) and gt 3 subgenomic replicon (B) with the above mentioned LAMP reactions and primer sets. The TP of AP Rev had a median of 27.2 minutes with the gt 1 template, while the AP Ori containing reaction had a slightly slower median TP of 27.9 minutes. The fastest median TP was without any AP at 24.8 minutes. The fastest TP with the gt 3 template was the AP Rev containing reactions at 28.5 minutes followed closely by AP Ori at 30 minutes. The slowest TP occurred without AP at 30.5 minutes. Both gt 1 and gt 3 reactions had no significant differences observed between any of the primers used. Therefore, the original AP was retained in future experiments.

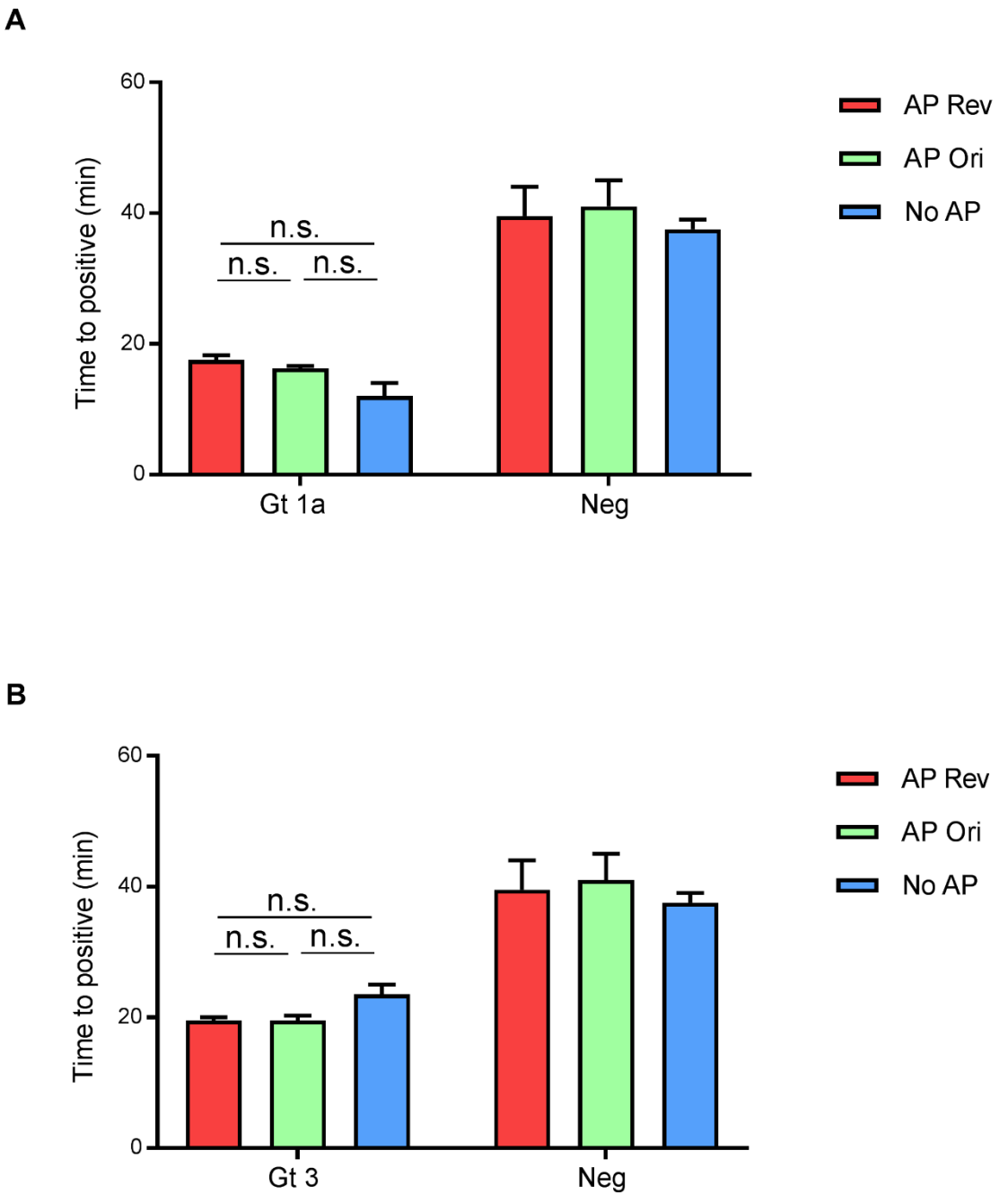

Figure 3.13 Evaluation of the new AP Reverse primer in gt 1a and gt 3 replicons
Time to detection was based on genotype 1a and 3 replicon standards at 10^6 and 10^5 copies/ml, respectively. All HCV-LAMP assays consisted of 0.8 µM FIP/BIP, 0.4 µM loop primers, 0.2 µM F3/B3 and 0.4 µM AP Ori/AP Rev (or no AP). Reactions were incubated for 45 minutes at 65°C. Values represent median with interquartile range. Graph represents data from two independent experiments in triplicate (replicon standard) or duplicate (No template control). Kruskal-Wallis test was used for statistical analysis between the AP Rev, AP Ori and No AP LAMP reactions with gt 1a and gt 3 templates with no significance detected (p=0.0594 and p=0.0635, respectively). A indicates results with gt 1a subgenomic replicon and B indicates results with genotype 3a subgenomic replicon. AP Rev – Accelerating Reverse primer, AP Ori – Accelerating Original primer, No AP – No Accelerating primer. No amplification was given a TP of 45 minutes. Neg is the no template control reaction.

In order to further validate the accelerating ability of the AP, additional experiments were run either with or without AP and standard LAMP primers with the gt 2, JFH1, subgenomic replicon template. Figure 3.14 indicates that the median time to positive was reduced from 28.5 minutes to 21 minutes with AP, which was a significant difference (p=0.0286). Therefore, the AP was included in future experiments.

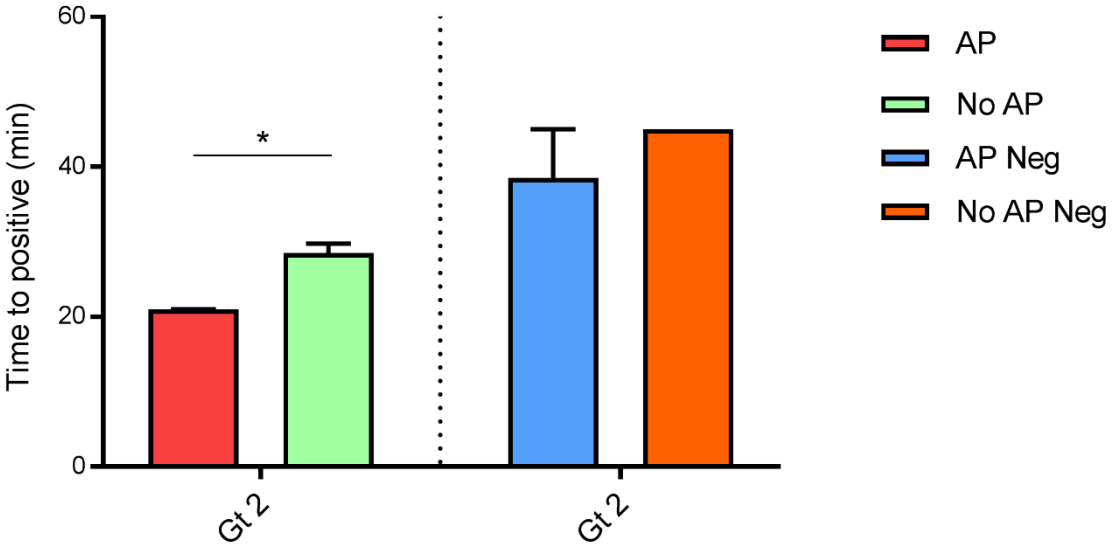

Figure 3.14 Effect of Accelerating Primer in published HCV LAMP in genotype 2
LAMP amplification products following amplification in real time incubated for 45 minutes at 65°C. Pos was JFH1 plasmid at 10^7 copies/ml and Neg was no template control. Published primers were used at concentration of 2 µM (FIP/BIP), 1 µM (FLP/BLP) and 0.2 µM (F3/B3). No AP Pos (blue) represents standard JFH1 with published HCV LAMP primers. AP Pos (green) represents standard JFH1 with published HCV LAMP primers with additional accelerating primer at 0.8 µM. The values represent the median. Graph represents data from two independent experiments in duplicate. Error bars represent interquartile range. Statistical analysis between the AP reactions and no AP reactions was performed using Mann Whitney test with significance detected (p=0.0286). Graph represents data from two independent experiments in duplicate.

In order to assess whether the F3 primer is needed for LAMP reactions, we repeated the LAMP assays with no F3 primer and compared it to reactions with the inclusion of F3 in gt 1a subgenomic replicon and gt 3 subgenomic replicon. Figure 3.15 shows the results of this experiment with the median TP of 15 minutes without F3 and only slightly slower median TP of 15.5 minutes with the original F3 primer in gt 1a. The results were similar for the gt 3 template with a TP of 20.5 minutes for no F3 reaction and 21.5 minutes for F3 containing reaction, respectively. The median TP of no template control without F3 was 45 minutes and 45 minutes with the F3 primer. Since the presence of F3 made no significant differences in the TP, the original F3 of the published primer set was kept in the future LAMP reactions without modifying the sequence to compensate for mismatches.

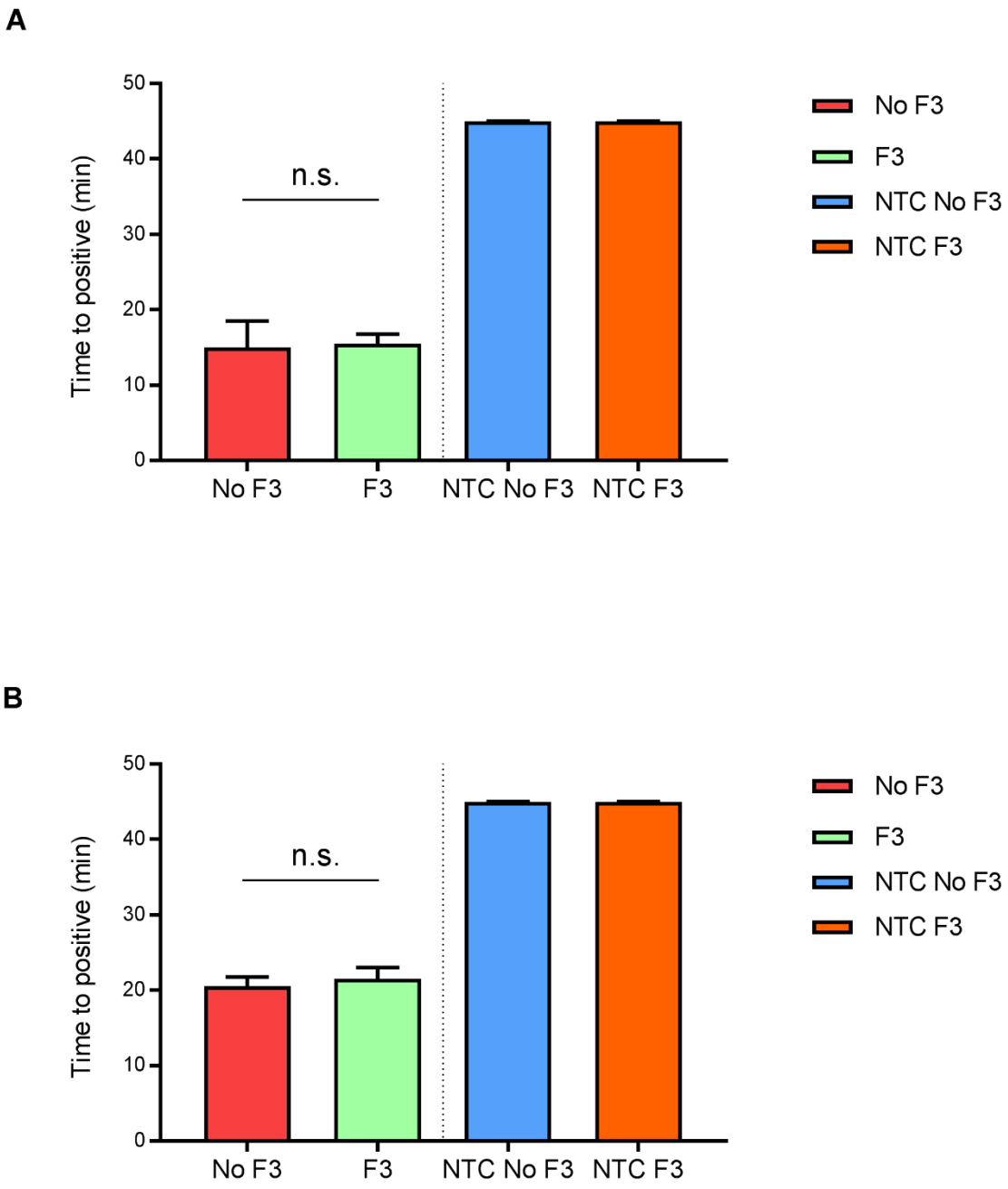

Figure 3.15 Evaluation of HCV LAMP reaction with and without F3 primer
Time to detection was based on genotype 1a (A) and 3 (B) replicon standards at 10^6 and 10^5 copies/ml, respectively. All HCV-LAMP assays consisted of 0.8 µM FIP/BIP, 0.4 µM loop primers, 0.2 µM F3/B3 (or 0.2 µM B3 only) and 0.4 µM AP/AP Rev (or no AP). Reactions were incubated for 45 minutes at 65°C. Values represent medians with interquartile range. Graph represents data from two independent experiments in duplicate. Mann Whitney test was used for statistical analysis between the different groups with no significance detected. F3 PAN represents the original pan genotypic F3 primer from the published primer set. NTC is the no template control. No amplification was given a TP of 45 minutes.

A new gt 3/6-specific FP primer was evaluated in a HCV LAMP assay by comparing the TP in minutes with LAMP assays containing the original FIP (FIP Ori) primer as well as a 50% mixture of the two (FIP 50/50). Figure 3.16 shows the mean TP of both FIP Ori and FIP G3/B were the same at 15.5 minutes while the FIP 50/50 mix LAMP reaction was slightly delayed – 18 minutes – for the gt 1a template although there were no significant differences between any of the primer groups. The mean TP for the gt 3 template for the LAMP reaction containing FIP G3/6 primer was 22.3 minutes while the FIP Ori reaction was slightly faster – 20.5 minutes. The 50/50 mixture LAMP reaction had a TP of 21.8 minutes although once again there was no significant differences between the primer groups. The mean TP of all no template controls were above 35 minutes although some error bar variability was large. Therefore, the FIP was kept in its original form for future reactions.

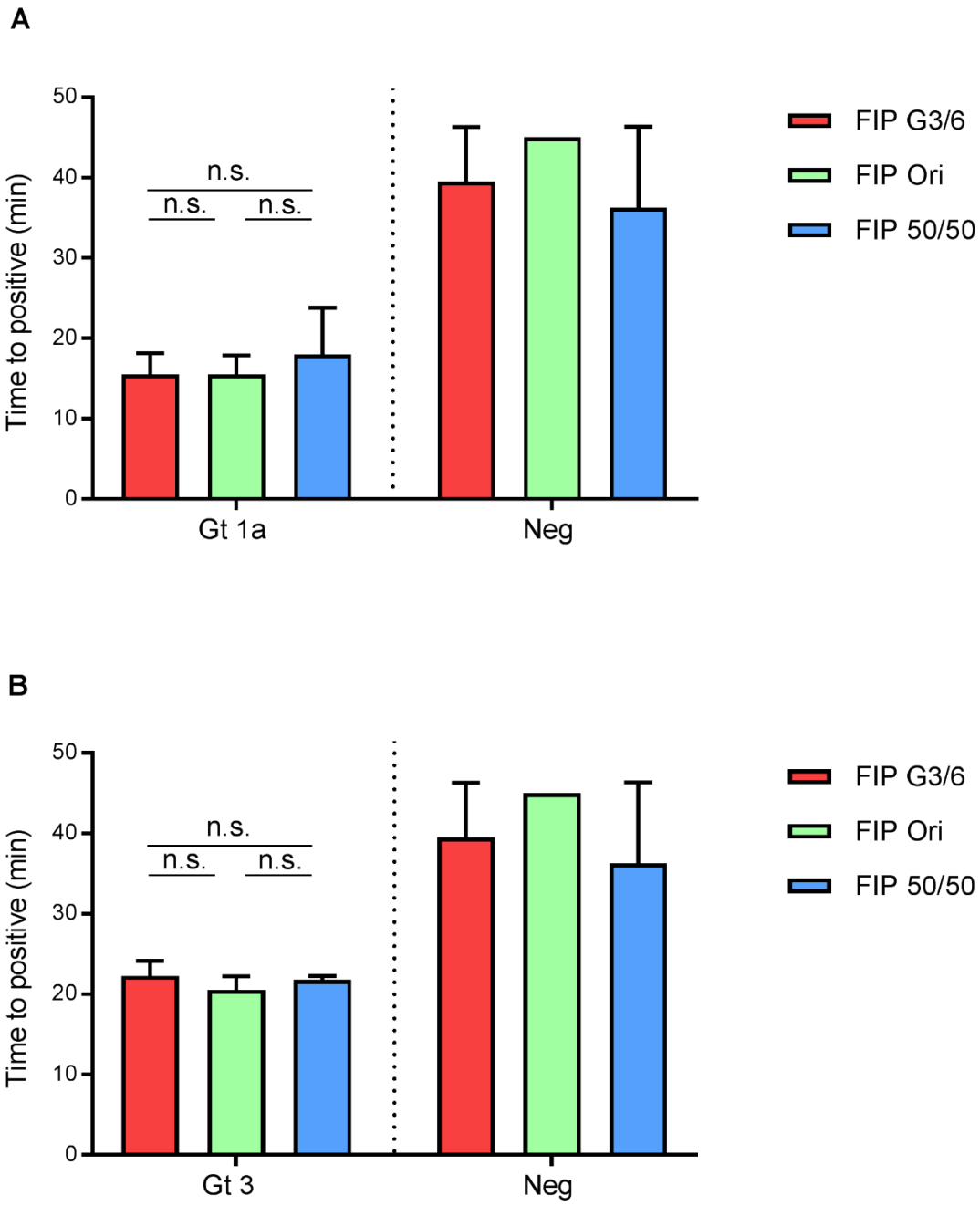

Figure 3.16 Evaluation of the HCV LAMP reaction with the new genotype-specific FIP
Time to positive was based on genotype 1a and 3 replicon standards at 10^6 and 10^5 copies/ml, respectively. All HCV-LAMP assays consisted of 0.8 µM FIP/BIP, 0.4 µM loop primers, 0.2 µM F3/B3 and 0.4 µM AP/AP Rev. FIP Ori is the original FIP from the published primer set and the FIP G3/6 is the new primer specifically designed to match gt 3 and 6. The FIP 50/50 reactions contained 0.4 µM of FIP Ori and 0.4 µM of FIP G3/6 Reactions were incubated for 45 minutes at 65°C. Graph represents data from two independent experiments in duplicate. Error bars represent ±SD. One-way ANOVA with Tukey's multiple comparisons test was used to test for significance between different primer groups with no significance detected (p=0.6028 for gt 1a and p=0.3101 for gt 3). Neg is the no template control. No amplification was given a TP of 45 minutes

The BIP primer was tested either as a 50% mix of two BIP primers or as the original BIP (BIP ori) with degenerate nucleotides in LAMP assays (Figure 3.17). The TP with gt 1a template was very similar for both of the reactions, 12.5 minutes and 13.5 minutes for BIP 50/50 and BIP Ori, respectively. The BIP 50/50 LAMP assay was slightly delayed with the gt 3 template with a mean TP of 23 minutes compared to a mean TP of 20.5 minutes with the LAMP assay containing the original BIP. The NTC had a mean TP of above 44 minutes with tight error bars. No statistical analysis was calculated as not enough replicates were performed. The BIP was, therefore kept in the original form for future reactions.

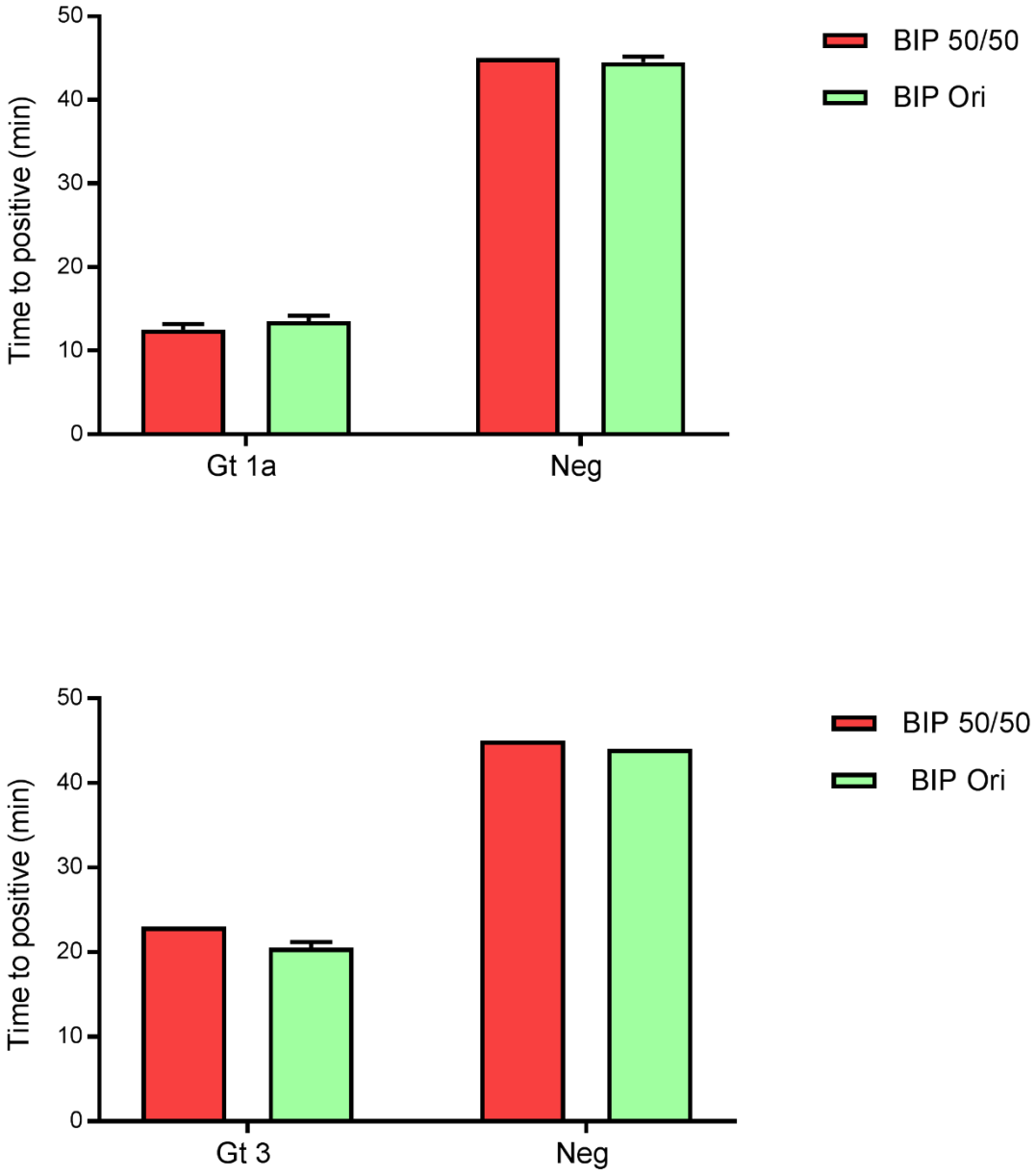

Figure 3.17 Evaluation of the HCV LAMP reaction with the new BIP mix
Time to positive was based on genotype 1a and 3 replicon standards at 10^6 and 10^5 copies/ml, respectively. All HCV-LAMP assays consisted of 0.8 µM FIP/BIP, 0.4 µM loop primers, 0.2 µM F3/B3 and 0.4 µM AP/AP Rev. BIP Ori is the original BIP from the published primer set. The BIP 50/50 reactions contained 0.4 µM of BIP Ori and 0.4 µM of new BIP. Reactions were incubated for 45 minutes at 65°C. Error bars represent ±SD. Neg is the no template control. No amplification was given a TP of 45 minutes. Graph represents data from a single experiment in duplicate.

3.1.1.3 Temperature selection

The optimal temperature for LAMP reactions was tested out with the ISO-001 master mix by running the reactions at 60°C and 65°C. Figure 3.18 shows that the 65°C had a shorter median TP of 27 minutes compared with 35.5 minutes at 60°C. Moreover, the difference in minutes between the two temperatures was significant (p=0.0286). Both NTC had a mean TP of 45 minutes. Therefore, future LAMP reactions were incubated at 65°C.

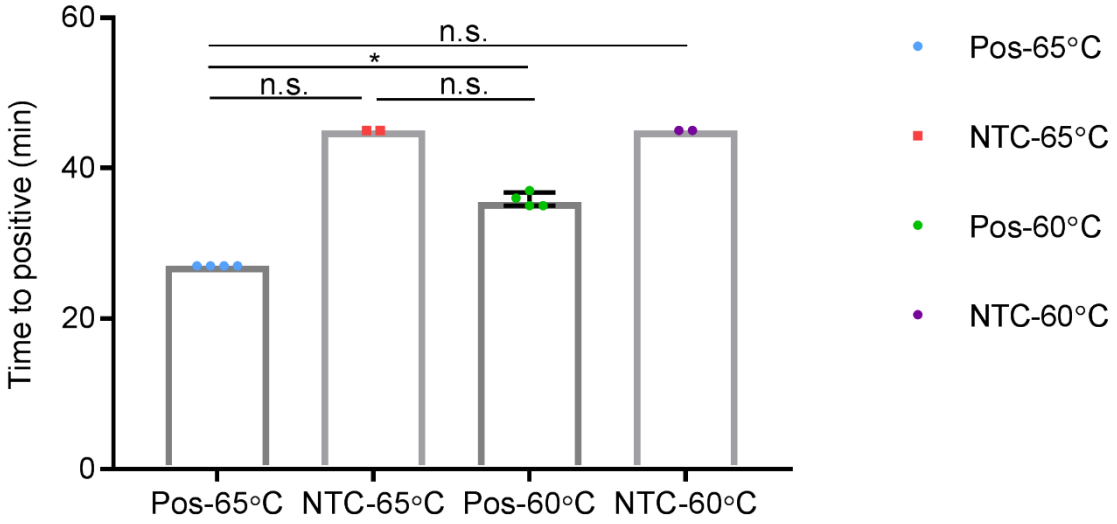

Figure 3.18 Optimisation of reaction temperature of LAMP assays based on real-time fluorescence over time
LAMP reactions were incubated at either 60°C or 65°C with 10^7 copies/ml of JFH1 subgenomic replicon or no template control (NTC) for 45 minutes. All reactions contained 8 units/µl of the GspSSD polymerase, 10x reaction buffer, 3.25 mM of $MgSO_4$, 1.1 mM of dNTPs, 1M of Betaine, 1x Evagreen dye and 6 µl of the template. LAMP primers were incubated at the following concentrations; 1.6 µM of FIP/BIP, 0.2 µM of F3/B3, 1 µM of FLP/BLP and 1 µM of AP. Nuclease free water was the NTC. Time to positive was determined based on relative fluorescence and no amplification was defined as 45 minutes. Values represent median with interquartile range. Statistical analysis was performed between the positive reactions at 60°C and 65°C using Mann Whitney test with significance detected (p=0.0286). The graph represents data from two independent experiments in duplicate.

The results of the temperature selection were later verified by running the products on gel electrophoresis. Figure 3.19 shows that both 60°C and 65°C LAMP incubations resulted in a characteristic smear with a banding patter appearing at the bottom in the positive controls. No smears or bands appeared in both of the LAMP reactions in the NTC. There were no differences in the banding pattern between the different temperatures other than the smear being more intense at 60°C than 65°C. Due to this the 65°C reactions appear to have four bands at different sizes compared to only three bands in the 60°C reactions. Thus, it was

not possible to tell what reaction temperature is better by looking at the end-point gel electrophoresis detection.

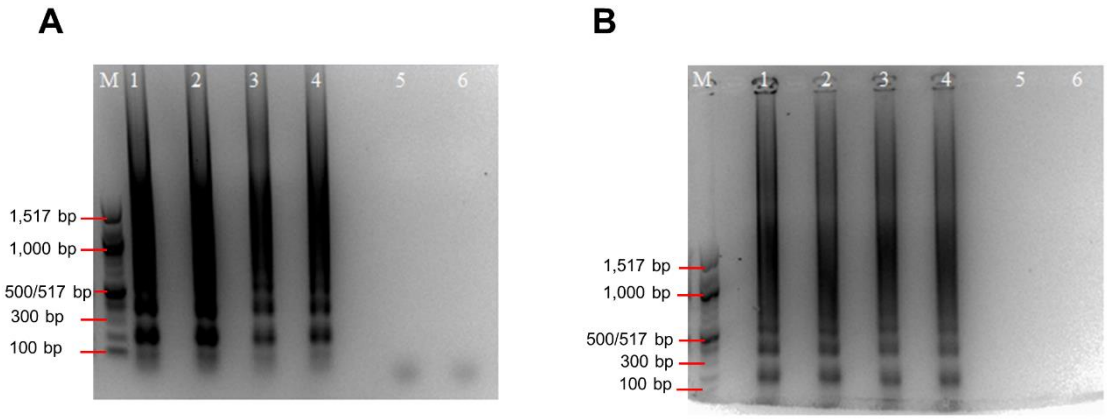

Figure 3.19 Optimisation of reaction temperature of LAMP assays based on gel electrophoresis
HCV LAMP amplification products are shown following incubation for 45 minutes at 60°C or 65°C and subsequent gel electrophoresis on 1% agarose gel stained with ethidium bromide. JFH1 plasmid in quadruplicate (n=4) at 10^7 copies/ml was used as the standard and nuclease-free water in duplicate (n=2) as a negative control. Published primers were used at a concentration of 1.6 µM (FIP/BIP), 1 µM (FLP/BLP) and 0.2 µM (F3/B3). A) Gel electrophoresis at 60°C (left) and B) at 65°C (right). *Lane M*; 100bp NEB ladder, *lane 1-4*; positive control, *lane 5-6*; negative control.

3.1.1.4 Concentration of dNTP and polymerase selection

As part of the optimisation of the HCV LAMP assay, different deoxynucleotide triphosphates (dNTPs) concentrations were tested in the reactions. In parallel, different polymerases were tested to find the optimal conditions for the HCV LAMP assay. Overall, three concentrations of dNTPs were tested; 0.4 mM, 0.9 mM and 1.4 mM, with three polymerases; two DNA polymerases from *Bacillus stearothermophilus, Bst* 2 (NEB) and *Bst* 3 (NEB) and *GspSSD* (Optigene). Figure 3.20 shows that the median TP for the Bst 2 with the positive control, JFH1, was 60, 60 and 58 minutes for 0.4 mM, 0.9 mM and 1.4 mM dNTP concentration respectively. The median TP for negative controls at all dNTP concentrations were the same, 60 minutes. Significant difference in the TP occurred between the positive control at 0.4 mM and the positive control at 1.4 mM of dNTP. The TP of *Bst* 3 polymerase was very similar for both negative and positive controls at the same concentrations. The fastest TP occurred at the highest dNTP concentration, 1.4 mM, at 26.5 minutes with the positive control compared with 32 minutes with the negative control. At 0.9 mM of dNTP, the median TP was 31 compared to 32 minutes with the negative control. At the lowest dNTP

concentration of 0.4 mM, the TP was 51.5 minutes while the TP of the negative control was slightly faster at 49.5 minutes. The only significant difference in TP occurred between the positive control at 0.4 mM and the positive control at 1.4 mM ($p=0.0050$). The quickest TP with the GspSSD enzyme occurred at 0.9 mM dNTP at 43 minutes followed by 51.65 minutes at 0.4 mM and 60 minutes at 1.4 mM. The GspSSD TP with the NTC was 60 minutes for all the concentrations tested. Significant differences were found between the positive control 0.9 mM dNTP and 1.4 mM dNTP ($p=0.0425$), the positive control at 0.9 mM and the NTC at 0.4 mM ($p=0.0208$), 0.9 mM ($p=0.0208$) and 1.4 mM ($p=0.0208$). Therefore, the GspSSD was the only polymerase which could detect the positive control with significant differences with the negative control TP. The best dNTP concentration was 0.9 mM. However, there were large variability in the TP in all three polymerases and dNTP concentrations tested with the positive control and further experiments were required.

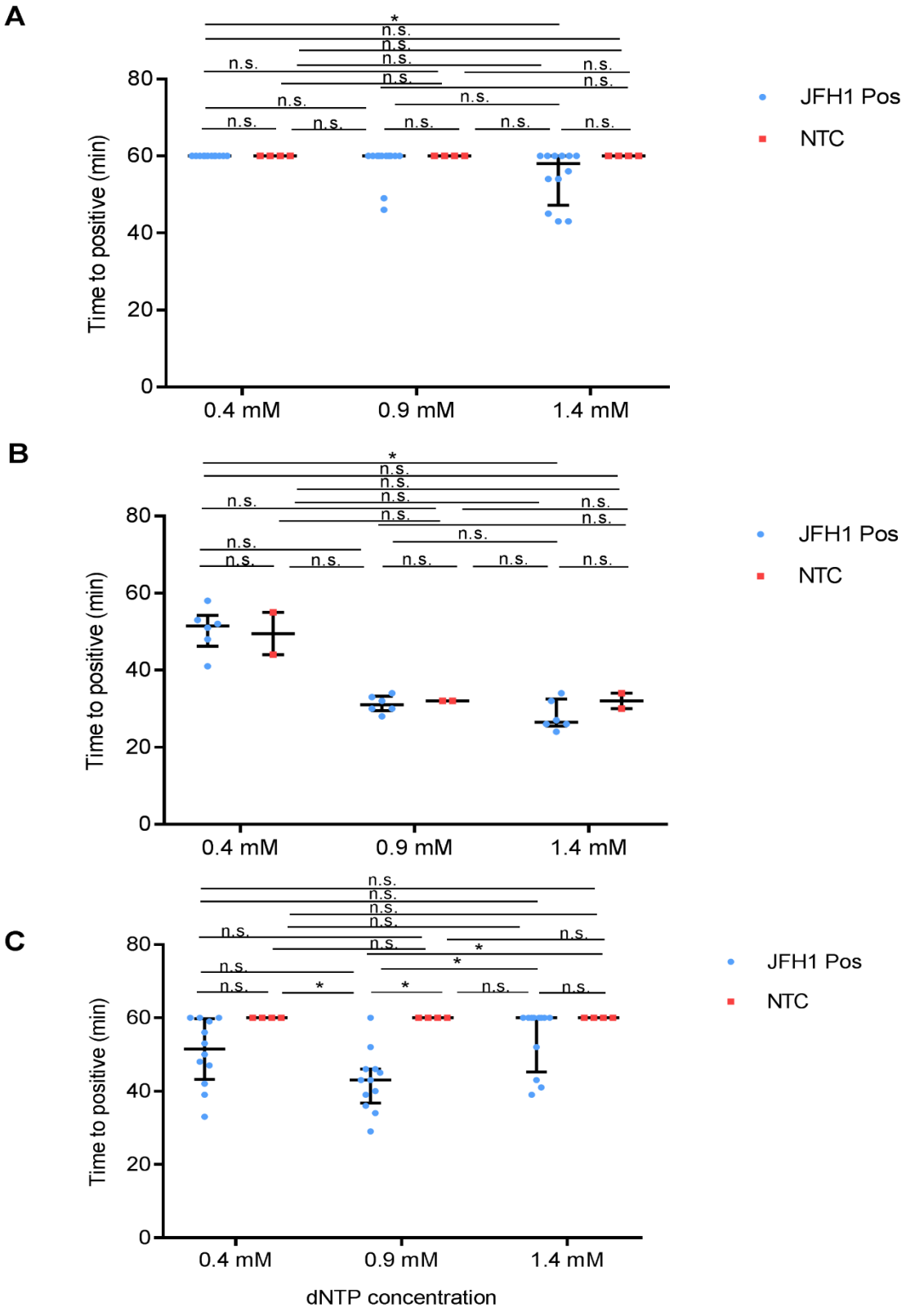

Figure 3.20 Evaluation of different polymerases and dNTP concentrations in the LAMP reaction
Three polymerases, *Bst* 2 (A), *Bst* 3 (B) and GspSSD (C) were tested for TP in LAMP reactions with three different dNTP concentrations, 0.4 mM, 0.9 mM and 1.4 mM. Time to positive in minutes was based on the gt 2 JFH1 subgenomic replicon template (JFH1) and the no template control (NTC) was the negative control. All LAMP assays consisted of 2 µM FIP/BIP, 1 µM loop primers, 0.2 µM F3/B3 and 1 µM AP The values represent the mean and the error bars represent ±SD. No amplification was defined as time to positive of 60 minutes. Kruskal-Wallis test with Dunn's multiple comparisons test was used for statistical analysis with significant differences indicated as follows: **** - p≤0.0001, *** - p≤0.001, ** - p≤0.01, * - p≤0.05, n.s. – not significant. Graphs represent four independent experiments in triplicate.

Next, serial dilutions of JFH1 template (10^6 copies/ml to 10^4 copies/ml) were tested in LAMP reactions using three polymerases, *Bst*, *Bst* 3 and GspSSD in order to select the most sensitive enzyme. Figure 3.21a shows that the median TP with *Bst* polymerase was 60 minutes for all dilutions as well as the negative control. Therefore, the *Bst* polymerase could not detect the JFH1 template. The *Bst* 3 polymerase had a median TP of 27 minutes, 29 minutes and 30 minutes for 10^6 copies/ml, 10^5 copies/ml and 10^4 copies/ml, respectively (Figure 3.21b). Therefore, the enzyme's TP did not differ significantly between template concentrations ($p>0.05$). The median TP of the negative control was 60 minutes, as it did not amplify. Unlike the *Bst* 3 polymerase, the GspSSD enzyme had an inverse relationship between the TP and the concentration of template – as the template concentration decreased the TP in minutes increased. The median TP for the 10^6 copies/ml was 32 minutes and 41 minutes for the 10^5 copies/ml. The median TP for the 10^4 copies/ml and the negative control was 60 minutes (Figure 3.21c). Significant differences in the TP were observed in the GspSSD polymerase between the 10^6 copies/ml and the 10^4 copies/ml ($p=0.0402$). There was also significant difference in the TP between the 10^6 copies/ml and negative control in the *Bst* 3 polymerase ($p=0.0228$). Therefore, the GspSSD polymerase was the only enzyme that showed decreasing TP in minutes with increasing template concentration. It was also the only polymerase that enabled a distinction between the negative and positive control (with no amplification in the no template control). Thus, the GspSSD polymerase was selected for future LAMP assays.

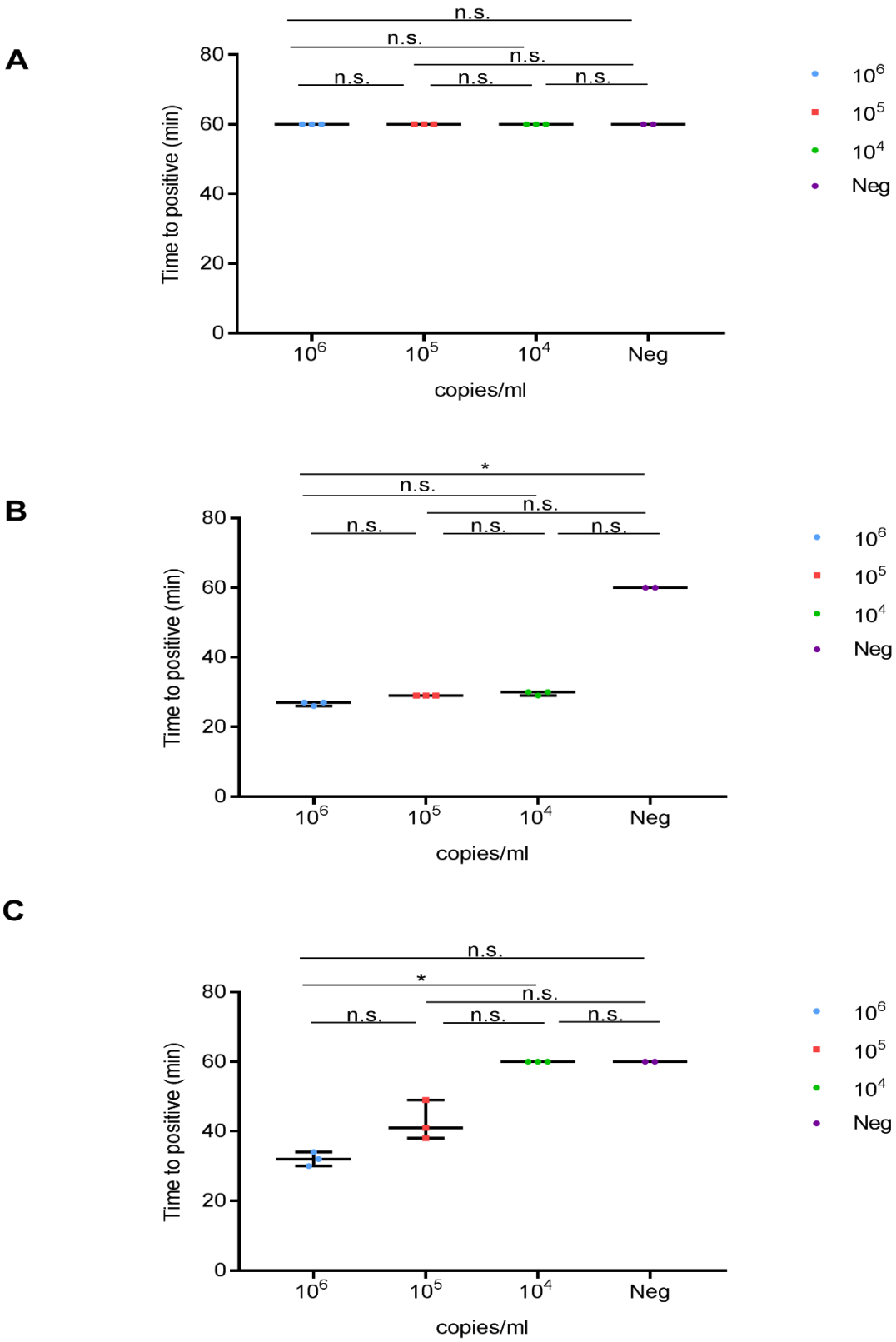

Figure 3.21 Evaluation of time to positive in three polymerases by serial dilutions of JFH1 replicon
Three polymerases, *Bst* (A), *Bst* 3 (B) and GspSSD (C) were tested for TP in LAMP reactions with three serial ten-fold dilutions of the JFH1 plasmid (10^6-10^4 copies/ml). All LAMP assays consisted of 2 µM FIP/BIP, 1 µM loop primers, 0.2 µM F3/B3 and 1 µM AP. The values represent the median and the interquartile range. Graphs represents a single experiment in triplicate. No amplification was defined as time to positive of 60 minutes. Kruskal-Wallis test with Dunn's multiple comparisons test was used for statistical analysis with significant differences indicated as follows: **** - p≤0.0001, *** - p≤0.001, ** - p≤0.01, * -p≤0.05, n.s. – not significant. Neg is the no template control.

3.1.1.5 Evaluation of master mixes and the false-positive rates in LAMP reactions

The high variability between replicates in LAMP reactions was addressed in the next set of experiments by performing LAMP reactions with isothermal master mixes containing the GspSSD enzyme (Optigene). Isothermal master mixes, ISO-001 and ISO-004, were tested with serial dilutions of the subgenomic replicon (10^8 copies/ml to 10 copies/ml) in order to provide more consistent results. Figure 3.22a indicates that the ISO-001 master mix was associated with detection between 10^8 copies/ml to 10^6 copies/ml with a TP of 19, 21 and 29.5 minutes, respectively. One of the replicates at 10^4 copies/ml was also detected, with a mean TP of 34.5 minutes. The TP for 10^5 copies/ml was 44 minutes, followed by 45 minutes TP for 10-10^3 copies/ml and the negative control. There was an inverse relationship between the TP and the copy number, as the template concentration decreased, the TP increased. The error bars were mostly tight between the replicates. Figure 3.22b shows the results from the ISO-004 master mix with a similar inverse relationship between the TP and copy number but only for the highest two concentrations, 10^8 and 10^7 copies/ml with mean TP of 24 and 30 minutes, respectively. The TP of all other concentrations were very similar with high variability. The TP of the negative control was 38 minutes, which overlapped with TP of reactions with templates ranging between 10 and 10^6 copies/ml. Therefore, the ISO-004 was associated with false positive results.

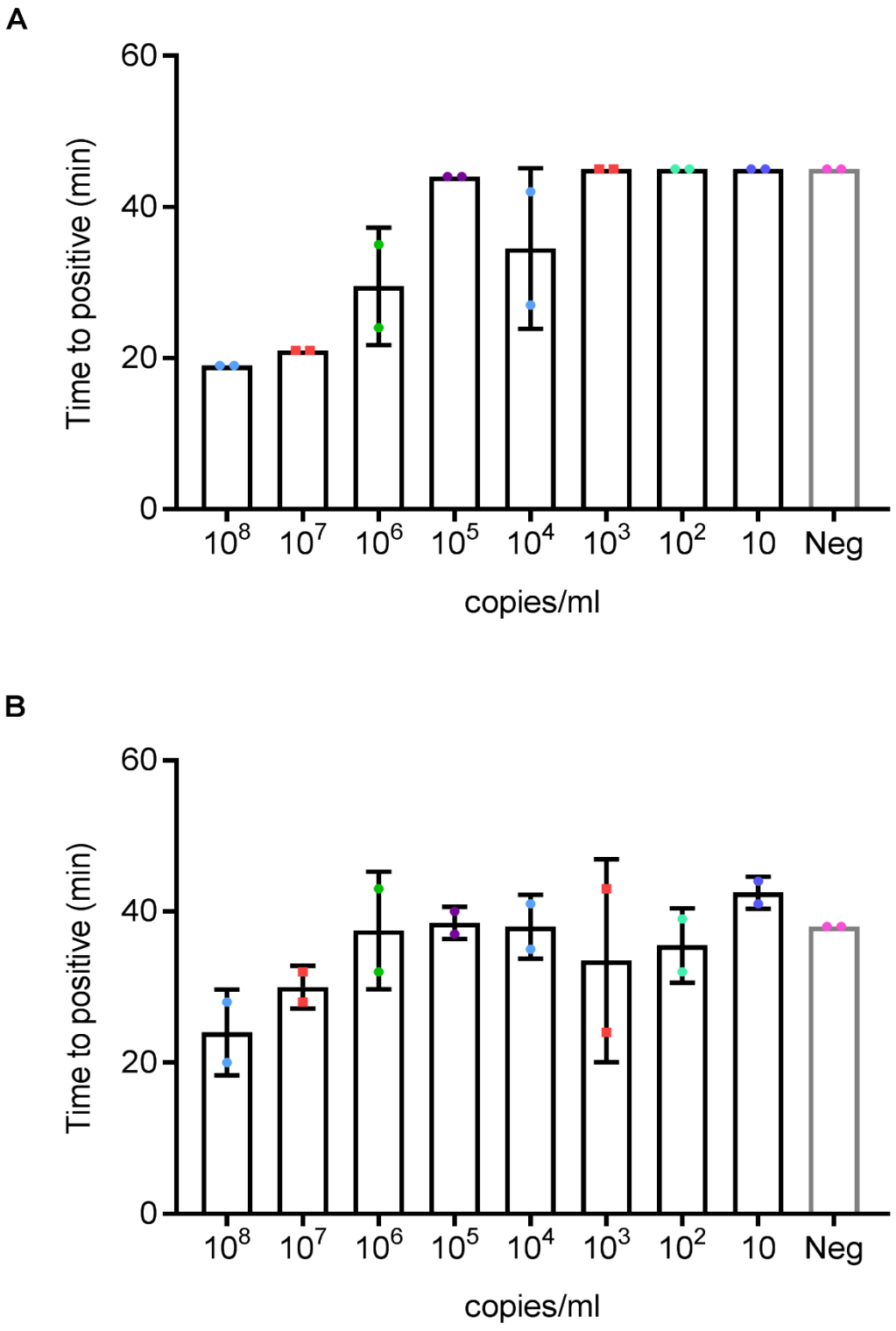

Figure 3.22 Evaluation of the ISO001 and ISO004 master mixes to reduce data variability in LAMP assays
LAMP reactions were incubated at 65°C for 45 minutes with serial ten-fold dilutions of the JFH1 plasmid (10^8-10 copies/ml) or no template (Neg). All LAMP assays consisted of 1.6 µM FIP/BIP, 0.8 µM loop primers, 0.4 µM F3/B3 and 0.8 µM AP The values represent the mean and the error bars represent ±SD. No amplification was defined as time to positive of 45 minutes. Graphs represent a single experiment in duplicate. A) LAMP reactions incubated with the ISO-001 master mix (Optigene). B) LAMP reactions incubated with the ISO-004 master mix (Optigene).

To check whether the false positives in LAMP reactions were caused by primer interactions, the next experiment was set up with the no template control only with the two master mixes, ISO-001 and ISO-004. Figure 3.23 shows that the ISO-001 master mix had no template amplification in one of the two replicates in the original primer set as well as the degenerate primer set after 45 minutes. The ISO-004 master mix had no template amplification after 40 minutes with both replicates of the original and degenerate primer sets.

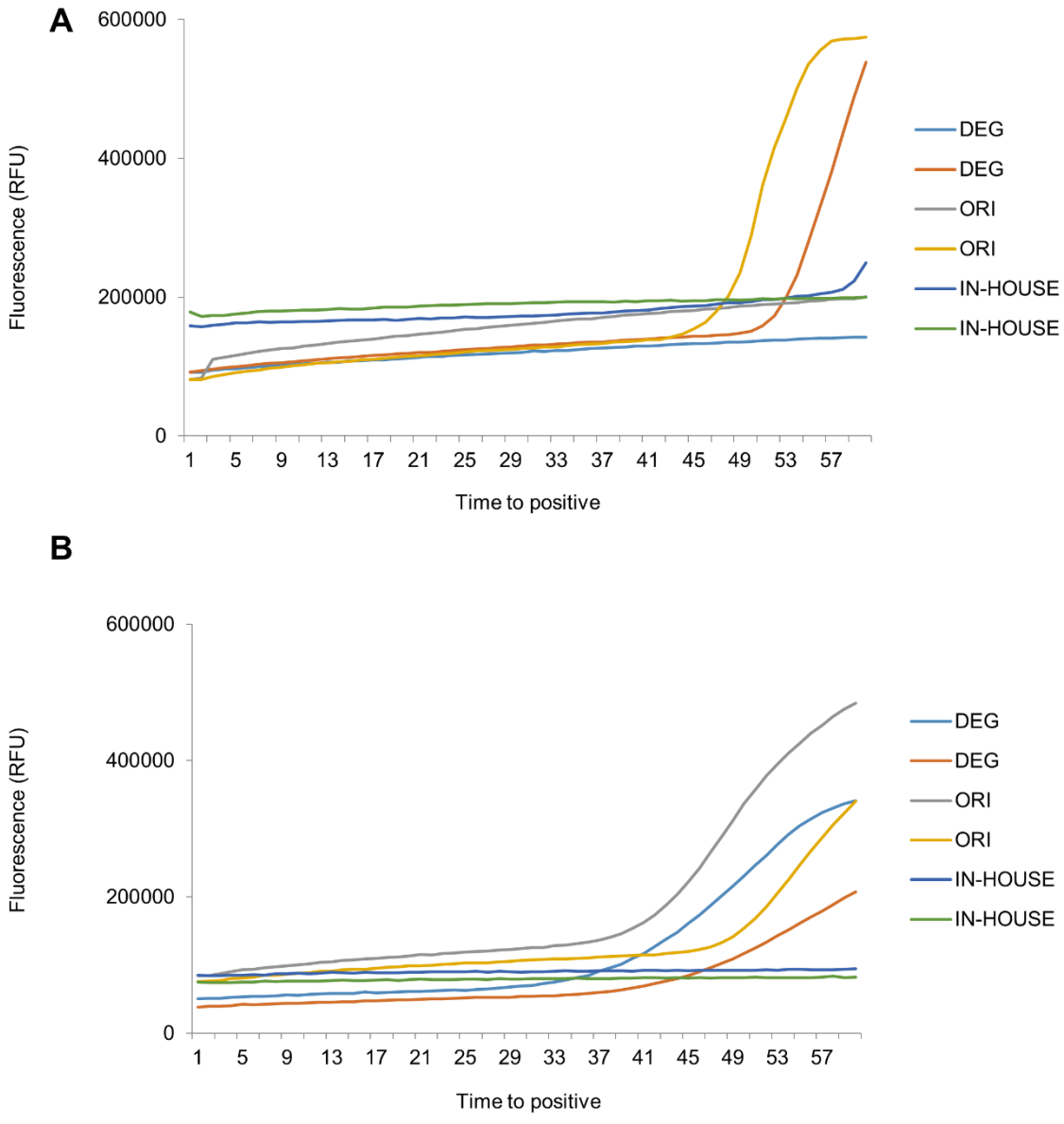

Figure 3.23 Evaluation of false positives in no template control LAMP reactions with ISO-001 and ISO-004
LAMP reactions were incubated at 65°C for 45 minutes with no template (Neg) to check for false positives. LAMP reactions used ISO-001 (A) or ISO-004 with three primer sets in duplicate; original published primers (ORI), degenerate published primers (DEG) and in-house primers (IN-HOUSE). All LAMP assays consisted of 1.6 µM FIP/BIP, 0.8 µM loop primers, 0.4 µM F3/B3 (and 0.8 µM AP for the published primer set). The values represent the fluorescence in relative fluorescence units (RFU).

Since only the published primer sets (and the modified published primers), resulted in no template amplification, the next experiment reduced the primer concentrations by half, following the instructions from the manufacturer (FIP/BIP reduced from 1.6 µM to 0.8 µM, loop primers/AP from 0.8 µM to 0.4 µM, and F3/B3 primers from 0.4 µM to 0.2µM). Figure 3.24 shows that only the ISO-001 had no-template amplification in one replicate of the degenerate primer set after 40 minutes of incubation. Therefore, the reduced primer concentration reduced the incidence of false positives and was used for future experiments.

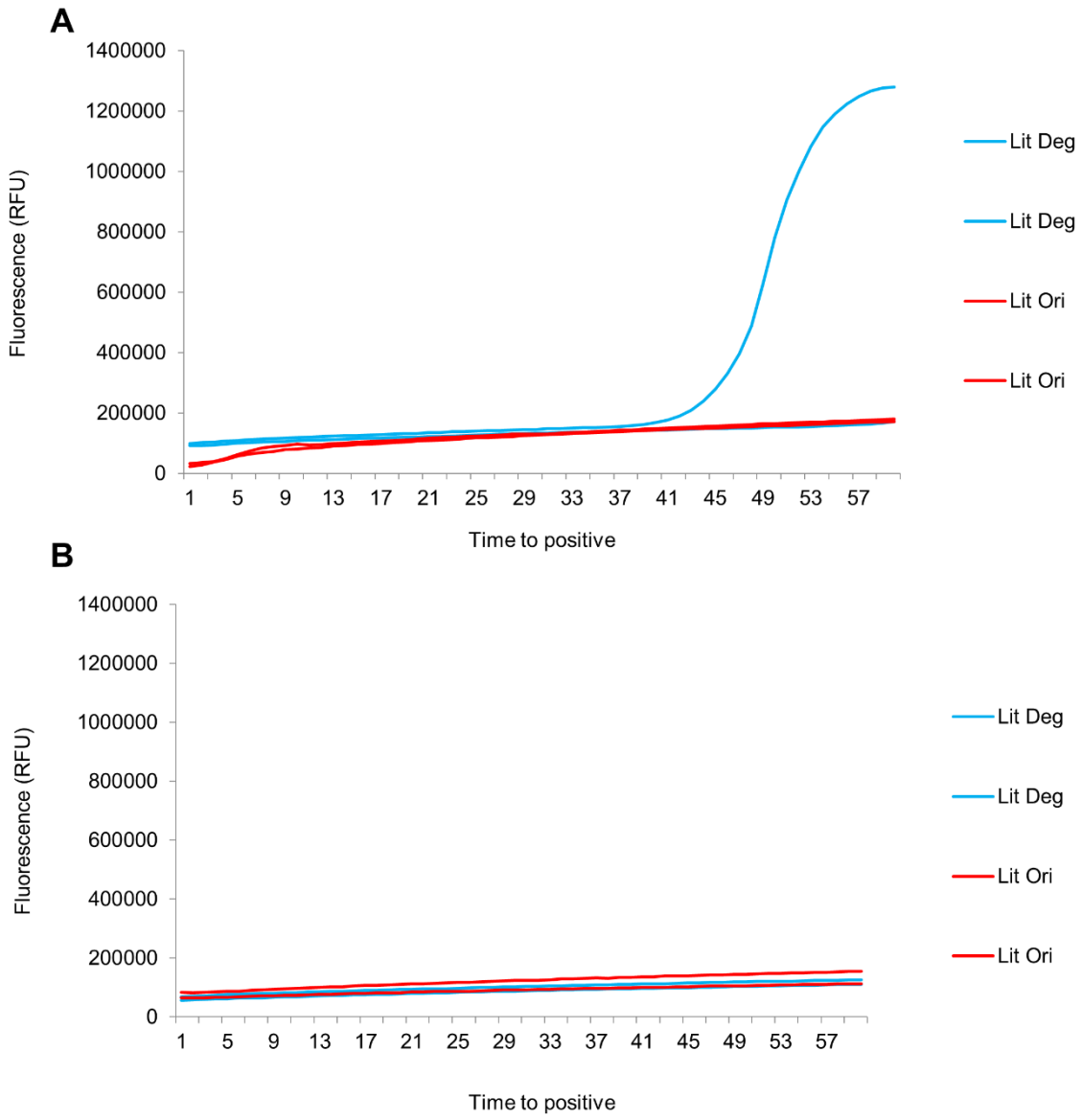

Figure 3.24 Evaluation of false positives in no template control LAMP reactions with reduced primer concentrations
LAMP reactions were incubated at 65°C for 60 minutes with no template (Neg) to check for false positives. LAMP reactions used ISO-001 (A) or ISO-004 with two primer sets in duplicate; original published primers (ORI) and degenerate published primers (DEG). All LAMP assays consisted of 0.8 µM FIP/BIP, 0.4 µM loop primers, 0.2 µM F3/B3 and 0.4 µM AP. The values represent the fluorescence in relative fluorescence units (RFU). Graphs represent a single experiment.

Next, the master mixes were compared by sensitivity in three clinical samples (AA09, AA11 and AA16) from the EAP, which were tested in previous experiments (see Figure 3.7). The other five samples from the EAP study were not tested as they were used up in previous experiments. Figure 3.25a shows that the ISO-001 master mix detected two replicates of the AA09 and AA16 in 60 minutes. The amplification curves of the AA16 samples were too flat to classify them as positives. The ISO-004, on the other hand, was able to detect all samples and replicates (AA09, AA11 and AA16) although the negative control also had a positive amplification within 30 minutes (Figure 3.25b).

Despite the better clinical sensitivity with the ISO-004 master mix, the ISO-001 was selected as the optimal master mix. This was because the ISO-004 was more prone to false positives which did not improve after the primer concentration reduction, as well as variability in serial dilution experiments.

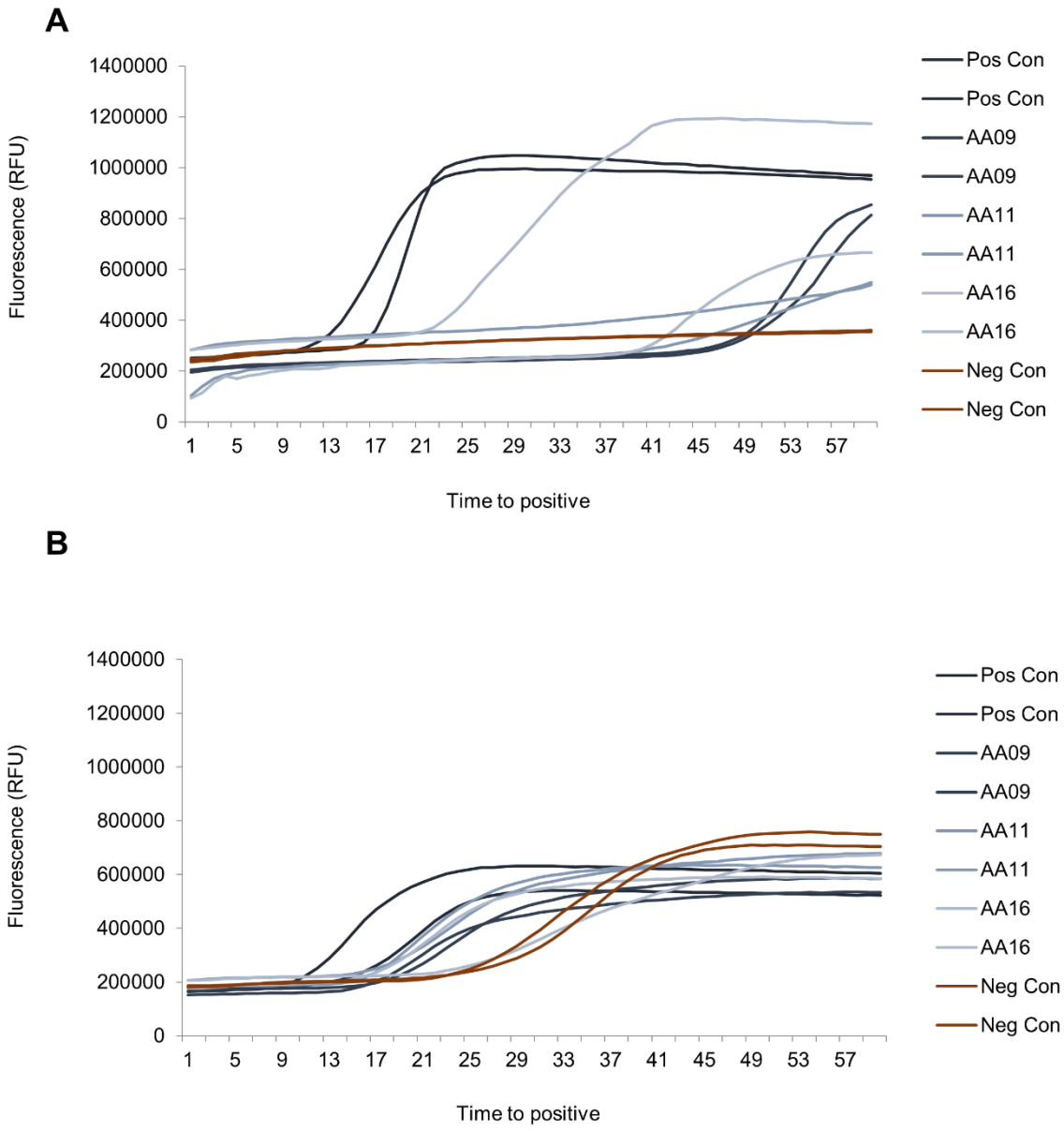

Figure 3.25 Comparison of clinical sensitivity between the ISO-001 and ISO-004 master mix in LAMP assays
The graph represents sensitivity with three clinical samples from chronically-infected HCV patients, AA09, AA11 and AA16, from the EAP. Primers were used at a concentration of 0.8 µM (FIP/BIP), 0.4 µM (FLP/BLP), 0.2 µM (F3/B3) and 0.4 µM (AP). The LAMP assay was incubated at 65°C for 60 minutes with ISO-001 (A) or ISO-004 (B). The diagrams represent fluorescence in relative fluorescence units (RFU) from one experiment with duplicate samples. Samples are colour-coded as indicated on the figure legend (right side of the graphs). Pos is positive control, JFH1 plasmid at 10^6 copies/ml, Neg is no template, negative control.

3.1.1.6 Selection of optimal primer concentration

To ensure the primer concentration recommended by the ISO-001 manufacturer was optimal, one further experiment was performed testing different concentrations of the following primer pairs: internal primers (IP, FIP and BIP), loop primers (LP, FLP and BLP) and external primers (EP, F3 and B3). Figure 3.26a indicates that the IP concentration did not significantly affect the mean TP. The mean TP for 1 µM, 1.6 µM and 2 µM IP was 20.7, 19.3 and 20.3 minutes, respectively with significant differences between all the concentrations and the NTC ($p=0.0002$ for all). The changes in concentrations of the loop primers (LP) also did not significantly change the mean TP with 21.3, 20 and 19.7 minutes for the 0.4 µM, 0.8 µM and 1 µM. Once again the only significant differences were observed between all the concentrations and the NTC ($p<0.0001$ for all) (Figure 3.26b). This was also true for the external primers (EP), the mean TP was 21.7, 20.7 and 22.3 minutes at 0.2 µM, 0.4 µM and 0.8 µM, respectively with significance between them and the NTC ($p<0.0001$ for all reactions). Therefore, there was no advantage of changing the primer concentration from the ISO-001 manufacturer's recommendations; 0.8 µM for FIP/BIP, 0.4 µM for FLP/BLP and 0.2 µM for F3/B3.

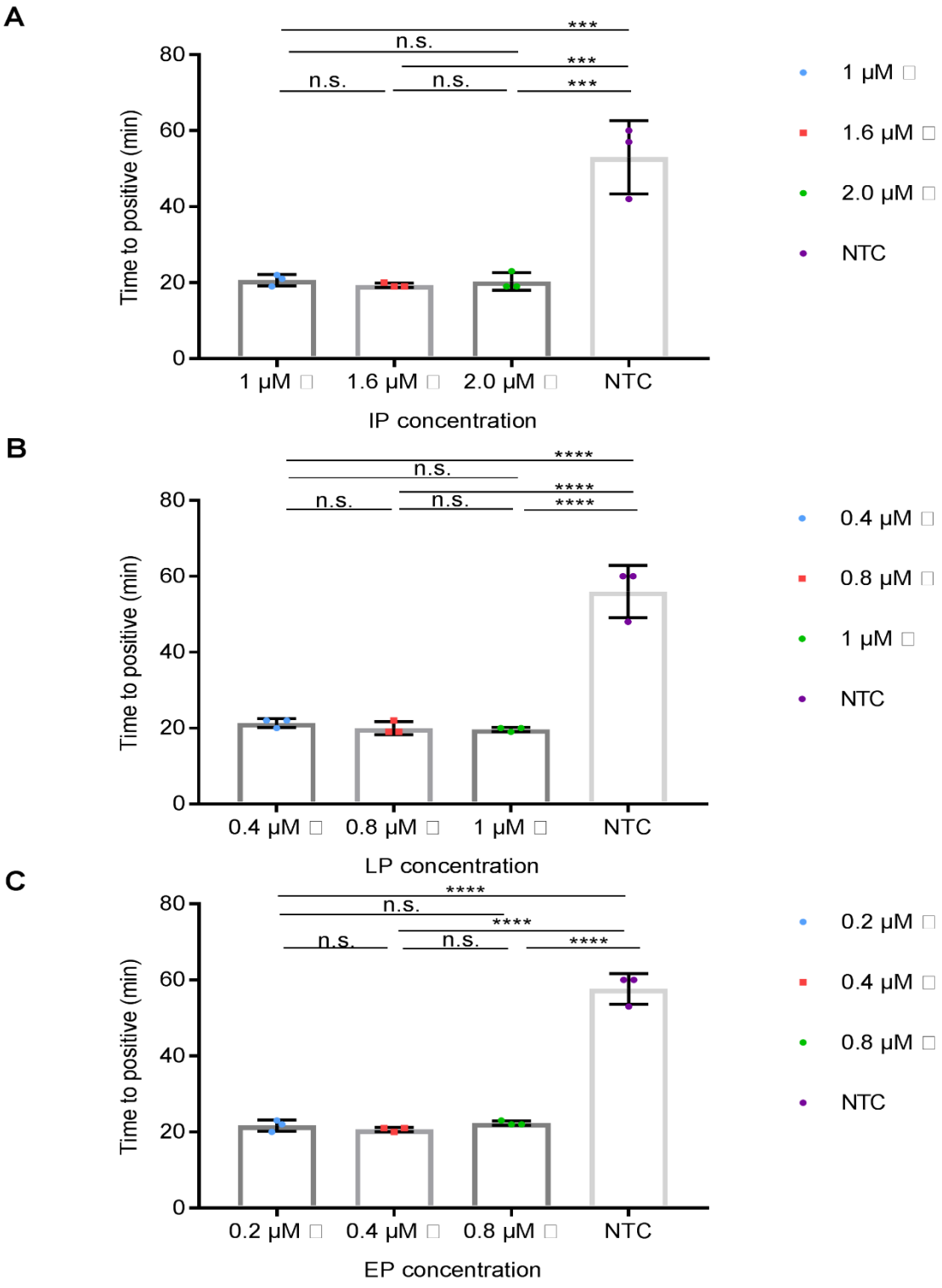

Figure 3.26 Evaluation of different primer pair concentrations in the ISO 001 master mix LAMP reactions
LAMP reactions were incubated at 65°C for 60 minutes with ISO-001 master mix and the subgenomic replicon or no template control (NTC). The values represent the mean and the error bars represent ±SD. Graph represent a single experiment in triplicate. One-way ANOVA with Tukey's multiple comparisons test was used for statistical analysis with significance indicated as follows: **** - p≤0.0001, *** - p≤0.001, ** - p≤0.01, * -p≤0.05, n.s.-not significant. No amplification was defined as TP of 60 minutes. A) LAMP reactions testing three concentrations of the internal primers (IP), FIP/BIP at 1 µM, 1.6 µM and 2 µM. Other primers were used at the following concentrations; 2 µM for FLP/BLP, 0.2 µM for F3/B3 and 1 µM for AP. B) LAMP reactions testing three concentrations of the loop primers (LP), FLP/BLP at 1 µM, 1.6 µM and 2 µM. Other primers were used at the following concentrations; 1 µM for FIP/BIP, 0.2 µM for F3/B3 and 1 µM for AP. C) LAMP reactions testing three concentrations of the external primers (EP), F3/B3 at 0.2 µM, 0.4 µM and 0.8 µM. Other primers were used at the following concentrations; 2 µM for FIP/BIP, 1 µM for FLP/BLP and 1 µM for AP.

The next experiment aimed to determine the optimal concentration of the AP as the manufacturer of the ISO-001 does not offer recommendations for additional primers. Figure 3.27 shows the results of testing three AP concentrations; 0.4 µM, 0.8 µM and 1.0 µM, with a mean TP of 22, 20.3 and 23 minutes, respectively. There were no significant differences between the different concentrations although all reactions were significantly different than the NTC ($p=0.0001$ for 0.4 µM and $p<0.0001$ for 0.8 µM and 1 µM, respectively). Therefore, future experiments used the lowest concentrations of 0.4 µM, which matched the concentrations of loop primers.

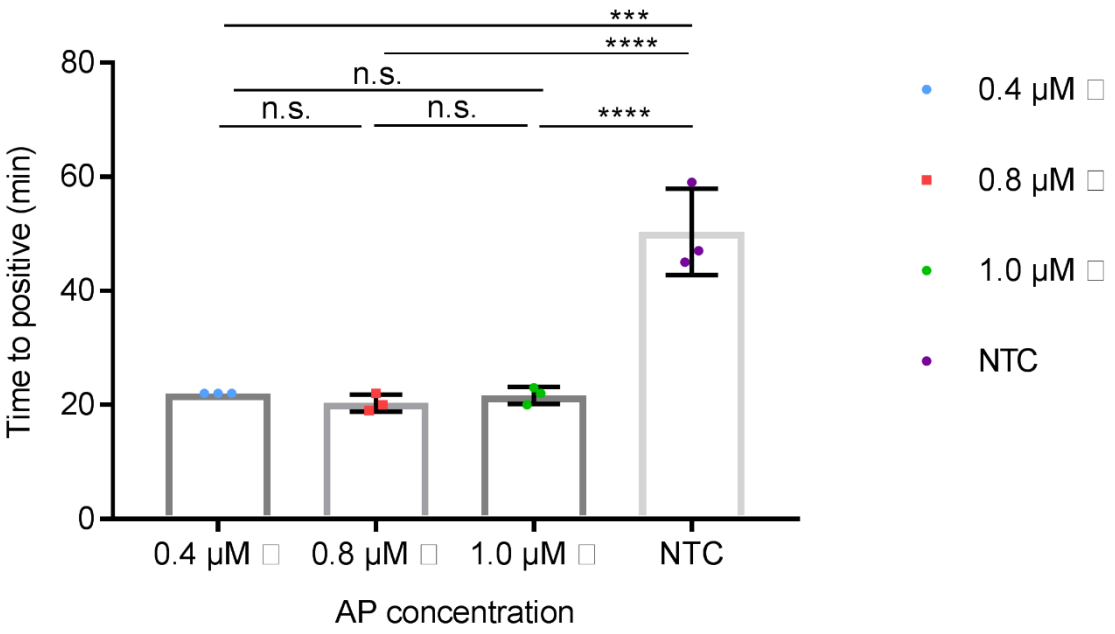

Figure 3.27 Evaluation of different AP concentration in ISO-001 master mix
LAMP reactions were incubated at 65°C for 60 minutes with ISO-001 master mix and the subgenomic replicon or no template control (NTC). The values represent the mean and the error bars represent ±SD. The graph represents a single experiment in triplicate. One-way ANOVA with Tukey's multiple comparisons test was used for statistical analysis with significance indicated as follows: **** - p≤0.0001, *** - p≤0.001, ** - p≤0.01, * -p≤0.05, n.s – not significant. No amplification was defined as TP of 60 minutes. LAMP reactions testing three concentrations of the Accelerating Primer (AP), at 0.4 µM, 0.8 µM and 1.0 µM. Other primers were used at the following concentrations; 2 µM for FIP/BIP, 0.2 µM for F3/B3 and 1 µM for FLP/BLP.

3.1.1.7 Summary of the HCV-LAMP optimisation experiments

In summary, the following conditions were tested in order to optimise the HCV LAMP assay; primer set, reaction temperature, polymerase selection, master mix selection and primer concentration (Figure 3.28). The published primer set were more sensitive than the in-house primers, both analytically and clinically. The published primer set was analysed for mismatches to all major HCV genotypes and a modified degenerate primer set was generated. However, the degenerate primer did not improve analytical or clinical sensitivity. Therefore, individual primers were analysed in experiments including a novel BLP, AP Rev, a 50% mix of BIP and a gt 3/6 specific FIP. The novel BLP resulted in significant improvement in TP in gt 3 samples and was therefore included in future LAMP assays. The GspSSD polymerase was better at HCV detection compared to the two *Bst* polymerases used in previous HCV LAMP assays. Variability and false positives were reduced by the use of the ISO-001 master mix and reducing the primer concentration to the one recommended by the manufacturer; 0.2 µM for EP, 0.4 µM for Loops, 0.4 µM for AP and 0.8 µM for IP.

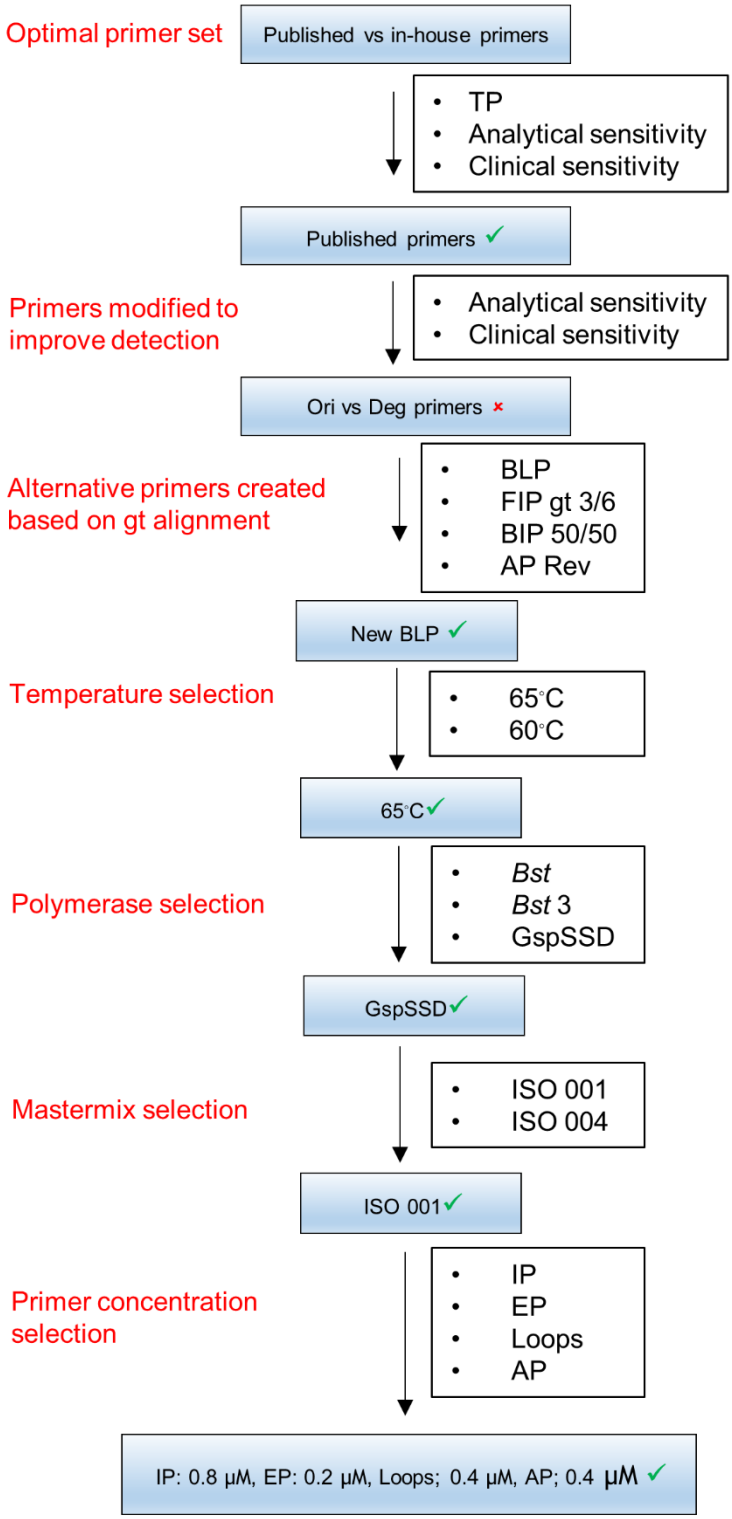

Figure 3.28 Flow chart summarising optimisation experiments for the HCV LAMP assay
TP – time to positive. Ori- original. Deg – degenerate. IP – internal primers, EP – external primers, AP – accelerating primer. FIP – forward internal primer. BIP – backward internal primer. BLP – backward loop primer.

3.1.2 Evaluation of sensitivity and specificity of LAMP vs qPCR

In the next set of experiments, the optimised LAMP reaction conditions were utilised in order to determine the assay's clinical sensitivity and specificity. A total of 52 anonymised RNA samples from HCV antibody-positive patients were tested from the West of Scotland Specialist Virology Centre. Table 3.5 summarises the sample numbers, names, gt and viral load in log_{10} IU/ml. The highest number of samples were from gt 1a (n=24), followed by gt 3 (n=18), unknown gt (n=8) and gt 1b (n=2). The viral load ranged between 3.04 to 7.3 log_{10} IU/ml although the viral load for some samples was unknown.

Table 3.5 Characteristics of RNA samples from the West of Scotland Specialist Virology Centre

Genotype	Name (16.71…)	Total number	Viral load range (log_{10} IU/ml)
1a	3173, 3642, 3854, 3968, 4241, 4628, 4668, 3479, 4883, 4961, 4964, 4970, 4986, 5063, 5077, 5126, 5150, 5292, 5349, 5377, 5512, 5525, 5383, 5465	24	4.36 to 7.3 or not known
1b	5042, 5224	2	5.4 to 6.19
3	3688, 3771, 4476, 4485, 4647, 4660, 4725, 4967, 4969, 5104, 5115, 5144, 5160, 5162, 5378, 5521, 5381, 5460	18	3.04 to 7.04 or not known
Unknown	4144, 4140, 4511, 4652, 4753, 5079, 3782, 5386	8	not known
Total		**52**	

In order to test the samples with the optimised HCV LAMP assay, the samples were reverse transcribed to cDNA. Sensitivity was calculated based on the results of an in-house HCV qPCR assay (Table 3.6). Three samples out of 52 tested negative on the qPCR assay and were used as negative controls. These samples were also negative on the HCV LAMP assay resulting in 100% specificity. The HCV LAMP assay detected all 23 gt 1 samples and two out of two samples of gt 1b which correlated with the qPCR. Out of 18 gt 3 samples and six unknown gt

samples detected by qPCR, the HCV LAMP assay detected 16 and 5, respectively. Thus, the HCV LAMP assay sensitivity was 93.8%.

Table 3.6 Comparative evaluation of HCV LAMP and RT-PCR on 52 samples

Genotype	No. of Samples	No. (%) of samples detected	
		HCV-LAMP (cDNA)	RT-PCR (cDNA)
1a	23	23	23
1b	2	2	2
3	18	16	18
Unknown	6	5	6
Total (Sensitivity)	49	46/49 (93.8%)	49/49 (100%)
Controls (Specificity)	3	0 (100%)	0 (100%)

In order to check whether gt had an effect on TP, all the replicates were divided by TP in minutes by gt, resulting in five distinctive groups. Figure 3.29 shows that shortest median TP occurred in gt 1a and 1b at 18 minutes, followed by unknown gt at 26 minutes and lastly by gt 3 at 28.5 minutes. Significant differences in TP in minutes were detected between gt 1a and gt 3 ($p<0.0001$), gt 1b and gt 3 ($p=0.0203$) and gt 1a and unknown gt ($p=0.0093$). The most variable TP was found in unknown gt.

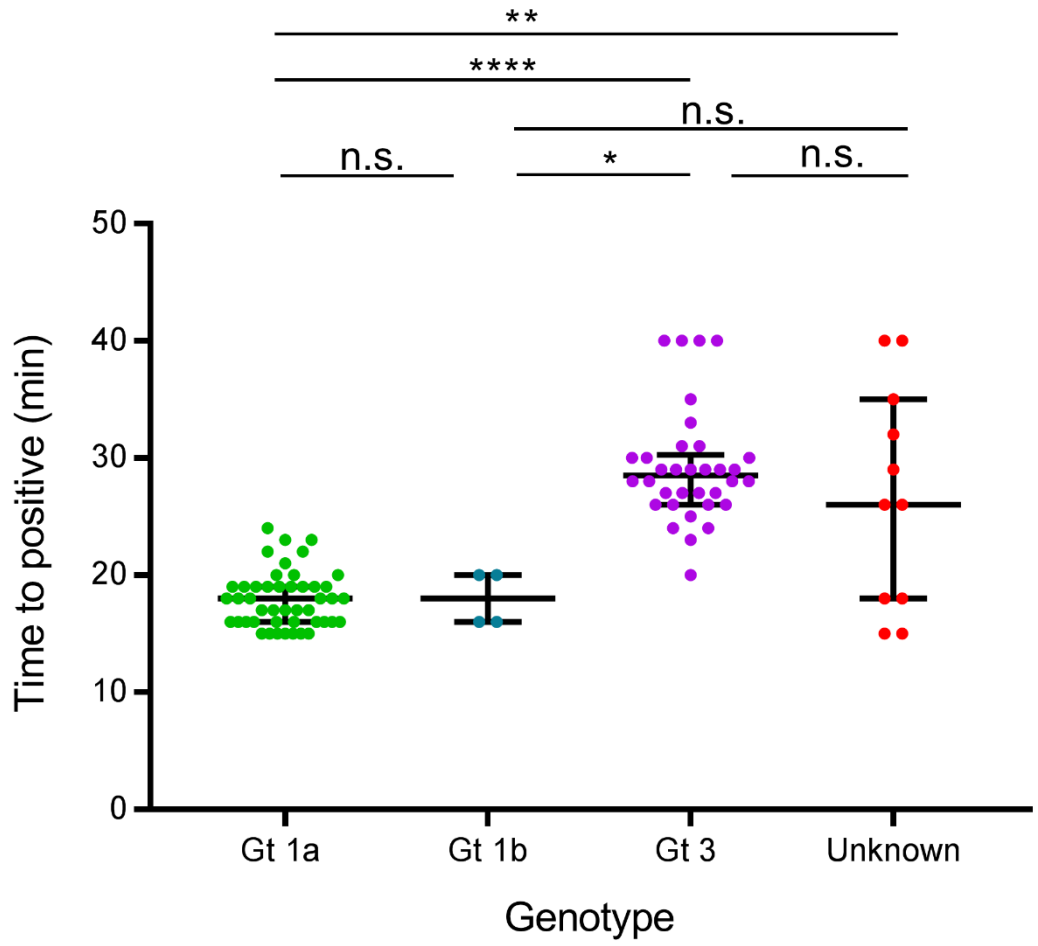

Figure 3.29 The effect of genotype on time to positivity by LAMP
LAMP reactions were incubated for 40 minutes at a stable temperature of 65◦C and changes in fluorescence recorded every minute cycle. The time to positive in minutes for LAMP and HCV cDNA samples divided into groups based on genotypes 1a, 1b, 3 and unknown genotypes. Time to positive in minutes was calculated as at least three times increase in standard deviation of fluorescence from mean baseline fluorescence (relative fluorescence units). Each point on the graphs represents a replicate of a sample run in duplicate. Lines indicate median and interquartile range. False negative samples were recorded as time to positive reaction of 40 minutes. Statistical analysis was performed using a non-parametric Kruskal Wallis with Dunn's multiple comparisons test. * - $p \leq 0.05$, ** - $p \leq 0.01$, *** - $p \leq 0.001$, **** - $p \leq 0.0001$, n.s. – not significant.

Next, the TP in minutes was divided by three groups determined by different viral loads, namely: 3.04-4.94 $\log_{10}$ IU/ml, 5.02-5.95 $\log_{10}$ IU/ml and 6.0-7.3 $\log_{10}$ IU/ml. Figure 3.30 shows that the shortest TP occurred in the highest viral load group (6.0-7.3 log10 IU/ml) with median TP of 19 minutes, followed by 21 minutes in the next largest group (5.02-5.95 $\log_{10}$ IU/ml) and 25.5 minutes in the lowest viral load group (3.04-4.95 $\log_{10}$ IU/ml). This data correlates with previous experiments were increasing TP in minutes was associated with decreasing concentration of template. No significant differences were observed between any of the groups.

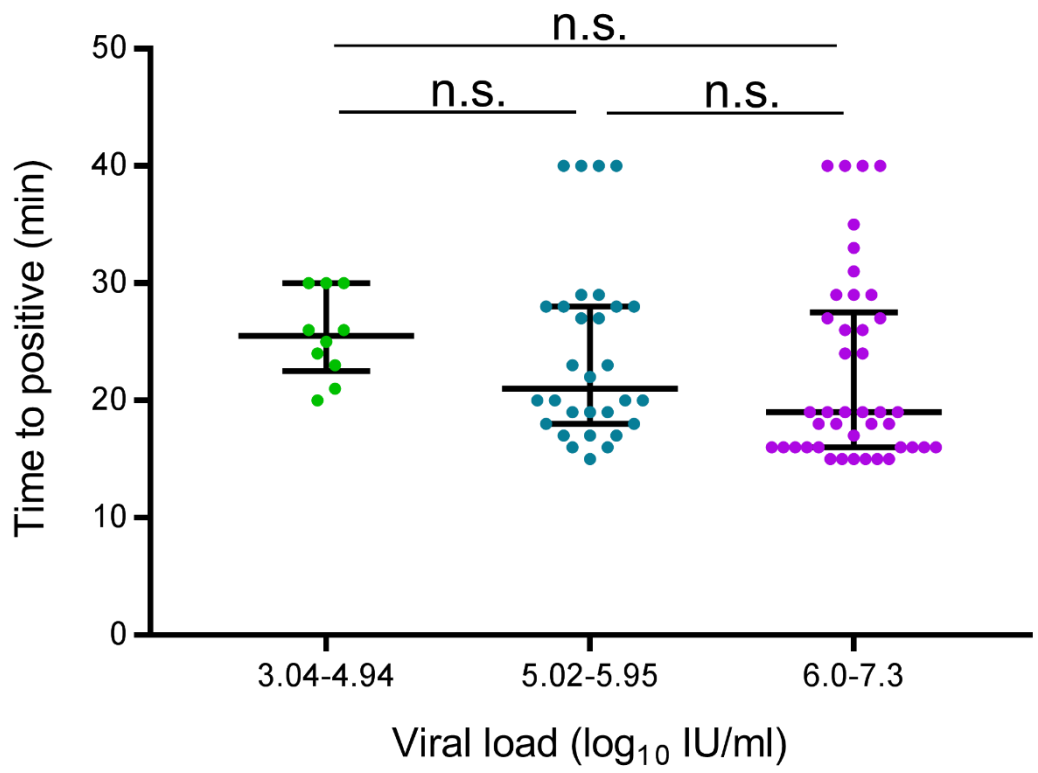

Figure 3.30 The effect of viral load on time to positive of LAMP assays
LAMP reactions were incubated for 40 minutes at a stable temperature of 65°C and changes in fluorescence recorded every minute cycle. The time to positive in minutes for HCV LAMP and cDNA/dsDNA samples was divided into three groups based on viral load (log_{10}IU/ml). Groups included viral loads of 3.04-4.94, 5.02–5.95 and 6.0–7.3 log_{10}IU/ml. Samples with unknown viral loads were excluded from the analysis. Time to positive in minutes was calculated as at least three times increase in standard deviation of fluorescence from mean baseline fluorescence (relative fluorescence units). Each point on the graphs represents a replicate of a sample run in duplicate. Lines indicate median and interquartile range. False negative samples were recorded as time to positive reaction of 40 minutes. Statistical analysis was performed using a non-parametric Kruskal Wallis with Dunn's multiple comparisons test. * - $p \leq 0.05$, ** - $p \leq 0.01$, *** - $p \leq 0.001$, **** - $p \leq 0.0001$.

3.1.2.1 Double-blind clinical evaluation study

The above experiments showed that LAMP could be used to detect HCV from clinical samples. However, the experiments were limited by the use of cDNA (requiring preceding RNA extraction and cDNA synthesis steps). In addition, very few HCV negative samples were tested and therefore specificity could not be accurately calculated.

In order to better assess clinical sensitivity and specificity, 100 HCV positive plasma samples and 100 HCV negative plasma samples were tested following double-blinding to eliminate bias. Since the ISO-001 master mix (Optigene) had very limited reverse transcriptase activity, an alternative master mix ISO-001-RT was used for the double-blind study. Table 3.7 summarises the results from the double-blind study on positive HCV samples by genotype and viral load-based detection by three different assays, namely, RT-LAMP based on the detection of RNA directly by ISO-001-RT master mix, LAMP based on the detection of cDNA converted from RNA using ISO-001-RT master mix and RT-PCR based on cDNA detection.

Table 3.8 summarises the sensitivity and specificity of the three assays. Overall 96, 97 and 96 samples out of 100 were detected by RT-LAMP, LAMP and RT-PCR, respectively, resulting in sensitivities of 96%, 97% and 96%, respectively. Specificity of the RT-LAMP assay was 91%, 90% for the LAMP assay and 100% for the RT-PCR assay. False positives were detected in RT-LAMP and LAMP assays (nine and ten samples, respectively) while none were found in the RT-PCR test.

False negatives occurred in different genotypes namely, gt 1, three in all three assays used, gt 3 samples, one in both LAMP assays and two in RT-PCR, one in gt 4 in RT-LAMP and one in unknown gt in all assays. When looking at different viral loads, most false negatives were found in the lowest viral load group, 1.7-3.95 $\log_{10}$ IU/ml (two by both LAMP assays and three by RT-PCR) although one false negative occurred in RT-LAMP in the 5.2-5.98 $\log_{10}$ IU/ml group and one in the unknown viral load group by all three assays.

Table 3.7 Detection of HCV positive samples by three different assays in the double-blind study

	Detection by method			
	RT-LAMP	LAMP	RT PCR	Samples (%)
HCV genotype				
1	25	25	25	26 (26 %)
2	14	14	14	14 (14%)
3	22	22	21	23 (23%)
4	21	22	22	22 (22%)
5	3	3	3	3 (3%)
6	1	1	1	1 (1%)
7	1	1	1	1 (1%)
Unknown	9	9	9	10 (10%)
Viral load range (log_{10} IU/ml)			Total	100
1.7-3.95	3	3	2	5 (5%)
4.4-4.85	12	12	12	12 (12%)
5.2-5.98	36	37	37	37 (37%)
6.05-6.97	37	37	37	37 (37%)
Unknown	8	8	8	9 (9%)
			Total	100

Numbers highlighted in blue indicate false negatives. Experiments were performed in duplicate and at least one positive replicate was interpreted as a positive result.

Table 3.8 Sensitivity and specificity of different HCV assays used in the double-blind study

Method	RT-LAMP	LAMP	RT-PCR
True Positive	96	97	96
False Negative	4	3	4
Total (Sensitivity)	100 (96%)	100 (97%)	100 (96%)
True Negative	91	90	100
False Positive	9	10	0
Total (Specificity)	100 (91%)	100 (90%)	100 (100%)

Abbott RealTime HCV assay was used as the gold standard reference.

Next the impact of gt and viral load on the TP on both HCV RT-LAMP and LAMP was assessed. Most of HCV positive samples were detected within 30 minutes, regardless of the gt for both RNA and cDNA

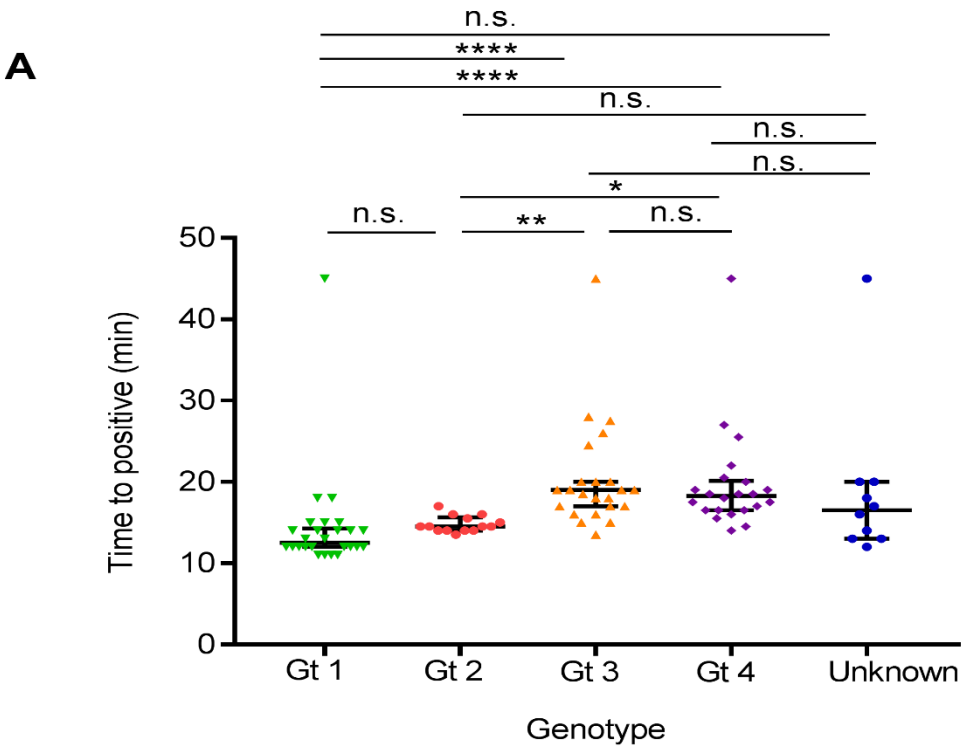

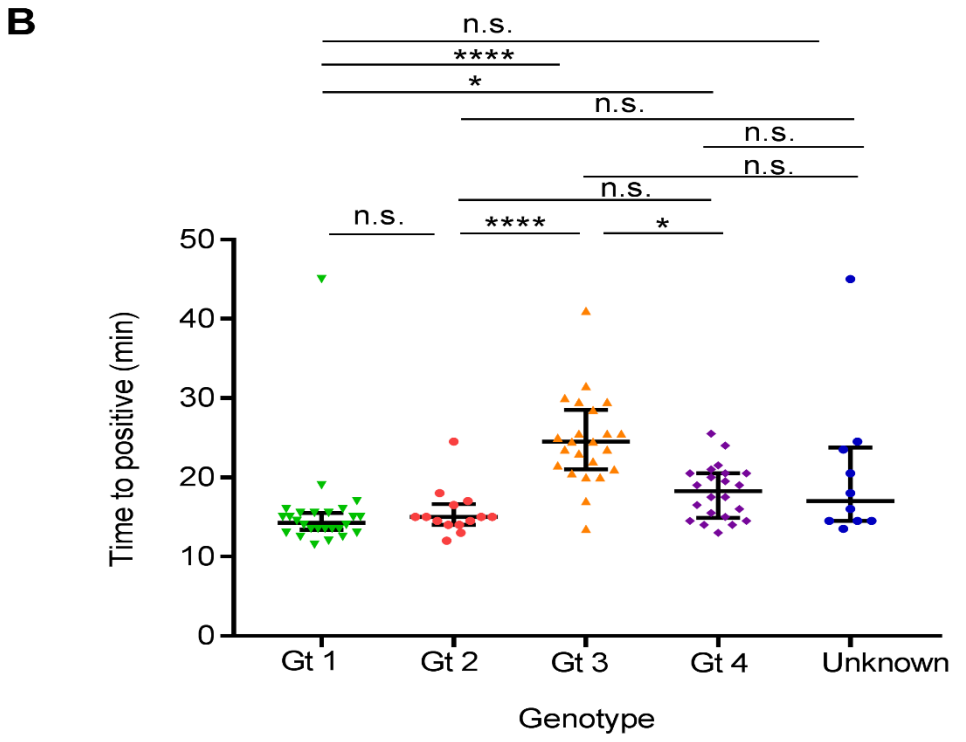

Figure 3.31).The shortest TP for RNA samples was observed in gt 1, (median of 12.5 minutes) followed by gt 2 (14.5 minutes), unknown gt (16.5 minutes), gt 4 (18.3 minutes) and gt 3 (19 minutes). The order of gt based on shortest median TP was the same for cDNA samples with gt 1 (median of 14.3 minutes) followed by gt 2 (15 minutes), unknown gt (17 minutes), gt 4 (18.3 minutes) and gt 3 (24.5 minutes). Significant differences in RNA samples were detected between gt 1 and gt 3 ($p<0.0001$), gt 1 and gt 4 ($p<0.0001$), gt 2 and gt 3 ($p=0.0058$) and gt 2 vs gt 4 ($p=0.0170$). Similarly in cDNA samples, significant differences in TP were detected between gt 1 and gt 3 ($p<0.0001$), gt 1 and gt 4 ($p=0.0360$), gt 2 and gt 3 ($p<0.0001$) and gt 3 vs gt 4 ($p=0.0258$).

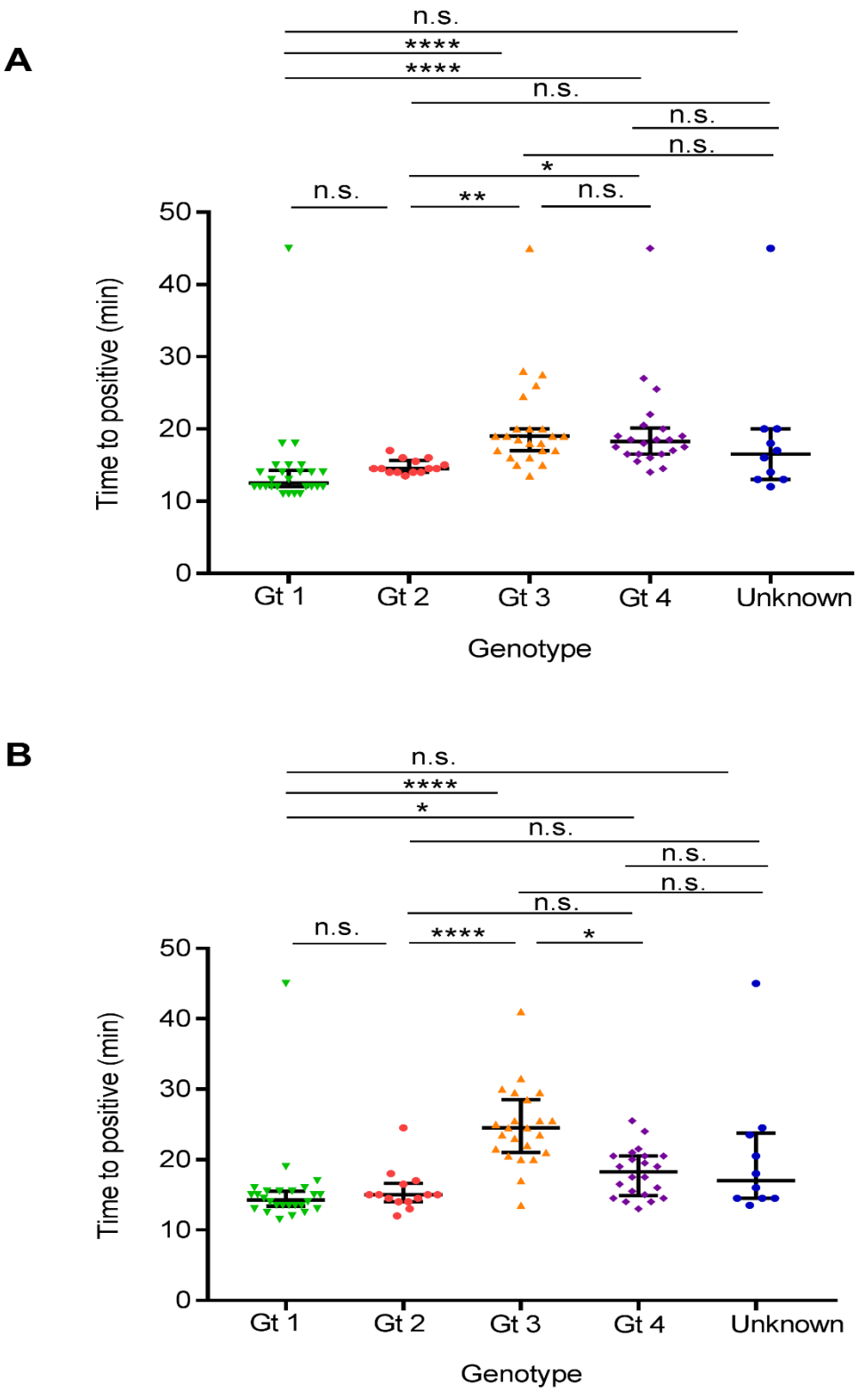

Figure 3.31 The effect of genotype on time to detection of HCV LAMP reactions in the double-blind study
LAMP reactions were incubated for 45 minutes at 65°C and changes in fluorescence recorded every minute cycle. TP in minutes was calculated as at least three times increase in SD of fluorescence from mean baseline fluorescence in relative fluorescence units. Each point on the graphs indicates the mean of a sample run in duplicate from a single double-blind experiment. Lines indicate median with interquartile range. No amplification was recorder as TP of 45 minutes. Statistical analysis was performed using a non-parametric Kruskal-Wallis with Dunn's multiple comparisons test. * - $p \leq 0.05$, ** - $p \leq 0.01$, *** - $p \leq 0.001$, **** - $p \leq 0.0001$, n.s. – not significant. A. The TP in minutes for RT-LAMP and HCV RNA samples divided into groups based on genotypes 1-4 and unknown genotypes. B. The TP in minutes for LAMP and HCV cDNA samples divided into groups based on gt 1-4 and unknown gt.

The impact of viral load on TP in both RNA and cDNA samples was tested in Figure 3.32. There was an inverse relationship between viral load and TP in minutes, as the viral load increased, the TP in minutes decreased for both RNA and cDNA samples. For RNA samples the median TP was 26, 18, 16.5 and 14.5 minutes for 1.7-3.95 log_{10} IU.ml, 4.4-4.85 log_{10} IU.ml, 5.2-5.98 log_{10} IU.ml and 6.05-6.97 log_{10} IU.ml, respectively. For cDNA samples the median TP was 28.5, 18, 16.5 and 14.5 minutes for 1.7-3.95 log_{10} IU.ml, 4.4-4.85 log_{10} IU.ml, 5.2-5.98 log_{10} IU.ml and 6.05-6.97 log_{10} IU.ml, respectively. Significant differences in RNA samples were observed between 1.7-3.95 log_{10} IU.ml group and 6.05-6.97 log_{10} IU.ml ($p=0.0095$) as well as between the 4.4-4.85 log_{10} IU.ml and 6.05-6.95 log_{10} IU.ml ($p=0.0301$). This was also true for cDNA samples with p values of 0.0032 and 0.0492, respectively.

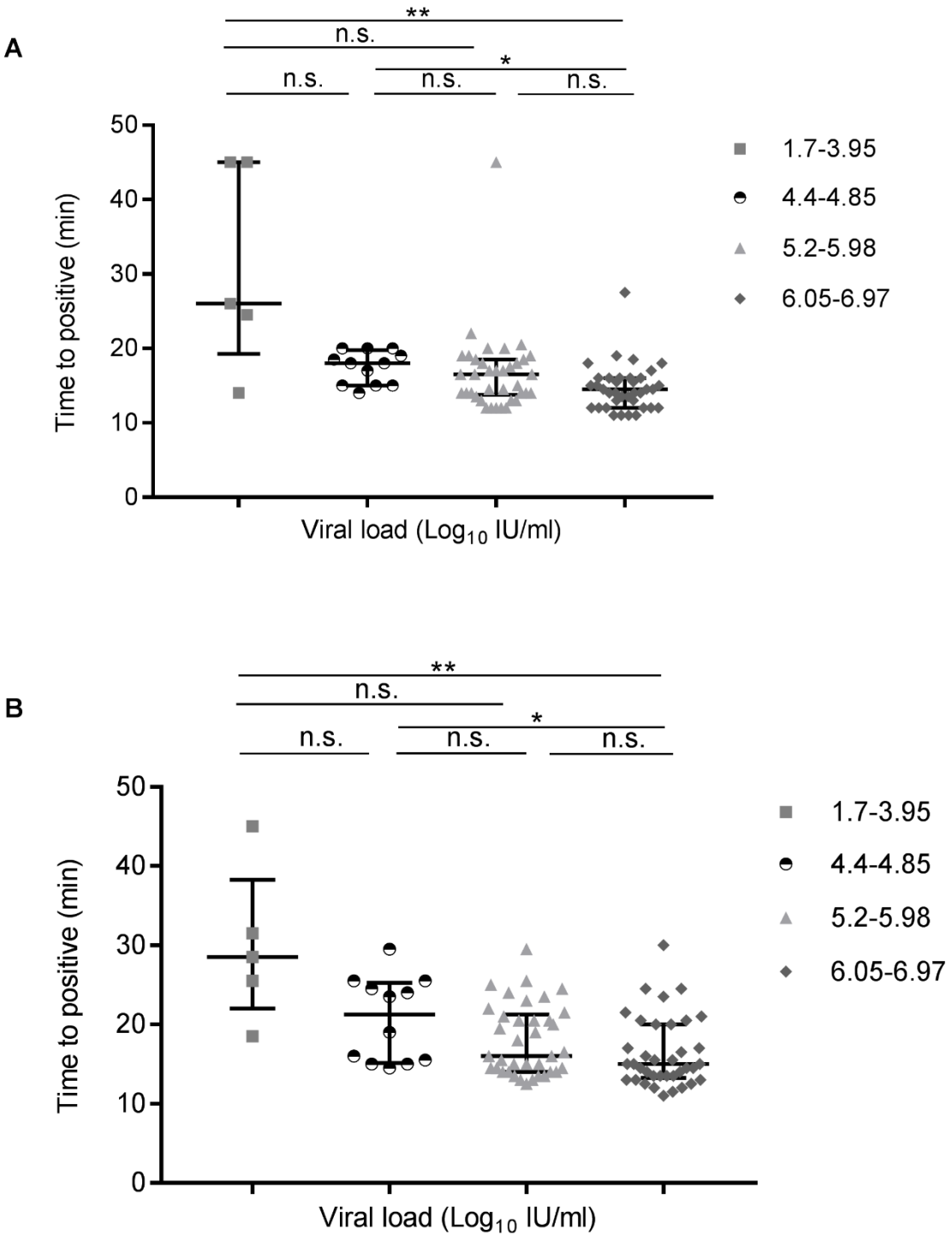

Figure 3.32 The effect of viral load on time to detection of LAMP reactions in the double-blind study
LAMP reactions were incubated for 45 minutes at 65°C and changes in fluorescence recorded every minute cycle. TP in minutes was calculated as at least three times increase in SD of fluorescence from mean baseline fluorescence in relative fluorescence units. Each point on the graphs indicates the mean of a sample run in duplicate from a single double-blind experiment. Lines indicate median with interquartile range. No amplification was recorded as TP of 45 minutes. Statistical analysis was performed using a non-parametric Kruskal-Wallis with Dunn's multiple comparisons test. * - $p \leq 0.05$, ** - $p \leq 0.01$, *** - $p \leq 0.001$, **** - $p \leq 0.0001$, n.s – not significant. A. The TP in minutes for RT-LAMP and HCV RNA samples divided into four groups based on viral load (log_{10} IU/ml). Groups included viral loads of 1.7-3.95, 4.4–4.85, 5.2–5.98, 6.05–6.97 log_{10} IU/ml. Samples with unknown viral loads were excluded from the analysis. B. The TP in minutes for LAMP and HCV cDNA samples divided into four groups based on viral load (log_{10} IU/ml). Groups included viral loads of 1.7-3.95, 4.4–4.85, 5.2–5.98 log_{10} IU/ml.

Since all medians of the viral load and gt groups were within 30 minutes, the next set of experiments assessed for the most suitable detection time to achieve optimal sensitivity and specificity. Receiver operating characteristic (ROC) curves for both LAMP assays and the RT-PCR assay were used to determine how well they distinguish between diseased and non-diseased individuals at different TP in minutes or Ct values, respectively. The area under the curve was 0.97, 0.97 and 0.99 for RT-LAMP, LAMP and RT-PCR, respectively (Figure 3.33,

Figure 3.34 and Figure 3.35). In <29 minutes the sensitivity and specificity of RT-LAMP was 95% (95% CI of 88.7% to 98.4%) and 94% (95% CI of 87.4% to 97.8%) (Figure 3.33). The LAMP assay on the other hand, had a sensitivity and specificity of 95% (95% CI of 99.7% to 98.4%) and 92% (95% CI of 84.8% to 96.5%) in <29.8 minutes (

Figure 3.34). The closest cut-off to comply with the WHO criteria for POC test (minimum of 90% sensitivity and >98% specificity) occurred in <24.8 minutes for RT-LAMP, with sensitivity and specificity of 90% (95% CI of 82.4% to 95.1%) and 98% (95% CI of 93% to 99.8%). For the LAMP assay it occurred in <26.8 minutes with a sensitivity and specificity of 92% (95% CI of 84.8% to 96.5%) and 98% (95% CI of 93% to 99.8%). Thus, the RT-LAMP assay was run without prior conversion of cDNA to RNA and for a maximum incubation time of 30 minutes. For the RT-PCR assay, the cut off of <30.8 Ct resulted in a sensitivity of 97% (95% CI of 91.5% to 99.4%) and 100% specificity (95% CI of 96.4% to 100%) (Figure 3.35).

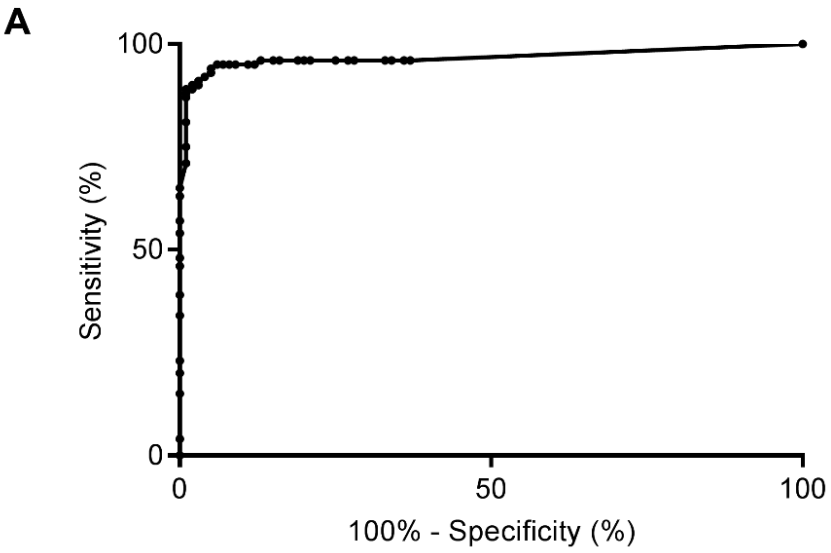

Area under the ROC curve	
Area	0.9669
Std Error	0.01435
95% CI	0.9388 to 0.995
P value	<0.0001

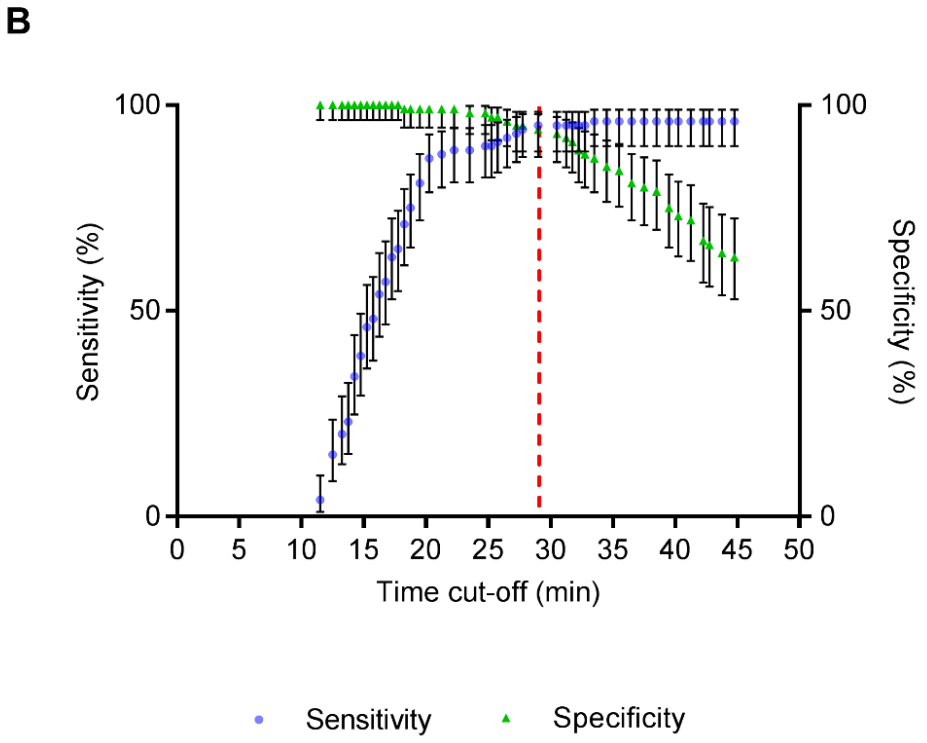

Figure 3.33 ROC curve for RT-LAMP assay based on RNA samples
ROC curves were based on the mean TP of 100 HCV positive and 100 HCV negative samples – the 16 NTC samples for the extraction were excluded. ROC curve demonstrates the area under the curve and standard error (Std error), 95% confidence intervals (95% CI) and the p value. A. ROC curve analysis for RT-LAMP and RNA samples. B. Graphed sensitivity and specificity with 95% confidence and triangles indicate specificity with 95% confidence intervals. The dashed line indicates the cut-off time in minutes for RT-LAMP, where sensitivity and specificity were at the highest point.

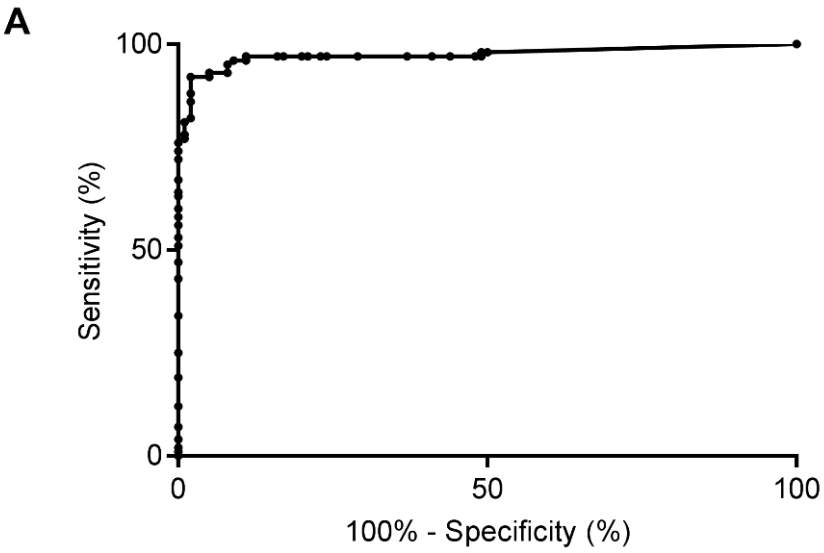

Area under the ROC curve	
Area	0.9735
Std Error	0.01219
95% CI	0.9496 to 0.9973
P value	<0.0001

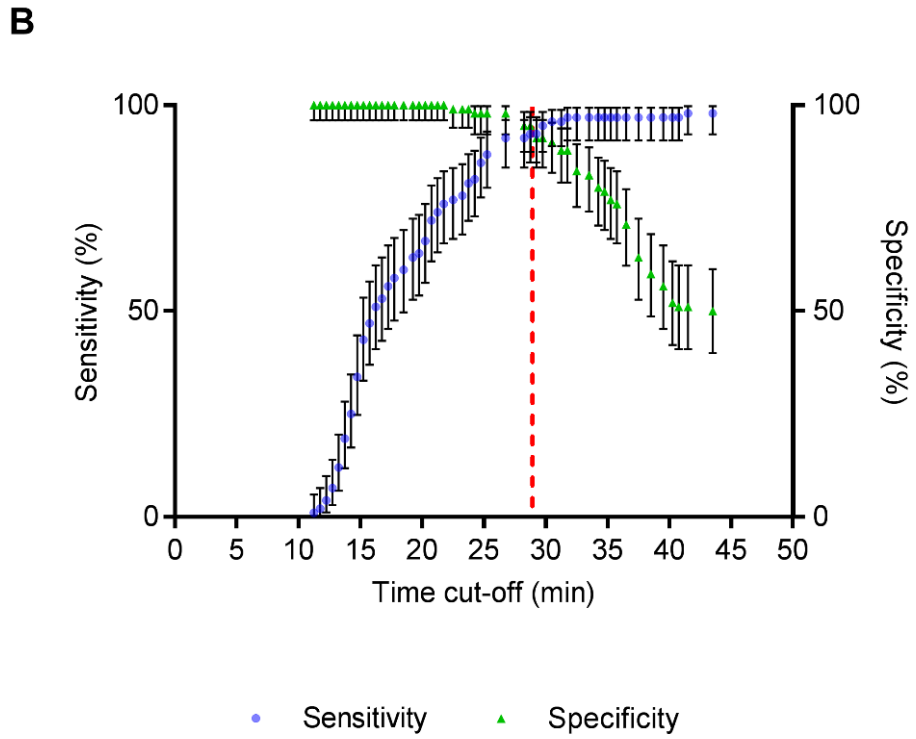

Figure 3.34 ROC curve for LAMP assay based on cDNA samples
ROC curves were based on mean TP of 100 HCV positive and 100 HCV negative samples – the 16 NTC samples for the extraction were excluded. ROC curve demonstrates the area under the curve and standard error (Std. error), 95% confidence intervals (95% CI) and the p value. A. ROC curve analysis for LAMP and cDNA samples. B. Graphed sensitivity and specificity with 95% confidence and triangles indicate specificity with 95% confidence intervals. The dashed line indicates the cut-off time in minutes for LAMP, where sensitivity and specificity were at the highest point.

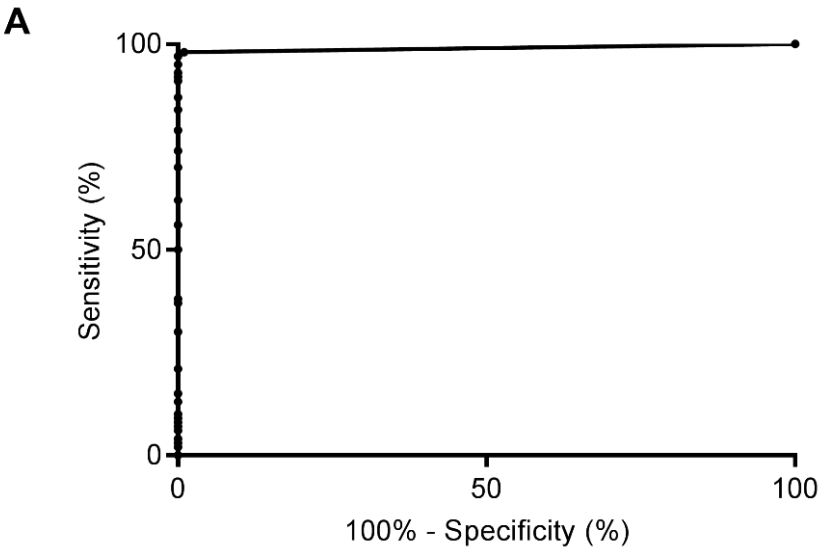

Area under the ROC curve	
Area	0.9899
Std Error	0.008186
95% CI	0.9738 to 1.006
P value	<0.0001

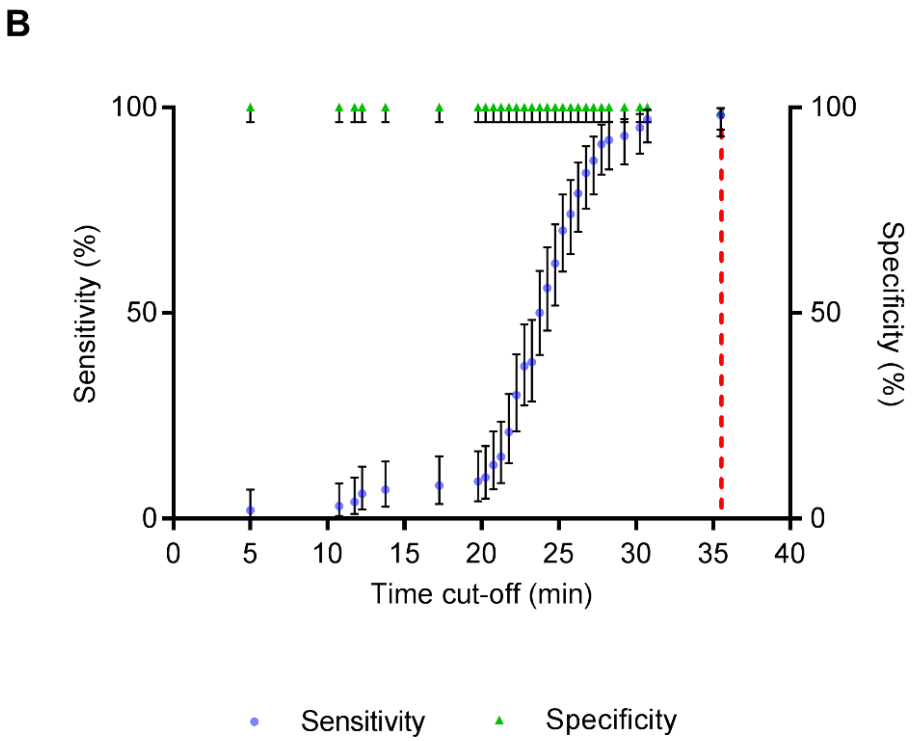

Figure 3.35 ROC curve for RT-PCR from cDNA samples and time cut-off determination
ROC curves were based on mean Ct values of 100 HCV positive and 100 HCV negative samples – the 16 NTC samples for the extraction were excluded. ROC curve demonstrates the area under the curve and standard error (Std error), 95% confidence intervals (95% CI) and the p value. A. ROC curve analysis for RT-PCR and cDNA samples. B. Graphed sensitivity and specificity with 95% confidence and triangles indicate specificity with 95% confidence intervals. The dashed line indicates the cut-off time in minutes for RT-PCR, where sensitivity and specificity were at the highest point.

3.1.2.2 Assessment of visual detection of HCV LAMP products

The RT-LAMP assay was highly sensitivity and specific but was incubated with laboratory equipment to allow for detection and subsequent interpretation of results. The next set of experiments aimed to identify a suitable detection system to allow for result interpretation by the naked eye without laboratory equipment. Colorimetric detection was evaluated through the use of Leuco-Crystal Violet (LCV) as previously published (S Miyamoto et al. 2015). LCV is a colourless liquid that turns violet upon contact with double-stranded DNA such as the products of LAMP reactions. Figure 3.36 shows that the LAMP reaction with the LCV mixture appears almost colourless to the naked eye, prior to the addition of the template. Following the addition of JFH1 to tubes 1-3 (in serial ten-fold dilutions) and NTC to tube 4, a slight tint of purple appears particularly in the last mixture. After the incubation of the LAMP reaction at 65 C for 30 minutes, the tubes containing HCV template turned deep purple (tubes 1-3) while the NTC tube is a light purple colour. While there is a slight colour difference between the positive and the negative controls, it was not clear enough to distinguish between them.

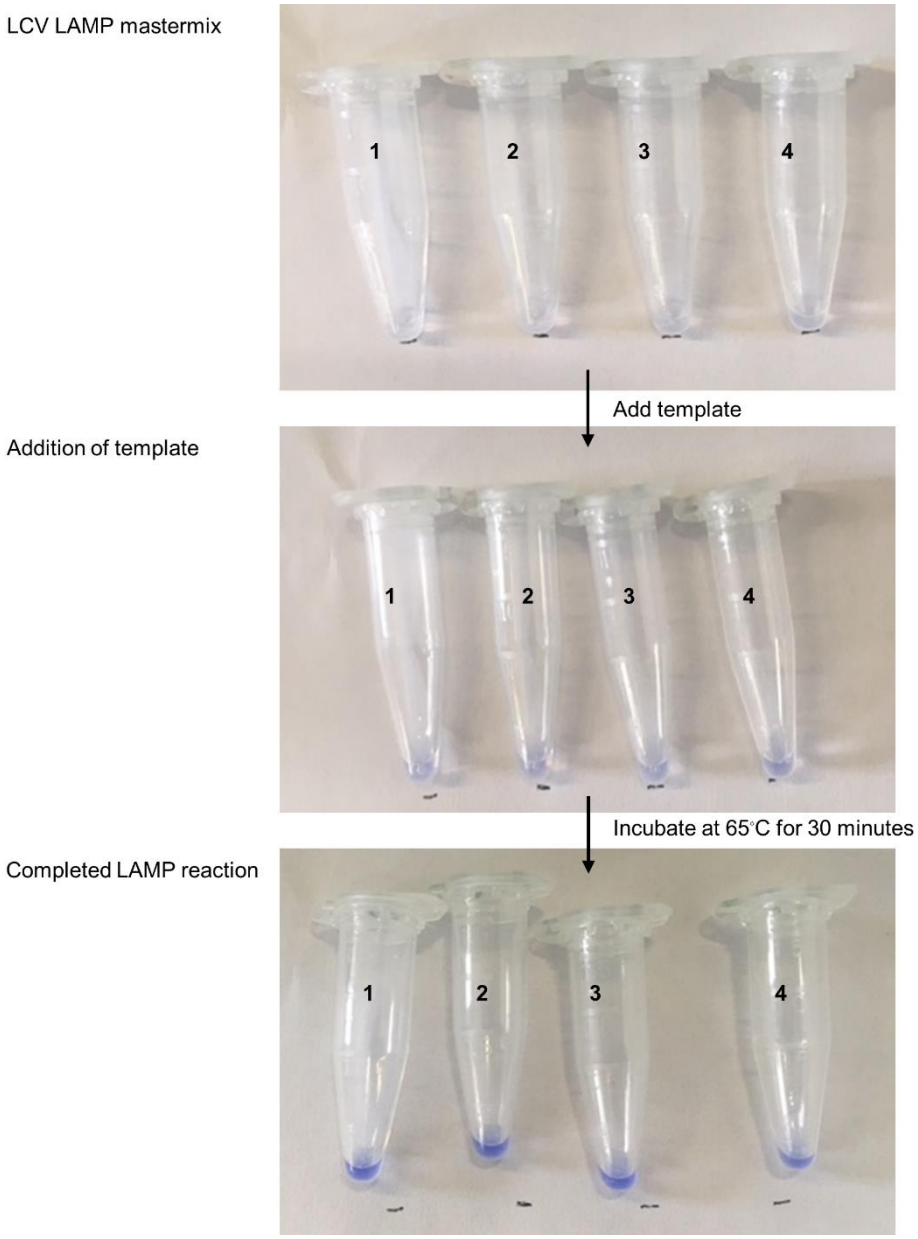

Figure 3.36 The use of Leuco Crystal Violet for colorimetric detection of LAMP products
A mixture containing 0.5 mM Crystal Violet, 30 mM Sodium sulphite and 5 mM of β-Cyclodextrin was aliquoted in 5 µl aliquots in Eppendorf tubes and subsequently dried out at 50°C for 30 minutes. Holes were drilled into the lids of the Eppendorf tubes to allow for vacuum-removal of moisture for one hour. Top Panel - LAMP master mix added to the LCV mixture. Middle Panel – LAMP master mix with LCV mixture following the addition of template. Bottom Panel – LAMP reaction following the incubation at 65°C for 30 minutes. Tubes 1-3 – Serial ten-fold dilutions of 1 ng/µl of JFH1 subgenomic replicon, tube 4 – no template control.

LCV was therefore not considered a suitable method to distinguish between positive and negative reactions and thus other naked-eye detection methods were explored. Figure 3.37 illustrates the use of the WarmStart Colorimetric master mix from NEB. The master mix changes colour from pink to yellow upon DNA amplification in a LAMP reaction. Results were compared directly with the ISO-001 reaction based on fluorescence (Figure 3.37a). This resulted in a clear distinction between positive template and the no template control, the former appearing yellow while the latter stayed pink. The ISO-001 was noted to have a faster TP. The ISO-001 reactions containing gt 1 template were detected just after 12 minutes, while the WarmStart Colorimetric master mix started to turn a tinge of yellow around 15 minutes. A clear positive did not appear until 20 minutes when both positive control-containing tubes turned bright yellow. Alternative methods of naked-eye detection were explored in future experiments based on the previously optimised ISO-001 master mix.

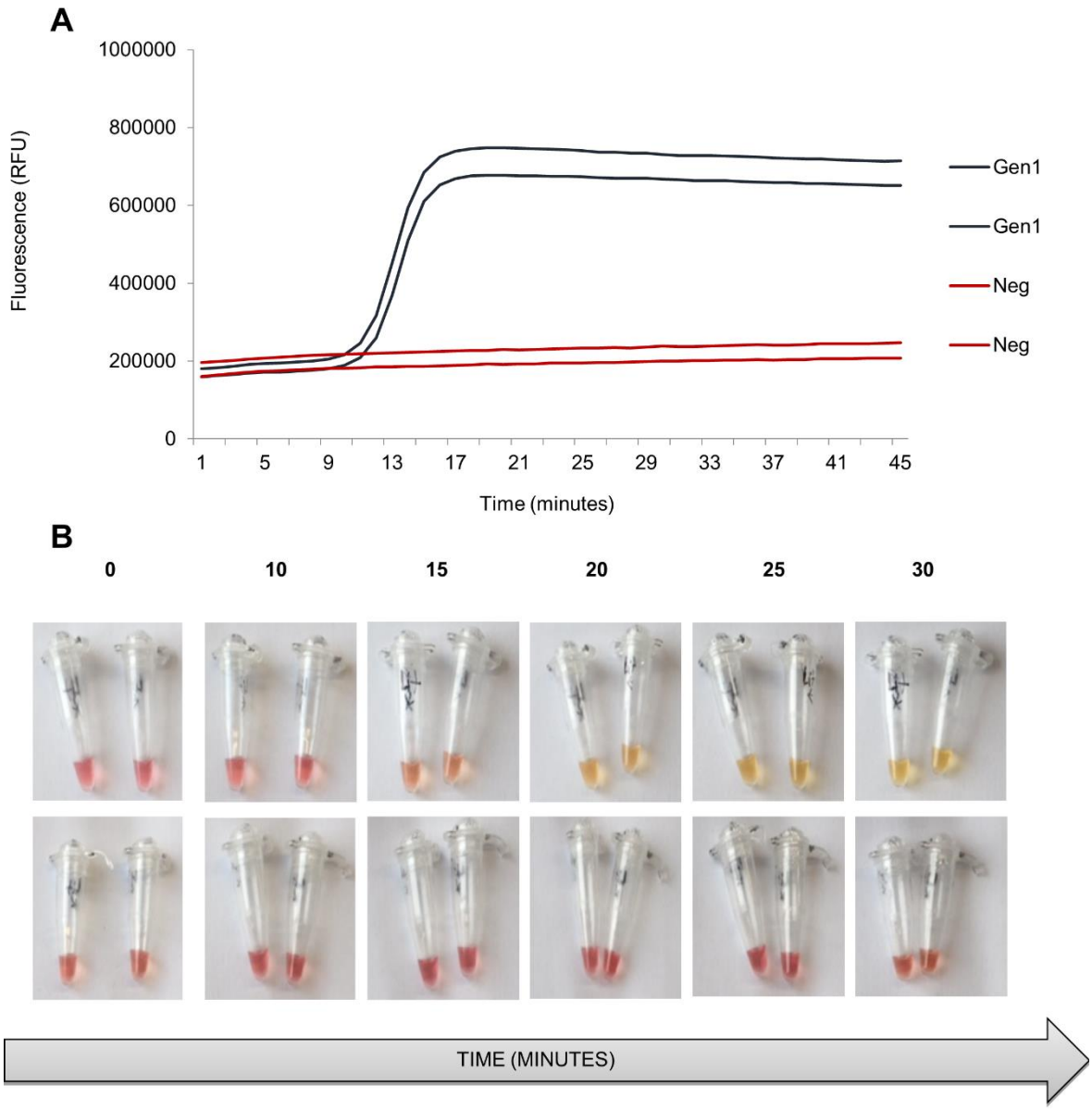

Figure 3.37 The use of WarmStart colorimetric master mix for the detection of LAMP products.
Direct comparison of the detection of LAMP products by the ISO-0001 master mix (Optigene) based on relative fluorescence and the WarmStart colorimetric master mix (NEB) based on changes in colour. A. The ISO-001 master mix contained 0.8 µM of FIP/BIP, 0.4 µM of FLP/BLP, 0.4 µM of AP and 0.2 µM of F3/B3 primers. The reactions were incubated for 45 minutes at 65°C with the gt 1 subgenomic replicon template (blue lines) or no template control (red lines). B. The WarmStart colorimetric master mix contained 1.6 µM of FIP/BIP, 0.4 µM of FLP/BLP, 0.4 µM of AP and 0.2 µM of F3/B3 primers as per manufacturer's instructions. The reactions were incubated for 45 minutes at 65°C with the gt 1 subgenomic replicon template (top panel) or no template control (bottom panel). A positive reaction was indicated by a colour change from pink to yellow. No amplification was indicated by no changes and pink colour by the end of the reaction. Pictures were taken at 5 minutes intervals starting from 0 to 30 minutes. Diagrams represent data from a single experiment in duplicate.

3.1.2.3 Lateral-flow based detection

The next method explored for the naked-eye detection of LAMP products was the use of lateral-flow strips. Two primers of the Loop primers were labelled – one with Biotin and one with FITC – as described in the Materials and Methods, thus allowing for only double-stranded LAMP product detection. The optimised ISO-001 master mix was used and the entire reactions were added to individual strips for analysis. Figure 3.38 shows the results following the addition of LAMP products from a positive control and negative control reaction as well as addition of water to the nucleic-acid detection strips. The Positive control strips produced two intense bands – one at the control line and one at the test line. The negative control and the no LAMP control produced only one band at the control line and no bands at the test line. Therefore, the nucleic-acid detection strips were used in future experiments as a naked-eye detection method for LAMP products to be used without laboratory equipment.

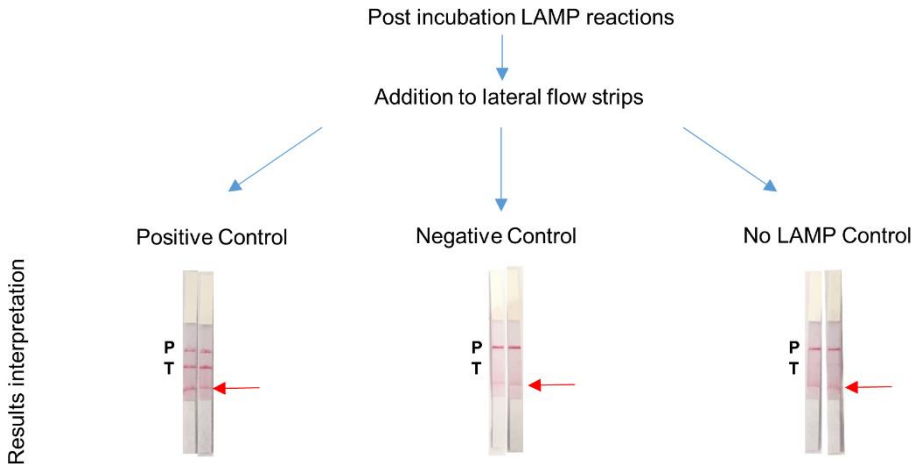

Figure 3.38 Detection of LAMP products based on lateral flow devices
LAMP reactions with the ISO-001 master mix contained 0.8 µM of FIP/BIP, 0.4 µM of FLP/BLP, 0.4 µM of AP and 0.2 µM of F3/B3 primers. The FLP and BLP primers were labelled with FITC and Biotin, respectively to allow for lateral flow LAMP product detection as described in Materials and Methods. The reactions were incubated for 40 minutes at 65°C with the subgenomic replicon template (Positive Control) or no template control (Negative Control). Post-incubation the entire volume of the LAMP reaction was dispensed onto the conjugate pad. The lateral flow strips were topped up with nuclease free water, until the moisture reached the red line (marked by the red arrows). No LAMP Control did not contain any LAMP reactions, but nuclease-free water only. Results were interpreted after 5-10 minutes and photographs taken using a smartphone camera. Letter P indicates the internal positive control line and letter T indicates the test line. One band indicates no amplification and two bands indicate positive amplification of the target.

The next experiment aimed to determine whether the lateral flow strips results correlate with the results from relative fluorescence and gel-electrophoresis end-point detection based on the ISO-001 master mix. Serial ten-fold dilutions of the JFH1 subgenomic replicon were made starting from 4.1 $\log_{10}$ copies/reaction (approximately 12500 copies) and finishing at 2.9 $\log_{10}$ copies/reaction (approximately 390 copies). Figure 3.39 shows that the lowest copy number/reaction detected was the same for each method used – 2.6 $\log_{10}$ copies/reaction In the fluorescence detection significant differences in the TP were detected between the no template control (N) and all reactions containing the JFH1 plasmid at all concentrations ($p<0.0001$).

.

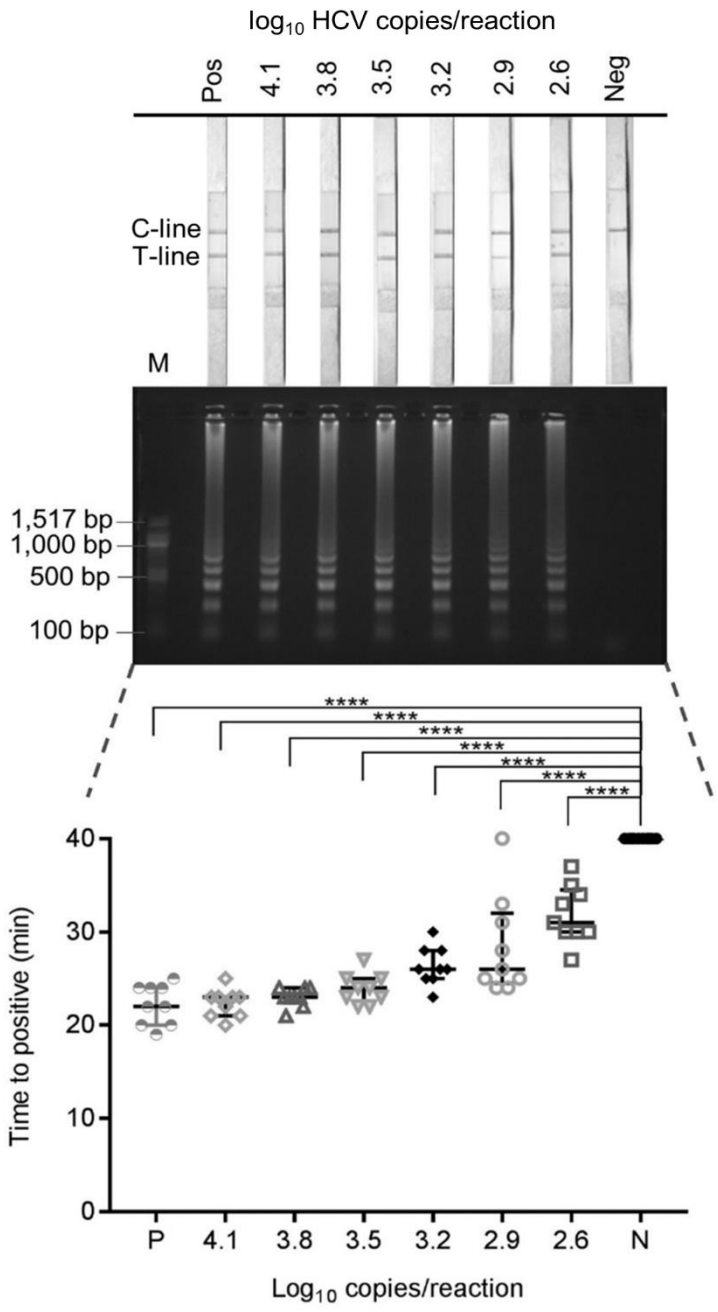

Figure 3.39 Analytical sensitivity of the lateral flow strips compared to other detection methods
LAMP assays were incubated for 40 minutes and the results detected by one of three methods; nucleic acid detection strips (top panel), gel electrophoresis (middle panel) and increase in fluorescence over time (bottom panel). Serial dilutions of plasmid sub-genomic JFH1 replicon were used to determine the analytical sensitivity of the LAMP assay. The figure represents three independent experiments ran in duplicate (gel electrophoresis/lateral flow strips) or triplicate (increase in fluorescence over time. The copy number per reaction (log_{10}) were calculated based on the DNA mass and plasmid length on the NEB online calculator; https://nebiocalculator.neb.com/#!/dsdnaamt, accessed on 25/03/2019. Top panel – positive reactions on the nucleic acid detection strips are indicated by two bands at T and C lines, negative by one band at the C line. T- test line, C – control line Pos – positive HCV control sample, Neg – negative no template control. Middle panel – M indicates 100bp NEB DNA ladder with markers displayed on the left of the bands. Bottom panel - Time to positive in minutes was calculated as ten times increase in standard deviation of fluorescence from mean baseline fluorescence (relative fluorescence units). Experiments were conducted in triplicate and performed three times. Each symbol indicates one LAMP reaction. Black lines indicate median with interquartile range. Negative results were recorded as time to detection of 40 minutes. Statistical analysis was performed using a parametric one-way ANOVA. . * - $p \leq 0.05$, ** - $p \leq 0.01$, *** - $p \leq 0.001$, **** - $p \leq 0.0001$ - P – positive HCV control sample, N – negative no template control.

To validate the LAMP assay results produced on the lateral flow strips, the intensity of each test line and control line from the serial dilution experiment was quantified and compared to the intensity of the test line and control line of the NTC lateral flow strip. Figure 3.40 shows the results displayed as the percentage intensity of the control line divided by the test line from each concentration of template. The percentage intensity of the reactions containing template ranged between 99.5% and 104.0% while the NTC had a mean percentage intensity of 88.0%. Moreover, there were significant differences between all reactions containing template and the NTC ($p<0.0001$).

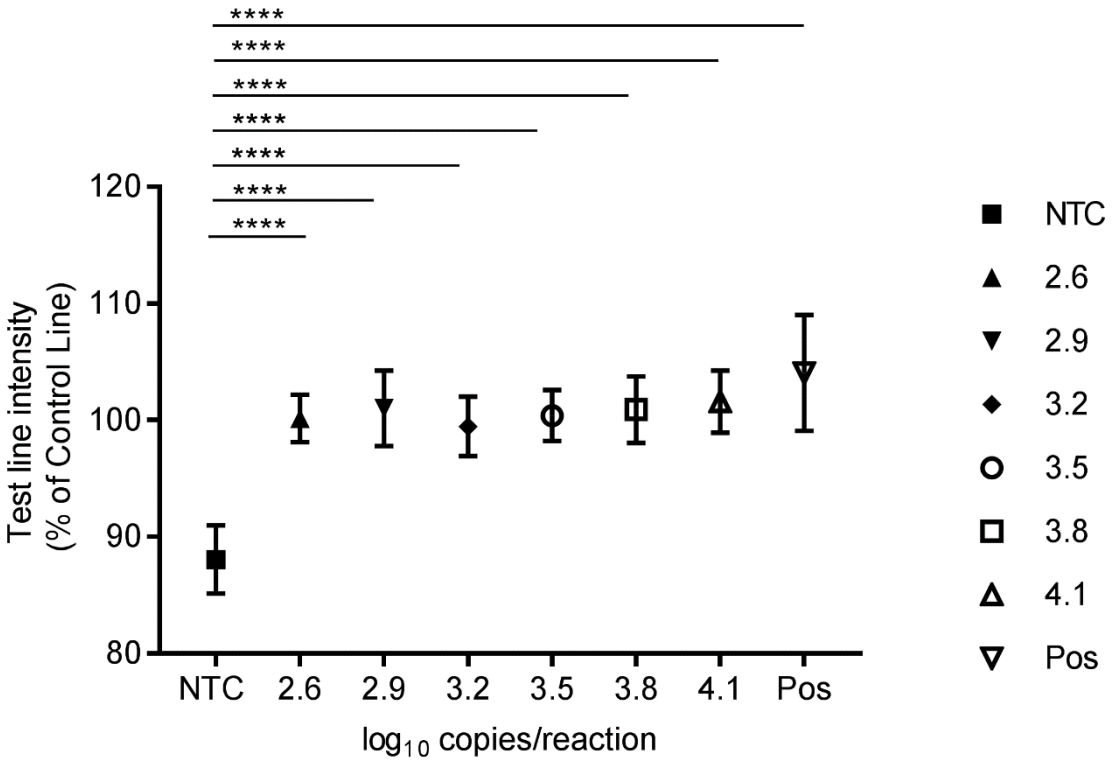

Figure 3.40 Percentage of the test line intensity of the lateral flow strips from serial dilutions of template
Intensity of the lateral flow test lines represented by a percentage of the control line for each concentration of template. The JFH1 plasmid was serially diluted from 4.1 $\log_{10}$ IU/ml to 2.6 $\log_{10}$ IU/ml and included in the LAMP assay reaction. No template control (NTC) was the LAMP master mix reaction containing only water, which acted as the negative control. All LAMP reaction products were added to lateral flow strips and topped up with water. Data represent mean and SD± from three experiments in duplicate. Image J software was used to calculate intensity of each control and test line on lateral flow strips. Statistical analysis between the NTC and template dilutions was performed using a parametric one-way ANOVA with Dunnet's multiple comparisons test. . * - $p \leq 0.05$, ** - $p \leq 0.01$, *** - $p \leq 0.001$, **** - $p \leq 0.0001$, n.s. – not significant, - P – positive HCV control sample, N – negative no template control.

Previous experiments indicated that 30 minutes of incubation produces high sensitivity and specificity. Therefore, the limit of detection of the LAMP assay was calculated based on a 30-minute incubation period. Figure 3.41 shows that at 3.15 $\log_{10}$ copies/reaction (95% CI of 2.96-4.04) there is a 95% probability of obtaining a positive result within the 30 minutes incubation period. Therefore, the limit of detection within 30 minutes was 3.15 $\log_{10}$ copies/reaction or approximately 1426 copies.

A

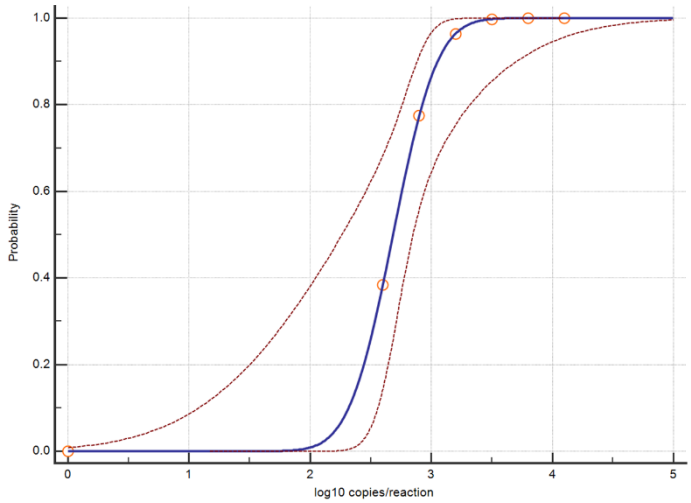

B

Probability	log_{10} Copies/reaction	95% Confidence interval	
0.010	2.01719	0.067351	2.36980
0.020	2.09532	0.33239	2.41800
0.025	2.12220	0.42345	2.43471
0.05	2.21252	0.72880	2.49146
0.10	2.31666	1.07920	2.55852
0.20	2.44275	1.49938	2.64387
0.25	2.49066	1.65695	2.67835
0.50	2.68398	2.26240	2.84796
0.75	2.87731	2.69542	3.19000
0.80	2.92521	2.75885	3.31861
0.90	3.05131	2.88194	3.70105
0.95	3.15544	2.96186	4.03860
0.975	3.24576	3.02469	4.33787
0.980	3.27264	3.04270	4.42763
0.990	3.35078	3.09386	4.68971

Figure 3.41 Determination of the limit of detection based on probit regression analysis
The probit sigmoid dose-response curve was calculated producing values of the dose variable that corresponds to probabilities in MedCalc Software version 19. Data represent grouped variables from previously calculated TP at different concentrations from 0 to 4.1 log_{10} copies/reaction. Replicates with TP of ≤30 minutes at each concentration were converted to number of positives out of a possible nine replicates**. A)** Dose-response graph with concentration in log_{10} copies/ml against probability ranging from 0-1 (blue line) with 95% CI (red lines). Red circles indicate the entered data values**. B)** Dose-response table with limit of detection corresponding to the probability value of 0.95 as based on a previously published definition (Anderson 1989).

3.1.3 Lateral flow device development

The lateral flow nucleic acid detection strips showed that they can easily be interpreted by the naked-eye while also correlating with the results from other detection methods such as gel electrophoresis and fluorescence over time. Thus far, the strips were used separately from the LAMP reaction, leaving them exposed to potential contaminants from reaction to reaction as well as the environment. The next section therefore explores connecting both stages of LAMP reaction –incubation at 65°C and the detection stage by the lateral flow strips – by designing a prototype devices based on laser cutting from acrylic glass otherwise known as Poly (methyl-methacrylate) or PMMA.

3.1.3.1 Single test devices

Initial lateral flow devices were designed as single tests enabling them to fit into standard heat block racks for Eppendorf tubes thus allowing an easy incubation step. Preliminary designs were modified from templates received through personal communication (Miss Alice Garrett). Figure 3.42 shows the first two designs containing the LAMP chamber connected to the chamber containing the lateral flow strip through a thin channel. Throughout the incubation period of 30 minutes at 65°C, the bottom portion of the device containing the LAMP chamber was inserted into a heat block or water bath while the lateral flow strips remained at room temperature. Evaporation was prevented by the use of valves (chambers filled with oil or filter paper) to stop leakage of moisture to the lateral flow strips prior to finishing the LAMP reaction. The water chamber is located at the extreme end of the channel away from the lateral flow chamber, which acts as a finger pump following the incubation period. Applying pressure on the water chamber allows the liquid to travel upward carrying LAMP products towards the lateral flow strips, which can then be used for detection purposes. The final part of each design consists of a top layer with inlets for inserting liquids into the Water and LAMP chambers. The two layers were sealed together with acetone as described in Materials and Methods. Following the addition of liquids to all chambers, both sides of the devices were sealed by PCR cover films to prevent evaporation and leakage. While Design 1 could be inserted into an Eppendorf rack in a water bath or heat block, the devices produced were prone to breaking due to the large water chamber (Figure 3.42). Thus, Design 2 had a

narrower, more elongated chamber which successfully prevented breakages. The inlets were also reduced in size. Design 2's LAMP and water chambers were filled with a coloured dye to inspect for leakage and evaporation of liquid during an incubation period at 65°C for 15 minutes. Evaporation of the liquid was apparent and the insertion of the liquids through the inlets created air bubbles suggesting further optimisations of the designs would be required.

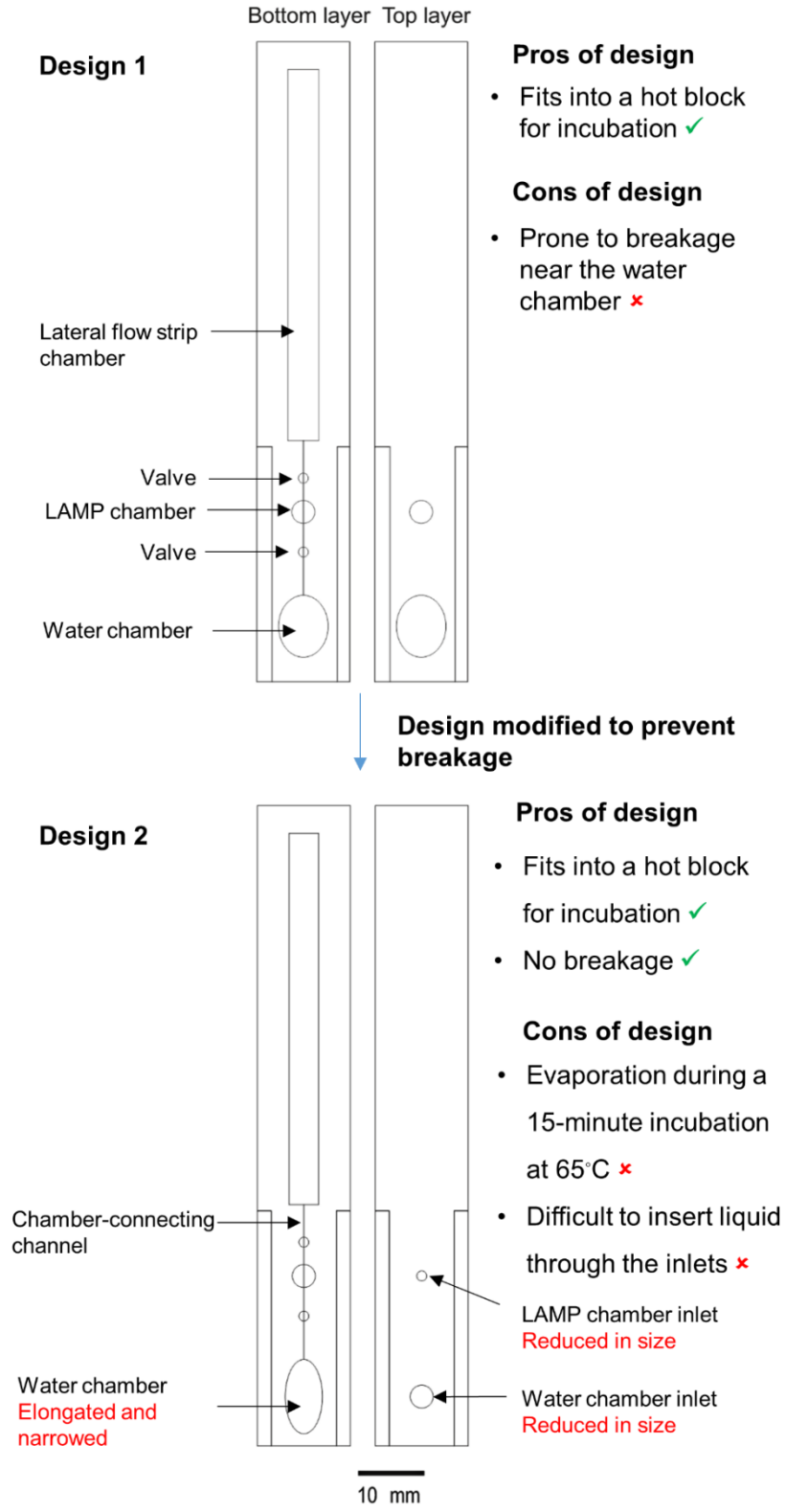

Figure 3.42 The pros and cons of the first two single lateral flow devices
The two lateral flow devices, Design 1 and Design 2, consisted of two laser-cut layers of 2mm-thick PMMA joined together by acetone and incubated under a heavy weight at room temperature for 24 hours. Devices were designed in CorelDraw software Version 2013. Red text indicates the modifications made to the design to improve the function of the device. The water chamber could hold up a volume of 100 µl of water while the LAMP chamber had a capacity of 25 µl.

Designs 3 and 4 contained improvements from the initial lateral flow devices as shown on Figure 3.43. To prevent evaporation, the valves in Design 3 were filled with paraffin wax instead of oil/filter paper. The inlets were also increased in size to allow for easier insertion of liquids into the reaction chambers. While the paraffin wax successfully prevented evaporation during a 65°C incubation, it blocked the channel due to melting and upright position of the device during the reaction. This blockage prevented the finger pump from functioning and therefore these lateral flow devices could not be used for detection of LAMP products. Furthermore, insertion of liquid remained challenging and often resulted in overflowing of the chambers despite the increased size of the inlets. In addition, while the lateral flow devices were inserted into the water bath/heat block, the LAMP chamber was exposed above water/metal. To prevent blockage and evaporation, Design 4 was modified by inserting parafilm into the valves. The LAMP chamber was elongated and narrowed to allow for easier insertion of the master mix and template. It was also moved downwards along with the corresponding inlet in order to keep the entire reaction at constant temperature below the metal or water surface in the heat block/water bath, respectively. While evaporation and blockage were successfully prevented by the insertion of parafilm, leakage of the devices were frequent and insertion of liquid through the inlet to the LAMP chamber remained challenging.

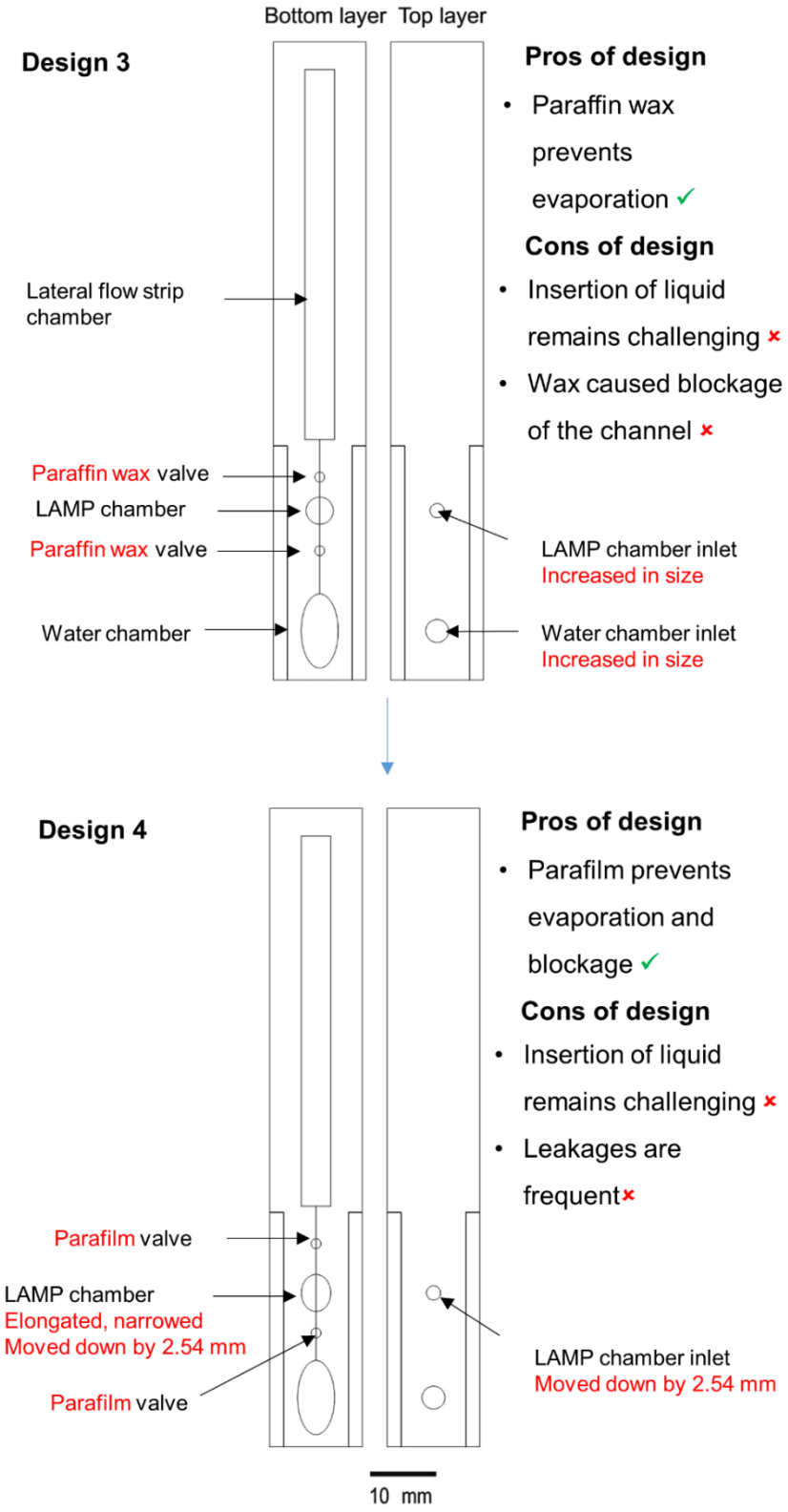

Figure 3.43 Improvements to the single test lateral flow devices
The two lateral flow devices, Design 3 and Design 4, consisted of two laser-cut layers of 2mm-thick PMMA joined together by acetone and incubated under a heavy weight at room temperature for 24 hours. Devices were designed in CorelDraw software Version 2013. Red text indicates the modifications made to the design to improve the function of the device. The Water chamber could hold up a volume of 100 µl of water while the LAMP chamber had a capacity of 25 µl.

3.1.3.2 Multiple test devices

Since all LAMP reactions were run in parallel with positive and negative controls, a minimum of three lateral flow strips were required per sample. Therefore, the next design focused on including four lateral flow strips, one for positive control, one for negative control and two for the sample run in duplicate. Since the previous acetone-sealed devices were prone to leaking, the multiple test device consisted of one layer of PMMA sealed on both sides by acetate films (Figure 3.44). To prevent problems with evaporation, the water and LAMP chambers were joined together into one chamber. The channel was also reduced in length to allow the LAMP products to be easily propelled into the lateral flow chamber following the incubation period. The device on Figure 3.44 was evaluated by incubating at 65°C for 30 minutes with a green food dye to allow for monitoring of evaporation. The results indicate that while none of the lateral flow devices started prematurely, evaporation into the lateral flow chamber was apparent.

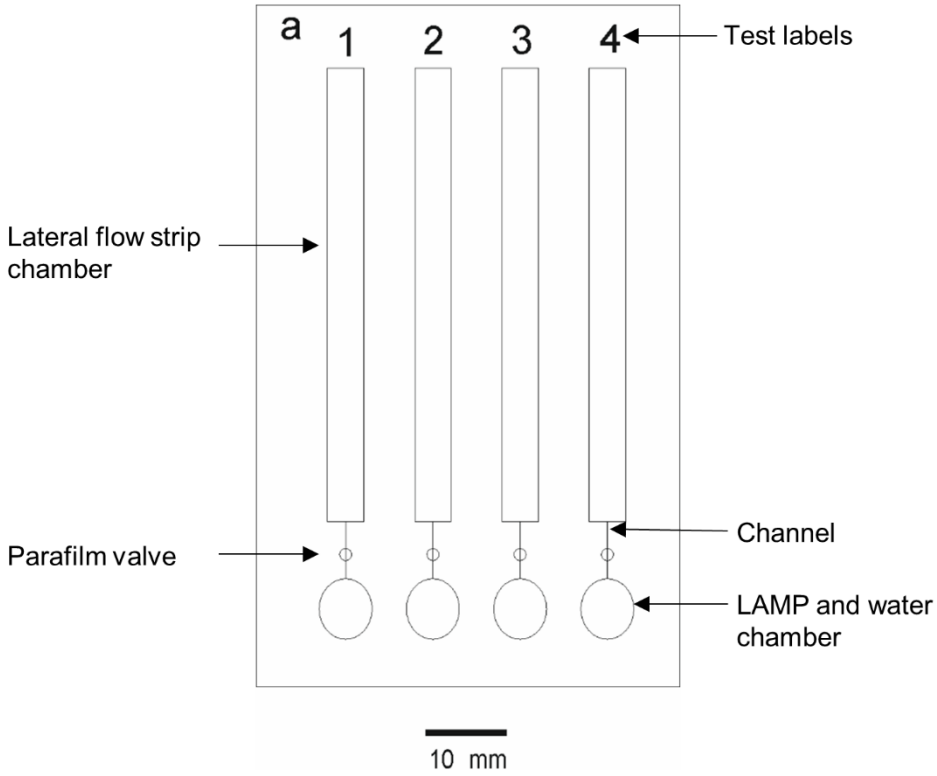

Figure 3.44 The first design of a multiple test lateral flow device
The lateral flow device was designed using CorelDraw software Version 2013 and laser cut out of 2mm-thick PMMA. The device consisted of four lateral flow chambers and LAMP reaction chamber with a single channel and a parafilm valve. The two sides of the device were sealed with acetate films with the inlet for insertion of liquid cut out with 2mm-thick biopsy puncher. Following the addition of the master mix and template (50 µl in total) into the LAMP/water chamber the device was sealed with another layer of PCR plate cover.

To prevent the problems associated with evaporation the next lateral flow devices were modified by elongating the channel connecting the LAMP chamber and the lateral flow chamber (Figure 3.45). While this design successfully prevented evaporation one of the four lateral flow strips could not be activated during the experiment – the water from the water chamber could not be entirely moved onto the lateral flow strip by the finger pump. Furthermore, the LAMP/water chamber could hold up to 100 µl of liquid – four times the amount of LAMP master mix used in previous experiments.

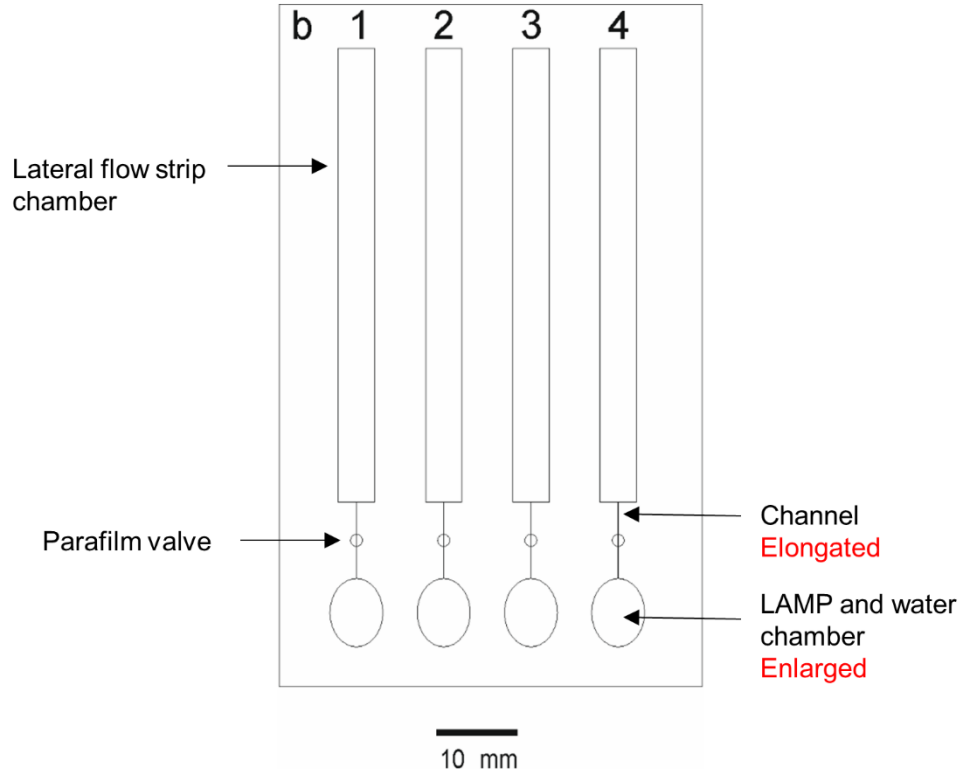

Figure 3.45 The second design of a multiple test lateral flow device
The lateral flow device was re-designed using CorelDraw software Version 2013 and laser cut out of 2mm-thick PMMA. The device consisted of four lateral flow chambers and LAMP reaction chamber with a single channel and a parafilm valve. The channel was elongated and the LAMP chamber enlarged. The two sides of the device were sealed with acetate films with the inlets for insertion of liquid cut out with 2mm-thick biopsy puncher. Following the addition of the master mix and template into the LAMP/water chamber (100 µl in total) the device was sealed with another layer of PCR plate cover.

In order to reduce the volume of LAMP reaction used the LAMP chamber and water chamber were separated in the next design (Figure 3.46). Two parafilm valves were included on either side of the LAMP chamber to prevent evaporation. Despite this, one of the lateral flow strips started to run prior to the end of the incubation period because of excessive evaporation. Therefore, an alternative approach to parafilm as a valve was evaluated in future lateral flow devices.

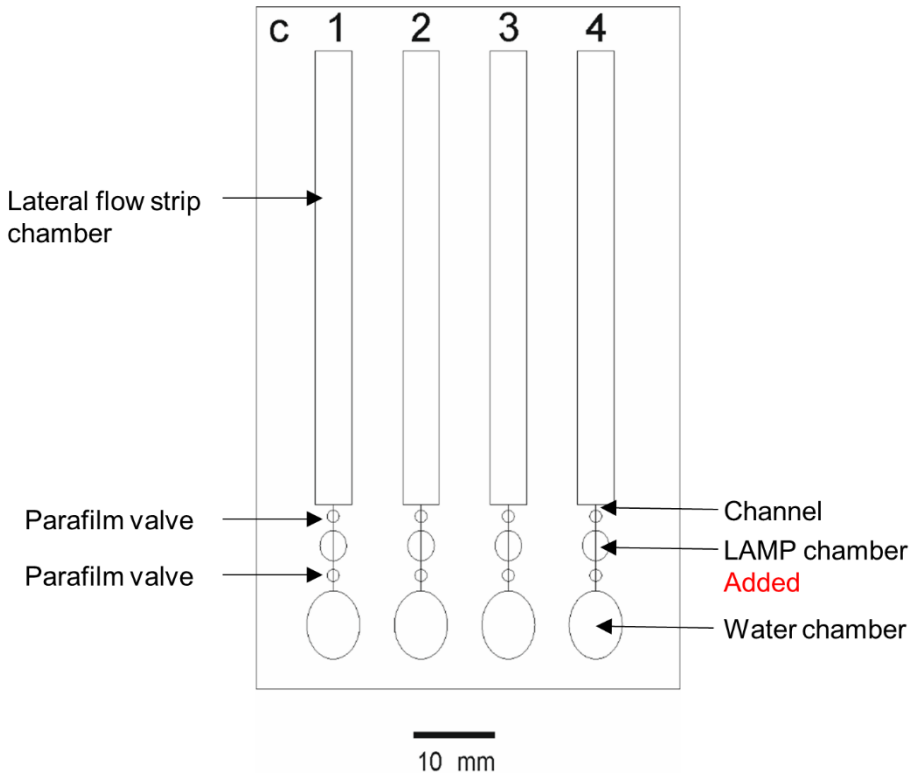

Figure 3.46 The third design of multiple test lateral flow device
The lateral flow device was designed using CorelDraw software Version 2013 and laser cut out of 2mm-thick PMMA. The device consisted of four lateral flow chambers and LAMP reaction chamber with a single channel and a parafilm valve. The device was improved by separating the water and LAMP chamber into two separate chambers. The two sides of the device were sealed with acetate films with the inlets for insertion of liquid cut out with 2mm-thick biopsy puncher. Following the addition of the master mix and template into the LAMP (25 µl in total), and water into the water chamber (100 µl), the device was sealed with another layer of PCR plate cover.

The final lateral flow device eliminated the use of valves and parafilm by using an elongated and curved channel connecting the LAMP chamber and the water chamber (Figure 3.47). An additional channel was added between the LAMP chamber and the lateral flow chamber to eliminate the risk of evaporation. To solve the issue with insertion of LAMP reagents the LAMP chambers were reshaped to resemble a rectangle rather than oval or circle. The water chamber was also elongated and less liquid was added as a final precaution for evaporation issues (80 µl instead of 100 µl). Due to elongations of several elements in the design the entire device was elongated. This design provided consistent results between experiments involving incubations at 65°C and LAMP reactions with positive and no template controls and was therefore used in future experiments.

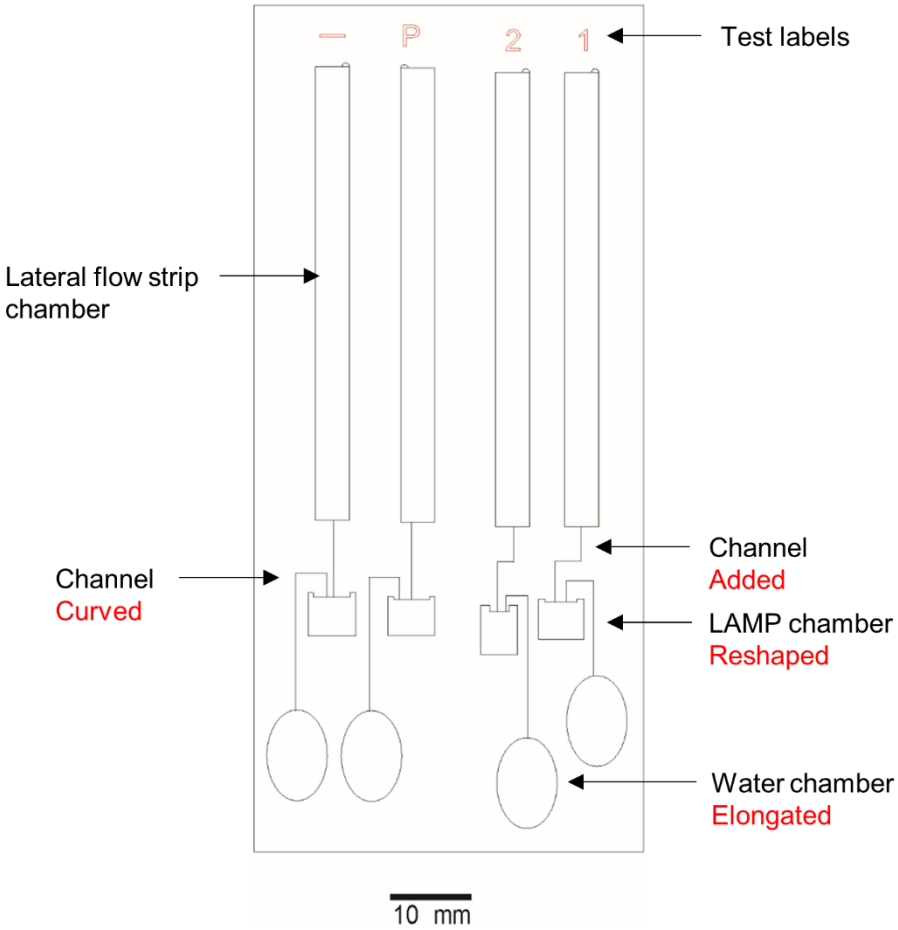

Figure 3.47 The final lateral flow design
The lateral flow device was designed using CorelDraw software Version 2013 and laser cut out of 2mm-thick PMMA. The device consisted of four lateral flow chambers and LAMP reaction chamber with two channels. The device was improved by changing the shape of the LAMP chamber to a rectangle and elongating and curving one of the channels to prevent evaporation. The two sides of the device were sealed with acetate films with the inlets for insertion of liquid cut out with 2mm-thick biopsy puncher. The inlet for the insertion of liquid was cut out on the opposite side to the LAMP chamber inlet. Following the addition of the master mix and template into the LAMP (25 µl in total), and water into the water chamber (80 µl), the device was sealed with another layer of PCR plate cover on both sides of the device. The device was based on a template provided by Dr Xiaoxiang Yan. Modifications were applied with help of Dr Shantimoy Kar.

The workflow of the LAMP reaction incubation within the lateral flow devices is illustrated on Figure 3.48. Briefly, after the insertion of lateral flow strips into the appropriate chambers the device is sealed with acetate film on both sides. The chambers are prefilled through 2 mm diameter holes on either side of the devices with 80 µl of water (water chamber), 20 µl of LAMP master mix and 5 µl of template (LAMP chamber). The inlet holes are then sealed on both sides of the device with a strip of acetate film. The entire device is inserted into a heat block or water bath for 30 minutes at 65°C. Following the incubation period, the device is inverted and the lateral flow strips started by pressing on the water chamber now acting as a water pump. The results are read within 5 to 10 minutes.

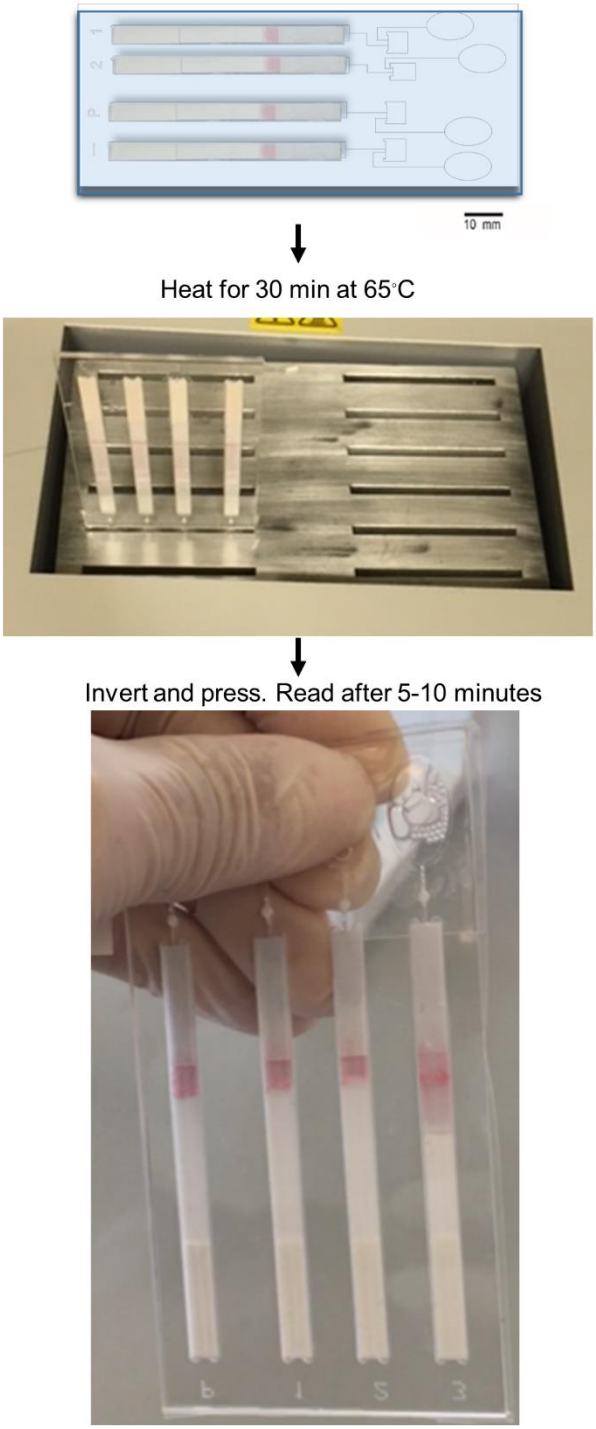

Figure 3.48 The workflow for LAMP reaction incubation in the lateral-flow devices
Following the addition of lateral flow strips, the LAMP master mix, template and water are inserted through the inlet holes on either side of the device. The entire device is sealed with acetate film (blue layer) and inserted upright into a heat block for 30 minutes at 65°C. Following the incubation period the device is removed, inverted and pressure applied on each water chamber until the liquid reaches the conjugate pad line (marked red on the lateral flow strips). The lateral flow strips are left for 5-10 minutes to develop and results are read within 5-10 minutes.

3.1.4 Development of a point-of-care extraction system

The development of the HCV LAMP-based POC test demonstrated the ability to detect LAMP products from template with minimal equipment namely, a water bath and nucleic-acid detection strips for naked-eye based product detection. However, for a complete sample to answer POC test an efficient extraction system is required with minimal or no laboratory equipment. Therefore, the next experiments looked into the development of an efficient extraction platform including the use of microfluidic devices and detection of products directly from raw sample material.

3.1.4.1 Evaluation of LAMP amplification from serum samples

Before proceeding with the development of an extraction system, it was important to evaluate whether LAMP can amplify nucleic acid directly from raw sample material. For this purpose, the first experiment involved spiking serial ten-fold dilutions of JFH1 plasmid (10^5, 10^6 and 10^7 copies/reaction) into serum from a healthy donor. Figure 3.49 shows that serially diluted JFH1 in water had decreasing TP with increasing concentration of template; NTC with median TP of 45 minutes, 10^5 copies/reaction with median TP of 21 minutes, 10^6 copies/reaction with median TP of 18 minutes and 10^7 copies/reaction with median TP of 15 minutes. Significant differences were observed between the NTC and 10^6 copies/reaction ($p=0.0104$) and 10^7 copies/reaction ($p<0.0001$) and between 10^5 copies/reaction and 10^7 copies/reaction ($p=0.0273$). When the template was diluted in serum the median TP was delayed in some cases with no amplification occurring at all; NTC with median TP of 45 minutes, 10^5 copies/reaction with median TP of 41 minutes, 10^6 copies/reaction with median TP of 36 minutes and 10^7 copies/reaction with median TP of 31 minutes. The same was also true for the template diluted in heat-inactivated serum with median TP of NTC of 45 minutes, 42.5 minutes in 10^5 copies/ml and 45 minutes for both 10^6 and 10^7 copies/reaction with no amplification occurring in the last two. No significant differences in median TP were noted in either serum or heat-inactivated serum samples. However when Triton X-100 was added to the serum samples, amplification with significant differences in median TP was observed. The NTC had a median TP of 45 minutes while the 10^5 copies/reaction, 10^6 copies/reaction and 10^7 copies/reaction had a median TP of 44, 38 and 35

minutes, respectively. Significant differences were observed between the NTC and 10^6 copies/ml ($p=0.0180$) and 10^7 copies/reaction ($p<0.0001$) and between 10^5 copies/reaction and 10^7 copies/reaction, the same as in the water diluent. Therefore, while Triton X-100 in serum did result in amplification extraction methods for a portable HCV POC test were explored in order to improve the TP.

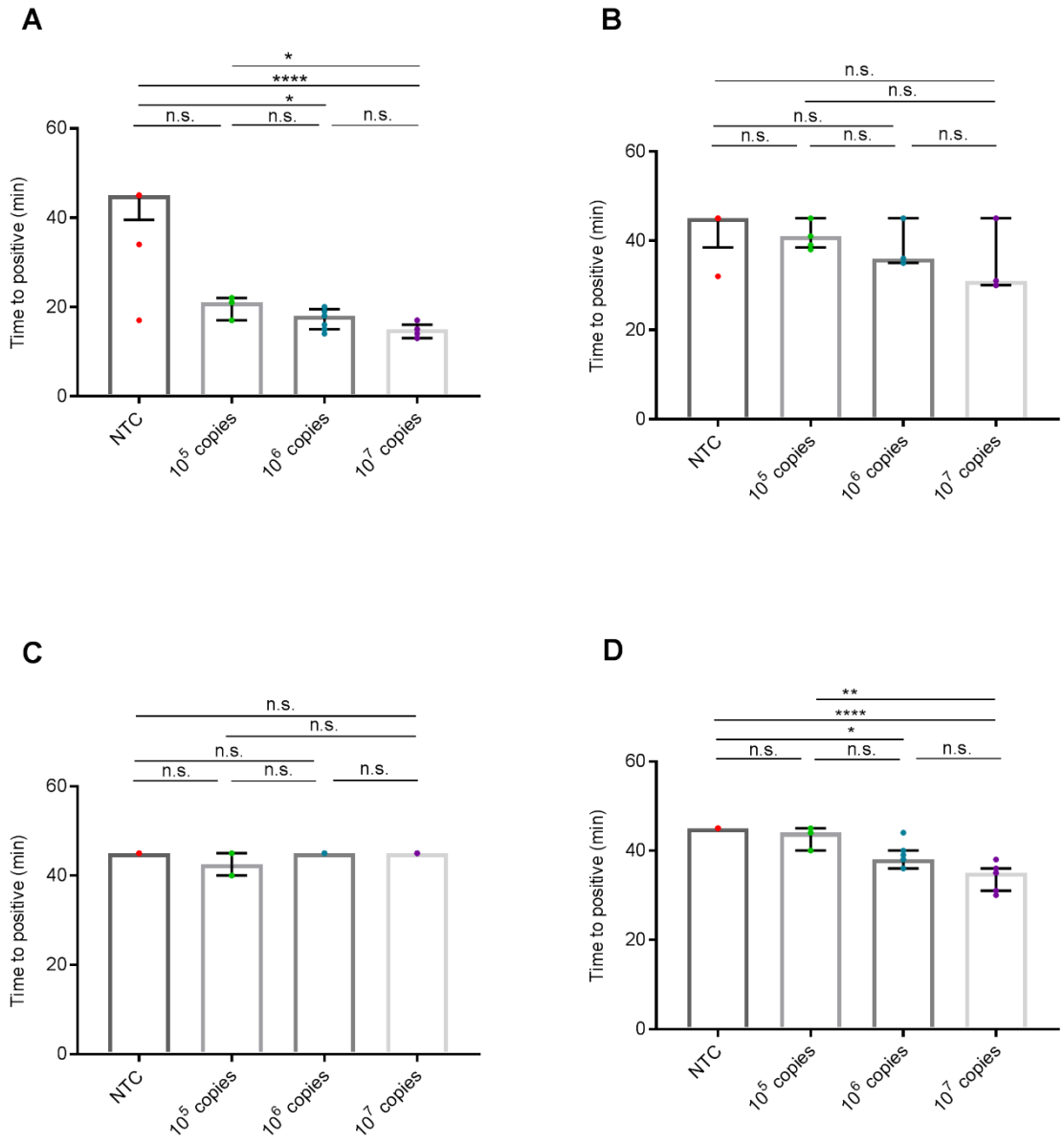

Figure 3.49 Evaluation of LAMP amplification from spiked serum samples
Healthy serum sample or water were spiked with serial 10-fold dilutions of JFH1 plasmid at 10^5 copies, 10^6 copies and 10^7 copies/reaction. LAMP reactions contained 2 µl of template and the following primer concentrations: 0.8 µM of FIP/BIP, 0.4 µM of FLP/BLP, 0.4 µM of AP and 0.2 µM of F3/B3 primers LAMP reactions were incubated for 40 minutes at 65°C and changes in fluorescence recorded every minute cycle. Lines indicate median with interquartile range. No amplification was recorded as TP of 45 minutes. Graphs represents two independent experiments in triplicate or duplicate (Graph C). Statistical analysis was performed using a non-parametric Kruskal-Wallis with Dunn's multiple comparisons test. * - $p \leq 0.05$, ** - $p \leq 0.01$, *** - $p \leq 0.001$, **** - $p \leq 0.0001$, n.s. – not significant. A) Nuclease-free water used as diluent for spiking JFH1 at different concentrations. NTC is no template control. B) Healthy control serum used as diluent for spiking JFH1 at different concentrations. C) Heat-inactivated healthy control serum used as diluent for spiking JFH1 at different concentrations. Heat inactivation was carried out at 56◦C for 30 minutes. D) Serum with 0.05% Triton-X 100 used as diluent for spiking JFH1 at different concentrations.

3.1.4.2 Magnetic bead-based extraction

Since the lateral flow detection method was based on a laser-cut PMMA device, the preliminary extraction devices were made using the same method. The principle relied on creating different chambers for each stage of the RNAdvance RNA extraction protocol excluding the DNAse stage and the last two washes. The nucleic acid extracted can be transported between the different chambers by the use of magnetic beads and a strong magnet. Figure 3.50 shows a prototype PMMA device with four layers stacked together and attached with the use of acetone. The top layer was sealed with acetate film following the insertion of dyed liquids and clear water solution separated by thin channels filled with paraffin wax (Figure 3.50b). The use of paraffin wax and acetone sealing prevented leakages between the different compartments even when the entire device was moved and inverted. Following the incubation period at 65°C for 5 minutes the paraffin wax melted allowing for the mixture of liquids as is evident by the colour changes in the chambers. However, the melted paraffin wax has entered the elution chamber contaminating the solution. Therefore, an improvement of the device was required.

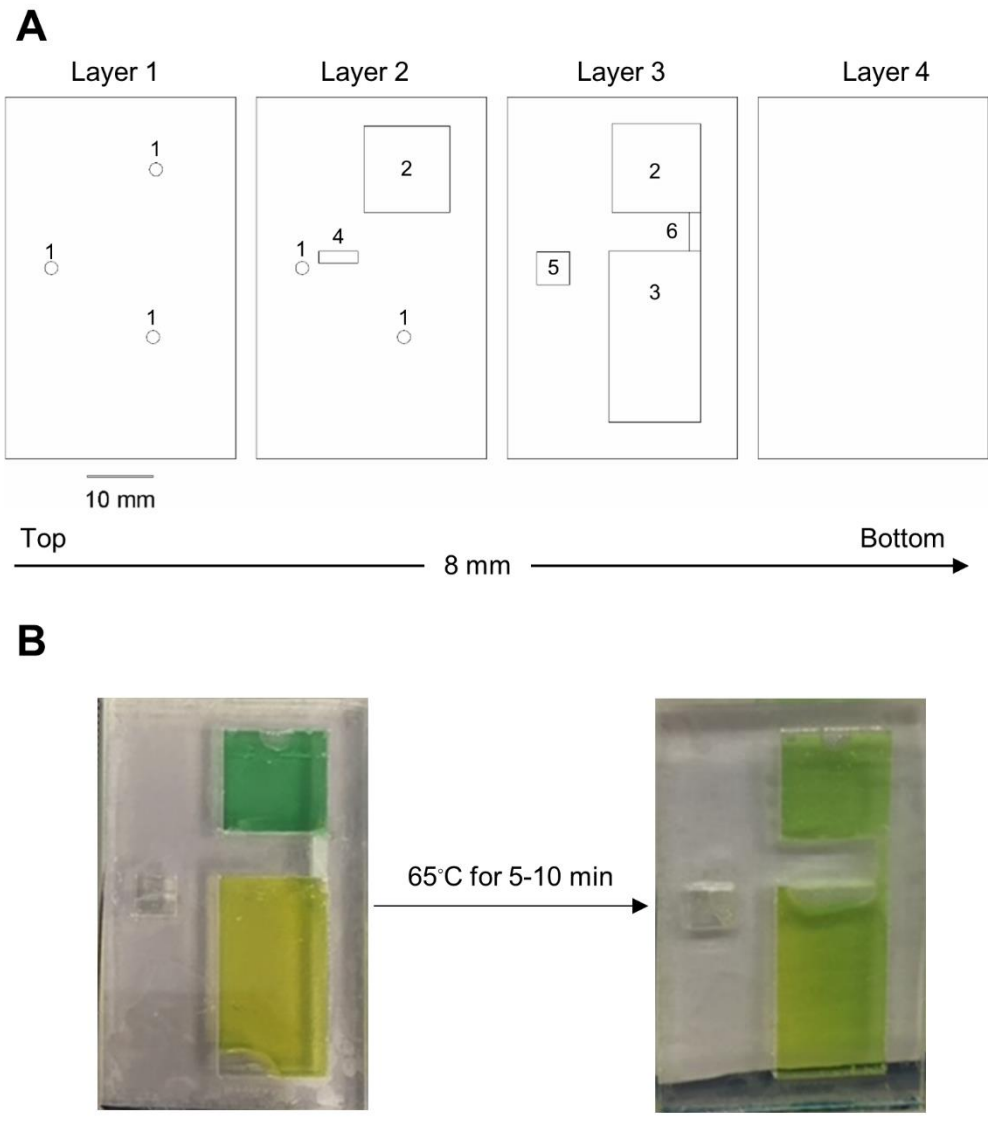

Figure 3.50 The use of paraffin wax as a valve in PMMA-based nucleic-acid extraction devices
A) The diagram shows a prototype laser-cut PMMA device for nucleic acid extraction consisting of four layers stacked on top of each other. The arrow indicates the direction of stacking of 2mm-layers from top to bottom and sealed together with acetone. The numbers indicate different elements of the device required for the RNA extraction; 1 – inlets for insertion of liquids, 2 – lysis chamber, 3 – wash chamber, 4 – channel connecting chambers, 5 – elution chamber and 6 – channel connecting lysis and wash chambers. B) The picture shows the assembled device sealed on one side with acetate film with green and yellow dyes inserted into lysis and wash chambers, respectively. The connecting channel was pre-filled with paraffin wax to prevent mixture of liquid. Following the incubation at 65◦C for 5 minutes the wax melts and the liquids mix.

The next device eliminated the use of paraffin wax as a valve in channels. The fluidic manipulation was instead controlled by narrowing of the channels connecting chambers and the use of acetate film to allow for finger pumps to be incorporated into the device. Figure 3.51 shows the proposed devices A-D with different channel widths – 0.6 mm, 0.8 mm, 1.0 mm and 1.2 mm. The device chambers were reshaped to resemble circular shapes rather than rectangles which prevented trapping of magnetic beads between the different extraction stages. The layers were reduced from four to two covered with acetate films once again facilitating the use of pressure-induced fluidic manipulation via finger pumps. Despite the use of acetate films and fewer PMMA layers the liquid did not flow freely between the lysis chamber and binding chamber. Moreover, applying pressure to the lysis chamber facilitated leakage. The chambers accommodated smaller volumes than the ones stated in the RNAdvance protocol; 100 µl for the lysis chamber, 300 µl for the bind chamber and 200 µl for wash chamber. Thus, further device improvements were required to resolve the above-mentioned problems. Channel widths were modified to 1.5 mm, 2.0 and 2.5 mm with the 2.5 mm allowing for free movement of liquid between the lysis chamber and the bind chamber once the device was upright.

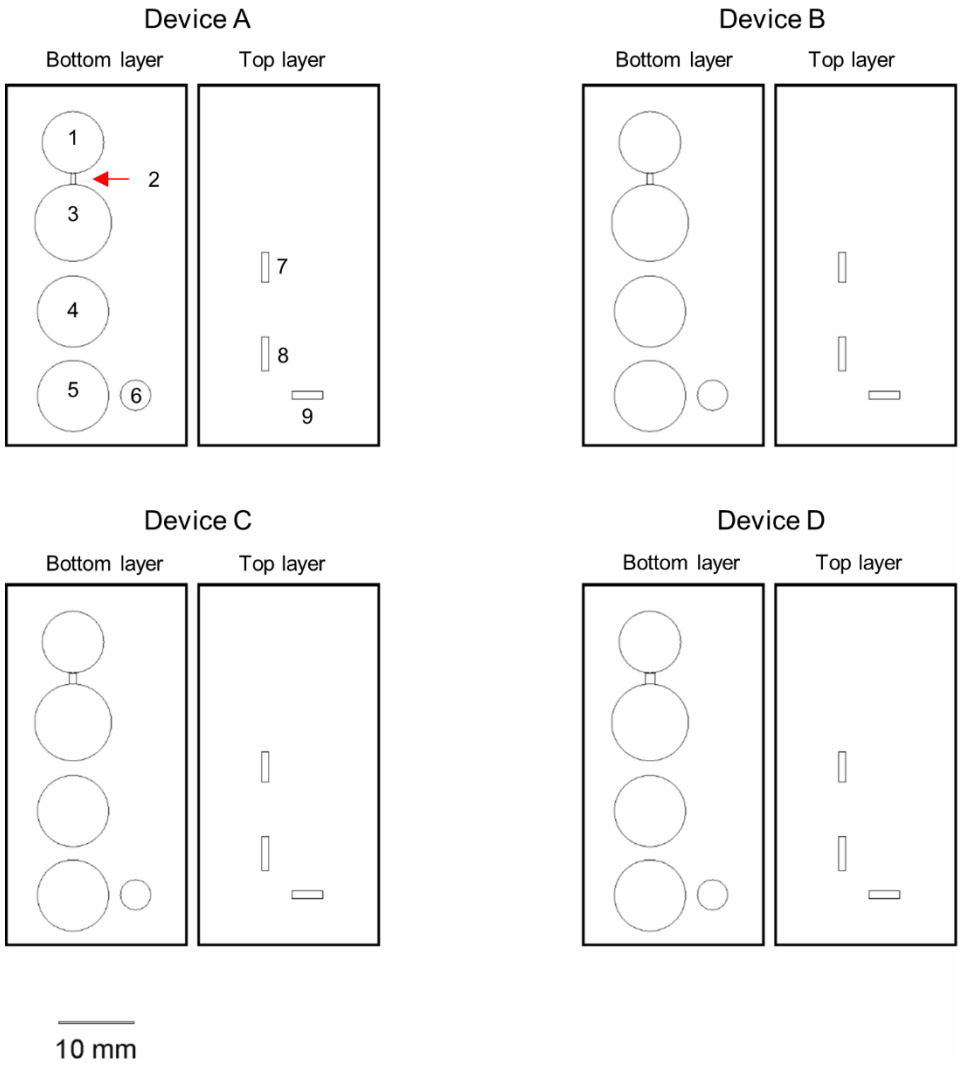

Figure 3.51 Alterations of width of channels for fluidic manipulation between the chambers
The improved PMMA-extraction device contained circular-shaped chambers and two 2-mm layers sealed with acetone and covered with acetate films. The numbers indicate different elements of the PMMA device, namely; 1 – lysis chamber, 2 - connecting channel 3 – bind chamber, 4 –wash 1 chamber, 5 – wash 2 chamber, 6 – elution chamber, 7-9 – channels connecting chambers. Devices A-D differed in the widths of the channel indicated by the red arrow; 0.6 mm, 0.8 mm, 1.0 mm, 1.2 mm, respectively.

The next device tested more channel widths by checking the following three; 2.2 mm, 2.3 mm and 2.4 mm (Figure 3.52). The wash chambers and the elution chamber were moved sideways to prevent the mixing of the solutions, particularly the wash solutions and elution. In addition, the elution chamber was moved to the top layer while all the remaining chambers remained on the bottom. Inlets were inserted into the design to insert the liquids into the different chambers. An additional dry chamber was inserted in the top layer next to the elution chamber to prevent the wash solution from mixing with the elution. The chambers could now accommodate larger volumes as the bottom layer's thickness was changed from 2 mm to 3 mm and the shapes on designs

were enlarged. The 2.4 mm was the only width of channel which allowed free-movement of solutions between the chambers although only upon applying additional pressure on the acetate film. Therefore, the 2.5 mm width was kept for future devices. Upon the addition of beads into the bind chamber (No. 3) some magnetic beads were left behind on the sides of the chambers when a magnet was applied. In addition, magnetic beads reached the elution chamber only in Device C although not completely dry. Therefore, further changes were required to resolve the above-mentioned issues.

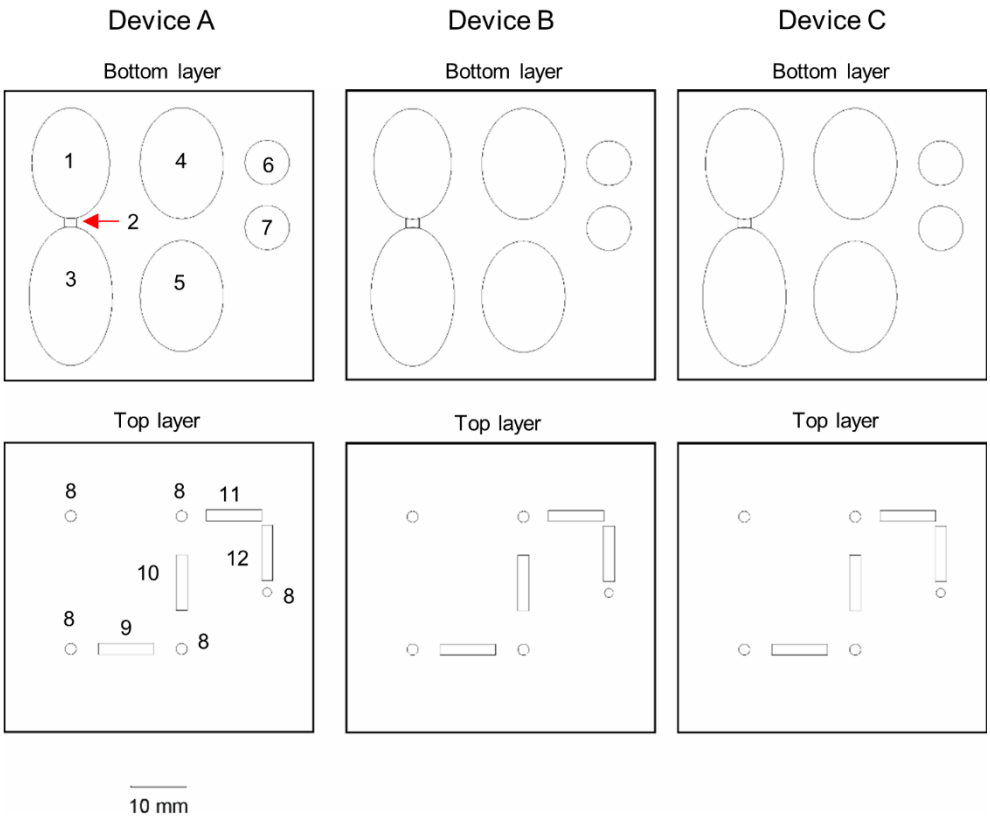

Figure 3.52 Further optimisations of the PMMA-device accommodating for larger buffer volumes
Diagrams represents three devices (A, B, C) with different widths of the channel connecting lysis and binding chambers (2.2 mm, 2.3 mm and 2.4 mm, respectively). The red arrow points to the modified channel. The device volumes were increased by changing the thickness of the bottom layer from 2 mm to 3 mm and enlarging the chambers. The top layer was 2 mm-thick and was sealed with acetone to the bottom layer. The assembled device was sealed with two layers of acetate films. The numbers indicate different compartments of the devices; 1- lysis chamber, 2 – channel, 3 – bind chamber, 4 –and 5 – wash 1 and 2 chambers, 6 – dry chamber 7 – elution chamber, 8 – inlets for inserting liquid, 9-12 – connecting channels.

The next device's channels were modified by including a funnel-shape at the entry point to prevent magnetic beads from trapping between the chambers (Figure 3.53). In addition, all channels were moved to the bottom layer while the elution channel and dry chamber stayed on the top. Contamination of the elution chamber was prevented by keeping the dry chamber and by the addition of two additional neighbouring chambers – the LAMP chamber and the water chamber. The purpose of the water chamber was to propel the elution onto the magnetic beads once they reach the dry chamber and then directly into the LAMP master mix once pressure is applied. Following the assembly of three devices mixing of the lysis and bind solutions were only possible when the device was tilted sideways and pressure applied to the lysis chamber. It was also noted that liquids could move more freely to chambers underneath them rather than to chambers located to the side. While some beads managed to reach the dry chamber they could not be moved by pressure or magnet to the LAMP chamber. Some also carried residual wash buffer to the dry chamber upon assistance with the magnet. No water entered the dry chamber upon applying pressure to the water chamber, eliminating the possibility of efficient elution. Therefore, more changes were made to the designs for future extraction devices.

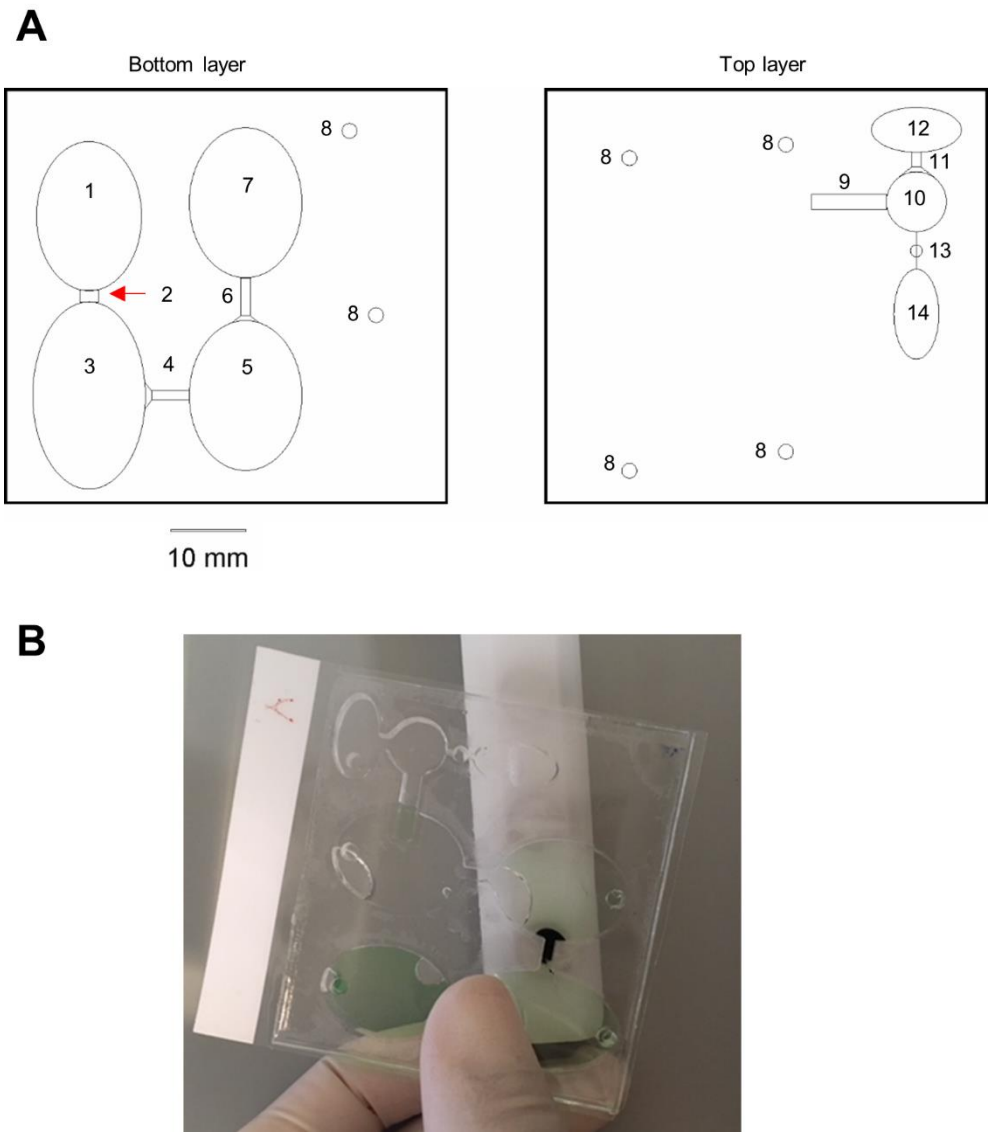

Figure 3.53 Prevention of contamination in the elution chamber and the movement of magnetic beads
A) Diagram shows the modified device consisting of two layers of PMMA sealed together with acetone and covered with acetate films on either side. The channel connecting bind chamber and lysis chamber had a width of 2.5 mm. The entry points of the channels contained funnels to allow for movement of magnetic beads. The numbers indicate different compartments of the device, 1 – lysis chamber, 2 – connecting channel, 3 – bind chamber, 4 – funnel channel, 5 wash chamber 1, 6 – funnel channel, 7 – wash chamber 2, 8 – inlets for inserting liquid, 9 connecting channel, 10 – dry chamber, 11 – funnel channel, 12 – LAMP chamber, 13 – channel with paraffin valve, 14 – water chamber. **B**) The demonstration of movement of magnetic beads through the funnel channel with the assistance of a magnet.

The final design of the PMMA-based nucleic-acid extraction device integrated the lateral flow detection strip on the top layer of the device (Figure 3.54). The lysis and LAMP chambers were intentionally protruding to allow for insertion into a heat block for the incubation stages. The chambers were enlarged to compensate for the insertion of 200 µl of sample material into the lysis chamber. The lysis and bind chamber were separated by a valve containing agarose gel, allowing for the solutions to mix only upon incubation of the lysis stage of the extraction procedure. A mock extraction test was performed by inserting

nuclease-free water as sample and all buffers required for the RNAdvance extraction protocol into the chambers (excluding the DNase stage and two subsequent washes). The acetate film covering the lysis buffer was prone to leaking especially upon applying pressure following the incubation period. The solutions of the lysis chamber could only be mixed with the bind solution upon shaking the device in a sharp-downward motion. The agarose gel has successfully separated the two layers until after the lysis incubation but the movement of magnetic beads was restricted to the bottom layer of the device. Only some of the beads reached the LAMP chamber. Therefore, alternative approaches to RNA extraction were explored which are discussed in the next section.

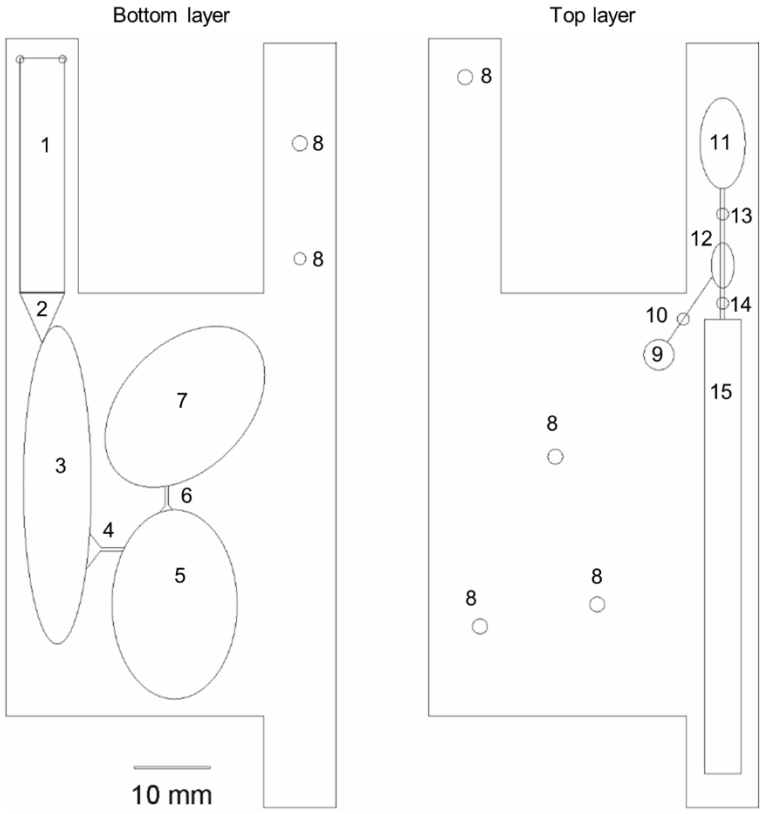

Figure 3.54 Integration of the lateral flow strip with the PMMA-based extraction device
The prototype extraction device was integrated with a single nucleic-acid detection strip on two different layers. The extraction layer was 3 mm thick and the lateral flow layer was 2 mm thick. The device was assembled by sealing the two layers with acetone and covering both sides with acetate films. The numbers indicate different compartments of the device; 1 – lysis chamber, 2 – agarose gel valve, 3 – bind chamber, 4 – funnel channel, 5 – wash 1 chamber, 6 – funnel channel, 7 – wash 2 chamber, 8 – inlets for inserting liquids, 9 – entry chamber, 10 – connecting channel with paraffin valve, 11 – water chamber, 12 – LAMP chamber, 13, 14 – connecting channels with paraffin valves, 15 – lateral flow chamber.

3.1.4.3 Origami-based paper extraction

The alternative method of extraction was based on a filter-paper based microfluidic device as described previously for DNA testing (Xu, Nolder, et al. 2016) (See Materials and Methods). This method relies on printing wax on filter paper where the black patterns represent hydrophobic water-repellent areas and white represent the hydrophilic, 'water-loving' areas. The printed pattern and appropriate folding allows for the manipulation of liquids in predefined manner hence the name 'origami'. Figure 3.55 shows the folding pattern required for the extraction of nucleic acid from raw sample material such as blood and plasma while Figure 3.56 shows the attachment of the paper device with the lateral flow detection device. The lysis of the raw material is carried out in an Eppendorf tube where magnetic beads are added. Following vigorous mixture of the raw material with magnetic beads the magnetic beads are transferred onto the paper device (white circle on panel 5) with the wash panel (no. 6) folded underneath on top of absorbent material (such as tissue paper). Wash buffer is added onto the magnetic beads allowing for impurities to be captured into the area underneath and the absorbent material. The wash panel (no. 6) is torn off and the magnetic beads are folded over onto panel 4, which is subsequently folded onto panel 3 and 2. Elution buffer is subsequently added onto the magnetic beads and the nucleic acid is carried in a downward manner towards panel 2. The eluted nucleic acid is captured by filter paper cut out into circular discs (4 mm in diameter) which are placed directly underneath the hydrophilic circles on panel 2. Panel 1 serves as a guide which allows the paper device to be attached onto the lateral flow device. The guide panel sits underneath the plastic device and is attached by double-sided tape. The cut-out discs with captured nucleic acid are inserted into the LAMP reaction chambers (pre-filled with the LAMP master mix) via a sterile pipette filter tip through the cut out inlets (Figure 3.56).

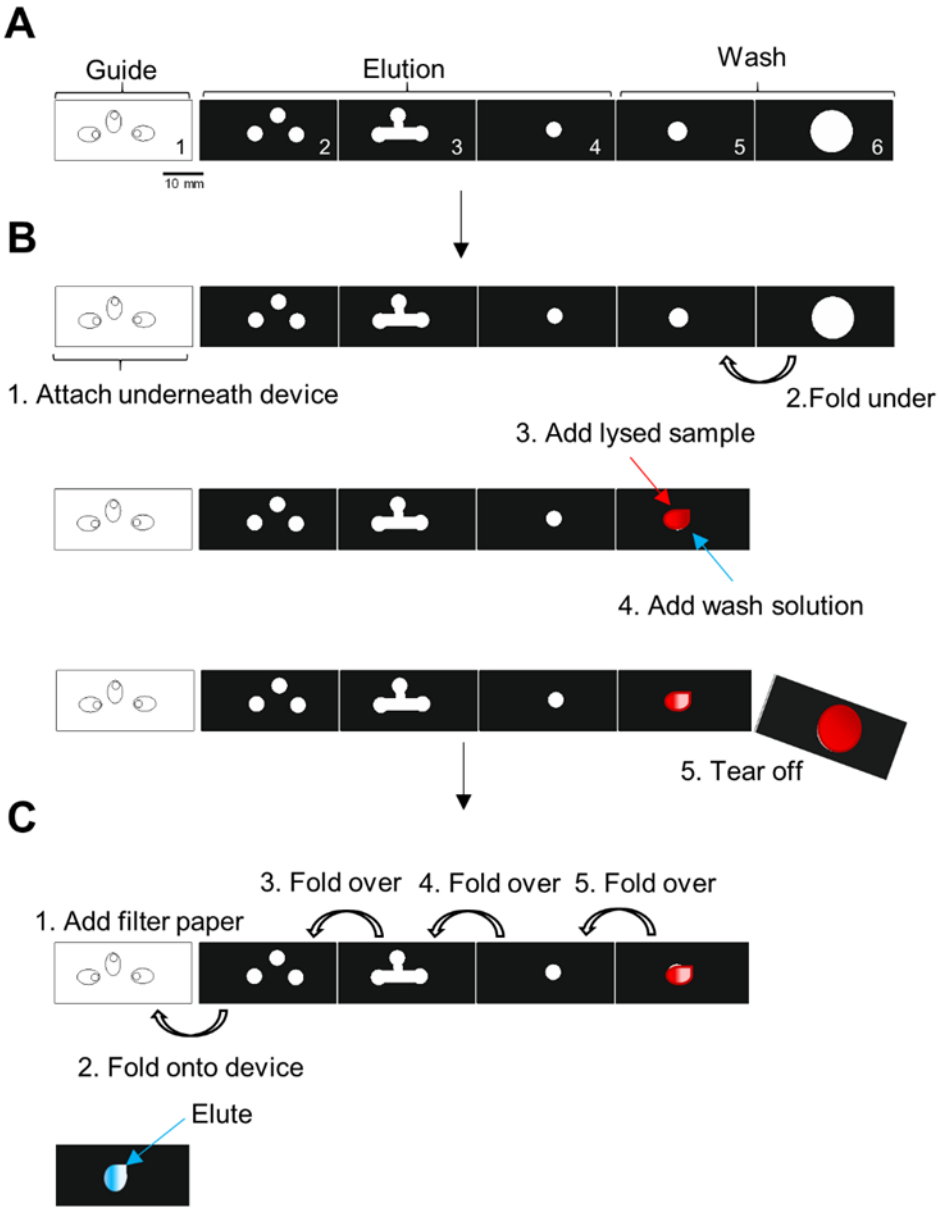

Figure 3.55 Schematic representation of the folding steps of the filter-paper devices
The filter paper is folded in a pre-defined manner to allow for fluidic manipulation during the nucleic-acid extraction process. The arrows indicate the folding direction. Scale bar on diagram A is applicable to all sections. A) The 6-panel filter-paper device. Panel 1 is used as a guide for direct attachment to the lateral flow device by double-sided tape. Panels 2-4 are distribution channels used for the elution step. Panels 5-6 are required for the wash step. B) Wash step. Panel 6 is folded underneath panel 5, which receives the magnetic beads from the lysed sample. Wash buffer is added to panel 5 to wash any impurities and panel 6 is discarded. C) Elution step. Three 4x4 mm discs are cut out of filter paper and placed underneath panel 2 which is folded onto the lateral flow device's reaction chambers. Panel 5 is folded onto the remaining panels and the elution buffer is added allowing for distribution of liquid and capturing the nucleic acid on the filter paper discs.

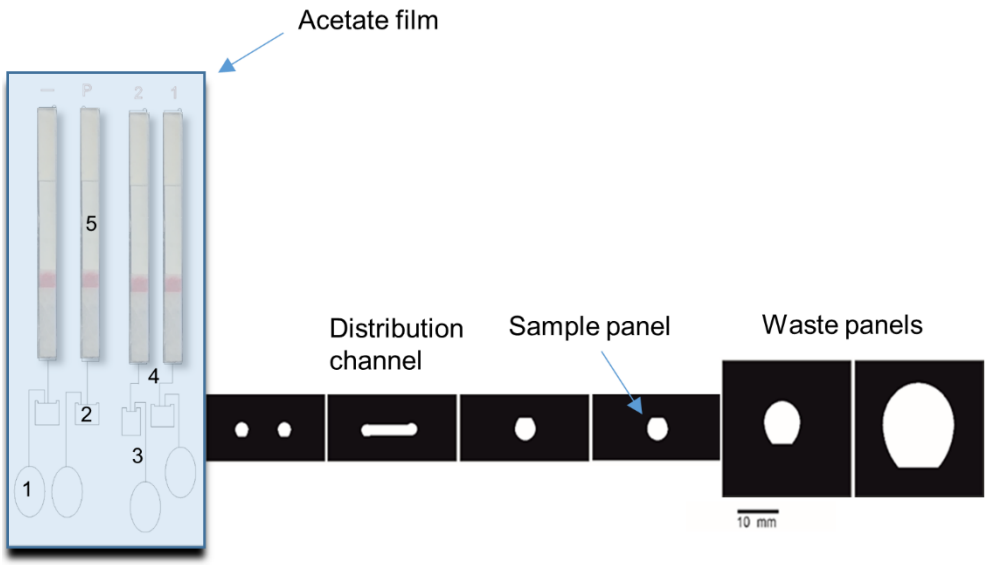

Figure 3.56 The assembly of the lateral flow device with the paper device
The diagram shows the complete HCV POC test from extraction stage to detection stage. The lateral flow device consists of four chambers including; negative control (-), positive control (+) and two duplicates for elution of the extracted samples (1 and 2) covered by acetate films. The numbers indicate different components of the lateral flow device, namely, 1-Water chamber (pre-filled with 80 µl of nuclease-free water), 2–LAMP chamber, 3-Channel connecting LAMP chamber with the water chamber, 4 –Channel connecting LAMP chamber with the lateral flow strip, 5 – lateral flow strip chamber. The filter paper consists of 6 nucleic acid extraction panels with panel 7 attached to the lateral flow device directly underneath the two LAMP chambers (labelled 1 and 2). The two rightmost panels act as waste absorbent within the white hydrophilic areas. The third rightmost panel is the sample addition zone and the three leftmost panels are used for the elution of nucleic acid. The pattern of the wax allows for distribution of the elution onto pre-cut circular filter-paper discs (4 mm in diameter), which are subsequently inserted into the LAMP chamber via the inlets. The LAMP chambers are filled with the LAMP master mix (and template for the positive and negative controls) before the entire device is sealed with acetate film.

Since the filter-paper based extraction system was developed for DNA rather than RNA, several optimization steps were required prior to testing the entire device. To prove the principle of extraction, the filter paper device was used to extract spiked HCV subgenomic replicon (10^8 copies/reaction) from a blood sample (5 µl of DNA into 15 µl of blood). In parallel DNA was extracted from a non-spiked blood sample with no template control acting as a negative control and subgenomic replicon (10^8 copies) used as a positive control. The extraction process relied on the same principle of folding paper as described in Figure 3.55, except glass fibre was used instead of magnetic beads. The filter paper containing eluted DNA was inserted directly into the qPCR tube. Successful extraction was confirmed through the use of HCV qPCR assay as described in Material and Methods. Figure 3.57 shows that the reactions containing the filter paper had raised fluorescence with no apparent amplification making the Ct undetermined. The no template control and the positive controls had the

expected results, no amplification and amplification occurring after 28 Cycles. The blood sample without addition of the subgenomic replicon also resulted in raised fluorescence and undetermined Ct values.

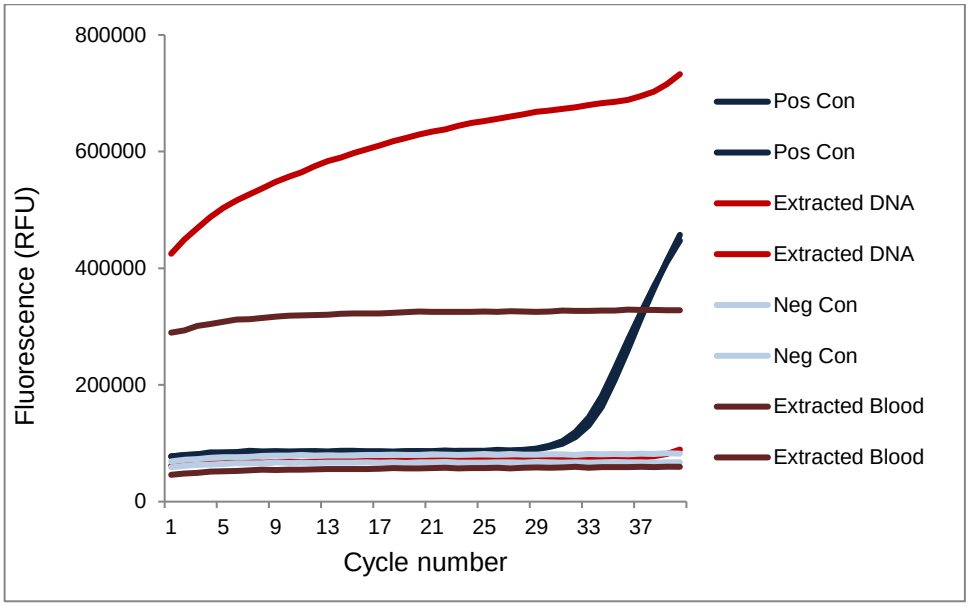

Figure 3.57 Filter-paper extraction from blood spiked with subgenomic replicon evaluated by qPCR
The extraction on paper was evaluated on the HCV qPCR assay as described in Materials and Methods. The graph shows increase in fluorescence in relative fluorescence units (RFU) over cycle number. The master mix contained either 2 µl of template, 10^8 copies/reaction of the subgenomic replicon in the positive control (Pos Con) or nuclease free water (Neg Con) or a circular disc of filter paper (4 mm in diameter) with eluted DNA in the Extracted Blood/DNA samples. The extracted DNA samples (in red) were spiked with 5 µl of the JFH1 subgenomic replicon into 15 µl of fresh blood. The extracted blood (in brown) acted as negative control and contained 20 µl of fresh blood. The samples were then mixed with 40 µl of lysis buffer 1, incubated at 95◦C for 1 minute and centrifuged briefly. An aliquot of 20 µl from each sample was then added onto the sample pad containing a 2mm-wide glass fibre disc. The samples were then washed with Ethanol and eluted in 20 µl of nuclease-free water as described on Figure 3.50 and Figure 3.56. The filter paper discs were then inserted to the sides of qPCR tubes. Data were collected from two independent experiments in duplicate.

Since the paper extraction experiment from the subgenomic replicon led to inconclusive results, an alternative method of evaluating extraction efficiency was tested. The Mengovirus extraction kit allows for a more thorough comparison of several extracting procedures since it contains a whole RNA virus rather than only nucleic acid (See Materials and Methods). Therefore, the kit was used to compare RNA extraction from plasma based on the RNAdvance kit with and without the DNase stage. Figure 3.58a shows the standard curve of the extraction of the positive control diluted in 10-fold dilutions. The fit of the line was close to 1 (R^2 = 0.9338) with the efficiency of the standard curve of 106.5. The lowest mean Ct value was achieved by the extracted sample without DNase

treatment and its 10-fold dilution, 27.2 (±1.321) and 30.9 (±0.0313), respectively. The sample treated with DNase and its 10-fold dilution had mean Ct values of 31.2 (±0.086) and 34.4 (±0). The negative control Ct values were undetermined

A

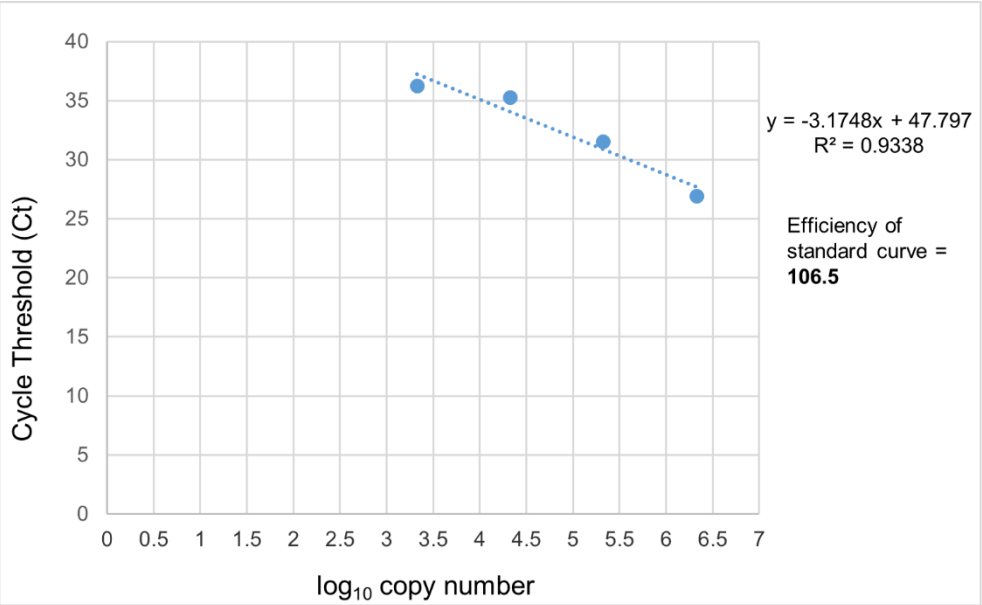

B

Sample	Mean Ct (±SD)
MV DNAse	31.2 (±0.086)
MV DNAse 1/10	34.4 (±0)
MV No DNAse	27.2 (±1.321)
MV No DNAse 1/10	30.9 (±0.313)
Neg Control	Undetermined

Figure 3.58 Comparison of DNase and no DNase RNA extraction from Mengovirus by qPCR assay
The experiment involved RNA extraction of 2130000 copies of Mengovirus (10 µl of stock solution) spiked into 330 µl of lysis buffer and Proteinase K (PK) solution. The standard protocol of the RNAdvance kit with or without DNase stage was used as the extraction method. The threshold cycle was determined by the Mengovirus kit qPCR assay as described in Materials and Methods. Four extractions were done in parallel; Mengovirus spiked into Lysis buffer (positive control), Mengovirus spiked into plasma with DNase treatment, Mengovirus spiked into plasma without DNase treatment and plasma alone (negative control). A) The graph shows the standard curve based on serial 10-fold dilutions of the eluted positive control (Lysis buffer spiked with Mengovirus). The samples were eluted into 20 µl of nuclease-free water, which acted as the first point of the standard curve. The equation of the line and the efficiency of the standard curve are shown on the rightmost side. B) The mean threshold cycle with the ±SD for each extraction (excluding the positive control) along with the 1/10 fold dilution of the elution. MV – Mengovirus. Experiments ran together with Dr Zoe O'Hara. Data were collected over two independent experiments in duplicate.

Since the RNAdvance kit could extract RNA from Mengovirus spiked into raw sample material (plasma), it was used for subsequent RNA extractions. The DNase step of the extraction was excluded as the Ct values without the DNase step were lower. To keep the extraction process on paper similar to the tube extraction procedure, the previously published filter paper design used for DNA extraction was modified as shown on Figure 3.59. To accommodate for the larger volume of wash buffer added (800 µl instead of 20 µl), an additional waste panel was added and both hydrophilic spots enlarged together with the hydrophobic region (Figure 3.59a and Figure 3.59b). Since the LAMP reactions from eluted samples was run in duplicate the number of distribution spots and the distribution channel were altered to accommodate two elution spots instead of three. Other minor changes to the filter paper were made to accommodate the progressive improvements made to the lateral flow detection device (see section 3.1.3).

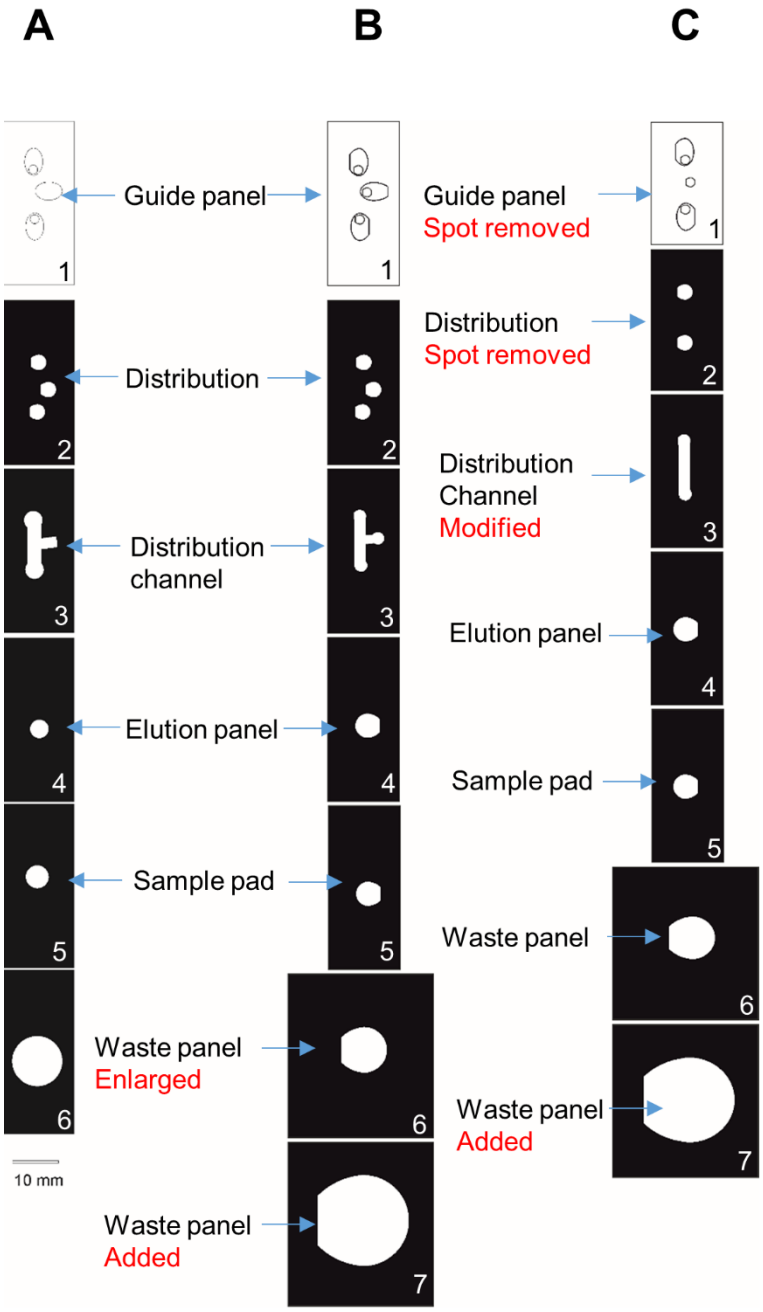

Figure 3.59 The modifications made to the filter paper device
Three filter-paper designs printed on wax paper to be used for RNA extractions. The black areas represent hydrophobic patterns and the white are hydrophilic allowing fluidic manipulation upon pre-defined folding patterns (See previous Figures). Design A was based on a template supplied by Miss Alice Garrett. Alterations made to design B and C were made in CorelDraw Version 2013. The changes included an additional Waste panel and enlargement of the Waste spots. Design C was the final design used for RNA extractions and differed from Design B in the distribution channel and the number of elution spots – reduced from three to two. The length of each panel on Design C was shortened by Dr Shantimoy Kar to save on the use of filter paper.

The next experiment involved the extraction of Mengovirus RNA from filter paper. As described previously, the extraction procedure started with the lysis stage in the tube; lysis buffer and PK were added to a sample spiked with Mengovirus (and one control sample without Mengovirus). The entire mixture was then incubated at 55°C for 15 minutes and magnetic beads added. Following the removal of the supernatant the first wash was carried out in the Eppendorf with an attached magnet leaving approximately 20 µl of the wash solution with magnetic beads. The magnetic beads were then transferred onto the sample pad and the remaining extraction procedures were the same as described in Figure 3.55 and Figure 3.56. The filter-paper discs containing Mengovirus RNA were transferred to 20 µl of nuclease-free water and vortexed vigorously. The resulting elution was then used as template for a Mengovirus qPCR reaction as described in Materials and Methods. The paper-extraction was run in parallel to standard RNAdvance extractions and controls. Table 3.9 shows the Ct values recovered from tube-based and paper-based RNAdvance extractions. The lowest mean Ct was observed in tube-based extraction with Mengovirus spiked directly into Lysis buffer, 29.8 (SD of ±1.811) followed by Mengovirus in Plasma treated with DNase, 30.6 (SD of ±2.34) and Mengovirus in Plasma (DNase untreated) at 30.9 (SD of ±0.266). Paper-based extraction did recover RNA from Mengovirus although the mean Ct was high, 34.7 (SD of ±0.631). Both negative controls in tube and paper were undetermined (non-spiked Plasma samples).

Table 3.9 Comparison of standard and paper-based extraction based on the RNAdvance kit by qPCR

	Method of Extraction Mean Ct (±SD)	
Sample	Tube-based	Paper-based
MV* in Lysis buffer	29.8 (±1.811)	
MV* in Plasma	30.9 (±0.266)	34.7 (±0.631)
MV* in Plasma (DNase-treated)	30.6 (±2.34)	
Plasma	Undetermined	Undetermined

*MV – Mengovirus. Table represents two independent experiments ran in duplicate.

The next experiment involved the integration of the entire sample-to answer process on the filter paper/lateral flow device platform from three HCV positive samples (P37, P49, P19) and two HCV negative samples (N92, N87) from the double-blind study. In parallel, an extraction control, human gene BRCA LAMP reaction as described in Materials and Methods, was run on the filter paper/lateral flow device platform on two samples, one HCV positive and one HCV negative (P49 and N87). Figure 3.60a shows that the internal extraction control, BRCA showed a positive result in one out of two replicates in the N87 sample and two negative replicates in the P49 sample. The NTC was negative on both devices containing N87 and P49 samples. For the HCV sample extraction test only the HCV negative samples produced expected results (N92 and N87), namely the positive controls were positive, NTC were negative and the two replicates on both devices were negative (Figure 3.60b). In all HCV positive samples (P37, P19, P49) all NTC and positive controls were positive. Only one sample with the highest viral load, P37 (6.18 $\log_{10}$ IU/ml), was positive in both of the replicates although the test bands were faint. The remaining two HCV positive samples, P19 and P49, were negative in both replicates and had viral loads of 5.33 and 5.22 $\log_{10}$ IU/ml, respectively.

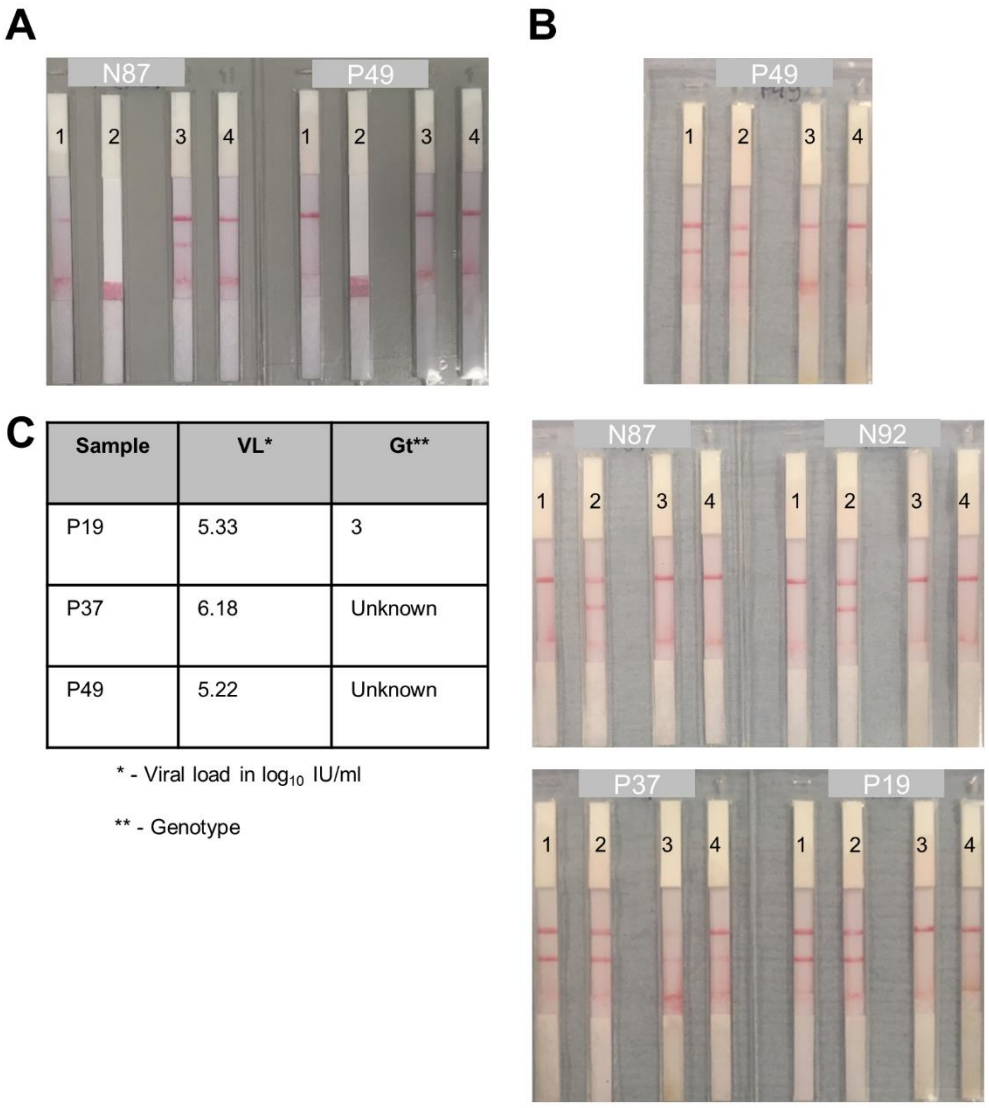

Sample	VL*	Gt**
P19	5.33	3
P37	6.18	Unknown
P49	5.22	Unknown

* - Viral load in log_{10} IU/ml

** - Genotype

Figure 3.60 Paper-based extraction and lateral flow device detection of HCV positive and control samples
The extraction protocol was based on RNAdvance Blood kit with omission of the DNase stage as described in Materials and Methods. The samples were eluted from magnetic beads on the filter paper with 30 µl of nuclease-free water onto two circular discs, 4mm in diameter, which were then inserted into the lateral flow device's LAMP chambers with a sterile pipette tip. The entire paper device was discarded and the master mix added to the LAMP chambers along with the template for NTC and Positive controls. The devices were incubated upright in a water bath at 65°C for 30 minutes. The grey boxes represent the name of each sample inserted into the device. Numbers indicate different reactions, namely 1 – NTC, 2 – Positive Control containing 1 ng of JFH1 subgenomic replicon, 3 and 4 – lateral flow strips containing the products from the two replicates extracted on filter paper. A) The results from extraction control LAMP reaction based on the BRCA human gene acting as an internal control on one HCV negative and one HCV positive sample. BRCA LAMP master mix contained the BRCA primers as described in the Materials and Methods. The BRCA extraction control did not use the Positive Control (No. 2 lateral flow device). B) The results from extracting three HCV positive and two HCV negative samples based on the HCV RT-LAMP assay. C) Table showing the viral loads and genotypes of the HCV positive samples used in the extraction. Data were collected over a single experiment.

3.1.5 Discussion

Recent advances in direct-acting antiviral (DAA) treatments for HCV have moved us closer than ever before to the goal of HCV elimination by 2030. However, treatment can only be administered following linkage to care after diagnosis of infection. The WHO states that only 19% of those infected are aware of their status and the lack of a sensitive and specific POC test is a major hurdle (WHO 2017). In this thesis, I aimed to progress the development of a POC test for the diagnosis of HCV using an isothermal amplification method called reverse-transcriptase loop mediated isothermal amplification or RT-LAMP.

3.1.5.1 LAMP is a powerful candidate for a POC test

In recent years, many efforts have concentrated on the development of a POC test with a user-friendly format and minimal hands-on time requirements in order to facilitate immediate diagnosis of HCV infection and immediate linkage to care for treatment. Standard of care enzyme immunoassays such as the OraQuick® HCV Rapid Antibody Test, a POC assay which can be used on saliva, blood or plasma samples directly (Lee et al. 2010) offer both high sensitivity and specificity and a quick turnaround time of 20 minutes. However, they do not distinguish between active or past infection. Furthermore, HCV antibodies develop within 4-10 weeks after exposure, causing some acute infections to be undiagnosed (Mondelli, Cerino & Cividini 2005). Immunosuppressed individuals such as HIV co-infected patients tend to have delayed seroconversion making traditional diagnostic methods even less sensitive (Thomson et al. 2009). The major disadvantage is therefore the need for a follow-up test to confirm the presence of viral nucleic acid or antigen. Real-time PCR and other molecular-based assays are the gold-standard method in HCV diagnostics, but are limited by the need for sophisticated equipment and the requirement for highly skilled personnel (Germer & Zein 2001). In contrast LAMP can be performed at a constant temperature with minimum equipment requirements, thereby drastically reducing diagnostic costs while retaining high sensitivity and specificity (Mori & Notomi 2009). Many other isothermal amplification assays have been developed in recent years including nucleic acid sequence-based amplification (NASBA) and rolling circle amplification. However LAMP is by far

the most popular method for POC testing as is evident by over 3000 thousand publications on PubMed by January 2019.

3.1.5.2 Optimisation of LAMP conditions significantly improves HCV-LAMP detection accuracy

In this study, attempts were made to optimise LAMP diagnostic accuracy by optimising reaction conditions and primer design. Further, we aimed to develop a method for the use of RNA directly, removing the need for cDNA synthesis.

In the initial optimisation experiments of this study, published LAMP primers were more sensitive both clinically and analytically than an in-house primer set for genotype 1. Interestingly the sensitivity of these was high, despite numerous mismatches in the primer sequences in comparison to no mismatches in the in-house primer set. In contrast, optimisation significantly improved the detection of genotype 3 HCV.

The authors of the original study used only a small number of samples (n=25) from a limited number of gts, gt 1b and 2a, and thus did not evaluate detection in gt 3 infected patients. Standard LAMP assays and their polymerases do not have 3'- 5' exonuclease activity and therefore mismatches at the 3' end have detrimental effects on the assay performance (Notomi et al. 2015). This is evident in this study where a mismatch in the 3'end of the BLP primer resulted in a significant delay in the time to positive of gt 3 samples. Therefore I have introduced a novel loop primer (BLP) to optimise the previously published primer set (Yang et al. 2011). This significantly reduced time to detection for the gt 3 standard from 21.5 minutes to 17 minutes. Genotype 3 comprises 25% of all HCV cases globally, which is only surpassed by gt 1 infections comprising 44%% of all patients (Blach et al. 2017). As gt 3 is the second most common gt both in the UK and worldwide, the HCV LAMP assay described here has the potential to improve clinical and POC testing for a large number of cases.

Previous studies have shown that optimal primer design for LAMP is critical but complex (Nagamine, Hase & Notomi 2002; Notomi et al. 2000a). It is often necessary to test several primer sets produced by LAMP primer design software prior to finding one efficient for the assay (Torres et al. 2011). It is therefore possible that the initial in house primer set was not optimal for a number of

reasons. Both primer sets were based on the most conserved area of the HCV genome, namely the 5'UTR, which is widely used as a target in gold-standard HCV detection assays (Drexler et al. 2009). The suboptimal nature of the in house primers may also be related to the complex secondary structures found in the 5'UTR region (Shi & Lai 2006). The published HCV LAMP primer set was selected based on the presence of an additional accelerating primer (AP) as well as the authors' consideration of the secondary structures of the 5'UTR when designing the primer set (Yang et al. 2011). Despite numerous HCV LAMP studies published in recent years, only the authors of the published primers have taken the complex structures into account when designing primers, and thus their primers were selected for further development in this study (Kargar et al. 2012; Nyan & Swinson 2016; Wang et al. 2011; Yang et al. 2011; Zhao, Liu & Sun 2017). While some novel primers, FIP, BIP 50/50 and AP Rev, did not substantially improve the time to positive, it provides insight into the assay's dynamics with mid-primer mismatches. The findings presented here imply that as long as each primer does not contain multiple mismatches at the 3'end, the time to positive of the assay is not significantly delayed. This is because despite the mismatches present in the published primer set, high sensitivity was reported both in this thesis and in the original study. Moreover, compensating for mismatches by introducing degenerate base pairs did not significantly improve time to detection. However, in previous studies, mismatches in LAMP primers significantly affected the sensitivity and efficient amplification of the target often resulting in false negatives (Wong et al. 2018). Designing perfectly matching primers for a pangenotypic assay is particularly challenging for viruses such as HCV which exist as a quasispecies due to the erroneous nature of the RNA polymerase leading to high variability between different genotypes and subtypes (Domingo & Perales 2018). One study has successfully resolved the issue of mismatching LAMP primers for a similarly diverse RNA virus, dengue, by the addition of a miniscule amount of a high-fidelity polymerase with proof-reading activity (Zhou et al. 2019).

The next series of experiments aimed to identify the optimal enzyme and reaction conditions for HCV LAMP. To the best of our knowledge all of the published HCV-LAMP assays have used 8U of *Bst* polymerase (NEB, UK), with the addition of AMV reverse transcriptase in some publications. We compared *Bst*

polymerase with an improved version of the polymerase – *Bst* 3.0 polymerase – and another polymerase (GspSSD, Optigene). There was no amplification with *Bst* polymerase in our assay, which reflects the reduced amplification speed, yield, salt tolerance, and thermostability of the enzyme compared with the latter two polymerases. Both of the *Bst* polymerases had a high false positive rate (due to the formation of non-specific product) and did not have an inverse relationship between concentration and positivity. The use of GspSSD and the corresponding master mix significantly improved the original assay. In this study, the time to positive of the positive control at a concentration of 10^6 copies/ml was always <15 min compared to a mean time to positive of 17.99 ±0.62 min in the original assay at a similar concentration of $5x10^5$ IU/ml (Yang et al. 2011).

End-point dilution was next used to determine the sensitivity of the assay. The lowest dilution detected by our HCV-LAMP assay was 10^2 copies/ml which was comparable to other studies which reported sensitivities of 50 and 10 IU/ml respectively (Wang et al. 2011; Yang et al. 2011). The slightly lower results detected in other studies may reflect the use of less divergent clinical samples, a higher false positive rate, a longer incubation time of 70 minutes compared to 30-60 minutes in this study, and the use of a shorter target sequence of 180 bp, compared with 207 bp and 273 bp in this study. This effect was additionally noted between the uses of shorter in-house primers (207 bp) compared with the previously published primer set (273 bp).

Regression analysis was used to estimate the limit of detection of the LAMP assay at 3.15 $\log_{10}$ copies/reaction or approximately 1426 copies/reaction using a 30-minute incubation period. Therefore the HCV LAMP assay fulfils the WHO criteria for a POC test with minimal limit of detection of 3000 IU/ml or below (WHO 2017).

It is likely that the sensitivity of the HCV LAMP assay could be further improved. This is because samples used in the initial clinical sensitivity and specificity evaluation were stored as RNA extracts for a prolonged period of time and subject to multiple freeze-thaw cycles. Previous studies suggests that RNA transcripts stored at -80°C are stable for up to 56 days while storage of viral RNA extracts for 3 years at -80°C results in a mean viral load reduction of 1.13 $\log_{10}$ IU/ml (Granados et al. 2017). Moreover, ten freeze-thaw cycles resulted in 0.5

log_{10} copies/µl decrease in viral load. This may be caused by nucleic-acid shearing, particularly in samples with low viral load (≤3.0 log_{10} copies/µl) or stored in small aliquots (Bellete et al. 2003; Granados et al. 2017). Future studies should aim to test the samples shortly after RNA extraction, which would mimic a POC set up.

3.1.5.3 HCV LAMP is highly sensitive and specific when applied to clinical samples

The next series of experiments described in this thesis included the first double blind LAMP analysis of sensitivity and specificity in clinical HCV positive and negative samples. Unlike other studies, varied viral loads and all major HCV gt were tested, including a recently identified gt 7 sample (Davis et al. 2019). The samples were obtained from virology reference laboratories and the viral load and gt were confirmed by the Abbott Real-Time HCV assay and sequencing. The viral load was further assessed by running RT-LAMP and LAMP assays in parallel with an in-house RT-PCR assay. All three samples undetected by LAMP were also undetected by the RT-PCR assay with an additional sample missed by the latter. Interestingly all of these samples had low viral loads of ≤3.95 log_{10} IU/ml which could have affected successful diagnosis. The most likely explanation for this is multiple freeze-thaw cycles of plasma samples and long-term storage leading to reduced viral load of the viral RNA, particularly in low viral load samples, as has been demonstrated before (Granados et al. 2017; Palyi et al. 2018).

Two of the HCV samples undetected by RT-LAMP but detected by LAMP and RT-PCR were gt 4. Significant differences in time to positive were noted between gt 4 and gt 1 and gt 2 samples using RT-LAMP. This difference in sample detection between RT-LAMP and LAMP/RT-PCR may be related to differences in the cDNA synthesis step of the assays. Both RT-PCR and LAMP protocols employed random hexamers for cDNA synthesis, while the RT-LAMP protocol used target-specific LAMP primers. Studies of cDNA synthesis efficiency based on the use of random hexamers vs target-specific primers have produced conflicting results (Pecoraro et al. 2013). Higher concentrations of both primer sets may result in improved reverse transcription (Miranda & Steward 2017). Furthermore, mismatches to gt 4 found in the alignment of primers with major HCV gt may also have reduced the sensitivity of the LAMP assay. The discrepancies in time to positive detection

could be explained by HCV alignment with gt 3/4 sequences showing a large number of mismatches to the published primer set. Full genome sequencing using NGS of undetected gt 3 and 4 samples to look for mismatches would be useful. Further optimisation of the assay by varying primers ratios could also improve both time to positive detection and overall sensitivity (Zhou et al. 2014).

The overall sensitivity of our HCV RT-LAMP assay in clinical testing was similar to that reported in other studies (96% in the initial evaluation compared to 95% and 90% in others (Kargar et al 2012, Wang et al 2011). However, other studies mostly evaluated samples from a distinct geographical region (for example Iran and China) with little genetic variation and limited gt 3 infected patient samples (Kargar et al 2012, Wang et al 2011 and Yang et al 2011). The WHO recommends a minimum diagnostic specificity of >98% and sensitivity of ≥90-95% for a HCV POC test (WHO. 2016b). This was fulfilled by RT-LAMP at a cut-off of <24.8 minutes (sensitivity of 90% and specificity of 98.3%) and LAMP at a cut-off of <26.8 min (sensitivity of 92% and specificity of 98.3%). A small number of false positive samples were detected by RT-LAMP and LAMP which were not confirmed by RT-PCR. False positives could indicate a slightly elevated risk of cross-contamination between different wells in the LAMP assay due to a larger volume of template compared to RT-PCR. Alternatively the complexity and the large number of primers in LAMP elevates the risk of primer-dimer formation in LAMP assays (Nagamine, Hase & Notomi 2002). This second finding has been evident in other LAMP studies where the authors frequently use melt curve analysis to distinguish between cross contamination and primer-dimers (Mao, Leung & Xin 2007; Wang et al. 2015). The problem can be overcome by improving LAMP primer design (Torres et al. 2011). Other studies used restriction enzymes or mathematical models to evaluate banding patterns on gel electrophoresis specific to the target sequence (Nagamine, Kuzuhara & Notomi 2002; Schneider, Blakely & Tripathi 2019; Yang et al. 2011). Additionally, reduced primer concentrations can reduce the number of false positives caused by primer dimers (Tone et al. 2017), and, the addition of dimethyl sulfoxide (DMSO) has reduced false positives in both LAMP and RT-PCR assays in previous studies (Wang et al. 2015). Overall, following optimisation, false positives did not occur frequently in this study (Wang et al. 2011; Yang et al. 2011). The specificity of the assay in

future studies could be improved by the addition of DMSO, running melt curve analysis or restriction enzyme digest and running the assay for the incubation time with optimal sensitivity and specificity prior to false positive development (<24.8 minutes for RT-LAMP).

3.1.5.4 Future work and applications of HCV LAMP

The current diagnostic algorithm for HCV relies on testing for anti-HCV antibodies and later sampling for HCV RNA to confirm active infection (Chevaliez & Pawlotsky 2006). Recently, two CE-IVD certified platforms (European Community's 'CE' mark for *in vitro* diagnostic medical devices) have been developed; GeneDrive and Cepheid Xpert. These assays both detect nucleic acid directly and have high sensitivity and specificity. They have significantly improved the armamentarium for HCV diagnosis. However both assays are limited by the requirement of technical expertise and the need for an initial significant financial investment (Lamoury et al. 2018; Alba Llibre et al. 2018). The current cost of the GeneDrive platform is $5000 and $30-40 for each HCV test. In contrast, the collaborators of the work involved in this thesis have previously estimated the cost of a similar LAMP assay for malaria at ≤$10 (Reboud et al. 2019). The incubation time from sample to answer is 1 hour and 40 minutes for the GeneDrive and 1 hour for the Cepheid Xpert assay. Although additional extraction steps are still required, the LAMP assay demonstrated here had optimal sensitivity and specificity within 25 minutes. Several LAMP assays have been developed into POC tests with both CE-IVD and WHO approval. For example, the *illumigene assay* for diagnosis of *C. difficile* demonstrated high sensitivity and specificity with minimal hands on time in 1 hour (Hong et al. 2014). Furthermore, a TB-LAMP assay has been recommended by the WHO as a replacement test for smear microscopy in tuberculosis patients (Global Tuberculosis Programme n.d.). The major advantages of these assays are minimal hands-on time, simplicity of use and a sample to diagnosis period of less than 1 hour (Bojang et al. 2016).

3.1.5.5 Development of POC LAMP platforms for clinical use

This study aimed to develop a POC test for HCV diagnosis based on the ASSURED criteria. One of the crucial aspects of a POC test is a user-friendly format. The

HCV-LAMP assay presented in this thesis used two easy to interpret methods to facilitate naked-eye visualization, namely pH-based colour change and a nucleic-acid detection strip based on FITC and biotin-labelled primers (FLP and BLP). Previous HCV LAMP studies visualize detection by gel electrophoresis or fluorescent dyes, which cannot be used directly in a POC format (Wang et al. 2011; Yang et al. 2011). Naked-eye detection methods such as SYBR Green I have also been assessed, but those are limited by additional steps or preparation requirements (Kargar et al. 2012). SYBR Green I is typically added after the incubation period increasing the chances of cross-contamination with LAMP products obtained during the reaction (Karthik et al. 2014). There is an array of other visualization methods available, which allow naked eye detection and offer a variety of sensitivities in a POC setting without the risk of contamination (Fischbach et al. 2015). However these are often limited by time-consuming preparation requirements.

To the best of our knowledge, our assay is the first study which utilizes a colorimetric master mix to detect HCV LAMP products. In contrast to other studies the target can be added directly to the master mix, without complex preparation, and incubated in a simple water bath for a LAMP reaction (Tanner, Zhang & Evans Jr. 2012). Previous studies have shown that thermos flasks containing boiled water can be used for carrying out LAMP reactions, thus further simplifying detection in resource-limited settings (Xu, Zhao, et al. 2016). Naked eye visualization of a clear colour change from pink to yellow can be carried out in as little as 15 minutes. This colorimetric detection relies on changes in pH detected by a pH indicator. The HCV-LAMP assay could also be used in a pH-detecting semiconductor assay, a method which has previously been used to detect HIV (Gurrala et al. 2016). The utility of this method must be balanced against the drawback that a colour change also occurs following the formation of primer dimers, resulting in a high false positive rate (Wang et al. 2017).

To the best of our knowledge, this study is also the first HCV LAMP assay based on a prototype lateral flow-based nucleic acid detection method. The lateral flow strip detection correlated with results obtained through gel electrophoresis and fluorescence-based detection. The use of target specific tags namely FITC on the loop forward primer and biotin on the loop backward primer were used to

reduce false positive results. This was demonstrated in another study comparing lateral flow detection with DNA binding dyes in end-point LAMP reactions as the former lead to false positives in primer-dimer amplification events (Wang et al 2017). In this study, a prototype hand-held detection device with a finger pump for ease of operation was developed to accommodate nucleic-acid detection strips (Peeling 2006). A similar device has previously been used for the rapid diagnosis of malaria in resource-limited settings (Reboud et al. 2019). Moreover, lateral flow strip-based detection of LAMP products has previously been demonstrated in an array of different infectious diseases including *Brucella* species, *Toxoplasma gondii* and *Mycobaterium* (Lalle et al. 2018; Li et al. 2019; Liu et al. 2019). The findings from these studies reflect the high sensitivity, specificity and user-friendly nature of lateral-flow strips, ideal for a POC test setting.

Due to time constraints, this study demonstrated the use of the prototype lateral flow device with HCV standards rather than clinical samples. Future work will utilise the samples from the double-blind study to evaluate the assay's performance in a clinical setting.

3.1.5.6 RNA extraction is required for optimal sensitivity and specificity of HCV LAMP assays

The last objective of this study was to overcome the need for a separate RNA extraction step prior to use of the prototype lateral-flow device.

An initial set of experiments demonstrated that LAMP can be used directly on serum samples with the only limitation being somewhat delayed amplification. This correlates with other LAMP studies that demonstrated amplification directly from serum, urine and blood, for example for the detection of Zika virus without significantly hindering reaction performance (Damhorst et al. 2015; Ihira et al. 2007; Lamb et al. 2018). Mengovirus was used as an internal extraction control by spiking serum samples prior to RNA extraction. Others have also successfully used Mengovirus to evaluate their extraction methods (Costafreda, Bosch & Pintó 2006; Martin et al. 1996). Mengovirus is non-pathogenic to humans, replicates well in cell culture and does not normally occur in human blood or plasma (Martin et al. 1996). In addition it is genetically distinct from

HCV making it a potential candidate as an internal RNA extraction control. Importantly, we also demonstrated that removal of the DNase step increases the efficiency of the assay and increases the concentration of extracted viral RNA as has been found in other studies (Norhazlin et al. 2015; Paska et al. 2019).Several experiments were performed to integrate a paper-based RNA extraction method with the prototype lateral flow LAMP device. This proved to be challenging with difficulty replicating results reliably with inconsistencies between the duplicate lateral flow strips. False positives were present in some negative controls, likely a result of cross-contamination from the neighbouring positive control due to high template concentration and design flaws. Future studies should further optimise the RNA extraction step. RNA extraction on paper is a fairly novel concept with only a limited number of studies reporting its success in literature. One study demonstrated the use of paper as a suitable RNA extraction platform for LAMP reaction in an impressive 30-second protocol (Zou et al. 2017). Other studies looked at RNA extraction on paper for viruses like Ebola and Zika in conjugation with isothermal amplification including Recombinase Polymerase Amplification and LAMP, respectively (Kaarj, Akarapipad & Yoon 2018; Magro et al. 2017). The former study extracted RNA in a resource-limited setting using freeze-dried reagents. A similar paper platform in conjugation with a lateral-flow LAMP detection device was recently used in the field for the diagnosis of malaria (Reboud et al. 2019). Therefore, any of those protocols in conjugation with our highly sensitivity and specific HCV LAMP assay would help in the development of a novel POC test with a sample to detection time of <60 minutes. Paper is a particularly desirable platform for RNA extraction due to its low cost and ease of fluidic manipulation, for example via wax printing (Cate et al. 2015; Glavan et al. 2013; Martinez et al. 2007; Parolo & Merkoçi 2013). Paper platforms are also easy to transport and dispose of, for example by burning, reducing risks of contamination and infection.

The development of a user-friendly and sensitive HCV POC test would provide a significant advance for diagnosis of HCV in resource-limited settings and could also be used in high income countries in high risk groups including PWID and HIV infected MSM. Uptake of a novel POC test could significantly decrease loss to follow-up in these populations as a single visit would allow for diagnosis and linkage to care leading to immediate therapy (Linas et al. 2012; Martin et al.

2011). Diagnosis of HCV in PWID is significant as an estimated 10 million PWID have tested positive for anti-HCV antibodies in 148 countries (Nelson et al. 2011). Previous findings suggest that POC diagnosis is cost-effective in PWID and other high risk groups as well as resource-limited countries with high HCV prevalence, such as Egypt (Kim et al. 2015; Schackman et al. 2015). Since LAMP needs a constant incubation temperature of 60-65°C, reactions can be set up with minimal equipment requirements, as previously demonstrated by others (Jiang et al. 2018). Moreover, LAMP has successfully been used in a resource-limited setting for the diagnosis of malaria and foot-and-mouth disease amongst others (Howson et al. 2017; Reboud et al. 2019; Viana et al. 2018). Therefore, data demonstrated here and by other studies highlights LAMP assay's potential as a future POC test for HCV testing.

3.2 Studying the rare event of secondary spontaneous clearance

In a rare cohort of 201 patients infected acutely with HCV, the majority of whom were co-infected with HIV (see Materials and Methods for a detailed description), 19.4% (39/201) have spontaneously cleared their infection without receiving treatment (primary spontaneous clearance). The first 85 patients who did not spontaneously clear were treated with IFN alpha and RBV for a duration of 24-48 weeks according to local guidelines (Figure 3.61). The majority achieved a sustained virological response (SVR, 63/85; 74.1%). The remainder failed treatment, due to either null response (8/85; 9.4%), partial response (4/85; 4.7%) or viral relapse (8/85; 9.4%) (See Introduction for definitions). Unexpectedly, two patients spontaneously cleared HCV following viral relapse, a term hereon referred to as **secondary spontaneous clearance (SSC)**. The viral relapse strain in both patients was the same prior to and after treatment by sequencing, thus eliminating the possibility of reinfection (Abdelrahman et al. 2015). This novel phenomenon of SSC has never been described before in the natural history of HCV infection and thus the next chapter will explore the immunological mechanisms underlying this event in these two patients.

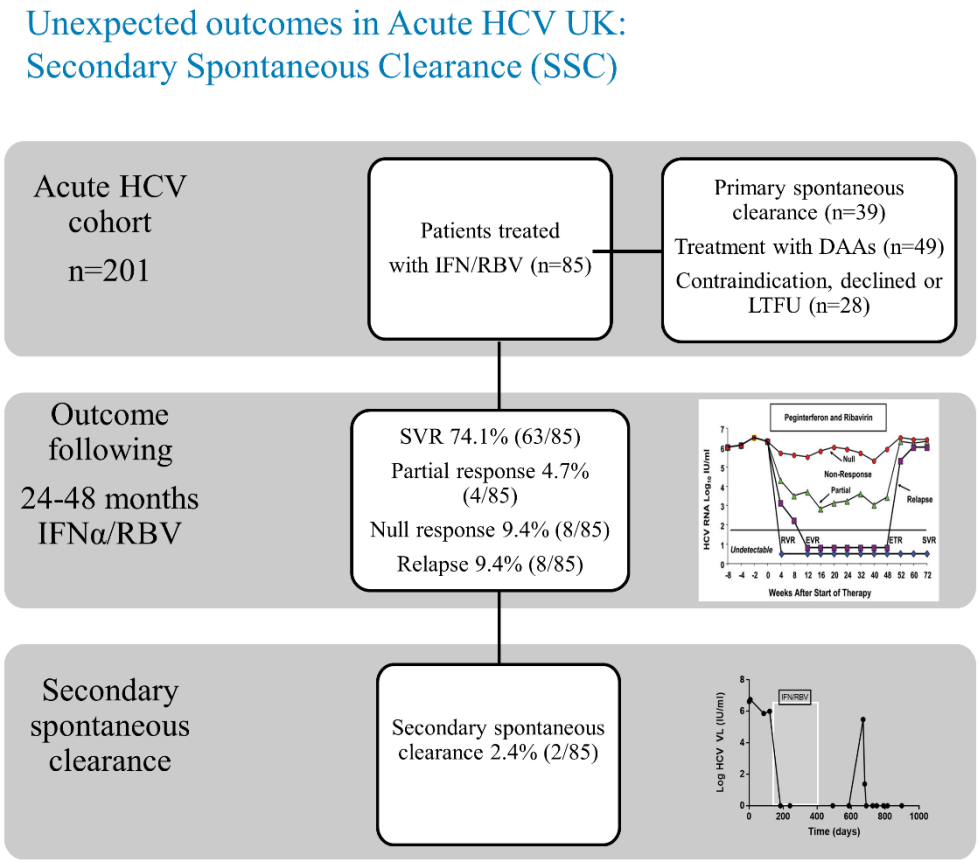

Figure 3.61 Outcomes in St Mary's cohort of acute HCV patients.
The acute HCV cohort consisted of 200 patients of MSMs. The first 85 treated patients received 24-48 weeks of IFNα and RBV. The graph on the bottom right corner indicates the typical viral load pattern during SSC. LTFU – loss to follow up, DAA – direct acting antivirals, SVR – sustained virological response.

3.2.1 Clinical parameters of secondary spontaneous clearers and control patients

The clinical history and longitudinal viral load data for both SSC patients and controls who failed treatment but did not spontaneously clear infection thereafter are shown in Figure 3.62 and Figure 3.63. Both cases 1 (P76) and 2 (P155) were patients recruited at St Mary's Hospital, London. Both were MSM and co-infected with HIV. At the time of initial HCV infection, the baseline CD4 count was 390 cells/mm3 and 560 cells/mm3, respectively (Figure 3.63). Case 1 had an undetectable HIV viral load on anti-retroviral (ARV) treatment and Case 2 seroconverted with HCV and HIV at the same time and was therefore not on Anti-Retrovirals (ARVs). Unprotected anal intercourse was considered the main risk of infection for both patients. The genotype was identified as 1a and 4d in P76 and P155, respectively.

The viral load for both cases at the first time-point post-infection (time point A; TPA) was greater than 10^6 IU/ml and decreased to 10^5 IU/ml at TPB for both patients. Both patients had a rapid virological response (RVR) on dual IFN/RBV therapy (HCV PCR neg <12 IU/ml at week 4 of therapy) but developed relapse at 12 and 24 weeks following end of treatment (Figure 3.62). History taking at the time of viral relapse (TPC for P76 and TPD for P155) indicated that neither patient had a risk of re-infection. Sanger sequencing of the E2 gene (P76, P155) and Illumina sequencing of the entire HCV genome (P155) suggested re-emergence of a pre-existing variant rather than re-infection (Table 3.10 and Table 3.11). Table 3.10 shows the amino acid alignment of the consensus E1E2 sequence from P76 at TPA (first PCR positive and EDI) and TPC (relapse) compared to the H77 reference sequence. The alignment revealed five amino acid changes between the baseline TPs and post-treatment time-point at relapse including: at position 223 from Threonine to Alanine (T223A), at position 386 from Valine to Phenylalanine (V386P), at position 401 from Glycine to Serine (G401S), at position 408 from Lysine to Arginine (L408A) and at position 574 from Asparagine to Aspartic acid (N574D). Unexpectedly 5 months following relapse in P76 and 7 months in P155, no HCV was detected suggesting secondary spontaneous clearance (TPD for P76 and TPE for P155).

In order to further investigate SSC, four patients that failed treatment and did not subsequently clear infection were selected as controls. These consisted of three relapse patients (P75, P101 and P131) and one null responder patient (P63). In each of these, a viral load of at least 10^5 IU/ml was present at the time of HCV diagnosis which did not decrease substantially over the course of 3 months in all treatment failure patients prior to treatment (Figure 3.62c-f). After the start of therapy, all relapse patients had an undetectable viral load, which later on returned to high titre at relapse (TPB for P75 and P101, TPC for P131). The null response patient (P63) had a high viral load, which did not change more than 2 log values over the course of treatment.

Since CD4/CD8 T cell ratios are frequently used to monitor immune activation in HIV/HCV co-infected patients, the CD4+ and CD8+ T cell counts were investigated throughout the course of infection (Kuniholm et al. 2016). Prior to treatment the nadir CD4 T cell count for P76 and P155 was 380 cells/mm^3 and 550 cells/mm^3, respectively (Figure 3.63). Similarly the nadir CD4+ T cell for control patients P75, P131, P101 and P63 were 220, 680, 590 and 320 cells/mm^3, respectively. The nadir CD4 T cell count during treatment for SSC, P76 and P155 were 180 cells/mm^3 and 420 cells/mm^3, respectively. At relapse, SSC patients had a steady increase in CD4+ cell count with nadir cell count of 430 cells/mm^3 for P76 and 510 cells/mm^3 for P155 which increased to 540 cells/mm^3 and 560 cells/mm^3, respectively around the time of SSC. Similarly, the nadir CD4 T cell count during treatment for control patients, P75, P131 and P101 were 260, 290 and 600 cells/mm^3, respectively. There was no CD4 T cell count measured during treatment for P63. Post treatment the nadir CD4 T cell count for control patients, P75, P131, P101 and P63 were 180, 550, 570 and 290 cells/mm^3, respectively.

The nadir CD8 T cell count for SSC (P76 and P155) pre-treatment was higher than the nadir CD8 T cell count in any control patients (P75, P131, P101 and P63), 1120/1330 cells/mm^3 compared to 470, 830, 930 and 640 cells/mm^3, respectively (Figure 3.63). The nadir CD8 T cell count during treatment decreased rapidly both in SSC patients, 160 and 690 cells/mm3, and control patients, 190, 330 and 590, respectively. No CD8 T cell counts were measurements were taken during treatment of P63. The nadir CD8 T cell counts post-treatment were higher in SSC patients (P76 and P155) at 690 cells/mm^3 and

1140 cells/mm^3, respectively compared to control patients, P75, P101 and P63 with cell counts of 150, 600 and 610 cells/mm3, respectively. The nadir CD8 T cell count post-treatment for P131 was higher than P76, but lower than P155 at 840 cells/mm^3. However, around the time of SSC the CD8 T cell count for P76 and P155 increased to 930 cells/mm^3 and 1230 cells/mm^3, respectively.

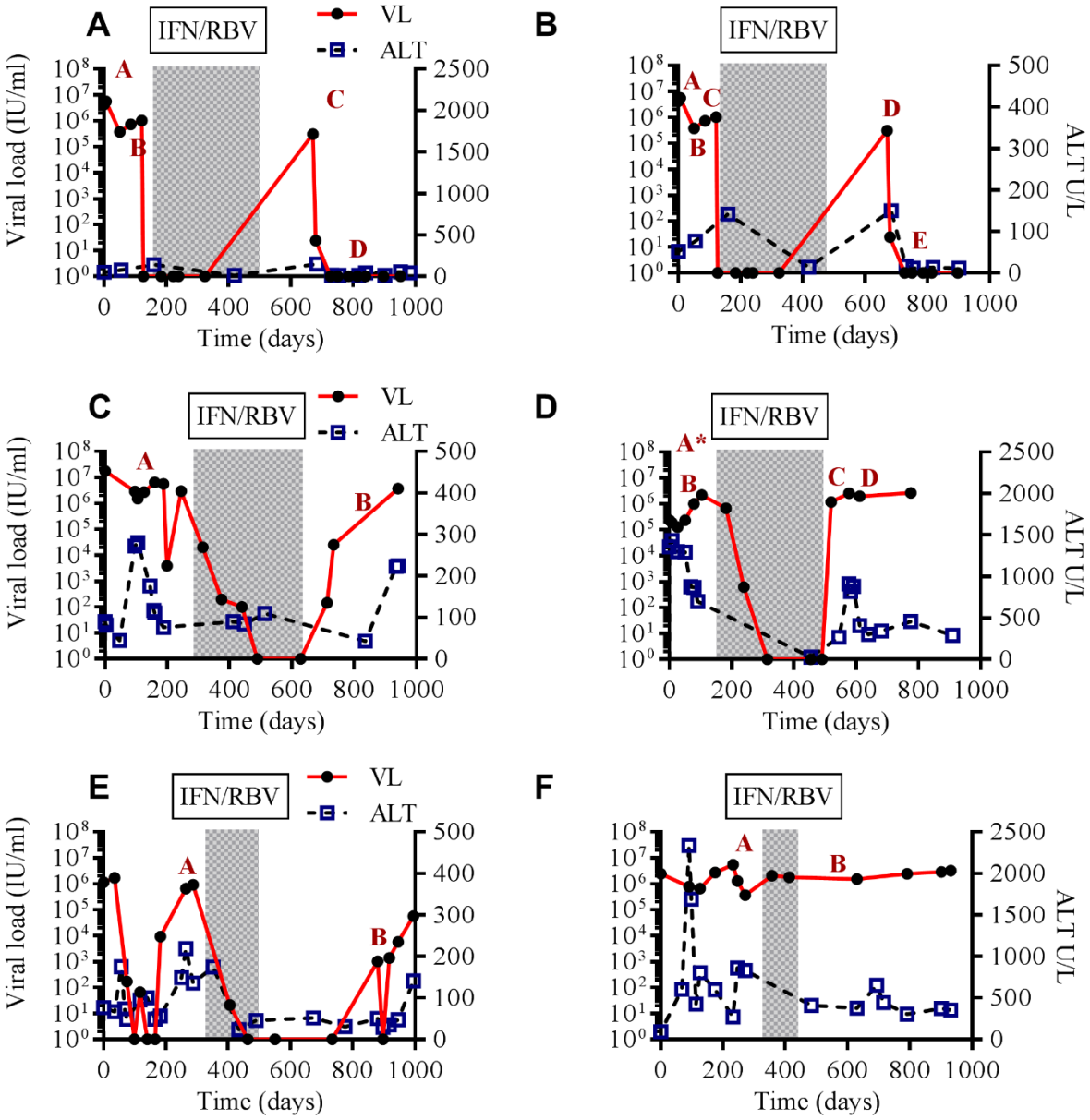

Figure 3.62 Viral loads and alanine aminotransferase levels of SSC and control patients
The graphs show the viral loads and alanine aminotransferase level for the first 1000 days post first HCV positive PCR in secondary spontaneous clearers (SSC) and treatment failure (TF) patients. The black dots on red lines indicate viral load levels in $\log_{10}$ IU/ml and the blue boxes on dashed lines represent alanine aminotransferase levels (ALT) in Units/Litre (U/L). The grey boxes indicate the duration of pegylated interferon (PEG-IFN) and ribavirin (RBV) treatment for each patient. Letters A-E indicate different time points (TP) during the infection of each patient. A. P76, a genotype 1a SSC at TPA and TPB pre-treatment and TPC and TPD post-treatment. B. P155, a genotype 4d SSC. TPA-TPC were pre-treatment and TPD and TPE post-treatment. C.P75, a genotype 1a relapse control at TPA pre-treatment and TPB post-treatment. D. P131, a genotype 1a relapse control. TPA and TPB were pre-treatment and TPC/TPD were post-treatment. A*-Time-point taken prior to first positive PCR. E. P101, a genotype 1a relapse control at TPA pre-treatment and TPB post-treatment. F. P63, a genotype 1a null responder control at TPA pre-treatment and TPB post-treatment.

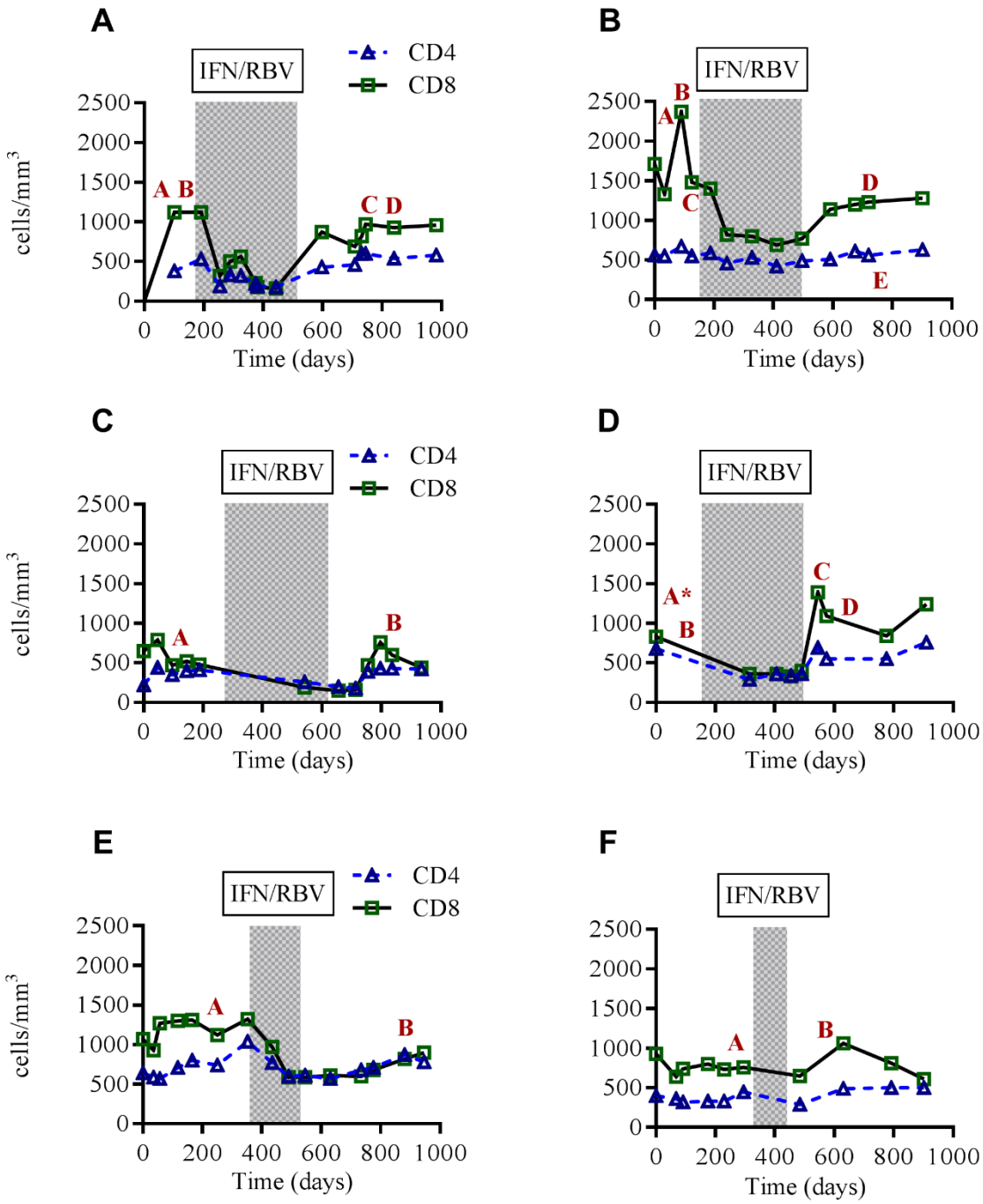

Figure 3.63 The CD4 and CD8 count of secondary spontaneous clearers and control patients.
The number of CD4 and CD8 T cells within the first 1000 days post first HCV positive PCR in secondary spontaneous clearers (SSC) and treatment failure (TF) patients. The triangles on dashed blue lines indicate CD4 T cell number in cells/mm3 and the squares on solid lines represent CD8 T cell number in cells/mm3. The grey boxes indicate the duration of pegylated interferon (PEG-IFN) and ribavirin (RBV) treatment for each patient. Letters A-E indicate different time points (TP) during the infection of each patient. A. P76 (genotype 1a) SSC. TPA and TPB pre-treatment and TPC and TPD post-treatment. B. P155, a genotype 4d SSC. TPA-TPC were pre-treatment and TPD and TPE post-treatment. C.P75, a genotype 1a relapse control at TPA pre-treatment and TPB post-treatment. D. P131, a genotype 1a relapse control. TPA and TPB were pre-treatment and TPC/TPD were post-treatment. A*-Time-point taken prior to first positive PCR. E. P101, a genotype 1a relapse control at TPA pre-treatment and TPB post-treatment. F. P63, a genotype 1a null responder control at TPA pre-treatment and TPB post-treatment.

Table 3.10 Amino acid alignment of consensus E1E2 sequences from patient 76

H77	171	-	G	C	S	F	S	I	F	L	L	A	L	L	S	C	L	T	V	P	A	S	A	Y	Q	V	R	N	S	S	G	L	Y	H	V	T	N	D	C	P	N	209
P76_TPA		M	-	G	C	S	F	S	I	F	L	L	A	L	L	S	C	L	T	V	P	A	S	A	Y	Q	V	R	N	S	T	G	L	Y	H	V	T	N	D	C	P	
P76_TPC		M	.	.	.	.	.	.	.	.	.	.	.	.	.	.	.	.	.	.	.	.	.	.	.	.	.	.	.	.	.	.	.	.	.	.	.	.	.	.	.	.	.	
H77	210	S	S	I	V	Y	E	A	A	D	A	I	L	H	T	P	G	C	V	P	C	V	R	E	G	N	A	S	R	C	W	V	A	V	T	P	T	V	A	T	R	249
P76_TPA		S	S	I	V	Y	E	A	D	D	A	I	L	H	T	P	G	C	V	P	C	V	R	E	G	N	T	S	R	C	W	V	A	V	T	P	T	V	A	T	R	
P76_TPC		.	.	.	.	.	.	.	.	.	.	.	.	.	**A**	.	.	.	.	.	.	.	.	.	.	.	.	.	.	.	.	.	.	.	.	.	.	.	.	.	.	.	.	
H77	250	D	G	K	L	P	T	T	Q	L	R	R	H	I	D	L	L	V	G	S	A	T	L	C	S	A	L	Y	V	G	D	L	C	G	S	V	F	L	V	G	Q	289
P76_TPA		D	G	N	L	P	T	K	H	L	R	R	H	I	D	L	L	V	G	S	A	T	L	C	S	A	L	Y	V	G	D	L	C	G	S	V	F	L	V	G	Q	
P76_TPC		.	.	.	.	.	.	.	.	.	.	.	.	.	.	.	.	.	.	.	.	.	.	.	.	.	.	.	.	.	.	.	.	.	.	.	.	.	.	.	.	.	.	
H77	290	L	F	T	F	S	P	R	R	H	W	T	T	Q	D	C	N	C	S	I	Y	P	G	H	I	T	G	H	R	M	A	W	D	M	M	M	N	W	S	P	T	329
P76_TPA		L	F	T	F	S	P	R	R	H	W	T	T	Q	D	C	N	C	S	I	Y	P	G	H	I	T	G	H	R	M	A	W	D	M	M	M	N	W	S	P	T	
P76_TPC		.	.	.	.	.	.	.	.	.	.	.	.	.	.	.	.	.	.	.	.	.	.	.	.	.	.	.	.	.	.	.	.	.	.	.	.	.	.	.	.	.	.	
H77	330	A	A	L	V	V	A	Q	L	L	R	I	P	Q	A	I	M	D	M	I	A	G	A	H	W	G	V	L	A	G	I	A	Y	F	S	M	V	G	N	W	A	369
P76_TPA		T	A	L	I	M	A	Q	L	L	R	I	P	Q	A	I	L	D	M	I	A	G	A	H	W	G	V	L	A	G	I	A	Y	F	S	M	V	G	N	W	A	
P76_TPC		.	.	.	.	.	.	.	.	.	.	.	.	.	.	.	.	.	.	.	.	.	.	.	.	.	.	.	.	.	.	.	.	.	.	.	.	.	.	.	.	.	.	
H77	370	K	V	L	V	V	L	L	L	F	A	G	V	D	A	E	T	H	V	T	G	G	S	A	G	R	T	T	A	G	L	V	G	L	L	T	P	G	A	K	Q	409
P76_TPA		K	V	L	V	V	L	L	L	F	A	G	V	D	A	H	T	V	I	T	G	G	S	S	A	R	T	T	Q	A	L	T	G	L	F	T	Q	G	A	K	Q	
P76_TPC		.	.	.	.	.	.	.	.	.	.	.	.	.	.	.	.	**F**	.	.	.	.	.	.	.	.	.	.	.	.	.	.	**S**	.	.	.	.	.	.	**R**	.	
H77	410	N	I	Q	L	I	N	T	N	G	S	W	H	I	N	S	T	A	L	N	C	N	E	S	L	N	T	G	W	L	A	G	L	F	Y	Q	H	K	F	N	S	449
P76_TPA		N	I	Q	L	I	N	T	N	G	S	W	H	I	N	R	T	A	L	N	C	N	D	S	L	Q	T	G	W	I	A	G	L	F	Y	A	N	R	F	N	S	
P76_TPC		.	.	.	.	.	.	.	.	.	.	.	.	.	.	.	.	.	.	.	.	.	.	.	.	.	.	.	.	.	.	.	.	.	.	.	.	.	.	.	.	.	.	
H77	450	S	G	C	P	E	R	L	A	S	C	R	R	L	T	D	F	A	Q	G	W	G	P	I	S	Y	A	N	G	S	G	L	D	E	R	P	Y	C	W	H	Y	489
P76_TPA		S	G	C	P	E	R	L	A	S	C	R	P	L	T	D	F	A	Q	G	W	G	P	I	S	H	T	S	E	G	G	P	D	Q	R	P	Y	C	W	H	Y	
P76_TPC		.	.	.	.	.	.	.	.	.	.	.	.	.	.	.	.	.	.	.	.	.	.	.	.	.	.	.	.	.	.	.	.	.	.	.	.	.	.	.	.	.	.	
H77	490	P	P	R	P	C	G	I	V	P	A	K	S	V	C	G	P	V	Y	C	F	T	P	S	P	V	V	V	G	T	T	D	R	S	G	A	P	T	Y	S	W	529
P76_TPA		P	P	K	P	C	G	I	V	P	A	K	S	V	C	G	P	V	Y	C	F	T	P	S	P	V	V	V	G	T	T	D	R	S	G	A	P	T	Y	S	W	
P76_TPC		.	.	.	.	.	.	.	.	.	.	.	.	.	.	.	.	.	.	.	.	.	.	.	.	.	.	.	.	.	.	.	.	.	.	.	.	.	.	.	.	.	.	
H77	530	G	A	N	D	T	D	V	F	V	L	N	N	T	R	P	P	L	G	N	W	F	G	C	T	W	M	N	S	T	G	F	T	K	V	C	G	A	P	P	C	569
P76_TPA		G	E	N	D	T	D	V	F	V	L	N	N	T	R	P	P	M	G	N	W	F	G	C	T	W	M	N	S	T	G	F	T	K	V	C	G	A	P	P	C	
P76_TPC		.	.	.	.	.	.	.	.	.	.	.	.	.	.	.	.	.	.	.	.	.	.	.	.	.	.	.	.	.	.	.	.	.	.	.	.	.	.	.	.	.	.	
H77	570	V	I	G	G	V	G	N	N	T	L	L	C	P	T	D	C	F	R	K	H	P	E	A	T	Y	S	R	C	G	S	G	P	W	I	T	P	R	C	M	V	609

P76_TPA		V	I	G	G	N	G	N	N	T	L	Y	C	P	T	D	C	F	R	K	H	P	E	A	T	Y	S	R	C	G	S	G	P	W	I	T	P	R	C	L	V	
P76_TPC		.	.	.	.	**D**	.	.	.	.	.	.	.	.	.	.	.	.	.	.	.	.	.	.	.	.	.	.	.	.	.	.	.	.	.	.	.	.	.	.	.	.	
H77	610	D	Y	P	Y	R	L	W	H	Y	P	C	T	I	N	Y	T	I	F	K	V	R	M	Y	V	G	G	V	E	H	R	L	E	A	A	C	N	W	T	R	G	649
P76_TPA		D	Y	P	Y	R	L	W	H	Y	P	C	T	I	N	Y	T	I	F	K	V	R	M	Y	V	G	G	V	E	H	R	L	E	A	A	C	N	W	T	R	G	
P76_TPC		.	.	.	.	.	.	.	.	.	.	.	.	.	.	.	.	.	.	.	.	.	.	.	.	.	.	.	.	.	.	.	.	.	.	.	.	.	.	.	.	.	.	
H77	650	E	R	C	D	L	E	D	R	D	R	S	E	L	S	P	L	L	L	S	T	T	Q	W	Q	V	L	P	C	S	F	T	T	L	P	A	L	S	T	G	L	689
P76_TPA		E	R	C	D	L	E	D	R	D	R	S	E	L	S	P	L	L	L	S	T	T	Q	W	Q	V	L	P	C	S	F	T	T	L	P	A	L	S	T	G	L	
P76_TPC		.	.	.	.	.	.	.	.	.	.	.	.	.	.	.	.	.	.	.	.	.	.	.	.	.	.	.	.	.	.	.	.	.	.	.	.	.	.	.	.	.	.	
H77	690	I	H	L	H	Q	N	I	V	D	V	Q	Y	L	Y	G	V	G	S	S	I	A	S	W	A	I	K	W	E	Y	V	V	L	L	F	L	L	L	A	D	A	729
P76_TPA																																											
P76_TPC		.	.	.	.	.	.	.	.	.	.	.	.	.	.	.	.	.	.	.	.	.	.	.	.	.	.	.	.	.	.	.	.	.	.	.	.	.	.	.	.	.	.	
H77	730	R	V	C	S	C	L	W	M	M	L	L	I	S	Q	A	E	A																								746
P76_TPA																																											
P76_TPC		.	.	.	.	.	.	.	.	.	.	.	.	.	.	.	.	.																								

Dots indicate conserved regions. Amino acid numbering is based on the H77 reference sequence (Accession Number AF009606), with H77 amino acid sequence marked in grey. Changes between the two time points are indicated in bold red type. Raw sequence data was supplied by Dr Rachael Swann.

Table 3.11 Amino acid alignment of consensus E1E2 sequence from patient 155

H77	**171**	-	G	C	S	F	S	I	F	L	L	A	L	L	S	C	L	T	V	P	A	S	A	Y	Q	V	R	N	S	S	G	L	Y	H	V	T	N	D	C	P	N	**209**
P155	TPA	M	G	C	S	F	S	I	F	L	L	A	L	L	S	C	L	T	V	P	A	S	A	Y	N	Y	R	N	S	S	G	V	Y	H	V	T	N	D	C	P	N	
P155	TPD	M	.	.	.	.	.	.	.	.	.	.	.	.	.	.	.	.	.	.	.	.	.	.	.	.	.	.	.	.	.	.	.	.	.	.	.	.	.	.	.	.	
H77	**210**	S	S	I	V	Y	E	A	A	D	A	I	L	H	T	P	G	C	V	P	C	V	R	E	G	N	A	S	R	C	W	V	A	V	T	P	T	V	A	T	R	**249**
P155	TPA	S	S	I	V	Y	E	A	D	H	H	I	L	H	L	P	G	C	V	P	C	V	R	V	G	N	K	S	T	C	W	V	S	L	T	P	T	V	A	A	P	
P155	TPD	.	.	.	.	.	.	.	.	.	.	.	.	.	.	.	.	.	.	.	.	.	.	.	.	.	.	.	.	.	.	.	.	.	.	.	.	.	.	.	.	.	
H77	**250**	D	G	K	L	P	T	T	Q	L	R	R	H	I	D	L	L	V	G	S	A	T	L	C	S	A	L	Y	V	G	D	L	C	G	S	V	F	L	V	G	Q	**289**
P155	TPA	Y	L	N	A	P	L	E	S	L	R	R	H	V	D	L	M	V	G	S	A	T	L	C	S	A	L	Y	I	G	D	V	C	G	G	A	F	L	V	G	Q	
P155	TPD	.	.	.	.	.	.	.	.	.	.	.	.	.	.	.	.	.	.	.	.	.	.	.	.	.	.	.	.	.	.	.	.	.	.	.	.	.	.	.	.	.	
H77	**290**	L	F	T	F	S	P	R	R	H	W	T	T	Q	D	C	N	C	S	I	Y	P	G	H	I	T	G	H	R	M	A	W	D	M	M	M	N	W	S	P	T	**329**
P155	TPA	L	F	T	F	R	P	R	R	H	W	T	T	Q	D	C	N	C	S	I	Y	T	G	H	I	T	G	H	R	M	A	W	D	M	M	M	N	W	S	P	T	
P155	TPD	.	.	.	.	.	.	.	.	.	.	.	.	.	.	.	.	.	.	.	.	.	.	.	.	.	.	.	.	.	.	.	.	.	.	.	.	.	.	.	.	.	
H77	**330**	A	A	L	V	V	A	Q	L	L	R	I	P	Q	A	I	M	D	M	I	A	G	A	H	W	G	V	L	A	G	I	A	Y	F	S	M	V	G	N	W	A	**369**
P155	TPA	A	T	L	V	L	A	Q	L	M	R	I	P	S	A	M	V	D	L	L	A	G	G	H	W	G	I	L	A	G	I	A	Y	F	S	M	Q	A	N	W	A	
P155	TPD	.	.	.	.	.	.	.	.	.	.	.	.	.	.	.	.	.	.	.	.	.	.	.	.	.	.	.	.	.	.	.	.	.	.	.	.	.	.	.	.	.	
H77	**370**	K	V	L	V	V	L	L	L	F	A	G	V	D	A	E	T	H	V	T	G	G	S	A	G	R	T	T	A	G	L	V	G	L	L	T	P	G	A	K	Q	**409**
P155	TPA	K	V	I	L	V	L	F	L	F	A	G	V	D	A	E	T	Q	V	T	G	G	Q	A	A	R	A	A	F	S	F	A	S	L	F	N	P	G	S	R	Q	
P155	TPD	.	.	.	.	.	.	.	.	.	.	.	.	.	.	.	.	.	.	.	.	.	.	.	.	.	.	.	.	.	.	.	.	.	.	.	.	.	.	.	.	.	
H77	**410**	N	I	Q	L	I	N	T	N	G	S	W	H	I	N	S	T	A	L	N	C	N	E	S	L	N	T	G	W	L	A	G	L	F	Y	Q	H	K	F	N	S	**449**
P155	TPA	N	I	Q	L	I	N	T	N	G	S	W	H	I	N	R	T	A	L	N	C	E	D	S	L	N	T	G	F	I	A	G	L	L	H	Y	N	K	F	N	S	
P155	TPD	.	.	.	.	.	.	.	.	.	.	.	.	.	.	.	.	.	.	.	.	.	.	.	.	.	.	.	.	.	.	.	.	.	.	**Y**	.	.	.	.	.	.	
H77	**450**	S	G	C	P	E	R	L	A	S	C	R	R	L	T	D	F	A	Q	G	W	G	P	I	S	Y	A	N	G	S	G	L	D	E	R	P	Y	C	W	H	Y	**489**
P155	TPA	S	G	C	P	E	R	L	A	S	C	S	S	L	D	S	L	Q	Q	G	W	G	P	L	G	T	Y	Q	A	N	E	S	D	T	R	P	Y	C	W	N	Y	
P155	TPD	.	.	.	.	.	.	.	.	.	.	.	.	.	.	.	.	.	.	.	.	.	.	.	.	.	.	.	.	.	.	.	.	.	.	.	.	.	.	.	.	.	
H77	**490**	P	P	R	P	C	G	I	V	P	A	K	S	V	C	G	P	V	Y	C	F	T	P	S	P	V	V	V	G	T	T	D	R	S	G	A	P	T	Y	S	W	**529**
P155	TPA	T	P	R	P	C	W	T	V	P	A	S	T	V	C	G	P	V	Y	C	F	T	P	S	P	V	V	V	G	T	T	D	R	L	G	V	P	T	Y	T	W	
P155	TPD	.	.	.	.	.	.	.	.	.	.	.	.	.	.	.	.	.	.	.	.	.	.	.	.	.	.	.	.	.	.	.	.	.	.	.	.	.	.	.	.	.	
H77	**530**	G	A	N	D	T	D	V	F	V	L	N	N	T	R	P	P	L	G	N	W	F	G	C	T	W	M	N	S	T	G	F	T	K	V	C	G	A	P	P	C	**569**
P155	TPA	G	E	N	E	T	D	V	F	L	L	N	T	T	R	P	P	R	G	A	W	F	G	C	T	W	M	N	S	T	G	F	T	K	S	C	G	G	P	P	C	
P155	TPD	.	.	.	.	.	.	.	.	.	.	.	.	.	.	.	.	.	.	.	.	.	.	.	.	.	.	.	.	.	.	.	.	.	.	.	.	.	.	.	.	.	
H77	**570**	V	I	G	G	V	G	N	N	T	L	L	C	P	T	D	C	F	R	K	H	P	E	A	T	Y	S	R	C	G	S	G	P	W	I	T	P	R	C	M	V	**609**

P155	TPA	S	V	T	_	T	N	N	G	T	W	G	C	P	T	D	C	F	R	K	H	P	E	A	T	Y	T	K	C	G	S	G	P	W	L	T	P	R	C	L	V	
P155	TPD	.	.	.	.	.	.	.	.	.	.	.	.	.	.	.	.	.	.	.	.	.	.	.	.	.	.	.	.	.	.	.	.	.	.	.	.	.	.	.	.	.	.	
H77	**610**	D	Y	P	Y	R	L	W	H	Y	P	C	T	I	N	Y	T	I	F	K	V	R	M	Y	V	G	G	V	E	H	R	L	E	A	A	C	N	W	T	R	G	**649**
P155	TPA	D	Y	P	Y	R	L	W	H	Y	P	C	T	V	N	Y	T	I	F	K	V	R	M	Y	V	G	G	I	E	H	R	L	D	A	A	C	N	W	T	R	G	
P155	TPD	.	.	.	.	.	.	.	.	.	.	.	.	.	.	.	.	.	.	.	.	.	.	.	.	.	.	.	.	.	.	.	.	.	.	.	.	.	.	.	.	.	.	
H77	**650**	E	R	C	D	L	E	D	R	D	R	S	E	L	S	P	L	L	L	S	T	T	Q	W	Q	V	L	P	C	S	F	T	T	L	P	A	L	S	T	G	L	**689**
P155	TPA	E	P	C	N	L	E	H	R	D	R	T	E	L	S	P	L	L	L	S	T	T	Q	W	Q	V	L	P	C	S	F	T	T	L	P	A	L	S	T	G	L	
P155	TPD	.	.	.	.	.	.	.	.	.	.	.	.	.	.	.	.	.	.	.	.	.	.	.	.	.	.	.	.	.	.	.	.	.	.	.	.	.	.	.	.	.	.	
H77	**690**	I	H	L	H	Q	N	I	V	D	V	Q	Y	L	Y	G	V	G	S	S	I	A	S	W	A	I	K	W	E	Y	V	V	L	L	F	L	L	L	A	D	A	**729**
P155	TPA	I	H	L	H	Q	N	I	V	D	V	Q	Y	L	Y	G	V	G	S	A	V	V	S	W	A	L	K	W	E	Y	I	V	L	A	F	L	L	L	A	D	A	
P155	TPD	.	.	.	.	.	.	.	.	.	.	.	.	.	.	.	.	.	.	.	.	.	.	.	.	.	.	.	.	.	.	.	.	.	.	.	.	.	.	.	.	.	.	
H77	**730**	R	V	C	S	C	L	W	M	M	L	L	I	S	Q	A	E	A																								**746**
P155	TPA	R	L	C	A	C	L	W	M	M	L	M	V	S	Q	V	E	A																								
P155	TPD	.	.	.	.	.	.	.	.	.	.	.	.	.	.	.	.	.																								

Dots indicate conserved regions. Amino acid numbering are based on H77 sequence (Accession Number AF009606) with H77 amino acid sequence marked in grey. Changes between the two time points are indicated in bold red type.

Figure 3.64 shows viral load, ALT level and treatment duration (Figure 3.64a), CD4 and CD8 T cell levels (Figure 3.64b) and the relationship between viral load and CD8: CD4 T cell ratio (Figure 3.64c) in P57. P57 was a patient added as an additional control for the purpose of Luminex analysis (See section 3.2.9). Although four time-points were used for the Luminex analysis (A-D) they were all taken prior to the patient receiving IFN/RBV treatment. The viral load of the patient was at the highest point at the time of diagnosis (TPA, >107 IU/ml) and remained high above 106 IU/ml prior to the patient receiving treatment (TPB-TPD). Over the course of therapy, the viral load steadily decreased until undetected levels after day 400. However, a relapse occurred post-treatment around day 600 where the viral load returned to high levels of above 106 IU/ml. The ALT levels pre-treatment fluctuated between 232 U/ml to 2316 U/ml at day 54 and 142, respectively, which rapidly decreased below 200 U/ml throughout and post-treatment. The CD4 and CD8 count displayed almost identical patterns throughout the first 1000 days following the first HCV PCR positive. Pre-treatment the CD4 and CD8 cell count increased from 710 cells/mm3 for both to 570 and 560 cells/mm3, respectively at day 293. Throughout the course of treatment the CD4/CD8 count dropped to 430 and 280 cells/mm3, respectively, raising up steadily after the treatment to 960 and 860 cells/mm3. The ratio of CD8 to CD4 T cells raised to around 1 prior to treatment and remained steady with minor fluctuations throughout the course of infection within the first 1000 days post infection.

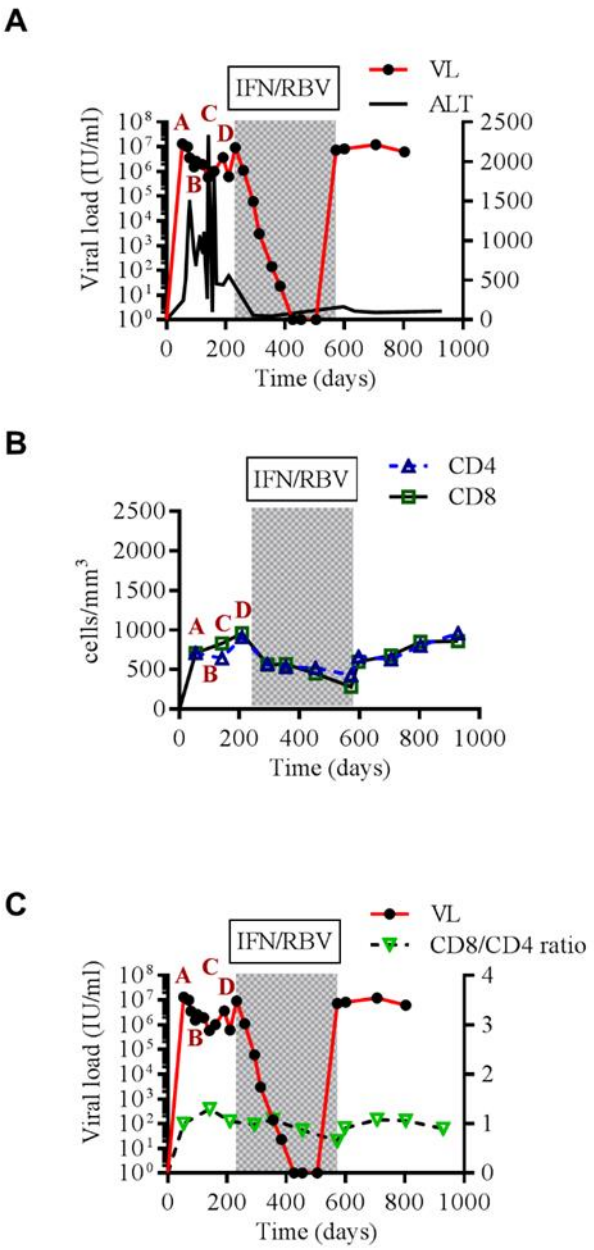

Figure 3.64 Natural history of HCV infection in patient 57.
The natural history of infection for the first 1000 days post first HCV positive PCR in relapse control patient 57 (P57). The black dots on red lines indicate viral load levels in $\log_{10}$ IU/ml. The grey boxes indicate the duration of pegylated interferon (PEG-IFN) and ribavirin (RBV) treatment. Letters A-D indicate different time points during the infection. A. The viral load level and alanine aminotransferase levels (ALT, U/L) in Units/Litre (indicated by the blue boxes on dashed lines) during the course of infection B. The number of CD4 and CD8 T cells. The triangles on dashed blue lines indicate CD4 T cell number in cells/mm^3 and the squares on solid lines represent CD8 T cell number in cells/mm^3. C. The ratio of CD8 to CD4 T cells during the course of HCV infection (numbers on right y-axis) in relation to viral load levels (red line with black dots).

3.2.2 Phylogenetic analysis of patient sequences

In order to distinguish relapse from reinfection in SSC patients, consensus sequences obtained by NGS at varying time-points pre- and post-treatment were aligned and used for phylogenetic analysis. The following treatment failure patients and their time points were also included on the phylogenetic tree: P63 TPA (021008), P63 TPB (110609), P75 TPA (210808), P75 TPB (091110), P101 TPA (161008), P131 TPA (260608), P131 TPB (260909) and P131 TPC (031210). Sequences from P76 samples were unavailable for NGS but E1E2 sequences were available from previous Sanger sequencing (carried out by Dr Rachael Swann). Figure 3.65 shows the phylogenetic tree for all acute HCV patients from the acute HCV cohort and revealed that the SSC failure patient samples clustered together with >60% bootstrap values (Figure 3.65b).

The E1E2 sequences from P76 clustered together in keeping with relapse rather than reinfection (bootstrap value of 100%). They have been referred to as '110606' and '200710' clones referring to the pre-treatment TPA and post-treatment TPC, respectively.

Since one of the SSC patients was infected with genotype 4d, we also looked at the phylogenetic analysis of all full genome sequences of genotype 4d infected patients in the acute HCV cohort and compared them to P155 time-point at the full genome level (Figure 3.65c). All dually infected or mixed infections were excluded from the analysis. Figure 3.65c shows that all P155 time-points including; TPA (181209), TPB (210110), TPC (220410), TPD (241011) are clustered together with a high level of confidence (>60% bootstrap value).

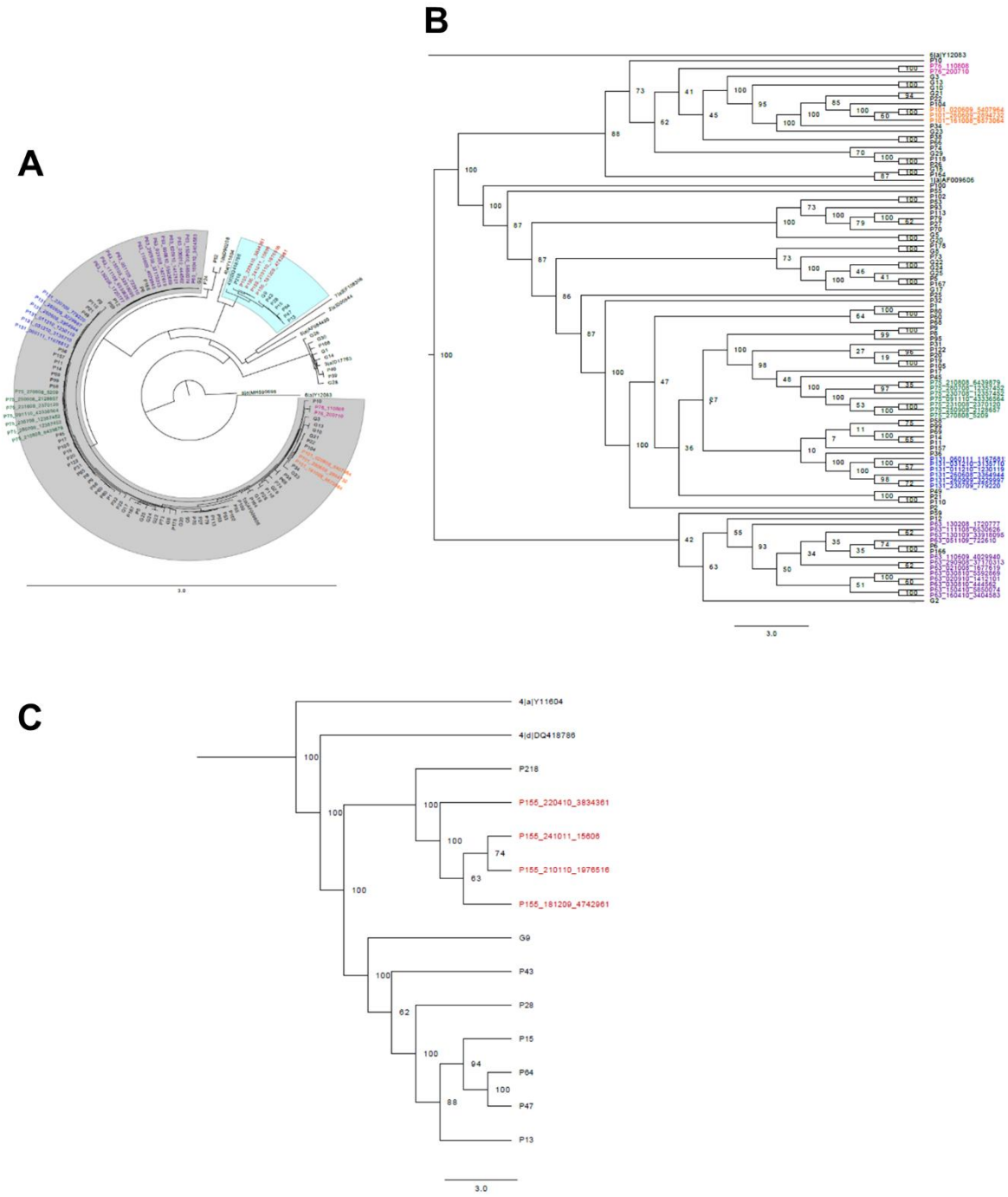

Figure 3.65 Phylogenetic tree of acute HCV patients from St Mary's cohort
Consensus sequences from the HCV open reading frame (ORF) were obtained by NGS on the Illumina Miseq platform as described in Materials and Methods. Mafft software was used for the alignment of the open reading frame of all acute HCV patients from the St Mary's cohort. Alignments were visually inspected and corrected manually as per requirements. The phylogenetic tree was generated using Raxml software with 500 bootstraps with a generalised time-reversible (GTR) + Gamma model. Secondary spontaneous clearers, P76 and P155 and treatment failure patients, P131, P101, P75, P63 are shown by coloured text indicated by the following colours: pink, red, blue, orange, green and purple, respectively. All time-points included for which NGS was successful. One example of a sequence at any time point was included for patients not analysed experimentally as part of this thesis. The tree was rooted at genotype 8a reference sequence (Accession number: MH590698). The numbers at the tree roots represent bootstrapping values (%).A – indicates the entire phylogenetic tree. Areas highlighted in grey are genotype 1a samples. Areas highlighted in blue are genotype 4 samples. B – Phylogenetic tree of the greyed out area from diagram A representing all genotype 1a samples. P76 samples represent E1E2 consensus sequenced obtained through Sanger sequencing by Dr Rachael Swann. C – Phylogenetic tree of the area highlighted in blue from diagram A representing all genotype 4 samples. Numbers at the end of sample names indicate the number of reads obtained through NGS. P76_110606_TPA, P76_200710 – TPB, P155_181209 – TPA, P155_210110 – TPB, P155_220410_TPC, P155_241011 – TPD, P63_021008 – TPA, P63_110609 – TPB, P75_210808 – TPA, P75_091110 –TPB, P131_260608 – TPA, P131_260909 – TPB, P131_031210 – TPC, P131_060111 – TPD

3.2.3 Generation of autologous pseudoparticles from patient samples

We hypothesised that humoral immune responses were active and may have contributed at least in part, to SSC. In order to study neutralising antibody responses, viral RNA was extracted from plasma from each SSC patient, converted to cDNA and nested PCR performed (using a directional tag and primers) in order to amplify the entire E1E2 sequence from one time-point pre-treatment and one time-point post-treatment. Purified E1E2 was then cloned into a pENTR/D-TOPO entry vector and subcloned into the phCMV expression vector in order to produce autologous HCV pseudoparticles (HCVpp). Purified IgG and plasma samples were then used to assess neutralisation against the autologous HCVpp. P76 (TPA and TPC) E1E2 sequences were previously amplified and cloned into both plasmid vectors, producing functional HCVpp in HEK-293T cells by Dr Rachael Swann.

The second SSC patient (P155) was infected with HCV genotype 4d, therefore the primers required modification for this genotype. In order to determine the different humoral immune responses pre and post-treatment, the aim of the nested PCR was to obtain at least one E1E2 from a pre-treatment time-point and one post-treatment. Table 3.12 outlines the experimental conditions required to optimise the PCR. The first experiments were carried out to optimise primer melting temperature (Tm) using the Phusion High Fidelity DNA polymerase protocol and online Tm calculator (NEB). Subsequently, DMSO was added in order to reduce the secondary structure of the starting material. As no cDNA product was obtained at the expected size (1890 bp), the PCR primers were further optimised. It was noted that the predicted Tm differed by more than 2°C for the inner primers. These were therefore modified to increase the Tm to 72°C, thus reducing chances of non-specific binding and amplification. Finally, since the final product size was >1500 bp, the extension time was increased from 30 seconds to 1 minute, and subsequently to 1 minute 30 seconds giving more time for the DNA polymerase to extend the fragment. These modifications resulted successful amplification of sequence obtained for P155 (TPA), as is indicated on Figure 3.66. No fragments above 1.5 kb were obtained for any other samples, although fragments <1000 bp were present.

Table 3.12 Experimental conditions for nested PCR for amplification of genotype 4d E1E2 (P155)

	Outer PCR (35 cycles)			Inner PCR (35 cycles)			Outcome
Exp	Anneal Tm/Time	Extension Tm/ Time	Primers	Anneal Tm/ Time	Extension Tm/Time	Primers	Amplification of E1E2 fragment
1	67°C/30 sec	72°C/1 min	Original	68°C/30 sec	72°C/1 min	Original	No
2	A. 67°C/30 sec B. 62°C/30 sec C* 62°C/30 sec	72°C/1 min	Original	68°C/30 sec	72°C/1 min	Original	No
3	A. 67°C/30 sec B. 62°C/30 sec	72°C/1 min 72°C/1 min	Original New	72°C/1 min 72°C/1 min	72°C/1 min 72°C/1 min	Original New	No
4	A. 68°C/1 min	72°C/1 min 30 sec	New	72°C/1 min	72°C/1 min 30 sec	New	Yes. P155 TPA

*Indicates the addition of DMSO. Primer Tm was based on NEB Tm calculator. Original primers (designed by Dr Rachael Swann) were modified according to the P155 consensus sequence following NGS (See Materials and Methods). New primers were extended to increase Tm for outer and inner primer sets to 72°C. Text highlighted in bold indicates the alternations between the different experiments. Exp –Experiment.

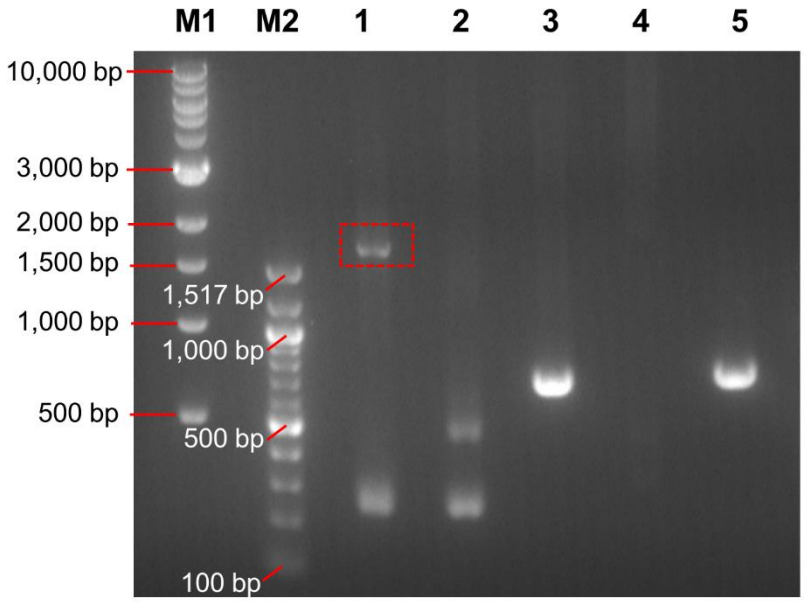

Figure 3.66 Gel electrophoresis showing amplification of P155 E1E2 sequence by nested PCR
Nested PCR was used to amplify P155 E1E2 from TPA, TPB, TPC and TPD at positions 1,2,3,4 respectively with no template control added at position 5. M1 and M2 represent 1 kb NEB ladder and 100 bp NEB ladder, respectively with markings on the left. The dashed red square indicates a PCR fragment of 1890 base pairs from P155 TPA, which was gel purified and sequenced.

The fragment from P155 TPA on Figure 3.66 was gel purified and cloned into the pENTR/D-TOPO vector as described in Materials and Methods. The cloning reaction resulted in five clones, which were grown overnight in selective media and DNA extracted. The samples were subsequently sent for Sanger sequencing in order to confirm that E1E2 sequences were present within the vector (Eurofins Genomics). Figure 3.67 shows the alignment of P155 TPA consensus sequence from target-enrichment NGS and the five clonal sequences for the first 100 base pairs of the insert determined by Sanger sequencing. 4/5 sequences had high similarity to the P155 TPA NGS consensus sequence, confirming that E1E2 was successfully inserted into the vector. Clone 3 was highly dissimilar and was not used for downstream processing.

Figure 3.67 Alignment of consensus sequence from P155 TPA with nested PCR inserts in pENTR/D-TOPO vector
A PCR fragment at the correct size (1725 base pairs) was gel purified and inserted into the pENTR/D-TOPO vector as described in Materials and Methods. The resulting colonies were sent for Sanger sequencing using the M13 forward and M13 reverse primers and aligned with the consensus sequence from P155 TPA (P155_NGS_1) obtained through NGS. The alignment shows the first 100 base pairs from the expected sequence of end of Core/start of E1E2 and five clones obtained through Sanger sequencing. Where mismatches occurred, chromatograms were visually inspected to confirm their presence. The letters in red show mismatches in the sequence, dashes indicate missing sequence. The numbers above the alignment are based on the start of the expected sequence and the numbers in brackets are based on nucleotide numbers from H77 reference genome (Accession number: AF009606)

The clones were next analysed to ensure that stop codons were not present within E1E2 as this would result in truncated protein expression on pseudoparticles. Figure 3.68 shows that none of the four clones analysed contained a stop codon. Clone 1 had two amino acid changes from the original P155 TPA NGS consensus: one at position 294 from Arginine to Glutamine (R294G) and one at 493 from Proline to Alanine (P493A). Clone 2 had one amino acid change at position 706 from Glycine to Alanine (G706A). Clones 4 and 5 had no amino acid changes from the NGS consensus sequence.

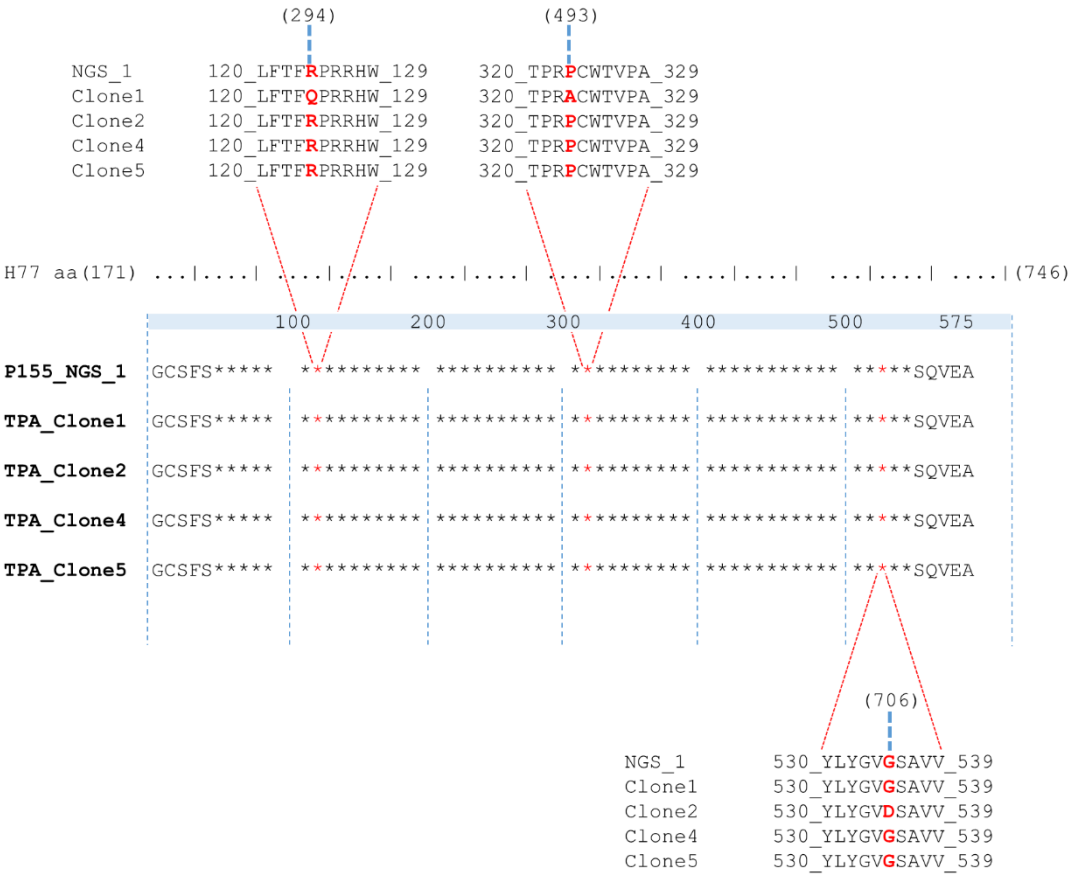

Figure 3.68 Amino acid changes in P155 TPA E1E2 pENTR/D-TOPO clones from consensus sequence
The entire amino acid sequence inserted into pENTR/D-TOPO vector was numbered 1-575. The numbers displayed in brackets indicate amino acid position based on H77 E1E2 sequence (Accession number: AF009606). Letters in bold red represent the position and the amino acid change in one of the clones. Only successfully transformed vectors were included in the analysis. The nucleotide sequence was manually translated into the amino acid sequence using Serial Cloner software.

Selected clones were subsequently recombined into the phCMV expression vector in order to obtain HCVpp by transfection of HEK-293T cells (See Materials and Methods). Sanger sequencing with a forward phCMV sequencing primer, provided by Dr Vanessa Cowton was used to confirm successful recombination. Figure 3.69 shows sequences obtained from Clones 4 and 5. Clones 1 and 2 failed sequencing.

```
      (171)  ....|....| ....|....| ....|....| ....|....| ....|....|
                      10         20         30         40         50
P155_NGS_1   GCSFSIFLLA LLSCLTVPAS AYNYRNSSGV YHVTNDCPNS SIVYEADHHI
TPA_Clone4   GCSFSIFLLA LLSCLTVPAS AYNYRNSSGV YHVTNDCPNS SIVYEADHHI
TPA_Clone5   GCSFSIFLLA LLSCLTVPAS AYNYRNSSGV YHVTNDCPNS SIVYEADHHI

             ....|....| ....|....| ....|....| ....|....| ....|....|
                      60         70         80         90        100
P155_NGS_1   LHLPGCVPCV RVGNKSTCWV SLTPTVAAPY LNAPLESLRR HVDLMVGSAT
TPA_Clone4   LHLPGCVPCV RVGNKSTCWV SLTPTVAAPY LNAPLESLRR HVDLMVGSAT
TPA_Clone5   LHLPGCVPCV RVGNKSTCWV SLTPTVAAPY LNAPLESLRR HVDLMVGSAT

             ....|....| ....|....| ....|....| ....|....| ....|....|
                     110        120        130        140        150 (320)
P155_NGS_1   LCSALYIGDV CGGAFLVGQL FTFRPRRHWT TQDCNCSIYT GHITGHRMAW
TPA_Clone4   LCSALYIGDV CGGAFLVGQL FT........ .......... ..........
TPA_Clone5   LCSALYIGDV CGGAFX.... .......... .......... ..........
```

Figure 3.69 Amino acid alignment of P155 TPA Clones after recombination into phCMV expression vector
Alignment of NGS consensus sequence of P155 from TPA and P155 TPA phCMV Clones to confirm successful recombination from entry vector to expression vector. Clones 1 and 2 failed sequencing and are not shown. The numbering in brackets is based on the amino acids from H77 E1E2 sequence (Accession number: AF009606). The alignment shows the first 150 amino acids from the expected sequence of end of Core/start of E1E2 and clones obtained through Sanger sequencing. The nucleotide sequence was manually translated into the amino acid sequence using Serial Cloner software.

Nested E1E2 PCR was successful for TPA from P155 but not subsequent time points. However, the sequence of subsequent time points was known from NGS. The TPA amino acid sequence pre-treatment and TPD amino acid sequence post-treatment were aligned in order to assess how many amino acids changes occurred between them as previously shown on Table 3.11. There was only one amino acid change throughout the entire sequence of the insert; a switch at position 443 from Histidine to Tyrosine (H443Y). Therefore, it was decided to perform site-directed mutagenesis to modify the nucleotide sequence in P155 TPA in phCMV expression vector, resulting in a subsequent amino acid change during expression of the E1E2 proteins on the HCVpp. Complementary primers were designed (see Materials and Methods) to span the mutation site with at least 9 nucleotides. The resulting plasmid was subsequently transformed into DH5α cells in selective media overnight, resulting in >100 colonies. Colonies were labelled site-directed mutagenesis 1-9 (SDM 1-9), their plasmid DNA extracted and sent for sequencing with a forward phCMV sequencing primer. Figure 3.70 shows an alignment of the original P155 TPA phCMV amino acid sequence translated from consensus sequence from NGS with P155 TPD NGS consensus sequence together with four SDM clones. Other SDM clones failed sequencing and are therefore not shown. Only 2/4 clones (SDM4 and SMD9) had a confirmed amino acid change from Histidine to Tyrosine at position 443 (H443Y). Sanger sequencing for the remaining clones, SDM2 and SDM4 terminated prior to reaching the mutation site and therefore it was not possible to determine whether the mutation was present. Therefore, clones SDM4 and SDM9 from SDM containing P155 TPD sequence and P155 TPA sequence were used for transfecting HEK-293T cells in order to obtain autologous HCVpp.

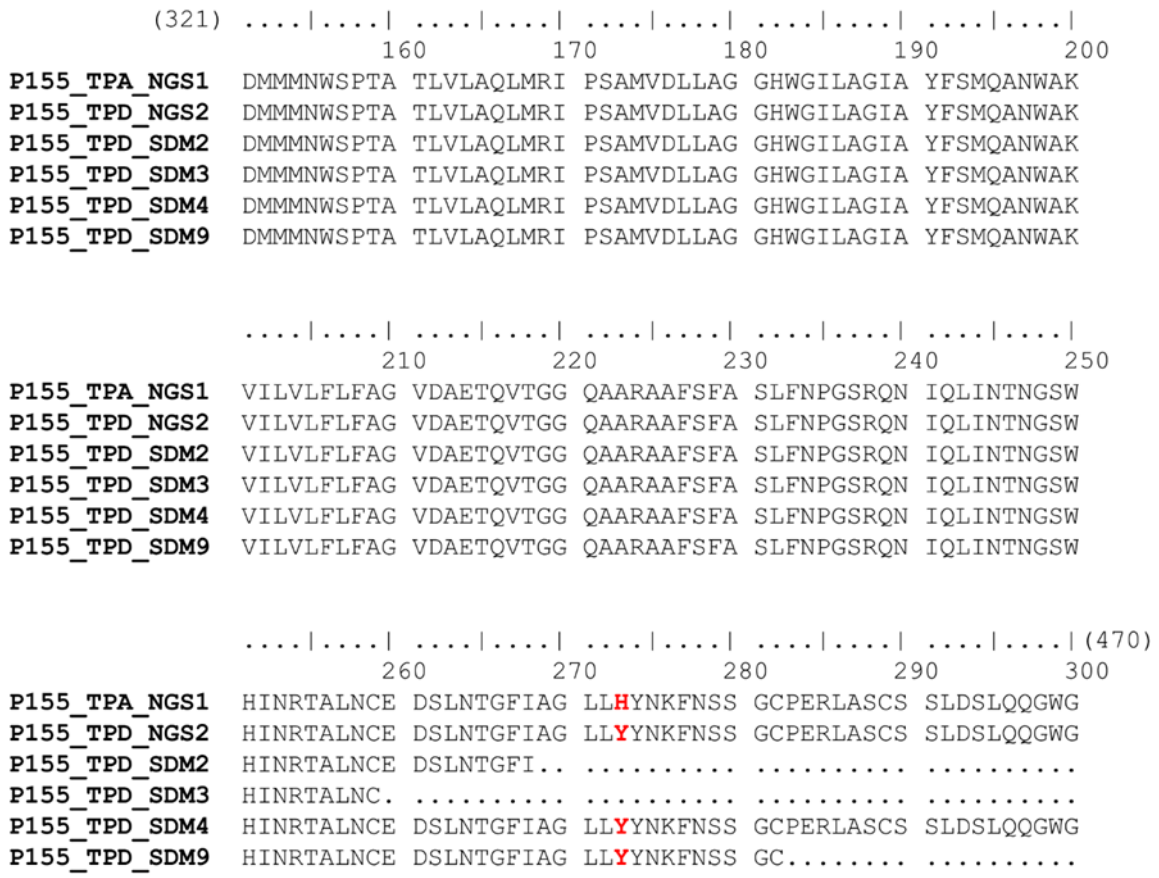

Figure 3.70 Alignment of consensus sequences from P155 in expression vector following site directed mutagenesis

Consensus sequences from P155 TPA and TPD obtained through NGS were aligned with phCMV expression vector clones following site directed mutagenesis to change one amino acid at position 273 (H to Y) marked in bold red text (See Materials and Methods). The numbers above amino acids are based on the length of the Core/E1E2 insert and the numbers in brackets are based on H77 sequence (Accession number: AF009606). Only Clones 4 and 9 had a confirmed amino acid change from H to Y thus representing P155 TPD. Sanger sequences from Clones 2 and 3 were terminated prematurely. Nucleotide sequences were translated manually into amino acids using Serial Cloner software. SDM – site directed mutagenesis, dots in the amino acid sequence represent no data available due to termination of Sanger sequence

In order to assess the neutralisation response during SSC, treatment failure patients were included in the experiments as controls. Attempts were made to obtain E1E2 from one time-point pre-treatment and one time-point post-treatment for three relapse controls (P75, P131 and P101) and one null patient (P63). Nested PCR for E1E2 was not performed on the relapse control P75, because samples were limited in volume (<0.5 ml). Instead, gene synthesis of TPA pre-treatment and TP-B post-treatment for P75 was used to obtain E1E2 sequences from the NGS consensus alignment shown in Table 3.13. This alignment revealed, that there were 10 amino acid changes between the baseline and post-treatment time points. Site-directed mutagenesis would have been possible in multiple stages but to save time, both genes were commercially synthesised. The amino acid differences from the two time-points included the following changes: position 386 from Tyrosine to Histidine (Y386H), position 391 from Serine to Asparagine (S391N), position 393 from Alanine to Glycine (A383G), position 395 from Threonine to Alanine (T395A), position 396 from Methionine to Alanine (M396A), position 397 from Serine to Alanine (S397A), position 399 from Isoleucine to Leucine (I399L), position 401 from Serine to Asparagine (S401N), position 408 from Arginine to Lysine (R408K) and position 531 from Glutamic acid to Aspartic acid (E531D). The gene synthesised E1E2 from both time-points were amplified by inner primers from the nested PCR and the fragments obtained inserted into the pENTR/D-TOPO vectors. Upon first attempt, two clones from each time point were sent for sequencing and one clone (C2) from TPB confirmed insertion of E1E2 into the vector. The transformation of TPA PCR product from gene synthesis was repeated with 11 clones following growth on Kanamycin selective medium. To minimise the number of Sanger sequencing reactions and time spent on the experiments, all clones were pre-screened for the correct product size using the M13 forward and M13 reverse sequencing primers based on the DreamTaq PCR assay (See Materials and Methods). This resulted in a sequence of around 2kb for Clones numbered 2, 5, 6 and 8-11. The successful transformation of E1E2 into the vector was confirmed by Sanger sequencing. Figure 3.71 shows the nucleotide alignment of NGS consensus sequences from P75 TPA and P75 TPB and the corresponding clones, which were successfully inserted into the pENTR/D-TOPO vector. Clones 2, 4, 5, 9 and 11 contained the E1E2 insert for P75 TPA and Clone 2 was the only one resembling P75 TPB. Clones were subsequently visually inspected throughout

the entire insert sequence to eliminate the possibility of stop codons. All unsuccessfully sequenced clones or clones containing stop codons were excluded from downstream processing.

Table 3.13 Amino acid alignment of E1E2 consensus sequence from patient 75.

H77		171	-	G	C	S	F	S	I	F	L	L	A	L	L	S	C	L	T	V	P	A	S	A	Y	Q	V	R	N	S	S	G	L	Y	H	V	T	N	D	C	P	N	209
P75_TPA			M	G	C	S	F	S	I	F	L	L	A	L	L	S	C	L	T	V	P	A	S	A	Y	Q	V	R	N	S	S	G	L	Y	H	V	T	N	D	C	P	N	
P75_TPB			.	.	.	.	.	.	.	.	.	.	.	.	.	.	.	.	.	.	.	.	.	.	.	.	.	.	.	.	.	.	.	.	.	.	.	.	.	.	.	.	.	.	
H77		210	S	S	I	V	Y	E	A	A	D	A	I	L	H	T	P	G	C	V	P	C	V	R	E	G	N	A	S	R	C	W	V	A	V	T	P	T	V	A	T	R	249
P75_TPA			S	S	I	V	Y	E	S	A	D	A	I	L	H	S	P	G	C	V	P	C	V	R	E	G	N	S	S	K	C	W	V	A	V	A	P	T	V	A	T	R	
P75_TPB			.	.	.	.	.	.	.	.	.	.	.	.	.	.	.	.	.	.	.	.	.	.	.	.	.	.	.	.	.	.	.	.	.	.	.	.	.	.	.	.	.	.	
H77		250	D	G	K	L	P	T	T	Q	L	R	R	H	I	D	L	L	V	G	S	A	T	L	C	S	A	L	Y	V	G	D	L	C	G	S	V	F	L	V	G	Q	289
P75_TPA			D	G	K	L	P	A	T	Q	L	R	R	H	I	D	L	L	V	G	S	A	T	L	C	S	A	L	Y	V	G	D	L	C	G	S	V	F	L	V	G	Q	
P75_TPB			.	.	.	.	.	.	.	.	.	.	.	.	.	.	.	.	.	.	.	.	.	.	.	.	.	.	.	.	.	.	.	.	.	.	.	.	.	.	.	.	.	.	
H77		290	L	F	T	F	S	P	R	R	H	W	T	T	Q	D	C	N	C	S	I	Y	P	G	H	I	T	G	H	R	M	A	W	D	M	M	M	N	W	S	P	T	329
P75_TPA			L	F	T	F	S	P	R	R	H	W	T	T	Q	D	C	N	C	S	I	Y	P	G	H	I	T	G	H	R	M	A	W	D	M	M	M	N	W	S	P	T	
P75_TPB			.	.	.	.	.	.	.	.	.	.	.	.	.	.	.	.	.	.	.	.	.	.	.	.	.	.	.	.	.	.	.	.	.	.	.	.	.	.	.	.	.	.	
H77		330	A	A	L	V	V	A	Q	L	L	R	I	P	Q	A	I	M	D	M	I	A	G	A	H	W	G	V	L	A	G	I	A	Y	F	S	M	V	G	N	W	A	369
P75_TPA			A	A	L	V	V	A	Q	L	L	R	V	P	Q	A	I	L	D	M	I	A	G	A	H	W	G	V	L	A	G	I	A	Y	F	S	M	V	G	N	W	A	
P75_TPB			.	.	.	.	.	.	.	.	.	.	.	.	.	.	.	.	.	.	.	.	.	.	.	.	.	.	.	.	.	.	.	.	.	.	.	.	.	.	.	.	.	.	
H77		370	K	V	L	V	V	L	L	L	F	A	G	V	D	A	E	T	H	V	T	G	G	S	A	G	R	T	T	A	G	L	V	G	L	L	T	P	G	A	K	Q	409
P75_TPA			K	V	L	V	V	M	L	L	F	T	A	V	D	A	E	T	Y	T	T	G	G	S	A	A	R	T	M	S	G	I	A	S	L	F	T	P	G	A	R	Q	
P75_TPB			.	.	.	.	.	.	.	.	.	.	.	.	.	.	.	.	**H**	.	.	.	.	**N**	.	**G**	.	**A**	**A**	**A**	.	**L**	.	**N**	.	.	.	.	.	.	**K**	.	
H77		410	N	I	Q	L	I	N	T	N	G	S	W	H	I	N	S	T	A	L	N	C	N	E	S	L	N	T	G	W	L	A	G	L	F	Y	Q	H	K	F	N	S	449
P75_TPA			N	V	Q	L	I	N	T	N	G	S	W	H	I	N	R	T	A	L	N	C	N	A	S	L	D	T	G	W	V	A	G	L	I	Y	H	H	K	F	N	S	
P75_TPB			.	.	.	.	.	.	.	.	.	.	.	.	.	.	.	.	.	.	.	.	.	.	.	.	.	.	.	.	.	.	.	.	.	.	.	.	.	.	.	.	.	.	
H77		450	S	G	C	P	E	R	L	A	S	C	R	R	L	T	D	F	A	Q	G	W	G	P	I	S	Y	A	N	G	S	G	L	D	E	R	P	Y	C	W	H	Y	489
P75_TPA			S	G	C	P	E	R	M	A	S	C	R	P	L	A	D	F	A	Q	G	W	G	P	I	S	Y	V	N	G	S	G	P	E	H	R	P	Y	C	W	H	Y	
P75_TPB			.	.	.	.	.	.	.	.	.	.	.	.	.	.	.	.	.	.	.	.	.	.	.	.	.	.	.	.	.	.	.	.	.	.	.	.	.	.	.	.	.	.	
H77		490	P	P	R	P	C	G	I	V	P	A	K	S	V	C	G	P	V	Y	C	F	T	P	S	P	V	V	V	G	T	T	D	R	S	G	A	P	T	Y	S	W	529
P75_TPA			P	P	K	P	C	G	I	V	P	A	Q	N	V	C	G	P	V	Y	C	F	T	P	S	P	V	V	V	G	T	T	D	K	S	G	A	P	T	Y	N	W	
P75_TPB			.	.	.	.	.	.	.	.	.	.	.	.	.	.	.	.	.	.	.	.	.	.	.	.	.	.	.	.	.	.	.	.	.	.	.	.	.	.	.	.	.	.	
H77		530	G	A	N	D	T	D	V	F	V	L	N	N	T	R	P	P	L	G	N	W	F	G	C	T	W	M	N	S	T	G	F	T	K	V	C	G	A	P	P	C	569
P75_TPA			G	E	N	D	T	D	V	F	V	L	T	N	T	R	P	P	L	G	N	W	F	G	C	T	W	M	N	S	S	G	F	T	K	V	C	G	A	P	P	C	
P75_TPB			.	**D**	.	.	.	.	.	.	.	.	.	.	.	.	.	.	.	.	.	.	.	.	.	.	.	.	.	.	.	.	.	.	.	.	.	.	.	.	.	.	.	.	
H77		570	V	I	G	G	V	G	N	N	T	L	L	C	P	T	D	C	F	R	K	H	P	E	A	T	Y	S	R	C	G	S	G	P	W	I	T	P	R	C	M	V	609

P75_TPA			N	I	G	G	V	G	N	K	T	L	Y	C	P	T	D	C	F	R	K	H	P	E	A	T	Y	S	R	C	G	S	G	P	W	V	T	P	R	C	L	V	
P75_TPB			.	.	.	.	.	.	.	.	.	.	.	.	.	.	.	.	.	.	.	.	.	.	.	.	.	.	.	.	.	.	.	.	.	.	.	.	.	.	.	.	.	.	
H77		610	D	Y	P	Y	R	L	W	H	Y	P	C	T	I	N	Y	T	I	F	K	V	R	M	Y	V	G	G	V	E	H	R	L	E	A	A	C	N	W	T	R	G	649
P75_TPA			D	Y	P	Y	R	L	W	H	Y	P	C	T	I	N	Y	T	L	F	K	V	R	M	Y	V	G	G	V	E	H	R	L	Q	V	A	C	N	W	T	R	G	
P75_TPB			.	.	.	.	.	.	.	.	.	.	.	.	.	.	.	.	.	.	.	.	.	.	.	.	.	.	.	.	.	.	.	.	.	.	.	.	.	.	.	.	.	.	
H77		650	E	R	C	D	L	E	D	R	D	R	S	E	L	S	P	L	L	L	S	T	T	Q	W	Q	V	L	P	C	S	F	T	T	L	P	A	L	S	T	G	L	689
P75_TPA			E	R	C	D	L	D	D	R	D	R	S	E	L	S	P	L	L	L	S	T	T	Q	W	Q	V	L	P	C	S	F	T	T	L	P	A	L	T	T	G	L	
P75_TPB			.	.	.	.	.	.	.	.	.	.	.	.	.	.	.	.	.	.	.	.	.	.	.	.	.	.	.	.	.	.	.	.	.	.	.	.	.	.	.	.	.	.	
H77		690	I	H	L	H	Q	N	I	V	D	V	Q	Y	L	Y	G	V	G	S	S	I	A	S	W	A	I	K	W	E	Y	V	V	L	L	F	L	L	L	A	D	A	729
P75_TPA			I	H	L	H	Q	N	I	V	D	V	Q	Y	L	Y	G	V	G	S	S	I	V	S	W	A	I	K	W	E	Y	V	I	L	L	F	L	L	L	A	D	A	
P75_TPB			.	.	.	.	.	.	.	.	.	.	.	.	.	.	.	.	.	.	.	.	.	.	.	.	.	.	.	.	.	.	.	.	.	.	.	.	.	.	.	.	.	.	
H77		730	R	V	C	S	C	L	W	M	M	L	L	I	S	Q	A	E	A																									746
P75_TPA			R	I	C	S	C	L	W	M	M	L	L	I	S	Q	A	E	A																									
P75_TPB			.	.	.	.	.	.	.	.	.	.	.	.	.	.	.	.	.																									

Dots indicate conserved regions. Amino acid numbering are based on the E1E2 H77 reference sequence (Accession Number AF009606) with H77 amino acid sequence marked in grey. Changes between the two time points are indicated in bold red type.

Figure 3.71 Alignment of consensus sequence from P75 TPA and B with PCR inserts in pENTR/D-TOPO vector
A PCR fragment of 1728 base pairs was gel purified and inserted into the pENTR/D-TOPO vector as described in Materials and Methods. The resulting colonies were pre-screened with DreamTaq PCR sent for Sanger sequencing and aligned with the consensus sequences from P155 TPA (P75_TPA_NGS) and P155 TPB (P75_TPB_NGS) obtained through NGS. The alignment shows the first 100 base pairs from the expected sequence of end of Core/start of E1E2 from six clones. The sequences highlighted in bold belong to P75 TPB. The letters in bold show mismatches in the sequence. The numbers above the alignment are based on the start of the expected sequence and the numbers in brackets are based on nucleotide numbers from H77 reference genome (Accession number: AF009606)

The P75 TPA and TPB clonal sequences were subsequently recombined into the phCMV expression vector. Two clones from each recombination plate were selected and the plasmid DNA extracted as previously described (Materials and Methods). Figure 3.72 shows the alignment of the P75 consensus sequence from TPA and TPB with the corresponding successfully sequenced clones. Overall, there were two clones from TPB, C2.1 and C2.2, which did not contain mismatches from the TPB consensus sequence. For TPA, clones C5.1, C9.1 and C9.2 matched the TPA consensus sequence.

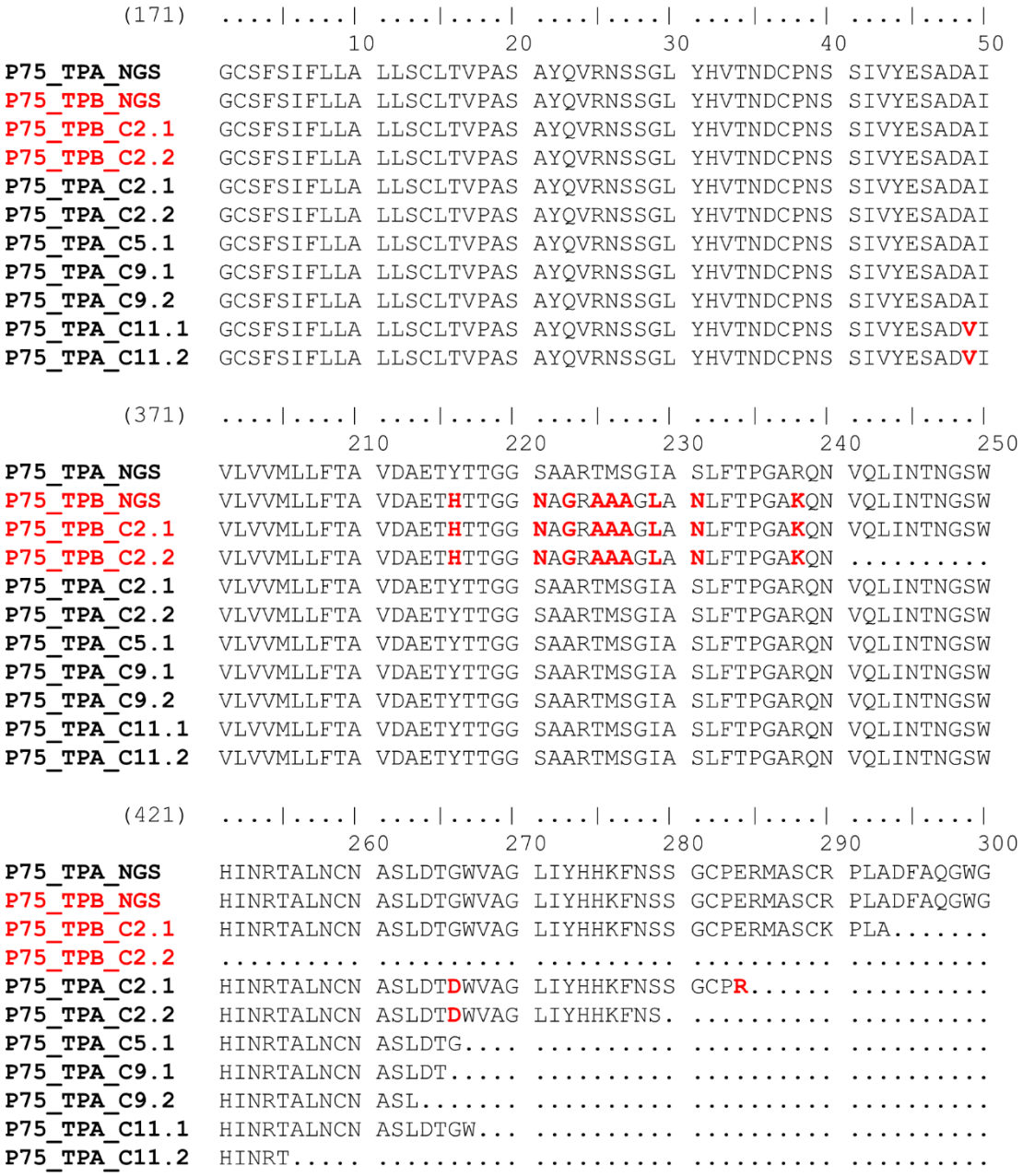

Figure 3.72 Confirmation of successful recombination into phCMV expression vector by P75 TPA and TPB
The alignment shows three different stretches of 50 base pairs along the expected E1E2 sequence in areas where amino acid changes occurred, from two clones from P75 TPB obtained successfully through Sanger sequencing. The sequences highlighted in red belong to P75 TPB. The letters in bold red show mismatches in the sequence with relation to the original NGS sequence or to TPA NGS consensus sequence. The numbers above the alignment are based on the start of the expected amino acid sequence and the numbers in brackets are based on amino acid numbers from H77 reference genome (Accession number: AF009606). Unsuccessful sequenced clones were excluded from the alignment. Dot indicate lack of sequence due to termination of Sanger sequencing.

Nested PCR for E1E2 was performed for the remaining relapse patients, P131 and P101 and the null responder, P63. While a fragment of the correct size for E1E2 was successfully obtained for P63 TPA, both time-points for P131 and P101 were not successfully amplified The fragment was gel purified and inserted into the pENTR/D-TOPO vector using selective media, which resulted in 16 colonies. Clones numbered 3, 6 and 13 had a positive PCR fragment above 1.5kb and were sequenced. Figure 3.73 shows the alignment of P63 NGS consensus sequences from TPA and TPB with clones 3, 6 and 13 obtained through Sanger sequencing. All three clones had high similarity to the consensus sequence. Only clone 13 (C13) differed by two amino acid: one change at position 358 from Glycine to Aspartic acid (G358D) and one from Arginine to Histidine at position 444 (R444H). P63 TPB NGS consensus sequence had the same amino acid change at position 444 (R444H) when compared to P63 TPA NGS consensus sequence as well as a second amino acid change from Glutamine to Lysine at position 408 (Q408T). It was not clear whether Clones 3 and 6 had the same Arginine to Histidine mutation at position 444, as both sequences terminated prior to this amino acid position.

```
       (221) ....|....| ....|....| ....|....| ....|....| ....|....|
                    60         70         80         90        100
P63_TPA_NGS   LHTPGCVPCV REGNTSRCWV AVTPTVATKD GKLPTTQLRR HIDLLVGSAT
P63_TPB_NGS   LHTPGCVPCV REGNTSRCWV AVTPTVATKD GKLPTTQLRR HIDLLVGSAT
P63_TPA_C3    LHTPGCVPCV REGNTSRCWV AVTPTVATKD GKLPTTQLRR HIDLLVGSAT
P63_TPA_C6    LHTPGCVPCV REGNTSRCWV AVTPTVATKD GKLPTTQLRR HIDLLVGSAT
P63_TPA_C13   LHTPGCVPCV REGNTSRCWV AVTPTVATKD GKLPTTQLRR HIDLLVGSAT

       (271) ....|....| ....|....| ....|....| ....|....| ....|....|
                   110        120        130        140        150
P63_TPA_NGS   LCSALYVGDL CGSVFLVGQL FTFSPRRHWT TQDCNCSIYP GHITGHRMAW
P63_TPB_NGS   LCSALYVGDL CGSVFLVGQL FTFSPRRHWT TQDCNCSIYP GHITGHRMAW
P63_TPA_C3    LCSALYVGDL CGSVFLVGQL FTFSPRRHWT TQDCNCSIYP GHITGHRMAW
P63_TPA_C6    LCSALYVGDL CGSVFLVGQL FTFSPRRHWT TQDCNCSIYP GHITGHRMAW
P63_TPA_C13   LCSALYVGDL CGSVFLVGQL FTFSPRRHWT TQDCNCSIYP GHITGHRMAW

       (321) ....|....| ....|....| ....|....| ....|....| ....|....|
                   160        170        180        190        200
P63_TPA_NGS   DMMMNWSPTT ALVVAQLLRI PQAIVDMIAG AHWGVLAGMA YFSMVGNWAK
P63_TPB_NGS   DMMMNWSPTT ALVVAQLLRI PQAIVDMIAG AHWGVLAGMA YFSMVGNWAK
P63_TPA_C3    DMMMNWSPTT ALVVAQLLRI PQAIVDMIAG AHWGVLAGMA YFSMVGNWAK
P63_TPA_C6    DMMMNWSPTT ALVVAQLLRI PQAIVDMIAG AHWGVLAGMA YFSMVGNWAK
P63_TPA_C13   DMMMNWSPTT ALVVAQLLRI PQAIVDMIAG AHWGVLADMA YFSMVGNWAK

       (371) ....|....| ....|....| ....|....| ....|....| ....|....|
                   210        220        230        240        250
P63_TPA_NGS   VLVVLLLFAG VDANTYVTGG TAGRVTAGLT GLFSPGAQQN IQLINTNGSW
P63_TPB_NGS   VLVVLLLFAG VDANTYVTGG TAGRVTAGLT GLFSPGAKQN IQLINTNGSW
P63_TPA_C3    VLVVLLLFAG VDANTYVTGG TAGRVTAGLT GLFSPGAQQN IQLINTNGSW
P63_TPA_C6    VLVVLLLFAG VDANTYVTGG TAGRVTAGLT GLFSPGAQQN IQLINTNGSW
P63_TPA_C13   VLVVLLLFAG VDANTYVTGG TAGRVTAGLT GLFSPGAQQN IQLINTNGSW

       (421) ....|....| ....|....| ....|....| ....|....| ....|....|
                   260        270        280        290        300
P63_TPA_NGS   HINRTALNCN DSLNTGWLAG LIYRHRFNSS GCPERLASCR RLTDFAQGWG
P63_TPB_NGS   HINRTALNCN DSLNTGWLAG LIYHHRFNSS GCPERLASCR RLTDFAQGWG
P63_TPA_C3    HINRTALNCN DSLNTGWLAG LIY..... .......... ..........
P63_TPA_C6    HINRTALNCN DSLNTGWLAG LIY..... .......... ..........
P63_TPA_C13   HINRTALNCN DSLNTGWLAG LIYHHRFNSS GCP..... ..........
```

Figure 3.73 Alignment of consensus sequence from P63 TPA and TPB with pENTR/D-TOPO clones from P63 TPA
The alignment shows successful Sanger sequencing results from P63 TPA pENTR/D-TOPO clones and two consensus sequences from P63 TPA and TPB. The letters in bold red show mismatches in the sequence with relation to the original NGS sequence or to TPA NGS consensus sequence. The numbers above the alignment are based on the start of the expected amino acid sequence and the numbers in brackets are based on amino acid numbers from H77 reference genome (Accession number: AF009606). Unsuccessful sequenced clones were excluded from the alignment. Dot indicate lack of sequence due to termination of Sanger sequencing.

The amino acid differences between TPA and TPB were determined by comparing the consensus sequence from NGS, in order to perform site-directed mutagenesis either on the entry vector clones or directly on the phCMV gateway expression vector. This would allow to obtain both P63 TPA and TPB sequences. Table 3.14 shows the amino acid alignment of reference H77 HCV sequence with P63 TPA and TPB. There were two amino acid changes from pre-treatment to post-treatment; one at position 408 from Glutamine to Lysine (Q408K) and one at position 444 from Arginine to Histidine (R444H), the same as the amino acid change Clone 13 contained. Based on this finding, complementary primers were made spanning the mutations of at least 9 bases on either side.

To maximise the success rate, site directed mutagenesis was performed on all three clones (Clone 3, 6 and 13). Since the R444H mutation was already present in Clone 13, the focus was on obtaining the Q408K mutation. Site-directed mutagenesis was performed on the entry vectors, the results of which were confirmed by DreamTaq PCR as described in Materials and Methods. Only site-directed mutagenesis clones containing fragments at the correct size (1728 nucleotides, confirmed by gel-electrophoresis) were subsequently recombined into phCMV expression vector and sent for confirmatory sequencing. Figure 3.74 shows the amino acid alignment of P63 TPA and TPB NGS consensus sequences compared to the phCMV Clones obtained following site-directed mutagenesis. The G1 sense sequencing primer was used for Sanger sequencing rather than the phCMV sequencing primer in order to prevent premature termination as the two altered amino acids were located in the middle of E1E2. A total number of six clones were obtained following site-directed mutagenesis and recombination. Clones had high similarity to the original consensus sequence TPA, apart from C13.1, which contained a total of eight amino acid changes. These amino acid changes included: Glycine to Aspartate at position 358 (G358D), Leucine to Proline at position 372 (L372P), Leucine to Methionine at position 456 (L456M), Arginine to Histidine at position 444 (R444H), Arginine to Proline at position 456 (R461P), Serine to Proline at position 471 (S471P), Alanine to Valine at position 475 (A475V) and Aspartic acid to Glutamate at position 481 (D481E). Due to the numerous changes, this clone was excluded from further experiments. Clones C1.4.1 and C.2.4.1 differed by two and three amino acids respectively when compared to P63 TPA consensus sequence. Both had the same amino acid changes at position 408 from Glutamine to Lysine (Q408K) and position 444 from

Arginine to Histidine (R444H) which were the desired amino acid changes required to change P63 TPA to TPB. Therefore C1.4.1 and C2.4.1 were used for future transfections in order to produce HCV pseudoparticles. The C2.4.1 clone also contained an amino acid change from Proline to Serine at position 498 (P498S). Overall all clones contained the amino acid change at position 444 from Arginine to Histidine (R444H) and therefore no recombined sequence resembled the P63 TPA consensus sequence completely. Therefore, new complementary primers were designed spanning approximately 10 nucleotides on each side of the mutation at position 444 (based on H77 amino acid sequence), in order to be used for site-directed mutagenesis directly on the phCMV expression vector. The template clones used were C2.A.6, C2.B.6 and C1.A.3, which contained the original Q408 amino acid resembling P63 TPA NGS consensus sequence. Following site-directed mutagenesis on phCMV vector as described in Materials and Methods, clones were screened for complete E1E2 by DreamTaq PCR as previously stated, which resulted in five clones with fragments above 1.5 kb. Two of the clones were subsequently sent for Sanger sequencing with the G1 sense forward primer. The results of the experiment are shown on Figure 3.75 and reveal the successful mutation of amino acid Histidine to Arginine at position 444. The clones 2A.6 and 2B.6 also contained the amino acid Glutamine at position 408, resembling P63 TPA NGS consensus sequence. Therefore, the two clones were ready for downstream processing.

Table 3.14 Amino acid alignment of consensus E1E2 sequences from patient 63

H77	171	-	G	C	S	F	S	I	F	L	L	A	L	L	S	C	L	T	V	P	A	S	A	Y	Q	V	R	N	S	S	G	L	Y	H	V	T	N	D	C	P	N	209
P63_TPA		M	G	C	S	F	S	I	F	L	L	A	L	L	S	C	L	T	V	P	A	S	A	Y	Q	V	R	N	S	S	G	L	Y	H	V	T	N	D	C	P	N	
P63_TPB		.	.	.	.	.	.	.	.	.	.	.	.	.	.	.	.	.	.	.	.	.	.	.	.	.	.	.	.	.	.	.	.	.	.	.	.	.	.	.	.	.	
H77	210	S	S	I	V	Y	E	A	A	D	A	I	L	H	T	P	G	C	V	P	C	V	R	E	G	N	A	S	R	C	W	V	A	V	T	P	T	V	A	T	R	249
P63_TPA		S	S	I	V	Y	E	A	A	D	A	I	L	H	T	P	G	C	V	P	C	V	R	E	G	N	T	S	R	C	W	V	A	V	T	P	T	V	A	T	K	
P63_TPB		.	.	.	.	.	.	.	.	.	.	.	.	.	.	.	.	.	.	.	.	.	.	.	.	.	.	.	.	.	.	.	.	.	.	.	.	.	.	.	.	.	
H77	250	D	G	K	L	P	T	T	Q	L	R	R	H	I	D	L	L	V	G	S	A	T	L	C	S	A	L	Y	V	G	D	L	C	G	S	V	F	L	V	G	Q	289
P63_TPA		D	G	K	L	P	T	T	Q	L	R	R	H	I	D	L	L	V	G	S	A	T	L	C	S	A	L	Y	V	G	D	L	C	G	S	V	F	L	V	G	Q	
P63_TPB		.	.	.	.	.	.	.	.	.	.	.	.	.	.	.	.	.	.	.	.	.	.	.	.	.	.	.	.	.	.	.	.	.	.	.	.	.	.	.	.	.	
H77	290	L	F	T	F	S	P	R	R	H	W	T	T	Q	D	C	N	C	S	I	Y	P	G	H	I	T	G	H	R	M	A	W	D	M	M	M	N	W	S	P	T	329
P63_TPA		L	F	T	F	S	P	R	R	H	W	T	T	Q	D	C	N	C	S	I	Y	P	G	H	I	T	G	H	R	M	A	W	D	M	M	M	N	W	S	P	T	
P63_TPB		.	.	.	.	.	.	.	.	.	.	.	.	.	.	.	.	.	.	.	.	.	.	.	.	.	.	.	.	.	.	.	.	.	.	.	.	.	.	.	.	.	
H77	330	A	A	L	V	V	A	Q	L	L	R	I	P	Q	A	I	M	D	M	I	A	G	A	H	W	G	V	L	A	G	I	A	Y	F	S	M	V	G	N	W	A	369
P63_TPA		T	A	L	V	V	A	Q	L	L	R	I	P	Q	A	I	V	D	M	I	A	G	A	H	W	G	V	L	A	G	M	A	Y	F	S	M	V	G	N	W	A	
P63_TPB		.	.	.	.	.	.	.	.	.	.	.	.	.	.	.	.	.	.	.	.	.	.	.	.	.	.	.	.	.	.	.	.	.	.	.	.	.	.	.	.	.	
H77	370	K	V	L	V	V	L	L	L	F	A	G	V	D	A	E	T	H	V	T	G	G	S	A	G	R	T	T	A	G	L	V	G	L	L	T	P	G	A	K	Q	409
P63_TPA		K	V	L	V	V	L	L	L	F	A	G	V	D	A	N	T	Y	V	T	G	G	T	A	G	R	V	T	A	G	L	T	G	L	F	S	P	G	A	Q	Q	
P63_TPB		.	.	.	.	.	.	.	.	.	.	.	.	.	.	.	.	.	.	.	.	.	.	.	.	.	.	.	.	.	.	.	.	.	.	.	.	.	.	.	.	**K**	.	
H77	410	N	I	Q	L	I	N	T	N	G	S	W	H	I	N	S	T	A	L	N	C	N	E	S	L	N	T	G	W	L	A	G	L	F	Y	Q	H	K	F	N	S	449
P63_TPA		N	I	Q	L	I	N	T	N	G	S	W	H	I	N	R	T	A	L	N	C	N	D	S	L	N	T	G	W	L	A	G	L	I	Y	R	H	R	F	N	S	
P63_TPB		.	.	.	.	.	.	.	.	.	.	.	.	.	.	.	.	.	.	.	.	.	.	.	.	.	.	.	.	.	.	.	.	.	.	.	**H**	.	.	.	.	.	.	
H77	450	S	G	C	P	E	R	L	A	S	C	R	R	L	T	D	F	A	Q	G	W	G	P	I	S	Y	A	N	G	S	G	L	D	E	R	P	Y	C	W	H	Y	489
P63_TPA		S	G	C	P	E	R	L	A	S	C	R	R	L	T	D	F	A	Q	G	W	G	S	I	S	Y	A	N	G	S	G	P	D	E	R	P	Y	C	W	H	Y	
P63_TPB		.	.	.	.	.	.	.	.	.	.	.	.	.	.	.	.	.	.	.	.	.	.	.	.	.	.	.	.	.	.	.	.	.	.	.	.	.	.	.	.	.	
H77	490	P	P	R	P	C	G	I	V	P	A	K	S	V	C	G	P	V	Y	C	F	T	P	S	P	V	V	V	G	T	T	D	R	S	G	A	P	T	Y	S	W	529
P63_TPA		P	P	R	P	C	G	I	V	P	A	K	S	V	C	G	P	V	Y	C	F	T	P	S	P	V	V	V	G	T	T	D	R	S	G	A	P	T	Y	S	W	
P63_TPB		.	.	.	.	.	.	.	.	.	.	.	.	.	.	.	.	.	.	.	.	.	.	.	.	.	.	.	.	.	.	.	.	.	.	.	.	.	.	.	.	.	
H77	530	G	A	N	D	T	D	V	F	V	L	N	N	T	R	P	P	L	G	N	W	F	G	C	T	W	M	N	S	T	G	F	T	K	V	C	G	A	P	P	C	569
P63_TPA		G	E	N	D	T	D	V	F	V	L	N	N	T	R	P	P	L	G	N	W	F	G	C	T	W	M	N	S	T	G	F	T	K	A	C	G	A	P	P	C	
P63_TPB		.	.	.	.	.	.	.	.	.	.	.	.	.	.	.	.	.	.	.	.	.	.	.	.	.	.	.	.	.	.	.	.	.	.	.	.	.	.	.	.	.	
H77	570	V	I	G	G	V	G	N	N	T	L	L	C	P	T	D	C	F	R	K	H	P	E	A	T	Y	S	R	C	G	S	G	P	W	I	T	P	R	C	M	V	609

P63_TPA		V	I	G	G	M	G	N	N	T	L	R	C	P	T	D	C	F	R	K	H	P	E	A	T	Y	S	R	C	G	S	G	P	W	I	T	P	R	C	M	V	
P63_TPB		.	.	.	.	.	.	.	.	.	.	.	.	.	.	.	.	.	.	.	.	.	.	.	.	.	.	.	.	.	.	.	.	.	.	.	.	.	.	.	.	.	
H77	610	D	Y	P	Y	R	L	W	H	Y	P	C	T	I	N	Y	T	I	F	K	V	R	M	Y	V	G	G	V	E	H	R	L	E	A	A	C	N	W	T	R	G	649
P63_TPA		D	Y	P	Y	R	L	W	H	Y	P	C	T	I	N	Y	T	T	F	K	V	R	M	Y	V	G	G	V	E	H	R	L	E	A	A	C	N	W	T	R	G	
P63_TPB		.	.	.	.	.	.	.	.	.	.	.	.	.	.	.	.	.	.	.	.	.	.	.	.	.	.	.	.	.	.	.	.	.	.	.	.	.	.	.	.	.	
H77	650	E	R	C	D	L	E	D	R	D	R	S	E	L	S	P	L	L	L	S	T	T	Q	W	Q	V	L	P	C	S	F	T	T	L	P	A	L	S	T	G	L	689
P63_TPA		E	R	C	D	L	E	D	R	D	R	S	E	L	S	P	L	L	L	S	T	T	Q	W	Q	V	L	P	C	S	F	T	T	L	P	A	L	S	T	G	L	
P63_TPB		.	.	.	.	.	.	.	.	.	.	.	.	.	.	.	.	.	.	.	.	.	.	.	.	.	.	.	.	.	.	.	.	.	.	.	.	.	.	.	.	.	
H77	690	I	H	L	H	Q	N	I	V	D	V	Q	Y	L	Y	G	V	G	S	S	I	A	S	W	A	I	K	W	E	Y	V	V	L	L	F	L	L	L	A	D	A	729
P63_TPA		I	H	L	H	Q	N	I	V	D	V	Q	Y	L	Y	G	V	G	S	S	I	A	S	W	A	I	K	W	E	Y	V	V	L	L	F	L	L	L	A	D	A	
P63_TPB		.	.	.	.	.	.	.	.	.	.	.	.	.	.	.	.	.	.	.	.	.	.	.	.	.	.	.	.	.	.	.	.	.	.	.	.	.	.	.	.	.	
H77	730	R	V	C	S	C	L	W	M	M	L	L	I	S	Q	A	E	A																								746
P63_TPA		R	V	C	S	C	L	W	M	M	L	L	I	S	Q	A	E	A																								
P63_TPB		.	.	.	.	.	.	.	.	.	.	.	.	.	.	.	.	.																								

Dots indicate conserved regions. Amino acid numbering are based on H77 sequence (Accession Number AF009606) with H77 amino acid sequence marked in grey. Changes between the two time points are indicated in bold red type.

```
      (321)  ....|....| ....|....| ....|....| ....|....| ....|....|
                     160        170        180        190        200
P63_TPA_NGS  DMMMNWSPTT ALVVAQLLRI PQAIVDMIAG AHWGVLAGMA YFSMVGNWAK
P63_TPB_NGS  DMMMNWSPTT ALVVAQLLRI PQAIVDMIAG AHWGVLAGMA YFSMVGNWAK
P63_2A.6     DMMMNWSPTT ALVVAQLLRI PQAIVDMIAG AHWGVLAGMA YFSMVGNWAK
P63_2B.6     DMMMNWSPTT ALVVAQLLRI PQAIVDMIAG AHWGVLAGMA YFSMVGNWAK
P63_C13.1    DMMMNWSPTT ALVVAQLLRI PQAIVDMIAG AHWGVLADMA YFSMVGNWAK
P63_C1A.3    DMMMNWSPTT ALVVAQLLRI PQAIVDMIAG AHWGVLAGMA YFSMVGNWAK
P63_C1.4.1   DMMMNWSPTT ALVVAQLLRI PQAIVDMIAG AHWGVLAGMA YFSMVGNWAK
P63_C2.4.2   DMMMNWSPTT ALVVAQLLRI PQAIVDMIAG AHWGVLAGMA YFSMVGNWAK
      (371)  ....|....| ....|....| ....|....| ....|....| ....|....|
                     210        220        230        240        250
P63_TPA_NGS  VLVVLLLFAG VDANTYVTGG TAGRVTAGLT GLFSPGAQQN IQLINTNGSW
P63_TPB_NGS  VLVVLLLFAG VDANTYVTGG TAGRVTAGLT GLFSPGAKQN IQLINTNGSW
P63_2A.6     VLVVLLLFAG VDANTYVTGG TAGRVTAGLT GLFSPGAQQN IQLINTNGSW
P63_2B.6     VLVVLLLFAG VDANTYVTGG TAGRVTAGLT GLFSPGAQQN IQLINTNGSW
P63_C13.1    VPVVLLLFAG VDANTYVTGG TAGRVTAGLT GLFSPGAQQN IQLINTNGSW
P63_C1A.3    VLVVLLLFAG VDANTYVTGG TAGRVTAGLT GLFSPGAQQN IQLINTNGSW
P63_C1.4.1   VLVVLLLFAG VDANTYVTGG TAGRVTAGLT GLFSPGAKQN IQLINTNGSW
P63_C2.4.2   VLVVLLLFAG VDANTYVTGG TAGRVTAGLT GLFSPGAKQN IQLINTNGSW
      (421)  ....|....| ....|....| ....|....| ....|....| ....|....|
                     260        270        280        290        300
P63_TPA_NGS  HINRTALNCN DSLNTGWLAG LIYRHRFNSS GCPERLASCR RLTDFAQGWG
P63_TPB_NGS  HINRTALNCN DSLNTGWLAG LIYHHRFNSS GCPERLASCR RLTDFAQGWG
P63_2A.6     HINRTALNCN DSLNTGWLAG LIYHHRFNSS GCPERLASCR RLTDFAQGWG
P63_2B.6     HINRTALNCN DSLNTGWLAG LIYHHRFNSS GCPERLASCR RLTDFAQGWG
P63_C13.1    HINRTALNCN DSLNTGWLAG LIYHHRFNSS GCPERMASCR PLTDFAQGWG
P63_C1A.3    HINRTALNCN DSLNTGWLAG LIYHHRFNSS GCPERLASCR RLTDFVQGWG
P63_C1.4.1   HINRTALNCN DSLNTGWLAG LIYHHRFNSS GCPERLASCR RLTDFVQGWG
P63_C2.4.2   HINRTALNCN DSLNTGWLAG LIYHHRFNSS GCPERLASCR RLTDFAQGWG
      (471)  ....|....| ....|....| ....|....| ....|....| ....|....|
                     310        320        330        340        350
P63_TPA_NGS  SISYANGSGP DERPYCWHYP PRPCGIVPAK SVCGPVYCFT PSPVVVGTTD
P63_TPB_NGS  SISYANGSGP DERPYCWHYP PRPCGIVPAK SVCGPVYCFT PSPVVVGTTD
P63_2A.6     S--------- ---------- ---------- ---------- ----------
P63_2B.6     SISYANGSGP DERPYCW--- ---------- ---------- ----------
P63_C13.1    PISYVNGSGP E--------- ---------- ---------- ----------
P63_C1A.3    SISYANGSGP DERPYCWHYP PRPCGIVPAK ---------- ----------
P63_C1.4.1   SISYANGSGP DERPYCWHYP PRPCGIVPAK ---------- ----------
P63_C2.4.2   SISYANGSGP DERPYCWHYP PRPCGIVSA- ---------- ----------
```

Figure 3.74 Amino acid alignment of P63 consensus with phCMV clones following site-directed mutagenesis
The alignment shows successful Sanger sequencing results from P63 phCMV clones following site-directed mutagenesis and two consensus sequences from P63 TPA and TPB based on the G1a Inner sense primer. Where mismatches occurred, chromatograms were visually inspected to confirm their presence. The letters in bold red show mismatches in the sequence with relation to the original NGS sequence or to TPA NGS consensus sequence. The numbers above the alignment are based on the start of the expected amino acid sequence and the numbers in brackets are based on amino acid numbers from H77 reference genome (Accession number: AF009606). Unsuccessful sequenced clones were excluded from the alignment. Dashes indicate lack of sequence due to termination of Sanger sequencing.

```
      (221)  ....|....| ....|....| ....|....| ....|....| ....|....|
                    60         70         80         90        100
P63_TPA_NGS  LHTPGCVPCV REGNTSRCWV AVTPTVATKD GKLPTTQLRR HIDLLVGSAT
P63_TPB_NGS  LHTPGCVPCV REGNTSRCWV AVTPTVATKD GKLPTTQLRR HIDLLVGSAT
P63_2A.6     LHTPGCVPCV REGNTSRCWV AVTPTVATKD GKLPTTQLRR HIDLLVGSAT
P63_2B.6     LHTPGCVPCV REGNTSRCWV AVTPTVATKD GKLPTTQLRR HIDLLVGSAT

      (271)  ....|....| ....|....| ....|....| ....|....| ....|....|
                   110        120        130        140        150
P63_TPA_NGS  LCSALYVGDL CGSVFLVGQL FTFSPRRHWT TQDCNCSIYP GHITGHRMAW
P63_TPB_NGS  LCSALYVGDL CGSVFLVGQL FTFSPRRHWT TQDCNCSIYP GHITGHRMAW
P63_2A.6     LCSALYVGDL CGSVFLVGQL FTFSPRRHWT TQDCNCSIYP GHITGHRMAW
P63_2B.6     LCSALYVGDL CGSVFLVGQL FTFSPRRHWT TQDCNCSIYP GHITGHRMAW

       (321) ....|....| ....|....| ....|....| ....|....| ....|....|
                   160        170        180        190        200
P63_TPA_NGS  DMMMNWSPTT ALVVAQLLRI PQAIVDMIAG AHWGVLAGMA YFSMVGNWAK
P63_TPB_NGS  DMMMNWSPTT ALVVAQLLRI PQAIVDMIAG AHWGVLAGMA YFSMVGNWAK
P63_2A.6     DMMMNWSPTT ALVVAQLLRI PQAIVDMIAG AHWGVLAGMA YFSMVGNWAK
P63_2B.6.   DMMMNWSPTT ALVVAQLLRI PQAIVDMIAG AHWGVLAGMA YFSMVGNWAK

       (371) ....|....| ....|....| ....|....| ....|....| ....|....|
                   210        220        230        240        250
P63_TPA_NGS  VLVVLLLFAG VDANTYVTGG TAGRVTAGLT GLFSPGAQQN IQLINTNGSW
P63_TPB_NGS  VLVVLLLFAG VDANTYVTGG TAGRVTAGLT GLFSPGAKQN IQLINTNGSW
P63_2A.6     VLVVLLLFAG VDANTYVTGG TAGRVTAGLT GLFSPGAQQN IQLINTNGSW
P63_2B.6     VLVVLLLFAG VDANTYVTGG TAGRVTAGLT GLFSPGAQQN IQLINTNGSW

       (421) ....|....| ....|....| ....|....| ....|....| ....|....|
                   260        270        280        290        300
P63_TPA_NGS  HINRTALNCN DSLNTGWLAG LIYRHRFNSS GCPERLASCR RLTDFAQGWG
P63_TPB_NGS  HINRTALNCN DSLNTGWLAG LIYHHRFNSS GCPERLASCR RLTDFAQGWG
P63_2A.6     HINRTALNCN DSLNTGWLAG LIYRHRFNSS ---------- ----------
P63_2B.6     HINRTALNCN DSLNTGWLAG LIYRHRFNSS ---------- ----------
```

Figure 3.75 Amino acid alignment of P63 and Sanger sequenced clones following second site directed mutagenesis
The alignment shows successful Sanger sequencing results from P63 phCMV clones following site-directed mutagenesis and two consensus sequences from P63 TPA and TPB based on the G1a Inner sense primer. Site-directed mutagenesis was performed on clones 2A.6 and 2B.6 in order to obtain a change of amino acid Histidine to Arginine at position 444. Where mismatches occurred, chromatograms were visually inspected to confirm their presence. The letters in bold red show mismatches in the sequence with relation to TPA NGS consensus sequence. The numbers above the alignment are based on the start of the expected amino acid sequence and the numbers in brackets are based on amino acid numbers from H77 reference genome (Accession number: AF009606). Unsuccessful sequenced clones were excluded from the alignment.

Envelope sequences from one time-point pre-treatment and one time-point post-treatment from P155, and two treatment failures, P75 and P63, were successfully recombined into the phCMV gateway expression vector and subsequently transfected into HEK-293T cells. The HEK-293T cells were harvested and the infectivity of each HCVpp tested on Huh7 cells as described in Materials and Methods.

3.2.4 Infectivity testing of HCVpp

The infectivity testing ensured that HCVpp were functional for the subsequent autologous neutralisation assays. Luminescence signal in relative light units was normalised to background or Huh7 cell signal only (set at 1). The infectivity of each HCVpp was measured as the increase from the mean of the background or control (x mean control). Only HCVpp with a signal increase of >10 times the control were considered functional. Figure 3.76 shows that the signal increase from control mean differed between different HCVpp. P155 TPA clone 1B had an increase of >10 times the control but <100 times, while 2B did not cross the desired threshold of a working HCVpp (Figure 3.76a). The two other clones from TPA, 4B and 6B, had infectivity of >300 times from the background and were therefore used for future experiments. Figure 3.76b looked at infectivity of P155 TPB clones, which were not as infectious as TPA clones reaching <100 times infectivity of control for SDM2 and SDM3 and >100 times infectivity for SDM4 and SDM9. Since SDM4 and SDM9 had the highest infectivity for P155 TPB and they had a confirmed amino acid change by Sanger sequencing from TPA to TPB (see Figure 3.70), they were used for subsequent neutralisation assays. The infectivity of P75 TPA was >400 times the control mean for Clone 2.2 and >100 times the control mean for Clone 9B. P75 TPB Clones 2.1 and 2.2 were both >200 more infectious than the background (Figure 3.76c). None of the P63 clones at either time-points produced working HCVpp of infectivity >10 times control mean, even though the positive control was >200 times the control mean (Figure 3.76d).

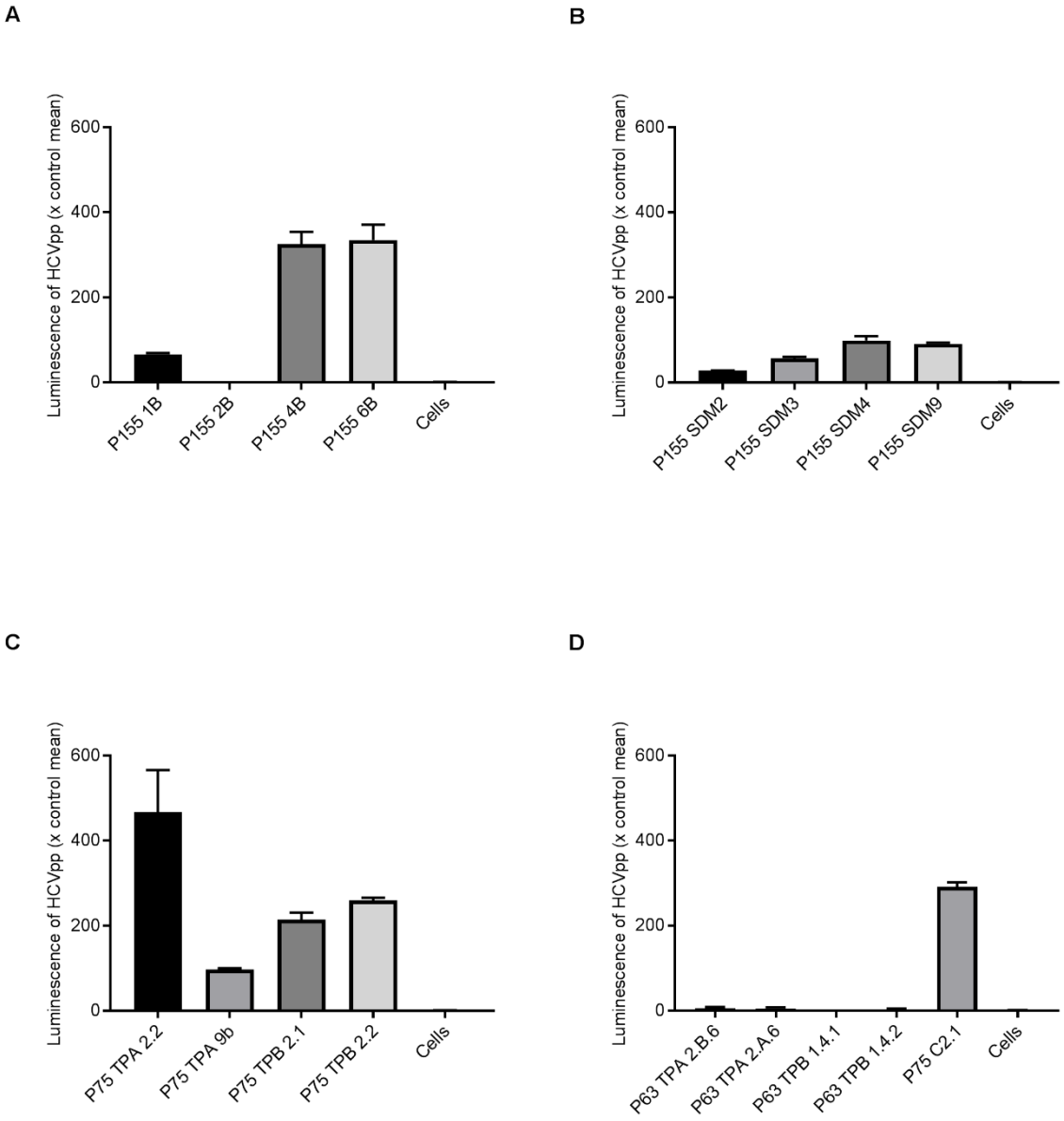

Figure 3.76 Infectivity of autologous HCV pseudoparticles from P155 and two control patients
Huh7 cells were infected with HCVpp bearing E1E2 sequences from secondary spontaneous clearer P155 and two treatment failures (P75 and P63). At 72 hours, cells were lysed and luciferase activity determined as described in Materials and Methods. The bars represent mean relative luminescence of HCVpp times control mean (fold change from mean luminescence of uninfected cells) and error bars represent ±SEM. HCVpp were used for functional assays if relative luminescence was >10x background (uninfected Huh7 cells). HCVpp were tested in triplicate over two experiments. A. Infectivity testing of all clones bearing E1E2 from P155 TPA. B. Infectivity testing of all clones bearing E1E2 from P155 TPD. SDM – site directed mutagenesis.

3.2.5 Evaluation of E1E2 production by GNA ELISA

Since none of the P63 HCVpp were infectious in Huh7 cells, it was decided to establish whether the transfections were successful, resulting in the production of E1E2. For this purpose, a Galanthus nivalis agglutin (GNA) ELISA was used to capture HEK-293T cell lysate from the transfections resulting in HCVpp. E1E2 sequences were detected by a linear epitope binding antibody, AP33 (provided by Dr Arvind Patel). The conditions of the GNA ELISA were optimised as described in Section 3.2.8. Figure 3.77 shows, that despite no positive infectivity signal above background luminescence, E1E2 proteins were detected in the P63 TPA transfected lysates. The signal of the absorbance was >10 times that of the mean Healthy Controls and E1E2 negative cell lysates. Since transfections were successful no further attempts were made at obtaining a functional P63 pseudoparticle and autologous neutralisation experiments were not performed for this sample.

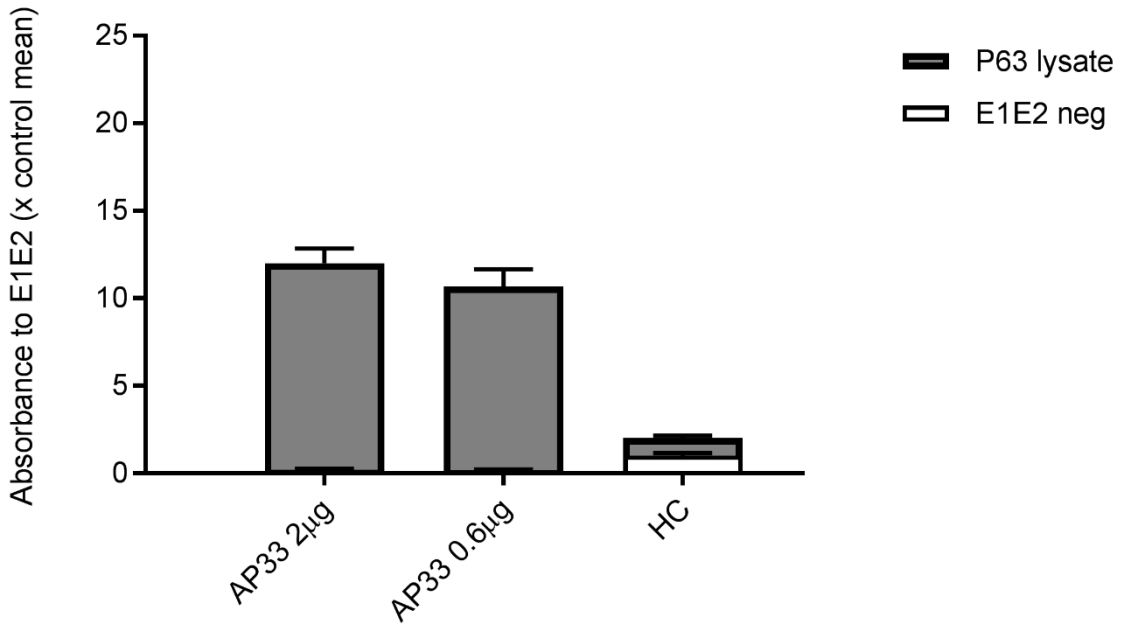

Figure 3.77 Detection of P63 E1E2 from transfected HEK-293T cells by GNA ELISA
HEK 293T cell lysate from P63 TPA was captured by 0.25 µg/well GNA in PBSA on ELISA plates. Plates were blocked with 2% skimmed milk PBST for 2 hours. Optimised concentration of the humanised monoclonal antibody, AP33 (h-AP33) were used in order to detect the presence of E1E2. E1E2 negative HEK 293T cell lysate (E1E2 neg) and purified IgG from healthy control 10 (HC10) and acute healthy control (AHC) were used as negative controls. Absorbance was calculated by normalising to healthy controls (fold change from the mean absorbance). Anti-human IgG HRP antibody (Sigma A0170) at 1/10000 in PBST was added for h-AP33 and healthy controls. TMB substrate was used for ELISA development and absorbance read at 450 nm. Graphs represent mean value of two experiments in duplicate with standard error mean (±SEM).

3.2.6 Whole genome analysis of patient sequences by next generation sequencing and Sanger sequencing

Humoral immune responses may act in concert with T cell responses during adaptive immunity to HCV. We therefore looked for evidence of immune selection both within and out with envelope by examining HCV evolution throughout the course of infection using full genome sequencing by NGS. Due to scarcity of samples we were unable to obtain whole genome sequencing data for P76 time-points although E1E2 sequences were available from Sanger sequencing. In P76 five amino acid changes were noted within E2, three of which sit in the HVR1. In P155, four amino acid changes were noted within E2, three of which sit in key antibody neutralising epitopes (E430K, H443Y, V524A) although only one was present at the post-treatment TPD (H443Y) (Table 3.15). In contrast control patients, P75, P131 and P63, only had one amino acid change located in a neutralising antibody epitope; E531D, S417N, R444H, respectively. P155 also had changes in consensus sequence in other areas of the genome, most of which occurred at the later TPD including, NS2 (n=1), NS3 (n=2), NS4A (n=1), NS5A (n=2) and NS5B (n=3). Interestingly all of these amino acid changes with the exception of one (I2723) occurred in known T cell epitopes. Similarly, relapse control patients, P75 and P131, also had changes in other areas of the genome including; p7 (P75, n=1), NS2 (P75, n=2, P131, n=1), NS3 (P75, n=3, P131, n=2), NS4A (P75, n=1), NS5A (P75, n=4, P131, n=5) and NS5B (P75, n=2). Most of these changes also occurred in epitopes associated with T cell responses against HCV. P63 had no changes in the HCV consensus sequence outside the E2 gene.

Table 3.15 Evolution of HCV genome sequences between patient time points.

Patient ID		Region of HCV genome															
	Time Point	E2				P7	NS2		NS3		NS4A	NS5A		NS5B	
		Amino acid changes													
P76	A	T223* K408*	V386* N574	G401*											
	C	T224A K408R	V386F N574D	G401S											
P155	A	F399*	E430#	H443#	V524#		A1020*		R1050*	S1091*	L1662*	A2148*	V2505*	T2696* S2720*	N2609* I2723
	B														I2723V
	C	F399L	E430K		V524A					S1091C	L1662I			S2720N	
	D			H444Y			A1020T		R1050K			A2148T	V2505I	T2696I	N2609D I2723V
P75	A	Y386* M396* R408*	S391* S397* E531#	A393* I399*	T395* S401*	V760*	A937*	T945*	A1332* P1621	V1408*	V1687*	M2079* R2276*	I2252* V2375*	Q2485*	D2486*
	B	Y386H M396A R408K	S391N S397A E531D	A393G I399L	T395A S401N	V760A	A937V	T945A	A1332V P1621S	V1408A	V1687I	M2079T R2276L	I2252V V2375A	Q2485H	D2486N
P131	A	V392* V603*	L399*	P405*	S417#		V895		Q1067*	A1113*		N2218* I2252* A2412	D2220* D2413		
	B	S417N													
	C	V392A V603I	L399F	P405Q	S417N		V895I		Q1067H			N2218D I2252V A2412G	D2220N D2413G		
	D	V603I			S417N		V895I		Q1067H	A1113V		N2218D I2252V	D2220N		
P63	A	Q408*	R444#												
	B	Q408K	R444H												

TPA was used as a baseline for each patient and compared to later time point(s) for different genes of the HCV genome. Numbers are based on amino acid reference sequence of genotype 1a, H77 (accession number AF009606) * indicates T cell epitopes, # indicates neutralising antibody epitope, red indicates epitope in the HVR1/2, blue indicates epitope in IgVR. Crossed out areas indicate lack of sequencing data. Sequencing data for P76 supplied by Dr Rachael Swann

The analysis of amino acid changes by NGS over time revealed a large number of changes in the T cell epitopes from pre-treatment time-points to post-treatment time-points (Table 3.15). Figure 3.78 shows the viral load patterns and the duration of treatment 1000 days post the first HCV PCR positive in relation to the calculated CD8 to CD4 T cell ratio for SSC, P76 (A) and P155 (B) and treatment failures, P75 (C), P131 (D), P101 (E) and P63 (F). During the pre-treatment phase of SSC patients and P75, the CD8 to CD4 ratio was above 2 and steadily decreasing throughout the first 200 days and later throughout the course of treatment (Figure 3.78a-c). Similarly, the ratio of P101 for the first 500 days post HCV detection, was also decreasing, but mostly remained below 2 (Figure 3.78e). P63 had a fluctuating CD8 to CD4 ratio, which rarely exceeded 2, but always remained above 1 (Figure 3.78f). The pattern of P131 within the pre-treatment phase (first 500 days post HCV diagnosis) was difficult to predict due to missing data points, although the ratio of CD8 to CD4 mostly remained steady above 1, but below 2 (Figure 3.78d). Post-relapse, the ratio of SSC patients increased rapidly and remained steady above 1.5 for P76 and above 2 for P155. This pattern was not observed in any other patient. At the time of relapse, the CD8 to CD4 of P75 and P131 increased rapidly subsequently decreasing. The ratio of P101 did not increase at the time of relapse and was slowly decreasing towards 1 post-treatment. Lastly, although the null patient ratio of CD8 to CD4 T cells did increase slightly post-treatment there was a rapid decrease following TPB toward 1.

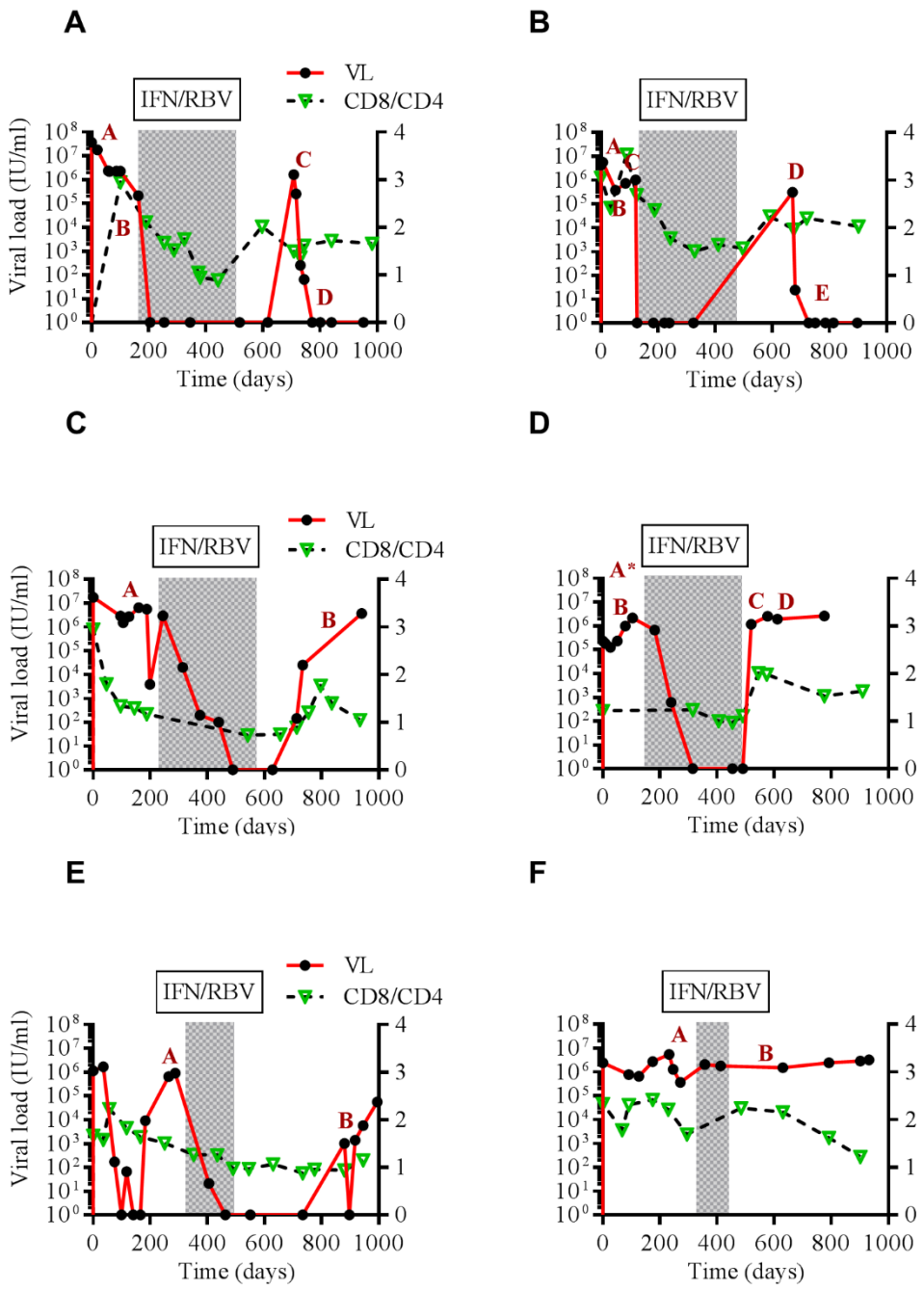

Figure 3.78 The ratio of CD8 to CD4 T cells in secondary spontaneous clearers and control patients
The ratio of CD4 and CD8 T cells within the first 1000 days post first HCV positive PCR in secondary spontaneous clearers (SSC) and treatment failure (TF) patients. The triangles on dashed lines indicate CD8 to CD4 T cell ratio numbers and the black dots on solid red lines represent viral load in $\log_{10}$ IU/ml. The grey boxes indicate the duration of pegylated interferon (PEG-IFN) and ribavirin (RBV) treatment for each patient. Letters A-E indicate different time-points during the infection of each patient. A. P76, a genotype 1a SSC at TPA and TPB pre-treatment and TPC and TPD post-treatment. B. P155, a genotype 4d SSC. TPA-TPC were pre-treatment and TPD and TPE post-treatment. C.P75, a genotype 1a relapse control at TPA pre-treatment and TPB post-treatment. D. P131, a genotype 1a relapse control. TPA and TPB were pre-treatment and TPC/TPD were post-treatment. A*- time-point taken prior to first positive PCR. E. P101, a genotype 1a relapse control at TPA pre-treatment and TPB post-treatment. F. P63, a genotype 1a null responder control at TPA pre-treatment and TPB post-treatment.

3.2.7 Neutralising antibody responses in SSC and controls

We hypothesized that humoral immune responses were active and may have contributed at least in part, to viral clearance. We focused on studying antibody responses to the envelope glycoproteins as they are required for cell entry through interaction with CD81 and SRB1 receptors and known targets for neutralizing antibodies (Op De Beeck et al. 2004). For this purpose, purified IgGs from all patients at multiple time-points pre-treatment and post-treatment were tested for neutralisation using the HCVpp system.

3.2.7.1 Neutralising antibody responses against heterologous HCVpp

The general HCVpp panel, containing representative examples from genotype 1a, 1b, 2a, 2b, 3a and 4a (as described in Materials and Methods) were used for the assessment of breadth of neutralisation of SSC and all control patients at pre-treatment and post-treatment time-points.

At pre-treatment time-points, SSC patients displayed no or weak neutralization to all genotypes Figure 3.79a and Figure 3.79b). Similarly to SSC, relapse controls, P75, P131 and P101, and the null responder, P63, all displayed weak or no neutralisation patterns to all genotypes tested at the pre-treatment time-points (Figure 3.79c-f). In contrast, IgG from later time-points from P76 showed broad neutralisation against all genotypes other than genotype 3 (Figure 3.79a). This neutralisation pattern was not shown by any other patient including the g4d infected SSC (Figure 3.79b-f). There was increase in neutralisation over time against g1a and g4 HCVpp for P155, although it was mostly below the 50% cut off (Figure 3.79.b). Control patients increase in neutralisation was also limited mostly to two genotypes, but was also below the 50% cut off (Figure 3.79c-f). A robust increase in neutralisation of >50% was only noted in the null control patient; P63, but only for genotype 1a (Figure 3.79f).

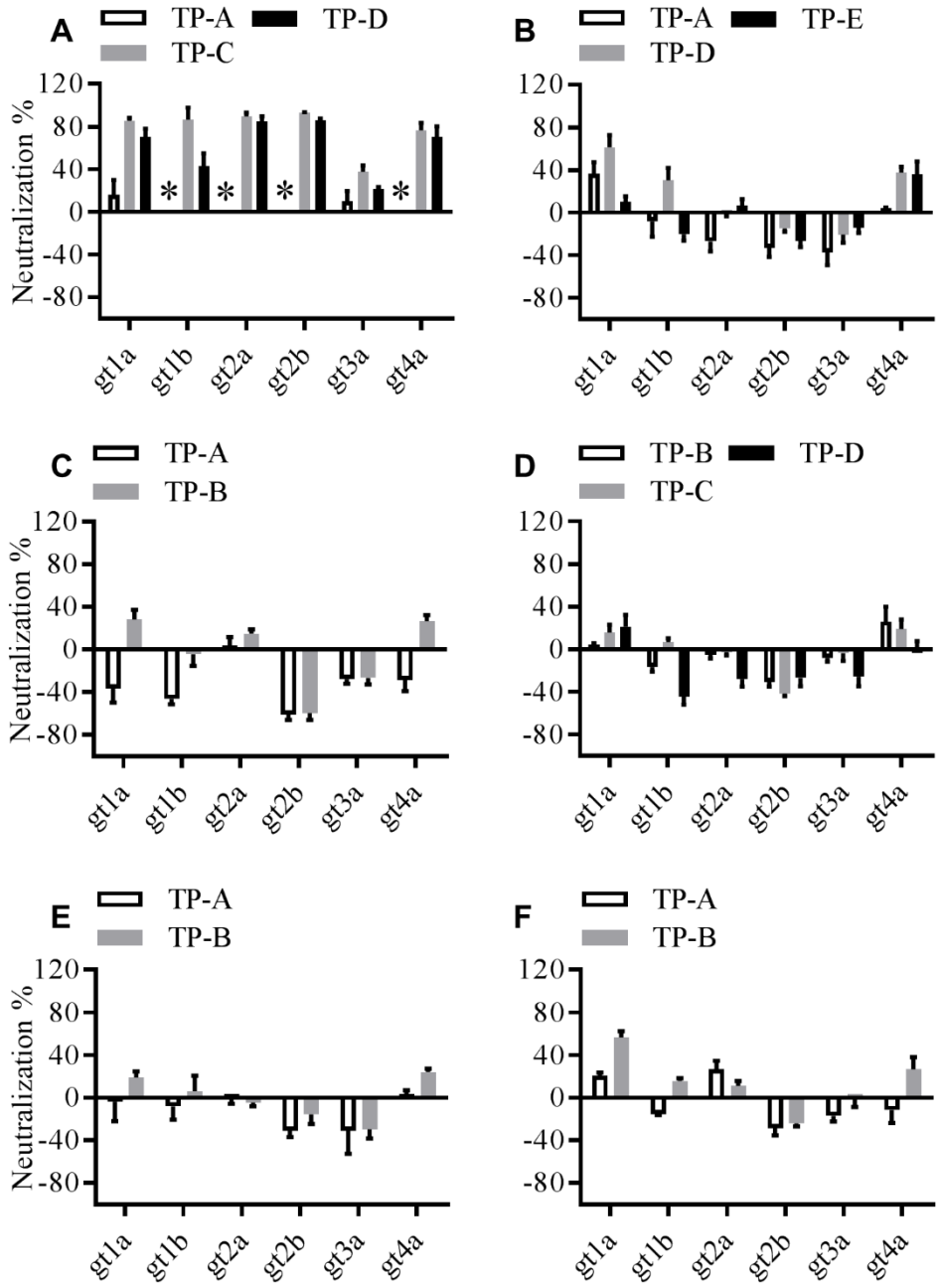

Figure 3.79 Neutralisation of standard HCV E1E2 sequences by purified IgG
Pseudoparticles bearing E1E2 proteins from a standard genotype (gt) panel (1a, 1b, 2a, 2b, 3a and 4a) were generated as described in Materials and Methods. Purified IgG from different patients and time-points were tested for their ability to prevent HCVpp infection at a concentration of 100 µg/ml. Positive neutralisation occurred if a reduction of at least 50% in relative light units was achieved. Error bars represent mean and standard error of the mean (±SEM). Graph represent data from 3-6 independent experiments in duplicate, A. Neutralisation pattern from secondary spontaneous clearer, P76.* indicates that there was insufficient IgG from TPA to test for neutralisation against gt 1b, 2a, 2b and 4a HCVpp. Data collected by Dr Rachael Swann B. Neutralisation pattern from secondary spontaneous clearer, P155. C. Neutralisation pattern from relapse control, P75. D. Neutralisation pattern from relapse control, P131. E. Neutralisation pattern from relapse control, P101. F. Neutralisation pattern from null control, P63.

3.2.7.2 Neutralising antibody responses against autologous HCVpp

Next we tested plasma neutralisation against HCVpp bearing autologous envelope sequences generated as described above. In order to obtain the neutralisation titre, functional HCVpp (as confirmed by the above infectivity assays) for pre-treatment and post-treatment time-points of P76, P155 and P75 were incubated with serial dilutions of plasma from various time-points during the course of infection. Due to volume constraints for each patient sample, purified IgGs were not utilised for autologous neutralisation experiments. Figure 3.80 shows autologous neutralisation of HCVpp from P76 at TPA (first HCV PCR positive) and TPC (relapse), which was generated by Dr Rachael Swann. Figure 3.81 shows the autologous neutralisation pattern of P155 HCVpp at TPA (First HCV PCR positive) and TPD (relapse), while Figure 3.82 shows autologous neutralisation of P75 HCVpp from TPA, pre-treatment and TPB, post-treatment. In all patients, plasma from TPA did not prevent HCVpp cell entry although a low level of neutralisation was noted in the relapse control P75 (<40% neutralisation) (Figure 3.82). Protection against TPA autologous HCVpp was displayed with plasma from TPC and TPD in P76 with IC_{50} results of 1: 2506 and 1:500, respectively (Figure 3.80a). This neutralisation pattern was also present in plasma from TPC and TPD against P76 TPC HCVpp with an IC_{50} 1:5076 and 1:167, respectively (Figure 3.80b).In samples from the second SSC patient (P155), TPD (relapse time-point) and TPE (SSC time-point) plasma neutralised the early TPA HCVpp with an IC_{50} of 1:131 and 1:149, respectively (Figure 3.81a). Similarly, at TPD the P155 HCVpp was only neutralised by the plasma samples from TPD and TPE achieving a slightly reduced IC_{50} values of 1:59 and 1:116, respectively (Figure 3.81b). P75 displayed a very similar pattern, with neutralisation of HCVpp from TPA by plasma sample from TPB, post-treatment (Figure 3.82a). The IC_{50} for that plasma time-point and HCVpp was lower than that of P76; 1:556. For the post-treatment HCVpp (TPB), the IC_{50} value was reduced to 1:333 (Figure 3.82b).

A

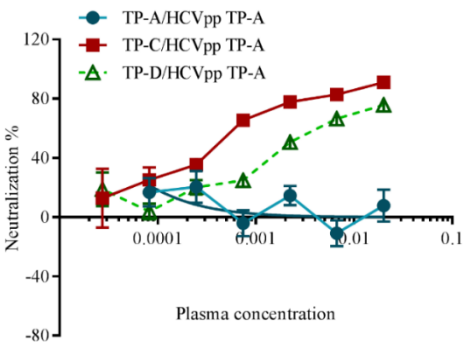

Timepoint	IC_{50}
A	N/A
C	1:2506
D	1:500

B

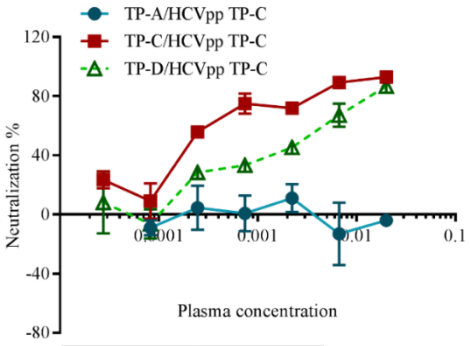

Timepoint	IC_{50}
A	N/A
C	1:5076
D	1:167

Figure 3.80 Plasma neutralisation of HCVpp bearing glycoproteins from autologous P76 sequences.
The graphs show percentage (%) reduction of relative light units on luciferase assay of HCVpp infection compared to no plasma control. Plasma from all time-points was heat-inactivated and serially diluted. IC_{50} values are displayed below the graphs in tables. Error bars represent mean with standard error of the mean (±SEM). Graphs represent data from four independent experiments in duplicate.A. Pseudoparticle bearing the consensus from SSC, P76, E1E2 TPA. B. Consensus sequence from P76 E1E2 TPC. Data collected by Dr Rachael Swann.

A

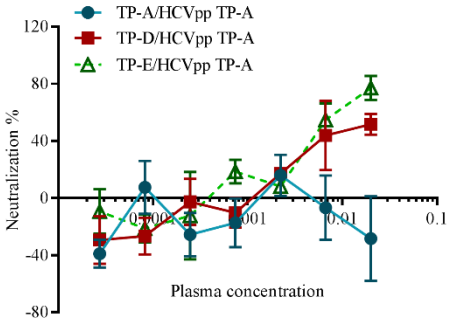

Timepoint	IC_{50}
A	N/A
C	1:131
D	1:149

B

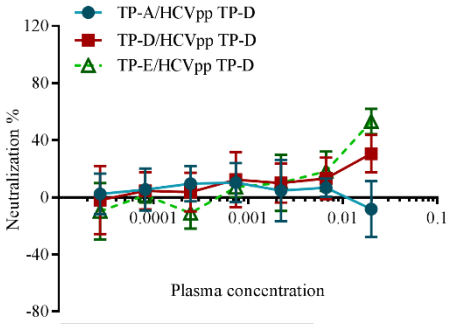

Timepoint	IC_{50}
A	N/A
D	1:59
E	1:116

Figure 3.81 Plasma neutralisation of HCVpp bearing glycoproteins from autologous P155 sequences
The graphs show percentage (%) reduction of relative light units on luciferase assay of HCVpp infection compared to no plasma control. Plasma from all time-points was heat-inactivated and serially diluted. IC_{50} values are displayed below the graphs in tables. Error bars represent mean with standard error of the mean (±SEM). Graphs represent data from six independent experiments in duplicate. A. Pseudoparticles bearing the consensus sequence from SSC, P155 E1E2 from TPA. B. Pseudoparticles bearing the consensus sequence from SSC, P155 E1E2 from TPD.

A

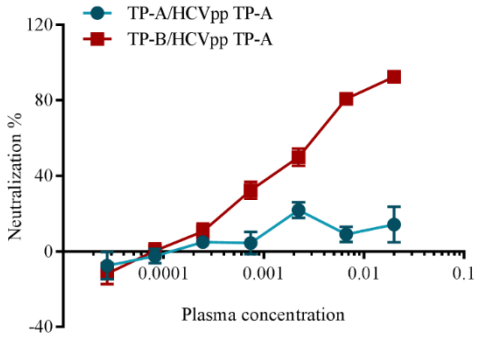

Timepoint	IC_{50}
A	N/A
B	1:556

B

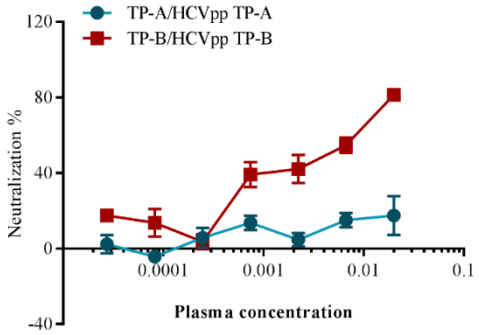

Timepoint	IC_{50}
A	N/A
B	1/333

Figure 3.82 Plasma neutralisation of HCVpp bearing glycoproteins from autologous P75 sequences
The graphs show percentage (%) reduction of relative light units on luciferase assay of HCVpp infection compared to no plasma control. Plasma from all time-points was heat-inactivated and serially diluted. IC_{50} values are displayed below the graphs in tables. Error bars represent mean with standard error of the mean (±SEM). Graphs represent data from six independent experiments in duplicate. A. Pseudoparticles bearing the consensus sequence from relapse control, P75, E1E2 from TPA. B. Pseudoparticles bearing the consensus sequence from relapse control, P75, E1E2 from TPB.

The genotype 4d-infected SSC, P155, had three pre-treatment time-points available for analysis (TPA, TPB and TPC). The neutralisation pattern of plasma from TPA was evaluated in the above section (See Figure 3.81).We therefore looked at the neutralisation pattern of the remaining two time-points (TPB and TPC) against HCVpp from TPA and TPD (Figure 3.83a and Figure 3.83b). Even at the highest concentration of plasma, both TPB and TPC did not reach a neutralisation of 50% or more against TPA HCVpp (Figure 3.83a). No IC_{50} values were therefore calculated. However, neutralisation levels increased gradually from TPA to TPC (Figure 3.81a and Figure 3.83a). In contrast, using the TPD HCVpp, neutralisation did not increase between TPB and TPC, indicating Ab escape (Figure 3.83b).

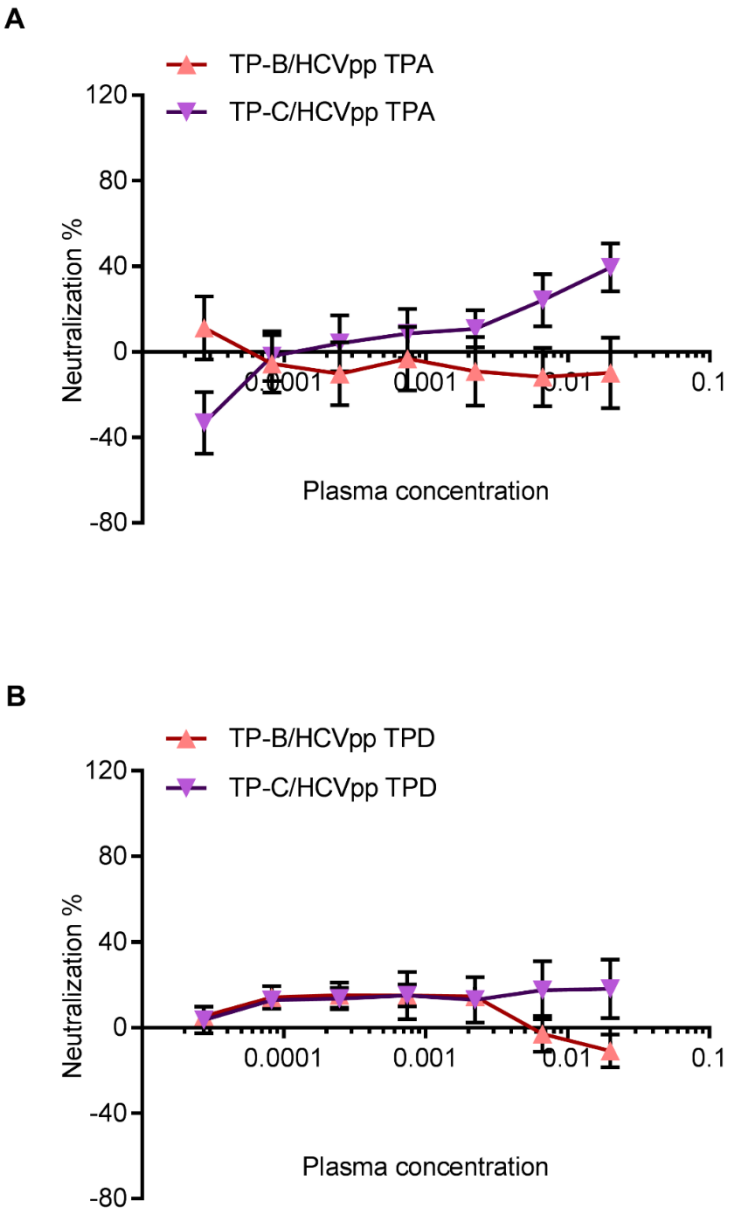

Figure 3.83 Plasma neutralisation of HCVpp bearing glycoproteins from autologous P155 pre-treatment sequences
The graphs show percentage (%) reduction of relative light units on luciferase assay of P155 HCVpp infection compared to no plasma control. Plasma from all time-points was heat-inactivated and serially diluted. Error bars represent mean with standard error of the mean (±SEM). Graphs represent data from six independent experiments in duplicate. Neutralisation was performed against P155 samples from two pre-treatment plasma TPA and TPB. A. Pseudoparticle bearing the consensus from secondary spontaneous clearer, P155, E1E2 TPA. B. Pseudoparticle bearing the consensus sequence from P155 E1E2 TPD.

3.2.8 Evaluation of E1E2 binding antibodies by GNA ELISA

3.2.8.1 Optimisation of E1E2 GNA ELISA

Since different neutralisation patterns emerged across the patients tested, it was important to establish whether E1E2 antibodies were present in all cases. A previously described Galanthus nivalis agglutin (GNA) ELISA method was used to capture HCV glycoproteins. GNA binds specifically with glycans on the HCV glycoproteins as well as other heavily glycosylated enveloped viruses. Therefore, GNA coated plates were used to capture HEK 293T cell lysates from the same HCV genotypes as the ones used in the genotype neutralisation panel (section 3.2.6).

Since there was a limited volume of patient samples available, the ELISA conditions were optimised prior to testing for E1E2 antibodies in patients' time-points. Firstly, the concentration of positive control for all ELISA tests was determined. AP33 is a mouse monoclonal antibody, which binds to a linear epitope in HCV envelope. Moreover, AP33 is known to bind to a conserved epitope and was therefore used as a positive control. A serial dilution of AP33 was performed ranging from 0.0025 µg to 8 µg for genotypes 1a, 1b, 3a and 4 in order to determine the optimal concentration for GNA capture ELISA (Figure 3.84). We aimed to establish a concentration that would not fall above absorbance/optical density (O.D) of 4 within 20-30 minutes after the addition of substrate. This is because the plate reader does not quantify the products accurately above that absorbance. The 20-30 minutes incubation allows enough time for antibodies to bind E1E2 even at small concentrations.

The optimal concentration of AP33 should be at least 3 times above the background or blank absorbance, enabling a good signal to noise ratio. Figure 3.84 shows that the optimal concentration for gt 1a was lower than other genotypes at ≥0.3 µg. Concentrations of ≥2 µg for gt 1b, gt 3a and gt 4 had absorbance at least 3 times above the blank, but below 4 and were therefore used for future experiments.

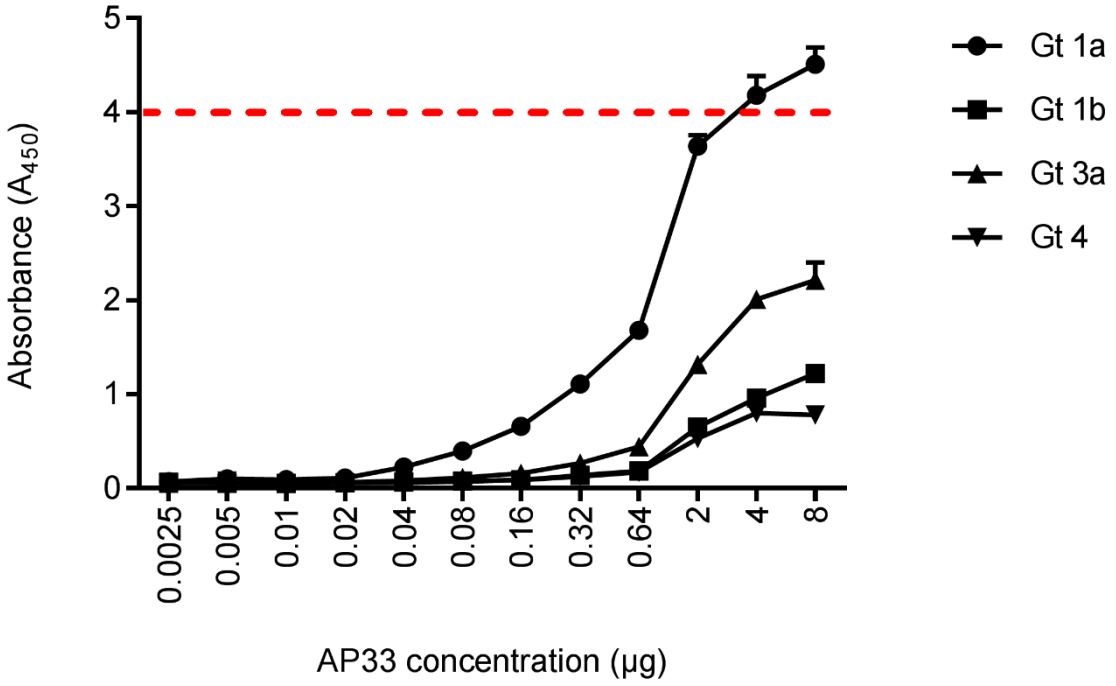

Figure 3.84 Optimal concentration of AP33 antibody for GNA ELISA
HEK 293T cell lysates from genotypes 1a (gt 1a), genotype 1b (gt 1b), genotype 3a (gt 3a) and genotype 4 (gt 4) were captured by 0.25 µg/well GNA in PBSA. Plates were blocked with 2 % skimmed milk powder in PBST for 2 hours. AP33 was serially diluted from 8µg to 0.0025µg in PBST in order to establish the optimal concentration. Anti-mouse HRP conjugate (Sigma A4416) was used at 1/1000 dilution in PBST as a secondary antibody followed by TMB substrate and absorbance was read at 450 nm. The dashed red line indicates the maximum absorbance for quantification of product by the plate reader. Each point represents mean value of a duplicate with standard error mean (±SEM). Values were considered positive if at least three times higher than the absorbance of the blank (no AP33 added). For gt 1a positive values were at ≥0.2 µg, gt 1b at ≥2 µg, gt 3a at ≥0.16 µg and gt 4 at ≥0.32 µg. Graph represents data from two independent experiments.

The serial dilution experiment established an optimal concentration of a positive control mouse-monoclonal antibody, AP33. However, the purpose of the ELISA assays was to establish whether antibodies to E1E2 were present in human subjects. Therefore, a humanised AP33 anti-E2 monoclonal antibody was used, ensuring the same secondary antibody for both patients and positive control. The optimal concentration of mouse AP33 (m-AP33) established above was compared with the same concentration of humanised AP33 (h-AP33) against different genotypes. Two negative controls were also added –purified IgGs from healthy controls at a concentration of 100 µg/ml and lysate from HEK 293T cells transfected without E1E2 (E1E2 neg). The negative controls were used to help in confirming whether the signal was specific to HCV envelope glycoprotein. Figure 3.85 shows that absorbance of m-AP33 correlated well with h-AP33 at the same concentrations and was specific to all HCV genotype as there was minimal absorbance observed in E1E2 negative lysate (<0.5 O.D). Absorbance of both AP33 antibodies was below 1 for genotype 1b and genotype 4, thus minimising the signal to noise ratio between the genotype and E1E2 neg lysate. This was particularly true for h-AP33, which had higher E1E2 neg absorbance possibly related to the use of a different secondary antibody. Both healthy controls had absorbance of around or above 1 O.D. to HCV and E1E2 negative lysate. The absorbance of healthy controls were similar to AP33 and therefore were not suitable as a negative control.

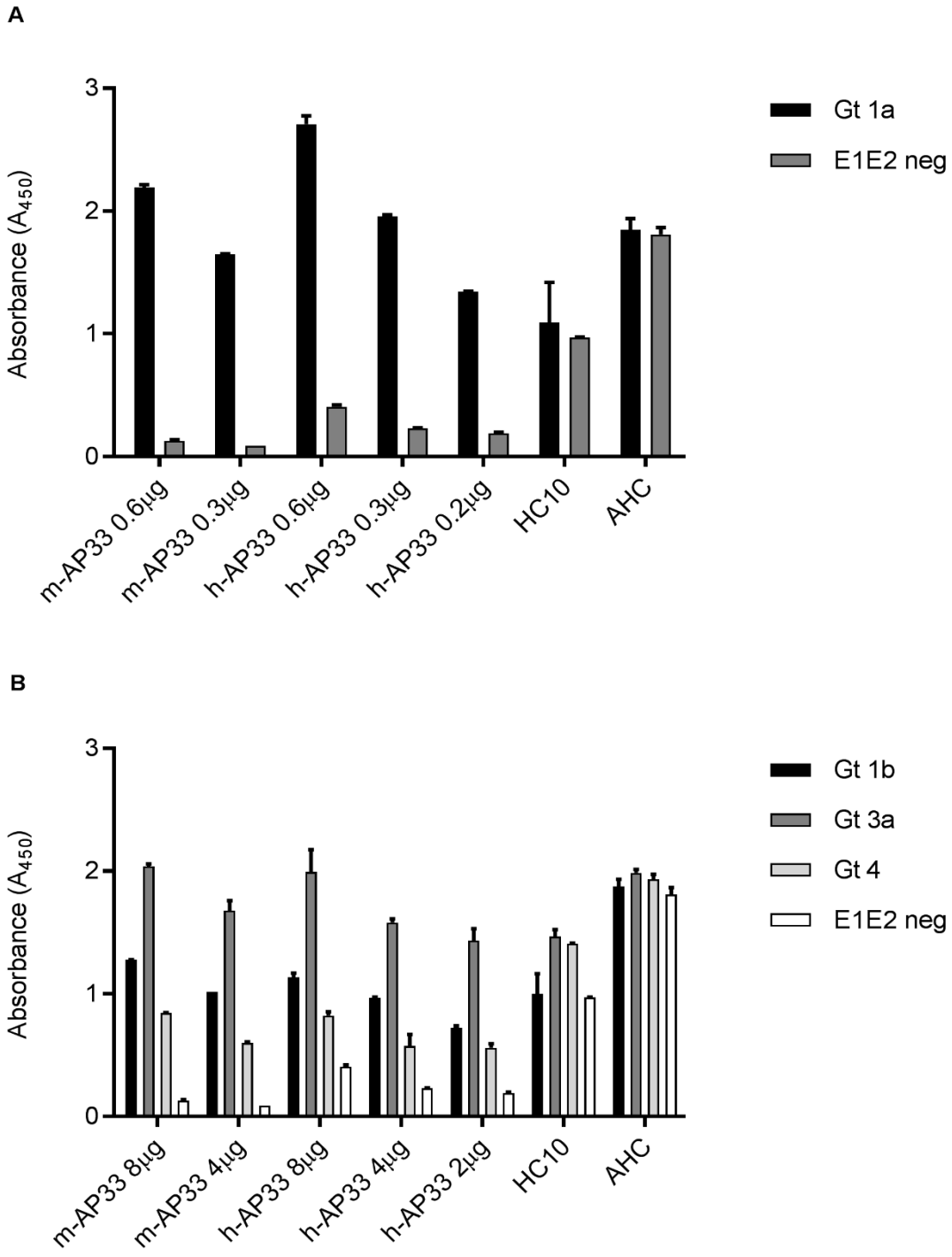

Figure 3.85 Comparing mouse AP33 and humanised AP33 monoclonal antibody binding
HEK 293T cell lysates from different genotypes were captured by 0.25 µg/well GNA in PBSA on ELISA plates. Plates were blocked with 2 % skimmed milk PBST for 2 hours. Previously established optimal mouse AP33 (m-AP33) concentrations along with the same humanised AP33 (h-AP33) concentration (plus one lower dilution) were used as positive controls. E1E2 negative HEK 293T cell lysate and purified IgG from healthy control 10 (HC10) and acute healthy control (AHC) were used as negative controls. Anti-mouse HRP conjugate (Sigma A4416) was added at 1/1000 dilution in PBST as a secondary antibody for m-AP33 and anti-human IgG HRP antibody (Sigma A0170) at 1/10000 in PBST was added for h-AP33 and healthy controls. TMB substrate was used for ELISA development and absorbance read at 450 nm. Graphs represent mean value of two experiments in duplicate with standard error mean (±SEM). A. Absorbance at 450 nm from gt 1a and E1E2 negative lysates. B. Absorbance at 450 nm from gt 1b, gt 3a, gt 4 and E1E2 negative lysates.

The next set of experiments aimed to improve the signal to noise ratio by two methods: first by reducing background signal in negative healthy control samples and second by increasing the positive signal from AP33 especially for gt 1b and gt 4 lysates. In order to establish whether the high background was limited to the two healthy controls tested, a screen of seven (n=7) different healthy control samples was performed (Figure 3.86). Figure 3.86 shows, that absorbance of AP33 was >1 only in gt 1a lysate. Absorbance without lysate or with E1E2 neg control was <0.5, thus ensuring a good signal to noise ratio. The same secondary antibody (Sigma A0170) used for h-AP33 was also used for healthy controls. Despite this, all healthy controls had absorbance >1 for gt 1a, E1E2 neg and no lysate controls. New healthy control (NHC), healthy control 5 (HC5) and healthy control 7 (HC7) had absorbance >3, much higher than the positive control. Therefore, the high background signal was present in all healthy control samples and therefore further optimisation was required.

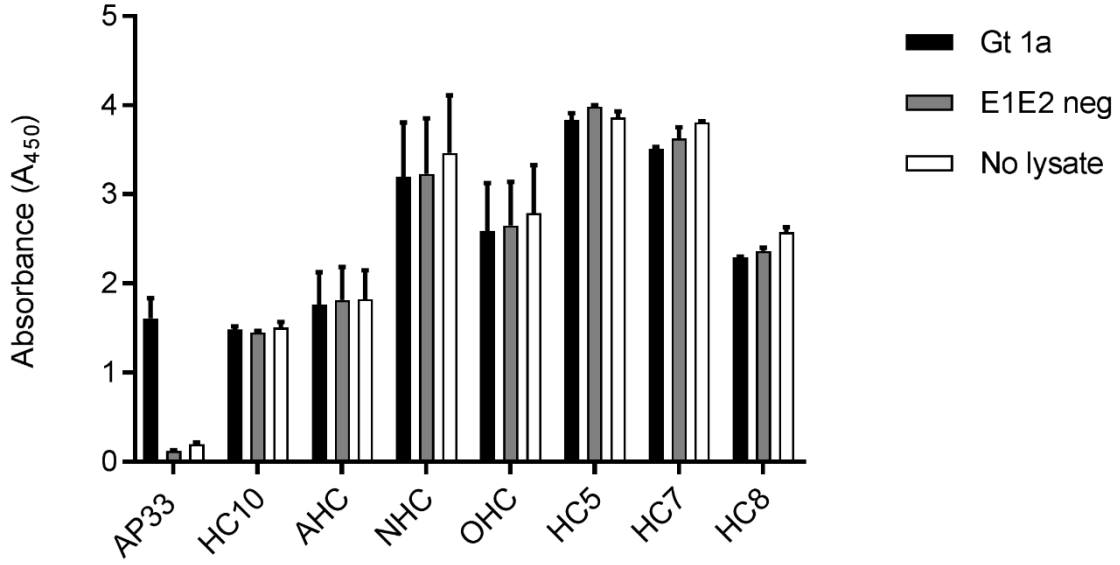

Figure 3.86 Screen of purified IgG from healthy control samples
Healthy controls (n=7) were screened to select for negative control with the best signal to noise ratio. HEK 293T cell lysate from genotype 1a and E1E2 negative control were captured by 0.25 µg/well GNA in PBSA on ELISA plates. Plates were blocked for 2 hours with 2% skimmed milk PBST. Humanised AP33 (h-AP33) at 0.6 µg/well in PBST was used as a positive control. Anti-human IgG HRP antibody (Sigma A0170) at 1/10000 in PBST was added as a secondary antibody. TMB substrate was used for ELISA development and absorbance read at 450 nm. Graphs represent mean value of two experiments in duplicate with standard error mean (±SEM). Signal to noise was determined by comparing absorbance from gt 1a and E1E2 neg lysate or no lysate. HC10 – healthy control 10, AHC – acute healthy control, NHC – new healthy control, OHC – old healthy control, HC5 – healthy control 5, HC7 – healthy control 7, HC8 – healthy control 8.

3.2.8.2 Improving signal to noise ratio in GNA ELISA

No distinction between gt 1a lysate, E1E2 neg and no lysate control may suggest unspecific binding of purified IgGs from healthy controls. Unspecific binding sites were blocked by using 2% skimmed milk powder, which was incubated with all ELISA plates for at least two hours after the addition of GNA. Therefore, 2% skimmed milk PBST was used as a diluent throughout the ELISA experiment in an attempt to reduce the background in healthy controls. Humanised AP33 and one healthy control (AHC) were tested on a variety of lysates (gt 1a, gt 3a, gt 4 and E1E2 neg) (Figure 3.87). The skimmed milk powder reduced the absorbance in healthy control to <0.5 for all lysates tested, while maintaining a signal of >2 for h-AP33 and <0.5 for E1E2 neg control. The signal in AP33 was therefore still specific to HCV E1E2. Therefore, 2% skimmed milk PBST was kept as a diluent for future experiments.

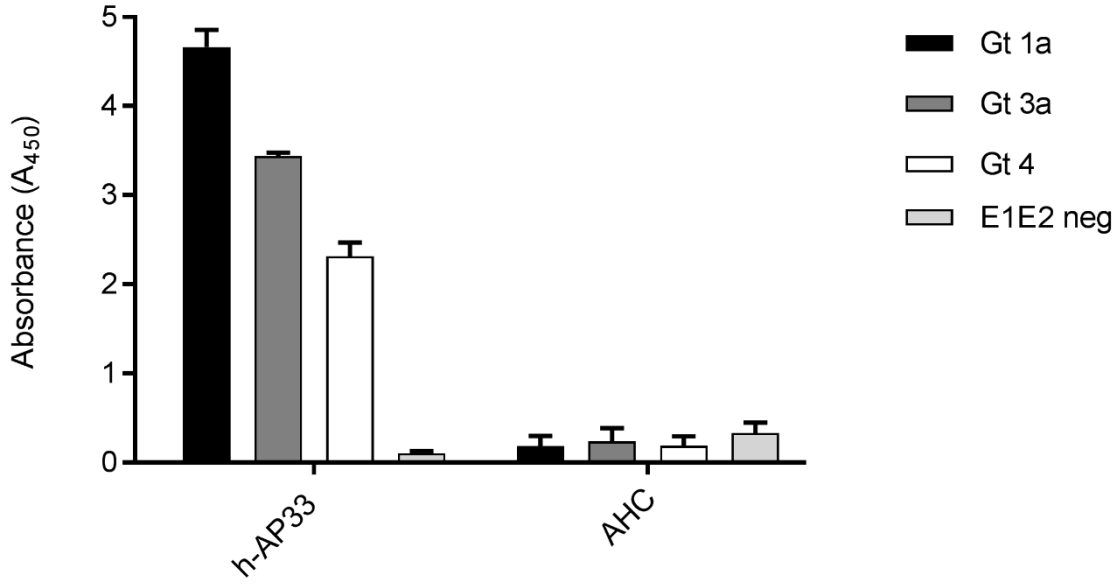

Figure 3.87 Reducing noise in healthy controls for GNA capture ELISA
HEK 293T cell lysate from gt 1a, gt 3a, gt 4 and E1E2 negative control were captured by 0.25 µg/well GNA in PBSA on ELISA plates. Plates were blocked for 2 hours with 2% skimmed milk PBST. The 2% skimmed milk PBST was kept as a diluent throughout all steps of the ELISA experiment to reduce background. Humanised AP33 (h-AP33) at 0.3 µg/well in PBST was used as a positive control. Anti-human IgG HRP antibody (Sigma A0170) at 1/10000 in PBST was added as a secondary antibody. TMB substrate was used for ELISA development and absorbance read at 450 nm. Graphs represent mean value of two experiments in duplicate with standard error mean (±SEM). Signal to noise was determined by comparing absorbance from AP33 and Acute healthy control (AHC) for all genotypes.

The reduction of background in healthy controls ensured a better signal to noise ratio. To further maximise the likelihood of detecting E1E2 antibodies in patients' purified IgG samples, steps were taken to increase the positive signal. Since transfections produce different amounts of E1E2, it was possible to increase the positive signal by screening different lysates for the highest concentration of antigen. Lysates from genotypes 1a, 3a, 4a and E1E2 neg control were obtained through personal communication from three different users (Dr Vanessa Cowton/V, Dr Anna Owsianka/A, and Weronika/W) and subsequently screened with the same concentration of h-AP33 (Figure 3.88) at three different dilutions (1:3, 1:6, 1:9 in PBST). Figure 3.88 shows, that lysates from user A from all genotypes consistently achieved absorbance of >1 at all three dilutions. The gt 1a lysate from user V also reached absorbance of >1 at all three dilutions.

Only the 1:3 dilution from A user lysates achieved absorbance of >2 for all genotypes. Therefore, gt 1a, gt 3a and gt 4 lysates from user A were used for future studies at 1:3 dilution in PBST. E1E2 neg lysates had consistent absorbance of <0.5 regardless of the user and therefore all were used for future experiments.

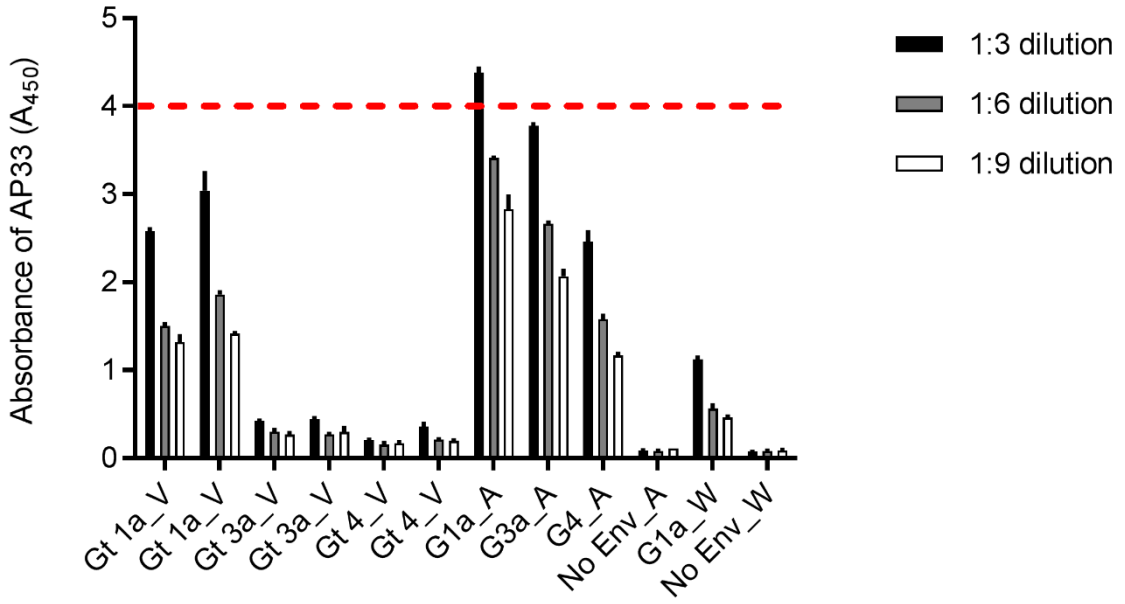

Figure 3.88 Screen of lysates from three users for optimal absorbance in GNA capture ELISA
HEK 293T cell lysates from E1E2 neg, gt 1a, gt 3a and gt 4 were captured by 0.25 µg/well GNA in PBSA. Lysates were obtained through personal communication from three different users indicated by letters (V – Dr Vanessa Cowton, A – Dr Anna Owsianka and W – Weronika). Lysates were diluted 1/3, 1/6 and 1/9 in PBST to determine the optimal dilution with the best signal to noise ratio. Plates were blocked with 2 % skimmed milk powder in PBST for 2 hours. The 2% skimmed milk PBST was kept as a diluent throughout all steps of the ELISA experiment. Humanised AP33 (h-AP33) at 0.3 µg/well in PBST was used as a positive control to screen for optimal lysate with the highest absorbance. Anti-human IgG HRP antibody (Sigma A0170) at 1/10000 in PBST was added as a secondary antibody. TMB substrate was used for ELISA development and absorbance read at 450 nm. Graphs represent mean value of two experiments in duplicate with standard error mean (±SEM). The dashed red line indicates the maximum absorbance for quantification of product by the plate reader. Each point represents mean value of a duplicate with standard error mean (±SEM).

The next experiment aimed to determine whether the signal to noise ratio could be improved further by decreasing the dilution factor of the anti-human HRP secondary antibody. The secondary antibody was diluted 1/10,000 as in previous experiments and compared with a lower dilution of 1/5,000 (Figure 3.89a/b, respectively). Figure 3.89 shows, that at 1/5000 dilution the absorbance of h-AP33 is higher for all genotypes tested (gt 1a, gt 3a and gt 4) than at 1/10,000 dilution. More importantly, the increase of the positive signal does not result in a noticeable increase in absorbance from the AHC negative control, or the background absorbance. The signal to background ratio was better with the 1/5000 dilution of the secondary antibody and therefore the new dilution factor was kept for future GNA capture ELISA experiments.

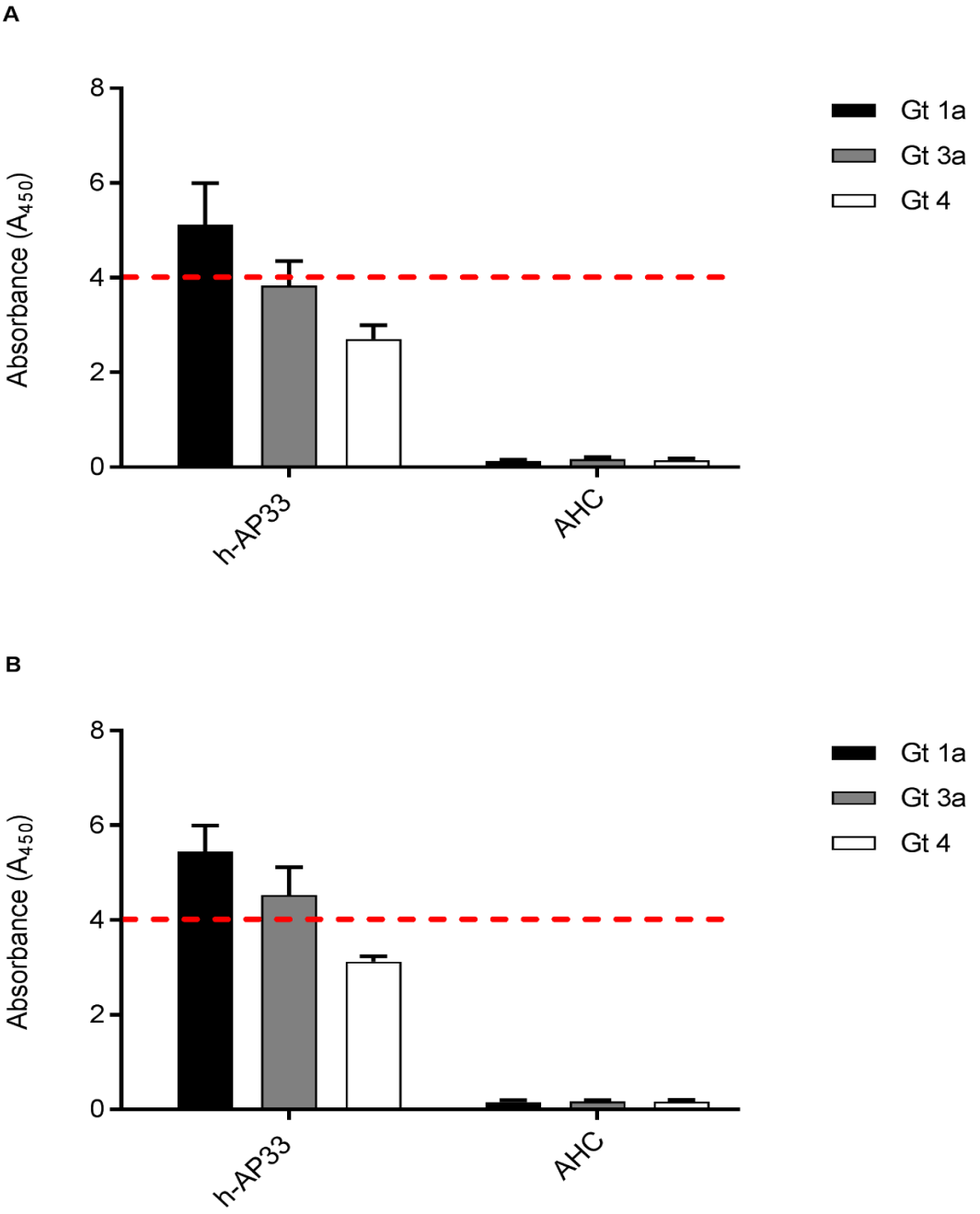

Figure 3.89 Optimisation of secondary antibody concentration for GNA capture ELISA
HEK 293T cell lysates from gt 1a, gt 3a and gt 4 were captured by 0.25 µg/well GNA in PBSA. Lysates were diluted 1/3 in PBST and the plates blocked with 2 % skimmed milk for 2 hours. The 2% skimmed milk PBST was kept as a diluent throughout all steps of the experiment. Humanised AP33 (h-AP33) at 0.3 µg/well in PBST was used as a positive control and AHC as a negative control to screen for optimal secondary antibody concentration. TMB substrate was used for ELISA development and absorbance read at 450 nm. Graphs represent mean value in duplicate with standard error mean (±SEM). The dashed red line indicates the maximum absorbance for quantification of product by the plate reader. Each point represents mean value of a duplicate with standard error mean (±SEM).A. Secondary anti-human IgG HRP antibody (Sigma A0170) at 1/10000 in PBST. B. Secondary anti-human IgG HRP (Sigma A0170_ antibody at 1/5000 in PBST

3.2.8.3 Genotype specific binding

The optimised conditions of the GNA capture ELISA were used to determine the presence of E1E2 binding antibodies in SSC and control patients at different time-points. Since the sample volume from each time-point were limited, testing for binding was initially performed only against two major genotypes for all patients, namely gt 1a and 3a, which were also used for the heterologous neutralisation panel. At baseline (TPA) weak binding to both genotype 1a and 3a was noted for both SSC and control patients tested (Figure 3.90). In contrast, purified IgG from later time-points showed increased binding to E1E2 from baseline, with significant differences in gt 1a binding for all patients tested ($P \leq 0.05$). The genotype 1a infected SSC (P76) and two treatment failures (P75 and P63) showed absorbance of >5 times mean control absorbance for gt 1a at later time-points. Interestingly, the gt 1a infected SSC, P76, showed a decrease in binding from TPC to TPD for both gt 1a and gt 3a. The secondary spontaneous clearer, P155 and two control patients (P75 and P63) also showed significant increase in binding to genotype 3a at later time-points. Despite this significant increase in binding, the difference in absorbance of P155 between TPA and TPC/D/E was minimal and did not exceed 5 times mean control absorbance.

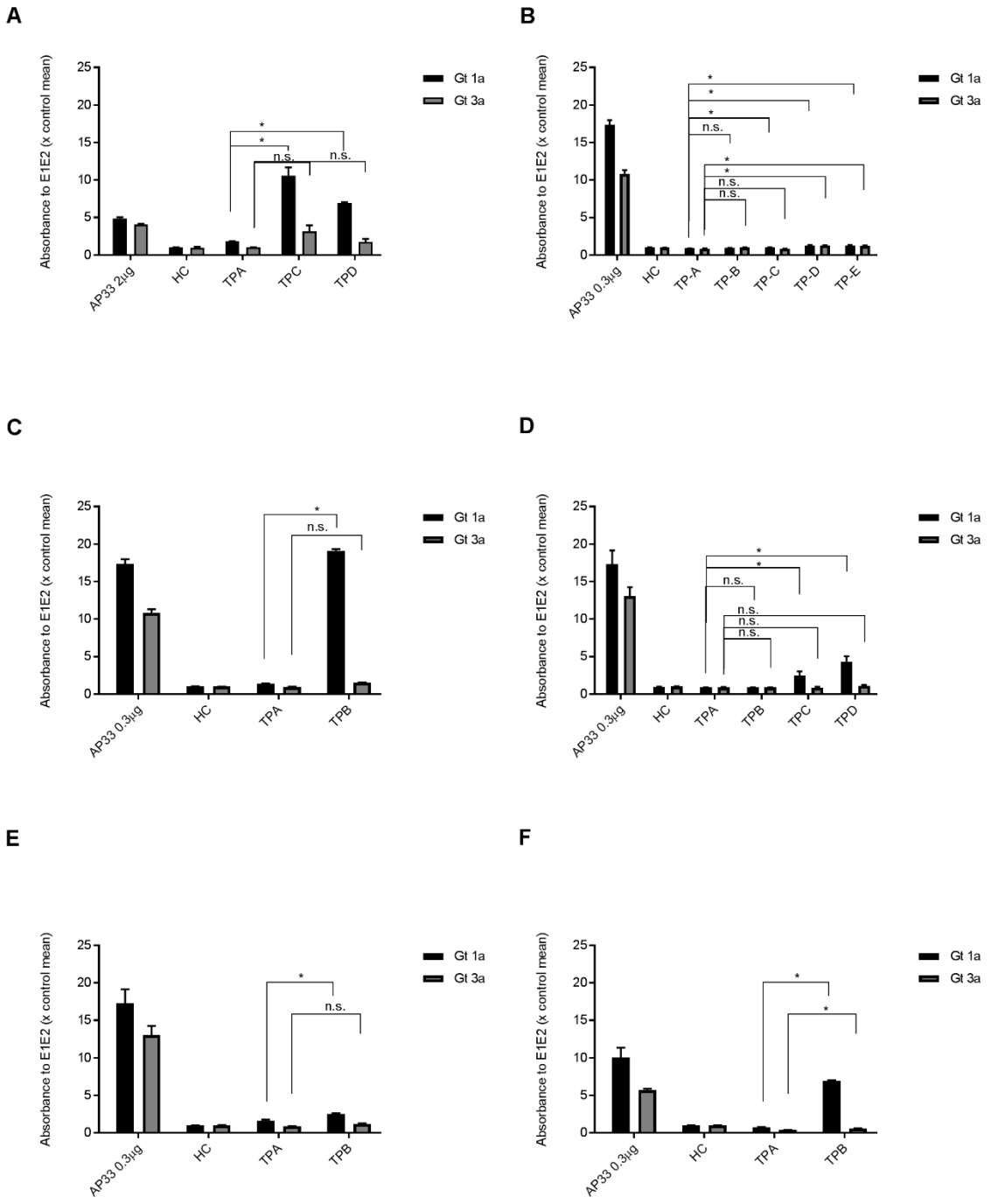

Figure 3.90 Relative binding of purified IgG to genotype 1a and 3a E1E2 lysates
Graphs show absorbance of purified IgG at 200 µg/well (A) or 100 µg/well (B-F) to HEK-293T cell lysates containing E1E2 from gt 1a and gt 3a. Humanised AP33, a monoclonal antibody specific for a conserved, linear epitope in E2, was used as positive control at concentrations shown on each graph. Absorbance was normalised to healthy controls (HC) used as the negative control (fold change from mean absorbance). Error bars represent the standard error mean (±SEM). Statistical differences in absorbance between baseline (TPA) and later time-point were determined using the Wilcoxon rank sum test. * - P≤0.05, **- P≤0.01, ***-P≤0.001, n.s – not significant. A. Relative binding of P76, gt 1a SSC. Experimental data supplied by Dr Rachael Swann. Results shown are from a single experiment in duplicate. B. Relative binding of P155, gt 4d SSC C. Relative binding of P75, gt 1a relapse control. D. Relative binding of P131, gt 1a relapse control. E. Relative binding of P101, gt 1a relapse control. F. Relative biding of P63, gt 1a null control. Unless otherwise stated results shown are from at least two experiments in duplicate.

Since P155 was infected with gt 4d, further experiments were performed to compare binding to gt 4a and the autologous gt 4d used in the neutralisation assays. Since increase of absorbance in P155 was minimal in gt 1a and gt 3a, additional negative control in the form of E1E2 neg lysate was added in order to show that binding was specific to HCV E1E2. A serial dilution of AP33 was added for gt 4a and gt 4d to minimise the chances of positive control absorbance exceeding 4 before time-point absorbance shows a good signal to noise ratio. While AP33 concentration for gt 4a remained the same as that for gt 1a and gt 3a (0.3 µg/well) with two further dilutions, AP33 concentration for gt 4d was increased based on results from infectivity experiments in section 3.2.4.

Figure 3.91a shows that binding to gt 4a at TPA and TPB was weak with overlapping error bars of patient absorbance and healthy control absorbance. The relative binding started increasing overtime prior to initiation of treatment at TPC with significant differences between baseline TPA and TPD/TPE ($P \leq 0.05$). There are minimal differences between absorbance to gt 4a and E1E2 neg control lysate at TPA-TPC further supporting weak binding at early time-points. There was a slight decrease of absorbance to gt 4a from relapse TPD to secondary spontaneous clearance TPE with non-overlapping absorbance to E1E2 neg lysate. In contrast, absorbance to autologous gt 4d is weak at early TPA and TPB, but the error bars from HC and E1E2 neg lysate do not overlap with gt 4d absorbance (Figure 3.91b). Moreover, there is a larger increase in absorbance at TPC-TPE to gt 4d than any other gt tested, reaching more than 10 times mean control absorbance. No significant differences were detected between baseline TPA and later time-points. Binding to E1E2 neg lysate was minimal at TPC-TPE compared to gt 4d and there was a decrease of absorbance from TPC (pre-treatment) to TPD (post-treatment, relapse). There was a final increase of absorbance to gt 4d from TPD, post treatment to TPE when secondary spontaneous clearance occurred.

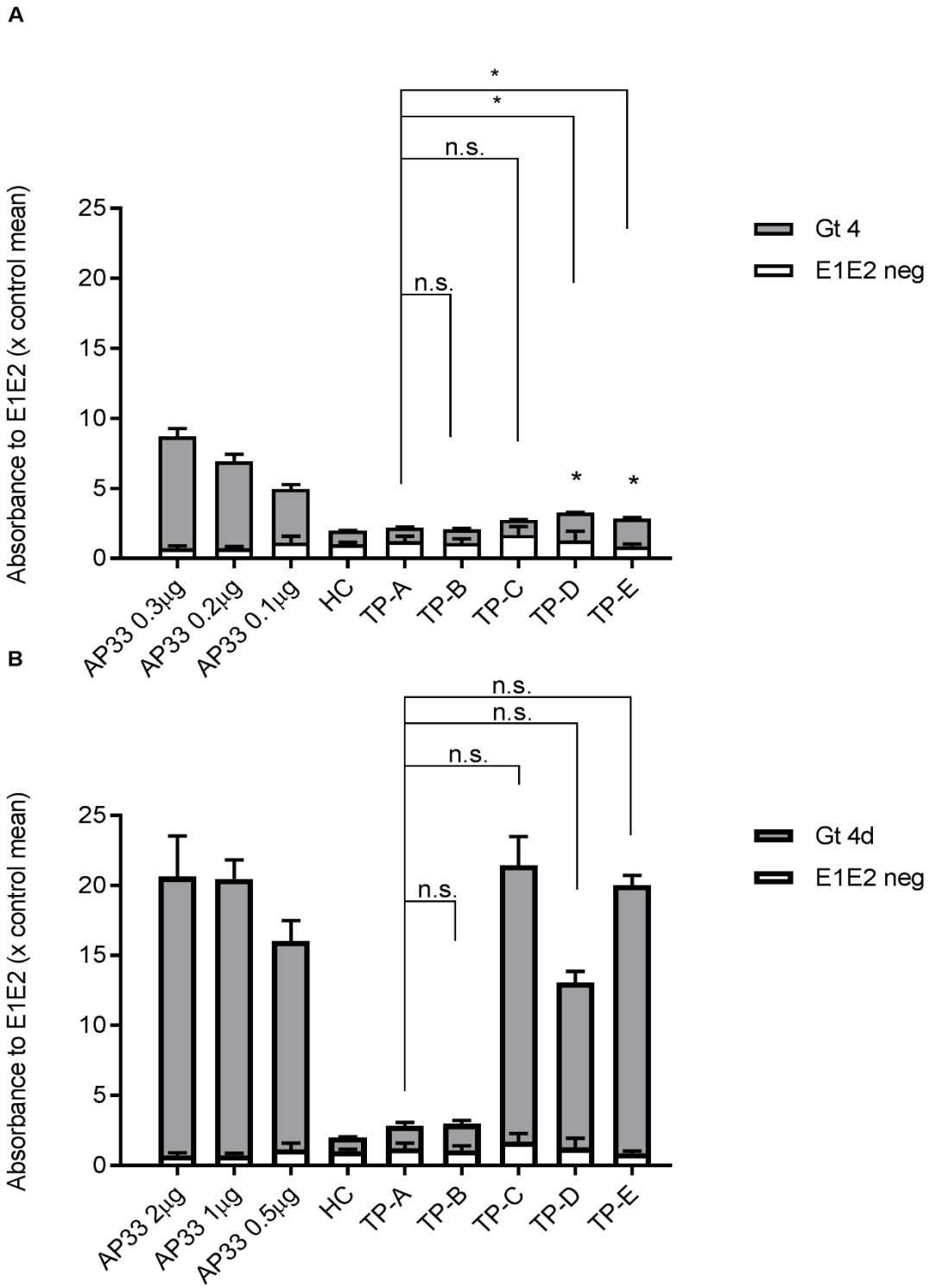

Figure 3.91 Relative binding of purified IgG from P155 to genotype 4a and 4d E1E2 lysates
Graphs show absorbance of purified IgG from genotype 4d infected P155 at 100 µg/well to HEK-293T cell lysates containing E1E2 from gt 4a (A) and autologous gt 4d from TPA (B). Humanised AP33 was used as positive control at concentrations shown on each graph. Absorbance was normalised to healthy controls (HC) (fold change in mean absorbance). HC were used as the negative control. E1E2 negative HEK 293T cell lysates was used as an additional negative control. Error bars represent ±SEM. Statistical differences between baseline (TPA) and later time-point were determined using the Wilcoxon rank sum test. * - P≤0.05, **- P≤0.01, ***-P≤0.001, n.s. – not significant. A. Results shown are from at least two experiments in duplicate. B. Results shown are from a single experiment in duplicate due to the paucity of samples.

3.2.9 Luminex analysis of cytokine and chemokine profiles of SSC

Both the NGS analysis of time-points amino acid changes in patients over time and the CD8 to CD4 ratio indicated, that T cell responses may play a crucial role in SSC. We therefore performed a Luminex experiment in order to analyse the unique cytokine and chemokine profile of patient plasma samples at pre-treatment and post-treatment time-points. Due to the scarcity of samples, P76 was only analysed at TPD pre-treatment, while P155 had all time-points included. For treatment-failure patients, there was enough sample present for the following patients pre-treatment: P75 (TPA), P131 (TPA, B), and P63 (TPA) and post-treatment: P131 (TPC), P63 (TPB). Therefore, we added another treatment failure patient to increase the number of time-points analysed. P57 was a treatment failure (relapse) patient from St Mary's Acute HCV cohort and was added to the Luminex analysis.

For the Luminex experiment the analysis was divided by SSC and treatment failure patients as well as pre-treatment time-points and post-treatment time-points. Cytokines and chemokines associated with Th1 (T helper cell 1) immune responses pre-treatment were analysed first (Figure 3.92). This included: Granulocyte macrophage colony stimulating factor (GM-CSF), Interferon gamma (IFN gamma), Chemokine (C-C motif) lectin 20 (CCL20), Interleukin 2 (IL2) and Interleukin 28 (IL-28). Figure 3.92 shows that the median concentration of SSC pre-treatment time-points of all cytokines and chemokines tested was higher than that of the treatment failures (controls). The median of GM-CSF for SSC was 1.2 ng/ml compared to 0 ng/ml for controls ($p = 0.0001$). Significant differences between SSC and control patients were also noted for all other cytokines and chemokines; IFN-gamma with median of 148.3 ng/ml for SSC and 17.7 ng/ml for controls ($p < 0.0001$), CCL20 with median of 153 ng/ml for SSC and 30.9 ng/ml for controls ($p = 0.0003$), IL-2 with median of 68.8 ng/ml for SSC and 0 ng/ml for controls ($p = 0.0015$) and IL-28 with median of 3.29 ng/ml for SSC and 0.8 ng/ml for treatment failures ($p < 0.0001$).

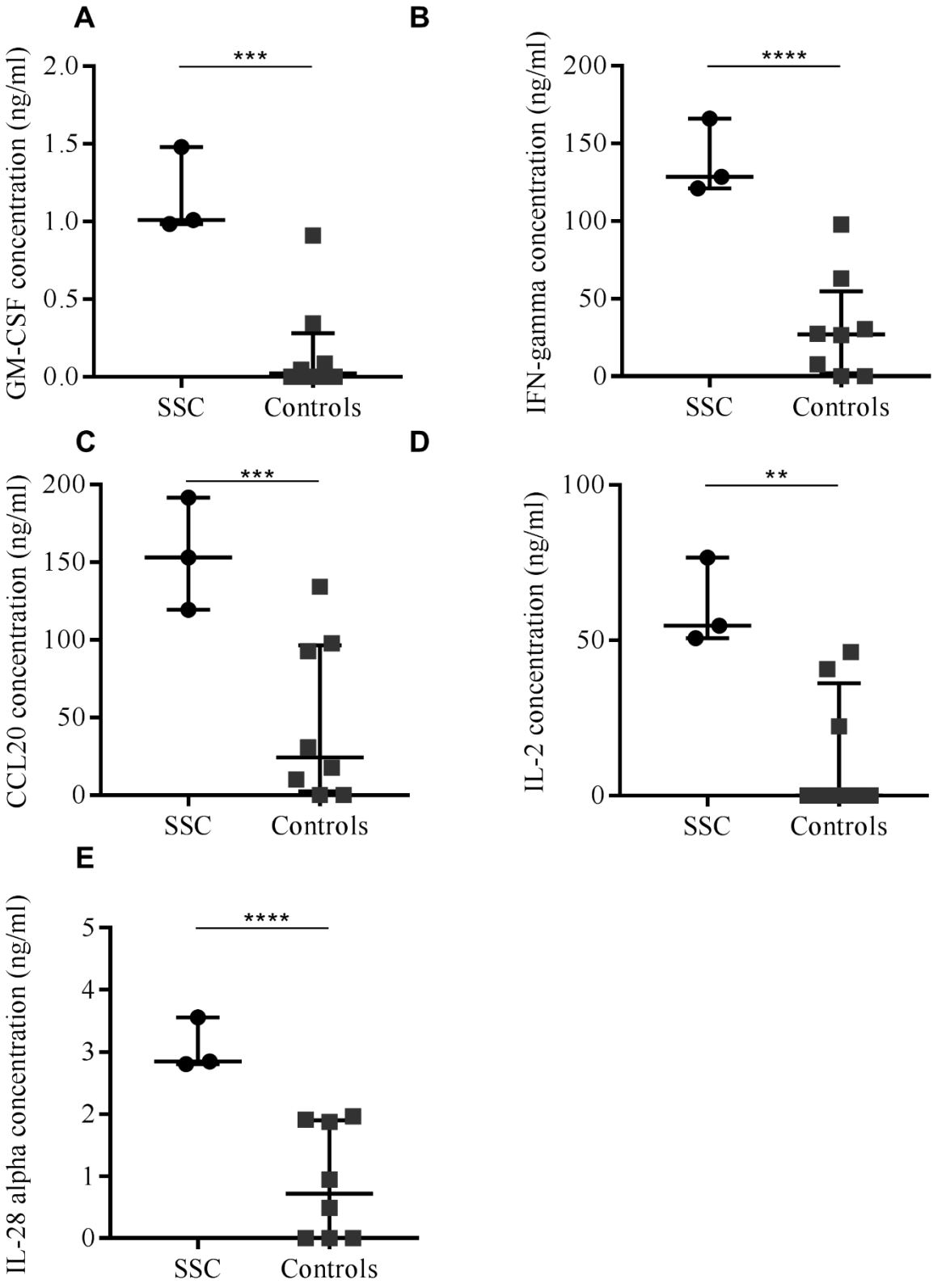

Figure 3.92 Luminex analysis of Th1 responses pre-treatment in SSC and control patients
Plasma concentrations (ng/ml) of various cytokines and chemokines associated with Th-1 responses in SSC and treatment failures (controls) in the pre-treatment time-points. Graphs represent median with interquartile range from a single experiment conducted in duplicate. Non-parametric Mann-Whitney statistical analysis was performed between SSC and control patients. For some values the bead count was below the recommended by the company (<30). A. Plasma concentration of Granulocyte-macrophage colony-stimulating factor (GM-CSF) with significant differences between SSC and control patients (p=0.0001). B. Plasma concentrations of Interferon gamma (IFN-gamma) with significant differences between SSC and controls (p<0.0001). C. Plasma concentrations of Chemokine (C-C motif) lectin 20 (CCL20) with significant differences between SSC and controls (p=0.003). D. Plasma concentrations of Interleukin 2 (IL-2) with significant differences between SSC and controls (p=0.005). E. Plasma concentrations of Interleukin 28 (IL-28) alpha with significant differences between SSC and controls (p<0.0001).

Next, the Luminex analysis focused on the same Th1 response associated cytokines and chemokines in SSC and treatment failures, this time looking into the post-treatment time-points. Figure 3.93 shows, the medians and the interquartile ranges were overlapping for the following cytokines and chemokines: GM-CSF, CCL20, IL-2 and IL-28. The median concentration of IFN-gamma was higher in treatment failures post-treatment than SSC (median value of 101.6 ng/ml and 56.92 ng/ml, respectively). However, no significant differences were noted between SSC and treatment failures post-treatment for any of the cytokines and chemokines.

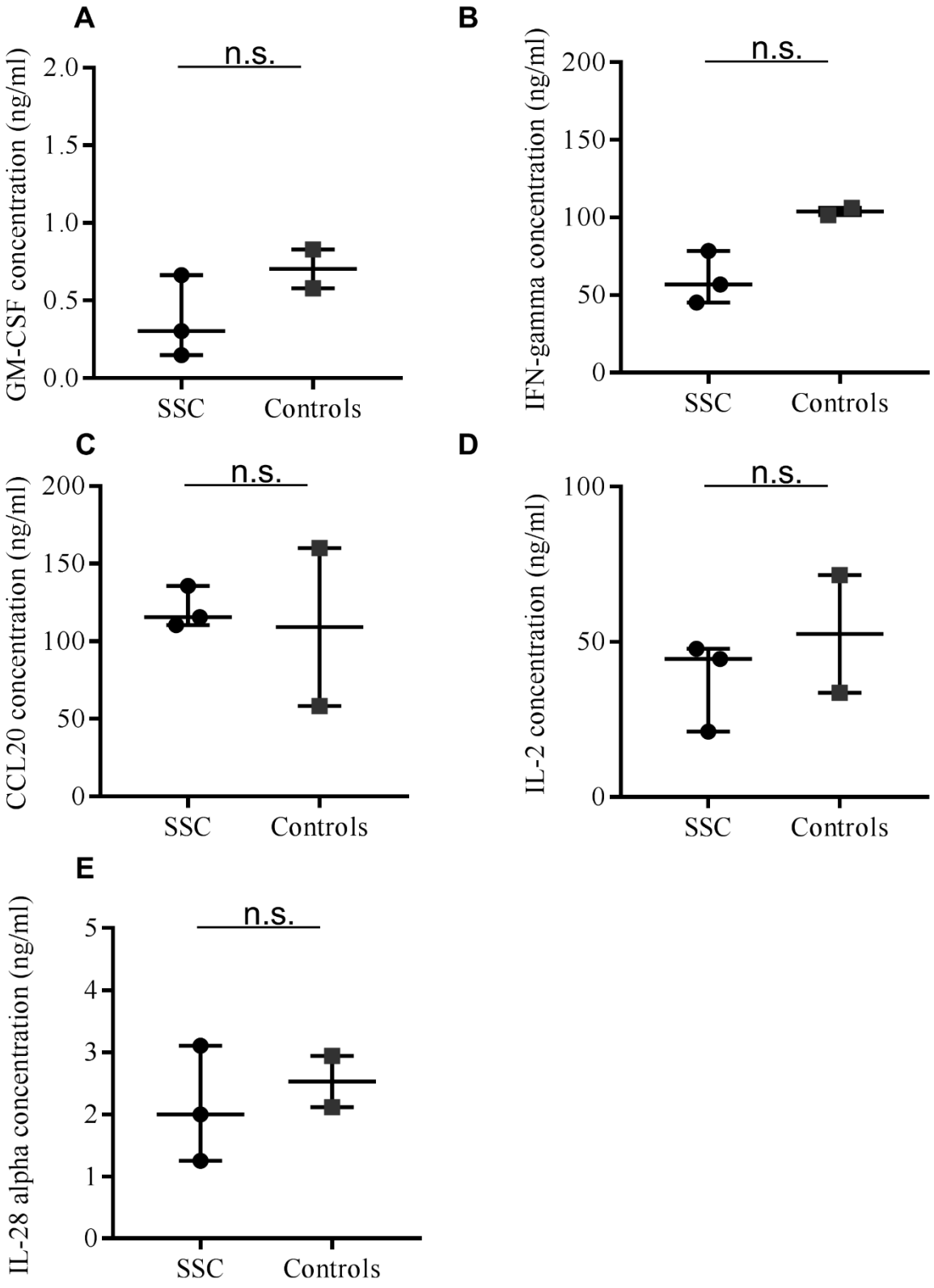

Figure 3.93 Luminex analysis of Th1 responses post-treatment in SSC and control patients
Plasma concentrations (ng/ml) of various cytokines and chemokines associated with Th-1 responses in SSC and treatment failures (controls) in the post-treatment time-points. Graphs represent median with interquartile range from a single experiment conducted in duplicate. Non-parametric Mann-Whitney statistical analysis was performed between SSC and control patients. For some values the bead count was below the recommended by the company (n<30). A. Plasma concentration of Granulocyte-macrophage colony-stimulating factor (GM-CSF) with no significant differences between SSC and control patients (p=0.7619). B. Plasma concentrations of Interferon gamma (IFN-gamma) with no significant differences between SSC and controls (p=0.2571). C. Plasma concentrations of Chemokine (C-C motif) lectin 20 (CCL20) with no significant differences between SSC and controls (p=0.6429). D. Plasma concentrations of Interleukin 2 (IL-2) with no significant differences between SSC and controls (p=0.7143). E. Plasma concentrations of Interleukin 28 (IL-28) alpha with no significant differences between SSC and controls (p<0.6095).

Figure 3.94 looked at the Luminex analysis on non-Th1 response associated cytokines and chemokines in SSC and treatment failures at pre-treatment time-points. The median concentrations for SSC were significantly higher than the median concentrations of treatment failure pre-treatment time-points for the following cytokines: IL-9 (45.5 ng/ml and 0 ng/ml, respectively, p=0.0008) IL-23 (17 ng/ml vs 1.3 ng/ml, respectively, p=0.0007) IL-6 (122.9 ng/ml and 0 ng/ml, respectively, p=0.0003) and TNF-alpha (53.6 ng/ml and 19.9 ng/ml, respectively, p=0.0043). The median and interquartile range did not overlap between SSC and treatment failures for any non-Th1 response associated cytokines. However, post-treatment analysis of the same non-Th1 cytokines between SSC and treatment failures showed overlapping medians and interquartile ranges with no significant differences (Figure 3.95). The median concentration of IL-9 was 15.8 ng/ml for SSC post-treatment and 35.68 ng/ml (p=0.1667) while the median concentration of IL-23 was 10.73 ng/ml and 11.61 ng/ml, respectively (p>0.9999). The median concentration for IL-6 for SSC post-treatment was 120 ng/ml and 68.7 ng/ml for treatment failures (p=0.2571) while the median concentration for TNF-alpha was 39.4 ng/ml and 49.3 ng/ml, respectively (p>0.9999).

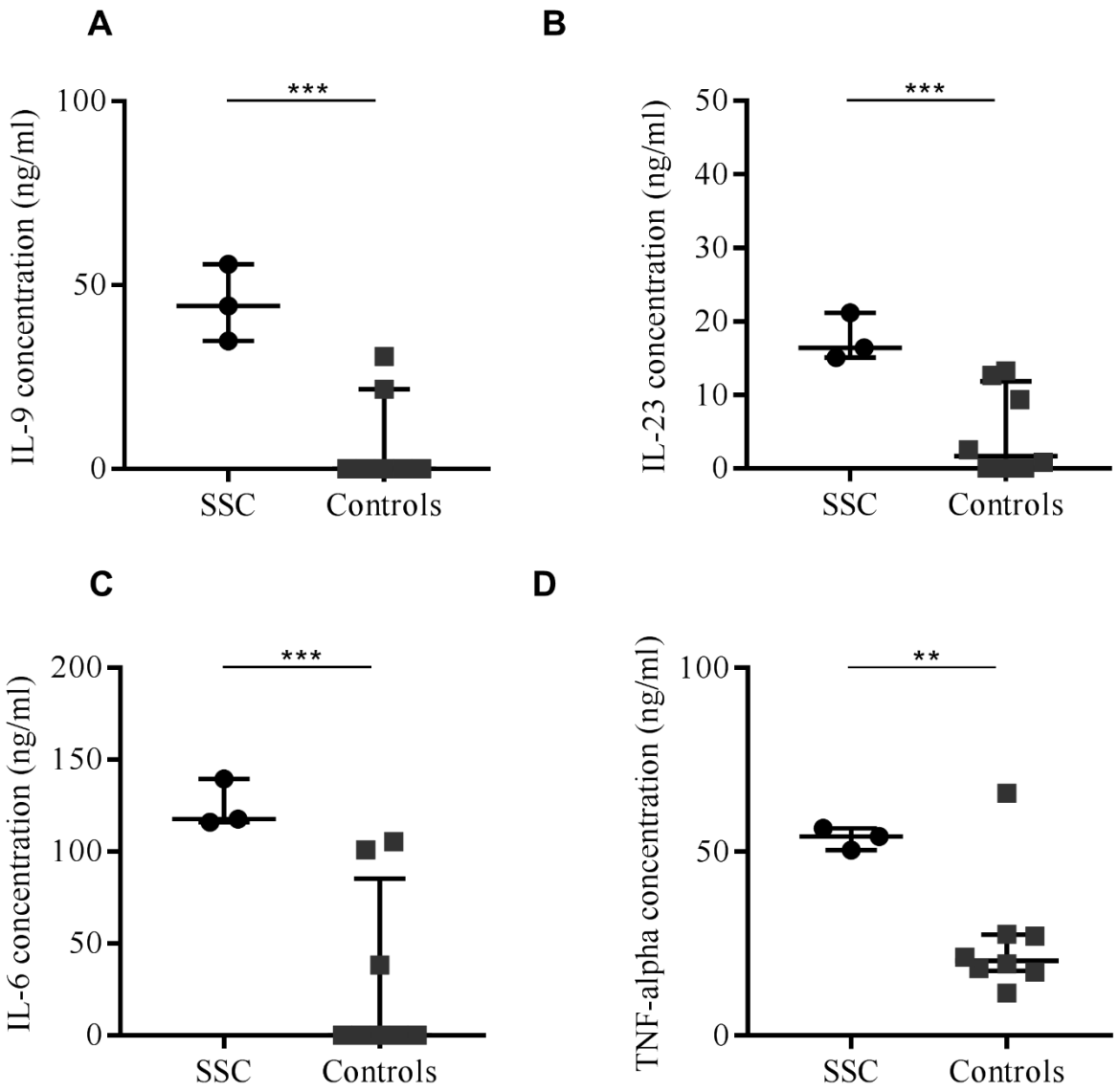

Figure 3.94 Luminex analysis of non-Th1 responses pre-treatment in SSC and control patients
Plasma concentrations (ng/ml) of various cytokines associated with non Th-1 responses in SSC and treatment failures (controls) in the pre-treatment time-points. Graphs represent median with interquartile range from a single experiment conducted in duplicate. Non-parametric Mann-Whitney statistical analysis was performed between SSC and control patients. For some values the bead count was below the recommended by the company (n<30). A. Plasma concentration of Interleukin 9 (IL-9) with significant differences between SSC and control patients (p=0.0008). B. Plasma concentrations of Interleukin 23 (IL-23) with significant differences between SSC and controls (p=0.0007). C. Plasma concentrations of Interleukin 6 (IL-6) with significant differences between SSC and controls (p=0.0003). D. Plasma concentrations of Tumor necrosis factor alpha (TNF-alpha) with significant differences between SSC and controls (p=0.0043).

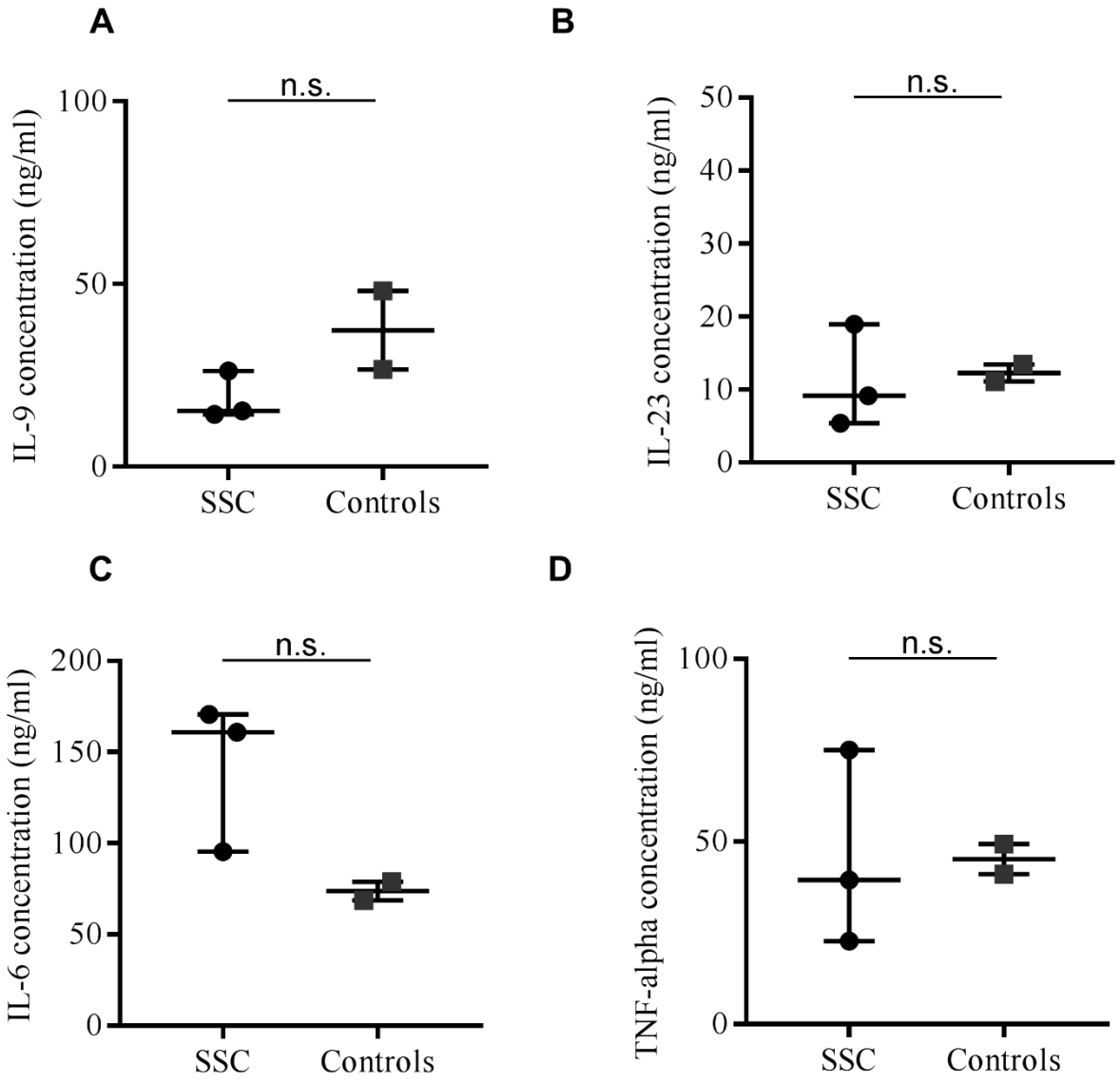

Figure 3.95 Luminex analysis of non-Th1 responses post-treatment in SSC and control patients
Plasma concentrations (ng/ml) of various cytokines associated with non Th-1 responses in SSC and treatment failures (controls) in the post-treatment time-points. Graphs represent median with interquartile range from a single experiment conducted in duplicate. Non-parametric Mann-Whitney statistical analysis was performed between SSC and control patients. For some values the bead count was below the recommended by the company (n<30). A. Plasma concentration of Interleukin 9 (IL-9) with no significant differences between SSC and control patients (p=0.0). B. Plasma concentrations of Interleukin 23 (IL-23) with no significant differences between SSC and controls (p>0.9999). C. Plasma concentrations of Interleukin 6 (IL-6) with no significant differences between SSC and controls (p=0.2571). D. Plasma concentrations of Tumor necrosis factor alpha (TNF-alpha) with no significant differences between SSC and controls (p>0.9999).

Table 3.16 lists all other cytokines and chemokines tested during the Luminex experiment at pre-treatment and post-treatment time-points in SSC and treatment failure patients. This analysis included classical Th2 related cytokines including: IL-33, IL-21, IL-4, IL-5, IL-25 and IL-31 as well as Th1 related cytokines, IL-13, and Th17; IL-17F, IL-17A and IL-22. Other cytokines tested included: IL-10, IL-12p70, IL-15, IL-1 beta, IL-27 and TNF-beta. None of the cytokines showed significant differences in concentration at either pre-treatment time-points or post-treatment time-points between SSC and treatment failures.

Table 3.16 Plasma cytokine concentrations pre and post-treatment in SSC and TF

Cytokine	Mean concentration (ng/µl ±SD)			
	SSC		Treatment failures	
	Pre	Post	Pre	Post
IL_17F	0·17 (±0·02)	0·13 (±0·14)	0·07 (±0·10)	0·11 (±0·01)
IL-10	10·64 (±4·2)	11·86 (±7·54)	6·43 (±10·37)	2·13 (±2·14)
IL-12p70	16·59 (±11·38)	31·35 (±28·81)	14·78 (±17·65)	10·78 (±6·20)
IL-13	195·29 (±94·61)	234·27 (±111·86)	130·59 (±105·50)	108·6 (±95·06)
IL-15	42·55 (±25·5)	70·71 (±46·73)	34·72 (±46·53)	18·97 (±3·86)
IL-17A	34·42 (±17·68)	51·47 (±22·17)	23·13 (±25·14)	20·84 (±8·05)
IL-22	0·39 (±0·35)	1·71 (±1·73)	0·55 (±0·54)	0·3 (±0·42)
IL-1beta	13·05 (±6·96)	20·67 (±17·45)	12·18 (±12·57)	21·05 (±24·67)
IL-33	45·49 (±20·7)	138·47 (±130·47)	43·4 (±38·7)	26·49 (±11·44)
IL-21	85·5 (±32·34)	103·04 (±75·39)	53·079 (±60·55)	86·34 (±9·59)
IL-4	1·4 (±0·81)	0·67 (±0·39)	0·22 (±0·21)	0·24 (±0·33)
IL-5	10·52 (±5·58)	15·49 (±14)	8·84 (±10·01)	7·87 (±3·27)
IL-25	0·23 (±0·13)	1·17 (±1·42)	0·27 (±0·25)	0·13 (±0·11)
IL-27	1·87 (±0·48)	3·95 (±3·64)	1·04 (±0·99)	1·45 (±0·05)
IL-31	0·13 (±0·06)	0·59 (±0·67)	0·14 (±0·13)	0·1 (±0·05)
TNF-beta	0·11 (±0·09)	0·17 (±0·13)	0·1 (±0·10)	0·08 (±0·03)

3.2.10 Discussion

The elimination of HCV may require the development of a vaccine as well as upscaling of diagnosis and treatment. The likelihood of developing a vaccine is hampered by a lack of studies of the immune response during early HCV infection. This series of experiments was carried out to investigate the immune response during "secondary spontaneous clearance" (SSC), a previously undescribed phenomenon of spontaneous resolution of HCV following post-treatment relapse.

Two cases of SSC were identified in the same longitudinal cohort of patients with acute HCV infection and HIV co-infection. Both presented with a similar clinical picture but with two different HCV genotypes. Studying the adaptive immune responses in these two SSC patients presented a unique opportunity to evaluate a natural vaccine model. In traditional vaccine studies, animal-models are primed with an antigen and boosted several weeks following this, often with an alternative vector. This leads to protective immune responses that prevent subsequent infection following experimental exposure (Dahari, Feinstone & Major 2010a). We hypothesised that the initial acute HCV infection in patients with SSC reflected a 'prime' followed by viral suppression on treatment and a 'boost' occurring during relapse after treatment. Apart from humans, the chimpanzee and the tree shrew are the only animal models for human HCV infection although studies on the former have ceased since 2013 for ethical reasons and the latter do not support chronic infection (Amako et al. 2010; Feng et al. 2017; Lanford et al. 2001). In previous studies, chimpanzees displayed protective immune responses upon challenge with recombinant proteins and exposure to viruses of a similar strain suggesting that an HCV vaccine may be an achievable goal (Dahari, Feinstone & Major 2010b; Major et al. 2002). The two cases of SSC provided a rare opportunity of a natural example of such an experiment. Patients with treatment failure from the same cohort that did not demonstrate SSC were used as control subjects.

3.2.10.1 Viral and clinical parameters during secondary spontaneous clearance

Although SSC post treatment relapse has never been described before, spontaneous resolution of HCV infection has been described during early and late

infection. For example, HIV and HCV co-infected patients have been reported to spontaneously clear infection in the chronic phase of infection following HIV ARV therapy (Falconer et al. 2008; Grint et al. 2017; De Rosa et al. 2006). In one study, 0.59% of HIV-HCV-co-infected cases (3/509) resolved chronic HCV infection following HIV suppression (Frias et al. 2017). Elevation of CD4+ T cell counts occurred following the initiation of therapy in two out of three cases from nadir counts of 267 and 148 cells/ml to 651 and 529 cells/ml, respectively. In another study, a rapid increase of CD4+ cell count was associated with viral clearance (Algoud et al. 2017). An elevation of CD4+ T cells of a similar magnitude occurred in one of the cases of SSC patients (P76); from a nadir count of 180 cells/ml during HCV IFN/RBV treatment to 540 cells/ml at the time of spontaneous resolution. A smaller elevation occurred in the second SSC patient (P155) with a nadir count of 420 cells/ml to 560 cells/ml around the resolution time-point, although the CD4+ T cell count remained relatively stable throughout treatment. It is therefore possible that cases of SSC and spontaneous resolution of chronic infection are more common in HIV co-infected patients because of unstable CD4+ T cell counts. Similar unusual outcomes of spontaneous resolution would easily be missed, because of infrequent monitoring of viral loads post treatment failure, at least until patients are reconsidered for therapy.

In addition to CD4+ T cells, the CD8+ T cell count pattern was unique to SSC patients when compared to TF patients, apart from P131 which showed a similar pattern, with a steady increase following treatment relapse. CD8+ T cells are known to play a crucial part in viral clearance of HCV. In chimpanzees, CD8+ T cell depletion has been used to demonstrate their protective role in re-infection. Anti-CD8+ depletion resulted in persistently high viral loads, despite the presence of memory CD4+ T cells and antibodies. Viral clearance occurred following the re-emergence of CD8+ T cells (Shoukry 2003). In another study, sustained virological responses to IFN/RBV therapy in chronic patients correlated with high frequency and stronger HCV-specific CD8+ T cell responses (Caetano et al. 2008). Furthermore, cases of spontaneous clearance have been reported in re-infected patients post IFN/RBV treatment even though they have failed to resolve their initial infection (Grady et al. 2013). This finding suggests a partial protective immune response may be induced following treatment, which may

have also played a role in SSC. Moreover, it is well known that upon re-infection, the incidence of spontaneous clearance is higher in patients who have spontaneously resolved their primary infection, a finding which is also supported by experiments in chimpanzees (Bassett et al. 2001; William O Osburn et al. 2014). It is therefore possible that high CD8+ T cell counts and reconstitution of CD4+ T cells post relapse in SSC cases contributed to spontaneous resolution of infection. While phylogenetic analysis of the SSC patient samples clearly revealed the presence of the same virus pre and post treatment, it cannot be excluded that the patients were re-infected with the same strain of the virus, although one patient reported no high risk activities for re-infection and the other reported only anonymous sexual partners reducing the risk of being re-infected with the same strain.

3.2.10.2 Neutralising antibodies play a role in secondary spontaneous clearance, but are also present in control patients

We hypothesized that humoral immune responses were active and may have contributed, at least in part, to viral clearance, as sequence analysis of patient derived envelope sequences (an antibody target) at baseline and later time points demonstrated that the majority variant differed by 5 and 1 amino acids for P76 and P155, respectively indicating positive immune pressure in this region. P76 showed broadly-reactive cross-genotypic neutralising antibody responses against a heterologous HCVpp panel. P155 had evidence of lower cross-neutralising responses, including to the genotype 4a pseudoparticle in the heterologous panel. There was evidence however of a strong response to autologous genotype 4d HCVpp. The lack of broadly neutralizing antibodies in P155 to other genotypes could be related to dual seroconversion with HCV and HIV, resulting in an impaired immune response to HCV. In order to evaluate the responses in controls, patients from the same cohort who had not responded to treatment were assessed. We found that these E1E2 sequences were also variable over time and that control patients also developed neutralising antibodies although of lower magnitude.

This is supported by the binding ELISA experiment where a significant increase in binding to g4 over-time was noted, although it was not as strong as that observed in P76. This is possibly related to the assay (based on g4a

pseudoparticles) and the difference in the sequence of envelope glycoproteins between genotype 4a and genotype 4d. Interestingly binding to genotype 4d over time was higher in P155 at TP-C (pre-treatment) as well as TP-D and TP-E post-treatment. Neutralisation was also observed in plasma samples from TP-C, TP-D and TP-E against the TP-A HCVpp with increasing potency at the later the time-points. Similarly, P76 showed no neutralisation with plasma from TP-A against either TP-A or TP-D HCVpp, only later time-points (TP-C and TP-D) demonstrated potent neutralisation. This demonstrates that a delayed immune response evolved following the IFN/RBV treatment. Previous studies have demonstrated that IFN-based therapy leads to restoration of adaptive immune responses. Such responses are characterised by an increase in the frequency and strength of CD4+ T helper cell responses with a Th1 predominance (Kamal et al. 2002). The development of neutralising antibody responses is in turn dependent on efficient CD4+ T helper cell responses (Spaan et al. 2015).

For E1E2, three amino acids changes in P76 and one amino acid change in P155 occurred within the HVR1, a known target for humoral responses (Ray et al. 1999). HVR-1 mutations also occurred in 9 out of 10 amino acid changes of E1E2 for P75, 3/5 amino acids in P131 and 1 out of 2 amino acids in P63. The high diversity of the HVR-1 has been shown to act as an immunological decoy or shield elucidating strong antibody responses away from the key neutralising antibody epitopes (Bankwitz et al. 2010; Prentoe et al. 2014). Cell culture-based experiments demonstrated that viruses were significantly more susceptible to neutralization following the removal of HVR-1 from the E2 glycoprotein (Prentoe et al. 2016). Therefore, targeting of several amino acids within the HVR in the control patients, particularly P75, may explain the lack of cross neutralising antibodies against the heterologous HCVpp panel and may imply viral escape from the immune system. This is further supported by the lower IC_{50} value of P75 plasma sample post-relapse against the autologous post-treatment HCVpp when compared to the SSC case, P76.

Although one of the SSC, P76, had several amino acid changes within the HVR-1, cross-competition experiments with neutralising Abs performed by Dr Rachael Swann demonstrated that antibodies at the post-relapse time-point targeted multiple CD81 binding epitopes which although located in the HCV envelope, are highly conserved across genotypes (results not part of this thesis). Thus, it is not

surprising that P76 developed potent cross-genotypic neutralising antibodies at the relapse time-point. In contrast the majority of P155's amino acid changes were located in neutralising antibody epitopes namely H430 and V524 at the relapse time-point and H444 at the SSC time-point. Previous studies on neutralising antibodies targeting the region 412-423 demonstrated their ability to neutralise both autologous HCVpp as well as binding of E2 to CD81 (Tarr et al. 2012). Furthermore, in one study a neutralising antibody, 1H8 targeting the region of 524-529 demonstrated that the same epitope enables E2 to interact with the CD81 receptor (Zhao et al. 2014). Therefore, although P155 did not have cross-genotypic neutralising antibodies in the HCVpp panel, the multiple changes within neutralising antibody epitopes post-treatment may imply a reduced fitness of the majority variant because of a reduced interaction with the key entry receptor, CD81. None of the control patients displayed as many changes in the amino acids associated with neutralising antibody episodes. It is therefore possible that SSC in the two patients has occurred through slightly different mechanisms; via broad, cross-reactive neutralising antibodies targeting CD81-binding epitopes in one and reduced ability to initiate CD81-binding due to loss of viral fitness in the other.

The importance of neutralizing antibodies in SSC is further supported by the experiments with autologous HCVpp. Although the pre-treatment plasma from both patients were unable to neutralise autologous HCVpp, potent neutralisation was noted and maintained in the post-treatment time-points against pre-treatment and post-treatment HCVpp. Unsurprisingly, the IC_{50} values were particularly high in P76 which displayed cross-reactive neutralisation. The reduced potency of neutralisation in P155 may be explained by additional mechanisms involved in SSC. This is supported by studies of primary spontaneous clearance which demonstrated that neutralising antibodies alone, rarely lead to spontaneous resolution of infection (William O Osburn et al. 2014; Pestka et al. 2007). In contrast potent T cell responses have been reported either alone or in conjugation with neutralising Abs in multiple studies associated with spontaneous resolution (Major et al. 2002; Spaan et al. 2015; Thomson et al. 2011).

Studies of primary spontaneous clearance have shown an association with early broadly neutralizing antibody responses (Bartenschlager et al.2010). Broadly

neutralising antibodies were displayed by P76, but not P155 or the control TF, P75, which was further supported by the more potent autologous neutralisation in P76 compared with the latter two patients. One of the limitations of this study was the lack of autologous HCVpp for other TF patients. Although an autologous HCVpp was obtained for P63, the sequence did not produce a functional HCVpp. Large scale studies demonstrated that functional HCVpp arise from a small proportion of all patients' glycoprotein sequences (approximately 24-27%) (Lavillette et al. 2005; Richard A. Urbanowicz et al. 2016). Moreover, even closely related sequences may have different outcomes in the production of functional HCVpp. A recent study by Urbanowicz *et al* suggests that the expression protocols have a direct effect on the functionality of pseudoparticles (Richard A Urbanowicz et al. 2016). Furthermore, the viral packaging construct may also affect functionality, a glycoprotein sequence functional in an MLV-based construct may not be functional in an HIV-based construct. Due to time constraints no other control patients' glycoprotein sequences were obtained. It is a time-consuming endeavour to obtain full-length E1E2 sequences via PCR and cloning as is evident by this and other studies (Lavillette et al. 2005; Richard A Urbanowicz et al. 2016; Richard A. Urbanowicz et al. 2016). Future work should focus on obtaining other control patients' glycoproteins via gene synthesis to speed up the production process, particularly for P131 due to the similar CD8+T cell pattern as the SSC patients.

3.2.10.3 Next generation sequencing revealed viral evolution within epitopes targeted by T cell responses

NGS data demonstrated the evolution of the viral consensus over different time-points for one of the SSC cases, P155, and TF patients, P131, P75 and P63. Due to scarcity of samples and low viral load at TPD, NGS data for P76 time-points were not obtained and only E1E2 data from Sanger sequencing were available as discussed above. Interestingly all of the amino acid changes in the non-structural proteins of P155 with the exception of one (I2723) occurred in known T cell epitopes. In addition the I2723V mutation occurred as a majority variant at TPB and TPD. None of the other mutations became fixed in the population in P155. Similarly, most of the changes in relapse control patients also occurred in epitopes associated with T cell responses against HCV although in P131 five out of eight amino acid changes in the non-structural proteins became fixed from

TPC to TPD. This may imply viral escape in the control patients but not in the SSC. Escape from T cell responses via amino acid changes in T cell epitopes has been associated with a narrow T cell receptor (TcR) repertoire with viral control linked to a broader repertoire (Meyer-Olson et al. 2004). This is reflected in the SSC patients who had mutations in all non-structural proteins unlike P131 who was limited to mutations in only three non-structural proteins at different time-points.

The outcome of SSC cases compared to TF may also be linked to the early timing of treatment. Both of the SSC cases received IFN/RBV therapy within 200 days after the first HCV PCR positive date whereas the TF did not receive therapy until >200 days after detection of infection. Longer exposure to HCV antigen may have contributed to T cell exhaustion associated with sustained expression of inhibitory receptors such as programmed cell death protein 1 (PD-1) which is characteristic in chronic infection (Bengsch et al. 2010; Raziorrouh et al. 2011; Urbani et al. 2006). Blocking the PD-1 receptor in chronically infected chimpanzees resulted in a significant reduction of the viral load although only in animals with previous broadly reactive T cell responses (Nakamoto et al. 2009). Spontaneous clearance in chronic infection was associated with appearance of neutralizing antibodies and a reversal of T-cell exhaustion (10). Since our patients showed evidence of neutralizing antibodies and a high CD4+ and CD8+ T cell count it is possible that both may play a role in this novel phenomenon. This is supported by the finding that none of the control patients had CD4+ and CD8+ T cell count as high as SSC at the time of relapse.

3.2.10.4 SSC is associated with varying cytokine/chemokine profiles

The Luminex assay is a powerful tool which enables one to look at the cytokine profile of plasma with minimal sample material. In this study the Luminex assay compared the cytokine profiles of SSC samples and TF samples at pre-treatment and post-treatment time-points. Interestingly, the pre-treatment samples of SSC had significantly elevated Th-1 response cytokines (and chemokines) when compared to pre-treatment samples from TF patients. These included IFN-gamma, IL-2 and IL-28 and the chemokines GM-CSF and CCL20. Out of these, IFN-gamma has important antiviral and pro inflammatory properties. One study demonstrated its ability to downregulate CLD1 expression and change the

distribution of CLDN1, SR-B1 and CD81 on the cell surface – all known cellular receptors involved in HCV entry (Evans et al. 2007; Pileri et al. 1998; Scarselli et al. 2002; Wei et al. 2009). Unsurprisingly, cells pre-treated with IFN-gamma demonstrated increased resistance to challenge with the HCV cell-culture model. Both IL-2 and IFN-gamma are known to be associated with spontaneous clearance. IFN-gamma related spontaneous resolution is linked with both NK and T cell-mediated inhibition of viral replication (Kokordelis et al. 2014). Moreover, IFN-gamma gene polymorphisms have been linked to HCV clearance namely the +2109 locus of the IFN-gamma gene. Single nucleotide polymorphisms GG or AG at this locus are associated with a favourable outcome (Sarvari et al. 2016). Favourable outcomes may be linked to IFN-gamma induction of Th-1 responses with a high frequency of HCV-specific T cells (Lechner et al. 2000b). In addition IFN-gamma is related to induction of chemokines which rehome T cells to the site of infection, namely hepatocytes.(Missale et al. 1996) Upregulation of T cells via major histocompatibility complex class I and II proteins and promotion of antigen processing are also linked to IFN-gamma production (Thimme et al. 2001b). Strong secretion of IL-2 by CD4+ T helper cells is linked to resolution of infection whereas chronic HCV is associated with an exhausted phenotype of CD4+ T cells and loss of IL-2 secretion (Blackburn & Wherry 2007; Semmo et al. 2005). In addition, IL-2 increases the activity of CD4+ T helper cells. Therefore, elevated levels of IL-2 and IFN-gamma in pre-treatment samples from SSC patients point to strong anti-viral responses and increased activity of CD4+ T helper cells. The role of CD4+ T cells in SSC in this study was implicated by a high CD8+ T cell to CD4+ T cell ratio in SSC compared to the control patients. The cytokine profiles of SSC at the pre-treatment time-points therefore demonstrate a favourable immunogenic profile which have likely led to spontaneous resolution post-treatment relapse. The role of the chemokines GM-CSF and CCL20 are not as clear in SSC. CCL20 is involved in homing of dendritic cells but it has also been strongly associated with fibrosis and progression to HCC in chronic HCV infection (Soliman et al. 2012). It is perhaps possible that increased levels of dendritic cells at the site of HCV infection led to increased antigen presentation to T lymphocytes leading to enhanced anti-HCV activity. On the other hand, GM-CSF is a chemokine which induced bone-marrow production of granulocytes including neutrophils. For this reasons several studies investigated the use of GM-CSF as an adjuvant to IFN-based therapy to prevent

neutropenia, one of the common side-effects of IFN/RBV treatment (Carreño et al. 1996). Interestingly, one study reported enhanced T helper cell functions and increased antibody titres upon addition of GM-CSF to a DNA-based vaccine (Lee, Cho & Sung 1998). Therefore, it is possible that elevated levels of these chemokines may be a unique feature of SSC patients which enhances the effects of the other elevated Th-1 related cytokines.

In addition to the Th-1 related cytokines and chemokines, pre-treatment samples from SSC showed significant elevation of IL-6, IL-9 and IL-23 when compared to pre-treatment time-points from TF patients. Interestingly IL-23 is normally produced by antigen presenting cells (such as dendritic cells) which do so in response to pathogen associated molecular patterns (PAMP) binding with their Toll-like receptors (Ashrafi Hafez et al. 2014; Wang et al. 2013). In turn the produced IL-23 promotes a pro-inflammatory response against HCV infection. The elevated IL-23 may therefore be related to increased chemotaxis of dendritic cells at the site of infection, induced by the elevated levels of GM-CSF in SSC. Elevated levels of IL-6 and IL-9 demonstrated contrasting results in studies. Some studies report elevated levels of IL-6 and IL-9 in treatment failure patients (Guzman-Fulgencio et al. 2012). This correlates with the findings of this study as SSC occurred in patients who failed IFN/RBV therapy. In contrast, one study looked at genome-wide association analysis which linked the IL-6 gene with spontaneous resolution of HCV (Waldron et al. 2016). It is therefore possible that elevated levels of both of these cytokines led to treatment failure of two patients who would otherwise spontaneously clear.

One of the limitations of the Luminex assay was the small number of samples present in the control group particularly in the post-treatment group. In addition, due to the scarcity of samples only P155 time-points were included in the pre-treatment analysis. It is possible that the observations made in the pre-treatment time-points in comparison with the control patients may only apply to one SSC patient. The Luminex assay was based on cytokine and chemokine concentrations in plasma samples. Therefore, they reflect the circulating levels of these immune regulators elucidated in response to a number of stimuli including pathogens and not just HCV. Future studies should therefore look into immune responses specific to HCV infection. One example of such technique is an ELISPOT assay where stimulation of PBMCs with HCV-specific peptides would

occur. Unfortunately PBMCs from the SSC and TF patients were limited. Future T cell assays would have to be based on post-treatment samples after successfully recalling patients back to the clinic.

3.2.10.5 Conclusions and future work

In conclusion, we have demonstrated that broadly neutralizing antibodies and cellular immune responses are crucial components in viral clearance following treatment relapse. SSC is a novel phenomenon in the natural history of HCV infection which, to our knowledge, has never been described before. SSC cases may be more frequent than once thought and studying the immune responses can significantly improve our understanding of viral control required for future vaccine studies. Elevated counts of CD4+ T and CD8+ T cells hinted at their importance in this novel phenomenon and may be related to fluctuations associated with HIV co-infections. The early onset of treatment with IFN/RBV may have possibly prevented T cell exhaustion. This is evident by the onset of robust neutralising antibodies at the time of relapse in SSC patients, as CD4+ T cells are required for effective B cell responses. These neutralising antibody responses may have contributed to viral clearance via the emergence of viral mutations in key CD81-binding epitopes inducing reduced fitness of the virus and/or blocking viral entry. Finally, numerous mutations in key T cell epitopes in one of the SSC patients hint at broadly reactive HCV specific T cell responses, facilitated by elevated levels of key Th1 cytokines in the pre-treatment time-points. Future studies should examine HCV-specific T cell response via ELISPOT and flow cytometry analysis in order to confirm the involvement of T cells in the viral clearance in post-treatment relapse.

References

A Guide to LAMP primer designing n.d., viewed 5 August 2019, <https://primerexplorer.jp/e/v4_manual/pdf/PrimerExplorerV4_Manual_1.pdf>.

Abdel-Hakeem, M.S. & Shoukry, N.H. 2014, 'Protective immunity against hepatitis C: Many shades of gray', *Frontiers in Immunology*.

Abdelrahman, T., Hughes, J., Main, J., McLauchlan, J., Thursz, M. & Thomson, E. 2015, 'Next-generation sequencing sheds light on the natural history of hepatitis C infection in patients who fail treatment', *Hepatology*, vol. 61, no. 1, 2014/05/07., pp. 88–97.

Afdhal, N., Reddy, K.R., Nelson, D.R., Lawitz, E., Gordon, S.C., Schiff, E., Nahass, R., Ghalib, R., Gitlin, N., Herring, R., Lalezari, J., Younes, Z.H., Pockros, P.J., Di Bisceglie, A.M., Arora, S., Subramanian, G.M., Zhu, Y., Dvory-Sobol, H., Yang, J.C., Pang, P.S., Symonds, W.T., McHutchison, J.G., Muir, A.J., Sulkowski, M., Kwo, P. & ION-2 Investigators 2014, 'Ledipasvir and Sofosbuvir for Previously Treated HCV Genotype 1 Infection', *New England Journal of Medicine*, vol. 370, no. 16, pp. 1483–93.

Afdhal, N., Zeuzem, S., Kwo, P., Chojkier, M., Gitlin, N., Puoti, M., Romero-Gomez, M., Zarski, J.-P., Agarwal, K., Buggisch, P., Foster, G.R., Bräu, N., Buti, M., Jacobson, I.M., Subramanian, G.M., Ding, X., Mo, H., Yang, J.C., Pang, P.S., Symonds, W.T., McHutchison, J.G., Muir, A.J., Mangia, A. & Marcellin, P. 2014, 'Ledipasvir and Sofosbuvir for Untreated HCV Genotype 1 Infection', *New England Journal of Medicine*, vol. 370, no. 20, pp. 1889–98.

Afdhal, N.H., McHutchison, J.G., Zeuzem, S., Mangia, A., Pawlotsky, J.-M., Murray, J.S., Shianna, K. V., Tanaka, Y., Thomas, D.L., Booth, D.R., Goldstein, D.B. & Pharmacogenetics and Hepatitis C Meeting Participants 2011, 'Hepatitis C pharmacogenetics: State of the art in 2010', *Hepatology*, vol. 53, no. 1, pp. 336–45.

Agnello, V., Abel, G., Elfahal, M., Knight, G.B. & Zhang, Q.-X. 1999, 'Hepatitis C virus and other Flaviviridae viruses enter cells via low density lipoprotein receptor', *Proceedings of the National Academy of Sciences*, vol. 96, no. 22, pp. 12766–71.

Al-Tahish, G., El-Barrawy, M.A., Hashish, M.H. & Heddaya, Z. 2013, 'Effectiveness of three types of rapid tests for the detection of hepatitis C virus antibodies among blood donors in Alexandria, Egypt', *J Virol Methods*, vol. 189, no. 2, 2013/04/02., pp. 370–4.

Algoud, M., Tissot-Dupont, H., Menard, A., Botta-Fridlund, D., Aherfi, S. & Colson, P. 2017, 'Spontaneous clearance of chronic hepatitis C virus infection in HIV-positive patients, southeastern France', *Clinics and Research in Hepatology and Gastroenterology*, vol. 41, no. 6, pp. e87–9.

Alter, H.J., Holland, P. V, Morrow, A.G., Purcell, R.H., Feinstone, S.M. & Moritsugu, Y. 1975, 'Clinical and serological analysis of transfusion-associated hepatitis.', *Lancet (London, England)*, vol. 2, no. 7940, pp. 838–41.

Alter, M.J. 2002, 'Prevention of spread of hepatitis C', *Hepatology*, vol. 36, no. 5B, pp. s93–8.

Alter, M.J., Coleman, P.J., Alexander, W.J., Kramer, E., Miller, J.K., Mandel, E., Hadler, S.C. & Margolis, H.S. 1989, 'Importance of heterosexual activity in the transmission of hepatitis B and non-A, non-B hepatitis.', *JAMA*, vol. 262, no. 9, pp. 1201–5.

Amadei, B., Urbani, S., Cazaly, A., Fisicaro, P., Zerbini, A., Ahmed, P., Missale, G., Ferrari, C. & Khakoo, S.I. 2010, 'Activation of Natural Killer Cells During Acute Infection With Hepatitis C Virus', *Gastroenterology*, vol. 138, no. 4, pp. 1536–45.

Amako, Y., Tsukiyama-Kohara, K., Katsume, A., Hirata, Y., Sekiguchi, S., Tobita, Y., Hayashi, Y., Hishima, T., Funata, N., Yonekawa, H. & Kohara, M. 2010, 'Pathogenesis of hepatitis C virus infection in Tupaia belangeri.', *Journal of virology*, vol. 84, no. 1, pp. 303–11.

Anderson, D.J. 1989, 'Determination of the lower limit of detection.', *Clinical Chemistry*, vol. 35, no. 10.

Angus, A.G.N. & Patel, A.H. 2011, 'Immunotherapeutic potential of neutralizing antibodies targeting conserved regions of the HCV envelope glycoprotein E2', *Future Microbiology*.

Ashrafi Hafez, A., Ahmadi Vasmehjani, A., Baharlou, R., Mousavi Nasab, S.D., Davami, M.H., Najfi, A., Joharinia, N., Rezanehad, H., Ali Ahmadi, N. & Imanzad, M. 2014, 'Analytical Assessment of Interleukin - 23 and -27 Cytokines in Healthy People and Patients With Hepatitis C Virus Infection (Genotypes 1 and 3a)', *Hepatitis Monthly*, vol. 14, no. 9, p. e21000.

Bankwitz, D., Steinmann, E., Bitzegeio, J., Ciesek, S., Friesland, M., Herrmann, E., Zeisel, M.B., Baumert, T.F., Keck, Z. y., Foung, S.K.H., Pecheur, E.I. & Pietschmann, T. 2010, 'Hepatitis C Virus Hypervariable Region 1 Modulates Receptor Interactions, Conceals the CD81 Binding Site, and Protects Conserved Neutralizing Epitopes', *Journal of Virology*, vol. 84, no. 11, pp. 5751–63.

Barnes, E., Folgori, A., Capone, S., Swadling, L., Aston, S., Kurioka, A., Meyer, J., Huddart, R., Smith, K., Townsend, R., Brown, A., Antrobus, R., Ammendola, V., Naddeo, M., O'Hara, G., Willberg, C., Harrison, A., Grazioli, F., Esposito, M.L., Siani, L., Traboni, C., Oo, Y., Adams, D., Hill, A., Colloca, S., Nicosia, A., Cortese, R. & Klenerman, P. 2012, 'Novel adenovirus-based vaccines induce broad and sustained T cell responses to HCV in man', *Science Translational Medicine*.

Bartenschlager, R., Ahlborn-Laake, L., Mous, J. & Jacobsen, H. 1994, 'Kinetic and structural analyses of hepatitis C virus polyprotein processing.', *Journal of virology*.

Bartenschlager, R., Cosset, F.-L. & Lohmann, V. 2010, *Hepatitis C virus replication cycle Hepatology Snapshot*, *Journal of Hepatology*.

Bartenschlager, R., Penin, F., Lohmann, V. & André, P. 2011, 'Assembly of infectious hepatitis C virus particles', *Trends in Microbiology*, vol. 19, no. 2, pp. 95–103.

Barth, H., Schäfer, C., Adah, M.I., Zhang, F., Linhardt, R.J., Toyoda, H., Kinoshita-Toyoda, A., Toida, T., van Kuppevelt, T.H., Depla, E., von Weizsäcker, F., Blum, H.E. & Baumert, T.F. 2003, 'Cellular Binding of Hepatitis C Virus Envelope Glycoprotein E2 Requires Cell Surface Heparan Sulfate', *Journal of Biological Chemistry*, vol. 278, no. 42, pp. 41003–12.

Bartosch, Birke, Dubuisson, J. & Cosset, F.-L. 2003, 'Infectious Hepatitis C Virus Pseudo-particles Containing Functional E1–E2 Envelope Protein Complexes', *The Journal of Experimental Medicine*, vol. 197, no. 5, pp. 633–42.

Bartosch, B, Dubuisson, J. & Cosset, F.L. 2003, 'Infectious hepatitis C virus pseudo-particles containing functional E1-E2 envelope protein complexes', *J Exp Med*, vol. 197, no. 5, 2003/03/05., pp. 633–42.

Bassett, S., Guerra, B., Brasky, K., Miskovsky, E., Houghton, M., Klimpel, G.R. & Lanford, R.E. 2001, 'Protective immune response to hepatitis C virus in chimpanzees rechallenged following clearance of primary infection', *Hepatology*, vol. 33, no. 6, pp. 1479–87.

Bassett, S.E., Lanford, R.E., Brasky, K.M. & Thomas, D.L. 1999, 'Viral persistence, antibody to E1 and E2, and hypervariable region 1 sequence stability in hepatitis C virus-inoculated chimpanzees', *Journal of Virology*.

Op De Beeck, A., Voisset, C., Bartosch, B., Ciczora, Y., Cocquerel, L., Keck, Z., Foung, S., Cosset, F.L. & Dubuisson, J. 2004, 'Characterization of functional hepatitis C virus envelope glycoproteins', *J Virol*, vol. 78, no. 6, 2004/03/03., pp. 2994–3002.

Beinhardt, S., Al-Zoairy, R., Kozbial, K., Stättermayer, A.F., Maieron, A., Stauber, R., Strasser, M., Zoller, H., Graziadei, I., Rasoul-Rockenschaub, S., Trauner, M., Ferenci, P. & Hofer, H. 2018, 'Long-term follow-up of ribavirin-free DAA-based treatment in HCV recurrence after orthotopic liver transplantation', *Liver International*, vol. 38, no. 7, pp. 1188–97.

Bellete, B., Flori, P., Hafid, J., Raberin, H. & Tran Manh Sung, R. 2003, 'Influence of the quantity of nonspecific DNA and repeated freezing and thawing of samples on the quantification of DNA by the Light Cycler.', *Journal of microbiological methods*, vol. 55, no. 1, pp. 213–9.

Bengsch, B., Seigel, B., Ruhl, M., Timm, J., Kuntz, M., Blum, H.E., Pircher, H. & Thimme, R. 2010, 'Coexpression of PD-1, 2B4, CD160 and KLRG1 on exhausted HCV-specific CD8+ T cells is linked to antigen recognition and T cell differentiation', *PLoS Pathogens*.

Bigger, C.B., Brasky, K.M. & Lanford, R.E. 2001, 'DNA Microarray Analysis of Chimpanzee Liver during Acute Resolving Hepatitis C Virus Infection', *Journal of Virology*, vol. 75, no. 15, pp. 7059–66.

Billerbeck, E., Wolfisberg, R., Fahnøe, U., Xiao, J.W., Quirk, C., Luna, J.M., Cullen, J.M., Hartlage, A.S., Chiriboga, L., Ghoshal, K., Lipkin, W.I., Bukh, J., Scheel, T.K.H., Kapoor, A. & Rice, C.M. 2017, 'Mouse models of acute and chronic hepacivirus infection', *Science*.

Di Bisceglie, A.M., Martin, P., Kassianides, C., Lisker-Melman, M., Murray, L., Waggoner, J., Goodman, Z., Banks, S.M. & Hoofnagle, J.H. 1989, 'Recombinant Interferon Alfa Therapy for Chronic Hepatitis C', *New England Journal of Medicine*, vol. 321, no. 22, pp. 1506–10.

Bjoro, K., Froland, S.S., Yun, Z., Samdal, H.H. & Haaland, T. 1994, 'Hepatitis C Infection in Patients with Primary Hypogammaglobulinemia after Treatment with Contaminated Immune Globulin', *New England Journal of Medicine*, vol. 331, no. 24, pp. 1607–11.

Blach, S., Zeuzem, S., Manns, M., Altraif, I., Duberg, A.-S., Muljono, D.H., Waked, I., Alavian, S.M., Lee, M.-H., Negro, F., Abaalkhail, F., Abdou, A., Abdulla, M., Abou Rached, A., Aho, I., Akarca, U., Al Ghazzawi, I., Al Kaabi, S., Al Lawati, F., Al Namaani, K., Al Serkal, Y., Al-Busafi, S.A., Al-Dabal, L., Aleman, S., Alghamdi, A.S., Aljumah, A.A., Al-Romaihi, H.E., Andersson, M.I., Arendt, V., Arkkila, P., Assiri, A.M., Baatarkhuu, O., Bane, A., Ben-Ari, Z., Bergin, C., Bessone, F., Bihl, F., Bizri, A.R., Blachier, M., Blasco, A.J., BrandÃ, C.E., Bruggmann, P., Brunton, C.R., Calinas, F., Y Chan, H.L., Chaudhry, A., Cheinquer, H., Chen, C.-J., Chien, R.-N., Seok Choi, M., Christensen, P.B., Chuang, W.-L., Chulanov, V., Cisneros, L., Clausen, M.R., Cramp, M.E., Craxi, A., Croes, E.A., Dalgard, O., Daruich, J.R., de Ledinghen, V., Dore, G.J., El-Sayed, M.H., ErgÃ, G., Esmat, G., Estes, C., Falconer, K., Farag, E., G Ferraz, M.L., Ferreira, P.R., Flisiak, R., Frankova, S., Gamkrelidze, I., Gane, E., GarcÃ, J., Ghafoor Khan, A., Gountas, I., Goldis, A., Gottfredsson, M., Grebely, J., Gschwantler, M., GuimarÃ rio, PessÃ es, Gunter, J., Hajarizadeh, B., Hajelssedig, O., Hamid, S., Hamoudi, W., Hatzakis, A., Himatt, S.M., Hofer, H., Hrstic, I., Hui, Y.-T., Hunyady, B., Idilman, R., Jafri, W., Jahis, R., Janjua, N.Z., JarÄ, P., Jeruma, A., Jonasson, G., Kamel, Y., Kao, J.-H., Kaymakoglu, S., Kershenobich, D., Khamis, J., Kim, Y.S., Kondili, L., Koutoubi, Z., Krajden, M., Krarup, H., Lai, M., Laleman, W., Lao, W., Lavanchy, D., Lã, P., Leleu, H., Lesi, O., Lesmana, L.A., Li, M., Liakina, V., Lim, Y.-S., Luksic, B., Mahomed, A., Maimets, M., Makara ly, Malu, A.O., Marinho, R.T., Marotta, P., Mauss, S., Memon, M.S., Mendes Correa, M.C., Mendez-Sanchez, N., Merat, S., Metwally, A.M., Mohamed, R., Moreno, C., Mourad, F.H., Mã, B., Murphy, K., Nde, H., Njouom, R., Nonkovic, D., Norris, S., Obekpa, S., Oguche, S., Olafsson ur, Oltman, M., Omede, O., Omuemu, C., Opare-Sem, O., H Ã, A.L., Owusu-Ofori, S., Oyunsuren, T.S., Papatheodoridis, G., Pasini, K., Peltekian, K.M., Phillips, R.O., Pimenov, N., Poustchi, H., Prabdial-Sing, N., Qureshi, H., Ramji, A., Razavi-Shearer, D., Razavi-Shearer, K., Redae, B., Reesink, H.W., Ridruejo, E., Robbins, S., Roberts, L.R., Roberts, S.K., Rosenberg, W.M., Roudot-Thoraval oise, Ryder, S.D., Safadi, R., Sagalova, O., Salupere, R., Sanai, F.M., Sanchez Avila, J.F., Saraswat, V., Sarmento-Castro, R., Sarrazin, C., Schmelzer, J.D., SchrÃ, I., Seguin-Devaux, C., Shah, S.R., Sharara, A.I., Sharma, M., Shevaldin, A., Shiha, G.E., Sievert, W.,

Sonderup, M., Souliotis, K., Speiciene, D., Sperl, J., StÃ, P., Stauber, R.E., Stedman, C., Struck, D., Su, T.-H., Sypsa, V., Tan, S.-S., Tanaka, J., Thompson, A.J., Tolmane, I., Tomasiewicz, K., Valantinas, J., Van Damme, P., van der Meer, A.J., van Thiel, I., Van Vlierberghe, H., Vince, A., Vogel, W., Wedemeyer, H., Weis, N., Wong, V.W., Yaghi, C., Yosry, A., Yuen, M., Yunihastuti, E., Yusuf, A., Zuckerman, E., Razavi, H. & Polaris Observatory HCV Collaborators, T. 2017, *Articles Global prevalence and genotype distribution of hepatitis C virus infection in 2015: a modelling study*.

Blackburn, S.D. & Wherry, E.J. 2007, 'IL-10, T cell exhaustion and viral persistence.', *Trends in microbiology*, vol. 15, no. 4, pp. 143–6.

Blight, K.J., Kolykhalov, A.A. & Rice, C.M. 2000, 'Efficient Initiation of HCV RNA Replication in Cell Culture', *Science*, vol. 290, no. 5498, pp. 1972–4.

Blight, K.J., McKeating, J.A., Marcotrigiano, J. & Rice, C.M. 2003, 'Efficient replication of hepatitis C virus genotype 1a RNAs in cell culture.', *Journal of virology*, vol. 77, no. 5, pp. 3181–90.

Bojang, A.L., Mendy, F.S., Tientcheu, L.D., Otu, J., Antonio, M., Kampmann, B., Agbla, S. & Sutherland, J.S. 2016, 'Comparison of TB-LAMP, GeneXpert MTB/RIF and culture for diagnosis of pulmonary tuberculosis in The Gambia', *Journal of Infection*, vol. 72, no. 3, pp. 332–7.

Borgia, S.M., Hedskog, C., Parhy, B., Hyland, R.H., Stamm, L.M., Brainard, D.M., Subramanian, M.G., McHutchison, J.G., Mo, H., Svarovskaia, E. & Shafran, S.D. 2018, 'Identification of a Novel Hepatitis C Virus Genotype From Punjab, India: Expanding Classification of Hepatitis C Virus Into 8 Genotypes', *J Infect Dis*, vol. 218, no. 11, 2018/07/10., pp. 1722–9.

Boulant, S., Vanbelle, C., Ebel, C., Penin, F. & Lavergne, J.-P. 2005, 'Hepatitis C Virus Core Protein Is a Dimeric Alpha-Helical Protein Exhibiting Membrane Protein Features', *Journal of Virology*.

Bowen, D.G., Shoukry, N.H., Grakoui, A., Fuller, M.J., Cawthon, A.G., Dong, C., Hasselschwert, D.L., Brasky, K.M., Freeman, G.J., Seth, N.P., Wucherpfennig, K.W., Houghton, M. & Walker, C.M. 2008, 'Variable Patterns of Programmed Death-1 Expression on Fully Functional Memory T Cells after Spontaneous Resolution of Hepatitis C Virus Infection', *Journal of Virology*.

Bowen, D.G. & Walker, C.M. 2005, 'Mutational escape from CD8+ T cell immunity: HCV evolution, from chimpanzees to man', *Journal of Experimental Medicine*.

Bresee, J.S., Mast, E.E., Coleman, P.J., Baron, M.J., Schonberger, L.B., Alter, M.J., Jonas, M.M., Yu, M.Y., Renzi, P.M. & Schneider, L.C. 1996, 'Hepatitis C virus infection associated with administration of intravenous immune globulin. A cohort study.', *JAMA*, vol. 276, no. 19, pp. 1563–7.

Brown, E.A., Zhang, H., Ping, L.-H. & Lemon, S.M. 1992, 'Secondary structure of the 5′ nontranslated regions of hepatitis C virus and pestivirus genomic RNAs', *Nucleic Acids Research*, vol. 20, no. 19, pp. 5041–5.

Bukh, J., Engle, R.E., Govindarajan, S. & Purcell, R.H. 2008, 'Immunity against the GBV-B hepatitis virus in tamarins can prevent productive infection following rechallenge and is long-lived', *Journal of Medical Virology*.

Bukh, J., Purcell, R.H. & Miller, R.H. 1992, 'Sequence analysis of the 5' noncoding region of hepatitis C virus.', *Proceedings of the National Academy of Sciences*, vol. 89, no. 11, pp. 4942–6.

Bumgardner, G.L., Heininger, M., Jiashun, L.I., Xia, D., Parker-Thornburg, J., Ferguson, R.M. & Orosz, C.G. 1998, 'A functional model of hepatocyte transplantation for in vivo immunologic studies', *Transplantation*.

Bumgardner, G.L., Jiashun, L.I., Heininger, M., Ferguson, R.M. & Orosz, C.G. 1998, 'In vivo immunogenicity of purified allogeneic hepatocytes in a murine hepatocyte transplant model', *Transplantation*.

Bumgardner, G.L., Li, J., Prologo, J.D., Heininger, M. & Orosz, C.G. 1999, 'Patterns of immune responses evoked by allogeneic hepatocytes: Evidence for independent co-dominant roles for CD4+ and CD8+ T-cell responses in acute rejection', *Transplantation*.

Buseri, F., Seiyaboh, E. & Jeremiah, Z. 2010, 'Surveying Infections among Pregnant Women in the Niger Delta, Nigeria', *J Glob Infect Dis*, vol. 2, no. 3, 2010/10/12., pp. 203–11.

Caetano, J., Martinho, A., Paiva, A., Pais, B., Valente, C. & Luxo, C. 2008, 'Differences in hepatitis C virus (HCV)-specific CD8 T-cell phenotype during pegylated alpha interferon and ribavirin treatment are related to response to antiviral therapy in patients chronically infected with HCV', *J Virol*, vol. 82, no. 15, 2008/05/16., pp. 7567–77.

Carreño, V., Carreño, V., Parra, A., Navas, S. & Quiroga, A.J. 1996, 'Granulocyte-macrophage colony-stimulating factor as adjuvant therapy for interferon α treatment of chronic hepatitis c', *Cytokine*, vol. 8, no. 4, pp. 318–22.

Cate, D.M., Adkins, J.A., Mettakoonpitak, J. & Henry, C.S. 2015, 'Recent Developments in Paper-Based Microfluidic Devices', *Analytical Chemistry*, vol. 87, no. 1, pp. 19–41.

Cavalheiro, N. de P., De La Rosa, A., Elagin, S., Tengan, F.M., Araújo, E.S.A. de & Barone, A.A. n.d., 'Hepatitis C: sexual or intrafamilial transmission? Epidemiological and phylogenetic analysis of hepatitis C virus in 24 infected couples.', *Revista da Sociedade Brasileira de Medicina Tropical*, vol. 42, no. 3, pp. 239–44.

Chen, J., Zhao, Y., Zhang, C., Chen, Hairong, Feng, J., Chi, X., Pan, Y., Du, J., Guo, M., Cao, H., Chen, Honghe, Wang, Z., Pei, R., Wang, Q., Pan, L., Niu, J., Chen, X. & Tang, H. 2014, 'Persistent hepatitis C virus infections and hepatopathological manifestations in immune-competent humanized mice', *Cell Research*.

Chevaliez, S. & Pawlotsky, J.-M. 2006, 'Hepatitis C Virus Serologic and Virologic Tests and Clinical Diagnosis of HCV-Related Liver Disease', *International Journal of Medical Sciences*, vol. 3, no. 2, pp. 35–40.

Chevaliez, S. & Pawlotsky, J.-M. 2018, 'New virological tools for screening, diagnosis and monitoring of hepatitis B and C in resource-limited settings', *Journal of Hepatology*, vol. 69, no. 4, pp. 916–26.

Choo, Q.L., Kuo, G., Ralston, R., Weiner, A., Chien, D., Van Nest, G., Han, J., Berger, K., Thudium, K. & Kuo, C. 1994, 'Vaccination of chimpanzees against infection by the hepatitis C virus.', *Proceedings of the National Academy of Sciences*.

Choo, Q.L., Kuo, G., Weiner, A.J., Overby, L.R., Bradley, D.W. & Houghton, M. 1989, 'Isolation of a cDNA clone derived from a blood-borne non-A, non-B viral hepatitis genome', *Science*, vol. 244, no. 4902, pp. 359–62.

Choo, Q.L., Richman, K.H., Han, J.H., Berger, K., Lee, C., Dong, C., Gallegos, C., Coit, D., Medina-Selby, R. & Barr, P.J. 1991, 'Genetic organization and diversity of the hepatitis C virus.', *Proceedings of the National Academy of Sciences of the United States of America*, vol. 88, no. 6, pp. 2451–5.

Choo, Q.L., Richman, K.H., Han, J.H., Berger, K., Lee, C., Dong, C., Gallegos, C., Coit, D., Medina-Selby, R., Barr, P.J. & al., et 1991, 'Genetic organization and diversity of the hepatitis C virus.', *Proceedings of the National Academy of Sciences of the United States of America*, vol. 88, no. 6, pp. 2451–5.

Conrad, C., Bradley, H.M., Broz, D., Buddha, S., Chapman, E.L., Galang, R.R., Hillman, D., Hon, J., Hoover, K.W., Patel, M.R., Perez, A., Peters, P.J., Pontones, P., Roseberry, J.C., Sandoval, M., Shields, J., Walthall, J., Waterhouse, D., Weidle, P.J., Wu, H., Duwve, J.M. & Centers for Disease Control and Prevention (CDC) 2015, 'Community Outbreak of HIV Infection Linked to Injection Drug Use of Oxymorphone--Indiana, 2015.', *MMWR. Morbidity and mortality weekly report*, vol. 64, no. 16, pp. 443–4.

Cooper, S., Erickson, A.L., Adams, E.J., Kansopon, J., Weiner, A.J., Chien, D.Y., Houghton, M., Parham, P. & Walker, C.M. 1999, 'Analysis of a successful immune response against hepatitis C virus', *Immunity*.

Costafreda, M.I., Bosch, A. & Pintó, R.M. 2006, 'Development, evaluation, and standardization of a real-time TaqMan reverse transcription-PCR assay for quantification of hepatitis A virus in clinical and shellfish samples.', *Applied and environmental microbiology*, vol. 72, no. 6, pp. 3846–55.

Cox, A.L., Mosbruger, T., Mao, Q., Liu, Z., Wang, X.-H., Yang, H.-C., Sidney, J., Sette, A., Pardoll, D., Thomas, D.L. & Ray, S.C. 2005, 'Cellular immune selection with hepatitis C virus persistence in humans', *The Journal of Experimental Medicine*.

Dahari, H., Feinstone, S.M. & Major, M.E. 2010a, 'Meta-Analysis of Hepatitis C Virus Vaccine Efficacy in Chimpanzees Indicates an Importance for Structural Proteins', *Gastroenterology*, vol. 139, no. 3, pp. 965–74.

Dahari, H., Feinstone, S.M. & Major, M.E. 2010b, 'Meta-Analysis of Hepatitis C Virus Vaccine Efficacy in Chimpanzees Indicates an Importance for Structural Proteins', *Gastroenterology*, vol. 139, no. 3, pp. 965–74.

Damhorst, G.L., Duarte-Guevara, C., Chen, W., Ghonge, T., Cunningham, B.T. & Bashir, R. 2015, 'Smartphone-Imaged HIV-1 Reverse-Transcription Loop-Mediated Isothermal Amplification (RT-LAMP) on a Chip from Whole Blood', *Engineering (Beijing, China)*, vol. 1, no. 3, pp. 324–35.

Davis, C., Mgomella, G.S., da Silva Filipe, A., Frost, E.H., Giroux, G., Hughes, J., Hogan, C., Kaleebu, P., Asiki, G., McLauchlan, J., Niebel, M., Ocama, P., Pomila, C., Pybus, O.G., Pepin, J., Simmonds, P., Singer, J.B., Sreenu, V.B., Wekesa, C., Young, E.H., Murphy, D.G., Sandhu, M. & Thomson, E.C. 2019, 'Highly Diverse Hepatitis C Strains Detected in Sub-Saharan Africa Have Unknown Susceptibility to Direct-Acting Antiviral Treatments', *Hepatology*, vol. 69, no. 4, 2018/11/06., pp. 1426–41.

Davis, G.L., Balart, L.A., Schiff, E.R., Lindsay, K., Bodenheimer, H.C., Perrillo, R.P., Carey, W., Jacobson, I.M., Payne, J., Dienstag, J.L., VanThiel, D.H., Tamburro, C., Lefkowitch, J., Albrecht, J., Meschievitz, C., Ortego, T.J. & Gibas, A. 1989, 'Treatment of Chronic Hepatitis C with Recombinant Interferon Alfa', *New England Journal of Medicine*, vol. 321, no. 22, pp. 1501–6.

Day, C.L., Lauer, G.M., Robbins, G.K., McGovern, B., Wurcel, A.G., Gandhi, R.T., Chung, R.T. & Walker, B.D. 2002, 'Broad Specificity of Virus-Specific CD4+ T-Helper-Cell Responses in Resolved Hepatitis C Virus Infection', *Journal of Virology*.

Dazert, E., Neumann-Haefelin, C., Bressanelli, S., Fitzmaurice, K., Kort, J., Timm, J., McKiernan, S., Kelleher, D., Gruener, N., Tavis, J.E., Rosen, H.R., Shaw, J., Bowness, P., Blum, H.E., Klenerman, P., Bartenschlager, R. & Thimme, R. 2009, 'Loss of viral fitness and cross-recognition by CD8+ T cells limit HCV escape from a protective HLA-B27-restricted human immune response', *Journal of Clinical Investigation*.

Deinhardt, F. 1967, 'STUDIES ON THE TRANSMISSION OF HUMAN VIRAL HEPATITIS TO MARMOSET MONKEYS: I. TRANSMISSION OF DISEASE, SERIAL PASSAGES, AND DESCRIPTION OF LIVER LESIONS', *Journal of Experimental Medicine*.

Denniston, M.M., Klevens, R.M., McQuillan, G.M. & Jiles, R.B. 2012, 'Awareness of infection, knowledge of hepatitis C, and medical follow-up among individuals testing positive for hepatitis C: National Health and Nutrition Examination Survey 2001–2008', *Hepatology*, vol. 55, no. 6, pp. 1652–61.

Ding, Q., von Schaewen, M., Hrebikova, G., Heller, B., Sandmann, L., Plaas, M. & Ploss, A. 2017, ' Mice Expressing Minimally Humanized CD81 and Occludin Genes Support Hepatitis C Virus Uptake In Vivo ', *Journal of Virology*.

Domingo, E. & Perales, C. 2018, 'Quasispecies and virus', *European Biophysics Journal*, vol. 47, no. 4, pp. 443–57.

Donahue, J.G., Muñoz, A., Ness, P.M., Brown, D.E., Yawn, D.H., McAllister, H.A., Reitz, B.A. & Nelson, K.E. 1992, 'The Declining Risk of Post-Transfusion Hepatitis C Virus Infection', *New England Journal of Medicine*, vol. 327, no. 6, pp. 369–73.

Dore, G.J., Law, M., MacDonald, M. & Kaldor, J.M. 2003, 'Epidemiology of hepatitis C virus infection in Australia.', *Journal of clinical virology : the official publication of the Pan American Society for Clinical Virology*, vol. 26, no. 2, pp. 171–84.

Dorner, M., Horwitz, J.A., Donovan, B.M., Labitt, R.N., Budell, W.C., Friling, T., Vogt, A., Catanese, M.T., Satoh, T., Kawai, T., Akira, S., Law, M., Rice, C.M. & Ploss, A. 2013, 'Completion of the entire hepatitis C virus life cycle in genetically humanized mice', *Nature*.

Dorner, M., Horwitz, J.A., Robbins, J.B., Barry, W.T., Feng, Q., Mu, K., Jones, C.T., Schoggins, J.W., Catanese, M.T., Burton, D.R., Law, M., Rice, C.M. & Ploss, A. 2011, 'A genetically humanized mouse model for hepatitis C virus infection', *Nature*.

Douam, F., Dao Thi, V.L., Maurin, G., Fresquet, J., Mompelat, D., Zeisel, M.B., Baumert, T.F., Cosset, F.L. & Lavillette, D. 2014, 'Critical interaction between E1 and E2 glycoproteins determines binding and fusion properties of hepatitis C virus during cell entry', *Hepatology*.

Dowd, K.A., Netski, D.M., Wang, X., Cox, A.L. & Ray, S.C. 2009, 'Selection Pressure From Neutralizing Antibodies Drives Sequence Evolution During Acute Infection With Hepatitis C Virus', *Gastroenterology*, vol. 136, no. 7, pp. 2377–86.

Drexler, J.F., Kupfer, B., Petersen, N., Grotto, R.M.T., Rodrigues, S.M.C., Grywna, K., Panning, M., Annan, A., Silva, G.F., Douglas, J., Koay, E.S.C., Smuts, H., Netto, E.M., Simmonds, P., Pardini, M.I. de M.C., Roth, W.K. & Drosten, C. 2009, 'A Novel Diagnostic Target in the Hepatitis C Virus Genome', P. Klenerman (ed.),*PLoS Medicine*, vol. 6, no. 2, p. e1000031.

Drummer, H.E., Boo, I., Maerz, A.L. & Poumbourios, P. 2006, 'A Conserved Gly436-Trp-Leu-Ala-Gly-Leu-Phe-Tyr Motif in Hepatitis C Virus Glycoprotein E2 Is a Determinant of CD81 Binding and Viral Entry', *Journal of Virology*.

Dubuisson, J., Helle, F. & Cocquerel, L. 2008, 'Early steps of the hepatitis C virus life cycle', *Cell Microbiol*, vol. 10, no. 4, 2007/12/18., pp. 821–7.

Dustin, L.B., Cashman, S.B. & Laidlaw, S.M. 2014, 'Immune control and failure in HCV infection-tipping the balance', *Journal of Leukocyte Biology*.

'EASL clinical practice guidelines: management of hepatitis c virus infection' 2016, *Journal of Hepatology*, vol. 60, no. 2, pp. 392–420.

Elmowalid, G.A., Qiao, M., Jeong, S.-H., Borg, B.B., Baumert, T.F., Sapp, R.K., Hu, Z., Murthy, K. & Liang, T.J. 2007, 'Immunization with hepatitis C virus-like particles results in control of hepatitis C virus infection in chimpanzees', *Proceedings of the National Academy of Sciences*, vol. 104, no. 20, pp. 8427–32.

Ember, S.W., Schulze, H., Ross, A.J., Luby, J., Khondoker, M., Giraud, G., Terry, J.G., Ciani, I., Tlili, C., Crain, J., Walton, A.J., Mount, A.R., Ghazal, P., Bachmann, T.T. & Campbell, C.J. 2011, 'Fast DNA and protein microarray tests for the diagnosis of hepatitis C virus infection on a single platform', *Anal Bioanal Chem*, vol. 401, no. 8, 2011/09/02., pp. 2549–59.

Ennishi, D., Terui, Y., Yokoyama, M., Mishima, Y., Takahashi, S., Takeuchi, K., Okamoto, H., Tanimoto, M. & Hatake, K. 2008, 'Monitoring serum hepatitis C virus (HCV) RNA in patients with HCV-infected CD20-positive B-cell lymphoma undergoing rituximab combination chemotherapy', *American Journal of Hematology*.

Erickson, A.L., Kimura, Y., Igarashi, S., Eichelberger, J., Houghton, M., Sidney, J., McKinney, D., Sette, A., Hughes, A.L. & Walker, C.M. 2001, 'The outcome of hepatitis C virus infection is predicted by escape mutations in epitopes targeted by cytotoxic T lymphocytes', *Immunity*.

Evans, M.J., von Hahn, T., Tscherne, D.M., Syder, A.J., Panis, M., Wölk, B., Hatziioannou, T., McKeating, J.A., Bieniasz, P.D. & Rice, C.M. 2007, 'Claudin-1 is a hepatitis C virus co-receptor required for a late step in entry', *Nature*, vol. 446, no. 7137, pp. 801–5.

Falconer, K., Gonzalez, V.D., Reichard, O., Sandberg, J.K. & Alaeus, A. 2008, 'Spontaneous HCV clearance in HCV/HIV-1 coinfection associated with normalized CD4 counts, low level of chronic immune activation and high level of T cell function', *Journal of Clinical Virology*, vol. 41, no. 2, pp. 160–3.

Falkowska, E., Kajumo, F., Garcia, E., Reinus, J. & Dragic, T. 2007, 'Hepatitis C Virus Envelope Glycoprotein E2 Glycans Modulate Entry, CD81 Binding, and Neutralization', *Journal of Virology*.

Falson, P., Bartosch, B., Alsaleh, K., Tews, B.A., Loquet, A., Ciczora, Y., Riva, L., Montigny, C., Montpellier, C., Duverlie, G., Pécheur, E.-I., le Maire, M., Cosset, F.-L., Dubuisson, J. & Penin, F. 2015, 'Hepatitis C Virus Envelope Glycoprotein E1 Forms Trimers at the Surface of the Virion', *Journal of Virology*.

Farci, P., Bukh, J. & Purcell, R.H. 1997, 'The quasispecies of hepatitis C virus and the host immune response.', *Springer seminars in immunopathology*, vol. 19, no. 1, pp. 5–26.

Farci, P., Shimoda, A., Wong, D., Cabezon, T., De Gioannis, D., Strazzera, A., Shimizu, Y., Shapiro, M., Alter, H.J. & Purcell, R.H. 1996, 'Prevention of hepatitis C virus infection in chimpanzees by hyperimmune serum against the hypervariable region 1 of the envelope 2 protein', *Proceedings of the National Academy of Sciences*, vol. 93, no. 26, pp. 15394–9.

Feld, J.J. & Hoofnagle, J.H. 2005a, 'Mechanism of action of interferon and ribavirin in treatment of hepatitis C', *Nature*, vol. 436, no. 7053, pp. 967–72.

Feld, J.J. & Hoofnagle, J.H. 2005b, 'Mechanism of action of interferon and ribavirin in treatment of hepatitis C', *Nature*, vol. 436, no. 7053, pp. 967–72.

Feng, Y., Feng, Y.-M., Lu, C., Han, Y., Liu, L., Sun, X., Dai, J. & Xia, X. 2017, 'Tree shrew, a potential animal model for hepatitis C, supports the infection and replication of HCV in vitro and in vivo', *Journal of General Virology*, vol. 98, no. 8, pp. 2069–78.

Firth, C., Bhat, M., Firth, M.A., Williams, S.H., Frye, M.J., Simmonds, P., Conte, J.M., Ng, J., Garcia, J., Bhuva, N.P., Lee, B., Che, X., Quan, P.L. & Ian Lipkin, W. 2014, 'Detection of zoonotic pathogens and characterization of novel viruses carried by commensal rattus norvegicus in New York city', *mBio*.

Fischbach, J., Xander, N.C., Frohme, M. & Glökler, J.F. 2015, 'Shining a light on LAMP assays— A comparison of LAMP visualization methods including the novel use of berberine', *BioTechniques*, vol. 58, no. 4.

Fisher, D.G., Hess, K.L., Erlyana, E., Reynolds, G.L., Cummins, C.A. & Alonzo, T.A. 2015, 'Comparison of Rapid Point-of-Care Tests for Detection of Antibodies to Hepatitis C Virus', *Open Forum Infect Dis*, vol. 2, no. 3, p. ofv101.

Folgori, A., Capone, S., Ruggeri, L., Meola, A., Sporeno, E., Ercole, B.B., Pezzanera, M., Tafi, R., Arcuri, M., Fattori, E., Lahm, A., Luzzago, A., Vitelli, A., Colloca, S., Cortese, R. & Nicosia, A. 2006, 'A T-cell HCV vaccine eliciting effective immunity against heterologous virus challenge in chimpanzees', *Nature Medicine*.

Forns, X., Payette, P.J., Ma, X., Satterfield, W., Eder, G., Mushahwar, I.K., Govindarajan, S., Davis, H.L., Emerson, S.U., Purcell, R.H. & Bukh, J. 2000, 'Vaccination of Chimpanzees With Plasmid DNA Encoding the Hepatitis C Virus(HCV) Envelope E2 Protein Modified the Infection After Challenge With Homologous Monoclonal HCV', *Hepatology*, vol. 32, no. 3, pp. 618–25.

Frank, C., Mohamed, M.K., Strickland, G.T., Lavanchy, D., Arthur, R.R., Magder, L.S., El Khoby, T., Abdel-Wahab, Y., Aly Ohn, E.S., Anwar, W. & Sallam, I. 2000, 'The role of parenteral antischistosomal therapy in the spread of hepatitis C virus in Egypt.', *Lancet (London, England)*, vol. 355, no. 9207, pp. 887–91.

Freiman, J.M., Tran, T.M., Schumacher, S.G., White, L.F., Ongarello, S., Cohn, J., Easterbrook, P.J., Linas, B.P. & Denkinger, C.M. 2016, 'Hepatitis C Core Antigen Testing for Diagnosis of Hepatitis C Virus Infection', *Annals of Internal Medicine*, vol. 165, no. 5, p. 345.

Frey, S.E., Houghton, M., Coates, S., Abrignani, S., Chien, D., Rosa, D., Pileri, P., Ray, R., Di Bisceglie, A.M., Rinella, P., Hill, H., Wolff, M.C., Schultze, V., Han, J.H., Scharschmidt, B. & Belshe, R.B. 2010, 'Safety and immunogenicity of HCV E1E2 vaccine adjuvanted with MF59 administered to healthy adults', *Vaccine*.

Frias, M., Rivero-Juarez, A., Tellez, F., Perez-Perez, M., Camacho, A., Machuca, I., Lorenzo-Moncada, S., Lopez-Lopez, P., Rivero, A. & Grupo de Estudio de Hepatitis Virales (HEPAVIR) of the Sociedad Andaluza de Enfermedades Infecciosas (SAEI), for the G. de E. de H.V. (HEPAVIR) of the S.A. de E.I. 2017, 'Spontaneous clearance of chronic hepatitis C is rare in HIV-infected patients after effective use of combination antiretroviral therapy.', *PloS one*, vol. 12, no. 5, p. e0177141.

Fried, M.W., Shiffman, M.L., Reddy, K.R., Smith, C., Marinos, G., Gonçales, F.L., Häussinger, D., Diago, M., Carosi, G., Dhumeaux, D., Craxi, A., Lin, A., Hoffman, J. & Yu, J. 2002, 'Peginterferon Alfa-2a plus Ribavirin for Chronic Hepatitis C Virus Infection', *New England Journal of Medicine*, vol. 347, no. 13, pp. 975–82.

Fuller, M.J., Callendret, B., Zhu, B., Freeman, G.J., Hasselschwert, D.L., Satterfield, W., Sharpe, A.H., Dustin, L.B., Rice, C.M., Grakoui, A., Ahmed, R. & Walker, C.M. 2013, 'Immunotherapy of chronic hepatitis C virus infection with antibodies against programmed cell death-1 (PD-1)', *Proceedings of the National Academy of Sciences*, vol. 110, no. 37, pp. 15001–6.

Galun, E., Burakova, T., Ketzinel, M., Lubin, I., Shezen, E., Kahana, Y., Eid, A., Ilan, Y., Rivkind, A., Pizov, G., Shouval, D. & Reisner, Y. 1995, 'Hepatitis c virus viremia in scid→bnx mouse chimera', *Journal of Infectious Diseases*.

Gaudieri, S., Rauch, A., Park, L.P., Freitas, E., Herrmann, S., Pfafferott, K., Naidoo, K., James, I., Lucas, M., Mallal, S.A., Chapman, R., Furrer, H., Jeffrey, G., Cheng, W., Battegay, M., Weber, R. & Telenti, A. 2006, 'Evidence of viral adaptation to HLA class I-restricted immune pressure in chronic hepatitis C virus infection', *Journal of Virology*.

Germer, J.J. & Zein, N.N. 2001, 'Advances in the molecular diagnosis of hepatitis C and their clinical implications', *Mayo Clin Proc*, vol. 76, no. 9, 2001/09/19., pp. 911–20.

Glavan, A.C., Martinez, R. V., Maxwell, E.J., Subramaniam, A.B., Nunes, R.M.D., Soh, S. & Whitesides, G.M. 2013, 'Rapid fabrication of pressure-driven open-channel microfluidic devices in omniphobic RF paper', *Lab on a Chip*, vol. 13, no. 15, p. 2922.

Global Tuberculosis Programme n.d., *The use of loop-mediated isothermal amplification (TB-LAMP) for the diagnosis of pulmonary tuberculosis : policy guidance*.

Gottwein, J.M., Jensen, S.B., Serre, S.B.N., Ghanem, L., Scheel, T.K.H., Jensen, T.B., Krarup, H., Uzcategui, N., Mikkelsen, L.S. & Bukh, J. 2013, 'Adapted J6/JFH1-Based Hepatitis C Virus Recombinants with Genotype-Specific NS4A Show Similar Efficacies against Lead Protease Inhibitors, Alpha Interferon, and a Putative NS4A Inhibitor', *Antimicrobial Agents and Chemotherapy*, vol. 57, no. 12, pp. 6034–49.

Gottwein, J. M., Jensen, T.B., Mathiesen, C.K., Meuleman, P., Serre, S.B.N., Lademann, J.B., Ghanem, L., Scheel, T.K.H., Leroux-Roels, G. & Bukh, J. 2011, 'Development and Application of Hepatitis C Reporter Viruses with Genotype 1 to 7 Core-Nonstructural Protein 2 (NS2) Expressing Fluorescent Proteins or Luciferase in Modified JFH1 NS5A', *Journal of Virology*, vol. 85, no. 17, pp. 8913–28.

Gottwein, J.M., Scheel, T.K.H., Hoegh, A.M., Lademann, J.B., Eugen–Olsen, J., Lisby, G. & Bukh, J. 2007, 'Robust Hepatitis C Genotype 3a Cell Culture Releasing Adapted Intergenotypic 3a/2a (S52/JFH1) Viruses', *Gastroenterology*, vol. 133, no. 5, pp. 1614–26.

Gottwein, Judith M., Scheel, T.K.H., Jensen, T.B., Ghanem, L. & Bukh, J. 2011, 'Differential Efficacy of Protease Inhibitors Against HCV Genotypes 2a, 3a, 5a, and 6a NS3/4A Protease Recombinant Viruses', *Gastroenterology*, vol. 141, no. 3, pp. 1067–79.

Gower, E., Estes, C., Blach, S., Razavi-Shearer, K. & Razavi, H. 2014, 'Global epidemiology and genotype distribution of the hepatitis C virus infection', *J Hepatol*, vol. 61, no. 1 Suppl, 2014/08/03., pp. S45-57.

Grady, B.P., Schinkel, J., Thomas, X. V. & Dalgard, O. 2013, 'Hepatitis C Virus Reinfection Following Treatment Among People Who Use Drugs', *Clinical Infectious Diseases*, vol. 57, no. suppl_2, pp. S105–10.

Grakoui, A., Shoukry, N.H., Woollard, D.J., Han, J.-H., Hanson, H.L., Ghrayeb, J., Murthy, K.K., Rice, C.M. & Walker, C.M. 2003, 'HCV Persistence and Immune Evasion in the Absence of Memory T Cell Help', *Science*, vol. 302, no. 5645, pp. 659–62.

Grakoui, A, Shoukry, N.H., Woollard, D.J., Han, J.H., Hanson, H.L., Ghrayeb, J., Murthy, K.K., Rice, C.M. & Walker, C.M. 2003, 'HCV persistence and immune evasion in the absence of memory T cell help', *Science*, vol. 302, no. 5645, 2003/10/25., pp. 659–62.

Granados, A., Petrich, A., McGeer, A. & Gubbay, J.B. 2017, 'Measuring influenza RNA quantity after prolonged storage or multiple freeze/thaw cycles', *Journal of Virological Methods*, vol. 247, pp. 45–50.

Grebely, J., Lamoury, F.M.J., Hajarizadeh, B., Mowat, Y., Marshall, A.D., Bajis, S., Marks, P., Amin, J., Smith, J., Edwards, M., Gorton, C., Ezard, N., Persing, D., Kleman, M., Cunningham, P., Catlett, B., Dore, G.J., Applegate, T.L. & LiveRLife Study Group 2017, 'Evaluation of the Xpert HCV Viral Load point-of-care assay from venepuncture-collected and finger-stick capillary whole-blood samples: a cohort study', *The Lancet Gastroenterology & Hepatology*, vol. 2, no. 7, pp. 514–20.

Grint, D., Tedaldi, E., Peters, L., Mocroft, A., Edlin, B., Gallien, S., Klinker, H., Boesecke, C., Kokordelis, P. & Rockstroh, J. 2017, 'Hepatitis C virus (HCV) RNA profiles among chronic HIV/HCV-coinfected individuals in ESPRIT; spontaneous HCV RNA clearance observed in nine individuals', *HIV Medicine*, vol. 18, no. 6, pp. 430–4.

Grompe, M., Al-Dhalimy, M., Finegold, M., Ou, C.N., Burlingame, T., Kennaway, N.G. & Soriano, P. 1993, 'Loss of fumarylacetoacetate hydrolase is responsible for the neonatal hepatic dysfunction phenotype of lethal albino mice', *Genes and Development*.

GUIDELINES ON HEPATITIS B AND C TESTING 2017, viewed 2 July 2019, <https://apps.who.int/iris/bitstream/handle/10665/254621/9789241549981-eng.pdf;jsessionid=6439ECFE9481EF89E3E3094732DEB420?sequence=1>.

Gupta, E., Agarwala, P., Kumar, G., Maiwall, R. & Sarin, S.K. 2017, 'Point -of - care testing (POCT) in molecular diagnostics: Performance evaluation of GeneXpert HCV RNA test in diagnosing and monitoring of HCV infection', *Journal of Clinical Virology*, vol. 88, pp. 46–51.

Gurrala, R., Lang, Z., Shepherd, L., Davidson, D., Harrison, E., McClure, M., Kaye, S., Toumazou, C. & Cooke, G.S. 2016, 'Novel pH sensing semiconductor for point-of-care detection of HIV-1 viremia', *Sci Rep*, vol. 6, 2016/11/11., p. 36000.

Guzman-Fulgencio, M., Jimenez, J.L., Berenguer, J., Fernandez-Rodriguez, A., Lopez, J.C., Cosin, J., Miralles, P., Micheloud, D., Munoz-Fernandez, M.A. & Resino, S. 2012, 'Plasma IL-6 and IL-9 predict the failure of interferon- plus ribavirin therapy in HIV/HCV-coinfected patients', *Journal of Antimicrobial Chemotherapy*, vol. 67, no. 5, pp. 1238–45.

Hauri, A.M., Armstrong, G.L. & Hutin, Y.J.F. 2004, 'The global burden of disease attributable to contaminated injections given in health care settings', *International Journal of STD & AIDS*, vol. 15, no. 1, pp. 7–16.

Heckel, J.L., Sandgren, E.P., Degen, J.L., Palmiter, R.D. & Brinster, R.L. 1990, 'Neonatal bleeding in transgenic mice expressing urokinase-type plasminogen activator', *Cell*.

Helle, F., Goffard, A., Morel, V., Duverlie, G., McKeating, J., Keck, Z.-Y., Foung, S., Penin, F., Dubuisson, J. & Voisset, C. 2007, 'The Neutralizing Activity of Anti-Hepatitis C Virus Antibodies Is Modulated by Specific Glycans on the E2 Envelope Protein', *Journal of Virology*.

Hess, K.L., Fisher, D.G. & Reynolds, G.L. 2014, 'Sensitivity and specificity of point-of-care rapid combination syphilis-HIV-HCV tests', *PLoS One*, vol. 9, no. 11, 2014/11/07., p. e112190.

Hijikata, M., Kato, N., Ootsuyama, Y., Nakagawa, M. & Shimotohno, K. 1991, 'Gene mapping of the putative structural region of the hepatitis C virus genome by in vitro processing analysis.', *Proceedings of the National Academy of Sciences of the United States of America*, vol. 88, no. 13, pp. 5547–51.

HitOmi, Y., McDonnell, W.M., Killeen, A.A. & Askari, F.K. 1995, 'Sequence analysis of the hepatitis C virus (HCV) core gene suggests the core protein as an appropriate target for HCV vaccine strategies', *Journal of Viral Hepatitis*.

Honda, M., Brown, E.A. & Lemon, S.M. 1996, 'Stability of a stem-loop involving the initiator AUG controls the efficiency of internal initiation of translation on hepatitis C virus RNA.', *RNA (New York, N.Y.)*, vol. 2, no. 10, pp. 955–68.

Hong, G., Park, K.S., Ki, C.-S. & Lee, N.Y. 2014, 'Evaluation of the illumigene C. difficile assay for toxigenic Clostridium difficile detection: a prospective study of 302 consecutive clinical fecal samples', *Diagnostic Microbiology and Infectious Disease*, vol. 80, no. 3, pp. 177–80.

Hoofnagle, J.H., Mullen, K.D., Jones, D.B., Rustgi, V., Di Bisceglie, A., Peters, M., Waggoner, J.G., Park, Y. & Jones, E.A. 1986, 'Treatment of Chronic Non-A, Non-B Hepatitis with Recombinant Human Alpha Interferon', *New England Journal of Medicine*, vol. 315, no. 25, pp. 1575–8.

Horner, S.M. & Gale, M. 2013, 'Regulation of hepatic innate immunity by hepatitis C virus', *Nature Medicine*, vol. 19, no. 7, pp. 879–88.

Howson, E.L.A., Armson, B., Madi, M., Kasanga, C.J., Kandusi, S., Sallu, R., Chepkwony, E., Siddle, A., Martin, P., Wood, J., Mioulet, V., King, D.P., Lembo, T., Cleaveland, S. & Fowler, V.L. 2017, 'Evaluation of Two Lyophilized Molecular Assays to Rapidly Detect Foot-and-Mouth Disease Virus Directly from Clinical Samples in Field Settings', *Transbound Emerg Dis*, vol. 64, no. 3, 2015/12/01., pp. 861–71.

Hsu, M., Zhang, J., Flint, M., Logvinoff, C., Cheng-Mayer, C., Rice, C.M. & McKeating, J.A. 2003, 'Hepatitis C virus glycoproteins mediate pH-dependent cell entry of pseudotyped retroviral particles', *Proceedings of the National Academy of Sciences*, vol. 100, no. 12, pp. 7271–6.

Ihira, M., Akimoto, S., Miyake, F., Fujita, A., Sugata, K., Suga, S., Ohashi, M., Nishimura, N., Ozaki, T., Asano, Y. & Yoshikawa, T. 2007, 'Direct detection of human herpesvirus 6 DNA in serum by the loop-mediated isothermal amplification method', *J Clin Virol*, vol. 39, no. 1, 2007/03/23., pp. 22–6.

Jacobson, I.M., Gordon, S.C., Kowdley, K. V., Yoshida, E.M., Rodriguez-Torres, M., Sulkowski, M.S., Shiffman, M.L., Lawitz, E., Everson, G., Bennett, M., Schiff, E., Al-Assi, M.T., Subramanian, G.M., An, D., Lin, M., McNally, J., Brainard, D., Symonds, W.T., McHutchison, J.G., Patel, K., Feld, J., Pianko, S. & Nelson, D.R. 2013, 'Sofosbuvir for Hepatitis C Genotype 2 or 3 in Patients without Treatment Options', *New England Journal of Medicine*, vol. 368, no. 20, pp. 1867–77.

Jacobson, I.M., McHutchison, J.G., Dusheiko, G., Di Bisceglie, A.M., Reddy, K.R., Bzowej, N.H., Marcellin, P., Muir, A.J., Ferenci, P., Flisiak, R., George, J., Rizzetto, M., Shouval, D., Sola, R., Terg, R.A., Yoshida, E.M., Adda, N., Bengtsson, L., Sankoh, A.J., Kieffer, T.L., George, S., Kauffman, R.S., Zeuzem, S. & ADVANCE Study Team 2011, 'Telaprevir for Previously Untreated Chronic Hepatitis C Virus Infection', *New England Journal of Medicine*, vol. 364, no. 25, pp. 2405–16.

Jani, I. V., Meggi, B., Vubil, A., Sitoe, N.E., Bhatt, N., Tobaiwa, O., Quevedo, J.I., Loquiha, O., Lehe, J.D., Vojnov, L. & Peter, T.F. 2016, 'Evaluation of the Whole-Blood Alere Q NAT Point-of-Care RNA Assay for HIV-1 Viral Load Monitoring in a Primary Health Care Setting in Mozambique', A.M. Caliendo (ed.),*Journal of Clinical Microbiology*, vol. 54, no. 8, pp. 2104–8.

Jiang, X., Loeb, J.C., Manzanas, C., Lednicky, J.A. & Fan, Z.H. 2018, 'Valve-Enabled Sample Preparation and RNA Amplification in a Coffee Mug for Zika Virus Detection', *Angew Chem Int Ed Engl*, vol. 57, no. 52, 2018/10/26., pp. 17211–4.

de Jong, Y.P., Dorner, M., Mommersteeg, M.C., Xiao, J.W., Balazs, A.B., Robbins, J.B., Winer, B.Y., Gerges, S., Vega, K., Labitt, R.N., Donovan, B.M., Giang, E., Krishnan, A., Chiriboga, L., Charlton, M.R., Burton, D.R., Baltimore, D., Law, M., Rice, C.M. & Ploss, A. 2014, 'Broadly neutralizing antibodies abrogate established hepatitis C virus infection', *Science Translational Medicine*, vol. 6, no. 254, pp. 254ra129-254ra129.

Jost, S. & Altfeld, M. 2013, 'Control of Human Viral Infections by Natural Killer Cells', *Annual Review of Immunology*, vol. 31, no. 1, pp. 163–94.

Kaarj, K., Akarapipad, P. & Yoon, J.-Y. 2018, 'Simpler, Faster, and Sensitive Zika Virus Assay Using Smartphone Detection of Loop-mediated Isothermal Amplification on Paper Microfluidic Chips', *Scientific Reports*, vol. 8, no. 1, p. 12438.

Kamal, S.M., Fehr, J., Roesler, B., Peters, T. & Rasenack, J.W. 2002, 'Peginterferon alone or with ribavirin enhances HCV-specific CD4+ T-helper 1 responses in patients with chronic hepatitis C', *Gastroenterology*, vol. 123, no. 4, pp. 1070–83.

Kamal, S.M., Kassim, S., El Gohary, E., Fouad, A., Nabegh, L., Hafez, T., Bahnasy, K., Hassan, H. & Ghoraba, D. 2015, 'The accuracy and cost-effectiveness of hepatitis C core antigen assay in the monitoring of anti-viral therapy in patients with chronic hepatitis C genotype 4', *Aliment Pharmacol Ther*, vol. 42, no. 3, 2015/05/29., pp. 307–18.

Kania, D., Bekale, A.M., Nagot, N., Mondain, A.M., Ottomani, L., Meda, N., Traore, M., Ouedraogo, J.B., Ducos, J., Van de Perre, P. & Tuaillon, E. 2013, 'Combining rapid diagnostic tests and dried blood spot assays for point-of-care testing of human immunodeficiency virus, hepatitis B and hepatitis C infections in Burkina Faso, West Africa', *Clin Microbiol Infect*, vol. 19, no. 12, 2013/08/02., pp. E533-41.

Kant, J., Moller, B., Heyne, R., Herber, A., Bohm, S., Maier, M., Liebert, U.G., Mossner, J., Berg, T. & Wiegand, J. 2013, 'Evaluation of a rapid on-site anti-HCV test as a screening tool for hepatitis C virus infection', *Eur J Gastroenterol Hepatol*, vol. 25, no. 4, 2012/12/06., pp. 416–20.

Kapoor, A., Simmonds, P., Gerold, G., Qaisar, N., Jain, K., Henriquez, J.A., Firth, C., Hirschberg, D.L., Rice, C.M., Shields, S. & Lipkin, W.I. 2011, 'Characterization of a canine homolog of hepatitis C virus', *Proceedings of the National Academy of Sciences*, vol. 108, no. 28, pp. 11608–13.

Kargar, M., Askari, A., Doosti, A. & Ghorbani-Dalini, S. 2012, 'Loop-Mediated Isothermal Amplification Assay for Rapid Detection of Hepatitis C virus', *Indian J Virol*, vol. 23, no. 1, pp. 18–23.

Karthik, K., Rathore, R., Thomas, P., Arun, T.R., Viswas, K.N., Dhama, K. & Agarwal, R.K. 2014, 'New closed tube loop mediated isothermal amplification assay for prevention of product cross-contamination.', *MethodsX*, vol. 1, pp. 137–43.

Kasprowicz, V., Schulze zur Wiesch, J., Kuntzen, T., Nolan, B.E., Longworth, S., Berical, A., Blum, J., McMahon, C., Reyor, L.L., Elias, N., Kwok, W.W., McGovern, B.G., Freeman, G., Chung, R.T., Klenerman, P., Lewis-Ximenez, L., Walker, B.D., Allen, T.M., Kim, A.Y. & Lauer, G.M. 2008, 'High Level of PD-1 Expression on Hepatitis C Virus (HCV)-Specific CD8+ and CD4+ T Cells during Acute HCV Infection, Irrespective of Clinical Outcome', *Journal of Virology*.

Kato, T., Furusaka, A., Miyamoto, M., Date, T., Yasui, K., Hiramoto, J., Nagayama, K., Tanaka, T. & Wakita, T. 2001, 'Sequence analysis of hepatitis C virus isolated from a fulminant hepatitis patient', *J Med Virol*, vol. 64, no. 3, 2001/06/26., pp. 334–9.

Kato, T., Miyamoto, M., Date, T., Furusaka, A., Hiramoto, J., Nagayama, K., Tsai, N., Mizokami, M. & Wakita, T. 2004, 'Differences in hepatitis C virus core protein processing among genotypes 1 and 2', *Hepatology Research*.

Kelly, C., Swadling, L., Brown, A., Capone, S., Folgori, A., Salio, M., Klenerman, P. & Barnes, E. 2015, 'Cross-reactivity of hepatitis C virus specific vaccine-induced T cells at immunodominant epitopes', *European Journal of Immunology*.

Khan, A.G., Whidby, J., Miller, M.T., Scarborough, H., Zatorski, A. V., Cygan, A., Price, A.A., Yost, S.A., Bohannon, C.D., Jacob, J., Grakoui, A. & Marcotrigiano, J. 2014, 'Structure of the core ectodomain of the hepatitis C virus envelope glycoprotein 2', *Nature*, vol. 509, no. 7500, pp. 381–4.

Kim, D.D., Hutton, D.W., Raouf, A.A., Salama, M., Hablas, A., Seifeldin, I.A. & Soliman, A.S. 2015, 'Cost-effectiveness model for hepatitis C screening and treatment: Implications for Egypt and other countries with high prevalence', *Glob Public Health*, vol. 10, no. 3, 2014/12/04., pp. 296–317.

Kittlesen, D.J., Chianese-Bullock, K.A., Yao, Z.Q., Braciale, T.J. & Hahn, Y.S. 2000, 'Interaction between complement receptor gC1qR and hepatitis C virus core protein inhibits T-lymphocyte proliferation', *Journal of Clinical Investigation*.

Klenerman, P. & Thimme, R. 2012, 'T cell responses in hepatitis C: The good, the bad and the unconventional', *Gut*.

Kline, G.M., Shen, Z., Mohiuddin, M., Ruggiero, V., Rostami, S. & DiSesa, V.J. 1994, 'Development of tolerance to experimental cardiac allografts in utero', *The Annals of Thoracic Surgery*.

Klostranec, J.M., Xiang, Q., Farcas, G.A., Lee, J.A., Rhee, A., Lafferty, E.I., Perrault, S.D., Kain, K.C. & Chan, W.C. 2007, 'Convergence of quantum dot barcodes with microfluidics and signal processing for multiplexed high-throughput infectious disease diagnostics', *Nano Lett*, vol. 7, no. 9, 2007/08/21., pp. 2812–8.

Kokordelis, P., Krämer, B., Körner, C., Boesecke, C., Voigt, E., Ingiliz, P., Glässner, A., Eisenhardt, M., Wolter, F., Kaczmarek, D., Nischalke, H.D., Rockstroh, J.K., Spengler, U. & Nattermann, J. 2014, 'An effective interferon-gamma-mediated inhibition of hepatitis C virus replication by natural killer cells is associated with spontaneous clearance of acute hepatitis C in human immunodeficiency virus-positive patients', *Hepatology*, vol. 59, no. 3, pp. 814–27.

Kolykhalov, A.A., Feinstone, S.M. & Rice, C.M. 1996, 'Identification of a highly conserved sequence element at the 3' terminus of hepatitis C virus genome RNA.', *Journal of virology*, vol. 70, no. 6, pp. 3363–71.

Kong, L., Giang, E., Nieusma, T., Kadam, R.U., Cogburn, K.E., Hua, Y., Dai, X., Stanfield, R.L., Burton, D.R., Ward, A.B., Wilson, I.A. & Law, M. 2013, 'Hepatitis C Virus E2 Envelope Glycoprotein Core Structure', *Science*, vol. 342, no. 6162, pp. 1090–4.

Kong, L., Kadam, R.U., Giang, E., Ruwona, T.B., Nieusma, T., Culhane, J.C., Stanfield, R.L., Dawson, P.E., Wilson, I.A. & Law, M. 2015, 'Structure of Hepatitis C Virus Envelope Glycoprotein E1 Antigenic Site 314-324 in Complex with Antibody IGH526', *Journal of Molecular Biology*.

Kosack, C.S., Nick, S. & Shanks, L. 2014, 'Diagnostic accuracy evaluation of the ImmunoFlow HCV rapid immunochromatographic test for the detection of hepatitis C antibodies', *J Virol Methods*, vol. 204, 2014/04/15., pp. 6–10.

Kumthip, K. & Maneekarn, N. 2015, 'The role of HCV proteins on treatment outcomes', *Virology Journal*, vol. 12, no. 1, p. 217.

Kuniholm, M.H., O'Brien, T.R., Prokunina-Olsson, L., Augenbraun, M., Plankey, M., Karim, R., Sarkar, M., French, A.L., Pierce, C., Strickler, H.D. & Anastos, K. 2016, 'Association of Hepatitis C Virus Infection With CD4/CD8 Ratio in HIV-Positive Women.', *Journal of acquired immune deficiency syndromes (1999)*, vol. 72, no. 2, pp. 162–70.

Kupek, E. 2004, 'Transfusion risk for hepatitis B, hepatitis C and HIV in the state of Santa Catarina, Brazil, 1991-2001', *Brazilian Journal of Infectious Diseases*, vol. 8, no. 3, pp. 236–40.

Lalle, M., Possenti, A., Dubey, J.P. & Pozio, E. 2018, 'Loop-Mediated Isothermal Amplification-Lateral-Flow Dipstick (LAMP-LFD) to detect Toxoplasma gondii oocyst in ready-to-eat salad', *Food Microbiology*, vol. 70, pp. 137–42.

Lamb, L.E., Bartolone, S.N., Tree, M.O., Conway, M.J., Rossignol, J., Smith, C.P. & Chancellor, M.B. 2018, 'Rapid Detection of Zika Virus in Urine Samples and Infected Mosquitos by Reverse Transcription-Loop-Mediated Isothermal Amplification', *Sci Rep*, vol. 8, no. 1, 2018/03/02., p. 3803.

Lamoury, F.M.J., Bajis, S., Hajarizadeh, B., Marshall, A.D., Martinello, M., Ivanova, E., Catlett, B., Mowat, Y., Marks, P., Amin, J., Smith, J., Ezard, N., Cock, V., Hayllar, J., Persing, D.H., Kleman, M., Cunningham, P., Dore, G.J., Applegate, T.L. & Grebely, J. 2018, 'Evaluation of the Xpert HCV Viral Load Finger-Stick Point-of-Care Assay', *The Journal of Infectious Diseases*, vol. 217, no. 12, pp. 1889–96.

Lanford, R.E., Bigger, C., Bassett, S. & Klimpel, G. 2001, 'The Chimpanzee Model of Hepatitis C Virus Infections', *ILAR Journal*, vol. 42, no. 2, pp. 117–26.

Larrat, S., Bourdon, C., Baccard, M., Garnaud, C., Mathieu, S., Quesada, J.L., Signori-Schmuck, A., Germi, R., Blanc, M., Leclercq, P., Hilleret, M.N., Leroy, V., Zarski, J.P. & Morand, P. 2012, 'Performance of an antigen-antibody combined assay for hepatitis C virus testing without venipuncture', *J Clin Virol*, vol. 55, no. 3, 2012/08/21., pp. 220–5.

Lau, D.T. –Y., Negash, A., Chen, J., Crochet, N., Sinha, M., Zhang, Y., Guedj, J., Holder, S., Saito, T., Lemon, S.M., Luxon, B.A., Perelson, A.S. & Gale, M. 2013, 'Innate Immune Tolerance and the Role of Kupffer Cells in Differential Responses to Interferon Therapy Among Patients With HCV Genotype 1 Infection', *Gastroenterology*, vol. 144, no. 2, pp. 402-413.e12.

Lau, D.T., Kleiner, D.E., Ghany, M.G., Park, Y., Schmid, P. & Hoofnagle, J.H. 1998, '10-year follow-up after interferon-? therapy for chronic hepatitis C', *Hepatology*, vol. 28, no. 4, pp. 1121–7.

Lauer, G.M., Barnes, E., Lucas, M., Timm, J., Ouchi, K., Kim, A.Y., Day, C.L., Robbins, G.K., Casson, D.R., Reiser, M., Dusheiko, G., Allen, T.M., Chung, R.T., Walker, B.D. & Klenerman, P. 2004, 'High resolution analysis of cellular immune responses in resolved and persistent hepatitis C virus infection', *Gastroenterology*.

Lauer, G.M., Ouchi, K., Chung, R.T., Nguyen, T.N., Day, C.L., Purkis, D.R., Reiser, M., Kim, A.Y., Lucas, M., Klenerman, P. & Walker, B.D. 2002, 'Comprehensive Analysis of CD8+-T-Cell Responses against Hepatitis C Virus Reveals Multiple Unpredicted Specificities', *Journal of Virology*.

Lavillette, D., Tarr, A.W., Voisset, C., Donot, P., Bartosch, B., Bain, C., Patel, A.H., Dubuisson, J., Ball, J.K. & Cosset, F.L. 2005, 'Characterization of host-range and cell entry properties of the major genotypes and subtypes of hepatitis C virus', *Hepatology*, vol. 41, no. 2, 2005/01/22., pp. 265–74.

Law, J.L.M., Chen, C., Wong, J., Hockman, D., Santer, D.M., Frey, S.E., Belshe, R.B., Wakita, T., Bukh, J., Jones, C.T., Rice, C.M., Abrignani, S., Tyrrell, D.L. & Houghton, M. 2013, 'A Hepatitis C Virus (HCV) Vaccine Comprising Envelope Glycoproteins gpE1/gpE2 Derived from a Single Isolate Elicits Broad Cross-Genotype Neutralizing Antibodies in Humans', *PLoS ONE*.

Law, M. n.d., *Hepatitis C virus protocols*, 2019, 'edn 3', Humana Press, New York, USA.

Law, M., Maruyama, T., Lewis, J., Giang, E., Tarr, A.W., Stamataki, Z., Gastaminza, P., Chisari, F. V, Jones, I.M., Fox, R.I., Ball, J.K., McKeating, J.A., Kneteman, N.M. & Burton, D.R. 2008, 'Broadly neutralizing antibodies protect against hepatitis C virus quasispecies challenge', *Nature Medicine*, vol. 14, no. 1, pp. 25–7.

Lawitz, E., Mangia, A., Wyles, D., Rodriguez-Torres, M., Hassanein, T., Gordon, S.C., Schultz, M., Davis, M.N., Kayali, Z., Reddy, K.R., Jacobson, I.M., Kowdley, K. V., Nyberg, L., Subramanian, G.M., Hyland, R.H., Arterburn, S., Jiang, D., McNally, J., Brainard, D., Symonds, W.T., McHutchison, J.G., Sheikh, A.M., Younossi, Z. & Gane, E.J. 2013, 'Sofosbuvir for Previously Untreated Chronic Hepatitis C Infection', *New England Journal of Medicine*, vol. 368, no. 20, pp. 1878–87.

Lechner, F., Wong, D.K.H., Dunbar, P.R., Chapman, R., Chung, R.T., Dohrenwend, P., Robbins, G., Phillips, R., Klenerman, P. & Walker, B.D. 2000a, 'Analysis of Successful Immune Responses in Persons Infected with Hepatitis C Virus', *The Journal of Experimental Medicine*.

Lechner, F., Wong, D.K.H., Dunbar, P.R., Chapman, R., Chung, R.T., Dohrenwend, P., Robbins, G., Phillips, R., Klenerman, P. & Walker, B.D. 2000b, 'Analysis of Successful Immune Responses in Persons Infected with Hepatitis C Virus', *The Journal of Experimental Medicine*, vol. 191, no. 9, pp. 1499–512.

Lee, S.R., Kardos, K.W., Schiff, E., Berne, C.A., Mounzer, K., Banks, A.T., Tatum, H.A., Friel, T.J., Demicco, M.P., Lee, W.M., Eder, S.E., Monto, A., Yearwood, G.D., Guillon, G.B., Kurtz, L.A., Fischl, M., Unangst, J.L., Kriebel, L., Feiss, G. & Roehler, M. 2011, 'Evaluation of a new, rapid test for detecting HCV infection, suitable for use with blood or oral fluid', *J Virol Methods*, vol. 172, no. 1–2, 2010/12/25., pp. 27–31.

Lee, S.R., Yearwood, G.D., Guillon, G.B., Kurtz, L.A., Fischl, M., Friel, T., Berne, C.A. & Kardos, K.W. 2010, 'Evaluation of a rapid, point-of-care test device for the diagnosis of hepatitis C infection.', *Journal of clinical virology : the official publication of the Pan American Society for Clinical Virology*, vol. 48, no. 1, pp. 15–7.

Lee, S.W., Cho, J.H. & Sung, Y.C. 1998, 'Optimal induction of hepatitis C virus envelope-specific immunity by bicistronic plasmid DNA inoculation with the granulocyte-macrophage colony-stimulating factor gene.', *Journal of virology*, vol. 72, no. 10, pp. 8430–6.

Li, S., Liu, Y., Wang, Yue, Chen, H., Liu, C. & Wang, Yi 2019, 'Lateral flow biosensor combined with loop-mediated isothermal amplification for simple, rapid, sensitive, and reliable detection of Brucella spp.', *Infection and drug resistance*, vol. 12, pp. 2343–53.

Li, Y.-P., Ramirez, S., Jensen, S.B., Purcell, R.H., Gottwein, J.M. & Bukh, J. 2012, 'Highly efficient full-length hepatitis C virus genotype 1 (strain TN) infectious culture system', *Proceedings of the National Academy of Sciences*, vol. 109, no. 48, pp. 19757–62.

Lin, W., Kim, S.S., Yeung, E., Kamegaya, Y., Blackard, J.T., Kim, K.A., Holtzman, M.J. & Chung, R.T. 2006, 'Hepatitis C Virus Core Protein Blocks Interferon Signaling by Interaction with the STAT1 SH2 Domain', *Journal of Virology*.

Linas, B.P., Wong, A.Y., Schackman, B.R., Kim, A.Y. & Freedberg, K.A. 2012, 'Cost-effective screening for acute hepatitis C virus infection in HIV-infected men who have sex with men', *Clin Infect Dis*, vol. 55, no. 2, 2012/04/12., pp. 279–90.

Lindenbach, B.D. 2005, 'Complete Replication of Hepatitis C Virus in Cell Culture', *Science*, vol. 309, no. 5734, pp. 623–6.

Lindenbach, B.D., Meuleman, P., Ploss, A., Vanwolleghem, T., Syder, A.J., McKeating, J.A., Lanford, R.E., Feinstone, S.M., Major, M.E., Leroux-Roels, G. & Rice, C.M. 2006, 'Cell culture-grown hepatitis C virus is infectious in vivo and can be recultured in vitro', *Proceedings of the National Academy of Sciences*, vol. 103, no. 10, pp. 3805–9.

Liu, D., He, W., Jiang, M., Zhao, B., Ou, X., Liu, C., Xia, H., Zhou, Y., Wang, S., Song, Y., Zheng, Y., Chen, Q., Fan, J., He, G. & Zhao, Y. 2019, 'Development of a loop-mediated isothermal amplification coupled lateral flow dipstick targeting erm(41) for detection of Mycobacterium abscessus and Mycobacterium massiliense', *AMB Express*, vol. 9, no. 1, p. 11.

Liu, S., Chen, R. & Hagedorn, C.H. 2014, 'Direct visualization of hepatitis C virus-infected Huh7.5 cells with a high titre of infectious chimeric JFH1-EGFP reporter virus in three-dimensional Matrigel cell cultures', *Journal of General Virology*, vol. 95, no. Pt_2, pp. 423–33.

Liu, S., Xiao, L., Nelson, C., Hagedorn, C. & Hagedorn, C. 2012, 'A Cell Culture Adapted HCV JFH1 Variant That Increases Viral Titers and Permits the Production of High Titer Infectious Chimeric Reporter Viruses', S.K. Jang (ed.),*PLoS ONE*, vol. 7, no. 9, p. e44965.

Llibre, Alba, Shimakawa, Y., Mottez, E., Ainsworth, S., Buivan, T.-P., Firth, R., Harrison, E., Rosenberg, A.R., Meritet, J.-F., Fontanet, A., Castan, P., Madejón, A., Laverick, M., Glass, A., Viana, R., Pol, S., McClure, C.P., Irving, W.L., Miele, G., Albert, M.L. & Duffy, D. 2018, 'Development and clinical validation of the Genedrive point-of-care test for qualitative detection of hepatitis C virus', *Gut*, vol. 67, no. 11, pp. 2017–24.

Llibre, A, Shimakawa, Y., Mottez, E., Ainsworth, S., Buivan, T.P., Firth, R., Harrison, E., Rosenberg, A.R., Meritet, J.F., Fontanet, A., Castan, P., Madejon, A., Laverick, M., Glass, A., Viana, R., Pol, S., McClure, C.P., Irving, W.L., Miele, G., Albert, M.L. & Duffy, D. 2018, 'Development and clinical validation of the Genedrive point-of-care test for qualitative detection of hepatitis C virus', *Gut*, vol. 67, no. 11, 2018/04/05., pp. 2017–24.

Lohmann, V., Hoffmann, S., Herian, U., Penin, F. & Bartenschlager, R. 2003, 'Viral and cellular determinants of hepatitis C virus RNA replication in cell culture.', *Journal of virology*, vol. 77, no. 5, pp. 3007–19.

Lohmann, V., Korner, F., Dobierzewska, A. & Bartenschlager, R. 2001, 'Mutations in Hepatitis C Virus RNAs Conferring Cell Culture Adaptation', *Journal of Virology*, vol. 75, no. 3, pp. 1437–49.

Lohmann, V., Körner, F., Koch, J., Herian, U., Theilmann, L. & Bartenschlager, R. 1999, 'Replication of Subgenomic Hepatitis C Virus RNAs in a Hepatoma Cell Line', *Science*, vol. 285, no. 5424, pp. 110–3.

Lubelchek, R., Kroc, K., Hota, B., Sharief, R., Muppudi, U., Pulvirenti, J. & Weinstein, R.A. 2005, 'The Role of Rapid vs Conventional Human Immunodeficiency Virus Testing for Inpatients', *Archives of Internal Medicine*, vol. 165, no. 17, p. 1956.

Magder, L.S., Fix, A.D., Mikhail, N.N., Mohamed, M.K., Abdel-Hamid, M., Abdel-Aziz, F., Medhat, A. & Strickland, G.T. 2004, 'Estimation of the risk of transmission of hepatitis C between spouses in Egypt based on seroprevalence data', *International Journal of Epidemiology*, vol. 34, no. 1, pp. 160–5.

Magiorkinis, G., Magiorkinis, E., Paraskevis, D., Ho, S.Y.W., Shapiro, B., Pybus, O.G., Allain, J.-P. & Hatzakis, A. 2009, 'The Global Spread of Hepatitis C Virus 1a and 1b: A Phylodynamic and Phylogeographic Analysis', A.Y. Kim (ed.),*PLoS Medicine*, vol. 6, no. 12, p. e1000198.

Magro, L., Jacquelin, B., Escadafal, C., Garneret, P., Kwasiborski, A., Manuguerra, J.-C., Monti, F., Sakuntabhai, A., Vanhomwegen, J., Lafaye, P. & Tabeling, P. 2017, 'Paper-based RNA detection and multiplexed analysis for Ebola virus diagnostics', *Scientific Reports*, vol. 7, p. 1347.

Major, M.E., Mihalik, K., Fernandez, J., Seidman, J., Kleiner, D., Kolykhalov, A.A., Rice, C.M. & Feinstone, S.M. 1999, 'Long-term follow-up of chimpanzees inoculated with the first infectious clone for hepatitis C virus.', *Journal of virology*.

Major, M.E., Mihalik, K., Puig, M., Rehermann, B., Nascimbeni, M., Rice, C.M. & Feinstone, S.M. 2002, 'Previously infected and recovered chimpanzees exhibit rapid responses that control hepatitis C virus replication upon rechallenge.', *Journal of virology*, vol. 76, no. 13, pp. 6586–95.

Manns, M., Marcellin, P., Poordad, F., de Araujo, E.S.A., Buti, M., Horsmans, Y., Janczewska, E., Villamil, F., Scott, J., Peeters, M., Lenz, O., Ouwerkerk-Mahadevan, S., De La Rosa, G., Kalmeijer, R., Sinha, R. & Beumont-Mauviel, M. 2014, 'Simeprevir with pegylated interferon alfa 2a or 2b plus ribavirin in treatment-naive patients with chronic hepatitis C virus genotype 1 infection (QUEST-2): a randomised, double-blind, placebo-controlled phase 3 trial', *The Lancet*, vol. 384, no. 9941, pp. 414–26.

Mao, F., Leung, W.-Y. & Xin, X. 2007, 'Characterization of EvaGreen and the implication of its physicochemical properties for qPCR applications', *BMC biotechnology*, vol. 7, p. 76.

Marcellin, P. 1997, 'Long-Term Histologic Improvement and Loss of Detectable Intrahepatic HCV RNA in Patients with Chronic Hepatitis C and Sustained Response to Interferon-α Therapy', *Annals of Internal Medicine*, vol. 127, no. 10, p. 875.

Martin, L.R., Duke, G.M., Osorio, J.E., Hall, D.J. & Palmenberg, A.C. 1996, 'Mutational analysis of the mengovirus poly(C) tract and surrounding heteropolymeric sequences.', *Journal of virology*, vol. 70, no. 3, pp. 2027–31.

Martin, N.K., Vickerman, P., Foster, G.R., Hutchinson, S.J., Goldberg, D.J. & Hickman, M. 2011, 'Can antiviral therapy for hepatitis C reduce the prevalence of HCV among injecting drug user populations? A modeling analysis of its prevention utility', *J Hepatol*, vol. 54, no. 6, 2010/12/15., pp. 1137–44.

Martinez, A.W., Phillips, S.T., Butte, M.J. & Whitesides, G.M. 2007, 'Patterned Paper as a Platform for Inexpensive, Low-Volume, Portable Bioassays', *Angewandte Chemie International Edition*, vol. 46, no. 8, pp. 1318–20.

Mast, E.E., Hwang, L., Seto, D.S.Y., Nolte, F.S., Nainan, O.V., Wurtzel, H. & Alter, M.J. 2005, 'Risk Factors for Perinatal Transmission of Hepatitis C Virus (HCV) and the Natural History of HCV Infection Acquired in Infancy', *The Journal of Infectious Diseases*, vol. 192, no. 11, pp. 1880–9.

Mazumdar, B., Banerjee, A., Meyer, K. & Ray, R. 2011, 'Hepatitis C virus E1 envelope glycoprotein interacts with apolipoproteins in facilitating entry into hepatocytes', *Hepatology*.

McHugh, M.P., Wu, A.H.B., Chevaliez, S., Pawlotsky, J.M., Hallin, M. & Templeton, K.E. 2017, 'Multicenter Evaluation of the Cepheid Xpert Hepatitis C Virus Viral Load Assay', Y.-W. Tang (ed.),*Journal of Clinical Microbiology*, vol. 55, no. 5, pp. 1550–6.

McHutchison, J.G., Gordon, S.C., Schiff, E.R., Shiffman, M.L., Lee, W.M., Rustgi, V.K., Goodman, Z.D., Ling, M.-H., Cort, S. & Albrecht, J.K. 1998, 'Interferon Alfa-2b Alone or in Combination with Ribavirin as Initial Treatment for Chronic Hepatitis C', *New England Journal of Medicine*, vol. 339, no. 21, pp. 1485–92.

McMahan, R.H., Golden-Mason, L., Nishimura, M.I., McMahon, B.J., Kemper, M., Allen, T.M., Gretch, D.R. & Rosen, H.R. 2010, 'Tim-3 expression on PD-1+ HCV-specific human CTLs is associated with viral persistence, and its blockade restores hepatocyte-directed in vitro cytotoxicity', *Journal of Clinical Investigation*.

Membreno, F.E. & Lawitz, E.J. 2011, 'The HCV NS5B Nucleoside and Non-Nucleoside Inhibitors', *Clinics in Liver Disease*, vol. 15, no. 3, pp. 611–26.

Messina, J.P., Humphreys, I., Flaxman, A., Brown, A., Cooke, G.S., Pybus, O.G. & Barnes, E. 2015, 'Global distribution and prevalence of hepatitis C virus genotypes', *Hepatology*, vol. 61, no. 1, pp. 77–87.

Meuleman, P. & Leroux-Roels, G. 2008, 'The human liver-uPA-SCID mouse: A model for the evaluation of antiviral compounds against HBV and HCV', *Antiviral Research*.

Meunier, J.-C., Gottwein, J.M., Houghton, M., Russell, R.S., Emerson, S.U., Bukh, J. & Purcell, R.H. 2011, 'Vaccine-induced cross-genotype reactive neutralizing antibodies against hepatitis C virus.', *The Journal of infectious diseases*, vol. 204, no. 8, pp. 1186–90.

Meyer-Olson, D., Shoukry, N.H., Brady, K.W., Kim, H., Olson, D.P., Hartman, K., Shintani, A.K., Walker, C.M. & Kalams, S.A. 2004, 'Limited T cell receptor diversity of HCV-specific T cell responses is associated with CTL escape.', *The Journal of experimental medicine*, vol. 200, no. 3, pp. 307–19.

Micallef, J.M., Kaldor, J.M. & Dore, G.J. 2006, 'Spontaneous viral clearance following acute hepatitis C infection: a systematic review of longitudinal studies', *J Viral Hepat*, vol. 13, no. 1, 2005/12/21., pp. 34–41.

Michalak, J.P., Wychowski, C., Choukhi, A., Meunier, J.C., Ung, S., Rice, C.M. & Dubuisson, J. 1997, 'Characterization of truncated forms of hepatitis C virus glycoproteins', *Journal of General Virology*.

Mikkelsen, M., Holst, P.J., Bukh, J., Thomsen, A.R. & Christensen, J.P. 2011, 'Enhanced and Sustained CD8 $^{+}$ T Cell Responses with an Adenoviral Vector-Based Hepatitis C Virus Vaccine Encoding NS3 Linked to the MHC Class II Chaperone Protein Invariant Chain', *The Journal of Immunology*, vol. 186, no. 4, pp. 2355–64.

Miranda, J.A. & Steward, G.F. 2017, 'Variables influencing the efficiency and interpretation of reverse transcription quantitative PCR (RT-qPCR): An empirical study using Bacteriophage MS2', *Journal of Virological Methods*, vol. 241, pp. 1–10.

Missale, G., Bertoni, R., Lamonaca, V., Valli, A., Massari, M., Mori, C., Rumi, M.G., Houghton, M., Fiaccadori, F. & Ferrari, C. 1996, 'Different clinical behaviors of acute hepatitis C virus infection are associated with different vigor of the anti-viral cell-mediated immune response.', *Journal of Clinical Investigation*, vol. 98, no. 3, pp. 706–14.

Miyamoto, S, Sano, S., Takahashi, K. & Jikihara, T. 2015, 'Method for colorimetric detection of double-stranded nucleic acid using leuco triphenylmethane dyes', *Anal Biochem*, vol. 473, 2015/01/13., pp. 28–33.

Miyamoto, Shigehiko, Sano, S., Takahashi, K. & Jikihara, T. 2015, 'Method for colorimetric detection of double-stranded nucleic acid using leuco triphenylmethane dyes', *Analytical Biochemistry*, vol. 473, pp. 28–33.

Mohd Hanafiah, K., Groeger, J., Flaxman, A.D. & Wiersma, S.T. 2013, 'Global epidemiology of hepatitis C virus infection: new estimates of age-specific antibody to HCV seroprevalence.', *Hepatology (Baltimore, Md.)*, vol. 57, no. 4, pp. 1333–42.

Mondelli, M.U., Cerino, A. & Cividini, A. 2005, 'Acute hepatitis C: diagnosis and management', *Journal of Hepatology*, vol. 42, no. 1, pp. S108–14.

Mori, Y., Nagamine, K., Tomita, N. & Notomi, T. 2001, 'Detection of loop-mediated isothermal amplification reaction by turbidity derived from magnesium pyrophosphate formation', *Biochem Biophys Res Commun*, vol. 289, no. 1, 2001/11/16., pp. 150–4.

Mori, Y. & Notomi, T. 2009, 'Loop-mediated isothermal amplification (LAMP): a rapid, accurate, and cost-effective diagnostic method for infectious diseases', *Journal of Infection and Chemotherapy*, vol. 15, no. 2, pp. 62–9.

Morin, T.J., Broering, T.J., Leav, B.A., Blair, B.M., Rowley, K.J., Boucher, E.N., Wang, Y., Cheslock, P.S., Knauber, M., Olsen, D.B., Ludmerer, S.W., Szabo, G., Finberg, R.W., Purcell, R.H., Lanford, R.E., Ambrosino, D.M., Molrine, D.C. & Babcock, G.J. 2012, 'Human Monoclonal Antibody HCV1 Effectively Prevents and Treats HCV Infection in Chimpanzees', *PLoS Pathogens*.

Muchmore, E., Popper, H., Peterson, D.A., Miller, M.F. & Lieberman, H.M. 1988, 'Non-A, non-B hepatitis-related hepatocellular carcinoma in a chimpanzee.', *Journal of medical primatology*, vol. 17, no. 5, pp. 235–46.

Mvere, D., Constantine, N.T., Katsawde, E., Tobaiwa, O., Dambire, S. & Corcoran, P. 1996, 'Rapid and simple hepatitis assays: encouraging results from a blood donor population in Zimbabwe', *Bull World Health Organ*, vol. 74, no. 1, 1996/01/01., pp. 19–24.

Nagamine, K., Hase, T. & Notomi, T. 2002, 'Accelerated reaction by loop-mediated isothermal amplification using loop primers', *Mol Cell Probes*, vol. 16, no. 3, 2002/07/30., pp. 223–9.

Nagamine, K., Kuzuhara, Y. & Notomi, T. 2002, 'Isolation of Single-Stranded DNA from Loop-Mediated Isothermal Amplification Products', *Biochemical and Biophysical Research Communications*, vol. 290, no. 4, pp. 1195–8.

Nakamoto, N., Cho, H., Shaked, A., Olthoff, K., Valiga, M.E., Kaminski, M., Gostick, E., Price, D.A., Freeman, G.J., Wherry, E.J. & Chang, K.M. 2009, 'Synergistic reversal of intrahepatic HCV-specific CD8 T cell exhaustion by combined PD-1/CTLA-4 blockade', *PLoS Pathogens*.

Nattermann, J., Schneiders, A.M., Leifeld, L., Langhans, B., Schulz, M., Inchauspé, G., Matz, B., Brackmann, H.H., Houghton, M., Sauerbruch, T. & Spengler, U. 2005, 'Serum antibodies against the hepatitis C virus E2 protein mediate antibody-dependent cellular cytotoxicity (ADCC)', *Journal of Hepatology*.

Nelson, P.K., Mathers, B.M., Cowie, B., Hagan, H., Des Jarlais, D., Horyniak, D. & Degenhardt, L. 2011, 'Global epidemiology of hepatitis B and hepatitis C in people who inject drugs: results of systematic reviews', *Lancet*, vol. 378, no. 9791, 2011/08/02., pp. 571–83.

Netski, D.M., Mosbruger, T., Depla, E., Maertens, G., Ray, S.C., Hamilton, R.G., Roundtree, S., Thomas, D.L., McKeating, J. & Cox, A. 2005, 'Humoral immune response in acute hepatitis C virus infection', *Clin Infect Dis*, vol. 41, no. 5, pp. 667–75.

Neumann-Haefelin, C., McKiernan, S., Ward, S., Viazov, S., Spangenberg, H.C., Killinger, T., Baumert, T.F., Nazarova, N., Sheridan, I., Pybus, O., Von Weizsäcker, F., Roggendorf, M., Kelleher, D., Klenerman, P., Blum, H.E. & Thimme, R. 2006, 'Dominant influence of an HLA-B27 restricted CD8+ T cell response in mediating HCV clearance and evolution', *Hepatology*.

Nguyen, H., Sankaran, S. & Dandekar, S. 2006, 'Hepatitis C virus core protein induces expression of genes regulating immune evasion and anti-apoptosis in hepatocytes', *Virology*, vol. 354, no. 1, pp. 58–68.

Niebel, M., Singer, J.B., Nickbakhsh, S., Gifford, R.J. & Thomson, E.C. 2017, 'Hepatitis C and the absence of genomic data in low-income countries: a barrier on the road to elimination?', *The lancet. Gastroenterology & hepatology*, vol. 2, no. 10, pp. 700–1.

Nieva, J.L., Madan, V. & Carrasco, L. 2012, 'Viroporins: structure and biological functions', *Nature Reviews Microbiology*, vol. 10, no. 8, pp. 563–74.

Norhazlin, J., Nor-Ashikin, M.N.K., Hoh, B.P., Sheikh Abdul Kadir, S.H., Norita, S., Mohd-Fazirul, M., Wan-Hafizah, W.J., Razif, D., Rajikin, M.H. & Abdullah, B. 2015, 'Effect of DNase treatment on RNA extraction from preimplantation murine embryos', *Genetics and Molecular Research*, vol. 14, no. 3, pp. 10172–84.

Notomi, T., Mori, Y., Tomita, N. & Kanda, H. 2015, 'Loop-mediated isothermal amplification (LAMP): principle, features, and future prospects', *J Microbiol*, vol. 53, no. 1, 2015/01/06., pp. 1–5.

Notomi, T., Okayama, H., Masubuchi, H., Yonekawa, T., Watanabe, K., Amino, N. & Hase, T. 2000a, 'Loop-mediated isothermal amplification of DNA', *Nucleic Acids Res*, vol. 28, no. 12, p. E63.

Notomi, T., Okayama, H., Masubuchi, H., Yonekawa, T., Watanabe, K., Amino, N. & Hase, T. 2000b, 'Loop-mediated isothermal amplification of DNA', *Nucleic Acids Res*, vol. 28, no. 12, 2000/06/28., p. E63.

Nyan, D.-C. & Swinson, K.L. 2016, 'A method for rapid detection and genotype identification of hepatitis C virus 1–6 by one-step reverse transcription loop-mediated isothermal amplification', *International Journal of Infectious Diseases*, vol. 43, pp. 30–6.

Nyan, D.C., Ulitzky, L.E., Cehan, N., Williamson, P., Winkelman, V., Rios, M. & Taylor, D.R. 2014, 'Rapid detection of hepatitis B virus in blood plasma by a specific and sensitive loop-mediated isothermal amplification assay', *Clin Infect Dis*, vol. 59, no. 1, pp. 16–23.

Nyirenda, M., Beadsworth, M.B., Stephany, P., Hart, C.A., Hart, I.J., Munthali, C., Beeching, N.J. & Zijlstra, E.E. 2008, 'Prevalence of infection with hepatitis B and C virus and coinfection with HIV in medical inpatients in Malawi', *J Infect*, vol. 57, no. 1, 2008/06/17., pp. 72–7.

Organization, W.H. 2016a, *COMBATING HEPATITIS B AND C TO REACH ELIMINATION BY 2030*.

Organization, W.H. 2016b, 'Guidelines for the screening, care and treatment of persons with chronic hepatitis c infection. Section 5: Recommendations on Screening.', *Geneva: World Health Organization*, vol. 2016:43-9.

Osburn, W O, Snider, A.E., Wells, B.L., Latanich, R., Bailey, J.R., Thomas, D.L., Cox, A.L. & Ray, S.C. 2014, 'Clearance of Hepatitis C infection is associated with early appearance of broad neutralizing antibody responses', *Hepatology*, vol. 59, no. 6, pp. 2140–51.

Osburn, William O, Snider, A.E., Wells, B.L., Latanich, R., Bailey, J.R., Thomas, D.L., Cox, A.L. & Ray, S.C. 2014, 'Clearance of hepatitis C infection is associated with the early appearance of broad neutralizing antibody responses.', *Hepatology (Baltimore, Md.)*, vol. 59, no. 6, pp. 2140–51.

Ouyang, E.C., Wu, C.H., Walton, C., Promrat, K. & Wu, G.Y. 2001, 'Transplantation of human hepatocytes into tolerized genetically immunocompetent rats', *World Journal of Gastroenterology*.

Overturf, K., Al-Dhalimy, M., Tanguay, R., Brantly, M., Ou, C.N., Finegold, M. & Grompe, M. 1996, 'Hepatocytes corrected by gene therapy are selected in vivo in a murine model of hereditary tyrosinaemia type I', *Nature Genetics*.

Owsianka, A., Tarr, A.W., Juttla, V.S., Lavillette, D., Bartosch, B., Cosset, F.L., Ball, J.K. & Patel, A.H. 2005, 'Monoclonal antibody AP33 defines a broadly neutralizing epitope on the hepatitis C virus E2 envelope glycoprotein', *J Virol*, vol. 79, no. 17, 2005/08/17., pp. 11095–104.

Owsianka, A.M., Timms, J.M., Tarr, A.W., Brown, R.J.P., Hickling, T.P., Szwejk, A., Bienkowska-Szewczyk, K., Thomson, B.J., Patel, A.H. & Ball, J.K. 2006, 'Identification of Conserved Residues in the E2 Envelope Glycoprotein of the Hepatitis C Virus That Are Critical for CD81 Binding', *Journal of Virology*.

Pai, N.P., Dhurat, R., Potter, M., Behlim, T., Landry, G., Vadnais, C., Rodrigues, C., Joseph, L. & Shetty, A. 2014, 'Will a quadruple multiplexed point-of-care screening strategy for HIV-related co-infections be feasible and impact detection of new co-infections in at-risk populations? Results from cross-sectional studies', *BMJ Open*, vol. 4, no. 12, 2014/12/17., p. e005040.

Palyi, B., Magyar, N., Henczko, J., Szalai, B., Farkas, A., Strecker, T., Takacs, M. & Kis, Z. 2018, 'Determining the effect of different environmental conditions on Ebola virus viability in clinically relevant specimens', *Emerging Microbes & Infections*, vol. 7, no. 1, pp. 1–7.

Pantua, Homer, Diao, J., Ultsch, M., Hazen, M., Mathieu, M., McCutcheon, K., Takeda, K., Date, S., Cheung, T.K., Phung, Q., Hass, P., Arnott, D., Hongo, J.A., Matthews, D.J., Brown, A., Patel, A.H., Kelley, R.F., Eigenbrot, C. & Kapadia, S.B. 2013, 'Glycan shifting on hepatitis C virus (HCV) E2 glycoprotein is a mechanism for escape from broadly neutralizing antibodies', *Journal of Molecular Biology*.

Pantua, H, Diao, J., Ultsch, M., Hazen, M., Mathieu, M., McCutcheon, K., Takeda, K., Date, S., Cheung, T.K., Phung, Q., Hass, P., Arnott, D., Hongo, J.A., Matthews, D.J., Brown, A., Patel, A.H., Kelley, R.F., Eigenbrot, C. & Kapadia, S.B. 2013, 'Glycan shifting on hepatitis C virus (HCV) E2 glycoprotein is a mechanism for escape from broadly neutralizing antibodies', *J Mol Biol*, vol. 425, no. 11, 2013/03/06., pp. 1899–914.

Papatheodoridis, G., Thomas, H.C., Golna, C., Bernardi, M., Carballo, M., Cornberg, M., Dalekos, G., Degertekin, B., Dourakis, S., Flisiak, R., Goldberg, D., Gore, C., Goulis, I., Hadziyannis, S., Kalamitsis, G., Kanavos, P., Kautz, A., Koskinas, I., Leite, B.R., Malliori, M., Manolakopoulos, S., Matičič, M., Papaevangelou, V., Pirona, A., Prati, D., Raptopoulou - Gigi, M., Reic, T., Robaeys, G., Schatz, E., Souliotis, K., Tountas, Y., Wiktor, S., Wilson, D., Yfantopoulos, J. & Hatzakis, A. 2016, 'Addressing barriers to the prevention, diagnosis and treatment of hepatitis B and C in the face of persisting fiscal constraints in Europe: report from a high level conference', *Journal of Viral Hepatitis*, vol. 23, pp. 1–12.

Park, Y., Lee, J.-H., Kim, B.S., Kim, D.Y., Han, K.-H. & Kim, H.-S. 2010, 'New automated hepatitis C virus (HCV) core antigen assay as an alternative to real-time PCR for HCV RNA quantification.', *Journal of clinical microbiology*, vol. 48, no. 6, pp. 2253–6.

Parolo, C. & Merkoçi, A. 2013, 'Paper-based nanobiosensors for diagnostics.', *Chemical Society reviews*, vol. 42, no. 2, pp. 450–7.

Paska, C., Barta, I., Drozdovszky, O. & Antus, B. 2019, 'Elimination of bacterial DNA during RNA isolation from sputum: Bashing bead vortexing is preferable over prolonged DNase treatment.', *PloS one*, vol. 14, no. 3, p. e0214609.

Patel, A., Dunlop, J., Owsianka, A. & Cowton, V. 2015, 'Current and future prophylactic vaccines for hepatitis C virus', *Vaccine: Development and Therapy*, vol. 5, p. 31.

Patel, A.H., Wood, J., Penin, F., Dubuisson, J. & McKeating, J.A. 2000, 'Construction and characterization of chimeric hepatitis C virus E2 glycoproteins: analysis of regions critical for glycoprotein aggregation and CD81 binding', *J Gen Virol*, vol. 81, no. Pt 12, 2000/11/22., pp. 2873–83.

Pawlotsky, J.-M., Negro, F., Aghemo, A., Berenguer, M., Dalgard, O., Dusheiko, G., Marra, F., Puoti, M. & Wedemeyer, H. 2018, 'EASL Recommendations on Treatment of Hepatitis C 2018', *Journal of Hepatology*, vol. 69, no. 2, pp. 461–511.

Pecoraro, H.L., Spindel, M.E., Bennett, S., Lunn, K.F. & Landolt, G.A. 2013, 'Evaluation of virus isolation, one-step real-time reverse transcription polymerase chain reaction assay, and two rapid influenza diagnostic tests for detecting canine Influenza A virus H3N8 shedding in dogs', *J Vet Diagn Invest*, vol. 25, no. 3, 2013/03/29., pp. 402–6.

Peeling, R.W. 2006, 'Testing for sexually transmitted infections: a brave new world?', *Sexually transmitted infections*, vol. 82, no. 6, pp. 425–30, viewed 8 July 2019, <http://www.ncbi.nlm.nih.gov/pubmed/17151028>.

Penna, A., Pilli, M., Zerbini, A., Orlandini, A., Mezzadri, S., Sacchelli, L., Missale, G. & Ferrari, C. 2007, 'Dysfunction and functional restoration of HCV-specific CD8 responses in chronic hepatitis C virus infection', *Hepatology*.

Perz, J.F., Armstrong, G.L., Farrington, L.A., Hutin, Y.J. & Bell, B.P. 2006, 'The contributions of hepatitis B virus and hepatitis C virus infections to cirrhosis and primary liver cancer worldwide', *J Hepatol*, vol. 45, no. 4, 2006/08/02., pp. 529–38.

Pestka, J.M., Zeisel, M.B., Blaser, E., Schurmann, P., Bartosch, B., Cosset, F.-L., Patel, A.H., Meisel, H., Baumert, J., Viazov, S., Rispeter, K., Blum, H.E., Roggendorf, M. & Baumert, T.F. 2007, 'Rapid induction of virus-neutralizing antibodies and viral clearance in a single-source outbreak of hepatitis C', *Proceedings of the National Academy of Sciences*, vol. 104, no. 14, pp. 6025–30.

Petracca, R., Falugi, F., Galli, G., Norais, N., Rosa, D., Campagnoli, S., Burgio, V., Di Stasio, E., Giardina, B., Houghton, M., Abrignani, S. & Grandi, G. 2002, 'Structure-Function Analysis of Hepatitis C Virus Envelope-CD81 Binding', *Journal of Virology*.

Pietschmann, T., Kaul, A., Koutsoudakis, G., Shavinskaya, A., Kallis, S., Steinmann, E., Abid, K., Negro, F., Dreux, M., Cosset, F.-L. & Bartenschlager, R. 2006, 'Construction and characterization of infectious intragenotypic and intergenotypic hepatitis C virus chimeras.', *Proceedings of the National Academy of Sciences of the United States of America*, vol. 103, no. 19, pp. 7408–13.

Pileri, P., Uematsu, Y., Campagnoli, S., Galli, G., Falugi, F., Petracca, R., Weiner, A.J., Houghton, M., Rosa, D., Grandi, G. & Abrignani, S. 1998, 'Binding of Hepatitis C Virus to CD81', *Science*, vol. 282, no. 5390, pp. 938–41.

Pinto, R.M., Costafreda, M.I. & Bosch, A. 2009, 'Risk assessment in shellfish-borne outbreaks of hepatitis A', *Appl Environ Microbiol*, vol. 75, no. 23, 2009/10/13., pp. 7350–5.

Ploss, A., Evans, M.J., Gaysinskaya, V.A., Panis, M., You, H., de Jong, Y.P. & Rice, C.M. 2009, 'Human occludin is a hepatitis C virus entry factor required for infection of mouse cells', *Nature*, vol. 457, no. 7231, pp. 882–6.

Poordad, F., McCone, J., Bacon, B.R., Bruno, S., Manns, M.P., Sulkowski, M.S., Jacobson, I.M., Reddy, K.R., Goodman, Z.D., Boparai, N., DiNubile, M.J., Sniukiene, V., Brass, C.A., Albrecht, J.K. & Bronowicki, J.-P. 2011, 'Boceprevir for Untreated Chronic HCV Genotype 1 Infection', *New England Journal of Medicine*, vol. 364, no. 13, pp. 1195–206.

Powdrill, M.H., Tchesnokov, E.P., Kozak, R.A., Russell, R.S., Martin, R., Svarovskaia, E.S., Mo, H., Kouyos, R.D. & Gotte, M. 2011, 'Contribution of a mutational bias in hepatitis C virus replication to the genetic barrier in the development of drug resistance', *Proceedings of the National Academy of Sciences*, vol. 108, no. 51, pp. 20509–13.

Poynard, T., Bedossa, P., Chevallier, M., Mathurin, P., Lemonnier, C., Trepo, C., Couzigou, P., Payen, J.L., Sajus, M., Costa, J.M., Vidaud, M. & Chaput, J.C. 1995, 'A Comparison of Three Interferon Alfa-2b Regimens for the Long-Term Treatment of Chronic Non-A, Non-B Hepatitis', *New England Journal of Medicine*, vol. 332, no. 22, pp. 1457–63.

Prentoe, J., Jensen, T.B., Meuleman, P., Serre, S.B.N., Scheel, T.K.H., Leroux-Roels, G., Gottwein, J.M. & Bukh, J. 2011, 'Hypervariable Region 1 Differentially Impacts Viability of Hepatitis C Virus Strains of Genotypes 1 to 6 and Impairs Virus Neutralization', *Journal of Virology*, vol. 85, no. 5, pp. 2224–34.

Prentoe, J., Serre, S.B.N., Ramirez, S., Nicosia, A., Gottwein, J.M. & Bukh, J. 2014, 'Hypervariable Region 1 Deletion and Required Adaptive Envelope Mutations Confer Decreased Dependency on Scavenger Receptor Class B Type I and Low-Density Lipoprotein Receptor for Hepatitis C Virus', *Journal of Virology*, vol. 88, no. 3, pp. 1725–39.

Prentoe, J., Velázquez-Moctezuma, R., Foung, S.K.H., Law, M. & Bukh, J. 2016, 'Hypervariable region 1 shielding of hepatitis C virus is a main contributor to genotypic differences in neutralization sensitivity.', *Hepatology (Baltimore, Md.)*, vol. 64, no. 6, pp. 1881–92.

Prokunina-Olsson, L., Muchmore, B., Tang, W., Pfeiffer, R.M., Park, H., Dickensheets, H., Hergott, D., Porter-Gill, P., Mumy, A., Kohaar, I., Chen, S., Brand, N., Tarway, M., Liu, L., Sheikh, F., Astemborski, J., Bonkovsky, H.L., Edlin, B.R., Howell, C.D., Morgan, T.R., Thomas, D.L., Rehermann, B., Donnelly, R.P. & O'Brien, T.R. 2013, 'A variant upstream of IFNL3 (IL28B) creating a new interferon gene IFNL4 is associated with impaired clearance of hepatitis C virus', *Nature Genetics*, vol. 45, no. 2, pp. 164–71.

Raghuraman, S., Park, H., Osburn, W.O., Winkelstein, E., Edlin, B.R. & Rehermann, B. 2012, 'Spontaneous Clearance of Chronic Hepatitis C Virus Infection Is Associated With Appearance of Neutralizing Antibodies and Reversal of T-Cell Exhaustion', *The Journal of Infectious Diseases*, vol. 205, no. 5, pp. 763–71.

Ramirez, S., Li, Y.-P., Jensen, S.B., Pedersen, J., Gottwein, J.M. & Bukh, J. 2014, 'Highly efficient infectious cell culture of three hepatitis C virus genotype 2b strains and sensitivity to lead protease, nonstructural protein 5A, and polymerase inhibitors', *Hepatology*, vol. 59, no. 2, pp. 395–407.

Ray, R., Meyer, K., Banerjee, A., Basu, A., Coates, S., Abrignani, S., Houghton, M., Frey, S.E. & Belshe, R.B. 2010, 'Characterization of Antibodies Induced by Vaccination with Hepatitis C Virus Envelope Glycoproteins', *The Journal of Infectious Diseases*.

Ray, S.C., Wang, Y.M., Laeyendecker, O., Ticehurst, J.R., Villano, S.A. & Thomas, D.L. 1999, 'Acute hepatitis C virus structural gene sequences as predictors of persistent viremia: hypervariable region 1 as a decoy', *J Virol*, vol. 73, no. 4, 1999/03/12., pp. 2938–46.

Razavi, H., Waked, I., Sarrazin, C., Myers, R.P., Idilman, R., Calinas, F., Vogel, W., Mendes Correa, M.C., Hézode, C., Lázaro, P., Akarca, U., Aleman, S., Balık, İ., Berg, T., Bihl, F., Bilodeau, M., Blasco, A.J., Brandão Mello, C.E., Bruggmann, P., Buti, M., Calleja, J.L., Cheinquer, H., Christensen, P.B., Clausen, M., Coelho, H.S.M., Cramp, M.E., Dore, G.J., Doss, W., Duberg, A.S., El-Sayed, M.H., Ergör, G., Esmat, G., Falconer, K., Félix, J., Ferraz, M.L.G., Ferreira, P.R., Frankova, S., García-Samaniego, J., Gerstoft, J., Giria, J.A., Gonçales, F.L., Gower, E., Gschwantler, M., Guimarães Pessôa, M., Hindman, S.J., Hofer, H., Husa, P., Kåberg, M., Kaita, K.D.E., Kautz, A., Kaymakoglu, S., Krajden, M., Krarup, H., Laleman, W., Lavanchy, D., Marinho, R.T., Marotta, P., Mauss, S., Moreno, C., Murphy, K., Negro, F., Nemecek, V., Örmeci, N., Øvrehus, A.L.H., Parkes, J., Pasini, K., Peltekian, K.M., Ramji, A., Reis, N., Roberts, S.K., Rosenberg, W.M., Roudot-Thoraval, F., Ryder, S.D., Sarmento-Castro, R., Semela, D., Sherman, M., Shiha, G.E., Sievert, W., Sperl, J., Stärkel, P., Stauber, R.E., Thompson, A.J., Urbanek, P., Van Damme, P., van Thiel, I., Van Vlierberghe, H., Vandijck, D., Wedemeyer, H., Weis, N., Wiegand, J., Yosry, A., Zekry, A., Cornberg, M., Müllhaupt, B. & Estes, C. 2014, 'The present and future disease burden of hepatitis C virus (HCV) infection with today's treatment paradigm', *Journal of Viral Hepatitis*, vol. 21, pp. 34–59.

Raziorrouh, B., Ulsenheimer, A., Schraut, W., Heeg, M., Kurktschiev, P., Zachoval, R., Jung, M., Thimme, R., Neumann–Haefelin, C., Horster, S., Wächtler, M., Spannagl, M., Haas, J., Diepolder, H.M. & Grüner, N.H. 2011, 'Inhibitory Molecules That Regulate Expansion and Restoration of HCV-Specific CD4+ T Cells in Patients With Chronic Infection', *Gastroenterology*, vol. 141, no. 4, pp. 1422-1431.e6.

Reboud, J., Xu, G., Garrett, A., Adriko, M., Yang, Z., Tukahebwa, E.M., Rowell, C. & Cooper, J.M. 2019, 'Paper-based microfluidics for DNA diagnostics of malaria in low resource underserved rural communities', *Proceedings of the National Academy of Sciences*, vol. 116, no. 11, pp. 4834–42.

'Recommendations for prevention and control of hepatitis c virus (hcv) infection and hcv-related chronic disease. centers for disease control and prevention.' 1998, *MMWR. Recommendations and reports : Morbidity and mortality weekly report. Recommendations and reports*, vol. 47, no. RR-19, pp. 1–39.

Resolution WHA67.6. Hepatitis 2014, *In: Sixty-Seventh World Health Assembly. Agenda item 12.3, Geneva, 19-24 May 2014*, Geneva, viewed 25 July 2019, <www.who.int/hiv/pub/idu/targetsetting/en/index.html.>.

Roberts, E.A. & Yeung, L. 2002, 'Maternal-infant transmission of hepatitis C virus infection', *Hepatology*, vol. 36, no. 5B, pp. s106–13.

Roccasecca, R., Ansuini, H., Vitelli, A., Meola, A., Scarselli, E., Acali, S., Pezzanera, M., Ercole, B.B., McKeating, J., Yagnik, A., Lahm, A., Tramontano, A., Cortese, R. & Nicosia, A. 2003, 'Binding of the hepatitis C virus E2 glycoprotein to CD81 is strain specific and is modulated by a complex interplay between hypervariable regions 1 and 2.', *Journal of virology*, vol. 77, no. 3, pp. 1856–67.

Rooney, G. & Gilson, R.J. 1998, 'Sexual transmission of hepatitis C virus infection', *Sexually Transmitted Infections*, vol. 74, no. 6, pp. 399–404.

De Rosa, F.G., Audagnotto, S., Bargiacchi, O., Garazzino, S., Marucco, D.A., Veronese, L., Canta, F., Bonora, S., Sinicco, A. & Di Perri, G. 2006, 'Resolution of HCV infection after highly active antiretroviral therapy in a HIV–HCV coinfected patient', *Journal of Infection*, vol. 53, no. 5, pp. e215–8.

da Rosa, L., Dantas-Correa, E.B., Narciso-Schiavon, J.L. & Schiavon Lde, L. 2013, 'Diagnostic Performance of Two Point-of-Care Tests for Anti-HCV Detection', *Hepat Mon*, vol. 13, no. 9, 2013/11/28., p. e12274.

Russell, R.S., Kawaguchi, K., Meunier, J.-C., Takikawa, S., Faulk, K., Bukh, J., Purcell, R.H. & Emerson, S.U. 2009, 'Mutational analysis of the hepatitis C virus E1 glycoprotein in retroviral pseudoparticles and cell-culture-derived H77/JFH1 chimeric infectious virus particles', *Journal of Viral Hepatitis*, vol. 16, no. 9, pp. 621–32.

Saeed, M., Gondeau, C., Hmwe, S., Yokokawa, H., Date, T., Suzuki, T., Kato, T., Maurel, P. & Wakita, T. 2013, 'Replication of hepatitis C virus genotype 3a in cultured cells.', *Gastroenterology*, vol. 144, no. 1, pp. 56-58.e7.

Saeed, M., Scheel, T.K.H., Gottwein, J.M., Marukian, S., Dustin, L.B., Bukh, J. & Rice, C.M. 2012, 'Efficient replication of genotype 3a and 4a hepatitis C virus replicons in human hepatoma cells.', *Antimicrobial agents and chemotherapy*, vol. 56, no. 10, pp. 5365–73.

Sánchez-Quijano, A., Rey, C., Aguado, I., Pineda, J.A., Perez-Romero, M., Torres, Y., Leal, M. & Lissen, E. 1990, 'Hepatitis C virus infection in sexually promiscuous groups.', *European journal of clinical microbiology & infectious diseases : official publication of the European Society of Clinical Microbiology*, vol. 9, no. 8, pp. 610–2.

Sandgren, E.P., Palmiter, R.D., Heckel, J.L., Daugherty, C.C., Brinster, R.L. & Degen, J.L. 1991, 'Complete hepatic regeneration after somatic deletion of an albumin-plasminogen activator transgene', *Cell*.

Sarvari, J., Moattari, A., Pirbonyeh, N., Moini, M. & Hosseini, S.Y. 2016, 'The Impact of IFN-γ Gene Polymorphisms on Spontaneous Clearance of HCV Infection in Fars Province, Southern of Iran', *Journal of Clinical Laboratory Analysis*, vol. 30, no. 4, pp. 301–7.

Sautto, G., Tarr, A.W., Mancini, N. & Clementi, M. 2013, 'Structural and antigenic definition of hepatitis C virus E2 glycoprotein epitopes targeted by monoclonal antibodies', *Clinical and Developmental Immunology*.

Scarselli, E., Ansuini, H., Cerino, R., Roccasecca, R.M., Acali, S., Filocamo, G., Traboni, C., Nicosia, A., Cortese, R. & Vitelli, A. 2002, 'The human scavenger receptor class B type I is a novel candidate receptor for the hepatitis C virus', *The EMBO Journal*, vol. 21, no. 19, pp. 5017–25.

Schackman, B.R., Leff, J.A., Barter, D.M., DiLorenzo, M.A., Feaster, D.J., Metsch, L.R., Freedberg, K.A. & Linas, B.P. 2015, 'Cost-effectiveness of rapid hepatitis C virus (HCV) testing and simultaneous rapid HCV and HIV testing in substance abuse treatment programs', *Addiction*, vol. 110, no. 1, 2014/10/09., pp. 129–43.

von Schaewen, M., Ding, Q. & Ploss, A. 2014, 'Visualizing hepatitis C virus infection in humanized mice', *Journal of Immunological Methods*.

Scheel, T.K.H., Simmonds, P. & Kapoor, A. 2015, 'Surveying the global virome: Identification and characterization of HCV-related animal hepaciviruses', *Antiviral Research*.

Schneider, L., Blakely, H. & Tripathi, A. 2019, 'Mathematical model to reduce loop mediated isothermal amplification (LAMP) false-positive diagnosis', *ELECTROPHORESIS*, p. elps.201900167.

Scott, C. & Griffin, S. 2015, 'Viroporins: structure, function and potential as antiviral targets', *Journal of General Virology*, vol. 96, no. 8, pp. 2000–27.

Seeff, L.B. 2002, 'Natural history of chronic hepatitis C', *Hepatology*, vol. 36, no. 5B, pp. s35–46.

Semmo, N., Day, C.L., Ward, S.M., Lucas, M., Harcourt, G., Loughry, A. & Klenerman, P. 2005, 'Preferential loss of IL-2-secreting CD4+ T helper cells in chronic HCV infection', *Hepatology*, vol. 41, no. 5, pp. 1019–28.

Sharma, M., Al Kaabi, S., John, A.K., Al Dweik, N., Ullah Wani, H., Babu Thandassary, R., Derbala, M.F., Al Ejji, K., Sultan, K., Pasic, F., Al Mohannadi, M., Yacoub, R., Butt, M.T. & Singh, R. 2015, 'Screening for hepatitis C in average and high-risk populations of Qatar using rapid point-of-care testing', *United European gastroenterology journal*, vol. 3, no. 4, pp. 364–70.

Shen, F., Sun, B., Kreutz, J.E., Davydova, E.K., Du, W., Reddy, P.L., Joseph, L.J. & Ismagilov, R.F. 2011, 'Multiplexed quantification of nucleic acids with large dynamic range using multivolume digital RT-PCR on a rotational SlipChip tested with HIV and hepatitis C viral load', *J Am Chem Soc*, vol. 133, no. 44, 2011/10/15., pp. 17705–12.

Shi, S.T. & Lai, M.M.C. 2006, *HCV 5′ and 3′UTR: When Translation Meets Replication*, *Hepatitis C Viruses: Genomes and Molecular Biology*, Horizon Bioscience.

Shoukry, N.H. 2003, *Memory CD8(+) T Cells Are Required for Protection from Persistent Hepatitis C Virus Infection*, vol. 197, no. 12, pp. 1645–55.

Simmonds, P. 2004, 'Genetic diversity and evolution of hepatitis C virus - 15 years on', *Journal of General Virology*, vol. 85, no. 11, pp. 3173–88.

Smith, B.D., Teshale, E., Jewett, A., Weinbaum, C.M., Neaigus, A., Hagan, H., Jenness, S.M., Melville, S.K., Burt, R., Thiede, H., Al-Tayyib, A., Pannala, P.R., Miles, I.W., Oster, A.M., Smith, A., Finlayson, T., Bowles, K.E. & Dinenno, E.A. 2011, 'Performance of premarket rapid hepatitis C virus antibody assays in 4 national human immunodeficiency virus behavioral surveillance system sites', *Clin Infect Dis*, vol. 53, no. 8, pp. 780–6.

Smith, D.B., Bukh, J., Kuiken, C., Muerhoff, A.S., Rice, C.M., Stapleton, J.T. & Simmonds, P. 2014, 'Expanded classification of hepatitis C virus into 7 genotypes and 67 subtypes: updated criteria and genotype assignment web resource', *Hepatology*, vol. 59, no. 1, pp. 318–27.

Smith, D.B., Mellor, J., Jarvis, L.M., Davidson, F., Kolberg, J., Urdea, M., Yap, P.-L. & Simmonds, P. 1995, 'Variation of the hepatitis C virus 5' non-coding region: implications for secondary structure, virus detection and typing', *Journal of General Virology*, vol. 76, no. 7, pp. 1749–61.

Smyk-Pearson, S., Tester, I.A., Lezotte, D., Sasaki, A.W., Lewinsohn, D.M. & Rosen, H.R. 2006, 'Differential Antigenic Hierarchy Associated with Spontaneous Recovery from Hepatitis C Virus Infection: Implications for Vaccine Design', *The Journal of Infectious Diseases*.

Soliman, H.H., Nagy, H., Kotb, N. & Alm El-Din, M.A. 2012, 'The role of chemokine CC ligand 20 in patients with liver cirrhosis and hepatocellular carcinoma', *The International Journal of Biological Markers*, vol. 27, no. 2, pp. 125–31.

Spaan, M., Kreefft, K., de Graav, G.N., Brouwer, W.P., de Knegt, R.J., ten Kate, F.J.W., Baan, C.C., Vanwolleghem, T., Janssen, H.L.A. & Boonstra, A. 2015, 'CD4+CXCR5+ T cells in chronic HCV infection produce less IL-21, yet are efficient at supporting B cell responses', *Journal of Hepatology*, vol. 62, no. 2, pp. 303–10.

Stanaway, J.D., Flaxman, A.D., Naghavi, M., Fitzmaurice, C., Vos, T., Abubakar, I., Abu-Raddad, L.J., Assadi, R., Bhala, N., Cowie, B., Forouzanfour, M.H., Groeger, J., Hanafiah, K.M., Jacobsen, K.H., James, S.L., MacLachlan, J., Malekzadeh, R., Martin, N.K., Mokdad, A.A., Mokdad, A.H., Murray, C.J.L., Plass, D., Rana, S., Rein, D.B., Richardus, J.H., Sanabria, J., Saylan, M., Shahraz, S., So, S., Vlassov, V. V, Weiderpass, E., Wiersma, S.T., Younis, M., Yu, C., El Sayed Zaki, M. & Cooke, G.S. 2016, 'The global burden of viral hepatitis from 1990 to 2013: findings from the Global Burden of Disease Study 2013', *The Lancet*, vol. 388, no. 10049, pp. 1081–8.

Stapleton, J.T., Foung, S., Muerhoff, A.S., Bukh, J. & Simmonds, P. 2011, 'The GB viruses: A review and proposed classification of GBV-A, GBV-C (HGV), and GBV-D in genus Pegivirus within the family Flaviviridae', *Journal of General Virology*.

Steinmann, E., Penin, F., Kallis, S., Patel, A.H., Bartenschlager, R. & Pietschmann, T. 2007, 'Hepatitis C Virus p7 Protein Is Crucial for Assembly and Release of Infectious Virions', *PLoS Pathogens*, vol. 3, no. 7, p. e103.

Subramaniam, A.B., Gonidec, M., Shapiro, N.D., Kresse, K.M. & Whitesides, G.M. 2015, 'Metal-amplified Density Assays, (MADAs), including a Density-Linked Immunosorbent Assay (DeLISA)', *Lab Chip*, vol. 15, no. 4, 2014/12/05., pp. 1009–22.

Suppiah, V., Moldovan, M., Ahlenstiel, G., Berg, T., Weltman, M., Abate, M.L., Bassendine, M., Spengler, U., Dore, G.J., Powell, E., Riordan, S., Sheridan, D., Smedile, A., Fragomeli, V., Müller, T., Bahlo, M., Stewart, G.J., Booth, D.R. & George, J. 2009, 'IL28B is associated with response to chronic hepatitis C interferon-α and ribavirin therapy', *Nature Genetics*, vol. 41, no. 10, pp. 1100–4.

Suzuki, T. & Suzuki, R. 2016, 'Role of Nonstructural Proteins in HCV Replication', *Hepatitis C Virus I*, Springer Japan, Tokyo, pp. 129–48, viewed 22 June 2019, <http://link.springer.com/10.1007/978-4-431-56098-2_7>.

Swadling, L., Capone, S., Antrobus, R.D., Brown, A., Richardson, R., Newell, E.W., Halliday, J., Kelly, C., Bowen, D., Fergusson, J., Kurioka, A., Ammendola, V., Del Sorbo, M., Grazioli, F., Esposito, M.L., Siani, L., Traboni, C., Hill, A., Colloca, S., Davis, M., Nicosia, A., Cortese, R., Folgori, A., Klenerman, P. & Barnes, E. 2014, 'A human vaccine strategy based on chimpanzee adenoviral and MVA vectors that primes, boosts, and sustains functional HCV-specific T cell memory', *Science Translational Medicine*.

Takahashi, K., Asabe, S., Wieland, S., Garaigorta, U., Gastaminza, P., Isogawa, M. & Chisari, F. V. 2010, 'Plasmacytoid dendritic cells sense hepatitis C virus-infected cells, produce interferon, and inhibit infection', *Proceedings of the National Academy of Sciences*, vol. 107, no. 16, pp. 7431–6.

Tanaka, T., Kato, N., Cho, M.J. & Shimotohno, K. 1995, 'A Novel Sequence Found at the 3′-Terminus of Hepatitis C Virus Genome', *Biochemical and Biophysical Research Communications*, vol. 215, no. 2, pp. 744–9.

Tang, D, Tang, J., Su, B., Ren, J. & Chen, G. 2010, 'Simultaneous determination of five-type hepatitis virus antigens in 5 min using an integrated automatic electrochemical immunosensor array', *Biosens Bioelectron*, vol. 25, no. 7, 2009/12/22., pp. 1658–62.

Tang, Dianping, Tang, J., Su, B., Ren, J. & Chen, G. 2010, 'Simultaneous determination of five-type hepatitis virus antigens in 5min using an integrated automatic electrochemical immunosensor array', *Biosensors and Bioelectronics*, vol. 25, no. 7, pp. 1658–62.

Tanner, N.A., Zhang, Y. & Evans Jr., T.C. 2012, 'Simultaneous multiple target detection in real-time loop-mediated isothermal amplification', *Biotechniques*, vol. 53, no. 2, 2012/10/04., pp. 81–9.

Targett-Adams, P. & McLauchlan, J. 2005, 'Development and characterization of a transient-replication assay for the genotype 2a hepatitis C virus subgenomic replicon', *Journal of General Virology*, vol. 86, no. 11, pp. 3075–80.

Tarr, Alexander W., Owsianka, A.M., Jayaraj, D., Brown, R.J.P., Hickling, T.P., Irving, W.L., Patel, A.H. & Ball, J.K. 2007, 'Determination of the human antibody response to the epitope defined by the hepatitis C virus-neutralizing monoclonal antibody AP33', *Journal of General Virology*.

Tarr, A W, Owsianka, A.M., Szwejk, A., Ball, J.K. & Patel, A.H. 2007, 'Cloning, expression, and functional analysis of patient-derived hepatitis C virus glycoproteins', *Methods Mol Biol*, vol. 379, 2007/05/16., pp. 177–97.

Tarr, A W, Owsianka, A.M., Timms, J.M., McClure, C.P., Brown, R.J., Hickling, T.P., Pietschmann, T., Bartenschlager, R., Patel, A.H. & Ball, J.K. 2006, 'Characterization of the hepatitis C virus E2 epitope defined by the broadly neutralizing monoclonal antibody AP33', *Hepatology*, vol. 43, no. 3, 2006/02/24., pp. 592–601.

Tarr, Alexander W., Owsianka, A.M., Timms, J.M., McClure, C.P., Brown, Richard J.P., Hickling, T.P., Pietschmann, T., Bartenschlager, R., Patel, A.H. & Ball, J.K. 2006, 'Characterization of the hepatitis C virus E2 epitope defined by the broadly neutralizing monoclonal antibody AP33', *Hepatology*.

Tarr, Alexander W., Owsianka, A.M., Timms, J.M., McClure, C.P., Brown, Richard J. P., Hickling, T.P., Pietschmann, T., Bartenschlager, R., Patel, A.H. & Ball, J.K. 2006, 'Characterization of the hepatitis C virus E2 epitope defined by the broadly neutralizing monoclonal antibody AP33', *Hepatology*, vol. 43, no. 3, pp. 592–601.

Tarr, A.W., Urbanowicz, R.A., Jayaraj, D., Brown, R.J.P., McKeating, J.A., Irving, W.L. & Ball, J.K. 2012, 'Naturally Occurring Antibodies That Recognize Linear Epitopes in the Amino Terminus of the Hepatitis C Virus E2 Protein Confer Noninterfering, Additive Neutralization', *Journal of Virology*, vol. 86, no. 5, pp. 2739–49.

Thimme, R., Oldach, D., Chang, K.-M., Steiger, C., Ray, S.C. & Chisari, F. V. 2001a, 'Determinants of Viral Clearance and Persistence during Acute Hepatitis C Virus Infection', *The Journal of Experimental Medicine*, vol. 194, no. 10, pp. 1395–406.

Thimme, R., Oldach, D., Chang, K.-M., Steiger, C., Ray, S.C. & Chisari, F. V. 2001b, 'Determinants of Viral Clearance and Persistence during Acute Hepatitis C Virus Infection', *The Journal of Experimental Medicine*, vol. 194, no. 10, pp. 1395–406.

Thomas, D.L. & Seeff, L.B. 2005, 'Natural History of Hepatitis C', *Clinics in Liver Disease*, vol. 9, no. 3, pp. 383–98.

Thomas, D.L., Thio, C.L., Martin, M.P., Qi, Y., Ge, D., O'hUigin, C., Kidd, J., Kidd, K., Khakoo, S.I., Alexander, G., Goedert, J.J., Kirk, G.D., Donfield, S.M., Rosen, H.R., Tobler, L.H., Busch, M.P., McHutchison, J.G., Goldstein, D.B. & Carrington, M. 2009, 'Genetic variation in IL28B and spontaneous clearance of hepatitis C virus', *Nature*, vol. 461, no. 7265, pp. 798–801.

Thomson, E., Ip, C.L., Badhan, A., Christiansen, M.T., Adamson, W., Ansari, M.A., Bibby, D., Breuer, J., Brown, A., Bowden, R., Bryant, J., Bonsall, D., Da Silva Filipe, A., Hinds, C., Hudson, E., Klenerman, P., Lythgow, K., Mbisa, J.L., McLauchlan, J., Myers, R., Piazza, P., Roy, S., Trebes, A., Sreenu, V.B., Witteveldt, J., Barnes, E. & Simmonds, P. 2016, 'Comparison of Next-Generation Sequencing Technologies for Comprehensive Assessment of Full-Length Hepatitis C Viral Genomes', *J Clin Microbiol*, vol. 54, no. 10, 2016/07/08., pp. 2470–84.

Thomson, E.C., Fleming, V.M., Main, J., Klenerman, P., Weber, J., Eliahoo, J., Smith, J., McClure, M.O. & Karayiannis, P. 2011, 'Predicting spontaneous clearance of acute hepatitis C virus in a large cohort of HIV-1-infected men', *Gut*, vol. 60, no. 6, 2010/12/09., pp. 837–45.

Thomson, E.C., Nastouli, E., Main, J., Karayiannis, P., Eliahoo, J., Muir, D. & McClure, M.O. 2009, 'Delayed anti-HCV antibody response in HIV-positive men acutely infected with HCV', *AIDS*, vol. 23, no. 1, pp. 89–93.

Thorpe, L.E., Ouellet, L.J., Levy, J.R., Williams, I.T. & Monterroso, E.R. 2000, 'Hepatitis C Virus Infection: Prevalence, Risk Factors, and Prevention Opportunities among Young Injection Drug Users in Chicago, 1997–1999', *The Journal of Infectious Diseases*, vol. 182, no. 6, pp. 1588–94.

Timm, J., Lauer, G.M., Kavanagh, D.G., Sheridan, I., Kim, A.Y., Lucas, M., Pillay, T., Ouchi, K., Reyor, L.L., zur Wiesch, J.S., Gandhi, R.T., Chung, R.T., Bhardwaj, N., Klenerman, P., Walker, B.D. & Allen, T.M. 2004, 'CD8 Epitope Escape and Reversion in Acute HCV Infection', *The Journal of Experimental Medicine*.

Tone, K., Fujisaki, R., Yamazaki, T. & Makimura, K. 2017, 'Enhancing melting curve analysis for the discrimination of loop-mediated isothermal amplification products from four pathogenic molds: Use of inorganic pyrophosphatase and its effect in reducing the variance in melting temperature values', *Journal of Microbiological Methods*, vol. 132, pp. 41–5.

Tong, Y., Lavillette, D., Li, Q. & Zhong, J. 2018, 'Role of Hepatitis C Virus Envelope Glycoprotein E1 in Virus Entry and Assembly.', *Frontiers in immunology*, vol. 9, p. 1411.

Torres, C., Vitalis, E.A., Baker, B.R., Gardner, S.N., Torres, M.W. & Dzenitis, J.M. 2011, 'LAVA: an open-source approach to designing LAMP (loop-mediated isothermal amplification) DNA signatures.', *BMC bioinformatics*, vol. 12, p. 240.

Trivedi, S., Murthy, S., Sharma, H., Hartlage, A.S., Kumar, A., Gadi, S. V., Simmonds, P., Chauhan, L. V., Scheel, T.K.H., Billerbeck, E., Burbelo, P.D., Rice, C.M., Lipkin, W.I., Vandegrift, K., Cullen, J.M. & Kapoor, A. 2018, 'Viral persistence, liver disease, and host response in a hepatitis C-like virus rat model', *Hepatology*, vol. 68, no. 2, pp. 435–48.

Urbani, S., Amadei, B., Tola, D., Massari, M., Schivazappa, S., Missale, G. & Ferrari, C. 2006, 'PD-1 Expression in Acute Hepatitis C Virus (HCV) Infection Is Associated with HCV-Specific CD8 Exhaustion', *Journal of Virology*.

Urbanowicz, Richard A., McClure, C.P., Brown, R.J.P., Tsoleridis, T., Persson, M.A.A., Krey, T., Irving, W.L., Ball, J.K. & Tarr, A.W. 2016, 'A Diverse Panel of Hepatitis C Virus Glycoproteins for Use in Vaccine Research Reveals Extremes of Monoclonal Antibody Neutralization Resistance', *Journal of Virology*, vol. 90, no. 7, pp. 3288–301.

Urbanowicz, Richard A, McClure, C.P., King, B., Mason, C.P., Ball, J.K. & Tarr, A.W. 2016, 'Novel functional hepatitis C virus glycoprotein isolates identified using an optimized viral pseudotype entry assay.', *The Journal of general virology*, vol. 97, no. 9, pp. 2265–79.

Vaghi, V., Potrich, C., Pasquardini, L., Lunelli, L., Vanzetti, L., Ebranati, E., Lai, A., Zehender, G., Mombello, D., Cocuzza, M., Pirri, C.F. & Pederzolli, C. 2016, 'On-chip purification and detection of hepatitis C virus RNA from human plasma', *Biophys Chem*, vol. 208, 2015/06/21., pp. 54–61.

Varaklioti, A., Vassilaki, N., Georgopoulou, U. & Mavromara, P. 2002, 'Alternate translation occurs within the core coding region of the hepatitis C viral genome', *Journal of Biological Chemistry*.

Vassilaki, N., Friebe, P., Meuleman, P., Kallis, S., Kaul, A., Paranhos-Baccalà, G., Leroux-Roels, G., Mavromara, P. & Bartenschlager, R. 2008, 'Role of the hepatitis C virus core+1 open reading frame and core cis-acting RNA elements in viral RNA translation and replication.', *Journal of virology*, vol. 82, no. 23, pp. 11503–15.

Vernelen, K., Claeys, H., Verhaert, H., Volckaerts, A. & Vermylen, C. 1994, 'Significance of NS3 and NS5 antigens in screening for HCV antibody.', *Lancet (London, England)*, vol. 343, no. 8901, p. 853.

Viana, G.M.R., Silva-Flannery, L., Lima Barbosa, D.R., Lucchi, N., do Valle, S.C.N., Farias, S., Barbalho, N., Marchesini, P., Rossi, J.C.N., Udhayakumar, V., Póvoa, M.M. & de Oliveira, A.M. 2018, 'Field evaluation of a real time loop-mediated isothermal amplification assay (RealAmp) for malaria diagnosis in Cruzeiro do Sul, Acre, Brazil', *PLOS ONE*, vol. 13, no. 7, p. e0200492.

Wakita, T., Pietschmann, T., Kato, T., Date, T., Miyamoto, M., Zhao, Z., Murthy, K., Habermann, A., Kräusslich, H.-G., Mizokami, M., Bartenschlager, R. & Liang, T.J. 2005, 'Production of infectious hepatitis C virus in tissue culture from a cloned viral genome', *Nature Medicine*, vol. 11, no. 7, pp. 791–6.

Waldron, P.R., Belitskaya-Lévy, I., Chary, A., Won, J., Winters, M., Monto, A., Ryan, J., Lazzeroni, L.C. & Holodniy, M. 2016, 'Genetic Variation in the IL-6 and HLA-DQB1 Genes Is Associated with Spontaneous Clearance of Hepatitis C Virus Infection.', *Journal of immunology research*, vol. 2016, p. 6530436.

Walewski, J.L., Keller, T.R., Stump, D.D. & Branch, A.D. 2001, 'Evidence for a new hepatitis C virus antigen encoded in an overlapping reading frame', *RNA*.

Wandeler, G., Schlauri, M., Jaquier, M.-E., Rohrbach, J., Metzner, K.J., Fehr, Jan, Ambrosioni, J., Cavassini, Matthias, Stöckle, M., Schmid, Patrick, Bernasconi, Enos, Keiser, Olivia, Salazar-Vizcaya, L., Furrer, Hansjakob, Rauch, Andri, Aubert, V., Battegay, M., Bernasconi, E., Böni, J., Bucher, H.C., Burton-Jeangros, C., Calmy, A., Cavassini, M., Dollenmaier, G., Egger, M., Elzi, L., Fehr, J., Fellay, J., Furrer, H., Fux, C.A., Gorgievski, M., Günthard, H., Haerry, D., Hasse, B., Hirsch, H.H., Hoffmann, M., Hösli, I., Kahlert, C., Kaiser, L., Keiser, O., Klimkait, T., Kouyos, R., Kovari, H., Ledergerber, B., Martinetti, G., Martinez de Tejada, B., Metzner, K., Müller, N., Nadal, D., Nicca, D., Pantaleo, G., Rauch, A., Regenass, S., Rickenbach, M., Rudin, C., Schöni-Affolter, F., Schmid, P., Schüpbach, J., Speck, R., Tarr, P., Telenti, A., Trkola, A., Vernazza, P., Weber, R., Yerly, S. & Yerly, S. 2015, 'Incident Hepatitis C Virus Infections in the Swiss HIV Cohort Study: Changes in Treatment Uptake and Outcomes Between 1991 and 2013', *Open Forum Infectious Diseases*, vol. 2, no. 1, p. ofv026.

Wang, D.-G., Brewster, J.D., Paul, M. & Tomasula, P.M. 2015, 'Two methods for increased specificity and sensitivity in loop-mediated isothermal amplification.', *Molecules (Basel, Switzerland)*, vol. 20, no. 4, pp. 6048–59.

Wang, J.M., Shi, L., Ma, C.J., Ji, X.J., Ying, R.S., Wu, X.Y., Wang, K.S., Li, G., Moorman, J.P. & Yao, Z.Q. 2013, 'Differential Regulation of Interleukin-12 (IL-12)/IL-23 by Tim-3 Drives TH17 Cell Development during Hepatitis C Virus Infection', *Journal of Virology*, vol. 87, no. 8, pp. 4372–83.

Wang, Q.Q., Zhang, J., Hu, J.S., Chen, H.T., Du, L., Wu, L.Q., Ding, Y.Z., Xiong, S.H., Huang, X.C., Zhang, Y.H. & Liu, Y.S. 2011, 'Rapid detection of hepatitis C virus RNA by a reverse transcription loop-mediated isothermal amplification assay', *FEMS Immunol Med Microbiol*, vol. 63, no. 1, pp. 144–7.

Wang, Yi, Li, H., Wang, Yan, Zhang, L., Xu, J. & Ye, C. 2017, 'Loop-Mediated Isothermal Amplification Label-Based Gold Nanoparticles Lateral Flow Biosensor for Detection of Enterococcus faecalis and Staphylococcus aureus', *Frontiers in Microbiology*, vol. 8, p. 192.

Wei, X., Jia, Z.-S., Lian, J.-Q., Zhang, Y., Li, J., Ma, L., Ye, L., Wang, J.-P., Pan, L., Wang, P.-Z. & Bai, X.-F. 2009, 'Inhibition of Hepatitis C Virus Infection by Interferon-γ Through Downregulating Claudin-1', *Journal of Interferon & Cytokine Research*, vol. 29, no. 3, pp. 171–8.

Weiner, A.J., Geysen, H.M., Christopherson, C., Hall, J.E., Mason, T.J., Saracco, G., Bonino, F., Crawford, K., Marion, C.D. & Crawford, K.A. 1992, 'Evidence for immune selection of hepatitis C virus (HCV) putative envelope glycoprotein variants: potential role in chronic HCV infections.', *Proceedings of the National Academy of Sciences*, vol. 89, no. 8, pp. 3468–72.

Weiner, A.J., Kuo, G., Bradley, D.W., Bonino, F., Saracco, G., Lee, C., Rosenblatt, J., Choo, Q.L. & Houghton, M. 1990, 'Detection of hepatitis C viral sequences in non-A, non-B hepatitis.', *Lancet (London, England)*, vol. 335, no. 8680, pp. 1–3.

Wieland, S., Makowska, Z., Campana, B., Calabrese, D., Dill, M.T., Chung, J., Chisari, F. V. & Heim, M.H. 2014, 'Simultaneous detection of hepatitis C virus and interferon stimulated gene expression in infected human liver', *Hepatology*, vol. 59, no. 6, pp. 2121–30.

Wong, J.A.J.-X., Bhat, R., Hockman, D., Logan, M., Chen, C., Levin, A., Frey, S.E., Belshe, R.B., Tyrrell, D.L., Law, J.L.M. & Houghton, M. 2014, 'Recombinant Hepatitis C Virus Envelope Glycoprotein Vaccine Elicits Antibodies Targeting Multiple Epitopes on the Envelope Glycoproteins Associated with Broad Cross-Neutralization', *Journal of Virology*.

Wong, V.W., Wong, G.L., Chim, A.M., Cheng, T.F., Cheung, S.W., Lai, C.M., Szeto, K.J., Tsang, S., Wu, S.H., Yan, K.K., Hui, A.Y., Yiu, D.C., Wu, B.B., Cheung, D., Chung, C.S., Lai, C.W. & Chan, H.L. 2014, 'Targeted hepatitis C screening among ex-injection drug users in the community', *J Gastroenterol Hepatol*, vol. 29, no. 1, 2013/09/17., pp. 116–20.

Wong, Y.-P., Othman, S., Lau, Y.-L., Radu, S. & Chee, H.-Y. 2018, 'Loop-mediated isothermal amplification (LAMP): a versatile technique for detection of micro-organisms', *Journal of Applied Microbiology*, vol. 124, no. 3, pp. 626–43.

Wose Kinge, C.N., Espiritu, C., Prabdial-Sing, N., Sithebe, N.P., Saeed, M. & Rice, C.M. 2014, 'Hepatitis C Virus Genotype 5a Subgenomic Replicons for Evaluation of Direct-Acting Antiviral Agents', *Antimicrobial Agents and Chemotherapy*, vol. 58, no. 9, pp. 5386–94.

Wu, G.Y., Konishi, M., Walton, C.M., Olive, D., Hayashi, K. & Wu, C.H. 2005, 'A Novel Immunocompetent Rat Model of HCV Infection and Hepatitis', *Gastroenterology*, vol. 128, no. 5, pp. 1416–23.

Xu, G., Nolder, D., Reboud, J., Oguike, M.C., van Schalkwyk, D.A., Sutherland, C.J. & Cooper, J.M. 2016, 'Paper-Origami-Based Multiplexed Malaria Diagnostics from Whole Blood', *Angew Chem Int Ed Engl*, vol. 55, no. 49, 2016/08/25., pp. 15250–3.

Xu, G., Zhao, H., Cooper, J.M. & Reboud, J. 2016, 'A capillary-based multiplexed isothermal nucleic acid-based test for sexually transmitted diseases in patients', *Chem Commun (Camb)*, vol. 52, no. 82, 2016/10/11., pp. 12187–90.

Yamada, N., Tanihara, K., Takada, A., Yorihuzi, T., Tsutsumi, M., Shimomura, H., Tsuji, T. & Date, T. 1996, 'Genetic Organization and Diversity of the 3′ Noncoding Region of the Hepatitis C Virus Genome', *Virology*, vol. 223, no. 1, pp. 255–61.

Yanagi, M., Purcell, R.H., Emerson, S.U. & Bukh, J. 1997, 'Transcripts from a single full-length cDNA clone of hepatitis C virus are infectious when directly transfected into the liver of a chimpanzee', *Proceedings of the National Academy of Sciences of the United States of America*, vol. 94, no. 16, pp. 8738–43.

Yang, J., Fang, M.X., Li, J., Lou, G.Q., Lu, H.J. & Wu, N.P. 2011, 'Detection of hepatitis C virus by an improved loop-mediated isothermal amplification assay', *Arch Virol*, vol. 156, no. 8, 2011/05/13., pp. 1387–96.

Yasui, K., Wakita, T., Tsukiyama-Kohara, K., Funahashi, S.I., Ichikawa, M., Kajita, T., Moradpour, D., Wands, J.R. & Kohara, M. 1998, 'The native form and maturation process of hepatitis C virus core protein.', *Journal of virology*.

Yu, M. -y. W., Bartosch, B., Zhang, P., Guo, Z. -p., Renzi, P.M., Shen, L. -m., Granier, C., Feinstone, S.M., Cosset, F.-L. & Purcell, R.H. 2004, 'Neutralizing antibodies to hepatitis C virus (HCV) in immune globulins derived from anti-HCV-positive plasma', *Proceedings of the National Academy of Sciences*.

Yu, M., Peng, B., Chan, K., Gong, R., Yang, H., Delaney, W. & Cheng, G. 2014, 'Robust and Persistent Replication of the Genotype 6a Hepatitis C Virus Replicon in Cell Culture', *Antimicrobial Agents and Chemotherapy*, vol. 58, no. 5, pp. 2638–46.

Zeisel, M.B., Felmlee, D.J. & Baumert, T.F. 2013, 'Hepatitis C Virus Entry', *Current topics in microbiology and immunology*, vol. 369, pp. 87–112.

Zhang, L., Ding, B., Chen, Q., Feng, Q., Lin, L. & Sun, J. 2017, 'Point-of-care-testing of nucleic acids by microfluidics', *TrAC Trends in Analytical Chemistry*, vol. 94, pp. 106–16.

Zhao, N., Liu, J. & Sun, D. 2017, 'Detection of HCV genotypes 1b and 2a by a reverse transcription loop-mediated isothermal amplification assay', *J Med Virol*, vol. 89, no. 6, 2016/12/10., pp. 1048–54.

Zhao, Y., Chen, F., Li, Q., Wang, L. & Fan, C. 2015, 'Isothermal Amplification of Nucleic Acids', *Chemical Reviews*, vol. 115, no. 22, pp. 12491–545.

Zhao, Z., Zhong, L., Elrod, E., Struble, E., Ma, L., Yan, H., Harman, C., Deng, L., Virata-Theimer, M.L., Liu, P., Alter, H., Grakoui, A. & Zhang, P. 2014, 'A neutralization epitope in the hepatitis C virus E2 glycoprotein interacts with host entry factor CD81.', *PloS one*, vol. 9, no. 1, p. e84346.

Zhong, J., Gastaminza, P., Cheng, G., Kapadia, S., Kato, T., Burton, D.R., Wieland, S.F., Uprichard, S.L., Wakita, T. & Chisari, F. V. 2005, 'Robust hepatitis C virus infection in vitro', *Proceedings of the National Academy of Sciences*, vol. 102, no. 26, pp. 9294–9.

Zhou, D., Guo, J., Xu, L., Gao, S., Lin, Q., Wu, Q., Wu, L. & Que, Y. 2014, 'Establishment and application of a loop-mediated isothermal amplification (LAMP) system for detection of cry1Ac transgenic sugarcane', *Scientific Reports*.

Zhou, Y., Wan, Z., Yang, S., Li, Y., Li, M., Wang, B., Hu, Y., Xia, X., Jin, X., Yu, N. & Zhang, C. 2019, 'A Mismatch-Tolerant Reverse Transcription Loop-Mediated Isothermal Amplification Method and Its Application on Simultaneous Detection of All Four Serotype of Dengue Viruses', *Frontiers in Microbiology*, vol. 10, p. 1056.

Zou, Y., Mason, M.G., Wang, Y., Wee, E., Turni, C., Blackall, P.J., Trau, M. & Botella, J.R. 2017, 'Nucleic acid purification from plants, animals and microbes in under 30 seconds', *PLOS Biology*, vol. 15, no. 11, p. e2003916.